



Bicycling Science

David Gordon Wilson and Theodor Schmidt
with contributions by Jim Papadopoulos

“Full of interesting material to ponder
while pedaling down the road.”

— Jearl Walker, *American Journal of Physics*

fourth edition

Bicycling Science

Fourth Edition

David Gordon Wilson and Theodor Schmidt

with contributions by Jim Papadopoulos

**The MIT Press
Cambridge, Massachusetts
London, England**

© 2020 Massachusetts Institute of Technology

All rights reserved. No part of this book may be reproduced in any form by any electronic or mechanical means (including photocopying, recording, or information storage and retrieval) without permission in writing from the publisher.

This book was set in ITC Stone Serif Std and ITC Stone Sans Std by Toppan Best-set Premedia Limited.

Library of Congress Cataloging-in-Publication Data

Names: Wilson, David Gordon, 1928–2019 author. | Schmidt, Theodor (Bernhard), 1954– author. | Papadopoulos, Jim, contributor.

Title: *Bicycling science* / David Gordon Wilson and Theodor Schmidt ; with contributions by Jim Papadopoulos.

Description: Fourth edition. | Cambridge, Massachusetts ; London, England : The MIT Press, [2020] | Includes bibliographical references and index.

Identifiers: LCCN 2019024252 | ISBN 9780262538404 (paperback) | ISBN 9780262357531 (ebook)

Subjects: LCSH: Bicycles—Dynamics. | Bicycles—History. | Human powered vehicles.

Classification: LCC TL410 .W546 2020 | DDC 629.227/2015313—dc23

LC record available at <https://lccn.loc.gov/2019024252>

10 9 8 7 6 5 4 3 2 1

Contents

Preface vii

In Memoriam David Gordon Wilson xi

- 1 A Short History of Bicycling 1**
- 2 Human Power Generation 41**
- 3 Speed Achievements and Racing 129**
- 4 Power and Speed 171**
- 5 Bicycle Aerodynamics 213**
- 6 Rolling: Tires and Bearings 261**
- 7 Braking 319**
- 8 Steering, Balancing, and Stability 349**
- 9 Power Transmission and Hybrid Systems 393**
- 10 Special Human-Powered Machines 453**
- 11 Human-Powered Vehicles for Transportation 523**

Index 547

Preface

In 2017 The MIT Press asked me to consider bringing out a fourth edition of *Bicycling Science*. I was impressed with its confidence in the book and with the challenge that a fourth editing presented. The first three editions were lucky in that there was a great deal of interest, at the time they were published, in bicycles in general and in experimental innovative bicycles in particular. The International Human Powered Vehicle Association (IHPVA) was founded in the mid-1970s, leading to a wide variety of new designs and large increases in speeds and performances of new bicycle types. Bicycle speed records are nowadays regularly set at speeds of well over 80 mph, 135 km/h, 37.5 m/s. (These records are not wholly valid, because they can be set at the limits of permissible downslope, wind, and so on.) It is a potent time for bicycling, because many large cities have racks of standard bicycles that can be picked up fairly easily for rental use. Cars are facing greater restrictions because of the emissions that are still involved. Electric drive is becoming increasingly popular. Improvements are forecast in the types of batteries used for electric bicycles and for regular motor vehicles. More exercise is prescribed for greater health.

These major developments lead many to forecast a new period of greater use of bicycles in cities. Therefore, while there is no longer a sense of excitement over new types of bicycles, there is a sense that they have matured and can be quickly produced for wider use for the benefit of users and nonusers.

In the third version of this book, Jim Papadopoulos largely wrote the text of chapters 2, 4, 6, 8, and 10, which was insufficiently acknowledged. In this heavily revised fourth version, a great deal

of Jim's original material remains in chapters 2 and 8 and some in chapters 4 and 6.

I have been very lucky that Theo Schmidt (see figure 8.5) responded to an invitation to collaborate on the changes needed to produce the fourth edition. He and I have worked together in many IHPVA activities. We have both been chair of the IHPVA and editor of its technical journal *Human Power*, and we have worked together on the *Human Power eJournal*, of which Theo is currently the editor and also a member of the World Human Powered Vehicle Association rules and records committee. He earned a diploma in physics and astronomy at the University of Basel and graduated in physical oceanography and electronic engineering at the University of Wales. Theo joined the British human-powered vehicle club (BHPC), became vice-president of Future Bike in Switzerland, and participated in the Swiss Tour de Sol with his own vehicles, including an electric bicycle with a continuously variable transmission and a semiamphibious solar hybrid HPV. He started working on an extraordinary range of projects, including kite research and construction of early human and solar-powered vehicles and boats, on one of which, a semiamphibious HPV, he attempted to travel from London to Paris (but gave up before reaching the middle of the English Channel, then almost made it later on a solar boat without batteries). He has his own research and development company working in these broad areas, and some of his projects are illustrated in this edition. Readers will appreciate the experience and values that he has brought to the coverage.

David Gordon Wilson
Cambridge, Massachusetts, February 2019

I'm honored to have been invited by Dave Wilson and The MIT Press to help with this fourth edition of *Bicycling Science*, as I have neither Dave Wilson's literary writing style nor Jim Papadopoulos's mathematical engineering knowledge. But I think I'm a good editor, and this heavily revised new edition contains most of the material from the third edition and follows its structure, except for the chapter on materials and the appendixes, which we reluctantly left out of the book this time. Many thanks to the MIT Press staff for their patient help and to Nick Green (BHPC) and Michael Harrup (MITP) for proofreading and copyediting.

Most of the text and many drawings are those of Dave Wilson and Jim Papadopoulos from the third version, and there is also some new text from Dave. I've added some text and a great many updates, new references, and new figures.

There is now a great deal of information available on the internet, so much that relevant resources can be difficult to find amidst all that is there. We now include URLs (internet addresses) for most references that are actually available and interesting. Most are too long to type, so as a service to readers we've put a list of links at hupi.org/BS4/. (The Human Power Institute—on whose website the list resides—is the brainchild of the late Richard Ballantine, whom Dave and I helped to put the institute together, together with three former IHPVA board members or officers). Short, easy-to-type URLs (like that above) are mostly placed within the text instead of the reference section; your browser will add “https://” and perhaps “www” automatically. (Sometimes https:// will not work, and you must enter http:// manually.)

A note on units: equations without given units work in any consistent system. When units are given, we have tried to use those from the International System of Units (SI) where possible. However, we often also use customary units, especially for time (hours, etc.) and angles (degrees or slope). In these cases, formulas work only with the units given. A particular challenge for any technical text is the representation of weight. Even physicists often mix up an object's mass (kg, lb, sl), a relatively immutable basic property of all matter, with its weight (N, pdl, lbf), which is a somewhat variable force that the earth's gravity exerts of a mass. In this book we also switch somewhat randomly between the two, except in the section “Cycling on the Moon,” where the distinction is important. For quantities we try to give the most widely used units if not SI, for example, kilometers per hour for many cycling records, or sometimes miles per hour. It isn't scientific, and it isn't consistent, but it should, we hope, please a large spectrum of different readers.

Have a lot of fun!

Theodor Schmidt
Steffisburg, Switzerland, February 2019

In Memoriam David Gordon Wilson

David Gordon Wilson passed away on May 2, 2019, soon after he and Theo Schmidt submitted the final draft of the fourth edition of *Bicycling Science* to the Press. Mere days before, Dave and I met on MIT's campus to celebrate the completion of the revisions and look ahead to the book's publication. Most of the hour was spent in spontaneous conversation, talking about his love of bicycles, the New England terrain, the potential of wind power along the Roaring Forties in the Southern Hemisphere, and family. Editors generally disparage then delete lists of adjectives, but Dave's character lends itself to multiple superlatives: brilliant, irrepressibly curious, inventive, meticulous, kind, collaborative, civic-minded, resilient, funny, candid, and adventurous. These traits animate *Bicycling Science* and will charm readers new to the 2020 edition just as the book has charmed cycling aficionados since 1974. We at the MIT Press miss Dave and are proud to publish the fourth edition of *Bicycling Science*, through which his legacy continues.

Beth Clevenger
Senior Acquisitions Editor, Cambridge, Massachusetts

1 A Short History of Bicycling

Introduction

Those who are ignorant of history are not, in truth, condemned to repeat it, as George Santayana claimed. However, people do spend a great deal of time reinventing types of bicycles and components, and one purpose of this necessarily brief history is to give would-be inventors a glimpse of some of their predecessors. Sir Isaac Newton said that we make advances by standing on the shoulders of giants, but to do that, we must first know that there were giants and what they accomplished. Another purpose is to kill the many-headed Hydra of bicycling myths. People invent these myths—for instance, that Leonardo da Vinci or one of his pupils invented the chain-driven bicycle—for nefarious or self-serving or humorous purposes, and journalists and enthusiasts pick them up, and they almost instantly become lore, however false. Historians repeatedly denounce the fakes, but the amateur historians continue to report them as if they were true. These people seem to practice a crude form of democracy: if they read something in ten publications and the contrary in one, then the one reported most often is, they believe, correct.

We have become the disciples of a group of cycle historians that has become a powerful international movement having scholarly proceedings and meetings. The late Derek Roberts, the group's founder, wrote correction sheets for every new book incorporating cycling history, pointing out inaccuracies in detail. At the encouragement of the late John Pinkerton, a prominent member of the group and a publisher of cycling-history books, Roberts gathered these inaccuracies and corrections together and published *Cycling*

History—Myths and Queries (1991) in a further attempt to stem the tide of inaccurate versions of history. This present brief history endeavors to lay to rest previous myths and does its utmost not to create more. We have been graciously guided by Roberts, by Pinkerton, and by Hans-Erhard Lessing, a leading cycle historian, former curator, and university professor, who himself has documented several major bicycling myths (some quoted later in this chapter) previously regarded as historical facts. Others in this group who have been of particular help to us are Nick Clayton and David Herlihy. Cycle historians themselves are far from agreement on many aspects of their profession: cycle history is a field in which views are strongly held and defended and amateurs must tread with great care; we have greatly appreciated this group's advice, which has not always been unanimous.

There have been three significant periods in cycling history, each covered in more detail in this chapter. Despite the myths of supposed earlier two-wheelers, the first bicycle (a "running machine" that the rider straddled and propelled with his feet on the ground) was invented in Germany in 1817, and this is when the history of the bicycle and motorcycle begins. That first bicycle found a promising acceptance in several countries but was suppressed by the authorities in Mannheim (late 1817), Milan (1818), London, Philadelphia, New York (1819), and Calcutta (1820), so that by 1821 it had virtually died out (Lessing 2017). However, Lessing (2017) records "running-machine races in April 1829" in Munich "of 26 machines taking part." Others, including Pinkerton, believed that the enthusiasm for running machines was simply a fad of the rich and that it would come and go as such fashions do. Not until the early 1860s did someone in France add cranks and pedals to the front wheel of a running machine, at which point international enthusiasm redeveloped. If a modern bicycle is defined as a vehicle having two wheels in line connected by a frame on which a rider can sit, pedal, and steer so as to maintain balance, then this French running machine is the start of its history. The enthusiasm over this machine lasted much longer than that of 1817–1821. The front wheel was made progressively larger, and the high bicycle or "ordinary" was born. It was fun but it was dangerous, although Pinkerton, a long-time rider of high bicycles, believed the supposed dangers to be highly exaggerated. Designers and inventors tried for many years to arrive at a

safer machine. Success came with the so-called safety, first in 1878 with the Xtraordinary and the Facile, and reaching significant commercial success with John Kemp Starley's 1885 safeties, which, with Dunlop's pneumatic tires reinvented in 1888, became by 1890 very similar to the safety bicycle of today.

These, then, are the three principal developments that this short history discusses. It also mentions the tricycle period, the repeated enthusiasm for recumbent bicycles, and some modern developments.

Early History

It was through the use of tools that human beings raised themselves above the animals. In the broadest sense of the term, a tool might be something as simple as a stone used as a hammer or as complex as a computer controlling a spacecraft. The discussion here is concerned with the historical and mechanical range of tools that led to the bicycle, which—almost alone among major human-powered machines—came to use human muscles in a near-optimum way. A short review of the misuse of human muscle power throughout history (Wilson 1977) shows the bicycle to be a brilliant culmination of the efforts of many people to end such drudgery.

Many boats, even large ones, were muscle powered until the seventeenth century. Roman galleys had hundreds of "sweeps" in up to three banks. Figure 1.1 shows a large seventeenth-century galley having fifty-four sweeps, with five men on each. The men were likely to be criminals (real or supposed), chained to their benches. Overseers equipped with whips patrolled a central gangway to provide persuasion for anyone considered to be taking life too easy. These unfortunate oarsmen used muscle actions typical of those considered appropriate in the ancient world. The hand, arm, and back muscles were used the most, while the largest muscles in the body—those in the legs—were used merely to provide props or reaction forces. (These early oarsmen didn't have the sliding seat available to today's competitive rowers.) The motion was generally one of straining mightily against a slowly yielding resistance. With five men on the inboard end of a sweep, the one at the extreme end would have a more rapid motion than the one nearest to the pivot, but even the end man would probably be working at well

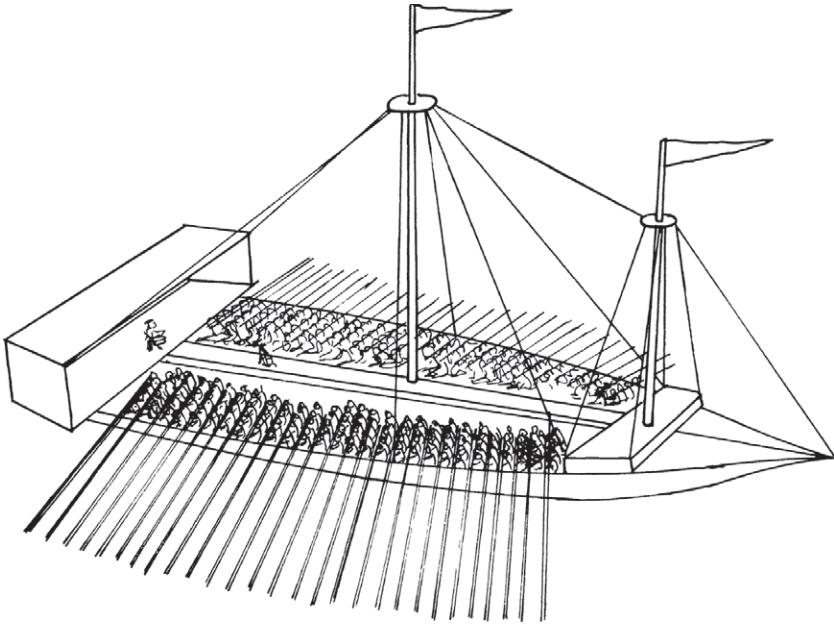


Figure 1.1

Early-seventeenth-century galley, with drummer in the stern and whip-bearing overseer on the central gangway. (From a drawing in the British Museum reproduced in the *Encyclopedia Britannica*, sketched by Dave Wilson.)

below his optimum speed. Muscle use in most farm work and forestry fell into the same general category. Hoeing, digging, sawing, chopping, pitchforking, and shoveling all employed predominantly the arm and back muscles, with little useful output from the leg muscles. In many cases, the muscles had to strain against stiff resistances; it is now known that muscles develop maximum power when they are contracting quickly against a smaller resistance, in what is termed a good *impedance match*. In the bicycling context specifically, this good impedance match might be called an *optimum gear ratio*.

One medieval example of the use of appropriate muscles in a good impedance match is the capstan, around which several people walked in a circle, pushing on radial arms, to winch in a rope. The capstan's diameter was chosen to provide comfortable working conditions, and each pusher could choose a preferred radial position

on the bar. The same principle has been reversed with the horizontal treadwheel. Inclining the treadwheel makes a more upright position possible, and the arms can push less. Finally we arrive at the vertical treadwheel, with a horizontal axis. Numerous configurations are possible, the most popular apparently the hamster drum type used in countless medieval cranes and mills, hence also the name *treadmill*, still used today for modern horizontal or inclined endless belts for exercise and ergometry.

Rarer is the outside-stair-cage type of treadmill suggested by Leonardo da Vinci for powering armaments. Later examples are also sinister, serving to enforce hard labor in penal institutes. They were “invented” by an English engineer, and ten large penal treadmills were constructed for the Brixton prison from 1821 onward, connected to two millstones and water pumps. Ten to twenty prisoners at a time could work each wheel for grinding flour. Unlike the galley sweeps, the capstans, or even the hamster drum type of treadwheels, all of which at least allowed workers some choice of force applied, the nefarious Brixton wheel design required each prisoner to exert exactly his own weight at the same rate as all the others. This rate was maintained by a centrifugal mechanism operating a bell (The Mirror 1822). The data given in Walton 2015 and Katch, McArdle, and Katch 1997 differ but do suggest that prisoners had to work at rates between about 120 W and 250 W for many hours per day, and being poorly nourished, often became ill. By midcentury, about one hundred English prisons, and a few in British colonies as well as in the United States, were so equipped, resulting in several maimed and killed prisoners (Vaver 2013). This form of punishment wasn’t discontinued until 1902. A working model survives, or was reconstructed, in South Africa (figure 1.2).

Augustino Ramelli proposed a number of novel or even unique treadmills, including what might be the only semirecumbent treadmill for a seated person (figure 1.3). The type of work involved may not have been pleasant, but it was far more congenial than that required of a galley slave or Victorian prisoner, and the view was better. Note the gearing: first stepped up, then heavily stepped down.

The first clearly human-powered vehicles known to history (if classes like wheelbarrows and carts pulled or pushed by men and women are excluded) were carriages supposedly propelled by



Figure 1.2

Triple treadmill used to punish prisoners at Breakwater Prison (now Breakwater Lodge), Cape Town, South Africa. (Photo by Lennon001, licensed CC-BY-SA 3.0.)

footmen, in France in the 1690s (Ritchie 1975, 16). (An alleged earlier effort by a pupil of Leonardo da Vinci has been convincingly shown by Lessing to be a fake.)

The First Bicycle

It seems likely that the most important discovery in the development of the bicycle was made by chance. Baron Karl von Drais, a resident of Mannheim, studied mathematics and mechanics in Heidelberg and invented a binary digit system, a paper-strip piano-music recorder, a typewriter, and—during a series of bad harvests after 1812—two human-powered “driving machines” on four wheels. In 1815 the Indonesian volcano Tambora exploded, expelling the greatest known mass of dust into the atmosphere (estimated at seven times the amount from Krakatoa in 1883) and making 1816 “the year without a summer” in central Europe and the New

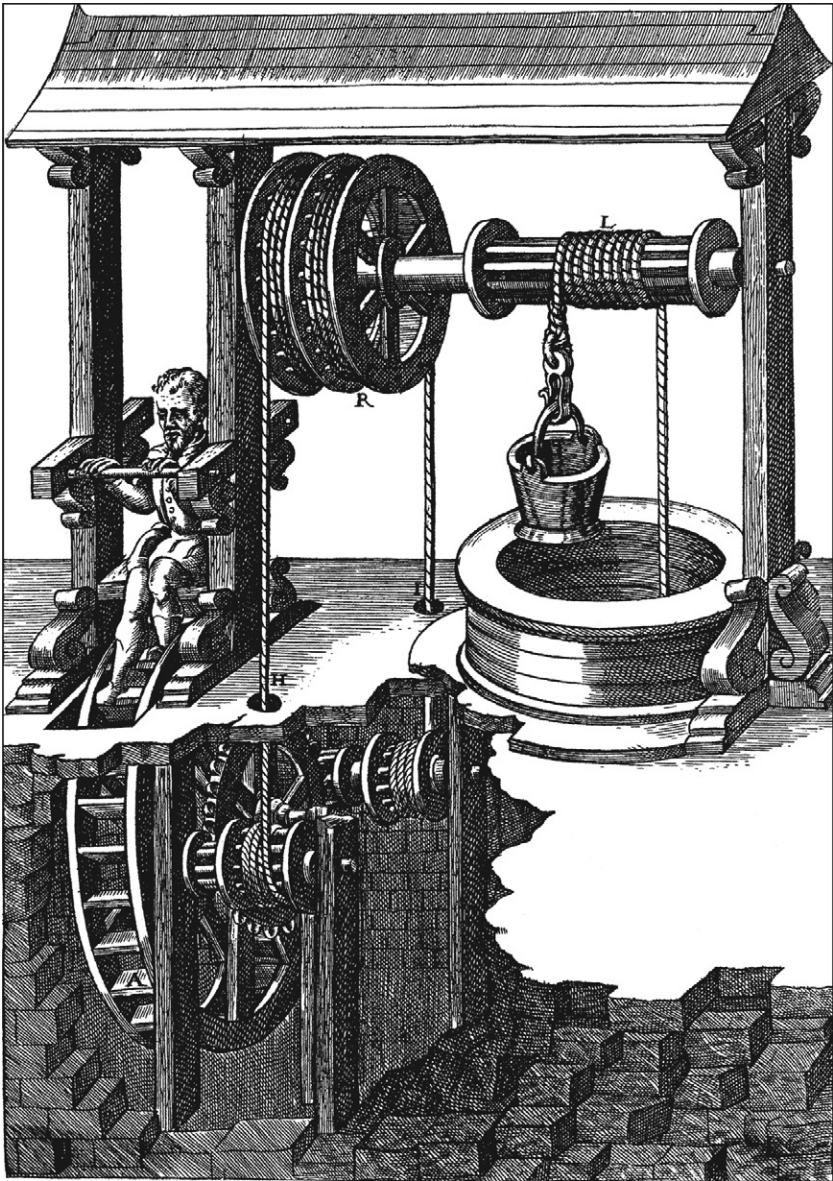


Figure 1.3
Semirecumbent treadmill powering geared winch. (From Gnudi and Ferguson 1987.)

England states. Starvation was widespread, and horses were killed for lack of fodder, the price of oats then playing the same role as the oil price fairly recently. Lessing (1995) believes that the consequent shortage of horses led von Drais to develop his two-wheeled “running machine” with front-wheel steering from the outset (figure 1.4). An earlier assumption was that he had no preconception that the steering would enable him to balance but simply thought that it would be a convenience. However, Lessing (1995, 130) makes a powerful argument that ice skating, which “had long been a means of travel and transport in the Netherlands with its many canals,” led to roller skating. Lessing quotes sources describing “a pair of skates contrived to run on small metallic wheels” to imitate ice skating on theater stages between 1761 and 1772. A preserved flyer for an outdoor demonstration between The Hague and Scheveningen in 1790 shows what appear to be the earliest in-line roller skates. These did not appear in technological magazines of the time, and it is therefore hard to tell if von Drais had knowledge of them. But von Drais was an ice skater himself, so balancing on one foot on a skate could have started him thinking about something larger, necessarily with steering. (As discussed later in the chapter, in 1863, James Plimpton patented roller skates that could be steered, which made him a multimillionaire [Lessing 1995].) A better-documented influence

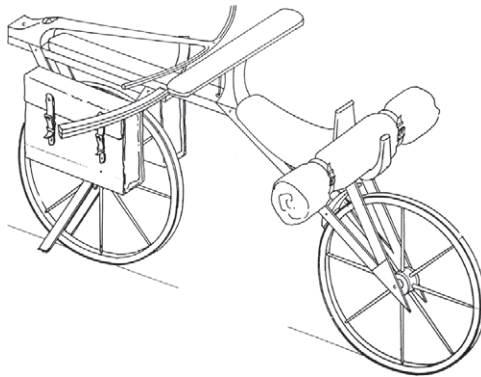


Figure 1.4

Draisienne or Draisine. Von Drais chose a wheel diameter of 690 mm (27 in). From von Drais’s plans by Joachim Lessing; the cloak and side panniers are reconstructed. (Courtesy of Hans-Erhard Lessing.)

was the rediscovery of the Chinese wheelbarrow (using even a sail) with its central wheel under the load, since this was a topic at the University of Heidelberg.

However it was attained, the major discovery in bicycle history had been made, and it was scarcely recorded. Von Drais's vehicle was, however, noted in the German newspapers in 1817 and those of the United Kingdom in 1818 and the United States in 1819. In Paris, where von Drais obtained a five-year patent, it was called *le vélocipède* (and in fact, from 1817 to 1870, the term *velocipede* was used in English for any foot-propelled vehicle) or *la draisienne*, and *Draisine* in German and English. In Britain it became known as the Pedestrian Accelerator and was nicknamed Hobby Horse (Street 1998). (Live horses needed constant care. These mechanical "horses" could be used or left at will and were thus treated as a hobby.)

Despite some initial skepticism and ridicule, von Drais was soon demonstrating that he could exceed the speed of runners and that of horse-pulled posts, even over journeys of two to three hours. His ability to balance when going down inclines and to steer at speed must have been important in this, and it awed the unathletic majority of the population. He indeed must have the principal claim to being the originator of balance on two wheels by steering.

Von Drais had many imitators. One was the London coachmaker Denis Johnson, who made a seemingly more elegant conveyance having a mainly iron rather than wooden frame (it was therefore heavier). It was soon called the Dandy Horse. Johnson set up a school in which young gentlemen could learn to ride. In the next year or so, use of the vehicle could be considered to have spread to clergymen, mailmen, and tradesmen, if contemporary cartoonists are to be taken seriously. However, its cost was too high for it to be used by any but the rich. In 1821, Lewis Gompertz fitted a swinging-arc ratchet drive to the front wheel (figure 1.5) so that the rider could pull on the steering handles to assist his feet. However, by this time so many restrictions had been put upon velocipedes that they lost their usefulness: "for they gave orders that those who rode velocipedes should be stopped in the streets and highways and their money taken from them. This they called putting down the velocipede by fines" (Davies 1837). John Pinkerton, in a 2001 communication to the senior author, indicated he believed that Davies

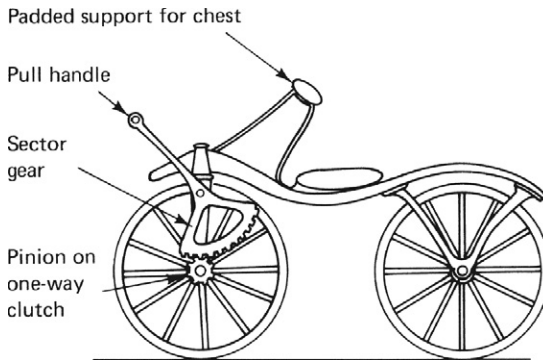


Figure 1.5
Gompertz's hand drive. (Sketched by Dave Wilson.)

was exaggerating: velocipede users were almost exclusively the very rich and therefore unlikely to be harassed.

Von Drais's premier place in what might be regarded as the three-step history of the development of the safety bicycle is assured, and it is relatively free from controversy. In contrast, the second and third steps (and "steps" seems an appropriate name, for they each resulted in "step-changes" in bicycle performance) are shrouded in some mystery and arguments among present-day proponents of one claimant or another.

In previous editions of this book, and in many other reputable books on bicycle history, including Ritchie 1975, credence has been given to a second step being taken in Dumfriesshire, Scotland, in 1839 or 1840 by Kirkpatrick Macmillan, who had been thought to have fitted cranks to the (large) rear wheel of a bicycle, with connecting rods going to swinging arms near the front-wheel pivot point. Alas, bicycle inventors seldom leave behind much incontrovertible evidence, and this is certainly true of Macmillan. His claimed development is reckoned by Nicholas Oddy (1990), Hans-Erhard Lessing (1991), and Alastair Dodds (1992) to be another myth. Lessing points out that in the chauvinistic atmosphere of that period (and later), unscrupulous people repeatedly manufactured "proofs" that someone from their own countries was the first to invent some notable device. (The velocipede credited to Macmillan by a relative, shown in figure 1.6, was actually the McCall velocipede of 1869, which belongs to the second step in our three-step history.)

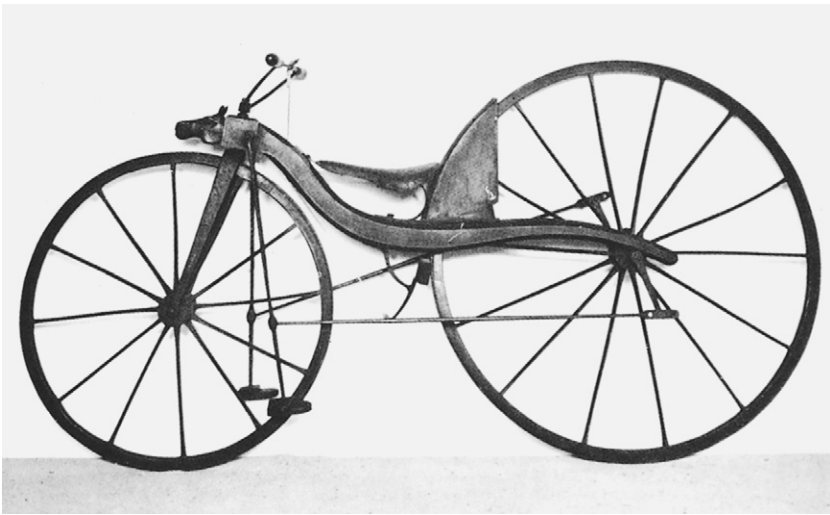


Figure 1.6

Copy of the velocipede attributed by some to Kirkpatrick Macmillan, built around 1869 by Thomas McCall of Kilmarnock. (Reproduced, with permission, from Ritchie 1975.)

However, others believe with conviction that Macmillan did in fact produce a rideable pedaled bicycle much earlier than this.

As implied earlier in the chapter, the Hobby Horse–velocipede “boom” had died down substantially by 1821. The second step in bicycle development had to wait until the 1860s (see the next section). Why so long? One can speculate that the countries in which two-wheeled vehicles had been developed and received with such enthusiasm—principally Germany, France, Netherlands, the United States, and Britain—were subsequently in the grip of railway mania. There was a new, fast way to travel, and this technology lured the creative dreams and efforts of inventors and mechanics away from the more mundane human-powered transportation. The parallels between this and what was to happen eighty years later, when the enthusiasm for the safety bicycle was to evaporate before the flaming passion for the automobile, are striking. Lessing (1995) points out that roller skating had lost its popularity on the arrival of the safety bicycle, with the rinks closing down in Europe, but not in the United States.

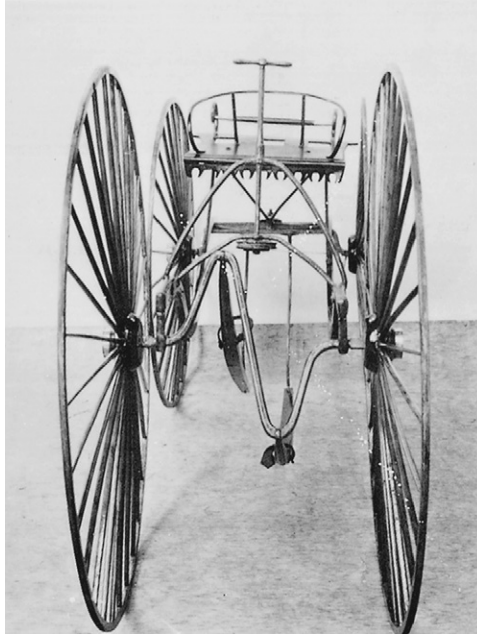


Figure 1.7

Sawyer four-wheeled velocipede. (Reproduced, with permission, from Ritchie 1975.)

It would be an exaggeration to claim that all development in human-powered vehicles stopped during this time, however. Such vehicles were used during the period by some enthusiasts (including Prince Albert, husband of Queen Victoria), but not extensively. The machines' size, weight, and cost and the poor roads of the time deterred walkers from changing their mode of travel. Willard Sawyer, a coachmaker in Kent, England, made increasingly sophisticated four-wheeled velocipedes, such as that shown in figure 1.7, and exported them around the world, from about 1840 to 1870 (McGurn 1999, 24–26). They too were used by a few enthusiasts, but no movement developed. Undoubtedly there were lone mechanics and inventors in various countries making what seemed to be improvements to the Draisine.

The Second Step: Pedaling Propulsion

The next step in bicycle development has become highly controversial. The second edition of this book added a chapter on bicycle



Figure 1.8

First commercial Michaux velocipede. (From Clayton 1998.)

history and credited Pierre Michaux with the significant step of adding pedals and cranks to the front wheel of a Draisine, thus initiating the astonishing period that lasted from the 1860s to the turn of the century when at least some parts of the earth appeared to have gone “bicycle crazy.” Michaux certainly produced pedaled velocipedes in increasing numbers in 1867–1869 (such as, for example, the one depicted in figure 1.8), but there appear to be a half-dozen other “first” originators, with no clear winning candidate for the title (see Hadland and Lessing 2014).

Whoever deserves the credit, there is no doubt about the results. A wild enthusiasm for *le vélocipède bicycle* started in Paris in 1868 and spread to Belgium, the Netherlands, Germany, the United States, and Britain. The first true bicycle boom was underway.

Why, and why then? Hans-Erhard Lessing claims that having learned to ride a bicycle during childhood, most of us are unable to understand the fear of balancing of former times (unless we try to teach cycling to an unknowing adult). This fear hindered earlier mechanics in thinking of two-wheelers with the rider’s feet permanently off safe ground. Sometime after Meyerbeer’s opera *Le prophète*,

with roller skaters on stage, promoted roller skating throughout the Continent in the 1840s, ice skaters developed the new art of figure skating. Trying to imitate this on roller skates created the need for “rocking” roller skates with rubber-block steering invented by a Bostonian, James Plimpton, in 1863. Plimpton’s empire of covered roller-skating rinks where the roller skates were rented, never sold, spanned the United States, Europe, and the whole Commonwealth. Roller skating became all the rage in the 1860s, and a large percentage of the rich learned to balance with both feet on wheels. Only on the basis of this broad balancing experience could someone on a two-wheeler ask: Why not take the feet off the ground permanently and put them on cranks? Moreover, Paris during this time got new macadamized boulevards that eased the use of the new machines, which had double the weight of the Draisines. But above all the machines were fun to ride, and thousands did so unimpeded by the authorities.

We might not find their experience so entrancing nowadays. The wooden wheels of the machines they rode had thick compression spokes and iron rims. It was only in the late 1860s that rubber was fastened onto the rims to cushion the harsh ride and ball bearings were first used to give easier running, although Davies (1837) mentions that some Draisines were fitted with “friction rollers” to lessen the friction. When French bicycle factories were subsequently required to turn to armaments in the Franco-Prussian war of 1870–1871, French leadership in bicycle development was lost (Ritchie 1975).

What of the apparent lack of American contributions to the mainstream of bicycle development? What happened to the Yankee genius in engineering and mechanics? The US Patent Office was in fact flooded with applications to patent improvements to velocipedes from 1868 on. French and British makers then found it necessary to follow the developments taking place across the Atlantic. In 1869 Pickering’s Improved Velocipedes were exported from New York to Liverpool. But the American craze, which *Scientific American* stated had made the art of walking obsolete, suddenly petered out in 1871, as quickly as it had started, leaving new businesses bankrupt and inventors with nowhere to go (Ritchie 1975). There was then a lull until 1877, when the high-wheel bicycle was imported from Europe. Colonel Albert Pope started manufacturing them in

the United States a year later. But conditions there were less conducive for bicycles than those in Europe, where the high bicycle enabled people to travel much farther than was comfortably possible on a velocipede. In Britain the roads were good enough for the country to be traversed from Lands End in southwest Cornwall to John O'Groats in northeast Scotland (924 mi; 1,490 km) in seven days (Ritchie 1975); in the United States the distances between towns were (except perhaps in New England) enormous, and the roads were poor. Accordingly, the bicycle did not have, and did not convey, as much freedom as in Europe, and the market was therefore smaller and far more dispersed than in Europe. It is doubtful that anyone in the United States used bicycles for long-distance travel except a few enthusiasts and people who wanted to set records.

Development was rapid in Britain, however, where production had been undertaken more to fill the unsatiated French demand than to supply any domestic market. James Starley (uncle of John Kemp Starley) used his sewing-machine factory to build up a thriving bicycle industry in Coventry and repeatedly assumed technical leadership in the area. The suspension or tension wheel was developed in Paris by Eugene Meyer in 1869 (Clayton 1997) and William Grout in 1870. At about the same time, Starley and William Hillman introduced the *lever-tension* wheel, with radial spokes and a lever for tensioning and torque transmission (figure 1.9), and in 1874 Starley patented the logical extension of this idea, the *tangent-tension* method of spoking, the standard spoking method to this day (shown in figures 1.13 and 1.17).

The High-Wheeler or Ordinary

With the advent of tension spoking, front wheels could be and were being made larger and larger to give a longer distance per pedal revolution and therefore greater speed. Starley patented his Ariel bicycle, which already had a larger-than-normal driving wheel, on August 11, 1870. (For a while, some French race organizers tried to restrict the diameter to about a meter [Dodge 1996, 58]—perhaps a harbinger of the restrictions later imposed by the Union Cycliste Internationale?) Starley and others recognized the advantages of using a geared step-up transmission, but experimenters found that



Figure 1.9
Starley-Hillman lever-tension wheel (circa 1870), shown by the late John Pinkerton in 2001. (Photo by Dave Wilson.)



Figure 1.10
Ordinary, high-wheeler, or penny-farthing. (From Sharp 1896.)

the available chains quickly froze up in the grit and gravel of contemporary roads. Soon front wheels were made as large as comfortable pedaling would allow, and one bought one's bicycle to fit one's inside leg length. The largest production "high-wheeler" or "ordinary" (also referred to as a "penny-farthing") would have a driving wheel about 60 inches (about 1.5 m) in diameter (figure 1.10). (In the English-speaking world, we still translate gear ratios into equivalent driving-wheel diameters, and this size corresponds to the middle gear of a typical modern bicycle. The French and others in Europe instead use *la developpement*, the wheel's circumference, the distance traveled in one full turn of the cranks.)

The 1870s were the years of the high-wheeler's dominance. By the end of the decade, top-level bicycles were made with ball bearings in both wheels and in the steering head, the rims and forks were formed from hollow tubing, the steer axis had been tilted to create a castering effect, the tire rubber was greatly improved over the crude type used in 1870, and racing bicycles had been reduced to under 30 lb (13.6 kg). A rideable ordinary weighing only 11 lb (5 kg) was produced in 1889.

The ordinary was responsible for the third two-wheeler passion, concentrated among the young upper-class men of France, Britain, and the United States and fostered by military-style clubs

with uniforms and even buglers (Dodge 1996, 82–88). The ordinary conferred unimagined freedom on its devotees; it also engendered antipathy on the part of the majority who didn't or couldn't bicycle. Part of that antipathy was envy. The new freedom and style were restricted to rich young men. Strict dress codes prevented all but the most iconoclastic of women from riding high-wheelers. Family men, even if they were still athletic, hesitated to ride because of the reported frequent severe injuries to riders who fell (some feel that these reports were exaggerated). Unathletic or short men were excluded automatically. Many prospective riders among these groups took instead to tricycles (Sharp 1896, 165–182), which for a time were produced in as many models as the ordinaries.

The need to serve this “extra-ordinary” market produced two technological responses. James Starley played a prominent role in the first, and his nephew, John Kemp Starley, in the second.

Tricycles and Quadracycles

The first of these responses was the development of practical machines of three or four wheels that eliminated the need to balance and allowed the rider to be seated in a comfortable, reasonably safe, and perhaps more dignified position. Such vehicles had been made at different times since at least the start of the century, but the old heavy construction made propelling them a formidable task. In fact, one or more servants, who in effect substituted for horses, allegedly often provided the motive power (there is considerable doubt about the truth of these reports). Women in conventional dress and relatively staid males could use Starley's Coventry Tricycle, patented by Starley's son and nephew in 1876 and produced by the Starleys for several years from 1877 on, with comparative ease. Early in the production run it was driven by a lever system and called the Coventry Lever. However, Starley had found a chain that worked, at least in the possibly more protected conditions of a tricycle, and produced later versions with rotary pedals; these were referred to as the Coventry Rotary (figure 1.11). The Coventry Tricycle and its successors had one large driving wheel on the left of the seat and two steering wheels, one in front and one behind, on the right. Starley saw the advantage, however, of a different arrangement, with two large driving wheels on either side of the rider(s) and a single

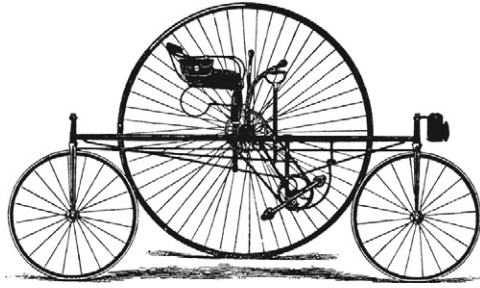


Figure 1.11
Starley's Coventry Rotary tricycle. (From Sharp 1896.)

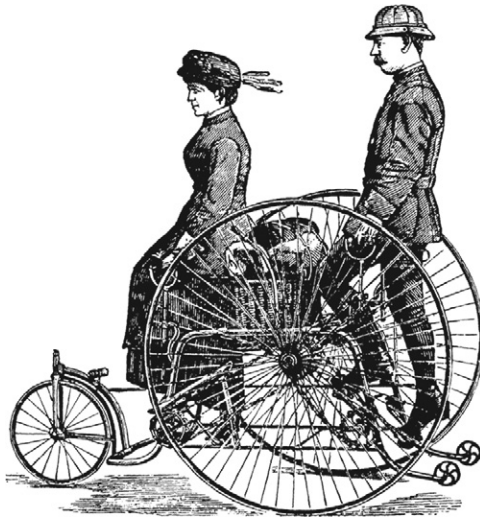


Figure 1.12
Starley's Royal Salvo tricycle. (From Sharp 1896.)

steering wheel in front. For this arrangement to work, however, power had to be transmitted to two wheels, which, during a turn, would be going at different speeds. To solve the problem, Starley reinvented the “balance gear” (Sharp 1896, 240–241), now known as the differential. Starley's Royal Salvo tricycle, which incorporated the improved design, became the predominant form—for single riders, for two sitting side by side, and even for one rider sitting behind the other (figure 1.12). This is not to say that there were no other

forms; tradesmen's carrier machines, for instance, with the steering wheel trailing the large driving wheels, used the reverse of this arrangement (Pinkerton 1983). But the front steerer was perceived as giving better control (one did not have to steer the rear wheel toward a pedestrian or a pothole to take avoiding action, as is necessary with rear steerers).

Gradually the tricycle's front wheel was made larger and the driving wheels smaller, as chain drives of increasing efficiency and reliability made possible. By 1884 or 1885, the front wheel was connected directly to the handlebars (figure 1.13), a simpler and more reliable arrangement than the rack-and-pinion and other indirect systems that had been used. The modern tricycle had evolved, with the modern riding position in which one sits or stands almost over the cranks and splits the body weight among handlebars, pedals, and saddle. (Today's modern tricycles and quadracycles are mostly recumbents with seats rather than saddles and are described in later chapters.)

Final Improvements to the Ordinary

This modern tricycle of late 1884 or early 1885 was also very similar to the emerging form of the modern bicycle. In fact, the second response to the exclusion of so many from the high-wheeler movement was the development of a configuration that would make a headfirst fall from a considerable height less likely, could be ridden in conventional dress, and did not require gymnastic abilities.

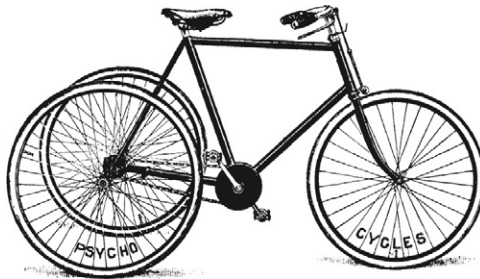


Figure 1.13

Early modern tricycle. (From Sharp 1896.)

Some improvements to the high-wheeler fulfilled only the first of these desiderata. Whatton bars (figure 1.14) were handlebars that came under the legs from behind, so that in the event of a pitch forward the rider could land feet first. (Cycle clubs—but not the police—recommended that riders of standard high-wheelers put their legs over the handlebars when going fast downhill, as in figure 1.15, for the same reason.) Some modern recumbent bicycles have similar handlebar arrangements. The American Star's designer took the approach of making over-the-handlebars spills much less likely by putting the bicycle's small wheel in front, giving it the steering function, and reducing the wheel size by using a lever-and-strap drive to the large wheel through one-way clutches (figure 1.16). Unfortunately, this innovation arrived too late to have much impact, in 1881, because by that time the true "safety" bicycle was evolving rapidly. Another type of bicycle that was safer to ride than the high ordinary was the "dwarf" front driver, such as Hillman's 1884 Kangaroo (figure 1.17 shows an 1886 Kangaroo Dwarf Roadster), with a geared-up drive to a smaller front wheel (Sharp 1896, 152, 158). Machines like the Kangaroo were offered because riders accustomed to front-drive machines did not always take kindly to the rear-drive safeties. Small-wheeled Bantam

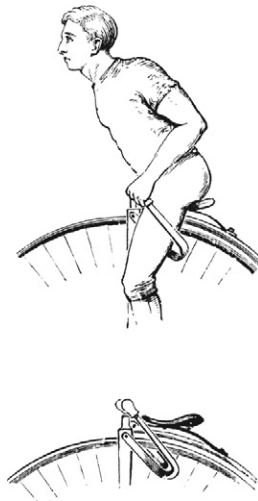


Figure 1.14

Whatton bars. (From *Cycling* 1887.)



Figure 1.15
“Coasting—Safe and Reckless.” (From *Cycling* 1887.)

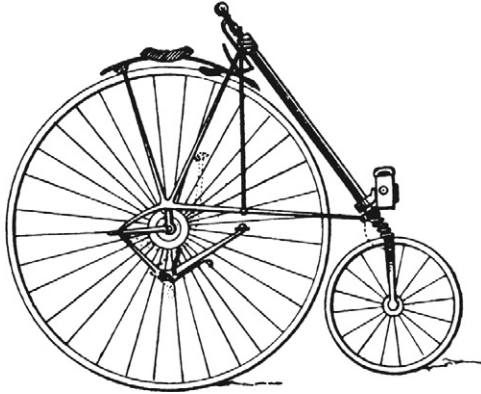


Figure 1.16
American Star, a treadle-action bicycle (1880). (From Baudry de Saunier 1892.)



Figure 1.17
1886 Kangaroo Dwarf Roadster. (From Sharp 1896.)

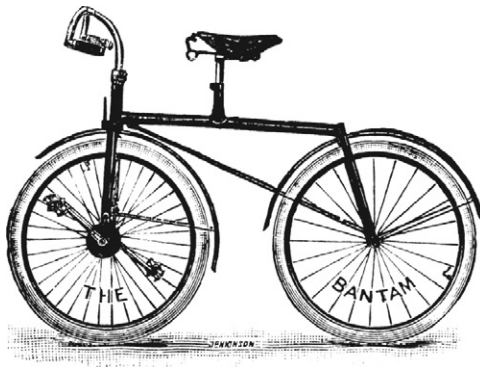


Figure 1.18
Bantam geared front-drive safety bicycle. (From Sharp 1896.)

bicycles with an epicyclic hub gear (figure 1.18) were marketed as late as 1900.

The Third Step: The Arrival of the Modern Safety Bicycle

It had long been recognized that it would be most desirable from the viewpoint of safety to have a bicycle's rider sitting between two wheels of moderate size. Many attempts at achieving this arrangement were made over the years. Rubber tires, variable gears,

freewheels, tubular frames, sprung wheels, and band brakes were shown at the first Paris velocipede show in 1869. But the direct ancestors of today's bicycles evolved rapidly in the one or two years before 1885, when several were shown in Britain's annual Stanley Bicycle Show. James Starley had died in 1881, but his nephew John Kemp Starley, working with William Sutton, produced a series of Rover safety bicycles (Pinkerton and Roberts 1998) in 1885 that, by the end of that year, had direct steering and something very close to the diamond frame used in most bicycles today (figure 1.19).

One major development in the mainstream flowing to the modern bicycle remained: the pneumatic tire, patented in 1888 by John Boyd Dunlop, a Scottish veterinarian in Belfast, although another Scot, R. W. Thomson, had patented pneumatic tires for horse-drawn vehicles in 1845 (UK Patent 10,990). Dunlop's early tires (made to smooth the ride of his son's tricycle) were crude, but by May 1889 W. Hume was using them in bicycle races in Belfast—and he won four out of four. Success in racing in those days gave a clear signal to a public confused by many diverse developments. Cyclists saw, as in the case of the safety versus the high-wheeled bicycle, a development that promised not only greater speed, or the same speed with less effort, but greater comfort and (especially) greater safety. Within eight years, solid tires had virtually disappeared from new bicycles, and Dunlop was a millionaire in pounds sterling.

With the arrival of the pneumatic-tired direct-steering safety bicycle, only refinements in components remained to be accomplished before the modern-day bicycle could be said to have fully developed.



Figure 1.19

Starley safety bicycle. (From Sharp 1896.)

Various types of epicyclic spur-gear variable-ratio transmissions for the brackets and rear hubs of chain-driven safety bicycles came on the market in Britain in the 1890s. Some heavier devices were available earlier for tricycles. The Sturmey-Archer three-speed hub (1902) was the predominant type, as it still is in many parts of the world (Hadland 1987), but it had many competitors. The derailleur or shifting-chain gear was developed in France and Britain in 1895 but was not popular. After further development by degrees in Europe, it was eventually accepted for racing in the 1920s (Berto, Shepherd, and Henry 1999).

Undoubtedly, much more will be discovered about the history of the modern traditional single-rider bicycle, and heretofore unrecognized inventors will receive the honor due them. Inquiring readers can find much more history than this book has space for in the excellent books referenced.

Waxing and Waning Enthusiasm

Although the enormous enthusiasm for the bicycle in most “Western, developed” countries in the 1890s waned sharply toward the end of the decade, that is not to state that the bicycle fell into wide disuse. Not many workers could afford bicycles, but well-to-do people used them for commuting and shopping, and later, in Europe at least, the “cloth-cap” (i.e., working) class used them also for sport and for weekend and vacation travel. The hapless senior author was not allowed to ride a bicycle until he was nine (and then he was allocated an old single-speed clunker), and he was given an old three-speed “sports” bike when he was eleven, in 1939, the year war was declared in Europe. Petrol (gasoline) was first rationed and then made unavailable for private use in Britain during World War II, and the bicycle was therefore used widely at the time. Riding with his elder brothers and mother and father was an important part of growing up. Going with his schoolboy friends to see local bomb damage and downed planes, to visit local towns for attractions such as swimming holes, and to plan increasingly longer trips ending with a 1,000 mi (1,600 km) tour into Scotland in 1944 were all liberating and character-forming activities. The camaraderie of European bicyclists everywhere made trips of any length very enjoyable.

The return to availability and affordability of motor fuel and cars after the Second World War ended reduced the bicycle in many Western countries to being used by children and what were seen as fringe groups. In the developing world, however, the bicycle was a necessity for anyone who could afford one. In most of these countries and especially in China, the proportion of person-trips and even of freight moved by bicycle was far higher than that carried by the railroads and road traffic.

A modern bicycle boom started in the United States about 1970, for reasons difficult to discern. (It followed rather closely the end of a two-year competition in the design of human-powered vehicles organized by the senior author that created considerable public interest at the time, which tempted him to puff himself up to take credit, just as the cock crows at the dawn he has obviously caused.) Annual sales of bicycles rose rapidly to exceed comfortably those of automobiles. The buyers were overwhelmingly middle-class, college-educated, and professional people, US bicyclers thereby contrasting with users in Britain. The bicycles were relatively lightweight models for road use; at the start, the popular style was the “English bicycle,” predominantly Raleigh three-speed models, but soon “English racers” (an increasing proportion actually being French and Japanese), later called “ten-speeds,” became fashionable, although we suspect that many of those purchased were not actually used much.

Although the bicycle represents a huge success story, its usage is again at a decline just when it is needed most, both for health and ecological reasons. Because worldwide usage is difficult to assess, Oke et al. (2015) examine the minimal bicycle ownership of private households in 150 countries. Overall the percentage of households that own at least one bicycle has in the last few decades decreased from about 60 to 40. In most parts of Africa and central Asia the proportion is about half of this, and in northern Europe as well as Burkina Faso, it is twice this figure. Standard bicycle usage may be in decline, but newer special forms of the bicycle, some of which we mention later in this chapter or in other chapters, are becoming more popular.

All-Terrain Bicycles

In 1970, at the time the enthusiasm for lightweight road bikes in the United States was increasing, a few enthusiasts in Marin County,

California (by coincidence also the decade-long home of the coauthor), began experimenting with old Schwinn clunkers for downhill off-road racing (Berto 1998). Others had done so in different countries before this, but they had not started a movement. Nearly thirty years later, Frank Berto interviewed nine then-young men who, in this small area of California, continued experimenting throughout the 1970s with configurations of bicycles that gave advantages first for fast purely downhill travel and later for cross-country and uphill riding. Several started companies to produce the designs they developed. Rather suddenly, “beginning around 1982, a sea change affected the sales of bicycles in America and Europe. The buyers switched from road bikes to all-terrain or ‘mountain’ bikes. Tires went from skinny to fat, and riders went from a crouched position on dropped handlebars to a more erect position on flat handlebars” (Berto 1998, 25). This second boom in bicycle popularity differed in character from the road-bike boom, because a far higher proportion of the bikes purchased were used to a significant extent. Perhaps most were not in fact used for off-road recreation but as extremely practical bikes for negotiating rough urban streets in commuting or shopping use. They left far behind their original heavy clunker image and became high-tech lightweights. They reached extraordinary levels of sophistication, many having front and rear suspension, wide-range twenty-seven-speed gears, hydraulic disk brakes, and frames made from aluminum, titanium, or carbon fiber. The technology developed for these so-called mountain bikes led the bicycle industry for some decades. Many bicycles today called “city bikes” have benefited from this technology.

Recumbents

One reason for discussing recumbents while excluding tandems, folding bicycles, pedicabs, or goods transporters (often themselves recumbents) from this discussion is that most modern record-breaking bicycles are recumbents. Another is that greater safety can result from the use of the recumbent riding position.

Many early cycles (particularly tricycles) placed their riders in a semirecumbent position. The early “boneshakers” with solid tires were often ridden with the saddle well back on the backbone spring and the feet at an angle considerably higher than that for the modern upright safety. In contrast with riders of the high-wheeler and of

the safety, who were told to position the center of gravity vertically over the center of the crank, semirecumbent riders sat in something like a chair and put their feet out forward on the pedals. The pedal-force reaction was taken not by the weight of the body (or when that was exceeded, by pulling down on the handlebars), but by the backrest.

The first known semirecumbent bicycle (that is, one in which riders' center of gravity is low enough relative to the front-wheel road contact point to make the possibility of their being thrown over the front wheel in an accident negligibly low) was built in Geneva by Charles Challand (von Salvisberg 1897, 47) sometime before 1895 (figure 1.20). On Challand's Normal Bicyclette, the rider sat rather high, directly over the rear wheel. In 1897 US Patent 577,895 was awarded to I. F. Wales for a somewhat strange-looking recumbent bicycle with hand and foot drive (figure 1.21) (Barrett 1972). An American named Brown constructed a much more modern-looking recumbent bicycle (figure 1.22), the Sofa Bicycle, and took it to Britain in 1901 (Dolnar 1902). By this time orthodoxy rested firmly with the traditional safety bicycle, and the derision that had successively greeted the Draisine, the velocipede, and the safety had been

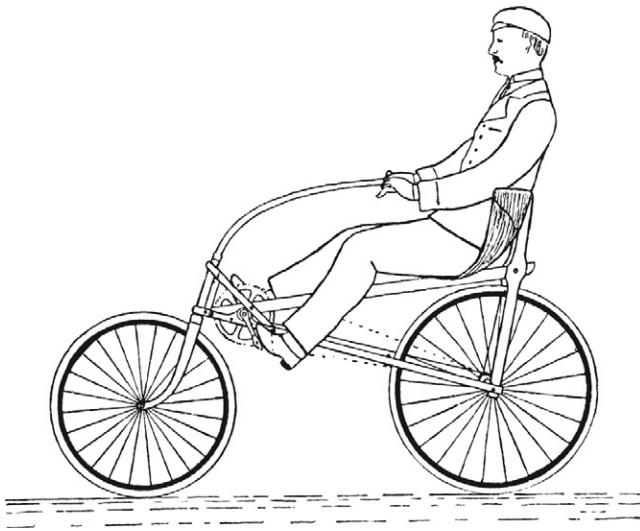


Figure 1.20

Challand's recumbent bicycle (1896). (From the *New York Times*, October 25, 1896.)

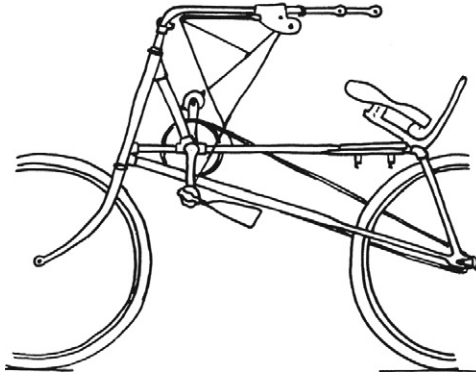


Figure 1.21

Design for hand-and-foot-powered recumbent patented by I. F. Wales in 1897. (Sketched by Frank Whitt.)

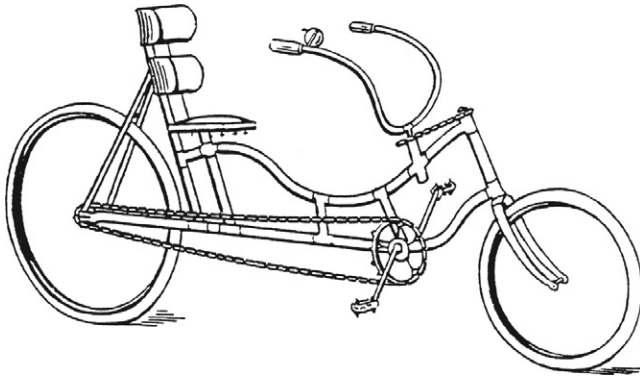


Figure 1.22

Brown's 1900 recumbent bicycle. (From a sketch of the Sofa Bicycle in *The Cyclist* [UK], November 13, 1901, 785.)

forgotten. Dolnar's review of the Brown recumbent in *The Cyclist* of January 8, 1902, was derisive to the point of sarcasm: "The curiously unsuitable monstrosity in the way of a novel bicycle shown in the single existing example of Mr. Brown's idea of the cycle of the future here illustrated ... fully show(s) the rider's position and the general construction of this crazy effort. ... The surprising fact is that any man in his sober senses could believe that there was a

market for this long and heavy monstrosity at the price of a hundred dollars (£20)."

Recumbents were then more successful in continental Europe. In 1921, after the First World War, the Austrian Zeppelin engineer (and later, car designer) Paul Jaray built recumbents in Stuttgart (Lessing 1998). The Swiss human-powered vehicle (HPV) club Future Bike has and occasionally uses its J-Rad (Future Bike 2018). It has swing-lever pedals with three leverages.

A racing recumbent called the Velocar (figure 1.23) was developed in France in 1931–1932 from four-wheeled pedaled vehicles of that name (Schmitz 1994). With a Velocar, a relatively unknown racing cyclist, Francis Faure, defeated the world champion, Henri Lemoine, in a 4 km pursuit race and broke track records that had been established on conventional machines ("The Loiterer" 1934).

At the time, a genuine orthodoxy pervaded the bicycle industry and the Union Cycliste Internationale (UCI), which controlled world bicycle racing. Instead of setting up a procedure and special category for machines such as the Velocar, the UCI, at the urging

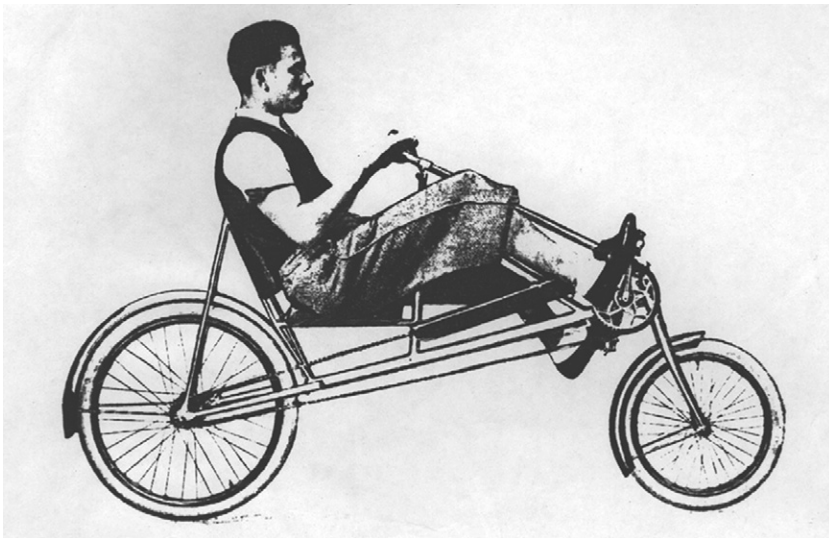


Figure 1.23

Velocar. (From an advertisement of a licensor.)

of the cycle trade, banned unconventional types of vehicles from organized competition, including recumbents like the Velocar. This decision denied novel ideas the opportunity of being tested and publicized through racing and thereby deterred experimentation and development.

Only with open-rule HPV competitions, which started in California in 1974 (and gave rise to the International Human Powered Vehicle Association and later other organizations) was the inventiveness of HPV designers again given an incentive in regard to recumbent design. With recumbent machines of a large variety of types now winning all classes of open races, the technological history of this type of vehicle, and of bicycles in general, is again being written. All recent single-person pedaled speed records for a streamlined bicycle (almost always a recumbent) over 200 m with a flying start have exceeded the motorway speed limits of most countries.

Although speed records continue to climb to levels never thought possible before, recumbents have never reached a significant market share in daily use, in spite of advantages they offer in safety and comfort. When given a chance to ride recumbent tricycles at shows, people line up and are excited, but they rarely buy them, for reasons of cost and space, compared to standard bicycles. Those with fairings, the velomobiles (see chapter 11), give excellent weather protection and are faster on the level, but slower steeply uphill, and their use is even more restricted than that of standard bicycles. Paradoxically, their large safety benefits, compared to standard bicycles, are not recognized, and they are instead compared to automobiles and regarded as extremely fragile.

Power-Assisted Bicycles

The first powered bicycle seems to have been Sylvester Roper's steam bicycle of 1868, and in 1881 Gustave Trouvé demonstrated an electrified Starley Coventry Tricycle (and in the same year also a boat and an unmanned airship!). The 1932 Philips Simplex was probably the first commercially available electric bicycle (e-bicycle), although patents and prototypes go back to 1895 (see timelines in Ron 2013 and Henshaw and Peace 2010). Electric power-assist systems for bicycles appeared beginning in 1896, with Hosea Libbey's

Velocipedrome, detailed in Desmond 2019. However, until 1932, manufactured powered bicycles used gasoline engines. They were similar in character to the mopeds still manufactured today, which have pedals only for emergency uses (such as engine malfunction, depletion of gasoline, and exceptionally steep hills) and sometimes for starting the engine. (In addition, having pedals puts the vehicles into different legal categories in many countries.) Although they are technically human-powered hybrid vehicles, most mopeds were and are not designed for actual use of the pedals: they have short cranks, only one gear, and suboptimal seating positions, and the rolling resistance of the tires is not conducive to attractive pedaling. The going is hard without the engine, and with it, the gear ratio is inappropriate for pedal operation. Even the famous Velo Solex is of this type: the pedals are used only for starting and when engine torque is insufficient on steep hills.

Such moped bicycles are not the subject of this book and even less so those without pedals, which quickly evolved into motorcycles or motor scooters and got heavier and heavier. Ironically, today some electric motor scooters, in a quirky retro-evolution, are fitted with hardly usable pedals, to enable them to be licensed as bicycles in some countries.

There is one notable exception, however. Physician and HPV pioneer Allan Abbott (who probably carried out more projects in different HPV fields than anybody else) was concerned with the unhealthy lifestyles many people were leading, as at the time there were as many as 250,000 premature deaths per year in the United States due to insufficient exercise. Because many of these people spent a great deal of time driving motor vehicles and had no time or energy left to exercise, Abbott suggested that they exercise *while driving*, by means of pedals. His goal here was not primarily to improve the vehicles' efficiency or reduce their environmental impact, and he therefore proposed fitting pedals even to powerful vehicles: gyms on wheels (see Abbott 1999). As a practical experiment in 1988 he fitted a bicycle with a small gasoline engine, but unlike in mopeds, in such a way that the engine would deliver power only when the rider pedaled: by connecting the engine's throttle to a spring-loaded chain tensioner on the pedal drive. Only with enough tension on the chain would the engine rev up and deliver torque through a centrifugal clutch. Abbott quickly found out that his bike was fun

to ride, more fun than the unpedaled mopeds with their inactive deadweight riders. Because the engine acted like a human-power amplifier, it rewarded the rider immediately with every turn of the pedal, especially when accelerating. With his flying hydrofoil colleague Alec Brooks (see chapter 10), Abbott later (1997) formed a company to market the first US “pedelec” e-bicycle (that is, a bicycle with an electric motor that runs only when the bicycle is pedaled), aptly named Charger.

The Coming of the Pedelecs

Other pioneers coinvented pedelecs around the same time. The first official mention of the principle involved in a pedal-driven e-bicycle is US Patent 3,884,317 to Augustus Kinzel in 1975, and US Patent 4,541,500 to Egon Gelhard in 1982 included a claim for the bicycle’s motor switching on above a road speed of 1 m/s. Yamaha invented its PAS Power Assist System in 1989, unveiled its first PAS bicycle in 1993, sold the first model (AX1, with a 235 W motor) in 1994, and had produced 200,000 PAS bicycles by mid-1997. PAS used torque and speed sensors to yield a true pedelec with a maximum power amplification of 200 percent (i.e., maximum 1:1 motor-to-human ratio, as required by Japanese regulations) up to 15 km/h and a gradual reduction to 0 percent at 24 km/h (see *Cyclepress* 1997).

PAS bicycles and similar pedelecs benefited from Japanese and European legislation designed to encourage them, up to a speed of 25 km/h. In Britain, this movement started in 1983 with the Electrically-Assisted Pedal Cycles Regulations, which allowed the free use of 200 W (250 W for tricycles) electric motors, provided they cut out at 15 mph (24 km/h) and the vehicles weighed less than 40 kg (60 kg for tricycles). In 2002 the European Union passed a similar directive with a cut-out of 25 km/h (15.6 mph), no weight restrictions, and a maximum power of 250 W, but with the difference that only pedelecs are allowed. The United States passed a rather different law in 2001 allowing 750 W motors and a top speed of 20 mph (32 km/h) for vehicles with functional pedals. In the same year Canada introduced regulations with the same speed restriction, but without the pedal requirement and with the motor power limited to 500 W. Both US states and Canadian provinces may impose additional legal requirements. Switzerland adopted the EU directive

for a time but introduced its own speed category in 1992 (see the next section) and today has several categories differing from all others. Thus in each of these countries, e-bicycles evolved differently, even if today they are mostly similar, even when fitted out or programmed differently. By the time you read this, things will have changed again.

Velocity and the “Fast Class”

The first really good pedelec in the Western world (maybe even the absolutely first commercial pedelec) was the Velocity, developed by Michael Kutter of Switzerland, who devoted most of his life to the project. The first commercial version was sold in 1992 (the coauthor helped with the assembly and promotion of the first batch of 30 and still has his). The principle was so good that apart from component and name changes by licensees (to Dolphin [figure 1.24]; to Swizzbee, starting in 2004; and to iZip [Currie], starting in 2008), nothing needed to be changed. However, Kutter died at an early age in 2015 and with him his small company. Although no longer sold, in the opinion of the coauthor, Kutter’s invention remains the best type of pedelec, even if others have caught up considerably these



Figure 1.24

Velocity Dolphin assisted human-powered bicycle. (Courtesy of Michael Kutter.)

twenty-five years later. It was probably the only mechanical series hybrid, and its functioning is explained in chapter 9.

Kutter also “invented” something else of importance, however: the legal specification dubbed “Swiss fast class.” Previously specifications for e-bicycles in Switzerland (and many other countries) were not clear. Mopeds could have 50 mL two-stroke engines limited to 30 km/h, pedals had to be fitted but did not have to be used, and a license, insurance, and a heavy helmet were—and still are—all required. In 1992, Kutter convinced the Swiss authorities to adopt legislation conforming to the system his Velocity employed, which at the time meant a maximum nominal 250 W motor that could propel the bicycle no faster than 20 km/h on its own. Pedal speed could, however, be added—this being a true series hybrid—and as in a pure bicycle, the top speed was not limited by law, but only by the rider’s fitness. Because of increasing air resistance with an unfaired bicycle (no fairings being allowed here), it is not possible to go much faster than about 50 km/h for any useful amount of time even when helped by a nominal 250 W motor; indeed, the coauthor reached only 48 km/h with his Velocity in 200 m speed trials in 1999 at Interlaken Airport, even slightly downhill at -0.33 percent slope. Type approval is required (i.e., a certificate of conformity), as well as a moped license and insurance, and no tandems, tricycles, or (as noted) fairings are allowed in this vehicle category. No helmet was then required, and even with 250 W it was easy to overtake the much more powerful but 30 km/h–limited mopeds and with wind in one’s hair escape their poisons and noise!

The Velocity turned out to be the fastest of all vehicles for trips of average length and in average traffic conditions from A to B, won most e-bicycle races, and was later adopted by the Los Angeles bicycle police, who bought 100 iZip Expresses in 2012 (see Hicks 2012), in order to be faster than their “clients.” The nominal motor power had by then been increased to 750 W for the North American market; top speeds (of the police model) of about 40 mph (~ 64 km/h) were reported.

Why is this unique vehicle, best of all pedelecs, no longer made? (This had happened already before Kutter’s death.) It wasn’t only the high price or the unreliability of some parts (the coauthor broke the slightly overstressed rear axle twice), but even more so the catching up and overtaking of competing firms.

Flyer, BionX, and Others

In particular the Flyer brand was marketed heavily in the late 1990s and soon became a synonym for the e-bicycle in Switzerland. Several successive manufacturers produced a bewildering range of Flyers and soon cornered the senior-citizen market. Fleets of rental Flyers became available in tourist areas, complete with battery-exchange points, tour suggestions, and also organized trips. Most models had a rather aggressive initial acceleration (which pleased new customers). Today most e-bicycles generally have a good “feel” irrespective of the type of system used, but they haven’t achieved the Velocity Dolphin’s semiautomatic operation. The coauthor’s family Flyer has a 14-speed Rohloff hub gear and requires frequent gear changing on every trip. Even models using the NuVinci variable gear need constant attention (see chapter 9). We hope therefore for a revival of the Velocity system someday. (At the time of writing, the first true automatics are starting to appear, and the NuVinci also has an automatic mode.) For a long time, Flyer used the popular Panasonic crankshaft-integrated motor, and now it also uses similar ones from Bosch. These large firms supply many pedelec manufacturers.

Up to 2018, the Canadian firm BionX produced a very easy-to-install pedelec kit with a gearless hub motor complete with rear wheel. With this kit, any bike shop or small firm (including the coauthor’s neighbor, who is a farmer) could sell its own brand of pedelec. The first models of BionX’s pedelec kit were freely programmable (two dozen parameters!) even to higher-than-legal speeds. (Today they are tamper-proof “black boxes” that self-deactivate, for example, if an attempt is made to change battery cells.) Another farmer-founded bicycle firm (Stromer) produced souped-up BionX-type pedelecs for new Swiss fast-class regulations implemented in 2014, which—although speeds are now limited to 45 km/h in pedelec mode—have raised the permissible power to 1 kW (hardly used; even top models are usually under 500 W). Although these pedelecs use motor systems of international brands, their development has taken place mainly in Switzerland, as the legality of fast pedelecs in other countries remains patchy, from tolerated to forbidden.

These and similar firms, along with independent promoters of pedelecs, eventually boosted sales enormously mainly in Switzerland and somewhat in Germany, where in 1992 Hannes Neupert

founded extraenergy.org, which assembled a large collection of available pedelecs, tested and displayed them all over Europe, and published data about them. In Great Britain, the Henshaw family, in *A to B Magazine* (atob.org.uk), tested and promoted e-bicycles on the British market (e.g., from Giant). In the United States Ed Benjamin surveyed and promoted e-bicycles at eCycle Electric (eCycleElectric.com) at least until 2014, estimating that sales had exceeded 170,000 per year. He had connections to China (as did Neupert) and found out that more than 200 million e-bicycles (in contrast to about 750,000 in Europe and the United States) had been produced there within a ten-year period! (These numbers probably include scooters and very low-performance bikes, however.)

China is now becoming an automobile country like the United States and many others, but in Switzerland fast pedelecs and slower e-bicycles (which unfortunately do not need to be pedelecs as in the European Union) have increased total bicycle usage, slowly leading to better supporting infrastructure. In traditional cycling countries that already have many cycle paths designed for low speeds, with many of them on sidewalks, fast pedelecs are less useful than they might otherwise be, as they can rarely be used at full speed. ExtraEnergy.org is therefore calling for North American-style speeds: a single free pedelec class limited to 32 km/h (20 mph) instead of the present 25 km/h (15.5 mph). The makers of assisted velomobiles and tandems, however, are calling for an assisted 45 km/h (28 mph) class instead of the present 25 km/h limit for these vehicles in Europe.

At the time of writing, e-bicycle usage is increasing rapidly in Switzerland, where e-bicycles accounted for one-third of all bicycle sales in 2018. Popular new types are e-mountain bikes and e-cargo bicycles and tricycles, in Switzerland and in other countries as well (see chapter 10).

References

Abbott, Allan V. 1999. "Health and the Reintegration of Physical Activity into Lifestyles in the New Millennium." In *Assisted Human Powered Vehicles* (Proceedings of the 4th Velomobile Seminar, Aula Interlaken, Switzerland, August 18, 1999), ed. Andreas Fuchs and Theo Schmidt, 21–33. Liestal: Future Bike Switzerland. <http://velomobileseminars.online>.

Barrett, Roy. 1972. "Recumbent Cycles." *The Boneshaker* (Southern Veteran-Cycle Club, UK), 227–243.

Baudry de Saunier, Louis. 1892. *Le cyclisme théorique et pratique*. Paris: Librairie Illustré.

Berto, Frank J. 1998. "Who Invented the Mountain Bike?" In *Cycle History: Proceedings of the 8th International Cycle History Conference, Glasgow, Scotland, August 1997*. San Francisco: Van der Plas.

Berto, Frank, Ron Shepherd, and Raymond Henry. 1999. *The Dancing Chain*. San Francisco: Van de Plas.

Clayton, Nick. 1997. "Who Invented the Penny-Farthing?" In *Cycle History: Proceedings of the 7th International Cycle History Conference, Buffalo, NY, 1996*. San Francisco: Van der Plas.

Clayton, Nick. 1998. *Early Bicycles*. Princes Risborough, UK: Shire.

Cyclepress. 1997. Japanese specifications statistics and information. Japanese, with English translation. Interpress, Tokyo.

Cycling. 1887. Badminton Library. London: Longman's, Green.

Davies, Thomas Stephens. 1837. "On the Velocipede." Address to the Royal Military College, Woolwich, UK. Reported, with notes by Hans-Erhard Lessing, in *The Boneshaker*, nos. 108 and 111 (1986).

Desmond, Kevin. 2019. *Electric Motorcycles and Bicycles: A History Including Scooters, Tricycles, Segways and Monocycles*. Jefferson, NC: McFarland.

Dodds, Alastair. 1992. "Kirkpatrick MacMillan—Inventor of the Bicycle: Fact or Fiction." In *Proceedings of the 3rd International Cycle History Conference*. Saint Etienne, France: Ville de Saint Etienne.

Dodge, Pryor. 1996. *The Bicycle*. Paris: Flammarion. http://pryordodge.com/The_Bicycle_Book.html.

Dolnar, Hugh. 1902. "An American Stroke for Novelty." *Cyclist* (London), January 8, 20.

Future Bike. 2018. "Das Sesselrad von Paul Jaray, Zeppelin-Konstrukteur und Erfinder der Stromlinienform für Autos." <http://futurebike.ch/page.asp?DH=2089&SE=jaray>.

Gnudi, Martha Teach, trans., and Eugene S. Ferguson, annotator. 1987. *The Various and Ingenious Mechanisms of Agostino Ramelli (1588)*. New York: Dover and Aldershot, UK: Scolar.

Hadland, Tony. 1987. *The Sturmey-Archer Story*. Self-published (UK).

- Hadland, Tony, and Hans-Erhard Lessing. 2014. *Bicycle Design*. Cambridge, MA: MIT Press.
- Henshaw, David, and Richard Peace. 2010. *Electric Bicycles*. Dorset, UK: Excellent Books. ExcellentBooks.Co.UK.
- Hicks, Eric. 2012. "IZip Express Review." *Electric Bike*, August 8. <http://www.electricbike.com/izip-express/>.
- Katch, Frank L., William D. McArdle, and Victor L. Katch. 1997. "Edward Smith (1819–1874)." History Makers (website). <http://www.sportsci.org/news/history/smith/smith.html>.
- Lessing, Hans-Erhard. 1991. "Around Michaux: Myths and Realities." In *Actes de la deuxième conférence internationale sur l'histoire du cycle*, St. Etienne, vol. 2. Ville de Saint-Etienne, France.
- Lessing, Hans-Erhard. 1995. "Cycling or Roller Skating: The Resistible Rise of Personal Mobility." In *Cycle History: Proceedings of the 5th International Cycle History Conference*. San Francisco: Van der Plas.
- Lessing, Hans-Erhard. 1998. "The J Wheel—Streamline Pioneer Paul Jaray's Recumbent." In *Cycle History: Proceedings of the 9th International Cycle History Conference, Ottawa, Canada, August 1998*. San Francisco: Van der Plas.
- Lessing, Hans-Erhard. 2017. Veteran-Cycle Club Cycling History, no. 8.
- "Loiterer, The." 1934. In "Velocar versus Normal," *Cycling*, March 2, 202.
- McGurn, Jim. 1999. *On Your Bicycle: The Illustrated Story of Cycling*. York, UK: Open Road.
- Mirror, The* (newspaper). 1822. "The Tread-Mill at Brixton." November 2.
- Oddy, Nicholas. 1990. "Kirkpatrick MacMillan, the Inventor of the Pedal Cycle, or the Invention of Cycle History." In *Proceedings of the 1st International Cycle History Conference, Glasgow*. Cheltenham, UK: Quorum.
- Oke, Olufolajimi, Kavi Bhalla, David C. Love, and Sauleh Siddiqui. 2015. "Tracking Global Bicycle Ownership Patterns." *Journal of Transport and Health* 2, no. 4: 490–501.
- Pinkerton, John. 1983. *At Your Service: A Look at Carrier Cycles*. Birmingham, UK: Pinkerton.
- Pinkerton, John, and Derek Roberts. 1998. *A History of Rover Cycles*. Birmingham, UK: Pinkerton.
- Ritchie, Andrew. 1975. *King of the Road: An Illustrated History of Cycling*. Berkeley, CA: Ten Speed.

- Roberts, Derek. 1991. *Cycling History—Myths and Queries*. Birmingham, UK: Pinkerton.
- Ron/Spinningmagnets. 2013. "Electric Bike History, Patents from the 1800's [to 1995]." *Electric Bike*, November 9. <https://www.electricbike.com/e-bike-patents-from-the-1800s/>.
- Schmitz, Arnfried. 1994. "Why Your Bicycle Hasn't Changed for 106 Years." *Human Power* 13, no. 3 (1994): 4–9; originally published in *Cycling Science* (June 1990). <http://www.ihpva.org/HParchive/PDF/46-v13n3-1998.pdf>.
- Sharp, Archibald. 1896. *Bicycles and Tricycles*. London: Longmans, Green. Reprint, Cambridge, MA: MIT Press, 1977.
- Street, Roger. 1998. *The Pedestrian Hobby-Horse at the Dawn of Cycling*. Christchurch, UK: Artesius.
- von Salvisberg, Paul. 1897. *Der Radfahrersport in Bild und Wort*. Munich. Reprint, Hildesheim, Germany: Olms, 1980.
- Vaver, Anthony. 2013. "Prisons and Punishments: The Failure of the Treadmill in America." Last modified February 27, 2013. Early American Crime (website). <http://www.earlyamericancrime.com/prisons-and-punishments/failure-of-the-treadmill>.
- Walton, Geri. 2015. "The Treadmill for Punishment." Geri Walton (website). <http://www.geriwalton.com/the-treadmill-for-punishment/>.
- Wilson, David Gordon. 1977. "Human Muscle Power in History." In *Pedal Power*, ed. James C. McCullagh. Emmaus, PA: Rodale.

2 Human Power Generation

Introduction

As a power producer, the human body has similarities and dissimilarities to an automobile engine. Energy is taken in through fuel (food and drink, in the case of humans). “Useful” energy is put out in the form of torque on a rotating crankshaft (in the case of cars) or in a variety of muscular movements (in the case of humans), and “waste” energy is dissipated as heat, which may be beneficial (for both) in cold weather. The two systems have peak efficiencies, the energy of movement divided by the energy in the fuel (for cars) or in the extra food used in working (for humans) remarkably close to one another, in the region of 20–30 percent. But automobile engines seldom work at peak efficiency, and in any case, they attain peak efficiency only close to full power, whereas the rider of a multi-speed bicycle can operate much closer to peak efficiency at all times. And whereas the automobile is powered by a “heat engine,” the human body is similar to a fuel cell, a device that converts chemical energy in fuel directly to work. Also, human output, unlike that of the automobile engine, changes over time because of fatigue, possibly hunger, and eventually the need for sleep. A human can draw on body reserves (i.e., stores of several different fuels); the piston engine can work steadily until the fuel runs out and then delivers nothing. Humans also vary greatly from one to another, and from one day to another, and from one life stage to another, in terms of the power output they can produce.

The authors’ intention in this chapter is to provide a basic understanding of how energy gets to the muscles of a bicycle’s rider and subsequently produces mechanical power at the pedals. The chapter

also comments on some bicycle configurations and mechanisms as they relate to the generation of human power. It takes the philosophical position that athletes do sophisticated things to maximize performance, many of which are not yet understood. Timing and direction of foot force, choice of crank length and gear ratio, when to stand up or “bounce” the upper body—all seem to diverge from simple logic. One is reminded of the agreement of the thermodynamicist and the practical engineer in stating that “science has learned more from the steam engine than the steam engine has learned from science.” (The second law of thermodynamics was formulated long after the first successful steam engines had been developed.)

Measuring Human Power Output

Exercise bicycles and ergometers of the pattern depicted in panel (a) of figure 2.1, in numerous variations, have been employed long and successfully. In these machines, the flywheel’s inertia minimizes crank-speed variations somewhat during brief variations in pedaling torque. For accurate work the wheel speed and the average braking torque must be measured precisely. One effective preelectronic measurement technique involves a band brake whose drag is set by a weight, theoretically giving unchanging, accurate data. However, generations of researchers have used simplistic calculations for the Monark-style brake band configuration shown in panel (b) of the figure; these calculations appear to overestimate force by 10–15 percent. Usually the force $F = F_T - F_S$ (the difference between the tight and slack parts) is simply assumed to be the same as the weight of the mass B , but the real relationship for a wrapped rope is $F = (1 - e^{-\Theta\mu}) F_T$, with Θ being the wrap angle and μ the coefficient of friction, which varies typically between 0.15 and 0.30. Other ergometer models using magnetic braking and electronic force sensing do not have this problem but need to be calibrated for accurate testing (see Zommers 2000, Gordon et al. 2004, Franklin et al. 2007, and especially Vandewalle and Driss 2015, which describes different friction ergometers with equations).

A different type of ergometer uses a bicycle mounted on a treadmill. Rider power at a given belt speed (figure 2.2) is controlled by the slope (or any rearward pull force, if used). The measured power

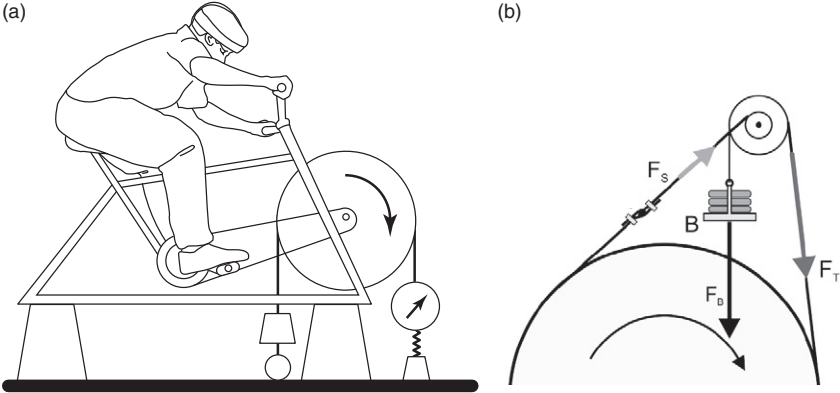


Figure 2.1
(a) How a belt tensioned between a spring scale and a weight can be used to produce and measure the tangential force on the wheel of a stationary bicycle; (b) the layout (in a larger scale) of the popular Monark-style ergometer using a differential pulley (both disks are connected) and weight-basket *B* attached to a brake rope wound around the flywheel. (Adapted from Vandewalle and Driss 2015, licensed CC-BY 4.0.)

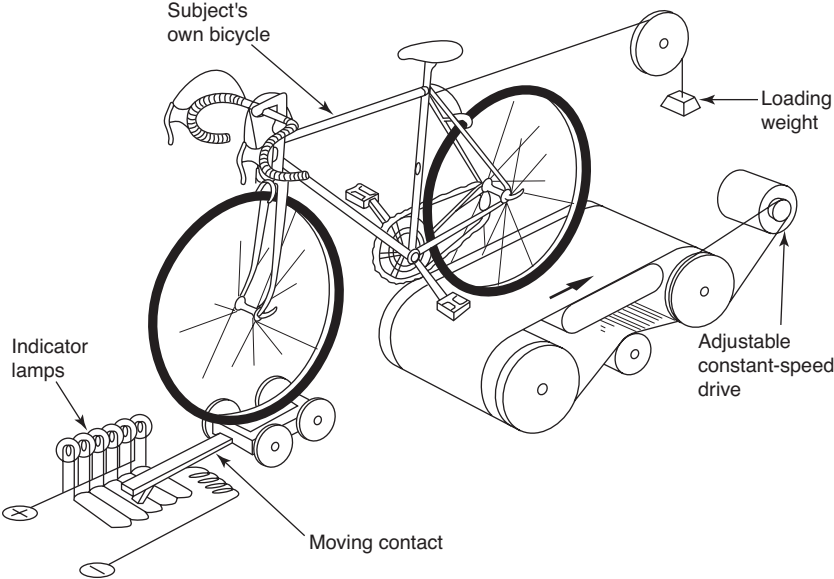


Figure 2.2
Muller ergometer (principle of operation). Load and speed are set; rider tries to keep center lamps lit. Run stops when rear-most lamp lights up.

includes rolling resistance and bicycle drive train efficiency and is thus slightly higher than the cyclist's power. It is shown here for historic reasons.

Much of the information presented in this chapter has been obtained through careful experiments, typically with ergometers. Most ergometers are pedaled in the same way as bicycles; other types are rowed, cranked, stepped, or walked. They are capable of precise energy measurements under the limitations mentioned. However, the following reservations about ergometer-based human-performance research must be kept in mind:

- People vary widely in performance, and unless very many are tested (seldom the case), the data cannot be generalized to the whole of humanity. There has also been a bias toward testing athletes (already self-selected for physical capability) and college students, predominantly male, in Western countries.
- Pedaling or rowing an ergometer usually feels different than riding a bicycle. It may take more than a month of regular use before someone becomes “proficient” on an ergometer. Muscle adaptation to full oxygen-using capability can take years of extensive training. Subjects are seldom given the opportunity to adapt for more than a few minutes (occasionally hours, but almost never more than that) to working an ergometer before tests are performed and measurements are taken.
- Quite apart from imperfect adaptation to an ergometer, the extant research in this area rarely follows a person's response to years of exercise from start to finish. Comparing a group of exercisers to a group of nonexercisers may suggest that exercise confers physical vigor, but the logic is weak: already-vigorous people may simply be the ones who tend to exercise. The proper test would be to track two equivalent groups as they followed different specified regimens.
- One reason pedaling an ergometer may feel strange is that the resistance to acceleration felt at the pedals (provided by a flywheel or other moving parts) is often much less than (as little as one-tenth of) the inertial resistance of the rider and bicycle, leading to a bothersome variation in pedal speed at substantial power levels. That is, it is often more like constant-torque pedaling as on a very steep hill climb, rather than constant-speed

pedaling, as when cycling fast. Tom Compton of the website Analytic Cycling (analyticcycling.com) has developed a “pedal-force simulator,” an electronically controlled brake that he says in this respect gives a bicycle on a roller-trainer almost the same feel as real cycling. Developers of electronic bicycles with pedal generators are faced with the same problem, which amounts to introducing virtual inertia into a system lacking sufficient real inertia.

- An ergometer bicycle is often fixed, whereas an actual bicycle can freely be tilted and moved relative to the pedaler, affecting body motions and forces.
- There are differences in posture between an ergometer and a bicycle: except on a recumbent, a competitive bicyclist must crouch to minimize aerodynamic drag, possibly restricting breathing. Crouching is unnecessary on an ergometer but should possibly be enforced in research studies if accurate comparison to road riding is desired.
- Subjects pedaling ergometers may not be given adequate cooling, and heat stress, as revealed by copious sweating, can limit their long-term output. There are exercisers on the market that dissipate most of the power via fans, thus simulating the square-law effect of wind resistance, but the airflow on such exercisers is not directed at the pedaler and in any case could not approach the cooling provided by the relative wind in real cycling.
- The motivation of competition (for maintaining a painful effort) can far exceed the stimulation of a laboratory setting.

Therefore, subjects are likely to achieve lower power output on ergometers (especially in the long term) than they could by pedaling or rowing their own familiar machines in a race that they want to win and cooled by their own apparent wind.

Most ergometers have frames, saddles, handlebars, and cranks similar to those of ordinary bicycles. The crank drives some form of resistance or brake in parallel with a flywheel, and the whole device is fastened to a stand, which remains stationary during use. Some ergometers can measure the output from hand cranking in addition to that from pedaling. Others permit various types of foot motion and body reaction, including rowing actions. The methods employed for power measurement range from the crude

to the sophisticated. One problem of ergometry is that human leg-power output varies cyclically (as does that of a piston engine) rather than being smooth (as with a turbine). Even in steady pedaling, a device indicating instantaneous power (pedal force in the direction of pedal motion, multiplied by pedal speed) would show peak values of perhaps 375–625 W, with an average of perhaps 250 W. Therefore, some form of electronic or mechanical averaging or both is usually employed, the simplest being the use of a flywheel. In some cases the subject is supposed to keep pedaling at a constant rate over 1–2 min to obtain accurate results; in other systems the power can be integrated and averaged electronically over any desired number of crank revolutions (Von Döbeln 1954; Lanooy and Bonjer 1956).

There are additional problems associated with the determination of very-short-duration extreme power levels (1–2 kW or even greater). It is very hard to hold power constant, and for the very shortest times, it is important to measure the work done over completed crank rotations only. The best-accepted high-power ergometer test is known as the Wingate anaerobic test (discussed later in the chapter), in which a high resistance is suddenly applied to a Monark-style ergometer and the pedaler immediately strives to pedal at maximum speed for 30 s, initially accelerating the flywheel dramatically, then allowing its speed to drop as fatigue sets in. Timing equipment determines the interval of each successive flywheel rotation, allowing average power during that rotation to be determined. Actually, it is better to average over crank rotations rather than wheel rotations, to smooth out the cyclic power variations occurring in each crank revolution. For the shortest times, simply using fast, accurate ergometer electronics that sense speed will also detect heretofore unexpectedly high peak power. For example, the ergometer record of nearly 2,400 W for 5 s (see Nüscheler 2009) is almost double the peak power indicated in the second edition of this book and well over the 1,500–1,700 W measured for football players doing staircase tests for durations of 2 s (Hetzler et al. 2010).

Sturdy old exercise bicycles with heavy, braked flywheels are very similar in function to laboratory-grade ergometers. They can be adapted for accurate power measurement, if the problem of controlling and measuring torque can be solved. Unfortunately,

energy-dissipating devices based on the losses of a small, tire-driven roller heat up the tire, changing the rolling resistance substantially. Magnetic (eddy-current) load units also heat up their conductive elements, increasing the electrical resistance and more than halving the initial magnetic torque. Temperature rise also tends to affect frictional brake drag, and even air fan devices can vary in resistance. Zommers (2000) describes how an ergometer using a small roller, inefficient generator, and resistance as load can nevertheless be calibrated to furnish accurate results. Whatever method is used for measuring, the unit must be designed to impose a torque that is essentially independent of friction coefficients and other temperature-dependent properties.

Some of the available test data on human power output are increasingly taken from subjects cycling on pavement, with various ingenious means used to measure work output (or oxygen consumption, which in steady state can be roughly related to work output, if calibrated in the lab, or both) (see figure 2.3). Measurements resulting from such setups may be more realistic than ergometer data and can give additional information, such as the onset of fat metabolization (Bergamin 2017). In such measurement schemes, however, someone wearing various sensors, in particular a breathing mask, is likely to find that the measurement apparatus creates a noticeable resistance to movement, breathing, or both and this will reduce performance somewhat (Davies 1962). Alternatively, cyclists' power output in closely monitored rides like popular cycle races can to some extent be determined indirectly and is sometimes displayed in television coverage.

Modern on-bicycle power-measuring systems such as Schoberer Rad Messtechnik (SRM) and PowerTap (see chapter 4) are free from the foregoing objections, and this has led to a very substantial rise in reported performances as more riders have used these systems, on their own bicycles, and especially in the heat of competition. This competition can be on the road, but increasingly cyclists "compete" on the internet, uploading their individual performances onto specific websites. This begs the question when we will start to see "virtual cyclist" data that are made up rather than measured.



Figure 2.3

Cyclist using breath-measuring equipment. Fitted out with gas sensors for oxygen and carbon dioxide, wearable metabolic systems can be used for indirect calorimetry. (Courtesy of Nijmegen University.)

Describing Pedaling Performance Quantitatively

Pedaling performance is usually described quantitatively by fixing a power level (usually by asking the subject to maintain a fixed pedaling speed at a given resistance) and determining the time to exhaustion. Different power levels can be sustained for durations anywhere between a few seconds and many hours. The results are often plotted as a power-duration curve, which seems to provide the best overall picture of a person's power-producing strengths and weaknesses.

Testing pedaling performance indoors, on an ergometer, has the advantage that the resistance is likely to be steady. Outdoors, even

“level-road” riding may involve periods of large variations, because of slight grades in the road, wind gusts, or accelerations.

Because individuals have different muscle mass, muscle makeup, inherited abilities, and state of conditioning, each will have a unique power-duration curve. When it comes to good athletic performance, some people are relatively stronger over particular durations and thus are better suited for events of those durations. This is partly why sprinters are not also climbers. (Another aspect of cycling performance, of course, is that different body types may have more or less aerodynamic drag, which is important in level riding, and more or less weight, which is important when riding uphill.)

Figure 2.4 shows power-duration data for “first-class athletes” and “healthy men” (designations in the original graph on which the figure is based) and for good cyclists. These data are referred to repeatedly throughout the book. They are derived from ergometer tests, from tests of bicyclists on bicycles, and from estimates based on the results of time-trial races. Each data point given is the maximum duration of pedaling at a certain power level: the curves do not reflect human power drop-off with time. The chain-dotted line estimates the best athletes’ maximum performance with an optimum mechanism. Unfortunately the subjects’ weights are seldom known, so specific power data cannot be given. Data for women are scarce and not comparable, because women are generally lighter, as the single data point given for a female athlete shows.

The top performances at different power levels are typically achieved by different types of individuals. The outer envelope reflects outstanding performances by rather large, strong men, with sprinters producing the short-time data and distance racers the longer-time results. However, the performance of any particular individual, in a given state of training and feeding, can be described by a curve of roughly similar form (see the next section). On-road on-bicycle power-measuring systems have become more sophisticated and numerous in recent years. They generally store complete logs of power versus time, and the underlying software can use the results of an ongoing ride to update the rider’s personal power-duration envelope.

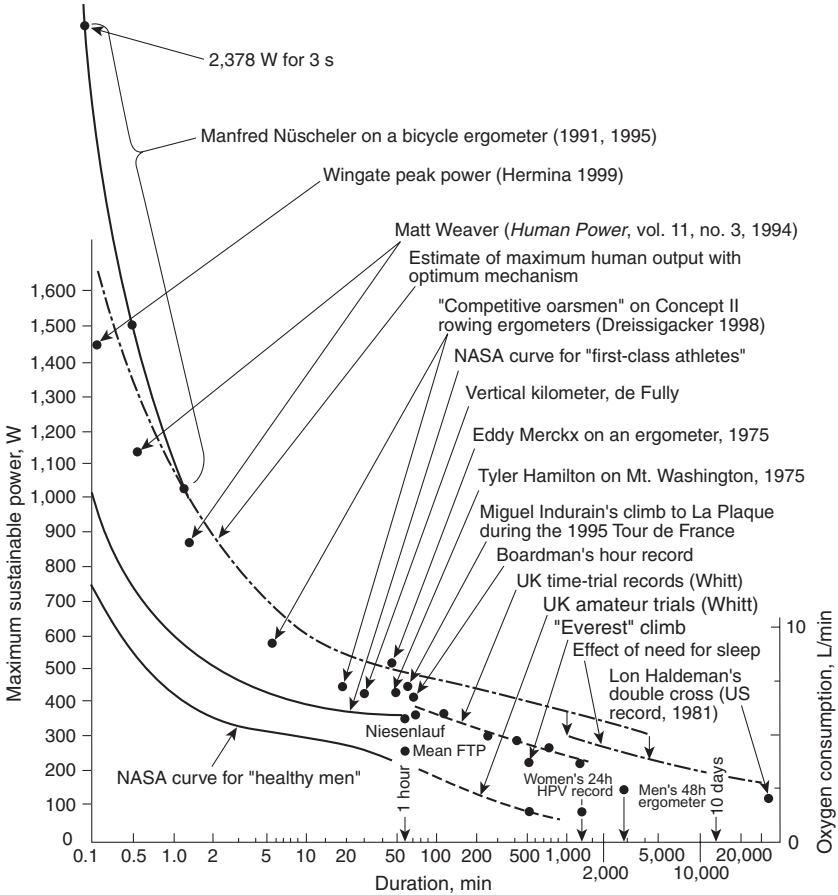


Figure 2.4

Human power output, principally by pedaling. Curves connect terminations through exhaustion in *constant-power* tests. A rough scale for oxygen consumption is also given. FTP: functional threshold power; HPV: human-powered vehicle. (Based on an original NASA chart with further data added. The “Mean FTP” data point is from Johnstone 2018 and assumes 75 kg men. The 48 h ergometer record is from *Book of Alternative Records* 2019.)

Critical Power: Fitting Curves to Power-Duration Pedaling Data

Individuals' power-duration curves have been subjected to a variety of curve-fitting efforts aimed at identifying the greatest power level that short-term tests suggest could be sustained "forever," which is commonly known as *critical power* (CP). Such efforts are interesting because they encapsulate data efficiently and permit mathematical approaches to performance optimization and also because they may reveal aspects of the physiological mechanisms governing endurance. A similar term is *functional threshold power* (FTP, defined as the power level that can be sustained for 1 h).

The simple regression used originally for such curve fitting of individual power-duration data appeared as a linear relationship between total work performed (that is, the selected power level times duration) and duration, in the form

$$\text{total work} = \text{anaerobic work capacity} + (\text{critical power} \times \text{duration}).$$

(Anaerobic work capacity, or AWC, refers to an amount of stored energy that can be released very quickly.) This equation embodies the simplified idea that any power beyond the pedaler's steady-state capacity is drawn from a nonreplenished finite energy reserve. Alternatively, this equation can be expressed as a linear relation between sustained power and duration: $\text{power} = (\text{AWC}/\text{duration}) + \text{CP}$.

A variety of research using such equations exhibits nice curve fits over ranges between 2 and 12 min, at power levels typically in the range from 200 to 400 W (obviously not championship power levels for those durations, which could be two to three times as great). In principle, two data points suffice to construct a straight-line relationship, but of course further trials are useful to demonstrate the variability and quality of fit. An initial guess at short-duration power settings, based on rider mass, might be 2 and 4 W/kg for an unfit person, 4 and 6 W/kg for a fit recreational cyclist, and 6 and 10 W/kg for a cycling champion. (Each of these power levels can be equated to a given vertical velocity from pedaling up a steep hill or running up flights of stairs.)

Gaesser et al. (1995) outline some criticisms of these simple correlations; for example, the erroneous implication that an individual's entire anaerobic work capacity can be depleted in a relatively short time span. In reality, some anaerobic work capacity will be held back, and the shortest-term maximum power will fall well below

predictions. Other researchers (see, e.g., Jenkins and Quigley 1990) have determined that a series of relatively short tests determines critical power well above the lactate threshold (described later) and that very few riders can sustain that intensity for even 30 min. Morton and Hodgson (1996, 500) review various proposed equations comprehensively and conclude that the model presented in the foregoing paragraphs “has a simple appeal, its parameters are well understood, and it has always been found to be a good fit to data over the 2- to 15-minute range. Extensions ... incorporate a more realistic representation of the human bioenergetic system, and fit data over a wider range of power and duration, from 5 s to 2 h.”

In principle, specialized power-duration curves could be developed for any particular conditions of interest, for example, with two different cadences or body positions, or before and after a preliminary fatiguing effort similar to a hill climb, or perhaps following a change in diet.

Actual power-duration data (or directly derived performance parameters such as critical power and anaerobic work capacity) seem more directly relevant for characterizing human performance improvements than physiological measurements such as lactate threshold, maximal oxygen uptake, or fuel efficiency. And such performance parameters are more easily measurable, requiring only a known-resistance exercise bicycle or an on-bicycle power-monitoring system.

Many cyclists have fitted their bicycles with power meters and exchange the resulting data online, often power-duration pairs, such as FTP. Johnstone (2018) posts FTP values that users of his web service say that they reach. For males, these values plot a nice Gaussian bell curve centered at about 3.5 W/kg, with the minimum at 1.5 W/kg and the maximum at 5.5 W/kg. For females, they result in an asymmetrical hill-shaped curve, also centered at about 3.5 W/kg, and with sharper cutoffs: minimum at 1.2 W/kg and maximum at 4.6 W/kg. Johnstone compares these curves with actual data mostly measured at shorter durations than 1 h. Because a full-hour test is very arduous and often impossible, training cyclists like to extrapolate from shorter tests, as explained earlier in the chapter, with a 20 min test having become a standard. How to do this is explained by Hunter Allen (2013), author of a standard training book with exercise physiologist Andrew Coggan. They use a 5 percent drop-off

in power between 20 and 60 min durations. Though many seem to have accepted this figure, the website *Fast Fitness.Tips* (2019) says it applies to athletes only and that 8 percent is more representative, with the figure even rising to 15 or 20 percent for untrained persons. This assertion seems plausible when one observes the rather short stamina of untrained people when cycling or hiking and corresponds to the drop-offs shown in the National Aeronautics and Space Administration (NASA) curves in figure 2.4: almost no drop-off for “first-class athletes” and about 50 W for “healthy men.” Coggan (2016) himself provides data for two hundred seasoned athletes that indicate a drop-off of 10 pp, or 14 percent, from 20 to 60 min, as well as a dozen or so personal measurements over a relatively large range. An online calculator from a company selling a fitness analysis system (Baron Biosystems 2018) allows the curves of figure 2.4 to be vaguely reproduced using just one to three data pairs.

Anaerobic Power: The Wingate Test and Alternatives

Anaerobic power is revealed in a person’s ability to leap or to sprint up a few flights of stairs. As described subsequently, it is governed by immediate and anaerobic energy stores in the specific muscles being used. The so-called immediate fuels are *adenosine triphosphate* (ATP) and *creatine phosphate* (or phosphocreatine), liberated through rapid partial metabolism of glycogen without oxygen. Because of the special problems presented by short-term, high-power ergometry, anaerobic power is not often assessed.

The most popular anaerobic power measurement is the Wingate anaerobic test, introduced by Ayalon, Bar-Or, and Inbar (1974) and further described by Inbar, Bar-Or, and Skinner (1996), which commonly uses a simple flywheel-style ergometer, braked by a weight-loaded friction band. In a typical protocol for the test, the rider stays seated, pedaling at 60 rpm with no resistance. For a gear ratio and wheel diameter with 5.9 m “development” (i.e., slippage past the brake in one pedal revolution), a sizable resistance equal to 8.5 percent of body weight is suddenly applied to the friction band, and the rider strives to produce maximum power (while remaining seated) for 30 s. Flywheel speed is measured every 5 s (or better yet, the time of every completed crank revolution is logged). A powerful sprinter may bring the pedal revolutions per minute (rpm) up

to 160 within the first few seconds of a test, only to have it drop to about 60 rpm by the end.

Apart from energy used to accelerate the flywheel and to cover transmission losses (which should be a small amount), a bicycle's pedaling power output is the wheel's peripheral speed times braking force. Three numbers need to be determined in order to calculate this output: the average speed (based on the total number of flywheel revolutions for the entire test) and the highest and lowest speeds (i.e., the highest and lowest average speeds over 5 s, respectively). From these and the resistance (known) are calculated 30 s average, peak, and minimum power (AP, PP, and MP, respectively). Finally, the fatigability index (FI), defined as the percentage drop from PP to MP, is also calculated. (Roughly speaking, PP corresponds to immediate fuel sources, whereas MP tends to approximate the maximum glycolytic power; see discussion later in the chapter.)

The Wingate test has typically been applied to noncyclist subjects to evaluate effects of diet or exercise. Naturally it is also used in evaluating elite competitors. However, ascertaining the true 5 s peak power directed to the flywheel, as would be revealed by on-bicycle power instrumentation such as PowerTap or SRM, is unlikely, in part because of the flywheel's inertia: during the violent initial acceleration, actual power may briefly reach twice the brake power or even more, and PP will be underestimated. (Initial acceleration does not affect MP and AP as much as it does PP.) In one example from Reiser, Broker, and Peterson (2000), inertial power correction yields PP values that are 20 percent higher. Such a correction, however, requires knowledge of the flywheel moment of inertia.

Another hindrance to true peak-power determinations is the relatively low resisting force felt at the pedals, usually less than half the body weight. To address this issue, Hermina (1999) tests fifteen elite road cyclists at brake resistances from 7.5 to 14.5 percent of body weight. At the lowest resistance the mean PP is 951 W, whereas at the greatest it is 1,450 W.

Franklin et al. (2007) examine a further criticism of the Wingate test performed on popular Monark-style ergometers. The basic Wingate test procedure uses a weight that applies tension to a brake band wrapped around the flywheel and assumes the resistance is equal to this weight. With models using a differential pulley as shown in figure 2.1, this is only approximately the case with friction

coefficients between the flywheel and the band or rope greater than about 0.3, but measurements reveal lower friction coefficients and overestimation of power by up to 12–15 percent. This means that much of the data up to the present day is inaccurate unless the exact method of measurement is documented.

Martin, Wagner, and Coyle (1997) devise an alternative to the Wingate test in which a Monark-style ergometer is modified to use flywheel acceleration alone (no brake) to determine the power. Thirteen subjects (average weight 80.6 kg) pedaled for 3–4 s (6.5 crank revolutions) starting from rest, with the instantaneous speed accurately measured, enabling the average and peak values for torque and power to be worked out without any direct torque or force measurements. Averaging over the best pedal-crank revolution yielded values of about 1.3 kW, or 16 W/kg. Figure 2.5 shows how instantaneous power (curve with peaks), as a function of instantaneous speed, varies strongly around the pedaling circle and between successive pedal revolutions (actually the revolution of one leg, or

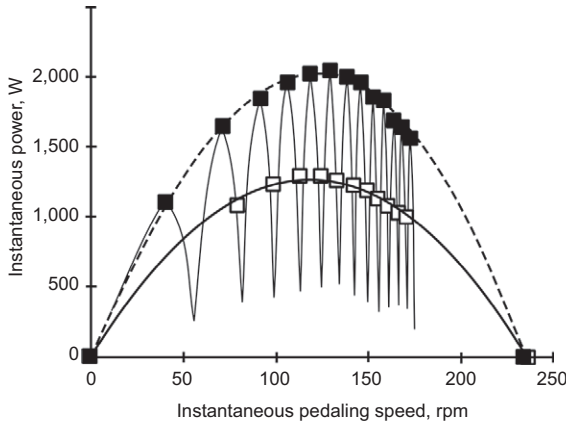


Figure 2.5

Average maximum power of thirteen active male subjects (solid squares, fitted curve represented by dashed line), instantaneous power of one subject (solid line with peaks), and average power of thirteen subjects over one pedal-crank revolution (unfilled squares, fitted curve represented by solid line), all as a function of instantaneous pedaling speed through 6.5 crank revolutions starting from zero over 3–4 s. (Adapted from Martin, Wagner, and Coyle 1997.)

half-revolutions), attaining the maximum during the third pedal revolution just before reaching 130 rpm.

Measuring the average power (P) between two times t_1 and t_2 is straightforward, as it is just the difference in kinetic energy (KE) at the two times divided by the period between the two times. The relationship to the moment of inertia I and the speedup of the flywheel is given by

$$P = \Delta KE / \Delta t = 0.5I (\omega_2^2 - \omega_1^2) / (t_2 - t_1).$$

All that is needed is a one-time calculation or measurement of the flywheel's I (~0.4 kg m² for the Monark model used) and a high-resolution recording of the instantaneous flywheel speed ω (in rad/s). The ratio of the pedal gear to the flywheel gear is chosen to get the desired range of pedaling speed (in this case ~7.4).

Another way to determine, for example, maximal 5 s power is on a fixed-speed (isokinetic), motor-driven ergometer. Averaging the measured torque of such an ergometer requires electronic instrumentation, and multiple tests are needed to obtain results for different cadences. Beelen and Sargeant (1992) use such an ergometer to show that peak power is commonly produced at 120–130 rpm, as Martin, Wagner, and Coyle also show; however, in 1995, the spinning champion Manfred Nüscheler produced his peak power, above 2,200 W, at 150 rpm (see Nüscheler 2009).

To sum up, the Wingate test, its variants, and other methods give somewhat different results, and the ergometers used in the testing are themselves subject to further variations and even errors, so computations of maximal anaerobic power are very approximate unless further documented with exactly what was measured.

Physiology of Pedaling: A Primer

The physiology of exercise, a complex subject, has evolved substantially from decade to decade as research has progressed. Neither of the book's authors nor its contributor was or is a researcher in this general field, so the book's attempt (in the following) to reconcile and summarize material published mostly during the 1980s risks criticism by experts in the field. Nevertheless the material seems worth presenting, because the subject is complicated and the field remains awash in mythology from still-earlier decades. The

presentation in this section is intended to prepare readers to gain insight from current and future exercise research.

For the big picture, the discussion here relies heavily on comprehensive texts by Åstrand and Rodahl (1977), Brooks, Fahey, and White (1996), and McArdle, Katch, and Katch (1996), all of which merit repeated study and some of which are available in new editions. McMahon (1984) engagingly presents many specialized details about muscle-fiber behavior. More recently, online discussion groups have offered a tremendous informal resource for the subjects of on-road power measurement technology, physiological determinants of performance, and related training recommendations.

Overview of How Muscles Work

Human muscle cells convert chemical potential energy into mechanical work, using a variety of fuels, originally derived from foodstuffs, that are stored in the body. Every muscle is composed of a large number of fibers (or cells) of three more or less distinct types. A platoon of such fibers, known as a motor unit, is assigned to each of the many nerves (*motor neurons*, or *motoneurons*) controlling a given muscle. These fibers may be visualized as extending from one muscle endpoint to the other, but this is not always accurate. A tilted fiber arrangement called *pennation* involves multiple fibers of shorter length, effectively creating a short, wide muscle. In pennation, fibers are angled to the direction of muscle contraction, rather than along this direction. This arrangement permits the connection of two long, overlapping tendons (tension elements that connect muscles to bones) with many short fibers, which increases the force a pennated muscle can exert compared to one with a smaller number of long fibers, but reduces its range of motion; it can't shorten to the same degree as the latter.

Muscles exert tension only (this physiological condition is termed *contraction*), and therefore can perform mechanical work only, as they shorten, drawing together their attachment points on two different bones. A limb or hand "pushes" only because the body has a system of levers (composed of bones), pivots (joints), tensioning cords (tendons), and antagonistic muscles, so that the pull of one set of muscles produces a movement of a limb or extremity in one direction and that of the other set in the other direction. Figure 2.6 shows a schematic representation of the main leg muscles.

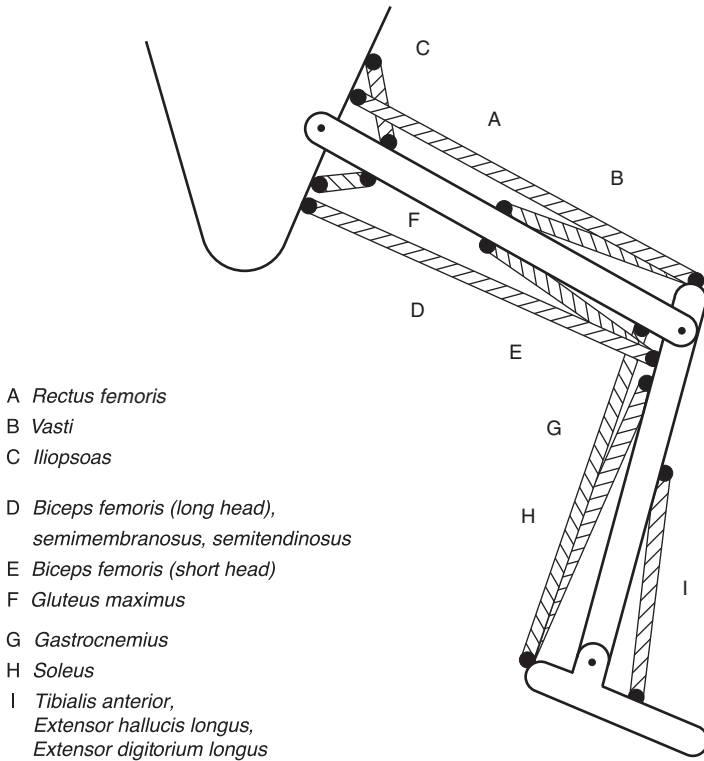


Figure 2.6

Stylized functional representation of the major muscles acting at the hip, knee, and ankle. (From Papadopoulos 1987.)

If a muscle actually lengthens while pulling (as occurs when one is lowering a barbell, for example, or slowly squatting), it is absorbing and dissipating work, rather than producing it. Such behavior is known as *eccentric contraction* or *negative work* and must be minimized if power or endurance is to be maximized. It is a matter of faith that humans, no less than animals, instinctively adjust their behavior to prevent energy from being lost in negative work.

Nerve stimuli, in the presence of a fuel, cause muscle contraction. Muscles use no fewer than six types of fuel (see the next section) individually or in combination, and the choice is not under conscious control. Instead, the power level the muscle user elects effectively “calls upon” the appropriate fuel choice or choices, at least

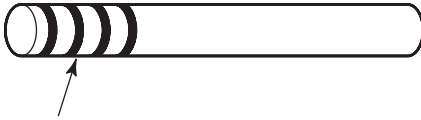
until depletion. In cycling specifically, at the very highest power levels for a given individual (generally above 1,500 W, or ~2 hp, for strong men), exhaustion occurs in just a few seconds. At a considerably lower power level, say 500 W, a strong rider may last a few minutes; at 350 W, an hour or longer; at 250 W, it may be possible to pedal all day. All these durations have analogs in cycling events: short match sprints (about 10 s), track time trials (a few minutes), hour and road time trials, and long road races, which can last even for days (e.g., the Race Across America).

After contracting briefly, a muscle fiber again relaxes. However, if a muscle is required to exert force for a longer time—for example, while supporting a weight—the nerve stimulating the motor unit involved will “fire” repeatedly, and if the firing period is shorter than the fiber relaxation time, the motor unit will exert a steady, maximal tension. During such “isometric” contraction, the muscle does not shorten. The fact that isometric contraction has a maximum tolerable duration is believed to arise from the blood vessels’ being squeezed, thus restricting the muscle’s blood supply. Even though the weight, in this example, is not being lifted during this time, and so in the thermodynamic sense no external work is being done, the muscle still requires energy either from its stores or from the bloodstream. To maximize external work and to minimize fatigue, isometric contractions should therefore be avoided as much as possible when bicycling.

Beyond the elementary picture of the muscle presented here lies the entire complex subject of exercise physiology, which must be explored to understand human bicycling performance.

The Six Muscle Fuels

As noted previously, muscles make use of six different types of fuels, some short acting and others usable for long durations. Figure 2.7 charts the movement and transformation of these six muscle fuels. All of the fuels involved are interconverted, transported, stored, and used differently. In addition, there are short-lived chemical intermediaries not discussed here that play crucial roles in human power production. A person’s fuel stores and the ability to transport fuel, oxygen, and waste products depend on genetics, training, and state of hunger or fatigue.



Contractile proteins in muscle fibers are powered solely by high-energy ATP

1. IMMEDIATE FUELS ATP stores in fibers (available ~3 s)
These ATP sources require no oxygen and produce no waste. There is therefore no transport delay but they must be continuously replenished. Efficiency to mechanical work ~50%.
 PCr stores in fibers (available ~10 s)

2. MEDIUM-TERM FUELS Carbohydrates of the $(CH_2O)_n$ variety, primarily glucose, its long-chain form glycogen, and its partially reacted forms pyruvate/lactate. (available ~2 h)
Sufficient glycogen is stored in the muscles for immediate use, giving two hours of high power, or a few minutes of extreme power. Glucose circulates in the blood for the use of muscles and the brain, delivered from the intestines or from breakdown of liver glycogen. Glycogen does not circulate.

There are two stages of carbohydrate use in muscles: Stage 1 is the fast nonoxidative (anaerobic) glycolysis/glycogenolysis to pyruvate, which has the greatest potential in FG or FOG fibers (see definition on p. 68). It delivers only 7 percent of the available energy in carbohydrate. No oxygen is required. Glycogen is in place. Glucose is brought in. This stage is potentially very powerful for one or two minutes. The excess unoxidized pyruvate accumulates as lactate. It must be cleared from working fibers. It enters neighboring fibers or is transported by blood to far fibers or the liver. May oxidize or reconstitute glycogen later. Inadequate transport or take-up limits high-power activity.

Stage 2 takes the oxidizable pyruvate at a limited rate to produce slow complete oxidation within the mitochondria of SO or FOG fibers to deliver the remaining 93 percent of energy. Oxygen supply is essential. Efficiency ~50% to ATP, i.e. ~25% to mechanical work.

3. LONG-TERM FUELS Fats (Lipids). Energy-rich compounds composed primarily of carbon and hydrogen that are stored throughout the body. (available several days and more)
These are mobilized and transported slowly to fibers. Oxygen is also required. They are used primarily by the weaker SO fibers. Fats are the main fuel while resting or gently exercising. High power levels suppress fat usage. Endurance training mobilizes fat and increases its usage at medium and high power, improves oxygen delivery and increases oxidizing structures, e.g., mitochondria.

Figure 2.7

Movement and transformation of the six muscle fuels.

Two Fast-Acting Fuels As noted previously, the so-called immediate fuels are adenosine triphosphate (ATP) and *creatine phosphate* (also phosphocreatine, or PCr). These are created within the muscle fibers from other fuels and do not release any harmful waste products requiring processing or removal other than heat. ATP is the only fuel used directly by a cell's contractile proteins; all other fuels are useful only insofar as they can regenerate ATP within the muscle fiber. ATP can be used as fuel without delay (no oxygen required)

and replenished just as rapidly through conversion of one of many other fuels.

Each muscle fiber stores enough ATP for about 2 to 5 s of all-out effort and enough PCr (which can be metabolized very rapidly without oxygen to form ATP) for about a further 10 s of ATP effort.

Because it can be utilized without any need for oxygen, a muscle fiber's stored reserve of ATP is an anaerobic energy source. It is the key resource used in leaping, or in accelerating from rest in a 100 m dash, or in lifting a maximal weight. At much lower power levels lasting minutes or longer, ATP is still the only fuel powering a muscle's contractile proteins; however, at such power levels it is generated at a steady rate (for example, by oxidation of other fuels), and the muscle fibers' net reserve is not depleted.

In a shortening contracted muscle, the transformation of ATP releases approximately equal amounts of heat and contractile work. That is, this final stage of the work-producing process has up to 50 percent efficiency.

Three Longer-Duration Carbohydrate Fuels In respect to intense efforts lasting 20 s through 2 h, three carbohydrates are of surpassing interest. These carbohydrates are the simple sugar *glucose* (essentially six carbon atoms combined with six water molecules); its stored form, the long-chain polysaccharide (starch) compound, *glycogen*; and its partially metabolized form, *lactate*. Glucose and glycogen can be used either aerobically (with oxygen, and slowly) or anaerobically (without oxygen, and far more quickly, but extremely incompletely). Anaerobic carbohydrate metabolism leaves behind high-energy lactate, either to be used immediately elsewhere or later (when oxygen is available) or to be reconstituted to glucose or glycogen. When used aerobically, the body's glucose and glycogen can provide power for a couple of hours. Alternatively, the glycogen in a muscle can be depleted anaerobically through conversion to lactate in just a few minutes.

Glucose reaches a muscle from the bloodstream, which it might enter from the digestive system or be released into from the liver, where it either is stored as glycogen or has been resynthesized from lactate. Glucose can be delivered to muscles only fast enough to supply up to one-third of the energy needs of intense steady-state exercise, so incoming glucose alone is not sufficient to produce high power levels. However, an adequate blood-glucose level is essential,

because glucose is also the primary fuel for the brain. If exercise depletes the body's supply of glucose, allowing levels in the blood to drop, a bicycle rider will feel weak and dizzy (hypoglycemic). Periodic intake of carbohydrates (for example, in a sugar drink) is effective in preventing this condition and is also somewhat beneficial for longer-duration exercise performance.

Once glucose enters a muscle cell (fiber), it can release energy in one or two steps. The first (anaerobic) step is to split in half to form two lactate molecules, with each half also giving up hydrogen to form *pyruvate*. It might be appropriate to term pyruvate a carbohydrate fuel also, but since it apparently is not stored or transported, it is presented here as a mere temporary intermediate compound. This decomposition, called *glycolysis* (a term also commonly misapplied to the splitting of muscle glycogen, which is more properly called *glycogenolysis*), releases only about 7 percent of the energy available in the glucose, but it can occur rapidly without using oxygen.

The second step proceeds in either of two ways. If the pyruvate is taken into the muscle cell's oxidative structure (mitochondria) and enough oxygen is also taken in, the other 93 percent of the energy is released aerobically in its conversion to water and carbon dioxide. This aerobic process of generating ATP produces roughly equal amounts of heat and available energy from the synthesized ATP, so that the steady-state formation of ATP is about 50 percent efficient. (The 50 percent efficiency of forming ATP aerobically and the 50 percent efficiency of using ATP to power the muscle, noted earlier in the chapter, lead to an overall aerobic "fuel efficiency of working" of about 25 percent.)

On the other hand, if the pyruvate is not oxidized in this way because there are too few mitochondria in the muscle cell to process the amount of pyruvate being produced, it simply regains its hydrogen to become lactate. The body must quickly clear lactate created in anaerobic glycolysis (more usually, glycogenolysis, since glucose cannot be delivered very quickly, and glycogen stored in the muscle is readily available) from the muscle fiber if it is to continue functioning. The accumulation of too much lactate in the blood will also put an end to exercise through the increasing pain that results as it accumulates.

In exercise at very high power levels, lactate concentrations in the blood may become unendurable within 30 s. However, at somewhat

lower power levels, it may take quite a few minutes to reach that condition, both because less lactate is being produced and because the body's lactate-removal system is able to handle most of it.

The essential point to remember is that glucose can be used either slowly and completely, achieving a high yield and medium power level, or rapidly but incompletely, achieving a low yield and high power for a short time only. Although an excessive accumulation of lactate prevents further work, lactate is far from a worthless poison: it is a highly significant fuel, since most of the energy of the precursor carbohydrate remains within it to be used. Apparently, lactate is reconverted to pyruvate, either in the liver, where it is further reconstituted to glucose, or in a muscle fiber, where it can be oxidized to perform work, or it can even be restored to glycogen. (The specific outcome apparently depends on a person's state of fatigue and level of hunger and whether exercise continues.) This highly mobile energy form's transport around the body for local use has been termed the *lactate shuttle* (Brooks, Fahey, and White 1996). However, the literature is not very definite on many issues collectively referred to as the *fate of lactate*.

As is discussed later in the chapter, some lactate is produced even at low and medium aerobic power levels. In exercise at a constant rate, the concentration of lactate in the blood will climb to a fixed level, usually less than 5 millimoles (mmol)/L, related to exercise intensity and removal rate. If lactate is produced at a rate greater than it can be cleared (stored, oxidized, or reconverted), then its concentration in the blood begins an upward trend that will eventually terminate working through the mechanisms just discussed. The critical exercise intensity that produces lactate at this rate is termed the *onset of blood-lactate accumulation* (OBLA) (McArdle, Katch, and Katch 1996).

In recent years it has been generally accepted that elevated lactate concentration defines the highest tolerable steady-state (i.e., over the range of 20 to 120 min) exercise intensity. However, a welter of terms and proposed definitions have somewhat muddied matters. Such concepts as the *lactate threshold* and *anaerobic threshold* (now considered a misnomer, because lactate elevation is not usually due to an inadequate oxygen supply) have also been defined, either when lactate reaches a specific concentration (4 mmol/L) or at the point at which the slope of the plotted relation between

steady-state concentration and exercise intensity increases. (The ventilatory threshold, or onset of panting, was originally believed to mirror the lactate threshold; however, Brooks, Fahey, and White [1996] have clarified that the near-simultaneous onset of panting as the lactate threshold is reached is mere coincidence.) Elite riders in a 10 to 15 min race may reach blood-lactate concentrations of 15 mmol/L, whereas in a 1 h race the lactate level is below 8 mmol/L because of the lower intensity of the power output.

Glucose is first in this section for reasons of simplicity, not of importance. Far more important to athletic muscle power than glucose itself is its starch, muscle glycogen, a long-chain polymer of glucose. Fuel for 1.5 or even 3 h of high aerobic power can be stored within working muscles in the form of glycogen, which unfortunately is incapable of moving from well-stocked fibers to others from which it has been depleted; its energy can be transported to other fibers only in the form of lactate. Muscle glycogen is typically 2 percent of a rider's muscle mass, if the rider is on a normal diet. It is one-quarter of this, or 0.5 percent, if the rider is on a low-carbohydrate diet, and it can be up to 4 percent after the depletion and overfeeding scheme known as *carbohydrate loading* or *glycogen supercompensation*. Glycogen is stored in muscles with three times its mass of water, so a person with 20 kg muscle mass engaging in carbohydrate loading may store up to 4 percent \times 4 \times 20 kg = 3.2 kg of glycogen with its accompanying water.

Muscle-stored glycogen can be degraded to pyruvate extremely rapidly compared to glucose, as glycogen does not have to travel through the bloodstream as glucose does. The pyruvate created through glycogen degradation can be used aerobically just as fast as the muscle mitochondria can process it (unless the oxygen supply is artificially restricted; see Coyle et al. 1983), and thus the combination of incoming glucose and muscle-stored glycogen produces higher aerobic power than incoming glucose alone.

To achieve power levels higher than a muscle's mitochondria and the body's oxygen-delivery systems can support, anaerobic glycogenolysis (pyruvate generation) can be increased to far higher levels than in aerobic work. In producing two or three times the maximum power level available through aerobic glycogenolysis, while releasing only 7 percent of the fuel's energy, anaerobic glycogenolysis evidently degrades glycogen thirty to forty times as fast as in complete

oxidation. Thus the anaerobic version of the process, in just a few minutes of intense effort, can deplete a store of glycogen sufficient for a 2 h aerobic effort, although rapid lactate accumulation may prevent this depletion from occurring all at once. The immediate aftermath is a painfully high blood concentration of lactate. (The time required to achieve a given lactate level depends, as noted earlier in the chapter, on how much the production rate exceeds the clearance rate.)

Fat: The Fuel for Very-Long-Duration Effort Fat is the final fuel in our list. Fats belong to a larger group called *lipids*. There are many different fatty compounds, composed principally of numerous carbon atoms with up to twice as many hydrogen atoms, plus relatively few atoms of oxygen. Because both its carbon and hydrogen are available to combine with oxygen, fat releases about twice as much energy per gram as carbohydrates. Furthermore, unlike glycogen, it is not stored with additional water. Body fat, our major energy store, is principally triglyceride, a glycerol molecule joining three fatty-acid molecules. For fat, which is not soluble in the blood, to travel in the bloodstream, the fatty acids are joined to proteins to form lipoproteins, which are.

Fat is used only aerobically and for most of us is solely a low-intensity fuel. It supplies most of the body's energy needs at rest and during exercise up to medium intensity. However, it takes considerable time to reach the muscles and is taken up by the muscle cells relatively slowly. At its greatest delivery rate, it supplies oxidative energy more slowly than muscle glycogen. However, the body holds enough stores for many days: fat stores can fuel weeks of effort. The typical human body stores 200 to 800 megajoules (MJ, ~50,000–200,000 kcal) as fat, because completely oxidized fat yields 37 kJ/g (9 kcal/g), enough energy for 100–200 h of hard work (or more realistically, 200–400 h of moderate work interspersed with rest). Stored glucose and glycogen can furnish only 1–2 percent of that amount of energy.

There are two opposite reasons to maximize fat utilization or *lipolysis* instead of using up carbohydrates: on one hand, to allow extremely long-duration efforts without “refueling,” and on the other, to lose weight. Although intense exercise will result in quick weight loss, it will mainly be in the form of carbohydrates and water. It is possible to metabolize an entire kilogram of glycogen in

a hard ride, which also means losing its associated 3 kg of water. As prolonged high-intensity effort is reckoned to inhibit fat utilization, exercise at that level may hardly touch the body's fat stores. In any case it is not possible to cycle at high power for long periods without replenishing glycogen with food, drink, or both. In exercise at low intensity, mainly fat is oxidized, but of course very little. This is good if it is necessary to carry on for days or weeks without food, but inefficient if the object is to get rid of body fat. In exercise at medium intensity, roughly half the energy used comes from fat, but in absolute terms its usage may be at a maximum of, say, 0.25 g/min (see Croci et al. 2014), so it would take about a whole week of daytime effort to lose 1 kg of fat.

Daley (2018), using research by Venables, Achten, and Jeukendrup (2005), has developed an online calculator for the ratio of fat to carbohydrate usage as a function of heart rate, for example, about 1:1 at 65 percent of maximum heart rate. (A rule of thumb for the maximum heart rate in beats per minute is 220 minus age in years.)

However, the foregoing statements must be further refined with respect to time: Güntner et al. (2017) show that it takes a while for the body's fat metabolism to begin and then it can stay high or increase even when resting, in especially pronounced cases, up to 3 hr after exercise if nothing is eaten, with strong variation from person to person. About one-third of the subjects Güntner and colleagues tested showed a significant increase after 1–1.5 hr, another third showed a slower linear increase from the beginning, and the final third little correlation. A compact breath sensor developed at ETH Zürich allows individuals easily to determine the onset of their lipolysis, as described by Bergamin (2017), thus removing the uncertainty. The sensor measures acetone, which correlates with lipolysis onset.

“Fat burning” is a widely and somewhat controversially discussed subject. Proponents say that repeated bouts of short, high-intensity (interval) training causes the body to rapidly shift into “fat-burning mode.” This assertion appears contradictory to the previous statements in favor of low-intensity steady-state training, but the contradiction can apparently be resolved through the use of both strategies. It might be worth pointing out, in the context of this book, that cycling for transportation and touring can usually provide both: hills and traffic lights (which involve accelerating

after stops) automatically motivate periods of high-intensity work, and level sections of terrain permit any desired rate of low-intensity work.

Muscle Fibers

A muscle is typically controlled by 50–500 nerves. Each nerve controls a bundle, or motor unit, of several hundreds or even thousands of muscle fibers, of which there are three types (discussed later in the section). Each fiber is a single hairlike cell (between 0.01 and 0.1 mm thick and sometimes as long as the muscle) containing a great many force-producing protein filaments known as *myofibrils*. The fibers in any one motor unit are all of the same fiber type, and those of each motor unit are intertwined with fibers from nearby motor units within the muscle. The proportion of each type of fiber, in a given muscle of a given person, is found to be mostly unalterable. Furthermore, the total number of fibers in a muscle is considered fixed early in life: muscle dimensional changes are due primarily to hypertrophy (increase in size) of the constituent fibers.

Three fairly distinct types of muscle fiber can be distinguished by chemically staining a muscle cross section: slow oxidative, fast glycolytic, and fast oxidative glycolytic. Each type differs in how it uses fuel and produces force and work, although the differences among them in these areas may not always be marked, as cells adapt through training: their behaviors are actually placed along a continuum. Any one muscle is composed of a mixture of the three types, all more or less adapted through training to either endurance (aerobic) or force or power (immediate and glycogenolytic) activities.

At one end of the spectrum, slow oxidative (SO) fibers (also known as Type 1 fibers) are richly supplied with oxygen-using mitochondria. They are reddish because of the oxygen-storing myoglobin they contain, as in the dark meat of a chicken. Endurance training can increase both the mitochondrial density of and the number of capillaries supplying oxygen to these fibers substantially. SO fibers are ideal for steady-state (endurance) activities, taking up oxygen at the highest rate to metabolize glucose, glycogen, or fat aerobically. They never grow very thick and exert relatively little force. They respond slowly to nervous stimulation and so are referred to as “slow-twitch” fibers. They have little ability to support rapid, oxygen-free liberation of carbohydrate energy (anaerobic glycolysis

or glycogenolysis). On the other hand, they are able to contract repeatedly without fatigue. Since this type of fiber actually produces steady muscle force through repeated contractions of individual fibers, postural muscles tend to be composed of SO fibers.

At the other extreme, fast glycolytic (FG) fibers (also known as Type 2b fibers) respond faster and more forcefully to nervous impulses. They largely lack both mitochondria and myoglobin and hence are pale, like the white meat of a chicken. They have a metabolic predilection for rapid anaerobic conversion of glucose or glycogen into lactate, producing high force and power with little delay (“fast twitch”). They are frequently described as “fatigable,” presumably through glycogen depletion or lactate accumulation. Through overload training, FG fibers can be enlarged in cross section, therefore increasing short-term muscle strength fueled either by carbohydrate or immediate sources (ATP and PCr). It has been suggested that glycogen stores can be higher in FG than in other types of fibers and that they are much better at using PCr.

A third type of fiber is the fastoxidative glycolytic (FOG, also known as Type 2a). It is believed that some FOG fibers may be converted from FG fibers as a result of endurance training. If so, they give up some glycolytic capacity for a substantial boost in aerobic ability. Textbooks describe FOG fibers as combining characteristics of SO and FG fibers.

As suggested earlier in the chapter, each power level muscles are commanded to exert invokes some combination of fuel transport and conversion mechanisms. Exhaustion of one resource or saturation with one waste that is not being removed fast enough will determine duration at any given power level. A lesser rate of using fuel or producing waste will therefore permit longer duration. Differences in the physiological mechanisms operating at different power levels would also be expected to alter the duration until exhaustion.

Fiber Recruitment The proper selection of muscle fibers to perform a given task is important. For example, short-term gains in weight-lifting ability can be attributed to improved fiber recruitment, rather than actual muscle-strength gains. If glycolytic motor units were recruited first for endurance (low-force) activities, they would quickly become depleted of glycogen without making use of much of the available oxygen. Although motor-unit recruitment is not directly under conscious control, it does seem to be a function of the central nervous system.

High-Power Aerobic Metabolism: Lactate Threshold and Glycogen Depletion

Not all of the physiological mechanisms defining an individual's power-duration curve have been studied to the same degree. Two that have received considerable attention, highest steady-state power (aerobic) and highest power sustainable for 1–2 min (anaerobic), relate to important types of cycling efforts.

High-power aerobic metabolism operates as follows: the highest power levels sustainable for about 30 min or longer are essentially steady state, neither using up any rapidly depleted resources nor increasingly accumulating painful lactate. From minute to minute, virtually all the power produced through such metabolism involves inhaled oxygen.

Carbohydrate stores—depletion of muscle glycogen or even blood glucose—often set the maximum duration of such high-intensity steady-state efforts. Sometimes other factors such as dehydration or cramping also play a role. Experiments described in textbooks comparing initial muscle glycogen to maximum possible duration of effort have amply confirmed that in well-trained endurance athletes, at least, muscle glycogen is the limiting resource that terminates hard steady-state effort (i.e., determines endurance). In addition, measurements of glycogen levels in both legs when only one leg is allowed to pedal (Åstrand and Rodahl 1977, chap. 14) show that glycogen is not mobile: the working leg depletes its stores and is exhausted, whereas the resting leg remains fully charged.

Increasing the energy delivered by the body's fat system or the pedaling rotations per minute (the reduction in pedal force reduces fast-twitch-fiber recruitment, with its associated anaerobic glycolysis) can reduce consumption of muscle glycogen in cycling. Furthermore, muscle glycogen stores can be supercharged through carbohydrate loading: depleting glycogen stores substantially over 2–4 days, then eating a superabundance of carbohydrates. This process has proved to double the levels of endurance achieved by normal well-fed but “unloaded” persons. Since muscle glycogen is also useful in shorter, more powerful efforts, carbohydrate loading would seem to be a useful practice for all but the shortest events. Since glycogen regeneration after consumption and depletion is supposed to take more than a day, an important question concerns the size of the glycogen stores that athletes can maintain in multiple-day events.

In the past, it was widely believed that the maximum rate at which fuel could be oxidized was set by the rate at which the lungs and the body's circulation could deliver oxygen to the working muscles and that this rate could be determined in a test of VO_2max (maximal oxygen consumption), as described by Daley (2018) and later in the chapter. However, at least for athletic endurance cyclists, this is no longer believed to be generally true. Instead, the rate of fuel oxidation seems to be limited by the somewhat lesser rate at which working muscles can oxidize fuels without excessive lactate production, which depends on the total mass of muscles being used, their fiber type, and their degree of adaptation (via mitochondria and capillaries) to oxidizing fats. The most effective fibers for taking up oxygen are the relatively weaker and slower-acting slow oxidative fibers. Appropriate training can double the capacity of these fibers to use oxygen. (Their weakness is not a problem for the cyclist, since the typical foot force produced in long cycling events is only about 10 percent of the maximum achievable pedaling force.)

As there is no obvious connection between the maximum steady rate at which muscles can take up oxygen and VO_2max , the latter ought to be power limiting in at least part of the population. (Coyle et al. [1983], discussing heart-disease patients, offer an extreme example of this.) However, even if this is true, individuals with limits set by VO_2max should be expected to be few among successful competitors (Brooks, Fahey, and White 1996). It is now believed that the blood-lactate level arising from the balance between lactate production of the working muscles and various mechanisms for clearing lactate determines the maximum work intensity most individuals can tolerate. A small amount of lactate is produced whenever pyruvate is available, that is, whenever carbohydrates are used as fuel. Much more is produced when SO fibers are required to produce more than a certain amount of energy from carbohydrates, or when FG fibers are recruited, or when a fiber has a poor oxygen supply. The rate of lactate production can then overwhelm the body's lactate-clearing capacity, which typically seems to occur quite independent of how much oxygen the circulation can deliver. Training reduces the amount of lactate produced at any given workload and increases the rate at which it can be used (cleared), therefore reducing the level of lactate in the blood. In

addition, training can increase the body's ability to tolerate elevated lactate levels.

Up until 1990, no consensus had been reached about precisely how to define the body's lactate threshold—for example, as a concentration level, as a slope change, or as an increase in concentration above the baseline. A seemingly rational definition is OBLA, the exercise intensity at which blood-lactate concentration can no longer remain steady: production exceeds clearance, and the blood-lactate concentration climbs inexorably until exercise ends.

There is good reason to expect that pedaling styles or devices that allow the use of a greater mass of muscles will increase a rider's maximum steady-state (i.e., aerobic) power level. Indeed, it is widely accepted that top Nordic skiers, who use their arms as well as their legs, tend to take up more oxygen than top cyclists and so produce greater steady-state power.

Riders are known to exhibit reduced aerobic power as they age. Figure 2.8 plots average speeds in 50 mi time trials versus age and estimates breathing capacity from the speeds.

Evaluations of pilots for the Massachusetts Institute of Technology (MIT) Daedalus flight in the 1980s yielded some interesting physiological data from a maximum-power long-term effort. These evaluations required the pilots to pedal for an estimated 4 h. As shown in figure 2.9 (Bussolari 1986–1987), two subjects were required to pedal at 70 percent of their maximum aerobic power and were monitored through measurements of their inhalation and exhalation and through blood samples taken periodically throughout the 4 h. They were allowed to drink as much as they wished. The solid lines in the various panels of the figure show the data for a female pilot who, according to Steven Bussolari, who conducted the study, had engaged in carbohydrate loading before the test and drank periodically throughout. She finished the 4 h in a condition good enough to have allowed her to continue for another 30–60 min. The dashed lines show the data for a male pilot who did not attempt carbohydrate loading, drank less than half the quantity of liquid that the female pilot consumed, and had to quit after 3.5 h because of leg soreness and cramping. As the figure shows, these discomforts were not brought on by a high lactate level.

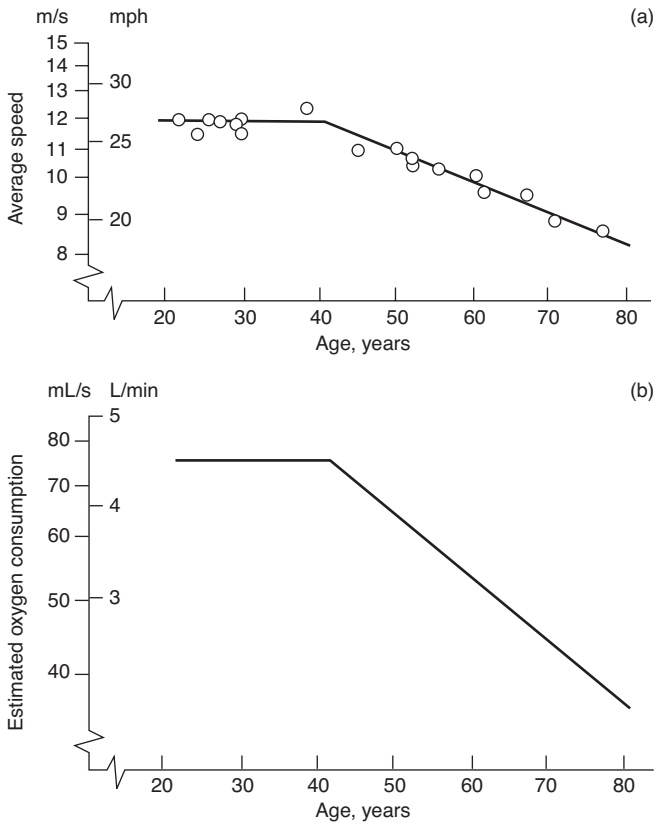


Figure 2.8

(a) Speeds and (b) estimated oxygen usage of 50 mi time trialists versus age. (Plotted by Dave Wilson from data supplied by Frank Whitt.)

High-Power Anaerobic Metabolism: Lactate Accumulation and Fast-Twitch-Fiber Population

In significant anaerobic efforts such as a sprint or climbing a short, steep hill, the muscles involved output far more power than the maximum aerobic power, by a factor of three to six, initially produced using the immediate fuels ATP and PCr. As those compounds are depleted, the power exerted by the muscles drops to a lower level, supplied primarily through the anaerobic glycogenolysis of muscle glycogen. As mentioned earlier, this results in a massive release of lactate.

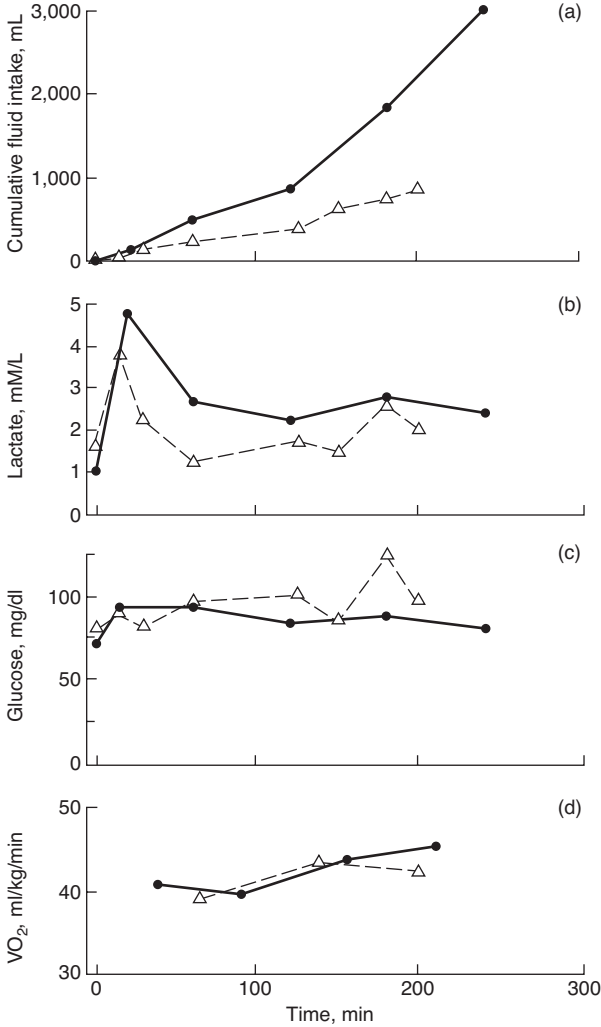


Figure 2.9 Measurements taken on two pilots for human-powered aircraft during a 4 h test at 70 percent of maximum aerobic power. (From Bussolari 1986–1987.)

When high-power work is performed for a very short time only, the glycogenolytic system is hardly engaged; the anaerobic fuel systems do not build up any lactate. This is one principle behind so-called interval training: great effort can be expended repeatedly, if the duration of such effort is kept short.

High-power anaerobic (both immediate and glycolytic) metabolism is predominant in the 5–20 s range of exercise duration. For lesser efforts, causing exhaustion in under 2 min, oxygen-derived power still represents less than 50 percent of the total energy expended (and some oxygen is already stored in muscle myoglobin), so an outstanding oxygen-using system is presumably of little value in such efforts.

Although lactate buildup ends high-power glycogenolysis, repeated intense efforts will actually deplete FG fibers of their glycogen. Therefore, to be able to perform a large number of sprints, for example, a superabundance of glycogen, which can be developed through carbohydrate loading, would be desirable.

A muscle's *anaerobic work capacity*, determined in critical-power curve fitting, suggests a rapidly deliverable “reserve quantity” of work. Presumably anaerobic work capacity can be approximated by measuring the stores of immediate fuels and adding an amount of muscle glycogen sufficient to raise blood lactate to intolerable levels when consumed. Some riders can tolerate higher lactate levels than others, however, and some riders can clear lactate faster than others. In addition, drinking a solution of bicarbonate of soda can help buffer blood lactate, thus permitting somewhat longer effort at very high power. (This is not considered to be doping, but it does have side effects in the intestinal tract.)

The fibers best adapted for brief, high-power activities are the FG and maybe the FOG fibers. Part of the adaptation of these fibers to these activities is a growth in volume (cross-sectional area) that provides for more work-producing protein and greater force, which shows up as a larger muscle. In addition, there are enzymes that catalyze the conversion of glycogen to lactate, and their levels must be adequate for this conversion to take place.

A high population of enlarged fast fibers is probably necessary to produce the maximum level of glycogenolytic power possible. However, the literature repeatedly stresses that this is not the whole story, inasmuch as some very strong people, including bicycle

sprinters, do not have particularly large muscles. It seems that the ability to recruit the proper fibers at precisely the right time is also important. Whether this facility is innate, as opposed to trainable, is little discussed in the literature.

Food and Efficiency

As explained earlier in the chapter, muscles have an overall aerobic fuel efficiency of about 25 percent. Tests performed by Pugh (1974) on bicyclists riding on an ergometer and on a track confirmed that the work produced accounted for about 25 percent of the extra fuel used. Bussolari (1986–1987) and Bussolari and Nadel (1989) quote 24 percent and give detailed measurements partly summarized in figure 2.10 (p. 86). In addition to the five rather similar pilots whose results are shown in the figure, Bussolari and Nadel tested twenty others and reported mechanical efficiencies between 18 and 34 percent at aerobically sustainable power levels, per body mass, of 3–5 W/kg. If the roughly 1 W/kg that is additionally required for basal metabolism (see discussion later in the chapter) is counted, the total efficiency is less, especially at low power levels. Zommers (2000) comprehensively summarizes food efficiency, and for pedaling about 60 rpm at low power right up to the anaerobic threshold, finds 22–24 percent for *net efficiency* or *working efficiency*. These terms use the total power metabolic input measured during exercise but then subtract that measured when sitting on the ergometer without exercise. See also the next section.

There are several ways of defining food's usable energy content (see FAO 2003). The values published in tables or on food packets generally use 37 kJ/g (9 kcal/g) for fat, 17 kJ/g (4 kcal/g) for carbohydrates and protein, and 8 kJ/g (2 kcal/g) for dietary fiber. Not all of this energy content is available to the body's muscles, however, as there are several losses. The largest is from digestion itself, which produces heat (*thermogenesis* or *thermic effect of food*), which reduces the previously quoted numbers somewhat depending on the actual food and individual—by up to 25 percent for proteins. Also, humans cannot digest practically any of the cellulose or lignin content in food (e.g., the insoluble parts of dietary fiber), so the energy contained in these is not counted in human nutrition.

Eating a 50 g snack bar with an energy content of 1 MJ (= 1 MWs \approx 0.278 kWh) per hour theoretically provides continuous 278 W

metabolic power or 69 W mechanical power for one hour, assuming 25 percent efficiency and not counting basal metabolism. That is enough for ordinary cycling.

At low power levels there is no immediate correlation between power and food eaten, as it is masked by considerable body stores and basal metabolism, so counting calories is not suitable for measuring performance except over long periods. However, food must be oxidized for the body to use it, and as the body stores only a few breaths' worth of oxygen, measuring oxygen usage during breathing is a far faster method for conducting such measurements.

Oxygen Uptake and Metabolism

Measuring oxygen (O_2) usage or carbon dioxide (CO_2) production is potentially a very powerful tool for revealing how much "fuel" is being metabolized to supply a person's total energy needs, and both O_2 usage and CO_2 production can be calculated through a process called *indirect calorimetry*. Knowing the *metabolic power* P_M (the rate of food-energy consumption) is useful on the one hand for planning food requirements and on the other hand for deriving the actual mechanical power provided by the muscles. The latter can be calculated as the difference between P_M measurements while working and at rest times aerobic muscular efficiency. The following observations are general but in part apply to standard air pressure near sea level and about room temperature. High-altitude effects are discussed in chapter 3.

For greatest precision the actual amounts of consumed O_2 and exhaled CO_2 are measured, that is, the volume per minute breathed times the diminution in O_2 concentration and the CO_2 increase in the exhaled air. The analysis can be performed either continuously with stationary or wearable equipment or after the exhaled air has been collected in a Douglas bag.

The same calculations can also reveal *which* fuel is being consumed. When carbohydrates are oxidized, every O_2 molecule is converted to a CO_2 molecule. Thus a 1:1 ratio of CO_2 to O_2 (the so-called *respiratory quotient*, or RQ) indicates a state of pure carbohydrate usage. On the other hand, when fats are oxidized, only about 70 percent of the O_2 forms CO_2 ; the rest creates water. Thus a $CO_2:O_2$ ratio of 0.7:1 indicates a state of pure lipid usage. For ratios between 0.7:1 and 1:1, the proportions of carbohydrate and fat usage (assuming

no oxidation of protein; see discussion later in this section) can be calculated. Fat oxidation yields 4.70 kcal/L (~19.7 kJ/L) O₂, whereas carbohydrates deliver 5.05 kcal/L (~21.1 kJ/L). Thus 1 L/min of O₂ consumed (which means breathing 20–25 L/min of air; see discussion later in this section) represents 352 W metabolic power for carbohydrates or 328 W for fat. If we subtract 80 W basal metabolic power (see discussion later in this chapter) and assume 25 percent efficiency, this represents 68 W mechanical power.

For intermediate metabolic values Weir (1949) devised a formula still in use today. A derivation for metabolic power P_M in watts is

$$P_M = MV \%CO_2 (2.72/RQ + 0.766),$$

in which MV is the minute volume (volume breathed per minute) in liters per minute, $\%CO_2$ the CO₂ in the expired air in percent, and RQ the respiratory quotient given in the preceding paragraph. (For P_M in kcal/d, multiply by 20.65.) If RQ is known or can be estimated or assumed, only one of the gases need be measured. The CO₂ rather than the O₂ concentration is specified in the equation because it is easier to measure. If an average value of $RQ = 0.85$ is used, a particularly simple approximation emerges: $P_M \approx 4 MV \%CO_2$.

Weir's exact formula includes a term for protein consumption, which could be determined by measuring urinary nitrogen. Proteins contain about 16 percent nitrogen, and 1 g in urine corresponds to almost 6 L of O₂ breathed. Consumed proteins deliver about as much energy as carbohydrates but have a lower RQ of 0.82. One needn't bother with the exact formula normally, as the food most people consume contains 11–14 percent protein (Weir 1949). The simplified Weir formula in the last paragraph is adjusted for 12.5 percent protein, and even if other amounts of protein are consumed, the resulting error is small. (Given a free choice, most people will tend to eat in such a way that protein supplies about 14 percent of their metabolic power. If one eats primarily protein-poor foods containing almost only carbohydrates and fat, one has to eat too much in order to achieve the 14 percent and will gain weight. Highly sugary drinks and energy bars may be good fuels for heavy cycling but are otherwise too protein deficient. Protein bars are also available, but nuts and dried fruit are likely to be healthier.)

Another caveat is in order: over the short term, not all energy is produced via oxidation. Brief, intense efforts rely on immediate

fuels and anaerobic glycogenolysis, and their oxygen cost is deferred. (And after exercise ends, changes in, for example, body temperature alter the basal metabolism, thus obscuring total fuel usage, because it is taken as being constant.) Oxygen measurements at unsustainable exercise intensities do not reflect steady state and must be interpreted cautiously.

Humans normally tend to exhale with a relatively constant CO₂ concentration of 4–5 percent (the coauthor 4.5–4.6 percent at rest). This is because the urge to breathe is already apparent at 5 percent and becomes very strong at 6 percent. At the other end of this range, CO₂ concentrations below 4 percent require deep or fast breaths even at rest, and “hyperventilating” at 3 percent is laborious.

If 5 percent is taken for the carbon dioxide concentration, the formula becomes $P_M \approx 20 MV$, or if 4 percent is selected, $P_M \approx 16 MV$, both for $RQ = 0.85$. Knipping and Moncrieff (1932) give $P_M = 14.63 MV$, which implies %CO₂ slightly above 4 percent, RQ slightly under 1, or both, as well as that 24 times the volume of O₂ absorbed must be breathed as air. For 5 percent CO₂ and $RQ = 1$, the figure is 20.

Measuring MV requires special equipment, so the foregoing rules of thumb are not very useful directly. However, measuring the *breathing rate* (BR, the respiratory frequency, or breaths per minute) is easy, and MV is BR times the *tidal volume* (TV, volume of a breath in liters). The latter is often taken to be 0.5 L for adults (or 7 mL/kg body mass) at rest. For $TV = 0.5$ L at 5 percent CO₂ and $RQ = 0.85$, metabolic power in watts is found to be $P_M \approx 10 BR$. At 4 percent CO₂ and $RQ = 1$, it would be about 7.3 BR.

These rough estimates can be refined somewhat, as TV itself increases with BR. To estimate power from BR alone requires a known relationship between MV and TV. While there is a considerable amount of data at resting metabolism (e.g., from hospital patients), there is little to be found at higher power levels. Mathur (2014) plots BR and TV versus mechanical power, compiling various sources. If a single function is fitted to these plots, an approximate curve fit gives P (not P_M !) $\approx 200 \ln(BR) - 515$, with the units used previously. For what type of person and which conditions this equation is meant to apply and how accurate it could be are not shown, but it works quite well for the 78 kg coauthor for medium power levels,

assuming that the resting metabolic rate (see discussion later in the chapter) is considered. Nicolò, Massaroni, and Passfield (2017) use a different approach and find a linear relationship from “fairly light” work at 65 percent of the subjects’ maximum breathing rate to the maximum “very very hard” work at the maximum breathing rate. To sum up, then, preceding paragraphs have given formulas for P_M , and this one, for (net) working P . Some of these formulas are given for use in the form of spreadsheets in Schmidt 2019.

Alternatively, once calibrated, a given individual’s heart rate (HR) can also provide an approximation of oxygen usage and power. For example, see Perez, Wisniewski, and Kendall 2016–2017, in which $P = 2.5 HR - 200$ approximates the measurements of two men using exercise bicycles, with P in watts and HR is in beats per minute.

If the oxygen usage rate is plotted for an increasing sequence of intensities of a particular exercise (allowing appropriate time for somewhat steady conditions to develop), the curve often shows a relatively sharp “knee” and levels out at an apparent maximum in oxygen uptake for that exercise. Even short, intense efforts can elicit the maximum uptake. This maximum rate of oxygen delivery, $VO_2\text{max}$, was long believed to represent a systemic (heart and lung) limitation on oxygen delivery. Although such a limitation surely does exist, it is more likely that a bicyclist’s $VO_2\text{max}$ actually represents the working muscles’ ability to take in oxygen. Different exercises, for example, have been found to lead to somewhat different values of $VO_2\text{max}$ for the same person.

$VO_2\text{max}$ may relate primarily to heart-stroke volume, which can be increased 10–15 percent with training, and blood hematocrit (red-cell concentration), which can be elevated through artificial means such as altitude training, blood doping, or use of the hormone erythropoietin (EPO). Even intense training cannot increase $VO_2\text{max}$ much, however, in those who are already pretty fit. Tables of normative values available from various sources suggest that the $VO_2\text{max}$ values of the very unfit are about half that of the very fit (at the same age), and that about the same factor applies to the old compared to the young (at the same fitness level), but that very fit old people are a bit better off than very unfit young people.

A focus on $VO_2\text{max}$ dominated exercise studies for a long time. Nowadays some version of the lactate threshold (e.g., OBLA) is seen as the trainable limit. $VO_2\text{max}$ is frequently well above this limit

(and in any event is not very trainable). This new perspective on performance determinants encourages a cautious optimism that employing more large muscles could permit bicycle riders to put out greater long-term power, perhaps even approaching their systemic limit to oxygen delivery. Bicycles with both hand and foot cranking are continually being reinvented to this end. The lack of notable racing-performance success with such bicycles hints at an array of difficult requirements, including a smooth energy-conserving pedaling motion and the ability to pedal and crank hard without disturbing the steering. (This is one arena in which ergometer-based success should clearly precede construction of an on-road prototype!). Although VO_2max does not obviously define maximum steady-state pedaling power, it cannot yet be ignored altogether as a determinant of athletic performance. Certainly ease of breathing has an effect on performance. This is also dependent on the pedaling position and is discussed further later in the chapter.

Energetics in Pedaling

In ideal circumstances, the (extra) energy cost of pedaling could be attributed directly to the work done on the pedals. However, in practice, some muscles (not necessarily in the leg) are used during pedaling in isometric or even in eccentric contraction. Furthermore, using or replenishing the various fuels that feed the muscles in use has various immediate and delayed metabolic costs. We do not know the relative contributions to fuel inefficiency of each such factor.

It is obvious that other, nonpedaling muscles are increasingly engaged at high-force or high-cadence pedaling. When force is high, a bicycle's rider must use these muscles to prevent being lifted from the saddle or slid along the seat. The same is true at high cadence, when the momentum of the descending thigh mass tends to straighten the leg fully and lift the rider from the saddle. But it doesn't seem that muscle use can be the only factor determining muscular fatigue. One of the main conundrums in studies of pedaling is why a lowered seat should so greatly harm performance, since the same work is being asked of the same muscles.

Quite a few muscles actuate the joints of the leg (see figure 2.6). Confusion about the functions of these muscles can be reduced by

first concentrating on the one-joint muscles, namely, those that cross just one joint. It can be seen that each joint has at least one muscle situated to extend it and an opposing muscle situated to flex it. These opposed pairs would not normally cocontract (i.e., exert opposing tensions simultaneously) when the goal is power production, because one would then be performing negative work, which irreversibly absorbs useful energy. (Cocontraction is instead a strategy used to enhance structural stiffness or to resist injury.)

What remains are two-joint muscles such as the *rectus femoris* and the long head of the *biceps femoris*, which exert torque about two joints without touching the intervening bone. The “logic” of these muscles can deviate from the simple logic of one-joint muscles. For example, both muscles just mentioned simultaneously shorten leg extensions such as those in jumping or pedaling. Therefore, in such motions, when these muscles are cocontracted, both perform positive work. (The initially surprising observation of these working muscles seeming to oppose each other is referred to as *Lombard's paradox*.)

Basal Metabolism

The human engine has an additional characteristic not generally found in machines: it can't be switched off, and some fuel must be consumed to keep it going even when it is at rest. (In this sense it is somewhat similar to a traditional steam plant, in which fuel must be burned continuously to keep steam pressure up even when no power is being delivered.) Human energy requirements are conventionally split into basal or resting metabolism and work metabolism.

Basal metabolism is usually expressed as the *basal metabolic rate* (BMR), but what is mostly meant is actually the slightly higher *resting metabolic rate* (RMR) (also called *resting energy expenditure* or REE). BMR involves a more complicated measurement representing really minimal bodily functions without digestion, and RMR represents the energy rate per day for normal living, but without physical activity. Both are usually given in kilocalories per day, or sometimes in kilojoules per hour, or in International System of Units (SI) units as power expressed in watts ($1 \text{ J/s} = 1 \text{ W}$). (Units common in the field require frequent conversions, as all usual time units from seconds to years are in use!) For example, $1,000 \text{ kcal/d}$ ($\sim 41.7 \text{ kcal/h} \sim 175 \text{ kJ/h}$) is $\sim 48.5 \text{ W}$, and 100 W is $\sim 2,065 \text{ kcal/d}$. The

first example would correspond to an old and small person, the latter to a young and large person. Besides those in age and size there are differences due to gender and ambient and body temperatures as well as clothing. Several predictive equations exist and are available in countless online BMR calculators. The best known are the older Harris-Benedict (Harris and Benedict 1918) and newer, similar Mifflin-St. Jeor equations, both of which take gender, age, and body height and weight as inputs, presumably with “normal” temperatures and clothing. The Mifflin-St. Jeor equation gives BMR in kilocalories per day as $(10 \times \text{weight in kilograms}) + (0.0625 \times \text{height in meters}) - (5 \times \text{age in years}) + 5$ (for men) or $- 161$ (for women). Lee and Kim (2012) list and compare these and a few other equations, but none seem to relate to the very important relationships between different temperatures and clothing, which can work in opposite directions: it is obvious that a cooler ambient temperature, lighter clothing, or both will increase metabolism, because more heat is lost from the skin. But a decrease in body core temperature of 1°C can cause a decrease in basal metabolism of 10–13 percent (see Landsberg et al. 2009). Lacking the results of unpleasant experiments, the question can be discussed (see, e.g., Selkov 2015) or the condition of a *thermoneutral environment*, in which a minimal BMR is defined to maintain core body temperature at 37°C , can be assumed.

The Weir formula given earlier in the chapter can also be used if breathing measurements are available. This gives the RMR if the subject is actually resting.

The main relationship is often expressed in terms of body (skin) surface area, for example, 936 (kcal/d)/m^2 ($\sim 45.4 \text{ W/m}^2$) for young adult males, 888 (43.0) for middle-aged males, and 864 (41.9) for adult women (McArdle, Katch, and Katch 1996). Body surface area has been related to height and mass by a number of correlations, for example, the formula from NASA 1969 (given only for men):

$$\text{Body area} = 0.007184 M^{0.425} (100 H)^{0.725},$$

in which body area is measured in square meters, height H in meters, and mass M in kilograms. (Typical body areas for average men are $1.5\text{--}2 \text{ m}^2$.) This leads to the estimate of $1,750 \text{ kcal/d}$ ($\sim 85 \text{ W}$) basal metabolism for a male of height 1.75 m and mass 75 kg , right between the Harris-Benedict and Mifflin-St. Jeor predictions.

Working Metabolism

The main part of the total metabolic rate P_M (described earlier) that is of interest here is that having to do with the mechanical work available for cycling. It can be derived by subtracting from P_M the metabolic rates not involved in productive work—that is, the BMR and thermic effect of food described earlier, and the thermic effect having to do with nonproductive movement that is not related to the cycling activity. What is left over after subtracting these can be called work metabolism or thermic effect of activity.

Work metabolism can be directly estimated as actual kilojoules or kilocalories of mechanical work divided by an efficiency factor, typically between 0.2 and 0.3. Each 100 W of mechanical power production thus requires a 333–500 W (280–430 kcal/h) rate of energy supply in food intake above that needed to maintain life and living. Thus where a normal meal of 500–1,000 kcal (or about 2–4 MJ) might be considered to supply 8 h of sedentary energy needs, an additional such meal is needed for each 1–2 h of cycling effort.

We acknowledge that our focus is mostly on the limits and potentialities of top athletic performances, generally involving people who may have embraced sport because they are naturally constituted for it. Of course, most pedaled distances are actually traveled by average persons at a far easier pace than that pursued in athletic competition and are less strenuous and more efficient.

Energy Cost of Cycling

From chapter 4 onward, this book examines in detail the various resistances affecting cycling and hence the energy cost for traveling a given distance or the power required for a given bicycle and speed. For the moment, taking typical values, two quite different examples are examined, with various different *system boundaries* each:

1. First, a person with a daily commuting distance of, say, 5 km (3 mi) at a speed of 15 km/h (9 mph), thus taking 20 min/d for this. Chapter 4 shows that the propulsive power required is approximately the same as the BMR described earlier, and if an efficiency of 25 percent from food to muscle power is assumed, four times this. Compared to the BMR of a whole day, however, the commute's energy cost is less than 6 percent of this, and because even an office job involves more metabolic power than just the BMR

(say, 20–40 percent extra), the food energy required for the commute is more likely to be 4 to 5 percent of the total amount. Affluent people, who have difficulty keeping their body weight anyway, will consider this small amount of energy “free.” Viewed just by itself, however, the trip costs roughly 400 kJ in food or 80 kJ/km or J/m, or if the BMR just during the trip time is included, roughly 100 J/m. It is low figures like this that give rise to claims of cycling being the most efficient form of transportation.

If the system boundary is widened further, the gray energy needed to produce the bicycle and the energy cost of the time required to earn money to pay for the bicycle could be included. If it is an expensive bicycle and the cyclist has a typical job that itself involves heavy energy use, the total energy cost of cycling is seen to be far from zero, but rather substantial, even if orders of magnitude less than that of owning or using a car.

2. Second, a hard-working professional cyclist, for example, a courier or racer, with, say, 8 h/d at several times the BMR. There is no question of this energy being “free.” If it is assumed that 150 km are covered during working hours at 150 kJ/km, about 23 MJ or 5,400 kcal food energy is required in addition to the food for living. As the latter is roughly three times less, it makes no great difference whether it is included in the energy for work or not. However, it does make a great difference whether the “whole cyclist” is considered part of the work purpose or not. If the former, the cyclist’s whole life, or at least his or her working life, must be included in the energy calculation, which then becomes extremely less efficient. In free societies, such costs are considered external, but somebody still has to pay for them.

Widening the system boundary further, the gray energy of even an expensive bicycle is less important than that of the food consumed. The latter can vary widely depending on what is eaten and how it is produced. Home-grown food can be nearly “free,” but a working cyclist won’t have the time or “energy” for this and will often buy highly processed foods that use up many times their food value to produce and transport. Viewed this way, employing a bicycle courier may not be more energy efficient than employing a courier using a motor vehicle, unless the cyclist both takes it easy and shops carefully for food.

This discussion shows that mainly the choice of system boundary determines whether cycling for a purpose (other than recreation or sport) can be considered energy efficient. It also gives a clue that “relaxed” cycling may be the most efficient overall, or perhaps “hybrid” cycling, as described in later chapters.

Experiments in the Amount of Breathing Oxygen Required

Detailed calculations relating to power as a function of oxygen breathed were presented earlier in the section “Oxygen Uptake and Metabolism.” The lungs of a young, average-weight male, at rest and not using any voluntary muscles, absorb roughly 5 mL/s (0.3 L/min) of oxygen, which corresponds to about 100 W thermal power. This quantity is in addition to any other absorption required by exercise. At the upper limits of steady-state aerobic athletic performance, more than 80 mL/s may be absorbed.

In ordinary air, 1 L of oxygen is found in about 4.8 L of air. However, about 24 L of air must be passed through the lungs for each liter of oxygen absorbed (see earlier calculation and Knipping and Moncrieff 1932). Thus, the human engine requires about 400 percent “excess” air. Most other engines, such as internal-combustion and steam engines, require only 5–10 percent excess air to ensure complete combustion of the fuel they consume. Gas turbines more nearly approach human lungs, taking in about 200 percent excess air. It should be stressed at this point that human metabolism does *not* operate like the described machines, which are heat engines and work by physically heating a material, which produces a force and an expansion. For the heat to flow through the machine, one part must be cooled to a lower temperature. Thermodynamics teaches us that the work capacity is tied to the available elevated temperature relative to that of the heat sink, often the environment, at a lower temperature. The fraction of the supplied energy transformed to work is limited by the second law of thermodynamics to $(T_2 - T_1)/T_2$ when temperature (T) is measured on the absolute scale. Therefore if the human body were a heat engine with $T_2 = 37^\circ\text{C} \approx 310\text{ K}$ and $T_1 = 20^\circ\text{C} \approx 293\text{ K}$, its maximal efficiency would be 5.5 percent. Because the body’s maximal efficiency is actually about 25 percent, which as a heat engine would require an upper temperature as high as boiling water, it is clear that it produces work in a different way, such as in a fuel cell, in which chemical energy can be converted

directly at a near-ambient temperature level. However, in both heat engines and fuel cells, energy not converted to power must appear as heat and be removed. (All animals, including humans, also excrete wastes that have some calorific heating value that should be included in a complete calculation.)

Figure 2.10 shows the relationship between oxygen absorbed and mechanical power delivered to the pedals for five volunteers piloting the human-powered aircraft Daedalus. Both the oxygen uptake and the power are given per kilogram of body mass, because of the importance of the power-to-mass ratio. For this series of tests a woman (other data for whom are given in figure 2.9) produced the best power-to-weight ratio, with “power” defined as 70 percent of the person’s maximal aerobic power, an output most endurance athletes can sustain for hours (some can achieve 80 percent). The final choices for volunteers were made among bicycling champions, who were taught piloting, which turned out to be easier than picking pilots and trying to make them into outstanding endurance athletes. The variation in oxygen uptake among the five individuals in good condition was not large.

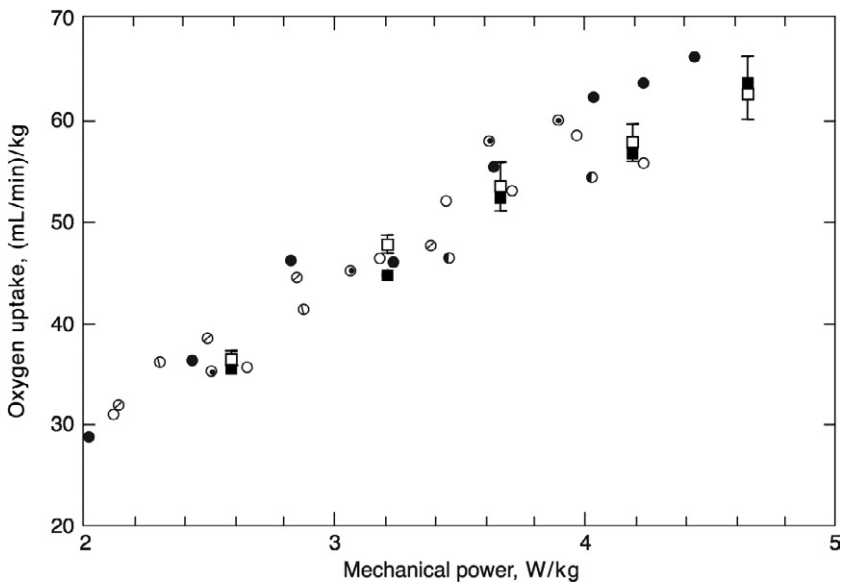


Figure 2.10

Measured oxygen uptake versus power delivered for five pilots (dots), and typical tests comparing power output by conventional (black squares) and semirecumbent (white squares) pedaling. (From Bussolari 1986–1987 and Bussolari and Nadel 1989.)

Although not a strict determinant of physical work capacity, maximal oxygen uptake is commonly used as a rough indicator of potential and a useful normalizing quantity. Most people should be able to work easily at one-third of maximal uptake, but exceeding two-thirds of maximal uptake for a long duration may require considerable training. For a nonathletic, not-young person, the maximum oxygen-absorption rate (i.e., VO_2max) is assumed to be about 50 mL/s or 3 L/min (approximately 60 percent that of an elite competitor; see, e.g., Daley 2018). When such a person, riding a bicycle, is using a third of this oxygen-breathing capacity, the power output is about 75 W (~ 0.1 hp). An average fit man or woman could work under these conditions for several hours without suffering fatigue to an extent that precludes reasonably rapid recovery. A power output of this kind propels a rider at approximately 5.5 m/s (20 km/h, 12.3 mph) on a lightweight touring bicycle on level ground. Figure 2.11 collects miscellaneous data on caloric expenditure of bicyclists given by Adams (1967), Harrison (1970), and others.

Breathing ability decreases with age. An athlete's peak breathing capacity comes at about age twenty, and as a rule of thumb, breathing capacity is halved by age eighty. Results of the 1971 UK 50 mi amateur time trials, in which the ages of the best "all-rounders" and of the "veterans" were given, are consistent with a breathing-based theory of performance. Panel (a) of figure 2.8 plots the average speed for each rider against the rider's age. As the figure shows, there is no recognizable falloff in performance up to age forty, after which there is a steady drop to that for the oldest competitor, aged seventy-seven. In panel (b) of the figure, these performances have been converted to breathing capacity, estimated using Whitt's (1971) method. When the curve is extrapolated to eighty years, the estimated breathing capacity is indeed very close to half the peak value. However, such reductions in performance with age could have a different explanation altogether: in today's society, even an athlete may be sedentary 85 percent of the time. Maybe the falloff shown in figure 2.8 occurs particularly when a person takes a sedentary job.

Up to a breathing rate of about 0.67 L/s (40 L/min), people tend to breathe through the nose if they have healthy nasal passages. Nasal passages usually open during exercise, even when someone has a heavy cold. Above this rate, the resistance to flow offered by

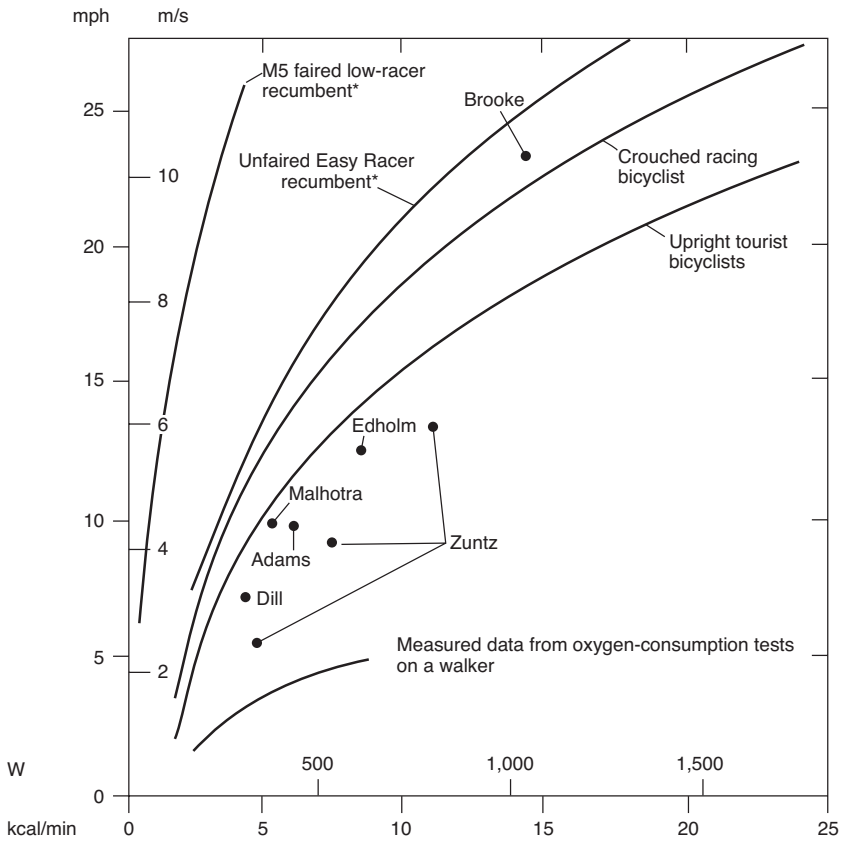


Figure 2.11

Bicyclists' gross caloric expenditure (metabolic power P_M). The measurements (dots, and curve for walker) presumably represent *total* P_M (including resting metabolic rate, or RMR) and the curves (from Whitt 1971) *net* P_M (excluding RMR), with an efficiency of 25 percent assumed.

even a healthy nose becomes penalizing, and mouth breathing is substituted. A normally healthy individual riding on the level in still air on a lightweight bicycle reaches this limiting rate for nasal breathing at about 14 mph (6.3 m/s).

Pedaling Forces

Up to this point the chapter has been concerned with the production of mechanical human power, but it has not yet described how

this power is actually transmitted to a wheel (propeller, etc.). Even if the mechanical transmissions are lossless, measurements show that more muscular power is involved than is actually available for propulsion, because the limbs' movements cannot at all times transmit their forces in an optimal manner. The following sections describe efforts to match optimally the kinetics of the human body to those of a bicycle or vehicle.

Average Thrust

A steadily riding racing bicyclist tends to use very consistent but moderate pedal thrusts, amounting to mean applied tangential forces of only about one-third to one-sixth of the rider's weight. The rider's peak vertical thrusts are greater (approximately 1.5 times the mean) but still relatively small. No doubt this type of movement enables the rider to maintain a steady seat position and steer steadily.

It is easy to calculate from a bicycle crank length and a given pedaling speed the average value of pedal thrust required to achieve a given power output on that bicycle. The peripheral pedal speed around the pedaling circle can be used in the equation *Average pedal propulsive force* (N) = *power* (W)/*foot speed* (m/s), which presumes that only one foot is pushing at a time. *Foot speed* is determined as revolutions per second times the circumference of the pedal circle (typically 1.07 m). (To convert from newtons to pounds force, divide by 4.45.)

Detailed Pedal-Force Data

Hull and his colleagues (Newmiller, Hull, and Zajac 1988; Rowe, Hull, and Wang 1998) have taken precise pedal-force measurements to a high art. To permit such measurements, specially designed pedals are instrumented with strain gauges and calibrated to measure force components in up to three directions and possibly also twisting moments tending to bend the pedal spindle. Angle sensors are used to determine the orientation of each pedal relative to the crank and of the crank relative to the bicycle. A computer logs all data, typically hundreds of times per second. Coyle et al. (1991) offer some pedal-force diagrams, and figure 2.12 shows one provided by Radlabor-Smartfit. Panel (a) shows total force vectors and demonstrates that much of the force does not contribute to propulsion,

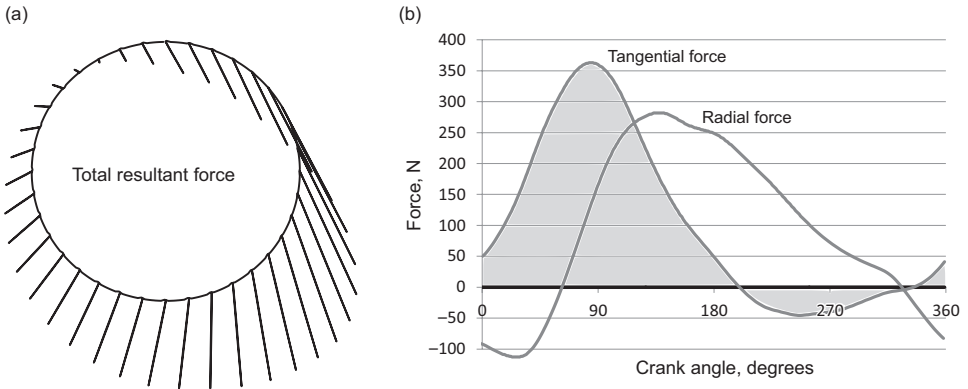


Figure 2.12

(a) Typical pedal-force pattern showing magnitude and direction of the total force of one foot on one pedal. (b) A different example with the force resolved into (noncontributing) radial and (effective) tangential components. (Adapted from Smartfit.bike diagrams of measured data, courtesy of Radlabor.de.)

mainly the radial components on the bottom half of the pedaling circle, shown in panel (b) graphed as a function of the crank angle. This isn't as bad as it looks, as legs are accustomed to providing large nonproductive forces at low energy cost, as when standing and walking. The tangential force provides power, represented by the shaded area in panel (b), in this case 340 W at a cadence of 96 rpm, for a rider using drop handlebars. This figure includes the small amount of negative power between crank angles of about 190° and 350°. If the latter is subtracted instead of added, the effective power reduces to about 275 W.

Because of such pedal- and crank-orientation issues, pedal force is not the simplest way to measure pedaling power; sprocket torque or chain tension is easier, or dedicated devices. Pedal-force diagrams are mainly used for analysis, custom bike fitting, and rehabilitation. Measuring pedals like the Smartfit Pedalforce are meant for laboratory ergometers and are particularly fast, allowing athletes or patients to view their pedaling patterns as they pedal and improve them with a kind of biofeedback. Fonda (2015) gives an account how such methods can improve pedaling. Predictive or simulation software such as the online pedaling model of AnalyticCycling.com can also generate pedal-force diagrams; the latter model, however, does not include the inertial effects of the moving limbs.

Some care is required for proper interpretation of such results. In principle, if someone not exerting any muscle forces (apart from keeping the ankles from flopping) is strapped onto a bicycle, for each stationary orientation of the cranks, the feet will apply some force to the pedals, primarily because of the weight of the thighs and the elasticity of the uncontracted muscles. The effect of muscle elasticity can be demonstrated by sitting relaxed on a bicycle with no chain. Trunk inclination affects the at-rest crank orientation. The direction of the net force is roughly along the line from knee to pedal. If a motor then drives the cranks (while the passive person is properly strapped to the saddle), additional pedal forces will be observed, mostly relating to the acceleration and deceleration of the thighs, acting in roughly the same directions. These dynamic foot forces can become very great as pedaling cadence is increased.

If these purely mechanical, non-power-producing forces are subtracted from the actual measured forces of a pedaling person, what remains are the muscular forces, which alone create propulsive power. The mechanical forces almost totally obscure the muscular forces at the top and bottom dead centers of the pedaling motion and also on the upstroke. (In steady-state power production, a person's slight tendency to lift while pedaling doesn't usually overcome the weight of the leg.)

Once the partially obscured nature of the pedaling forces is appreciated, one might ask about optimal magnitudes and directions for pushing around the pedaling cycle. With the many different muscles in the leg, each with its own size, fiber makeup, and state of fatigue, such optimalities may never be specified in general. However, there is a very important observation to be made: it is widely supposed that muscular force in pedaling should ideally be oriented along the pedal path (i.e., perpendicular to the crank); otherwise some amount of force will be "wasted." (In fact, the most common suggestion is that the total measured force should be kept tangent to the pedal path.) This supposition is generally invalid: the example of a piston engine shows that there is nothing inefficient about exerting a force along the connecting rod. As a general rule, better performance (power, efficiency, endurance) can be expected if the muscular force applied to the pedal is permitted to deviate somewhat in direction from tangency to the pedal path. In fact, Papadopoulos (1987), assuming only certain sets of muscles to

be active, shows that constraining the force direction leads to the performance of negative work by some muscles and the irreversible absorption of mechanical energy. Zommers (2000) researches ankling, that is, moving the ankle joint in addition to the knee and hip, and finds the efficiency to be lower than with “normal” pedaling.

Constrained motions (e.g., a fixed-length crank forcing the pedal to move in a circle) allow existing muscles to furnish their maximum power. *Unconstrained* motions (e.g., a crank that freely telescopes), however, require the pedaler to exert a total foot force exactly perpendicular to the crank (i.e., constrained *force*) and should severely reduce the rider’s power, although as a training aid, they may encourage certain underused muscles to develop greater strength. An upright-seated pedaler can turn the pedal cranks via any of a variety of distinct pedaling styles. Some styles involve strong tangential forces when the pedals are at their upper and lower extremes, or in contrast a “thrusting” style with brief high forces during the downstroke, or perhaps an unusual degree of lifting force (or leg-weight reduction) on the upstroke. Others involve additional phased pedal thrusts to counterbalance high-cadence bouncing at the saddle or control of foot-force direction to avoid slippage when there is nothing holding the foot to the pedal. Side force at the saddle, the handlebars, or both or a rotational couple of forces at the handlebars may result from high pedaling torque. Upper-body bobbing or fore-aft sliding are not unusual at high effort levels. Many other techniques or styles may be recognized, only some of which are for extreme (high-torque or high-cadence) situations.

As an example, consider stand-up pedaling. If all the cyclist’s body weight during stand-up pedaling is applied to each pedal in turn, then crank torque is a simple rectified (i.e., positive-only) sinusoidal function with a fixed amplitude. Even if the rider’s arms share in the work by tipping the bicycle (a good example of a nonmechanism way to add arm work), power is strictly related to the body weight times the speed of the descending pedal. How can one change the stand-up pedaling torque so as to adjust pedaling speed? To increase pedaling speed, one could obviously also pull up on the rising pedal and increase crank torque to any level. But pedaling more slowly is normally not possible without changing gears, pausing at each dead center, or applying negative work with the rising leg.

Effects of Body Position, Pedaling Motion, and Rate

Up to this point, the chapter has been concerned with the overall physiology of muscles and exercise and some general background on pedaling. It now takes up a variety of questions related to the specifics of pedaling. There is almost no theory to guide the discussion in this area, so the main thrust is to report on efforts to devise improved pedaling mechanisms. The mechanisms themselves are mainly described in chapter 9, but a start is made here with those that are thought to have specific physiological rather than only technical advantages (or disadvantages).

Pedaling and Rowing Motions

Harrison (1970) developed his curve for short-duration pedaling or cycling (curve 1 in figure 2.13) based on measurements taken

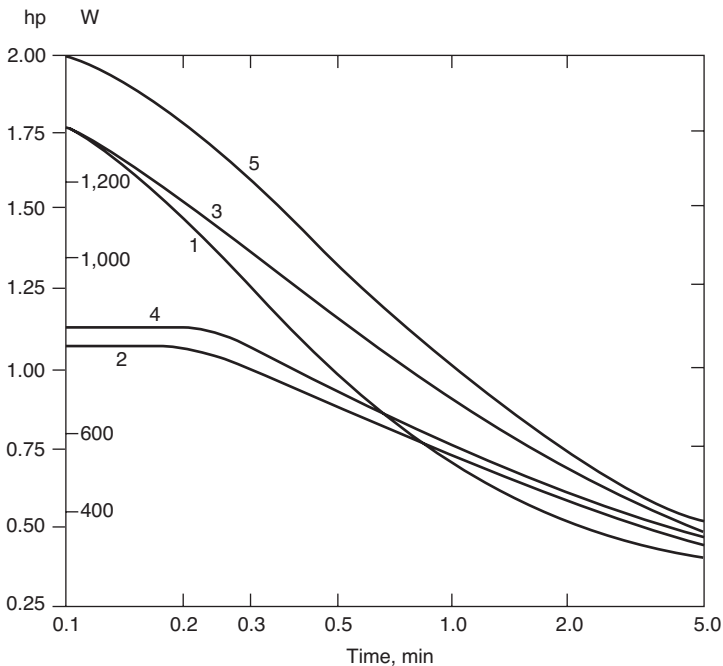


Figure 2.13

Peak human power output from various motions: cycling (curve 1), free (curve 2) and forced (curve 3) rowing with fixed feet, and free (curve 4) and forced (curve 5) rowing with seat fixed. (From Harrison 1970.)

from a group of active men, not record athletes. The significance of his results lies, therefore, in measurements of the relative power produced by the same individuals using different motions and mechanisms. Harrison's findings seem to be particularly significant because his subjects produced, in some cases, more power through motions to which they were unaccustomed than through bicycle pedaling, with which they were all familiar. The curves for linear ("rowing") foot and hand motion (curves 2 and 4) lie considerably below the cycling curve for short time durations but rise above it after 1 min.

Measurements taken on a rowing ergometer have an additional reason for showing a diminished power output: if the subject's feet are fixed with respect to the ground, as they are normally fixed with respect to the boat when one is rowing, there are large energy variations from the rower's accelerating and decelerating his body from rest positions at the ends of the stroke, something that occurs to only a minor extent in actual rowing (in which the light boat, rather than the heavy rower, does the accelerating and decelerating). It is actually possible for the rower to convert backward-moving kinetic energy to propulsive work, as long as the arms rather than the leg or trunk muscles are used to come to rest. However, to decelerate a boat's forward motion probably requires some negative work (in addition to elastic energy storage) in the leg and trunk muscles, particularly at high stroke rates. It is an interesting open question when such additional (but uncounted) power production, by a different set of muscles, is likely to reduce the desired power output. The simplest expectation is for fixed-power rowing endurance to be less when the feet are fixed to the stationary frame (curve 2) than when the seat is fixed and the feet are allowed to move (curve 4), as Harrison found.

Of great interest are Harrison's results for what he called "forced" rowing. He set up a mechanism that defined—that is, constrained—the ends of the rower's stroke and conserved the moving masses' kinetic energy, either with the feet fixed (curve 3) or the seat fixed (curve 5). A car engine's piston-crank-flywheel mechanism is of this type. With forced rowing and the seat fixed, considerably longer durations of power than with normal pedaling are obtained at all power levels. This apparently significant finding has not, to the authors' knowledge, been used to break any human-powered-vehicle

record. Indeed the known records carried out with a rowing bike (see rowingbike.com/en/records/) have used an unconstrained rowing mechanism.

Pedaling and Hand Cranking

The question frequently arises as to whether one can add hand cranking to pedaling and obtain a total power output equal to the sum of what one would produce using each mode independently, or at least somewhat more than by pedaling alone. Kyle, Caizzo, and Palombo (1978) show that for periods of up to 1 min, hand and foot cranking can generate 11–18 percent more power than foot cranking alone. The power produced is greater when the arms and legs are cranking out of phase than when each arm moves together with the leg on the same side. In later work, Powell and Robinson (1987), in tests of seventeen males and fifteen females, find that power production in a ramp test can be increased by more than 30 percent over pedaling alone when arm cranking is combined with pedaling. VO_2 max is higher for the combined arm-and-leg power than for leg power alone, supporting the statements made previously about the use of this measure. The chapter stated earlier that about half the advantage of combined arm-and-leg power over leg power alone is due to aerobic metabolism and half to anaerobic metabolism. Powell (1994) finds that in cranking at 50 W and 60 rpm, shorter cranks (100–125 mm) are less efficient than longer ones (125–165 mm). He also finds no significant difference between in-phase (parallel) cranking and out-of-phase cranking (like foot pedals), although they differ with respect to stability (torque in roll) and body restraints.

With hand cranking alone, power levels as shown in figure 2.14, in which general male athletes achieve 550–850 W with about four crank revolutions per second, male canoeists 1,000 W, and female canoeists 550 W, cranking slightly slower, are achievable. Neville, Pain and Folland (2009) conducted arm-cranking measurements on elite sailors, who must “grind” sail winches as quickly as possible. They found peaks of 1,400 W for 7 s at 120 rpm and 330 W for 3 min at 80 rpm, while the sailors were standing with the crank axis at about half the stature height. The crank length used was 0.25 m and the distance between the handles 0.44 m.

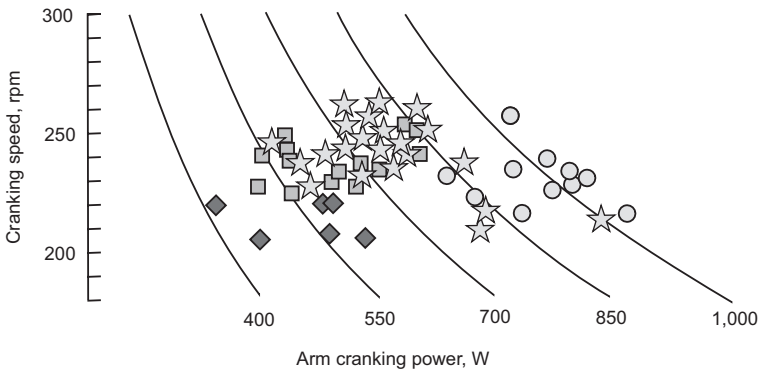


Figure 2.14

Parameters of the individual power-speed relationships (torque not shown) on a cranked ergometer with different types of sportsmen and sportswomen: male boxers (stars), male tennis players (squares), and female (diamonds) and male (circles) Olympic canoeists and kayakists. (Adapted from Driss and Vandewalle 2013, licensed CC-BY-SA 3.0.)

Upright and Recumbent Pedaling

Riders of recumbent bicycles sometimes claim advantages over standard positioning not only because of lower aerodynamic drag, but also because of freer breathing, as the bend in the recumbent position is less than that of the crouch imposed by a standard upright racing position. (This might not apply to *semirecumbent* positions corresponding to crouched positions but rotated 90°.) Specialist triathlon bicycles move the rider's body forward slightly in relation to the pedals, which reduces this bend.

Early measurements showed an apparent small reduction in power when a bicyclist switches from a conventional pedaling position to a recumbent one or no difference. Antonson (1987) studies the oxygen efficiency of recumbent and conventional bicycling positions at less than maximum workloads in thirty men: ten recumbent cyclists, ten cyclists used to conventional machines, and ten physically active noncyclists. Each is asked to pedal for 6 min at 52 W, followed by 6 min at 155 W, for each of the two positions, while being measured for oxygen consumption, ventilation, and heart rate. Antonson finds no significant differences in oxygen consumption or ventilation among the three groups, though the noncyclists are found to have a higher heart rate than those in the other

two groups. She finds no indication that either group of bicyclists benefits from being accustomed to one position or the other. Busso-lari and Nadel (1989) test twenty-four male and two female athletes in the two positions and find no significant difference in oxygen efficiency (figure 2.10). Egaña, Columb, and O'Donnell (2013) compare upright, various semirecumbent, and supine positions at high intensities and find little difference between the first two but less endurance in the supine position.

There are two pitfalls in particular to be avoided in such a comparison. One is in the definitions. The word *recumbent* is sometimes taken to mean supine, "flat on one's back," but more often to mean sitting as one does driving a car, a style more accurately referred to as *semirecumbent*. One would expect to produce a lower amount of power when on one's back. The *upright* posture can be taken as that used on an all-terrain bicycle or "sit-up" bike. One might expect a reduction in maximum aerobic power for the crouched racing position because of the restriction in breathing the position imposes, as has been speculated elsewhere. The other pitfall involves the question of accustomization, which is always difficult when a "new" position is being tested. It might take months of practice before one's muscles are adapted to a new position, yet in tests one is usually allowed only minutes to accustom oneself to a shift in position.

Backward Pedaling

The concept of pedaling backward instead of forward seems unnatural. However, Spinnetti (1987) experiments with low-power backward pedaling, then carries out careful measurements that show he can produce higher levels of short-duration maximum power pedaling backward (215 W) than forward (179 W) (figure 2.15). One should not draw conclusions on the basis of one series of tests on one person, but the power differential Spinnetti finds is intriguing. In the case of recumbents with a high bottom bracket (requiring "uphill" pedaling), the authors have found backward pedaling to be more pleasant, as the "power stroke" is angled downward more.

The next topic is a similarly unusual pedaling system that seems to allow increased power to be produced through involvement of more muscle groups.

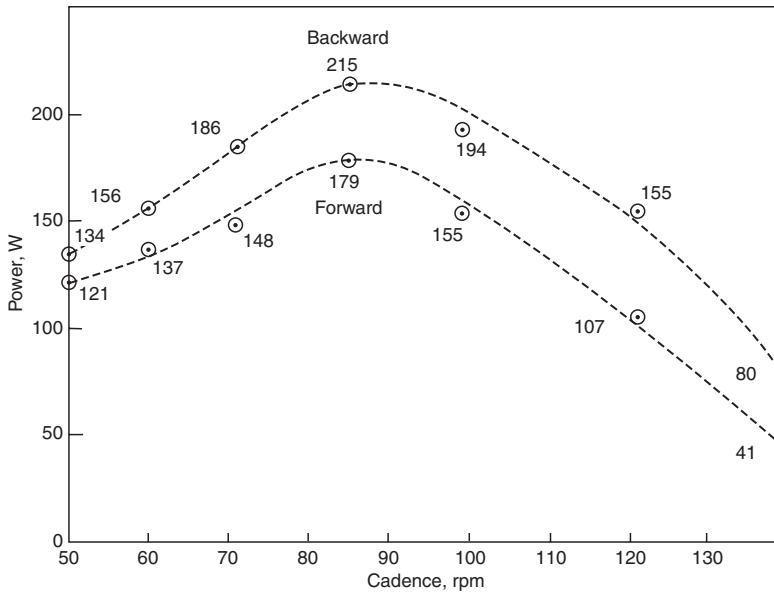


Figure 2.15

Maximum power produced versus revolutions per minute in forward and backward pedaling. (From Spinnetti 1987.)

PowerCranks and Active Involvement of the Lifting Muscles

One clever approach to involving additional major muscles in pedaling is that given by Frank Day's PowerCranks, which are built with one-way clutches so that each leg has to lift itself (helped neither by the counterbalancing weight nor by the down push of the other leg). Used only in training, they force some large muscles to develop that most people are content to leave uninvolved. PowerCrank.com claims an increase in power and hence cycling speed after some weeks of training; users and quite a few easily found studies support this assertion. Luttrell and Potteiger (2003) find in comparative tests that a PowerCranks group has significantly higher gross-efficiency values than a normal-crank group (e.g., 23.6 ± 1.3 percent versus 21.3 ± 1.7 percent), as well as significantly lower heart rates and VO_2 values. However, Burns (2008) finds no significant improvements for a PowerCranks group and less efficiency and economy compared to cycling with normal cranks.

It seems logical that training new muscles increases power and not surprising that efficiency in actual use doesn't increase or even

decreases. In contrast to the human arms, the human legs are “engineered” mainly for pushing and less for pulling.

Effect of Saddle Height

Using a single subject (a thirty-nine-year-old man, obviously not very athletic), Müller (1937) obtains the results shown in figure 2.16. For durations less than 0.5 h, he finds that the subject achieves at least one and a half times greater endurance at each power level when the saddle is raised 40–50 mm above the “normal” height, that for which the heel can just reach the pedal with the leg stretched and the posture upright. Equivalently, he can tolerate about 7 percent more power for each session. No less important, perhaps, is the dramatic 15–30 percent reduction in power, or 80 percent reduction in endurance, when the saddle is set 100 mm lower than normal.

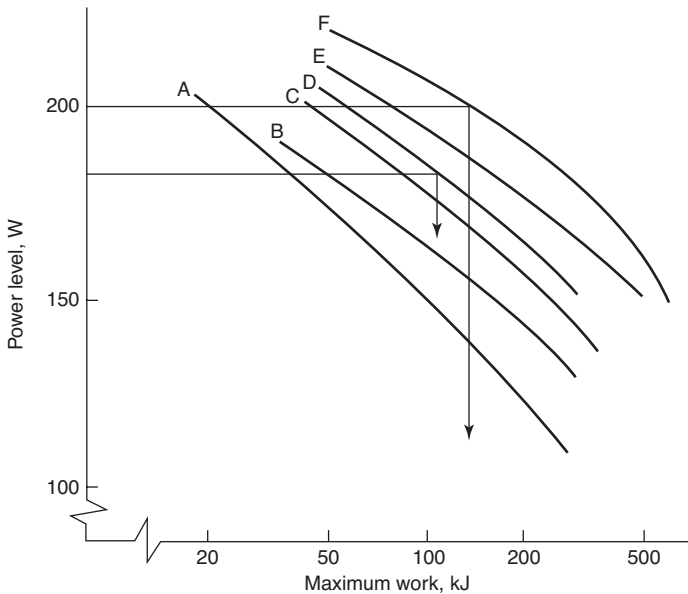


Figure 2.16

Effects on maximum work of saddle height and angle of seat tube from perpendicular: 100 mm below normal, 21° from perpendicular (curve A); 30 mm above normal, 8° from perpendicular (curve B); 40 mm below normal, 21° from perpendicular (curve C); 30 mm above normal, 43° from perpendicular (curve D); normal height, 21° from perpendicular (curve E); 30 mm above, 21° and 29° from perpendicular (curve F). (From Müller 1937.)

Similar research with more subjects by Hamley and Thomas (1967) shows maximal anaerobic power with the saddle height to the pedal spindle set, at its lowest position, at 109 percent, and AnalyticCycling.com's online model (using specified thigh, shin, and crank lengths and a fixed foot) shows a similar tendency, as well as that the maximum is a peaky one, with a sharp drop if the saddle height is increased further.

Peveler (2008) carries out measurements with groups of cyclists and noncyclists, comparing the 109 percent inseam recommendation with later ones specifying minimal knee angles between 25° and 35° (measured from a straight leg). He finds a poor correlation between these recommendations because of variations in limb proportions and a slight but significant efficiency maximum at the 25° knee angle, especially at aerobic power levels, as well as a mean personal preference of about 27° within the cyclist group.

With recumbent bicycles, seat height of course has different implications, and the main parameter to adjust is the more or less horizontal distance between the seat rest and the bottom bracket. Too and Landwer (2008) investigate this and other parameters.

Effect of Crank Length

The length of the cranks in conventional bicycles is fixed within narrow limits. With the saddle at the normal height above the pedals, as defined by Müller (1937), and with the pedals at a distance above the ground such that in moderate turns (when the bicycle will be inclined toward the center of the turn), the pedals do not contact the ground, and the saddle is then at a height at which the rider can just put the ball of one foot on the ground when stopped while still sitting on the saddle. The crank length is then chosen so that almost all riders will feel comfortable. This length is normally, for adult riders, taken as 165 mm (6.5 in) or 170 mm (6.7 in). Thus, the height above the ground of the bottom-bracket axle is fixed. An attempt to fit longer cranks will lead to a reduction in pedal clearance when cornering. (In a similar vein, it should be noted that the rider's need to fit the maximum wheel radius between his or her legs, in order to travel more distance with each pedal stroke, also drove the crank length for high-wheel bicycles downward.)

Few riders, then, have an opportunity to try long cranks, because each crank length strictly requires a frame specially designed for

that length. In this respect, bicycles with higher bottom brackets (those designed for off-road use, and even more so, recumbent bicycles), have an advantage. Most data on the effects of crank length are based on tests that have been taken on ergometers. But ergometer data can be regarded with suspicion, as has been implied, and this has certainly been true with regard to data on long cranks. So few people have been able to experiment with significantly longer cranks on actual bicycles that their impressions must also be treated with reserve.

The older literature describes several tests of different crank lengths and generally finds no advantage of particular lengths at normal pedaling speeds, a disadvantage of long cranks at high pedaling speeds, and an advantage of these in low-speed, high-torque pedaling. This is hardly surprising, but it is difficult to separate the effect of the crank length per se and the automatic effective “change of gear.” It is also not surprising that longer cranks are recommended especially for larger people. Nettally.com/palmk/crankset.html recommends cranks to be 0.216 times the inseam length and discusses this recommendation at length.

Müller and Grosse-Lordemann (1936) test the effect of crank lengths on an ergometer, employing only one subject. Their approach is to use three crank lengths—140, 180, and 220 mm—set the power output the subject must produce, and measure the maximum duration for which this output can be sustained. For all power levels, the subject is able to produce the most total work (that is, work for the longest periods) when using the longest cranks. At the highest power levels, the subject’s body efficiency (work output divided by energy input in food) is also highest when the longest cranks are used.

Harrison (1970) gives his five subjects, none of whom is particularly tall, an initial choice of crank length and finds that they prefer the longer cranks (177 and 203 mm; 7 and 8 in). Harrison intended to perform all of his tests at two different crank lengths; however, he finds from initial tests that “crank length played a relatively unimportant role in determining maximum power output” and uses just one (unspecified) length for most of his tests.

More recent data mostly confirm these earlier findings. Too (1998–1999) measures the anaerobic power outputs of six male subjects, aged twenty-four to thirty-five, employing the Wingate protocol (see the section earlier in the chapter on this), in conventional and

recumbent positions, using cranks from 110 to 265 mm in length. Too obtains the highest average power readings for 180 mm cranks for both positions. This crank length also yields the highest peak power for the conventional position, whereas the shortest cranks, 110 mm, allow the recumbent bicyclist to produce the highest peak power. For all crank lengths, peak and average power are higher in the recumbent position. This result seems at variance with earlier data quoted previously. Figure 2.17 summarizes the recumbent data (Too and Williams 2000). A newer study (Too and Williams 2017–2018) with upright cyclists produces a formula that suggests optimal crank lengths at peak power are shorter than normal.

In summary, as well as being impractical to increase on a conventional bicycle (no manufacturer currently seems to be making cranks whose lengths can be varied during use), crank length is apparently not of major importance in the quest for producing maximum power, although shorter-than-normal cranks appear indicated for high cadences and longer-than-normal ones for low cadences. However, for racers, even factors of seemingly minor importance can produce a win. To choose the optimum among all the factors involved is too detailed a topic for this book; a study

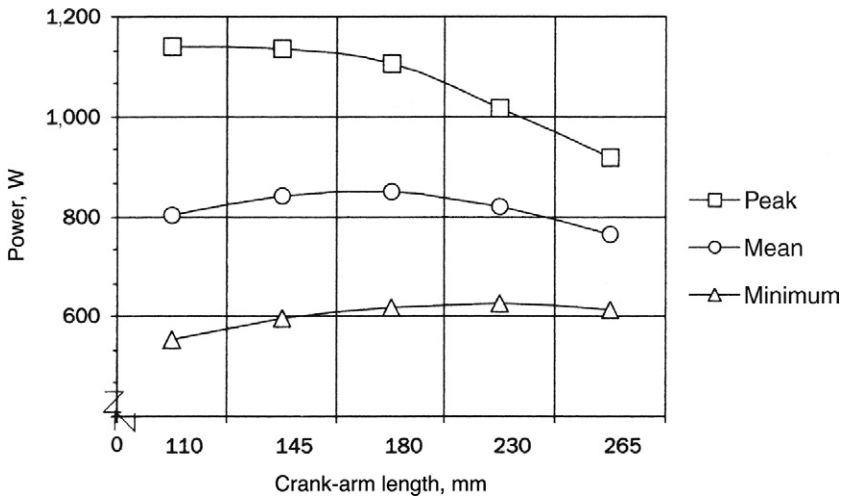


Figure 2.17

Peak, mean, and minimum power in recumbent pedaling as functions of crank length. (From Too and Williams 2000.)

of the references quoted and of others, existing and, undoubtedly, coming, is recommended.

Nonround Chainwheels

Elliptical chainwheels can be fitted to normal cranks, in which case the pedal motion remains circular, but of varying speed or gearing ratio. The usual purpose of elliptical chainwheels is to reduce the supposedly useless time during which the pedals are near the top and bottom dead centers. This orientation with the smallest size occurring at the dead centers is referred to as the “normal” one in this section. As a topic, they have some similarity to long cranks, in that there are fierce proponents and antagonists and little reliable data. Four of Harrison’s (1970) five subjects produce virtually identical output curves (power versus duration) using circular and elliptical chainwheels. One, apparently Harrison himself, produces about 12.5 percent more power with the elliptical chainwheel. All prefer the elliptical chainwheel for low-speed, high-torque pedaling. Harrison does not specify the degree of ovality of the chainwheel used but does state that the foot accelerations required are high. One of Harrison’s illustrations shows a chainwheel with a very high degree of ovality (about 1.45).

An elliptical chainwheel’s degree of ovality can be specified using the ratio of the major to the minor diameter of the underlying ellipse. In the 1890s, racing riders using elliptical chainwheels with ovalities of about 1.3 became disillusioned with their performances, and these chainwheels fell out of favor. In the 1930s the Thétic chainwheel, with an ovality ratio of 1.1, became quite popular. No deterioration of performance compared with that on a round chainwheel was recorded, and a small proportion of riders improved their performances by a few percent. According to a personal correspondence between Frank Whitt and the senior author in 1973, experiments with chainwheels having ovalities up to 1.6 have confirmed that high ovality (perhaps 1.2 or greater) decreases performance.

In the 1980s Shimano introduced a chainwheel, Biopace, that though nonround was not elliptical. The scientific background is given by Okajima (1983), who enables his group to determine the leg-joint torques for normal circular-chainwheel pedaling. Okajima points out that the knee has a period of strongly negative torque:

We saw two specific restrictions to be solved:

1. the difficulty of spinning, both in the motion and in the direction the force must be applied, restricts the speed of muscle contraction during pedaling to a rather slow rate, and requires the force to be on the high side, and
2. the knee joint is overused, while the hip joint is underused (the ankle is rather passive).

We decided that an appropriately uneven angular velocity pattern would reduce the loss of kinetic energy, and also make it easier for the rider to switch between the firing of different muscle groups at appropriate times (to be specific, at the reversal of knee torque).

Figure 2.18 shows the shapes of three chainwheels resulting from the Shimano study (used together in a triple chainwheel). As the figure shows, the eccentricity is not very pronounced and is turned in other direction from that of the elliptical chainwheels described earlier.

Various internet authors suggest a definitive advantage using Biopace chainwheels; others suspect marketing hype. Hansen et al. (2009) carry out comparative physiological tests on Biopace and circular chainwheels and record slightly lower lactate values with the Biopace. Van de Kraats (2018), in an extensive section on oval chainwheels, calls the Biopace “the maximal wrong choice” and

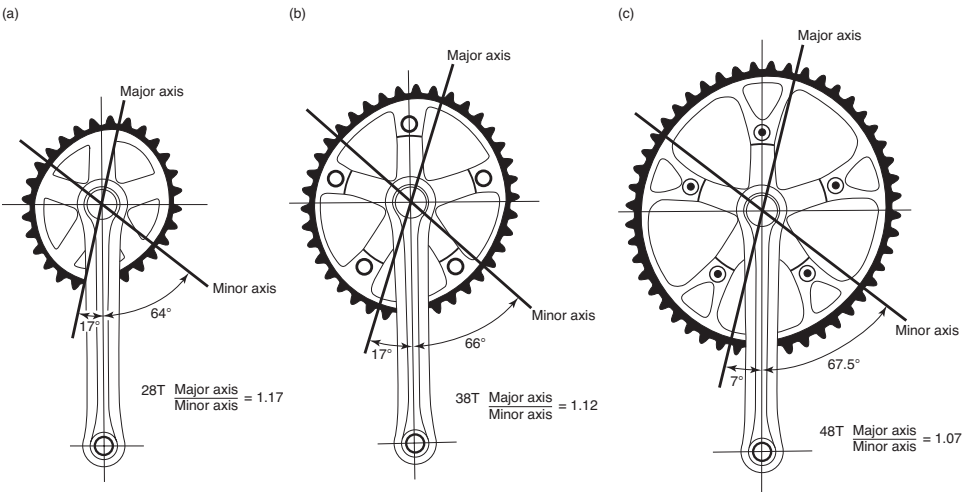


Figure 2.18 Biopace chainwheels with (a) 28, (b) 38, and (c) 48 teeth. (From Okajima 1983.)

lists recent arguments for the superiority of asymmetrical chainwheels with normal orientations and ovalities of about 1.1 and 1.2, including wins and records with the Osymetric chainwheel (1.2) (see figure 2.19) and the elliptical Q-ring (1.1). Van de Kraats describes (and links to) many further studies and models twelve chainwheels in an online simulator. A theoretical study by Rankin and Neptune (2008) suggests a 3 percent increase in power against circular from using normal elliptical chainwheels with eccentricities of 1.35, 1.3, and 1.25 at cadences of 60, 90 and 120 rpm, and at average powers of about 850–1,050 W.

A more versatile mechanism giving the same effect as a non-round sprocket was the Brown SelectoCam, also sold as the Stronglight Power-Cam (later Houdaille). In this mechanism, a bell-crank riding around a fixed central cam advanced and retarded the round chainring relative to the crank, twice each revolution, without the manufacturing om and chain-shifting disadvantages of a variable sprocket radius (see US Patent 4,281,845 [1981]).



Figure 2.19

A crankset with nonround Osymetric chainrings and 54 teeth. (Photo by Sam Sailor, licensed CC-BY-SA 4.0.)

Lever or Linear Drives

Many people have invented and reinvented forms of the linear drive, in which each foot pushes on (for instance) a swinging lever, with a strap or cable attached to the lever at a point along it that can be varied to give different gearing ratios. The cable is in turn attached, perhaps through a length of chain, to a freewheel on the back wheel and to a return spring (figure 2.20). The American Star high-wheeler (figure 1.16) had this type of drive, although its gear was not variable. Pryor Dodge has been gracious enough to allow us to reproduce the jacket photograph of his 1996 book *The Bicycle* (figure 2.21) showing a superb example of a swinging-lever drive. The drive’s manufacturer, Terrot, claimed at the time (the early 1900s) that the alternating levers avoided the dead point common with cranks and thus allowed for easier hill climbing. The coauthor’s experience with the Thuner Trampelwurm road train (see chapter 10) confirms this. This road train has various types of pedal drives, including unconstrained swinging “rowing” levers that are especially useful when strenuously climbing or accelerating from rest, because they can always be operated at a chosen phase and amplitude where maximum force is available. However, although there are no dead centers, there are jerky reversals of direction, and these drives thus are not very pleasant or efficient for normal (level) riding.

The overwhelming disadvantage of such swinging-lever drives is that the muscles must typically accelerate and decelerate the legs or arms in the same way as in shadowboxing (Wilson 1973). Harrison

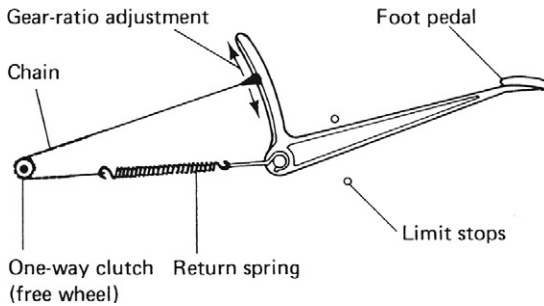


Figure 2.20
Swinging-lever drive. (Sketched by Dave Wilson.)



Figure 2.21

Sophisticated example of the swinging-lever drive of the Levocyclette, the earliest manufactured bicycle with ten speeds, manufactured by Terrot & Cie., Dijon, circa 1905. (From Dodge 1996; with the kind permission of Pryor Dodge, who provided a transparency.)

(1970) finds rather low outputs for motions of this type (figure 2.13). However, some believe that this disadvantage holds only for the most primitive embodiments: careful design should make it possible to oscillate the feet at high cadence with little loss. With geometrical slowing (a reducing sprocket radius or a drive linkage approaching its condition of zero mechanical advantage), kinetic energy is recaptured at the stroke end. (See figure 9.20 for the mechanism of the Thijs Rowcycle.)

With coupling between the left and right pedals, as in figure 2.21, one foot may lift the other in the same way as with a rotating crank. This still creates jerky reversals of no propulsion. Another

disadvantage in swinging-lever drives is the impossibility of wheeling so-equipped bicycles backward.

Constrained swinging-lever or linear drives do not have these disadvantages but do have dead centers that can prevent movement from rest. Once they are moving, the action is more or less sinusoidal and can achieve the highest effectiveness, according to figure 2.13 (“forced rowing”). However, as they are not connected via a freewheel, such drives take some skill to use, as the rider must synchronize to the phase given. This can be difficult, as people not used to treadle-driven sewing machines or railway draisines find out when starting to use such equipment. If a freewheel is used, one problem is exchanged for another. Although the rider can stop at any time, it is again possible to get stuck in a dead-center position, and not just at rest. The Thuner Trampelwurm road train also has some constrained swinging-lever pedals, and they are a nearly useless abomination compared to the other drives. A better design might change this.

Drives for Human-Powered Boats and Aircraft

Examining the physiological differences between the many ways of propelling traditional human-powered boats (HPBs) with oars and paddles is outside the scope of this book, but observations can be made on propeller drives for HPBs and human-powered aircraft (HPAs).

Unlike pedals for road vehicles, which at least when the rider is pedaling forward are in effect coupled rigidly to the road and therefore to the entire inertia of vehicle and rider, propeller drives *slip* with respect to the fluid they act on. Pedaling propellers with much slip is more at constant torque rather than constant speed, like pedaling a stationary exerciser without a flywheel. It is more difficult, or at least requires practice, to achieve high levels of *torque effectiveness* and *pedal smoothness*. The former is defined as the percentage of power delivered by the foot in the forward direction. A value of 100 percent implies pulling up on the upstroke. The latter is defined as the ratio of average power to peak power during a pedal revolution. A value of 100 percent implies no variation. See Johnstone 2014. In the case of propellers it is best to pedal at the peak of their efficiency curve, which implies little variation in speed and torque in the case of high-efficiency propellers of sufficient size.

When underway, such propellers slip only a few percent relative to their fluid and thus force pedaling at a certain speed relative to the vehicle speed, determined by the gear ratio, as with a bicycle. Cyclic variations in speed result immediately in large variations in torque and thrust and are thus coupled to the inertia of vehicle and rider. Pedaling then feels similar to pedaling on land, if the gearing is chosen well, and presumably much that has been said about land pedaling applies here also. However, as such propellers' efficiency curve has a pronounced peak, it is best to pedal smoothly enough to stay near this maximum during the entire pedal revolution.

Noncircular Cranking

Harrison (1970) shows that a constrained straight-line motion, with kinetic-energy conservation at the ends of the stroke, enables riders to produce greater short-term power than circular pedaling can generate. There has been limited but constant interest over more than a century in the question of whether a foot motion between circular and straight would be better than either of the two individually. Figure 2.22 shows the most common form of mechanism for producing such elliptical foot motions.

We have seen no results of ergometer tests of human power produced using such mechanisms. However, Miles Kingsbury in the United Kingdom has manufactured a modern form of such mechanisms, under the name K-drive, that has been used to win several races (Larrington 1999). Perhaps the K-drive's primary advantage lies in reducing the area swept out by the moving foot, so that a smaller, streamlined fairing may be used. In its present embodiment it adds weight and friction (because of several additional moving links), so the winning performances achieved with it must be regarded as significant.

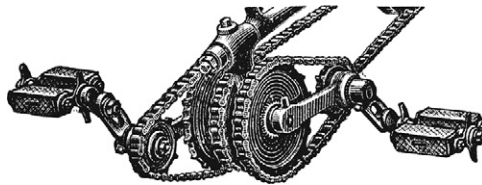


Figure 2.22

Mechanism for producing elliptical pedal paths. (From an 1890 German publication.)

Some Other Forms of Power Input

Mechanisms such as rotating hand cranks or rocking handlebars have been developed to allow riders to employ muscles other than the legs for propulsion. But perhaps surprisingly, conventional upright bicycles already offer this capability to some degree:

- When a cyclist is standing, tilting the bicycle away from the descending pedal enables the rider to perform substantial arm work easily. The diminution of pedal displacement at the given crank torque permits estimation of the amount of arm power exerted. For example, in tipping the bicycle from 15° right to 15° left, the arms are doing about 20 percent of the work, according to estimates made for this book. Presumably the legs can then push harder or move faster, for an overall increase in power output. A possible mechanical aid to arm work is a laterally movable saddle. When unlocked, such a saddle can bear the rider's weight but still permit the bicycle to be tipped forcefully by the arms.
- Pulling the torso forward (i.e., sliding along the saddle toward the handlebars) during each downstroke also enables a cyclist to use the arms powerfully at very low cadences and high torques.
- Especially when standing, a cyclist can leap upward with the assistance of the torso's uncoiling and push or pull somewhat vertically with the arms. (Not only can this technique add work produced by other muscles, but it makes it possible to convert low leg extension speeds to high, after which the rider descends on a straight, nonworking leg.)

Recumbents may be disadvantaged in this regard because they do not permit the rider to use additional muscles in this way. A spring-preloaded, rearward-slidable seat on a recumbent might provide a useful analog to the energy transformations of stand-up pedaling on an upright bicycle.

There are many ways of propelling skates, skateboards, and scooters, but we know of no data on measured efficiencies compared to pedaling, not even for the basic one-legged kicking thrust. Anybody who uses kick-cycles or modern Draisines, however, easily feels that these require more effort at the same speed, compared to pedaled vehicles. Reasons that come to mind are that the foot must be accelerated (backward) to at least road speed, and the other leg must be

partially bent. With skating movements this is also partly the case, but less so, as the thrust is more sideways, with higher force and less speed.

Thermal Effects (How Cyclists Keep Cool)

Bicycling can be hard work. For each unit of work put into the pedals, a bicyclist must get rid of about three units of heat in addition to the normal body heat from basal metabolism. It is as important that the body not become overheated when producing power as that it not lose more heat than can be replenished in cold conditions. As pointed out earlier in the book, the measurement of bicyclists' power output using ergometers is open to criticism because the conditions for heat dissipation on ergometers are critically different from those on bicycles. The performances of bicyclists riding in time trials and other long-distance races are, however, very amenable to analysis. Such time trials are of far longer duration than the few hours usually assumed (see, e.g., Wilkie 1960) as the maximum period over which data on human power output are available. Time trials (unpaced) are regularly held for 24 h periods; distances of 775 km (480 mi) are typical.

Bicycling generates a relative airflow of such magnitude that it bears little resemblance to the drafts produced by the small electric fans often used for cooling people pedaling ergometers, and these in turn can be much better than nothing. As a consequence, under most conditions of level cycling, the bicyclist works under cooler conditions than does an ergometer pedaler. At high speeds, most of the rider's power is expended in overcoming air resistance. Looking at this in a positive way, the power isn't all "wasted" but represents very effective cooling. Even if large cooling fans of the same power were used for ergometer experiments, the cooling effect would be less than that for the moving bicyclist.

Basic Cooling Mechanisms

The human body is cooled through four basic mechanisms: *radiation*, *convection*, *conduction*, and *perspiration*. The HyperPhysics website gives basic information about these mechanisms, with examples for an unclothed body at rest (see Nave 2018). Although its focus is space applications and not moving air as in cycling, NASA 1969

offers a detailed and comprehensive compilation on body thermal effects, including all the formulas and factors in this section and the next one, unless they are otherwise referenced.

Without wind and at or below room temperature, the primary cooling mechanism is heat radiation, and at elevated temperatures it is perspiration. The first three mechanisms noted in the previous paragraph can also absorb energy, that is, they can heat rather than cool the body. A further consideration is respiration or breathing, which can also cool the body through evaporation, like perspiration, and by a lesser amount, through convection.

Although each part of the skin cools differently, depending on orientation, exposure, and clothes, for approximations it is useful to know its total surface area. According to the formula given earlier, in the section “Basal Metabolism,” a man 1.8 m tall and weighing 80 kg has a skin area of 2 m², and one 1.5 m tall and weighing 50 kg, 1.43 m².

Heat-Transfer Data and Deductions

Skin of any color is an almost perfect (99 percent) “black body” radiator in the infrared. Heat radiation to the environment is very sensitive to actual temperatures, as they are raised to their fourth powers in the Stefan-Boltzmann equation typically used for calculating it. A skin area of 2 m² at a temperature of 34°C would radiate about 365 W into a 0°C environment, 133 W into 23°C, and 13 W into 33°C; at more than 34°C, energy would be absorbed, not lost. (In addition, if 10 percent of this area is exposed squarely to bright sunlight [~ 1 kW/m²], about 130–160 W [average white to average black skin] are absorbed.) Real figures are less, as some of the surfaces radiate toward each other (giving 65–75 percent of the total from crouched to semierect positions), and some like those of the fingers are rapidly cooled, thus decreasing radiation. Another caveat: the balance of infrared radiation occurs between the skin and a facing surface, which can be a wall, a canopy of leaves or material, a layer of humid air or a cloud, but not dry air, which is transparent to such radiation. An environment at thermal equilibrium might be more or less at air temperature, also with high humidity or a low cloud, but with a clear sky much of the heat of a surface facing upward is radiated into higher layers of the atmosphere with a much lower temperature: an infrared thermometer pointed at the clear sky can

show below-freezing temperatures even on a hot day. At night this is easily felt, and because of his or her orientation, a recumbent rider will radiate more heat than an upright cyclist. For clothed parts of the body, it is the outer surface temperature of the clothing that counts. Most fabrics are less perfect radiators (giving 70–80 percent of skin values), whereas reflective sheets (such as “rescue blankets”) radiate almost nothing themselves and reflect infrared radiation back to the skin.

If air temperature is higher than skin temperature, perspiration, the evaporation of sweat from the skin, and additionally, exhaled moisture are normally the only available means of cooling. Indeed the other mechanisms then all transport heat *into* the body. If 1 kg/h of water is evaporated without dripping or getting wiped away, this represents almost 675 W cooling power. Although this quantity is independent of the ambient air, the amount of evaporation possible is strongly dependent on the humidity. If humidity is very high, much of the sweat the body produces cannot evaporate and may instead drip away, removing far less heat. Wind strongly increases evaporation. According to Clifford, McKerslake, and Weddell (1959), evaporative cooling is proportional to $V^{0.63}$ (airspeed, measured from 0.6 m/s to 4 m/s) and also to the saturated vapor pressure at skin temperature (about 5 kPa) minus the ambient vapor pressure.

Convective cooling is proportional to surface area, the temperature difference between skin and air, and a heat transfer coefficient h_c , which is sensitive to airspeed and Reynolds number (see chapter 5), various other fluid-dynamic coefficients, and second-order conditions such as posture and airflow patterns. The third edition of this book showed that there can be greater than 100 percent variation in the local h_c in cross flow around a cylinder (such as an arm). In completely still air, there is no convection, and the (insulating) layer of air next to the skin nearly assumes its temperature. In this case, heat mainly flows by conduction through successive layers of still air. However, the slightest current, whether induced by the warm skin itself (buoyancy of locally heated air), movements of limbs, wind or fans, or the apparent wind of cycling itself, starts to remove this insulating air and raises the heat-transfer coefficient. Because of the many variables involved, an exact calculation is not possible, but various approximations have been proposed

for an overall coefficient as a function of airspeed. On the basis of their experiments in Antarctica, Siple and Passel (1945) propose an empirical formula: $h_c = 10.45 - V + 10\sqrt{V}$, in units of kilocalories per hour per square meter per degree Celsius, with airspeed V ranging from 2 to 20 m/s. The result can be multiplied by 1.1622 ... to yield the equivalent in SI units, that is, 23–35 W/(m² K) for the range specified. (This is explored further in the “Windchill” section later in the chapter). Colin and Houdas (1967) imply $h_c = 2.3 + 7.5 V^{0.67}$, which generates 14–58 W/(m² K) for the range specified. Although both formulas yield $h_c \approx 30$ W/(m² K) at $V = 7$ m/s, a typical cycling speed, this is coincidental, as the two groups took their measurements using different methods in different environments. Data from other researchers suggest functions more similar to those of Colin and Houdas. What all of this means is that 2 m² skin moving at 7 m/s at room temperature (i.e., 10 K cooler) is convectively cooled by about 600 W.

Heat transfer of course also depends on clothing. NASA 1969 expresses garments' thermal resistance garments in “Clo” units: 1 Clo = 0.155 K m²/W (for a 1.8 m² man) and represents comfortable indoor or light street clothing. Clo values vary from zero (nude) through 0.25 (underwear) and 2 (light winter clothing) to 7 (fox fur). 1 Clo will allow the average surface temperature of a person at rest to cool by about 5 K. The challenge for cycling clothing, however, is not high thermal resistance (apart from gloves and shoes in very cold conditions), but allowing perspiration without getting soaking wet.

The effect of adequate cooling may be inferred from Wilkie's (1960) finding, from experiments involving ergometer pedalers, that if it is necessary to exceed about 0.5 h of pedaling, subjects must keep their power output down to about 150 W (0.2 hp). However, peak performances in 24 h time trials can be analyzed using wind- and rolling-resistance data from chapters 5 and 6 to show that about 225 W (0.3 hp) are being expended over that period. The pedaler's exposure to moving air is principally responsible for the improvement in cooling. An ergometer pedaler who attempts a power output of 0.5 hp (373 W)—the same power output required to propel a racing cyclist doing a 40 km (25 mi) distance trial of nearly 1 hr—in normal laboratory ambient temperatures can expect to give up after perhaps 10 min and will be perspiring profusely.

Again the effect of moving air upon a pedaler's performance is very apparent.

In the design of heating and ventilating plants, the maximum heat load produced by a worker doing hard physical labor (the recommended room temperature for which is 55°F or 12.8°C) has long been accepted as 2,000 Btu/h (586 W) (Faber and Kell 1943). Most of the heat is lost through evaporation of sweat. If this includes 100 W basal metabolism and an efficiency of 25 percent is assumed, such a worker would produce about 122 W mechanical power. This would also seem to be an acceptable limit for pedaling ergometers or cycling very steeply uphill for long periods.

Figure 2.4 shows that athlete cyclists can exert greater than 400 W (0.54 hp) for periods of up to 1 h. A common range of endurance when pedaling ergometers at 0.5 hp (373 W) is 5–15 min (Whitt 1973), which again demonstrates vividly the value of flowing air in prolonging the tolerable period of hard work.

Even at lower speeds, the apparent wind can give enough cooling for relatively high-power cycling. For example, in a hill climb of the Grossglockner, Bill Bradley rode at about 5.4 m/s (12 mph) at a power output of 450 W, in high-temperature but low-humidity (40 percent) conditions.

Bicycling in Cold and Hot Conditions

A problem faced by advocates of bicycling as a means for daily commuting to and from work is that even temperate regions have days, and sometimes weeks, of extreme weather conditions during which bicycling may be unpleasant for many and impossible for some. There is no one set of temperature boundaries below and above which bicycling becomes impossible. Many fair-weather cyclists put their machines away for the winter when the morning temperatures drop to 10°C (50°F) and will not ride in business clothes at temperatures above 25°C (77°F). However, many hardier folk find bicycling still enjoyable at -15°C (5°F) to 35°C (95°F), or an even wider range of temperatures, also depending on wind and humidity. The main problem at temperatures below the lower end of this range seems to be the feet. The size of insulated footwear is limited to that which can fit on bicycle pedals, and it is a fairly common experience that, at -18°C (0°F), even when the trunk of the body is becoming overheated through exertion, the feet can become numb with cold.

Windchill Wind intensifies the effects of cold air. Weather forecasters often express these effects in terms of *windchill*: the air temperature that would have to exist, without wind (but at walking speed), to provide the same cooling to a human body as a particular combination of actual temperature and actual relative wind. The windchill temperatures tabulated by the US National Weather Service use an empirical formula giving the perceived temperature as a function of the actual temperature (assumed to be below 10°C or 50°F) and the wind speed (assumed above 1.3 m/s), for which there are many online calculators (see, e.g., Brice and Hall 2019 b). The following formula yields two results: first the windchill index in units of watts per square meter, after the original formula of Siple and Passel (1945) mentioned earlier:

$$\text{Windchill Index} = (11.622 V^{1/2} - 1.1622 V + 12.145) (33 - T),$$

in which V is the wind speed in meters per second and T the actual temperature in degrees Celsius. This is the formula for the heat-transfer coefficient given earlier, with kilocalories per hour converted to watts, multiplied by the difference between the ambient temperature and that of the skin (33°C). In 2001 the National Weather Service replaced this formula with the following one, which provides the windchill temperature in degrees Fahrenheit:

$$\text{Windchill Temperature} = 35.74 + 0.6215 T - 35.75 V^{0.16} + 0.4275 T V^{0.16},$$

in which V is the wind speed in miles per hour and T the actual temperature in degrees Fahrenheit. The calculator and information from Brice and Hall 2019b also give other units.

The Wikipedia article on windchill explains well the history and rationale of the method. Using calculators or published charts, one can find the effect on a rider's perceived temperature of bicycling into a relative wind. For instance, if the air temperature is -18°C (0°F) and one is bicycling into a relative wind of 5 m/s (11 mph), one is subjected to the same amount of cooling as if one were walking at a temperature of -27°C (-17°F). The calculated windchill index is about 1,650 W/m². Even if this is applicable only to skin exposed fully to the wind, it roughly shows what would happen to an unclothed human, and with what heat flux the body has to supply exposed skin (e.g., perhaps 40 W here for an exposed face). If the local blood supply cannot furnish this, the skin temperature

drops and frostbite ensues. This can also happen to the fingers if the gloves worn are too thin.

A cyclist's feet are particularly at risk because they are periodically traveling at a higher relative velocity (as they come over top dead center) and then at a lower velocity relative to the wind. Because the cooling relationship to relative wind is nonlinear, the average cooling effect is more severe. In particular, winter users of fast e-bicycles may suffer cold fingers, feet, and faces. As electric power is readily at hand, electrically heated gloves and shoes are a possibility.

The body core temperature of an adequately clothed cyclist is normally never at risk, as going faster normally produces more heat than is lost. An exception is going downhill, during which it is easy to lose a great deal of heat on long winter descents.

Heat and Humidity At higher temperatures, humidity becomes very important. The bicycle is highly prized for personal transportation and for local commerce throughout Africa and Asia. In northern Nigeria, for example (where the senior author lived for two years), the air is so dry throughout most of the year that the availability of water limits one's range on a bicycle more so than the temperature. The long-distance bicyclist Ian Hibell was able to ride through the Sahara (principally at night), limited again by his water supplies. He could not carry sufficient water for the longer stages between oases and relied on gifts of water from passing motor travelers. Even the United States occasionally experiences heat waves with a month or so of temperatures around 40°C, often coupled with high humidity. Yet some bicyclists continue to ride to work, even though bicyclists experience even higher ambient temperatures on roads.

The US National Weather Service has produced a *heat index* analogous to the windchill index just described, and in Canada, a similar *humidex* formula is in use. Both are well-described in Wikipedia articles; Brice and Hall 2019a (see also Weather Prediction Center 2014) provides a calculator and the underlying formula, too long to include here. The calculators and their associated formulas are used similarly to those for the apparent windchill temperature, except that relative humidity is entered instead of wind speed. For example, if the temperature is 40°C (104°F), the heat index formula returns those values for the perceived temperature if it is rather dry at, say, 22 percent relative humidity, or even a bit less if it is drier. But at 50 percent humidity, the felt temperature is about 55°C, with

a severe risk of heat stroke. Higher humidity values yield extreme results, but it is not quite clear for which ranges the heat index formula has been validated.

While cycling in temperature extremes is generally not much of a problem in level riding, this is not so for gradients. Cycling steeply uphill promotes heavy sweating. In warm conditions this is merely inconvenient or unpleasant, but in cold conditions the skin and clothes are moist just when their being so is most dangerous, for example, when cycling downward again, during which the evaporative cooling will be excessive unless additional clothing is donned. It is no wonder that the recent surge in popularity of e-bicycles has mainly been in hilly locales. The additional power permits uphill cycling with far better cooling, as well as cycling in business clothes without their becoming unduly moist.

There are caveats when using fast e-bicycles in hot or cold conditions, however. In the latter, any exposed or only thinly shielded skin is highly cooled, and the otherwise warm body may experience strong pain in those areas. In hot weather the cooling is so good that the body is motivated to cycle at especially high power levels. Sweat is produced but evaporates immediately and isn't noticed. The moment the rider stops and for a while afterward, sweat is still being produced, but evaporation decreases, and it starts dripping off. To avoid this, speed must be reduced well before stopping.

There are three lessons to be learned from the experience of the hardier riders who brace themselves for cycling against what seem to be extreme conditions. First, the promotion of good circulation through exertion helps the body cope with high temperatures and high humidity as well as with cold weather. Second, the relative airflow that bicycling produces is a major factor in making riding in hot weather tolerable and usually enjoyable. Third, the fact that so many riders choose to bicycle in extreme conditions (rather than being forced to do so by economic necessity) shows that many other healthy but more timid cyclists could push their limits with regard to conditions conducive to or comfortable for cycling without fear of harm.

Streamlined Vehicles

Normal unfaired bicycles and HPVs give optimal cooling in warm to hot conditions. Even better are those with sunroofs, like the

coauthor's 1985 solar-assisted tricycle, used with comfort in all sorts of conditions. With fairings, especially those of velomobiles or racing HPVs, which fully enclose the rider, most of this cooling is lost. Exposing at least the head or opening the canopy or the sides for ventilation helps considerably, but at the penalty of more air resistance, not acceptable for racing or record attempts and not ideal for velomobiles when it rains. Wichers Schreur (2004) provides an analysis and recommendations, showing that good interior ventilation is possible and if optimal ducts for the air intake are used, the power loss is under 1 W. Unfortunately at low speeds, for example, uphill, the airflow will be insufficient to prevent discomfort and heavy sweating.

Velomobiles can be fitted with small electric fans directed at the rider's head and shoulders. Even a few watts increase comfort enormously.

Racers of these vehicles are in greater danger of actually overheating, especially when large canopies also act as partial solar collectors. The rules for HPV racing or records prohibit cooling with stored energy, such as with the fans mentioned, ice, or precooled vests. They, do, however allow water sprays.

In cold conditions the fairings are thermally more advantageous, but ventilation is still required, especially to prevent the misting up of windshields.

Artificial Cooling

In addition to simple fans, wet cloths, or water sprays, it is in principle possible to wear clothes with built-in cooling elements. Vests are available that incorporate pads of *phase-change materials*. Water ice, the most common phase-change material, can absorb 334 kJ/kg when melting at 0°C, much more than the 10 kcal/kg (41.8 kJ/kg) absorbed by (nonevaporating) cooling water at 20°C that is heated by the skin to 30°C. Many other substances are available that melt at almost any desired temperature and mostly absorb between 160 and 230 kJ/kg. Evaporating water can, however, remove 2,260 kJ/kg, so a rider would have to use about 10 kg of phase-change materials to have the same effect as with optimal evaporative cooling with 1 kg of sweat or sprayed water.

The book's authors have never heard of its being done, for obvious practical reasons, but in principle clothes cooled by circulating

water (or heat pipes), connected to a radiator, could offer almost any desired degree of cooling for any length of time, without using up anything other than a small amount of power for a circulating pump. NASA 1969 goes into great detail on how this is accomplished in space suits. However, in hot conditions, a dry radiator wouldn't work, and a form of heat pump would be needed. This isn't quite as absurd as it sounds, as the theoretical coefficient of cooling power ($COP_{\text{cooling}} = T_c / [T_h - T_c]$, with cold and hot temperatures in Kelvin) could be greater than 30, so an efficient human-powered heat pump could cool with much more power than that needed to operate it, even though at least four times the operating power would appear additionally as heat.

References

- Adams, W. C. 1967. "Influence of Age, Sex and Body Weight on the Energy Expenditure of Bicycle Riding." *Journal of Applied Physiology* 22: 539–545.
- Allen, Hunter. 2013. "What Is FTP?" *Hunter Allen Power Blog*. January 9, 2013. <http://www.hunterallenpowerblog.com/2013/01/what-is-ftp.html>.
- Antonson, Ingrid. 1987. "Oxygen Cost of Submaximal Exercise in Recumbent and Conventional Cycling Positions." *Human Power* 6, no. 3 (Fall): 7, 17–18. <http://www.ihpva.org/HParchive/PDF/21-v6n3-1987.pdf>.
- Åstrand, Per-Olof, and Kåre Rodahl. 1977. *Textbook of Work Physiology*. 2d ed. New York: McGraw-Hill.
- Ayalon, A., B. Bar-Or, and Omri Inbar. 1974. "Relationships among Measurements of Explosive Strength and Anaerobic Power." In *Biomechanics IV: Proceedings of the Fourth International Seminar on Biomechanics, University Park, Pennsylvania*, ed. Richard C. Nelson and Chauncey A. Morehouse, 572–577. <https://www.researchgate.net/publication/306232114>.
- Baron Biosystems. 2018. Xert Fitness Signature calculator. <https://www.xertonline.com/calculator>.
- Beelen, Anita, and Anthony J. Sargeant. 1992. "Effect of Fatigue on Maximal Power Output at Different Contraction Velocities in Humans." *Journal of Applied Physiology* 71, no. 6 (January): 2332–2337. <https://www.researchgate.net/publication/21376724>.
- Bergamin, Fabio. 2017. "Breath instead of a Blood Test." Eidgenössische Technische Hochschule Zürich (ETHzürich), Zurich, Switzerland, October 10. <https://www.ethz.ch/en/news-and-events/eth-news/news/2017/10/breath-instead-of-a-blood-test.html>.

Book of Alternative Records. 2019. "Static Cycling, 48 Hours." <http://www.alternativerecords.co.uk/recorddetails.asp?recid=505>.

Brice, Tim, and Todd Hall. 2019a. "Heat Index Calculator." National Weather Service, National Oceanic and Atmospheric Administration, El Paso, TX. https://www.weather.gov/epz/wxcalc_heatindex.

Brice, Tim, and Todd Hall. 2019 b. "Wind Chill Calculator." National Weather Service, National Oceanic and Atmospheric Administration, El Paso, TX. https://www.weather.gov/epz/wxcalc_windchill.

Brooks, G. A., T. D. Fahey, and T. P. White. 1996. "Energetics and Athletic Performance." In *Exercise Physiology*, 2d ed., chap. 3. Mountain View, CA: Mayfield.

Burns, J. 2008. "Does T raining with PowerCrankTM Affect Economy of Motion, Cycling Efficiency, Oxygen Uptake and Muscle Activation Patterns in Trained Cyclists?" Master's thesis, School of Exercise, Biomedical and Health Sciences, Edith Cowan University, Perth, Australia. <http://ro.ecu.edu.au/theses/17>.

Bussolari, Steven R. 1986–1887. "Human Factors of Long-Distance HPA Flights." *Human Power* 5, no. 4 (Winter): 8–12. <http://www.ihpva.org/HParchive/PDF/18-v5n4-1986.pdf>.

Bussolari, Steven R., and Ethan R. Nadel. 1989. "The Physiological Limits of Long-Duration Human Power Production—Lessons Learned from the Daedalus P roject." *Human Power* 7, no. 4 (Summer): 1, 8–10. <http://www.ihpva.org/HParchive/PDF/25-v7n4-1989.pdf>.

Clifford, D., D. McKerslake, and J. L. Weddell. 1959. "The Effect of Wind Speed on the Maximum Evaporative Capacity in Man." *Journal of Physiology*, no. 147: 253–259. <https://doi.org/10.1113/jphysiol.1959.sp006240>.

Coggan, Andrew. 2016. "Power Drop Off Range 2 Mins–60 Mins: Comment." Timetrialling Forum (website), April 18. <http://www.timetriallingforum.co.uk/index.php?/topic/109887-power-drop-off-range-2mins-60mins/>.

Colin, Jean, and Yvon Houdas. 1967. "Experimental Determination of Coefficient of Heat Exchanges by Convection of the Human Body." *Journal of Applied Physiology* 22, no. 1: 31–38.

Coyle, Edward F., M. E. Feltner, Steven A. Kautz, M. T. Hamilton, Scott J. Mountain, A. M. Baylor, Lawrence D. Abraham, and G. W. Petrek. 1991. "Physiological and Biomechanical Factors Associated with Elite Endurance Cycling Performance." *Medicine and Science in Sports and Exercise* 23, no. 1: 93–107.

Coyle, Edward F., Wade H. Martin, A. A. Ehsani, James M. Hagberg, Susan A. Bloomfield, David R. Sinacore, and John O. Holloszy. 1983. "Blood Lactate Threshold in Some Well-Trained Ischemic Heart Disease Patients." *Journal of Applied Physiology* 54, no. 1 (January):18–23. <https://www.researchgate.net/publication/16373423>.

Croci, Ilaria, Fabio Borrani, Nuala Byrne, Rachel Wood, Ingrid Hickman, Xavier Chenevière, and Davide Malatesta. 2014. "Reproducibility of Fat_{max} and Fat Oxidation Rates during Exercise in Recreationally Trained Males." *PLoS ONE* 9, no. 6: e97930. <https://doi.org/10.1371/journal.pone.0097930>.

Daley, Jordan. 2018. "Fitness and Exercise Calculators." ShapeSense.com (website). <http://www.shapesense.com/fitness-exercise/calculators/>.

Davies, C. N., ed. 1962. *Design and Use of Respirators: Proceedings of a Joint Meeting of the Ergonomics Research Society and the British Occupational Hygiene Society, Held at Porton, 5 and 6 July, 1961*. New York: Pergamon.

Dodge, Pryor. 1996. *The Bicycle*. Paris: Flammarion.

Driss, Tarak, and Henry Vandewalle. 2013. "The Measurement of Maximal (Anaerobic) Power Output on a Cycle Ergometer: A Critical Review." *BioMed Research International* 2013: art. 5 89361. <https://www.hindawi.com/journals/bmri/2013/589361/>.

Egaña, Mikel, David Columb, and Steven O'Donnell. 2013. "Effect of Low Recumbent Angle on Cycling Performance, Fatigue, and $\dot{V}O_2$ Kinetics." *Medicine & Science in Sports & Exercise* 45, no. 4 (April): 663–672. <https://www.ncbi.nlm.nih.gov/pubmed/23135372>.

FAO (Food and Agriculture Organization). 2003. *Food Energy—Methods of Analysis and Conversion Factors: Report of a Technical Workshop, Rome, 3–6 December 2002*. Food and Nutrition Paper 77. Rome: Food and Agriculture Organization of the United Nations. <http://www.fao.org/docrep/006/Y5022E/y5022e00.htm>.

Faber, O., and J. R. Kell. 1943. *Heating and Air Conditioning of Buildings*. Chream, U.K.: Architectural Press.

FastFitness.Tips. 2019. "Cycling Myths Smashed." FastFitness.Tips (website). <http://www.fastfitness.tips/services>.

Fonda, Borut. 2015. "Cycling Biomechanics Optimisation." Cycling Science, Ljubljana, Slovenia. <http://www.cycling-science.si/cycling-biomechanics-optimisation-21-11-2015.html>.

Franklin, Kathryn L., Rae S. Gordon, Julien S. Baker, and Bruce Davies. 2007. "Accurate Assessment of Work Done and Power during a Wingate Anaerobic Test." *Applied Physiology, Nutrition, and Metabolism* 32: 225–32. <http://www.unm.edu/~rrobergs/478FranklinWingate.pdf>.

Gaesser, Glenn A., Tony J. Carnevale, Alan Garfinkel, Donald O. Walter, and Christopher J. Womack. 1995. "Estimation of Critical Power with Nonlinear and Linear Models." *Medicine and Science in Sports and Exercise* 27: 1430–38.

Gordon, R. S., K. L. Franklin, J. Baker, and B. Davies. 2004. "Accurate Assessment of the Brake Torque on a Rope-Braked Cycle Ergometer." *Sports Engineering* 7, no. 3 (September): 131–38. <https://doi.org/10.1007/BF02844051>.

Güntner, A. T., N. A. Sievi, S. J. Theodore, T. Gulich, M. Kohler, and S. E. Pratsinis. 2017. "Noninvasive Body Fat Burn Monitoring from Exhaled Acetone with Si-Doped WO₃-Sensing Nanoparticles." *Analytical Chemistry* 89, no. 19: 10578–10584. <http://dx.doi.org/10.1021/acs.analchem.7b02843>.

Hamley, E. J., and V. Thomas. 1967. "The Physiological and Postural Factors in the Calibration of the Bicycle Ergometer." *Journal of Physiology* 191: 55–57.

Hansen, Ernst Albin, Kurt Jensen, Jostein Hallén, John Rasmussen, and Preben K. Pedersen. 2009. "Effect of Chain Wheel Shape on Crank Torque, Freely Chosen Pedal Rate, and Physiological Responses during Submaximal Cycling." *Journal of Physiological Anthropology* 28, no. 6: 261–267. <https://doi.org/10.2114/jpa2.28.261>.

Harris, J. A., and F. G. Benedict. 1918. "A Biometric Study of Human Basal Metabolism." *Proceedings of the National Academies of Science USA* 4, no. 12: 370–373. <https://www.ncbi.nlm.nih.gov/pmc/articles/PMC1091498/>.

Harrison, J. Y. 1970. "Maximizing Human Power Output by Suitable Selection of Motion Cycle and Load." *Human Factors* 12, no. 3: 315–329.

Hermina, W. 1999. "The Effects of Different Resistance on Peak Power during the Wingate Anaerobic Test." M.S. thesis, College of Health and Human Performance, Oregon State University, Corvallis, OR. <https://ir.library.oregonstate.edu/downloads/zc77st11v>.

Hetzler, Ronald K., Rachele E. Vogelpohl, Christopher D. Stickley, Allison N. Kuramoto, Mel R. DeLaura, and Iris F. Kimura. 2010. "Development of a Modified Margaria-Kalamen Anaerobic Power Test for American Football Athletes." *Journal of Strength and Conditioning Research* 24, no. 4: 978–984. <http://www.unm.edu/~rrobergs/478Margaria1.pdf>.

Inbar, Omar, Oded Bar-Or, and James S. Skinner. 1996. *The Wingate Anaerobic Test*. Champaign, IL: Human Kinetics.

Jenkins, David G., and Brian M. Quigley. 1990. "Blood Lactate in Trained Cyclists during Cycle Ergometry at Critical Power." *European Journal of Applied Physiology* 61: 278–283.

Johnstone, David. 2014. "Torque Effectiveness and Pedal Smoothness." *Cycling Analytics* (blog). April 11, 2015. <https://www.cyclinganalytics.com/blog/2014/04/torque-effectiveness-and-pedal-smoothness>.

Johnstone, David. 2018. "How Does Your Cycling Power Output Compare?" *Cycling Analytics* (blog). June 7, 2018. <https://www.cyclinganalytics.com/blog/2018/06/how-does-your-cycling-power-output-compare>.

Knipping, H. W., and A. Moncrieff. 1932. "The Ventilation Equivalent of Oxygen." *Queensland Journal of Medicine* 25: 17–30. <https://academic.oup.com/qjmed/article/1/1/17/1598875>.

Kyle, C. R., V. J. Caizzo, and M. Palombo. 1978. "Predicting Human Powered Vehicle Performance Using Ergometry and Aerodynamic Drag Measurements." Paper presented at "Human Power for Health, Productivity, Recreation and Transportation," Technology University of Cologne, Cologne, Germany, September.

Landsberg, Lewis, James B. Young, William R. Leonard, Robert A. Linsenmeier, and Fred W. Turek. 2009. "Do the Obese Have Lower Body Temperatures? A New Look at a Forgotten Variable in Energy Balance." *Transactions of the American Clinical and Climatological Association* 120: 287–295. <https://www.ncbi.nlm.nih.gov/pmc/articles/PMC2744512/>.

Lanooy, C., and F. H. Bonjer. 1956. "A Hyperbolic Ergometer for Cycling and Cranking." *Journal of Applied Physiology* 9: 499–500. <http://citeseerx.ist.psu.edu/viewdoc/download?doi=10.1.1.919.7808&rep=rep1&type=pdf>.

Larrington, Dave. 1999. "Different Strokes?" *Human Power*, no. 48 (Summer): 25–27. <http://www.ihpva.org/HParchive/PDF/hp48-1999.pdf>.

Lee, Sun Hee, and Eun Kyung Kim. 2012. "Accuracy of Predictive Equations for Resting Metabolic Rates and Daily Energy Expenditures of Police Officials Doing Shift Work by Type of Work." *Clinical Nutrition Research* 1, no. 1: 66–77. <https://www.ncbi.nlm.nih.gov/pmc/articles/PMC3572798>.

Luttrell, Mark D., and Jeffrey A. Potteiger. 2003. "Effects of Short-Term Training Using Powercranks on Cardiovascular Fitness and Cycling Efficiency." *Journal of Strength and Conditioning Research* 17, no. 4 (November): 785–791. https://journals.lww.com/nsca-jscr/Abstract/2003/11000/Effects_of_Short_Term_Training_Using_Powercranks.26.aspx.

Martin, James C., Bruce M. Wagner, and Edward F. Coyle. 1997. "Inertial-Load Method Determines Maximal Cycling Power in a Single Exercise Bout." *Medicine and Science in Sports and Exercise* 29, no. 11 (November): 1505–1512. https://journals.lww.com/acsm-msse/Fulltext/1997/11000/Inertial_load_method_determines_maximal_cycling.18.aspx.

Mathur, Sunita. 2014. "Regulation of Ventilation during Exercise." Exercise Physiology: e-Learning Modules for MScPT, University of Toronto, Toronto, ON. <http://ptexphys.utorontoeit.com/respiratory-physiology/regulation-of-ventilation-during-exercise/>.

McArdle, W. D., F. I. Katch, and V. L. Katch. 1996. *Exercise Physiology: Energy, Nutrition, and Human Performance*. Baltimore: Williams and Wilkins.

McMahon, Thomas A. 1984. *Muscles, Reflexes, and Locomotion*. Princeton, NJ: Princeton University Press.

Morton, R. Hugh, and David J. Hodgson. 1996. "The Relationship between Power and Endurance: A Brief Review." *European Journal of Applied Physiology* 73: 491–502. <https://www.researchgate.net/publication/14388415>.

Müller, E. A. 1937. "Der Einfluß der Sattelstellung auf das Arbeitsmaximum und den Wirkungsgrad beim Radfahren" [The Influence of Saddle Height on Maximum Power and Efficiency of Bicycling]. Kaiser Wilhelm Institut für Arbeitsphysiologie, Dortmund-Münster, Germany.

Müller, E. A., and H. Grosse-Lordemann, H. 1936. "Der Einfluß der Leistung und der Arbeitsgeschwindigkeit auf das Arbeitsmaximum und den Wirkungsgrad beim Radfahren" [The Influence of Power and Working Speed on Maximum Power and Efficiency for Bicycles]. *European Journal of Applied Physiology* 9: 619–625. <https://www.researchgate.net/publication/238251597>.

NASA (National Aeronautics and Space Administration). 1969. "Thermal Environment." Paper 19690003109, Scientific and Technical Information Program, National Aeronautics and Space Administration, Washington, DC. https://ntrs.nasa.gov/archive/nasa/casi.ntrs.nasa.gov/19690003109_1969003109.pdf.

Nave, Rod. 2018. "Cooling of the Human Body." HyperPhysics (website). Department of Physics and Astronomy, Georgia State University, Atlanta. <http://hyperphysics.phy-astr.gsu.edu/hbase/thermo/coobod.html>.

Neville, V., M. T. G. Pain, and J. P. Folland. 2009. "Aerobic Power and Peak Power of Elite America's Cup Sailors." *European Journal of Applied Physiology* 106, no.1: 149–57. [https://dspace.lboro.ac.uk/dspace-jspui/bitstream/2134/6578/1/neville2009\[1\].pdf](https://dspace.lboro.ac.uk/dspace-jspui/bitstream/2134/6578/1/neville2009[1].pdf).

Newmiller, Jeff, Maury L. Hull, and F. E. Zajac. 1988. "A Mechanically Decoupled 2 Force Bicycle Pedal Dynamometer." *Journal of Biomechanics* 21, no. 5 (February): 375–386. <https://www.researchgate.net/publication/19738025>.

Nicolò, Andrea, Carlo Massaroni, and Louis Passfield. 2017. "Respiratory Frequency during Exercise: The Neglected Physiological Measure." *Frontiers in Physiology* 8: 922. <https://doi.org/10.3389/fphys.2017.00922>.

Nüscheler, Manfred. 2009. "Manfred Nüscheler—Roller Cycling Record Holder." Rekord-Klub Saxonia, Leipzig, Germany. <http://www.recordholders.org/en/records/roller1.html>.

Okajima, Shinpei. 1983. "Designing Chainwheels to Optimize the Human Engine." *Bike Tech* 2, no. 4: 1–7.

Papadopoulos, Jim. 1987. "Forces in Bicycle Pedaling." In *Biomechanics in Sport: A 1987 Update*, ed. R. Rekow, V. G. Thacker, and A. G. Erdman. New York: American

Society of Mechanical Engineers. http://ruina.tam.cornell.edu/research/topics/bicycle_mechanics/forces_bicycle_pedaling.pdf.

Parker, Jr., James F., and Vita R. West, eds. 1964. *Bioastronautics Data Book*. NASA SP-3006. Washington, DC: National Aeronautics and Space Administration.

Perez, Sergio E., Mark Wisniewski, and Jordan Kendall. 2016–2017. “Efficiency of Human-Powered Sail Pumping.” *Human Power eJournal*, no. 9: art. 23. <http://hupi.org/HPeJ/0023/HumanPoweredSailPumpingV7.pdf>.

Peveler, Will W. 2008. “Effects of Saddle Height on Economy in Cycling.” *Journal of Strength and Conditioning Research* 22, no. 4: 1355–1359. <https://www.ncbi.nlm.nih.gov/pubmed/18545167>.

Powell, Richard. 1994. “Arm Power Performance.” In *Proceedings of the Fourth International Human Powered Vehicle Scientific Symposium*. San Luis Obispo, CA: International Human Powered Vehicle Association.

Powell, Richard, and Tracey Robinson. 1987. “The Bioenergetics of Power Production in Combined Arm-Leg Crank Systems.” *Human Power* 6, no. 3 (Fall): 8–9, 18. <http://www.ihpva.org/HParchive/PDF/21-v6n3-1987.pdf>.

Pugh, L. G. C. E. 1974. “The Relation of Oxygen Intake and Speed in Competition Cycling and Comparative Observations on the Bicycle Ergometer.” *Journal of Physiology* (Physiological Society) 241:795–808. <https://doi.org/10.1113/jphysiol.1974.sp010685>.

Rankin, Jeffery, and Richard Neptune. 2008. “A Theoretical Analysis of an Optimal Chainring Shape to Maximize Crank Power during Isokinetic Pedaling.” *Journal of Biomechanics* 41: 1494–1502. <https://www.ncbi.nlm.nih.gov/pubmed/18395213>.

Reiser, Raoul F., Jeffrey P. Broker, and M. L. Peterson. 2000. “Inertial Effects on Mechanically Braked Wingate Power Calculations.” *Medicine and Science in Sports and Exercise* 32, no. 9: 1660–1664.

Rowe, T., Maury L. Hull, and E. L. Wang. 1998. “A Pedal Dynamometer for Offroad Bicycling.” *Journal of Biomechanical Engineering* 120, no. 1 (March):160–164. <https://www.researchgate.net/publication/13608754>.

Schmidt, Theodor. 2019. Online supplements to *Bicycling Science*, 4th ed. <http://hupi.org/BS4/>.

Selkov, Gene. 2015. “Answer: What Is the Relation of Body Temperature and Metabolism? If You Wear Minimal Clothes in Winter, Would Body Metabolism Work at an Accelerated Rate to Maintain Body Temperature, Leading to Weight Loss? Would It Be Vice Versa for Summer?” Quora (website). January 29, 2015. <https://www.quora.com/What-is-the-relation-of-body-temperature-and-metabolism>.

Siple, Paul A., and Charles F. Passel. 1945. "Measurements of Dry Atmospheric Cooling in Subfreezing Temperatures." *Proceedings of the American Philosophical Society* 89, no. 1 (April 30): 177–199.

Spinnetti, Ramondo. 1987. "Backward versus Forward Pedaling: Comparison Tests." *Human Power* 6, no. 3 (Fall): 1, 10–11. <http://www.ihpva.org/HParchive/PDF/21-v6n3-1987.pdf>.

Too, Danny. 1998–1999. "Summaries of Papers" (technical note). *Human Power*, no. 46 (Winter): 13–20. <http://www.ihpva.org/HParchive/PDF/hp47-n46-1998.pdf>.

Too, Danny, and Gerald Landwer. 2008. "Maximizing Performance in Human Powered Vehicles: A Literature Review and Directions for Future Research." *Human Power eJournal*, no. 5: art. 16. <http://hupi.org/HPeJ/0016/0016.html>.

Too, Danny, and Chris Williams. 2000. "Determination of the Crank-Arm Length to Maximize Power Production in Recumbent-Cycle Ergometry." *Human Power*, no. 51 (Fall): 3–6. <http://www.ihpva.org/HParchive/PDF/hp51-2001.pdf>.

Too, Danny, and Christopher D. Williams. 2017–2018. "Determination of the Optimal Crank Arm Length to Maximize Peak Power Production in an Upright Cycling Position." *Human Power eJournal*, no. 10: art. 25. <http://hupi.org/HPeJ/0025/Too-Williams-REV2-1.pdf>.

van de Kraats, Gert. 2018. "Efficient Pedaling on a Recumbent." *Cycle Vision* (website). <http://members.home.nl/vd.kraats/recumbent/pedal.html>.

Vandewalle, Henry, and Tarak Driss. 2015. "Friction-Loaded Cycle Ergometers: Past, Present and Future." *Cogent Engineering* 2, no. 1: 1029237. <http://dx.doi.org/10.1080/23311916.2015.1029237>.

Venables, Michelle C., Juul Achten, and Asker E. Jeukendrup. 2005. "Determinants of Fat Oxidation during Exercise in Healthy Men and Women: A Cross-Sectional Study." *Journal of Applied Physiology* 98, no. 1 (February): 160–167. <https://www.researchgate.net/publication/8377999>.

Von Döbeln, W. 1954. "A Simple Bicycle Ergometer." *Journal of Applied Physiology* 7: 222–224.

Weather Prediction Center. 2014. "The Heat Index Equation." Weather Prediction Center, National Centers for Environmental Prediction, National Weather Service, National Oceanic and Atmospheric Administration, College Park, MD. http://www.wpc.ncep.noaa.gov/html/heatindex_equation.shtml.

Weir, J. B. de V. 1949. "New Methods for Calculating Metabolic Rate with Special Reference to Protein Metabolism." *Journal of Physiology* (Physiological Society) 109, nos. 1–2 (August): 1–9. <https://www.ncbi.nlm.nih.gov/pmc/articles/PMC1392602/>.

Whitt, F. R. 1971. "A Note on the Estimation of the Energy Expenditure of Sporting Cyclists." *Ergonomics* 14, no. 3: 419–424.

Wilkie, D. R. 1960. "Man as an Aero-Engine." *Journal of the Royal Aeronautical Society* 64: 477–481. https://www.aerosociety.com/Assets/Docs/About_Us/HPAG/Papers/HP_wilkie.pdf.

Wichers Schreur, Ben. 2004. "The Ventilation of Streamlined Human-Powered Vehicles." *Human Power eJournal*, no. 1: art. 2. <http://hupi.org/HPeJ/0002/0002.htm>.

Wilson, S. S. 1973. "Bicycling Technology." *Scientific American* 228, no. 3 (March): 81–91.

Zommers, Alfred. 2000. "Variations in Pedalling Technique of Competitive Cyclists: The Effect on Biological Efficiency." PhD diss., Victoria University of Technology, Melbourne, Australia. <http://vuir.vu.edu.au/15742/>.

3 Speed Achievements and Racing

Introduction

This chapter summarizes cycling achievements as registered by various sports and record organizations and considers what might be possible in some theoretical scenarios. Speed achievements are intermingled with the sport of bicycle racing. As with most sports the goals here are not primarily about improving athletic records and associated technology or making scientific comparisons about them, but about competition, prestige, and money. Athletes, teams, and even nations compete with similar athletes (teams, nations), trying to be a bit better by improving both their bodies and their equipment to the extent that the sports organizations that administer the records allow. Finding new ways of doing this is considered legitimate, until the sports organizations decide to disallow or ban them, mostly for good reasons, but often simply to stay in control of the sport. Athletes or technologists then often attempt to cheat, or else form new sports or organizations. So there is competition not only between athletes and vehicle engineers, but also among ideas, groups, locations, and administrators.

This book is mainly interested in achievements in the scientific sense. The data acquired through bicycle racing are both invaluable and difficult to use, because mostly only relative achievements are recorded (e.g., “A was X seconds faster than B in event Y at site Z”) rather than complete data sets (e.g., “A achieved X with equipment Y under the conditions W and U”). The double variation possible (of both human and machine) makes it especially difficult to use the data obtained. As engineers, we are mainly interested in the machine (and in the following, we list vehicular records

mostly without naming the human “engine”), but sports achievements are usually about the human, team, or even team nationality. We include mainly records that exist for all types of bicycles—traditional, recumbent, partially and fully faired human-powered vehicles (HPVs)—but not from bicycle races on variable terrain. The data reported are only those known to us at the time of writing and are often rounded. Before listing these, we start by defining bicycles and event categories, taking a historical glimpse, and examining records for climbing.

Bicycle Definitions, Event Rules, and Organizations

Union Cycliste Internationale “Standard” Bicycles

The Union Cycliste Internationale (UCI) defines “standard” bicycles used for racing in a very strict manner, specifying the “upright” configuration, two wheels, a saddle and handlebars, and countless details (see UCI 2019). Aerodynamic improvements must include a structural function and be approved. No recumbent positions, no fairings, and no vehicles with more than two wheels are currently allowed. However, extreme environmental conditions with wind and slope are permissible, as they are the same for all participants on the same track or the same road race, and the object is not speed records per se. Nevertheless, the winning times in competitive cycle racing offer an indication of what is humanly possible. They are not strictly comparable, because in addition to the variables already mentioned, it is often unknown whether performance has been enhanced by drugs and if so, to what extent.

International Human Powered Vehicle Association and World Human Powered Vehicle Association HPVs

UCI-imposed restrictions disallow records by vehicles other than bicycles as defined by its rules. Therefore, the International Human Powered Vehicle Association (IHPVA) was founded in 1976 (both authors have acted as chairman at different times) specifically to explore the areas that the UCI has banned: recumbent positions, vehicles with more than two wheels, aerodynamic fairings. It imposes no restrictions on vehicle design except the requirement of brakes and helmets and, during races and speed trials, no form of energy storage except intrinsic kinetic energy (in spite of repeated

requests to open this up as well). As the goal is to compare vehicles, although including the human factor, not so much in races as in individual speed-record attempts, the permissible environmental conditions are closely regulated: a maximum of 6 km/h wind and $\frac{2}{3}$ percent downslope in the shorter sprints.

At the time of the IHPVA's formation, these tolerances were considered small, but today's record runs for sprints include about 200 W gravitational assist and theoretically some degree of wind assist. Whereas the latter has not been demonstrated in practice with land vehicles, the former has. As noted later in the chapter, currently only one site has been identified that is nearly optimal for sprints in this respect, in Nevada, and even before this was found, almost all record-setting sites were to be found in North America. For this reason an initiative was undertaken for rule changes that would allow competitive records on other continents, and in 1997 the IHPVA was reorganized to this effect, eventually resulting in a totally new organization formed in 2009, the World Human Powered Vehicle Association (WHPVA). Today the IHPVA focuses on the North American Nevada sprint records and the WHPVA on low-altitude hour records mainly in Europe. Since 2018 the WHPVA has recognized, in a new class, sprints with no net downslope.

World Recumbent Racing Association Partially Faired (and Unfaired) Recumbents

Neither the IHPVA nor the WHPVA has ever succeeded in defining categories for partially faired HPVs, which are administered by the World Recumbent Racing Association (WRRRA), founded in 2006. Partially faired vehicles, as defined by WRRRA, may have either a front fairing, like an aerodynamic windshield, or a rear fairing, like a faired tailbox, but not both at the same time. All current record-setting vehicles are equipped with rear fairings, but a decision has been made to also allow pedal-fairings together with rear fairings.

There are many more unfaired or partially faired than fully faired vehicles. The value of the vehicles in these rather vague categories is that the vehicles are of much greater practical use than either track bicycles or record-capable fully faired HPVs. Indeed their riders often use them on public roads and bike paths both for training and as a normal means of transport.

Human-Powered Speed Seen (Pre)Historically

Prehistoric humans running barefoot were probably able to reach or exceed the speeds of unaided humans today. The first technologies for increasing these speeds or their usefulness were perhaps footwear and clothes, as well as animal skins permitting sliding down snowy slopes, which many humans surely did, and also early sleds, skis, and ice skates. The invention of the wheel some thousands of years ago and the Draisine two centuries ago did not yet result in much of a human-speed improvement, with their maximums, perhaps 15 km/h, being mostly slower than peak speeds achieved in running or ice skating. However, the development of the bicycle soon improved this greatly, and that is what most of this chapter is about.

Climbing

Many types of essentially gravity-powered speed events and also practical locomotion are indirectly human powered if the required elevation is first gained by climbing up. Climbing records are also the purest and easiest way of measuring human power with a single resistance value, as all other resistances, which are usually mixed together and not easy to separate, are small or negligible in comparison to that arising from climbing, which is the vertical displacement that increases potential energy. The latter is simply the weight of bicycle and cyclist times the increase in elevation. The average power is then this value divided by the time taken for the climb. The equipment required is a timer, an altimeter (barometer or satellite) or chart, and a way of determining the total weight of bicycle and cyclist.

With cycling records for pure climbing, the object is to increase elevation while cycling up an arbitrary slope. The record for continuously climbing the equivalent height of Mount Everest (8,848 m) is about 8.75 h, or just over 1,000 m/h altitude gain. If a cyclist plus bicycle weighed 800 N, this would amount to an average power of 222 W. Other—healthier—awards are for the greatest altitude gain within a longer period, say, one month. These are not official, accurate records, but rather self-measured data shared online. Typically cycle-climbing enthusiasts climb from 50 km to well over 100 km in one month.

A single optimal slope angle for maximum vertical speed cannot be given, as it depends on several variables. *Bicycle elevators* allow pure vertical climbing with minimal air and (depending on construction) rolling resistances, but as is quickly realized when using one, the almost total lack of inertia requires constant-torque pedaling with a good technique to get past the pedal cranks' dead centers. Climbing on a road lessens this problem but increases the air resistance.

One can climb on foot unencumbered or while also transporting an additional payload (e.g., skis and boots, food, equipment, wood for cooking and heating a mountain refuge). The best unencumbered times up a flight of steps on the Swiss mountain Niesen (1.7 km vertical and ~3.1 km horizontal distance) are about 1 h for younger men (overall record 56 min in 2011; see Niesenlauf.ch). An internationally popular challenge is the vertical kilometer, which is undertaken in many places worldwide (see, e.g., en.wikipedia.org/wiki/Kilomètre_Vertical_de_Fully). The best times are just under 30 min.

Unfortunately with such climbing records the athletes' weights are not published, so the actual power levels achieved are unknown. Using the formula $P = (m g h)/t$ (in which m is the person's mass, g is the local gravity, h is the height climbed, and t is the time taken, which works in any consistent set of units), if it is assumed that these contestants weigh 75 kg and the local gravity is 9.8 m/s^2 , with some slight interpolations, the average power level is found to be about 420 W for 0.5 h and 350 W for 1 h durations.

If loads are neglected, the *specific* power can be worked out exactly in watts per kilogram even if the person's weight is unknown, using the formula $P = g h/t$. The 2017 vertical kilometer record was 1,733 s, for a specific power of 5.66 W/kg, and in the same way, just under 5 W/kg for the Niesenlauf.

Another question—How much load can be transported uphill and how much work can be done?—was intensively studied about 1780 by Charles-Augustin Coulomb (1820), who was not only a famous physicist, but also a civil engineer interested in how to build fortifications efficiently. He observed workers and soldiers ascending hills with and without loads. Men (described as strong and weighing 70 kg) carrying no extra weight could perform with a little over 2 megajoules (MJ) work per working day, lifting only their own bodies. This was of no direct use but could be if they were “climbing”

a treadmill. Men carrying optimal loads of a little more than 50 kg uphill could deliver about one-fourth of this, 500 kJ, as direct useful work, per working day. If we assume 20,000 s for actually doing this work per day, the men were performing at 100 W when not carrying a load or doing useful work at 25 W when carrying their 50 kg or greater loads uphill.

The Need for Speed

Men, especially, are always keen to go fast, with whatever means. *Maximum* speed in cycling is not very useful but commands the interest of millions of people worldwide. Few people, however, even know that *average* cycling speeds from one point to another in real urban or suburban transportation are higher than those using any other form of transportation, as is regularly shown in “commuter races,” as an internet search term like *Bicycle wins commuter race* shows. The authors have also found their bicycles fastest for most suburban trips. Power-assisted bicycles can be even faster, but only if the work time needed to pay for them is not used in the calculation, as they are more expensive and shorter-lived than normal bicycles. Also, the use of folding bicycles in multimode travel (including buses, trains, etc.) results in the fastest long-distance trips. (Alas, this is regrettably the only mention of folding bicycles in this book.) However, scientific or popular interest is generally focused exclusively on single-mode maximum speeds.

What speeds are achievable in cycling? The answer to this question depends on both the human factors described in chapter 2 and the amounts of resistance the chosen vehicle and conditions impose, as described in chapters 4, 5, and 6. But even more it depends on the way the conditions for measuring the speed are defined, in particular, the durations and slopes, and how kinetic and potential energy storage is managed. Important are the lengths and relative elevations of course sections and in addition, their absolute altitudes. The word *altitude* is usually used when the absolute value over sea level is of interest and the word *elevation* when it is the relative difference, for example, between start and finish, that is important.

Inertia as a Limit to Speed

Any cyclist starting from rest quickly realizes that initially, rolling and aerodynamic resistances are not important, but rather the force needed to accelerate, which can at first be as high as the limbs and bicycle transmission (for the particular gear ratio) can withstand. And the longer the duration needed to accelerate up to the top speed, the lower is the available human power and hence the lower this top speed, compared to the top speed achievable without having to accelerate first by human power. The latter could be measured only by already knowing at least its approximate value and accelerating to it using artificial means: a motor, a connected towing or pushing vehicle, or a spring or steep ramp. These procedures are actually carried out and are described later; they do not really represent pure instantaneous human power, however, but rather stored human power or hybrid power. Top human-power speed in practice is thus *not* that which a human could maintain for a few seconds, but rather an *optimization* between energy needed for acceleration and the top speed achievable after acceleration.

Much more than with motor vehicles, speed records for bicycles thus depend on the chosen duration or distance. The shortest distance is zero, or, say, that covered in 1–2 s, depending on which electronic measurement instruments are used. Measuring such a top speed is easy, as almost every cycling speedometer includes a maximum speed display: one just cycles as fast as one can and checks how well one has done afterward. But there are two important considerations. Does this speed (let's call it V_{\max}) represent the work done in accelerating up to it? If it does, the cyclist must beforehand accumulate $\frac{1}{2} m V_{\max}^2$ in kinetic energy (m being the mass of cycle and cyclist). This is in addition to the rate of work (power) needed to overcome the various resistances. If this work for acceleration is done *before* actually measuring V_{\max} as in the speedometer example, this implies a *flying start* at the beginning of the measurement. The distance between actually starting from rest and the start of the speed measurement, called the *run-up*, can be limited or unlimited. If it is strongly limited, the cyclist must accelerate fiercely and may not reach the V_{\max} potentially possible before timing begins. If it is unlimited, or if the limit is quite long, the cyclist is free to start slowly, build up speed gradually, and try to reach V_{\max} just when being timed. Thus V_{\max} is a function not just of cyclists' power

during a certain period and of the characteristics of the bicycles they're on, but also of how well the power is moderated in order to best match the human output to the measuring objective.

If the work of acceleration takes place *within* the distance being timed, this implies a *standing start* from rest. For very long distances or very slow bicycles, the time needed to accelerate to the desired speed is negligible, but in all other cases it clearly diminishes the measured average speed by some amount. If the distance is purposely chosen to be so short that mainly the period of acceleration counts, this is called a *drag race*. Traditionally the quarter-mile (402.34 m) from motor racing is used. However, the cycling event of this distance is not very popular, and the best time recorded (~27 s) goes back to 1992, on a streamlined supine bicycle, achieving an end speed of 46.7 mph (~75 km/h). More recently HPV racers have carried out tenth-of-a-mile (~160.9 m) drag races. Best times are around 17 s, a bit longer than a dog takes (see Recumbents.com 2016).

200-Meter Time Trials with Run-Up and Flying Start

Cycling records started before inexpensive and accurate instantaneous speed-measuring devices were available. Practical timing distances were defined that were long enough to enable manual stopwatches to be used, and the events were called *time trials*. For a long time the shortest distance, still used today, has been 200 m.

Invariably the 200 m time trial includes a flying start. The cyclists accelerate without being timed, with a run-up that may be of an unlimited or a specified distance. Usually the idea is that they have more or less reached their terminal speed when entering the 200 m timed section. Initially almost all the rider's power goes into acceleration, and at the terminal speed almost all is used for overcoming air and rolling resistance.

Length of Run-Ups

How long should a run-up be? Traditional 200 m time trials are carried out on *tracks*. A bicycle track or *velodrome* is a circuit of a specified length in the form of an oval that has transversely sloped banks to enable cyclists to ride fast and with the resulting lean still being more or less at a right angle to the surface. For track events

the allowable run-up, according to UCI Track Regulations (see UCI 2019), varies from 2 to 3.5 laps of the track, depending on its nominal length, amounting to 800–875 m. As the whole width of the track may be used, the actual length may be as much as 50 m longer. This is enough for UCI-defined bicycles in theory, because according to the equations and data presented in chapter 4, an athlete with constant 1,000 W power could reach terminal speed in under 1 min and would require about 770 m to do so. In practice power is not constant, so it will take a bit longer, but the example shows that the UCI has set limits based on experience of what can be achieved to get the best performance and does not restrict the top speed of UCI-defined bicycles very much.

When more efficient bicycles with aerodynamic fairings are involved, such run-up distances become far too small for such vehicles to reach their terminal velocities. Figure 3.1 shows how run-up distances increase when progressing from unfaired bicycles to partially faired recumbents and ultimately to fully faired speed machines optimized especially for record-setting events. The most aerodynamic HPVs need a run-up of about 10 km if powered with 500 W. Velodrome tracks, however, are not suitable for the high speeds such vehicles achieve. (For example, the 250 m velodrome in Grenchen, Switzerland, has a speed limit of 80 km/h. The track is 7.7 m wide and is banked 13° in the straights, 49° in the curves.) Therefore, events in which the highest speeds are achieved must use roads or at least *big circuits*. The latter are usually built for testing automobiles at similar and even higher speeds. The larger ones are ovals with about 8 km circuit length, so a single lap would be the minimum for well-streamlined HPVs. Given a choice, that is, with an unlimited run-up, cyclists may use even longer distances. The outside lanes in the curves of such motor-proving circuits are highly banked, but the radii of the innermost unbanked lanes are usually large enough that HPVs don't need to use the banks. This avoids problems with any strict maximum slope rules.

Slope and Profile Effects

Some observations about the meaning of a course's *slope* and *profile* are probably in order before their effects can be considered. At a small scale the meanings are unambiguous, as they correspond to what we expect in an orthogonal frame of reference, for example,

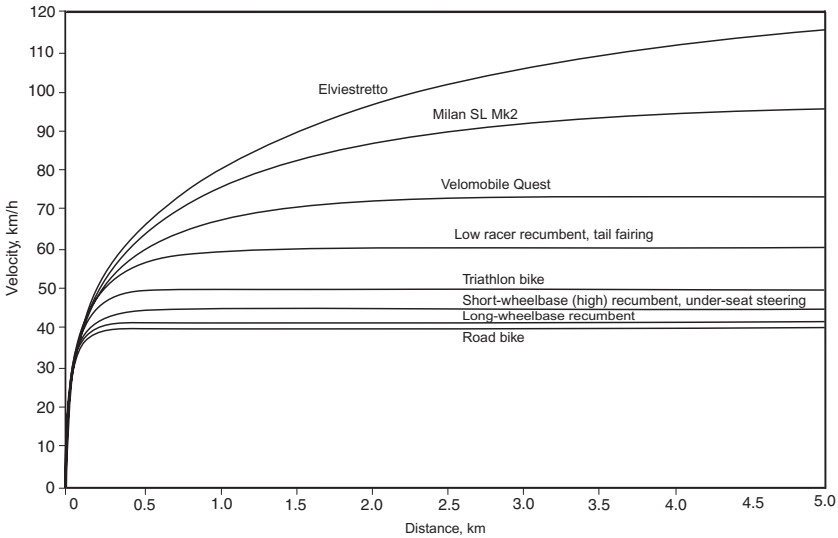


Figure 3.1

Plot of speed versus distance, illustrating by simulation the way various bicycles and tricycles, accelerating from rest, approach terminal velocity. The figure shows a road bike (lowest curve), then ever more aerodynamic vehicles up to a very optimized fully faired recumbent, which still hasn't reached full speed after a 5 km run-up. The cyclist's power output is taken to be constant at 500 W.

that a perfectly flat course viewed from the side is represented by a straight line at a constant elevation and that if there is a slope, it simply means that this line is tilted. The earth's surface, however, is not flat in this geometric sense, but curved, part of an approximate sphere with a circumference of about 40,000 km. More exactly, it follows an irregular body called the *geoid*, and this defines surfaces of equal elevation. The surface of a body of nonmoving water follows the geoid, as does a spirit level. A course's slope is thus relative to the geoid, even if the real profile is a curved or even wavy line. This ends up being largely irrelevant, however, even when satellite navigation equipment (which relates to a smoother ellipsoid model of the earth) is used, as the differences are automatically compensated for. The following discussion therefore uses the terms *flat* and *slope* in the usual sense, that is, *flat* means "having a constant elevation."

(In an attempt to help people realize all of this, the artist John K ormeling created what is probably the only large structure that is really flat in the orthogonal sense: the 9 km long Hollandweg near Groningen in the Netherlands. Compared to the geoid-following dike on which it is built, the ends are raised 1.6 m relative to the middle [see Schonen 2017]. A cyclist thus experiences a very slight downslope at the beginning and an upslope at the end.)

Surfaces other than frozen lakes or salt lakes always have elevation differences and hence slopes, which require extra propulsive power when they lie upward in the direction of motion (see chapter 4). A downward slope reduces the normal propulsive power required, sometimes to zero (coasting), or even renders it negative if power is removed as heat dissipated in the brakes. Differences of elevation give rise to two intermingled effects. One is the net harvestable potential energy $m g h$, given by the difference of elevation h between the start and finish of a course, $m g$ being the weight of the vehicle and rider. The second is the inherent exchange between the local potential and kinetic energies imposed by local slopes given by a course's elevation profile.

Pure-Gravity Records The maximum human end speed possible through the use of stored gravitational energy can easily be measured by climbing a hill and descending it. Without any equipment, a vertical drop into a body of water is already quite fast; nearly 60 m is possible without fatal injuries. The end speed of a frictionless fall would be $v = \sqrt{2 h g}$ or slightly over 34 m/s (~ 123 km/h or ~ 76 mph). Because there is considerable air drag, however, the actual speed will be less. A higher speed is possible with a higher cliff or slope and some means of braking, for example, a parachute (this is called *base jumping*) or cycling down a steep slope with a run-out permitting controlled braking. The records for this are, on a long snow slope with up to -70 percent gradient, 227 km/h with a bicycle and 255 km/h with skis at the same site (see Les Arcs 2012, Sport.ORF 2016, and Woodman 2017). Such records could be called truly if indirectly human powered if the cyclist (or skier) climbed the slope without motorized aid, which probably only divers and base jumpers do.

Gravity-Tolerated or -Assisted Records The usual object of bicycle speed trials is to remove the effects of gravity by using a course that

is as flat as possible, with a slope tolerance just great enough to allow sites available in practice. As mentioned previously, IHPVA/WHPVA rules for shorter time-trial events currently require a course's downward gradient to be no more than $\frac{2}{3}$ percent (except for the new WHPVA "pure human power class"; see definition later in the section "No-Gravity Records"), the "grandfathered" slope of the speedway used for early IHPVA events. Most motor speedways, roads, and runways have the same problem as this speedway: they are not completely flat, which has to do with the natural terrain, ground settlement, and the relative insensitivity of the powerful motor vehicles they are built for to slight gradients, so that it may not be worth the cost of getting rid of such gradients completely.

Before the effect that long, sloped run-ups have on high-speed records is examined, local-slope effects present on any not perfectly flat surface need to be mentioned. Even on round courses like tracks, or circuits with banks, or any not perfectly even stretch of road, and even when the start and finish of a course or section are at the same elevation—which does ensure no *net* harvest of potential energy—it is clear that any "hill" involves first a climb requiring either more power or a slower pace, and then a descent that either is faster or requires less or no power, and that with a "valley" it is the opposite way around. It is also plausible to assume that hills and valleys are either faster or slower than perfectly flat courses, but which is it, and under what conditions? The question is analytically elusive but well suited to computer simulations that allow an elevation profile to be entered as input. Some programs also allow a power profile to be entered, but the easier case is examined here: constant input power, which is not unrealistic, at least for mild elevation differences. The following examples using the program *Velocipedio* (described in chapter 4) are not proofs, but they demonstrate plausibilities.

Experience shows that cycling uphill is slow and downhill fast. It is plausible to assume that average of the uphill and downhill speeds of a course is slower than the speed of a level course, but is this so, and if so, by how much? Figure 3.2 simulates the speed of a road bike with a standard rider (total mass 85 kg) at constant 235 W, encountering a local 5 m hill (upslope and downslope each 167 m long, with grades of 3 and -3 percent, respectively). There are five distinct sections to this speed profile: first the constant

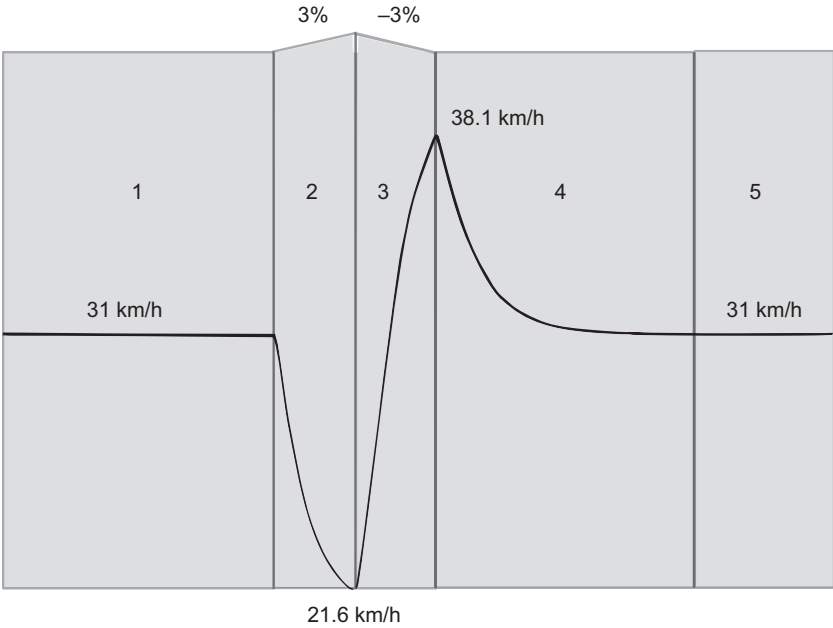


Figure 3.2

Five phases of speed variation as a function of distance, when a rider with a road bike (total 85 kg) overcomes a local elevation rising and descending 5 m over 2×167 m (simulation with constant 235 W). The average speed of phases 2, 3, and 4 is 30.3 km/h, which is (slightly) slower than without the hill (31 km/h).

steady-state speed of 31 km/h, then the climb slowing to 21.6 km/h, then the descent accelerating to 38.1 km/h, then the slowly decaying speed, until asymptotically the steady-state speed of 31 km/h is reached again.

Not shown explicitly in the figure is that the climb takes about 23 s, the descent 18 s, and the decay about 1 min. If the total distance of the three central phases is added and divided by their total time, the result shows an average speed of 30.3 km/h (or 29.3 km/h for phases 2 and 3), definitely slower than the 31 km/h without the hill, but perhaps by a smaller margin than expected. Where does the difference come from? It is due to the air drag's increasing with the square of the speed (see chapters 4 and 5). Therefore the greater drag during the portions in which the bike is traveling faster than average makes a greater difference than the lesser drag during

the portions in which it is traveling slower than average. Obviously one could come up with examples in which this is even more the case.

Note that taking just the hill itself, that is, phases 2 and 3, gives a much lower *average* speed at 27.6 km/h, but of course a much higher *exit* speed: 38.1 km/h. Basically phase 2 is the accumulation of potential energy, phase 3 the conversion of potential to kinetic energy, and phase 4 the conversion of kinetic energy to heat.

Therefore it is plausible that any local hill (or any number of hills) within a timed course leads to longer times and slower records; this would include the elevation involved in any banking a circuit might have. It is also plausible to assume that any modulation of a rider's power (without increasing average power) cannot change this. (This applies to single-vehicle time trials; for races involving multiple vehicles, other factors also apply, and courses' raised banks are and must be used for changing positions and overtaking.)

Hills (and banks) in *run-ups* are an entirely different matter. The distance and time used are irrelevant in open run-ups and are mostly secondary even in limited run-ups. What counts is the rider's speed when exiting the run-up and entering the course's timed section. Therefore the *location* of a hill in the run-up can make a great difference. If the hill or any number of hills are further away than the last phase of decay, they make no difference to the speed in the timed section, provided of course that there is no other downslope before the timed section. However, if the exit of the run-up is *within* the last phase of decay, the rider enters the timed section at a higher speed, and any associated record will be faster. This is indeed what happens in UCI 200 m track records: riders are allowed to use the banks and gain a little bit of speed swooping down from the final banked curve in the run-up. Although the use of banked curves increases the run-up's length, this extra does not count, as UCI run-ups are measured only in numbers of laps. Therefore, in a very strict sense, UCI 200 m track records from different-sized velodromes are not exactly comparable, quite apart from the additional question of the absolute altitude (air density) discussed later in the chapter.

In the case of the current IHPVA/WHPVA 200 m records for highly streamlined HPVs, hills in the run-up make a much greater

difference even though the maximum $\frac{2}{3}$ percent slope is less than the slopes achievable on the banks of velodromes. If a hill is at the very end of a run-up, the full amount of the previously stored kinetic energy is available in the timed section, minus the extra losses resulting from the higher speed. For an unlimited run-up, the extra length needed doesn't matter much, as there is no need for constant power, especially not for maximum power from the beginning. The hill can be climbed at low power, leaving even greater reserves for the descending phase. Even with rules that stipulate that the start be no higher than the finish, the rider could climb the upslope at a very leisurely pace and *effectively* start from the top. Therefore even hills with slopes of $\frac{2}{3}$ percent or less can produce considerably higher speeds than in their absence. An optimal course under the IHPVA/WHPVA rules would be an even slope of 1 in 150, 10–15 km long, which would result in a start of run-up that is as much as 100 m higher than the finish. On such a course, it might be opportune to accelerate with, say, 80 W to about 80 km/h, which would take about 5 km, then maybe even coast and rest for a short while, and then continue down at full power to an end speed of about 150 km/h. (There are sure to be better power “envelopes.”) Under such a scenario, the 100 m elevation times the vehicle-and-cyclist weight of, say, 1 kN (from 102 kg mass times g) represents an accumulated potential energy of 100 kJ. Such a perfect course probably doesn't exist, but one does exist of almost 9 km length and a very even downslope just over 0.6 percent, and it has indeed become the world's premier site for HPV top-speed events, producing astonishing speed records reviewed later in the chapter. It is on Highway 305 in the high Nevada desert (altitude about 1,400 m) some 34 km south of the small town of Battle Mountain.

Now what about dips or “valleys”? A similar simulation to the one just described, but with a 5 m valley instead, produces figure 3.3, which looks like a mirror image of figure 3.2 but shows different results. In this simulation, the average speed for the three central phases is only 21.7 km/h, whereas the two sloped phases (that is, the valley itself) produce an average speed of 32 km/h, as opposed to the 31 km/h steady-state speed. Therefore a valley within a course's timed section will *in general* lead to a *lower* course speed, but if it is located sufficiently near the finish for this to be *near the beginning of the phase of decay*, it will result in a *higher* course speed.

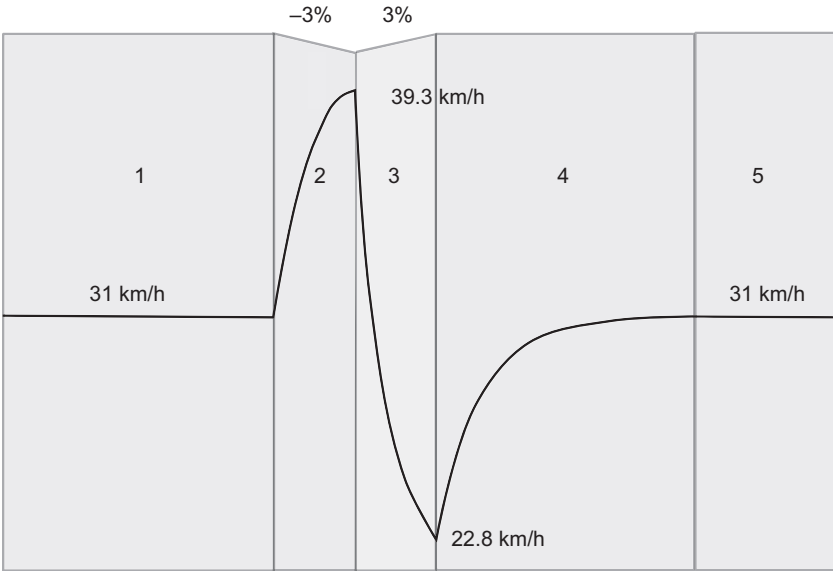


Figure 3.3

Five phases of speed variation when a rider with road bike (total 85 kg) rides through a 5 m local depression (simulation with constant 235 W). The average speed for phases 2, 3, and 4 is 21.7 km/h, which is *slower* than without the dip (31 km/h). The average speed of phases 2 and 3 is 32 km/h, which is *faster* than without the dip.

This higher course speed when there is a depression located near a course’s finish (or it represents the whole timed distance) can be plausibly explained by describing a special extreme case: the *brachistochrone* (figure 3.4), that is, the curve that, in a gravitational field and in the case of no friction and no power, allows a mass to move in the shortest time and with the fastest average speed from one point to another. Mathematically it is a cycloid and is $1/\pi$ as deep as its horizontal extension. Although in reality there is always some friction, the similarly shaped half-pipes used in skiing and skating and for BMX bikes show how it works in principle. For specific cases of friction, power, or both, there is likely to be an optimal curve for each set of conditions that is faster than any other curve or a straight line. Timed courses with such curves could thus yield the fastest possible speeds without the *net* exploitation of gravity, although there is considerable *momentary* use of gravity. Such courses allow a

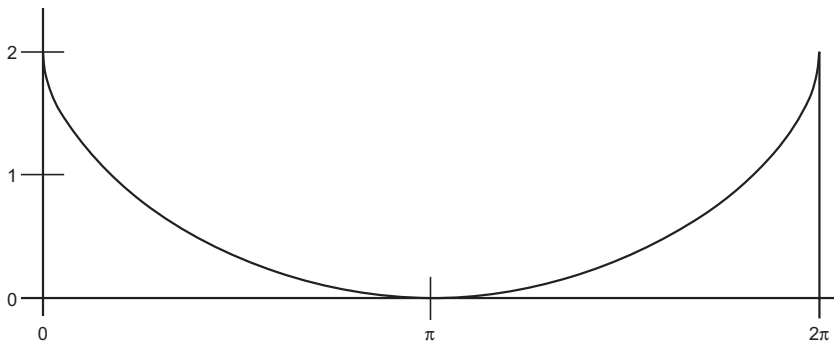


Figure 3.4

Cycloid curve called a *brachistochrone*, which describes the fastest path for a frictionless, powerless vehicle in an orthogonal gravitational field.

pretty optimal form of energy storage, as apart from friction losses the energy is completely returned to the system. In contrast that kinetic energy which is inherently stored in the vehicle's movement at the end of the course is entirely lost to the system after the rider crosses the finish line.

In an unlimited run-up, however, a brachistochrone (or any valley) is of no use, as the higher average speed doesn't count and gives rise to higher frictional losses that must be compensated for with extra human power.

No-Gravity Records The considerations outlined in the preceding section show how to specify slope conditions for record categories with no *net* gravity assist. This means that gravity or rather changes of potential energy may be used, like changes of kinetic energy, as a means of temporary storage, provided the energies at the start of the course, including run-up, are no higher than those at the finish of the course. Three conditions suffice for this:

- The finish must not be at a lower elevation than the start (including any run-up).
- A course's timed section course must not have any valleys (i.e., elevations lower than the finish), unless they are close enough to the start that the phase of speed decay is over before the finish. (Hills, on the other hand, are permissible in a course's timed section.)

- A run-up must not have any hills (i.e., no elevations higher than the start), unless they are close enough to the beginning that the phase of speed decay is over before the rider enters the timed section. (Valleys, on the other hand, are permissible in a course's run-up.)

In theory this allows closed circuits, really flat or upward-sloping routes, or any route with an S-shaped profile such that the run-up forms a valley and the timed section a hill. In practice, although every road has a large number of local S-shaped profiles, most will be too short or malproportioned to both satisfy these conditions and also be of the proper length for a desired record. However, there are likely to be a few that are suitable, and every closed circuit qualifies if its timed section represents its highest part. In 2018 the WHPVA published rules for a new “pure human-powered class” for sprints conforming to these principles. The records for this class will of course be slower than those for the traditional ones.

200-Meter UCI Track Records

The current (2013) best men's record with a UCI track bike over 200 m with a flying start is ~77.0 km/h, at an altitude of about 1,900 m. The women's record at the same location and in the same year is ~69.3 km/h. Records by other male athletes at lower altitudes are almost as fast (UCI 2014). (The effects of altitude are explored later in the chapter in the context of hour records.)

The records just mentioned and all following records are rounded and for informational purposes only. Mostly, records are given in only the most popular unit, kilometers per hour, even though meters per second would be better scientifically and miles per hour more popular in the United States. (For convenience, the conversions are as follows: $1 \text{ km/h} = 0.2777\dots \text{ m/s} = 0.621371 \text{ mph}$.)

200-Meter Partially Faired and Recumbent Records

As noted previously, there are many more unfaired or partially faired than fully faired vehicles. Typical records for unfaired and partially faired vehicles, from WRRRA 2019, all on outdoor, low-altitude velodromes, are as follows:

- unfaired, male: 63.16 km/h (2008),
- unfaired, female: 54.04 km/h (2009),

- tail-faired, male: 63.7 km/h (2009), and
- tricycle, male: 54.22 (2009).

Notably these are all considerably slower than the track bicycle records, which gives rise to some speculations: except when fitted with full fairings such as those shown in figure 3.5, recumbents are not as aerodynamically superior as usually assumed when compared to track bicycles and may be physiologically inferior for riders for the short durations involved. A further consideration is that top athletes are more likely to be found in the large field of traditional bicycle racing than in the niche of recumbent racing.

200-Meter Open Records

As of summer 2019, the fastest established speed over a distance of 200 m with a flying start and an unlimited run-up (in actuality, about 5 mi or 8 km), with a downslope of about 0.6 percent and an overall altitude of about 1,400 m, was greater than 40 m/s (89.5 mph, 144 km/h). If this run is simulated on a computer and the slope changed to zero, with everything else left unchanged, the achievable speed with no gravity assistance is about 35.5 m/s (~79.5 mph, ~128 km/h), either way an amazing achievement.

So far no records of this order have been established on flat or no-gravity courses, so what purely human-powered speeds are possible is still unknown, as mathematical corrections cannot completely represent all factors involved. All top records presently come from the almost optimally sloped Nevada site previously mentioned.

Longer-Distance Time Trial Records

Flying-start records are also maintained for a number of longer distances, notably 500 m, 1 km, and 1 mi, but records for these distances have not been tracked for both fully faired and partially faired recumbents, as well as for UCI-defined bicycles, so there is insufficient information to properly compare vehicles on courses of these lengths.

Open-Run-Up Conclusions

The preceding sections have shown that achieving the maximum possible speed with an unlimited run-up and a given vehicle and rider involves a careful optimization between the distance chosen and the cyclist's power. A 200 m record thus involves not only a

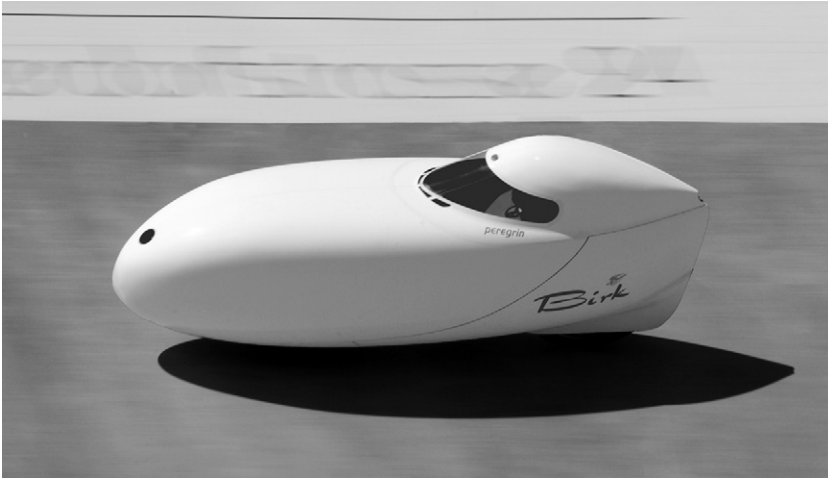


Figure 3.5

Charles Henry's PoB (Peregrin on Birk) fully faired racing HPV, with which Henry won several recent championships, even though he is nearly 60. When fitted out with rear-view mirrors, lights, and blinkers, this vehicle is usable on public roads, as it has flaps for putting one's feet down on the road. (Photo by Michael Ammann.)

low-drag, lightweight vehicle and maximum power for a certain duration, but also a good power “envelope”: optimal acceleration and perfect judgment to enable the rider to accelerate at full power just at the right distance and exit the timed section just before exhaustion—and also, as is shown later in the chapter, to choose the best altitude for doing it.

Time Trials with Standing Start

Longer time trials are carried out from a standing start, so that the rider must provide the energy required for acceleration within the course's timed section. Records are maintained for a number of distances, from 250 m through 500 m, as well as 1, 3, 4, 10, 100, and 1,000 km, although time trials for some of these distances are carried out as races, and for none of these distances are records maintained for both fully faired and partially faired recumbents, as well as UCI-defined bicycles (see Wikipedia 2019d; WHPVA 2019; WRRRA 2019; and IHPVA 2019). Records for distances covered in specific times seem more popular than those for times to cover a specific

distance, and the hour record (distance cycled in 1 h from a standing start) is the longest the UCI maintains and the most popular and best-documented category recorded for all vehicle types. The following are all hour records except where noted:

- The hour record for UCI-defined bicycles, since a rule change in 2014, has ranged between 51.11 km and 54.53 km (men) and between 46.27 and 48.00 (women). Two older and faster records, 55.29 km and 56.37 km, both for men, in 1994 and 1996, have not been surpassed since, because the types of bicycles and cycling positions then used (e.g., the “superman” position) are now banned.
- Unfaired recumbent: 57.64 km, “low altitude” (2016). This is a very extraordinary achievement, as not only is it longer than the partially faired record, but it also surpasses by a large margin the next-highest record by another man (50.53 km) and the record by a woman (46.35 km).
- Tail-faired recumbent (including faired pedals/shoes): 54.76 km, 450 m altitude (2017). (The same rider with pretty much the same vehicle achieved 248.19 km [41.36 km/h] in 6 h and 461.15 [38.43 km/h] in 12 h [both 2016].)
- Fully faired recumbent (prone position): 92.43 km, 120 m altitude (2016).

Effects of Altitude

The choice of a course’s overall altitude (elevation above sea level) allows an optimization between human performance and aerodynamic drag. The optimal altitude is also dependent on a trial’s duration, and the physiological studies discussed in this section relate to hour records.

As described in chapters 4 and 5, cycling speed in general is dependent on air density ρ , which is proportional to the local barometric air pressure P and inversely proportional to the absolute temperature T . The ideal gas law states that $\rho = P/(R - T)$, and in SI units the gas constant R has a value of about 287. Therefore at room temperature, ρ in kilograms per cubic meter is about 1.2 times P in bar (1 bar = 100 kilopascals); at somewhat below freezing, 1.3 times; and in the hot desert, 1.1 times. P is to a small extent dependent on a location’s current weather but is mainly dependent on its altitude above sea level. For example, at 4,000 m altitude, P is only 60–63

percent of its value at sea level. (There is some debate on the exact nature of the atmospheric model to use; see West 1996.) Therefore, a cyclist and bicycle at this altitude have a lower air resistance by about this amount and therefore, at the same power, a higher speed.

However, the partial pressure of oxygen at a given higher altitude is also lower by the same percentage, reducing the cyclist's maximum aerobic power. The function by which it is reduced, however, appears to be analytically elusive, so that Bassett et al. (1999) use an empirical analysis of athletes' data. They estimate that the ability of considerably acclimatized riders to consume oxygen, expressed as a percentage of $VO_2\text{max}$ at sea level, is reduced, in absolute percent, by approximately $1.9H + 1.122H^2$, in which H is the altitude in kilometers. This gives $VO_2\text{max}$ as 100 percent at sea level, 97 percent at 1 km, and 93 percent at 2 km, and for the 4 km example in the preceding paragraph, the athlete's $VO_2\text{max}$ has decreased to about 75 percent of the sea-level value.

The two effects working in opposite directions suggest an optimum at some altitude, which is clearly not at extremely high altitudes, where extra oxygen would be required even to survive, but plausibly higher than at sea level or the low altitudes where most velodromes or big circuits are located. Combining the Bassett equation with equations for cycling speed (similar to those given in chapter 4) and taking a low-altitude hour record of 56.4 km/h, figure 3.6, from Menn 2018, puts the optimum at about 3,200 m for acclimatized athletes, with a gain in speed greater than 5 percent.

Bassett et al. (1999), however, use a different resistance model and suggest that the optimum altitude for a UCI hour record is 2,000 m for unacclimatized athletes and 2,500 m for acclimatized ones. Cycling Power Lab (2018), referencing the same data, provides an online calculator, including a model for acclimatized (1 week) and unacclimatized elite cyclists, that shows that the optimum altitude is highly dependent on the chosen speed and power required for the type of bicycle and event. Depending on the parameters chosen, the optimum elevation calculated (for best speeds) can be sea level (for low speeds, e.g., hill climbs), at medium-high altitudes (e.g., bicycle hour record), or at 4,500 m or above (high speeds). This last calculation is extraordinary, as most unacclimatized lowlanders can move only very slowly at 4,500 m, as is borne out by Zubietta-Calleja et

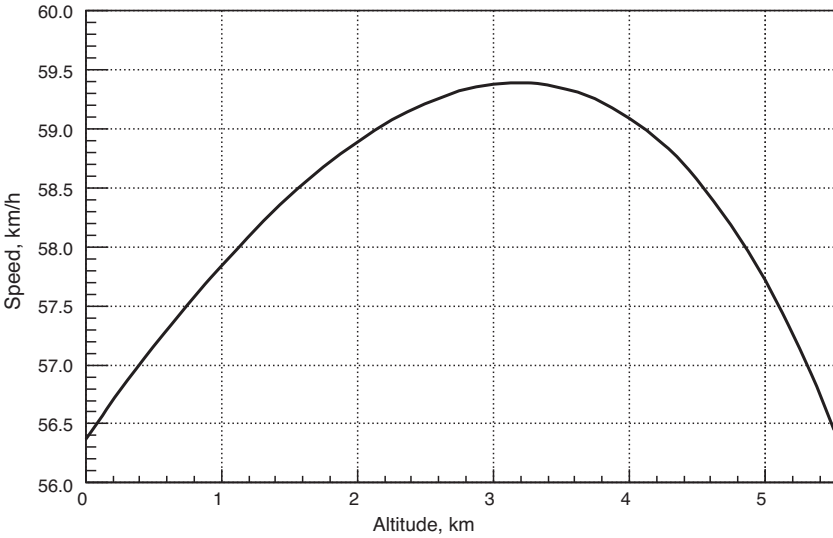


Figure 3.6
Predicted speeds for the hour record at various altitudes. (Figure by Wolfgang Menn [2018], using the formula given by Bassett et al. [1999]).

al. (2007), who suggest that full acclimatization at 4,000 m would take 6 weeks. It is reasonable to conclude either that the athletes studied are even more extraordinary individuals than expected or that the mathematical extrapolation into such rarified air does not take into account other effects that further weaken the human body.

However, the message is clear: for most speed events, there is a clear advantage at some medium-high altitude. It doesn't seem to matter to the UCI, but the HPV organizations debated fiercely for many years what to do about it, as many saw it as an unfair advantage in favor of cyclists from countries with higher mean elevations or of heavily sponsored athletes able to spend months on altitude training—or even more effective high-altitude *living* and low-level *training* (see Stray-Gundersen, Chapman, and Levine 2001). In the end, the organizations decided to list two separate categories, one each for high and low altitudes, with a cutoff elevation of 700 m between the two. This decision was finally adopted by all only in 2017, and the effect so far hasn't been great, with almost all recent short-distance records coming from the Nevada Highway 305 site at

over 1,400 m and all longer ones from velodromes and circuits well below 700 m.

Paced Records

A historically evolved specialty in cycle racing is *organized drafting*, both on the road, where teams can travel faster when close behind each other (see Trenchard 2012), and on tracks or velodromes, where the same applies but events also exist for cyclists paced close behind a very upright motorcyclist (see figure 3.7). The motorcycle-paced hour record seems to be 74.54 km (see Wikipedia 2019a), and various estimates are made for shorter peak speeds of about 100 km/h.

Blocken, Toparlar, and Andrianne (2016) show that even motorcycles (or cars) *behind* a cyclist can provide a substantial push (about 9 percent drag reduction at very short distances and ~4 percent at 1 m). They recommend increasing the present UCI rule's minimum of 10 m in following distance because of this advantage, and for safety reasons as well, there having been fatal accidents.



Figure 3.7

Motorcycle pacing, which allows cyclists to ride behind a standing motorcyclist and thus achieve speeds up to 100 km/h. (Photo by M. Engelbrecht, licensed CC-BY-SA-DE 3.0.)

Obviously, multiple cyclists pacing one another are faster than a single one, as described in chapter 5, and several events exploit this reality. Most are races, and the winners are published, but not always the times or speeds. The *team time trial* today usually involves one specified stage of a longer road race such as the Tour de France, with teams of six cyclists, or counts the fastest four of a larger team. Wikipedia (2019e) lists the best speeds for team time trials during the Tour de France as about 57.3 km/h over 67.5 km in 2005 and 57.8 km/h over 25 km in 2013. In track cycling, the *team pursuit* is carried out by four cyclists over 4 km, and the record as of 2019 stands at 63.1 km/h (Wikipedia 2019d).

Carrying the drafting idea to an extreme, some cyclists ride behind special motor vehicles fitted out with additional frontal area that removes practically all aerodynamic drag, so that the top speed measured reflects mainly rolling resistance; the vehicles are also accelerated initially by pulling. HPV pioneer and holder of several associated records Allan Abbott (see also chapters 1 and 10) told us (personal communication, 2018):

In terms of initial acceleration, all of the drafting cycling speed records over the past 50 years used some sort of help accelerating. Jose Meiffret before me was “pushed” initially by a motorcycle. I met Alf LeTourneur, who held the paced speed record before Meiffret, and he told me he was the last to have accelerated without some sort of push or pull. I was towed up to about 70 mph by a cable attached to the [towing] car. All of the subsequent paced records used an initial cable tow. ... I could ride my “Bonneville” bicycle from a standing start without assistance, however acceleration is VERY slow and a very long course would be needed. I would rather not have been towed for acceleration, however there was never enough room to get up to speed without assistance. In my case my car accelerated quite rapidly for the initial 0.25 mile, then detached and continued. ... There definitely is a “tail wind” vortex somewhere behind any pacing vehicle—the faster you go, the greater the tail wind.

Pacing may therefore do a bit more than remove aerodynamic drag. The present record for the “fastest bicycle speed in a slipstream” is 268.83 km/h (see Guinness World Records 2019).

Cycling on the Moon

The chapter now ventures into the hypothetical: cycling in a vacuum or even on the moon. Long evacuated tubes for rail vehicles are an old idea, and indeed a 1 mi version already exists in which

human-powered trips would be possible, but not very practical. Malewicki (1983) discusses the idea of a *moon bicycle*, which would benefit not only from a vacuum, but also from the moon's reduced gravity and hence reduced rolling resistance. The main resistance would then be primarily that from accelerating, assuming the cyclist has a road. According to a simulation, it would take a moon cyclist of 75 kg (including suit) on a 75 kg bicycle (including life-support system) equipped with tires with a coefficient of rolling resistance of 0.006 (see chapter 6) at a 75 W power level about 1 h and 100 km to reach a speed of 135 km/h or about 6.5 h and 1,000 km to reach the terminal speed of 170 km/h, with the limit due to rolling resistance. With less rolling resistance, the top speed would be higher, but it would take thousands of kilometers and many hours to reach at the same power level.

Because of the difficulties of cycling in space suits and the high cost of life-support systems, as well as the present lack of roads or tracks on the moon, cycling is not likely to be the first form of transportation for moon colonists. Also, the question of dynamics has not even been raised; on the moon, a bump might send a vehicle flying off great distances. However, solar-powered railway vehicles between moon bases would be quite likely, and these might have additional pedal drives for essential exercise and emergency use. And long-distance tracks laid through craters might benefit from gravitational acceleration and braking up and down the rims, as described earlier in the chapter. Or the opposite: controlled BMX-type flights over obstacles, but much longer! But maybe not: even if a cyclist's weight is only 17 percent of what it is on earth, his or her mass is the same, and crashing with any forward speed will be just as hard and potentially more dangerous.

Long Distances or Durations

Various organizations maintain a number of long-distance or long-duration records, such as the length of Great Britain; the breadth of the United States; 1 day, week, month, or year; 10,000 km; or 100,000 mi. These records are difficult to compare, because the rules vary and sleep is of course a major constraint. The Wikipedia (2019c) list of cycling records offers a good overview, as does worldultracycling.com. The furthest recorded distance in 24 h with a track bicycle is 941.8 km (585.25 mi) in 2017, and that with an

HPV 1,219 km (757.5 mi) in 2010. The record for 10,000 km yields a daily average of 441.6 km, and that for 100,000 mi, 380.5 km. Both were achieved by cycling daily on short round courses near the cyclist's home. Thus if the earth had a road going around it, with facilities, it would take 100 days to cycle around it, and with either HPVs or exceptional athletes, the idea of author Jules Verne's *Around the World in Eighty Days* could be carried out by cycling. The actual (2015) record stands at 123 days, but of course this includes crossing the oceans by airplane.

However, two complete vehicular human-powered circumnavigations have been recorded, using a variety of different vehicles, including an ocean pedal boat. One covered 75,000 km, nearly twice the minimal distance, between 1994 and 2007 (see Expedition 360 2007). The other traversed 66,300 km, using mainly rowing boats on the oceans, between 2007 and 2012 (see Eruç 2012).

Hybrid Power Sources

Records for vehicles with hybrid power sources are scientifically not very interesting, but of eminent practical interest. Therefore there have always been events for such vehicles that can make the best use of wind and sunlight and perhaps also store some of both for acceleration and hills. The Tour de Sol from 1985 to 1993 had a category for hybrid solar-human-powered vehicles (in which the coauthor participated half a dozen times), and in 2018 there was the 12,000 km (7,500 mi) Sun Trip solar bicycle race from Lyon in France to Ghangzou in China. The fastest entry took 49 days to complete the distance, for a 245 km daily average. The race started with 39 participants, about 30 of whom finished (see Phys.org 2018).

The goal in such events is not so much to get more speed—and indeed hybrid vehicles are usually slower—but rather to permit individual participation with practical and inexpensive vehicles. The human body with its many energy stores (see chapter 2) is more robust than solar-charged batteries being operated at the limit of their capabilities, and at the same time the solar assist allows the amount of food and camping equipment needed to be taken along without extreme exertion or support vehicles.

Records on Rails

Attempts to maximize cycling speed have so far focused on aerodynamics and tires, rather than on the surfaces on which they ride. Although the idea to use railway tracks for cycling came to mind early in the bicycle's development, most of these tracks are either being used by trains and not available officially or in a derelict condition. However, a few official speed competitions have taken place on good tracks and produced best sprint speeds of 70–70.5 km/h with a 1.5 km run-up (see figure 3.8 and chapter 10, p. 477). The low speed values compared to those for road vehicles reflect the smaller number of people and opportunities available to develop human-powered rail vehicles, as well as technical difficulties discussed in chapter 10.

A rail record of a different type was established by the Henshaw family: the greatest distance traveled by human power (including rider changes) in 12 h on a miniature railway track (7.25-inch gauge). They developed their own four-wheeled recumbent in 2006

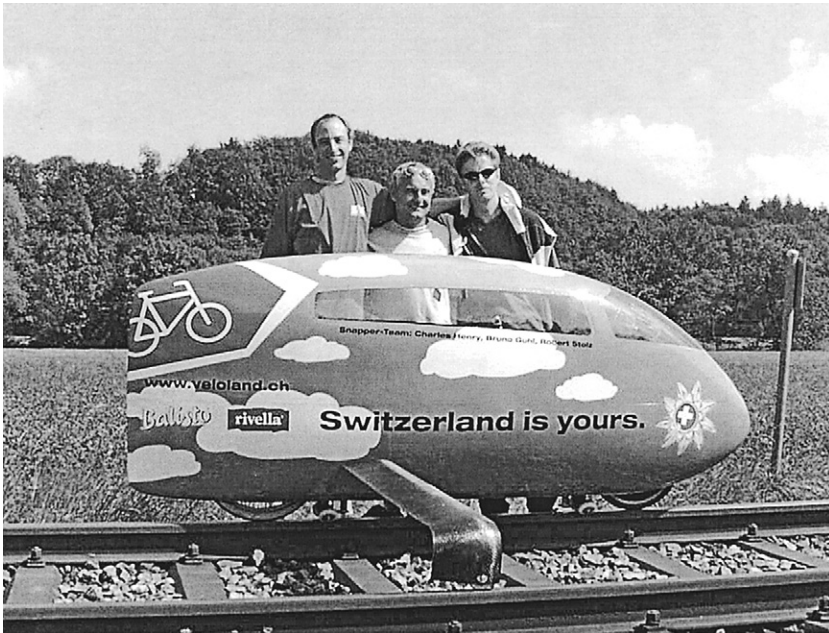


Figure 3.8

Record-breaking Snapper rail bike by Charles Henry. (Courtesy of Charles Henry.)

and attempted the record in 2018, covering 117.4 mi in 12 h, for an average speed of 9.78 mph (15.7 km/h, 4.37 m/s). This speed is slightly higher than those recorded for miniature motorized rail vehicles during 24 h (see Henshaw 2018).

Records on Ice and Snow

Cycling on ice is rarely done, not because of lack of traction, which is easily achieved with spiked tires, but because ice skating works so well. Cycling on snow is even more at a disadvantage compared to skiing, although new, very fat tires are changing this. Cycling on snow does, however, offer a special kind of speed record: the already-mentioned highest speed achieved on a bicycle downhill, more than 227 km/h (2017), much faster than on volcanic gravel at 172 km/h (2002), by the same person, Eric Barone. The fact that the record on snow is faster than the record on gravel may have more to do with safety concerns than rolling resistance, as he had a severe crash on the volcano and then switched entirely to snow.

Improving Performance: Progress or Cheating?

In cycling sports and with achievements such as records, there is both competition and a striving toward human and technological improvement. These are often considered exciting and innovative and thus are applauded. As soon as some regulatory body regulates against a particular improvement, however—absolutely or within specific categories—its further use is not recognized, and it is considered cheating or illegitimate (and may even be illegal). Sometimes new regulatory bodies are formed for a new sport or technology; then what was previously considered cheating becomes instead “forking” and thus accepted, at least by minorities. But what is in any case considered cheating by most is the purposeful use of clandestine improvements that are specifically banned.

Technological Improvements

Much of this book is about technical improvements to the bicycle, from pedals to chains, pneumatic tires, aerodynamic fairings, and recumbent seats. The UCI’s banning of the last two and the consequent formation of the IHPVA is mentioned at the beginning of this chapter. The UCI has since accepted some flexibility in its rigid

definition of “bicycle,” but it still bans recumbents and mechanically nonfunctional aerodynamic components, and events for recumbent bicycles and those equipped with such components, as well as some other vehicles, are administered by various HPV organizations. Here the problems continue, from defining *unfaired* and *partially faired* to many detailed questions even within the “open” categories that are meant to be as unrestricted by vehicle definitions as possible.

One difficult area is how much external nonhuman power is acceptable in racing and setting records. This type of power ranges from gravitational power, described in detail earlier in this chapter, to wind assistance (mentioned in chapter 5), to electric motors (covered in chapters 1 and 10 and later in this chapter) and electric power for gear shifting (allowed), to electric power for cooling purposes (not allowed). What is and isn’t allowed is determined by traditional (e.g., slope and wind rules) or commonsense reasons, as well as purely political reasons reflecting the majority opinion of decision makers at a particular time. Scientific reasons attempting to separate causes and effects as much as possible may underlie policy decisions but take second place to tradition, politics, and money.

A second related area that presents difficulties is that of stored energy. Assist motors powered by batteries, rubber bands, or flywheels, even if charged exclusively by human power only within a race or timed course, are not allowed except within certain special events or races. However, as explained earlier in the chapter, a cyclist may use large amounts of stored kinetic and potential energy acquired outside of a race’s timed sections.

Hidden motors and batteries are considered to be cheating in traditional cycle racing (*motor doping*, described later in the chapter). Racing or record categories for true hybrid vehicles like pedelecs are seldom proposed but do come up now and again, generally with limits on certain characteristics like motor power, battery type, and weight or solar-panel area. Cheating would consist of exceeding these limits and disguising that one was doing so, whereas certain other measures might be allowed, such as careful battery-cell selection and matching.

Another area in which conflicts occasionally surface are safety-related rules. Such rules are usually general and relatively lenient

(e.g., required “means of stopping,” “no sharp protrusions,” “helmet approved by a standards body.”) Helmets, however, present aerodynamic and physiological disadvantages, which provides motivation to violate helmet rules by using especially aerodynamic or thin but unapproved helmets. On the other hand, rules allow fully faired HPVs running solo on closed courses to be operated with very limited rider vision, or even with rider vision provided only through a closed-circuit video system, neither of which would normally be considered safe.

Safety rules are thus not always about safety per se, but about ensuring conditions are the same for everybody within a particular category. The use of helmets in particular can also be a requirement for some tracks and countries.

Human-Performance Improvement

More controversial than the technical issues just described are human-performance improvements, but the principle is the same: traditional and explicitly allowed measures are applauded or tolerated, whereas new methods not corresponding to majority thinking are banned or viewed with distaste. This is particularly true in the area referred to as *doping*, which is discussed later in the chapter. But first, what is accepted or allowed in regard to improving human performance? Among other things, the following are permitted:

- training (even using exotic, expensive, or potentially harmful methods)
- special foods and some chemical substances
- selection (teams or nations recruit especially able athletes)
- purchase (teams or nations employ the best athletes available)

Human performance can be enhanced considerably through the choice of food and drink and the consumption of supplementary substances, which can be eaten, drunk, breathed, or administered via skin contact or injections. Depending on context, traditions, and philosophical and political considerations, these can be defined as illegal, tolerated, or supported.

Examples of supported substances are “energy” foods or “isotonic” drinks that replenish the water, sugars, and salts consumed during activity. The record flight of the *Daedalus* (see chapter 10) depended on the consumption of about 5 L of a specially formulated drink. Or

in mountain climbing, the use of oxygen allows many more people to reach earth's highest peaks, or indeed even to survive at the high altitudes involved, than the few exceptional persons who can do so without it.

Then there are substances that in minimal quantities are an essential part of human nutrition but are also marketed as health supplements or "energy boosts," often combined with natural materials not part of normal diets. If there is no strong evidence for either harmfulness or effectiveness, such products are generally not regulated, and it is up to individuals or their physicians to consider their usage. The act of usage itself sometimes creates benefits even when the substances themselves are physiologically ineffective: this is known as the *placebo effect*.

One example of an illegal practice in sport, besides the use of banned drugs, is blood transfusions for the purpose of increasing the blood's oxygen-carrying capability; in the future, another might be genetic engineering. Such methods represent a first step in "dehumanizing" the normal human body. It may at some point be possible to incorporate into humans foreign genetic or artificial materials with enhanced properties. For example, high-performance hemoglobin based on that in lugworm blood is already being developed and is expected to save countless lives through uses in medicine. No doubt there will also be motivation to use this hemoglobin in sports as well.

There are numerous substances in between the clearly forbidden and the generally permitted. Some may be prohibited only during competition or above specified levels. Others are tolerated, such as stimulants like caffeine or nicotine or mild painkillers. Others are dangerous, giving no objective physical advantage yet harmful to the body, obviously also depending on the dosage. Stuart (2018) tests a variety of legal substances over six weeks and reports an increase in short-term power and a decrease in power in tests with 20 min duration, but he acknowledges possible errors in the latter result. He concludes that he would continue to take magnesium (an essential element found in many foods and dietary supplements) and beta-alanine, which buffers lactate production.

The less a substance can be considered traditional or harmless, the more likely its use will be defined as "doping" and be banned by sports' governing bodies or even governments. Many people

consider the use of such substances unethical. However, people also take dietary supplements and hormones, not necessarily to enhance performance in sports, but as preventive—for example “antiaging”—medicine. Yet some of these are banned. Thus the line between cheating and “normal use” is often a very fine one and can depend on the dosage and on the motivation behind the use.

Lance Armstrong’s acknowledged doping in apparently winning seven Tours de France has focused and intensified efforts to clean up the sport of cycling. This section attempts to determine how prevalent doping has been and to what extent it still is, what effect it has had on athletic performance, and what is being done to detect and prevent it.

How Long Has Doping Been Practiced in Bicycle Racing? There has been a widely held impression that doping became widespread in cycling only in the 1990s, but according to the French antidoping campaigner Jean-Pierre de Mondenard, “in the 1960s riders moved from one amphetamine to the next as they became detectable, and it’s no different now. There are around 20 products which remain undetectable and can be used to cheat. If you have undetectable substances on the market, they’re going to be used.” The sports writer William Fotheringham wrote in *The Guardian* on July 9, 2008, that the 1998 Tour de France should be known as “The Tour of Shame” because the leading team, Festina, was convicted of widespread doping and barred from racing. This affair generated enormous publicity and even its own Wikipedia article (see Wikipedia 2018b). The existence of doping in cycling has been confirmed through investigations into individuals whose performances have aroused suspicion, but in the aftermath of penalties imposed on Lance Armstrong and Alberto Contador for doping violations, some coaches and journalists have increased their assessments of its extent. Ross Tucker, writing in *The Science of Sport*, states that “in the past, doping exerted such a large effect on performance that it pushed performances beyond what is possible with normal physiology. Recent work by Pitsiladis suggests that EPO (erythropoietin) use improves endurance performance by around 5%, for relatively short-duration endurance.”

What Is the Extent of Doping in Bicycle Racing Now? With doping having been defined by the World Anti-Doping Agency (wada-ama.

org), in 2014 the UCI established the Cycling Independent Reform Commission and ordered an extensive study of doping in the sport and the surrounding investigative practices. According to the resulting report (see Marty, Nicholson, and Haas 2015), the commission “did not hear from anyone credible in the sport who would give cycling a clean bill of health” (88). A common response given to the commission, when it asked about doping on teams, was that probably three or four were clean, three or four were doping, and the rest were a “don’t know.” One respected cycling professional told the commission that he felt that even at that time, 90 percent of the peloton was still doping; another put it at 20 percent. Overall the commission’s report suggests the percentage of dopants at the time was likely to be between 14 percent and 39 percent. The last few years have seen incredible levels of doping in other sports by entire national teams and associated spying by national security agencies.

The term *doping* is derogatory. If there are substances that can be taken that enhance one’s performance and that have no known ill effects on the rider or others, they should surely be permitted, and indeed some are.

From a scientific point of view it would be important to know which performances are achieved with which methods. In this context, transparency would be more important than banning so many substances. Unfortunately this does not remove motivations to cheat anyway, with drugs that are undetectable, so performance enhancement cannot be ruled out with all but the most closely monitored performers. Doping is also banned by HPV organizations, but there are no tests to check riders’ honesty, leaving its effect on achievements recorded by such organizations undetermined. As there is no money to be gained in HPV racing, presumably the motivation to cheat is also less than in cycle racing. In regard to the top HPV records, however, the extent of doping-related cheating is simply not known.

How Can Drug Use Be Detected? In March 2014, Elliot Johnston wrote:

Dr. Yannis Pitsiladis of Glasgow University, whose team is funded by the World Anti-Doping Agency (WADA), revealed that they are on the brink of a revolutionary erythropoietin (EPO) detection breakthrough which will look for the effects of EPO in the body’s cellular anatomy rather than its presence in the bloodstream or

urine. Meanwhile, researchers at the University of Texas in Arlington, led by Dr. David Armstrong, unveiled a new screen for stimulants and steroids, which they claim is 1,000 times more sensitive than current detection methods. ... Both tests will increase the window of opportunity in which athletes can be caught using performance-enhancing drugs.

A number of high-tech systems for detecting doping are offered by the Pitsiladis team and others, and they can be very expensive, for example, as much as \$400 per test (see Witts 2017). Only well-sponsored events can afford testing at such high cost levels, so there is a race between prize-driven motivation to dope and measures to combat it.

Can Performance Indicate Doping? The question of whether athletic performance can serve as an indicator of doping could lead to painful uncertainties. Professor Ross Tucker, an exercise physiologist at the University of the Free State in South Africa, reported in 2013 on test data from the Cycling Power Lab website for a Tour de France “first big mountain finish: Ax 3 Domaines.” Two hypothetical riders, one weighing 64 kg and another 70 kg, were studied at 400 W pedaling power. The estimated time was 27 min for the heavier rider and 25.2 min for the lighter. Their data plots a little above the NASA curve for first-class athletes [in figure 2.4.]”

On the other hand, Wade Wallace, writing in *Cycling Tips* (2013), quotes the former Festina trainer Antoine Vayer in the publication *Not Normal*. According to Wallace, Vayer “took 21 of the most successful riders from LeMond to Armstrong to Evans, quantified their performances and then ranked them across an index of suspicion.” Vayer categorized as “suspicious” a power output of 410 W, “miraculous” an output above 430 W, and “mutant” an output above 450 W. Wallace quotes Vayer as saying that “of course, climbing up Alpe d’Huez in 30 minutes raises red flags, but these aren’t the types of margins we’re dealing with.”

The salient point here is that the data for several riders in figure 2.4 would be well into the mutant category. The book’s senior author entered all such outstanding achievements into this figure as the data became available and was reluctant to label Eddy Merckx or Miguel Indurain, champions who have been above suspicion, as dopers; he believed that Vayer was being too harsh. As former Australian and British swim coach Tim Kerrison is quoted in *Cycling Tips* (2013), “The best performances in every sport are outliers. So

the fact that you're an outlier alone, and the fact that the performance is exceptional alone, is not evidence that somebody is doping." A "power passport" that does not just record single events but monitors continuously an athlete's performance during training could provide stronger evidence of doping or not doping (see Hopper et al. 2016).

What Substances Are Used in Doping? The Cycling Independent Reform Commission report (Marty, Nicholson, and Haas 2015) noted earlier in the chapter, identifies "a move away from systematic, team-organised doping" (65) and suggests that riders now organize their own doping programs, often with the help of third parties who are primarily based outside the teams. New antidoping methods have forced riders to adopt doping techniques such as microdosing and, at elite level, they often have a sophisticated understanding of how and when to take substances to maximize the benefit while reducing the risk of getting caught.

The report includes a lengthy list of substances or medical products that the commission felt were either in use at the time or had been in use recently: "Some of the substances or methods used to enhance blood oxygen capacity or 'normalise' blood values are: Aicar, Xenon gas, ozone therapy, ITPP, Gas6, Actovegin, various forms of EPO such as CERA, 'Eprex', EPO zeta, EPO Retacrit, Neorecormon, and Albumina (to normalise blood values)" (62). It further lists a variety of products "that are used to increase muscle growth and recovery" (62), mainly growth hormones, but also the steroid Deca Durabolin, which dates back to the 1970s, and mentions Kenacort, a form of cortisone whose active agent, triamcinolone, was detected in Lance Armstrong's urine in testing for the 1999 Tour de France.

The report also details some "non-banned substances" (63) that the commission felt were being used to enhance performance. The following were highlighted as "substances that riders will take to gain an advantage: Viagra, Cialis and various nutritional supplements and homeopathic products: Testis, Coenzyme Compositum, Spirulina, Levothyroxine, Acetylcarnitine, Levocarnitine, Fructose; Levomefolate calcium, beta-alanine, iron products, Vitamin B12 and folic acids, Omega 3, and Oxazepam."

Some of these, such as vitamin B₁₂, are nutritional substances necessary for life. The book's coauthor takes at least four of the

substances in the list as dietary supplements, without participating in any competitive sports.

Then there were (legal) painkillers such as tramadol: a “narcotic-like pain reliever” (64), according to the report. Some of those interviewed told the commission that tramadol was used widely because it is an extremely strong painkiller—some felt that if a rider needed to take the product, he or she should not be riding. Some also thought that tramadol could cause impairment of judgment in a rider, which in turn could cause crashes. Legal in bicycle racing at the time the report was written, tramadol has now been banned (from 2019 onward).

How to deal with some of these substances, which in the right dosages are harmless or even healthy, is widely discussed. One widely held view is that despite their legitimate uses, such substances are still unfair in cycling competitions, because their use puts “pure” athletes at a disadvantage. An opposing view suggests that traditional training can be not only more harmful, if excessive, but also extremely time consuming, thus putting most nonprofessionals at a disadvantage. The same argument would apply to legal but expensive practices such as high-altitude training to build up hemoglobin.

Motor Doping

Electric–human power hybrid bicycles—often called *pedelecs* or *power bikes*, as described in other chapters of this book, have become very popular in recent years in many places. Although there exist some race categories for these and similar electrically assisted velomobiles, most cycle racing concentrates on pure athleticism, and from a scientific point of view, mixed power sources are not very interesting. Therefore almost all rules for cycling races and speed trials specify that no energy for propulsion can be stored in batteries, springs, and the like.

Whereas the first e-bicycles were cumbersome devices resembling mopeds or motorcycles, modern batteries allow a surprisingly small and light package and the consequent construction of bicycles with an unobtrusive or even invisible electric drive. One commercially available system is the Vivax Assist, which weighs about 2 kg, including a 1.3 kg, 270 Wh battery and is rated at 100 W for 100 min or 200 W briefly (though Stuart [2019] reckons considerably

less mechanical power in practice). The motor is completely hidden in the seat tube (> 32 mm) and engages the crankshaft through a bevel gear. The battery is normally housed in a saddlebag, but a “hidden performance package” is available with the battery in a fake water bottle and the controller in the seat post. The company recommends its drive as a general enhancement for sport cycling, for seniors, and for cycling in mixed groups. Aging sport cyclists especially like its invisibility. Many younger people consider assisted cycling to be cheating and look down upon utility e-cyclists. Many people take to normal pedelecs when they get old, but for some it is shameful, and they are happy to have a clandestine solution to their declining physical capacity.

Naturally this opportunity also motivates some racing cyclists to cheat (referred to as *motor doping*), and as in most races external power is clearly banned, the transgression is clearer than with the use of chemicals. The Cycling Independent Reform Commission report calls this “technical cheating” (Marty, Nicholson, and Haas 2015, 85) and considers it serious and not isolated. For the Tour of France 2018, the UCI raised the fine for using electrical assistance to a maximum of 1 million Swiss francs and greatly increased attempts at detection, with magnetic scanning, X-rays and thermal imaging—before, during and after the stages, throughout the three weeks of competition. Every one of these tests came back negative, as the UCI wrote in a press release. But in 2016, a rider in the 2016 Cyclocross World Championships was found to have a modified Vivax motor concealed in her bike, and two more incidents of the same kind have been reported since. Numerous allegations of motor usage have been forthcoming, but no actual proof has been found. Stuart (2019), writing in the UK magazine *Cyclist*, is not worried, reckoning that at least the known solutions are unlikely to escape scrutiny in professional cycle racing. The magazine also conducted a short hill-climb test featuring two similar amateurs, one on a 7 kg bicycle and the other on a 10 kg power-assisted one (see the video “Hidden Motor vs Super Bike” linked from Stuart 2019). The result was as expected (the bicycle with added battery power was faster), but by less than the difference between an average and a strong rider.

References

- Bassett, David R., Chester R. Kyle, Louis Passfield, Jeffrey P. Broker, and Edmund R Burke. 1999. "Comparing Cycling World Hour Records, 1967–1996: Modeling with Empirical Data." *Medicine and Science in Sports and Exercise* 31, no. 11 (November): 1665–1676. https://journals.lww.com/acsm-msse/Fulltext/1999/11000/Comparing_cycling_world_hour_records,_1967_1996_.25.aspx.
- Blocken, Bert, Yasin Toparlar, and Thomas Andrianne. 2016. "Aerodynamic Benefit for a Cyclist by a Following Motorcycle." *Journal of Wind Engineering and Industrial Aerodynamics* 155: 1–10. <https://doi.org/10.1016/j.jweia.2016.04.008>.
- Coulomb, Charles-Augustin. 1781/1820. "De plusieurs expériences destinées à déterminer la quantité d'action que les hommes peuvent fournir par leur travail journalier." English translation in Theo Schmidt, "Coulomb's Work on Human Power," *Human Power eJournal*, no. 8: art. 21 (2014). <http://hupi.org/HPeJ/0021/0021c.html>.
- Cycling Power Lab. 2018. Effects of altitude model. Cycling Power Lab (website). <http://www.cyclingpowerlab.com/effectsofaltitude.aspx>.
- Cycling Tips. 2013. "Can Performance Be Used as an Indicator of Doping?" <https://cyclingtips.com/2013/07/can-performance-be-used-as-an-indicator-of-doping/>.
- Eruç, Erden. 2012. "Human Powered Circumnavigation." <http://www.erdeneruc.com/human-powered-circumnavigation/>.
- Expedition 360. 2007. "Logbook." Expedition 360 (website). <http://www.expedition360.com/logbook/home.htm>.
- Guinness World Records. 2019. "Fastest Bicycle Speed in a Slipstream (Male)." Guinness World Records (website). [http://www.guinnessworldrecords.com/world-records/fastest-bicycle-speed-\(in-slipstream\)](http://www.guinnessworldrecords.com/world-records/fastest-bicycle-speed-(in-slipstream)).
- Henshaw, David. 2018. "Breaking Records: Guinness and the X4 Recumbent." *A to B* 121: 28–37. <http://www.atob.org.uk>.
- Hopker, J., L. Passfield, R. Faiss, and M. Saugy. 2016. "Modelling of Cycling Power Data and Its Application for Anti-doping." *Journal of Science and Cycling* 5, no. 2 (November). <http://www.jsc-journal.com/ojs/index.php?journal=JSC&page=article&op=view&path%5B%5D=267>.
- IHPVA (International Human Powered Vehicle Association). 2019. "IHPVA Official Speed Records: Index of Records." Revised February 1, 2019. International Human Powered Vehicle Association, San Luis Obispo, CA. <http://ihpva.org/hpvarech.htm>.
- Les Arcs. 2012. "Les Arcs—Activities." Sunshine World (website). https://web.archive.org/web/20120229090042/http://www.sunshineworldfrance.com/activities_les_arcs.php.

Malewicki, Douglas. 1983. "New Unified Performance Graphs and Comparisons for Streamlined Human Powered Vehicles." In *Proceedings of the Second International Human Powered Vehicle Symposium*, ed. Allan Abbott, 46–59. San Luis Obispo, CA: International Human Powered Vehicle Association.

Marty, Dick, Peter Nicholson, and Ulrich Haas. 2015. "Cycling Independent Reform Commission Report to the President of the Union Cycliste Internationale." <https://www.velonews.com/wp-content/uploads/2015/03/CIRC-Report-2015.pdf>.

Menn, Wolfgang. 2018. "The Hour Record at Altitude." <http://web.archive.org/web/20190428064153/http://www.wolfgang-menn.de/altitude.htm>.

Phys.org. 2018. "Belgian Wins Inaugural France to China Solar Bike Race." <https://phys.org/news/2018-08-belgian-inaugural-france-china-solar.html>.

Recumbents.com. 2016. "Drag Race Results WHPSC 9/18/2016." Recumbents.com. http://www.recumbents.com/wisil/whpsc2016/results.htm#DRAG_RACE_RESULTS.

Schonen, Rob. 2017. "Eindelijk komt er een echt rechte weg" [Finally Comes a Really Straight Road]. *Dagblad van het Noorden* (newspaper). <http://www.dvhn.nl/groningen/Eindelijk-komt-er-een-echt-rechte-weg-21940525.html>.

Sport.ORF. 2016. "Weltrekorde in italienischer Hand" [World Records in Italian Hands]. Sport.ORF.at. <https://sport.orf.at/stories/2248490/2248489/>.

Stray-Gundersen, J., R. F. Chapman, and B. D. Levine. 2001. "Living High–Training Low": Altitude Training Improves Sea Level Performance in Male and Female Elite Runners." *Journal of Applied Physiology* 91, no. 3: 1113–1120.

Stuart, Peter. 2018. "We Tried Legal Doping, and This Is What Happened." *Cyclist*, March 18. <http://www.cyclist.co.uk/in-depth/1224/we-tried-legal-doping-and-this-is-what-happened>.

Stuart, Peter. 2019. "Motor Doping Is Happening, and We've Tested It." *Cyclist*, April 23. <http://www.cyclist.co.uk/news/542/motor-doping-is-happening-and-weve-tested-it>.

Trenchard, Hugh. 2012. "The Complex Dynamics of Bicycle Pelotons." Unpublished manuscript, submitted June 5, 2012. Victoria, BC. Online. <https://arxiv.org/abs/1206.0816>.

UCI (Union Cycliste Internationale). 2014. "Historique des records hommes elite 21.10.2014" [Progression of Men's Elite Records].

UCI (Union Cycliste Internationale). 2019. Portal for UCI Technical Regulations. <https://www.uci.org/inside-uci/constitutions-regulations/regulations>.

West, John B. 1996. "Prediction of Barometric Pressures at High Altitudes with the Use of Model Atmospheres." *Journal of Applied Physiology* 81, no. 4: 1850–1854. <https://doi.org/10.1152/jappl.1996.81.4.1850>.

WHPVA (World Human Powered Vehicle Association). 2019. "Land—Men's 200 Meter Flying Start Speed Trial (Single Rider)." <http://www.whpva.org/land.html>.

Wikipedia. 2019a. "Dieter Durst." https://de.wikipedia.org/wiki/Dieter_Durst.

Wikipedia. 2019b. "Festina Affair." https://en.wikipedia.org/wiki/Festina_affair.

Wikipedia. 2019c. "List of Cycling Records." https://en.wikipedia.org/wiki/List_of_cycling_records.

Wikipedia. 2019d. "List of World Records in Track Cycling." https://en.wikipedia.org/wiki/List_of_world_records_in_track_cycling.

Wikipedia. 2019e. "Team Time Trial." https://en.wikipedia.org/wiki/Team_time_trial.

Witts, James. 2017. "The Future of Drug Testing in Cycling." *Cycling*, January 4. <http://www.cyclist.co.uk/in-depth/2042/the-future-of-drug-testing-in-cycling>.

Woodman, Oli. 2017. "Watch Eric Barone Hit 141 Mph in This Incredibly Sketchy Top Speed Run: Frenchman Tops His Own Speed Record." *Bikeradar*. <https://www.bikeradar.com/mtb/news/article/eric-barone-record-49423/>.

WRRRA (World Recumbent Racing Association). 2019. "200 Meter TT Velo—Non Faired." <http://www.recumbents.com/wrra/records.asp>.

Zubieta-Calleja, Gustavo R., Poul-Erik Paulev, L. Zubieta-Calleja, and G. Zubieta-Castillo. 2007. "Altitude Adaptation through Hematocrit Changes." *Journal of Physiology and Pharmacology: An Official Journal of the Polish Physiological Society* 58, suppl. 5, pt. 2 (December): 811–818. http://www.jpp.krakow.pl/journal/archive/11_07_s5/articles/86_article.html.

4 Power and Speed

Introduction

One of the first lessons one learns from bicycling is that more effort is required to ride fast, or uphill, or against the wind (than to ride at a more moderate speed on the level in calm conditions or with the wind at one's back). Chapter 2 characterized the power available from a pedaler for various durations. This chapter discusses what speed a given power level will enable a cyclist to achieve and under what circumstances cycling will be perceived as difficult. The chapter introduces the various kinds of drag, some of which are treated more fully in later chapters. It also explores the potential for riders to increase their speeds.

The object of pedaling, in scientific terms, is to exert a propulsive force (F_P) against the ground. To maintain a constant speed, the average magnitude of that force must equal the total force resisting forward motion, composed of

- air resistance (often called air drag) (F_A), from the motion of a bicycle relative to the air (depending on the bicycle speed and the wind speed, both relative to the ground);
- slope resistance (F_S), or what one would measure in terms of force if stationary on a hill, restrained from rolling by a spring scale parallel to the road surface;
- rolling resistance (F_R), from deformation and friction of the bicycle's rolling rubber tire and also from the deformation of the ground, if it is soft; and
- average bump resistance (F_B), on very rough surfaces.

An additional resisting force component (F_i) arises if a cyclist is accelerating, as a result of the inertia of the vehicle and rider masses. Mechanical friction in the bicycle's drive train could also be expressed as a force, but here it is treated as an efficiency and dealt with later in this section.

This balance of forces can be written as

$$F_P = F_A + F_S + F_R + F_B + F_i.$$

In this form, the equation assumes positive values for resisting forces, which could be modified by minus signs if required, for example, for an assisting slope or a strong tailwind. The value of F_P is usually unknown, as it is highly variable except perhaps when one is climbing vertically with a mechanical device, when F_P is almost totally composed of F_S (here the weight of the rider and ascending parts). In general, the quantity of interest is actually power: either the power required for a certain speed or acceleration or the power the rider is willing or able to exert.

The propulsive power P_P a cyclist provides at the driving wheel(s) equals the product of the propulsive force to the ground F_P and the velocity V of the bicycle relative to the ground. This is assuming no slipping of the tire on the road, as if it were a cogwheel on a toothed rack. (A rubber bicycle tire actually slips little on a hard surface, certainly less than automobile tires on roads, the latter doing so on the order of a few percent under appreciable torque.)

In this discussion, the bicycle's driving wheel delivers slightly less propulsive power P_P than the power P_F that the rider must produce by pedaling, which is equal to the tangential foot force times foot velocity, because of losses through transmission inefficiency, for example, chain and bearing losses. (Chapter 9 discusses transmission losses in more detail.) Propulsive power is often approximated as rider power. When greater precision is required, the equation to use is $P_P = P_F \eta$, in which the transmission efficiency η is usually between 0.85 and 0.97.

The power equation is thus (wheel power) $P_P = F_P V$ or (foot power) $P_F = F_P V/\eta$. The next sections will examine the components of F_P .

Air Resistance

In riding steadily on smooth, level pavement in still air, at or below jogging speeds (say, 3 m/s), the main resistance acting on a bicycle is

the rolling resistance of the tires. But as the bicycle's forward speed increases, aerodynamic drag grows quickly and becomes far more important.

The kind of air resistance most relevant to bicycling can be envisioned as consisting of two main components. One is that of pushing into and accelerating the air directly ahead of the rider, or bluff-body *pressure* drag. The other is that of sliding past the air, or *skin-friction* drag.

Air has a density (ρ) of very roughly 1 kg/m^3 . (See chapters 3 and 5 for a more precise measurement.) Each cubic meter of air a cyclist encounters is roughly comparable to (inelastically) colliding with a liter (or quart) container of, for example, milk: a parcel of air of that mass (m) is brought to about the vehicle's speed, then is pushed aside, where its kinetic energy is eventually lost, turned into heat. The cyclist must produce the force F_A during time t in order to accelerate the parcel to speed V (see figure 4.1), and it then has a kinetic energy of $\frac{1}{2} m V^2$ (from a standard physics formula). The parcel mass, assuming a cross section (frontal) area A , is $m = A V t \rho$, that is, the parcel volume times the air density. As the parcel is then "discarded" (in order to encounter the next parcel), its kinetic energy is lost. The work done (energy expended) in time t must also be F_A times the distance traveled, which is $V t$. Therefore $F_A V t = \frac{1}{2} m V^2 = \frac{1}{2} \rho A V t V^2$, or $F_A = \frac{1}{2} \rho A V^2$. Air drag is seen to increase as the square of the airspeed V and linearly with air density and frontal area. In still conditions the airspeed V has the same magnitude as the vehicle speed, but their directions are of course opposite.

This simple model assumes that cyclist and cycle with frontal area A encounter all air in the cross section perfectly and no more than this. This cannot be the case in reality, as the cross section A does not really punch a uniform profile through the air but entrains some air from outside of the cross section and does not accelerate all the air to the same velocity. However, it turns out that very bluff bodies do conform quite well to the preceding formula, whereas more rounded bodies like a sphere or a pointed cone experience only about half the drag for the same cross section A (see also figure 5.8). To model these variations, A is given an accompanying dimensionless coefficient of drag C_D , with the product $C_D A$ called the *drag area*. The latter is a useful quantity, as it is relatively easy to measure and allows vehicles to be compared even if their separate cross

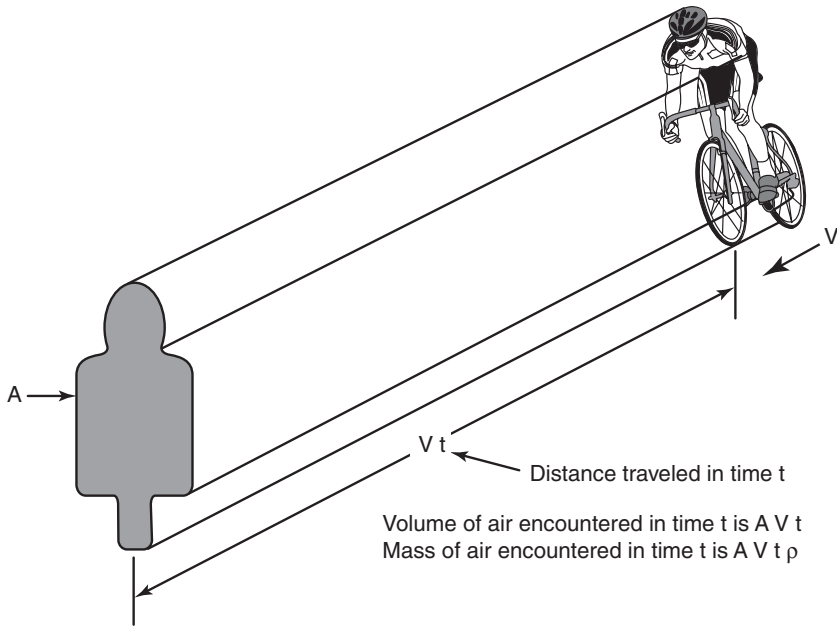


Figure 4.1
Mass of air encountered per second in cycling.

sections and drag coefficients are not accurately known or even relevant. A very large, very upright cyclist could just reach a drag area of 1 m^2 , an average racing cyclist a third of this, and cyclists on faired bicycles less than a tenth (see also table 5.1). The frontal coefficient of drag C_D by itself is also useful when it is known. It turns out that many bluff bodies, including the human one and long cylinders nearly square to the air flow, like parts of bicycle tubes and brake cables, have C_D values of about 1, making estimations quick to execute.

Our complete formula for air resistance is thus $F_A = \frac{1}{2} \rho C_D A V^2$. The derivation just given is full of assumptions and clearly does not represent a universal physical truth, but simply a very useful way of quantifying air drag. The concept is developed further in chapter 5, along with that of skin-friction drag, which becomes important when the streamlined fairings used to reduce the considerable air drag imposed by normal bicycles and their riders are considered.

Only when a streamlined fairing (smooth, with a rounded nose and tapered afterbody) virtually eliminates bluff-body drag is the

effect of skin-friction drag (intrinsically much lower in magnitude) worth considering. Skin friction can be reduced by minimizing the fairing's surface area, improving its surface smoothness, and trying to optimize the turbulence in the thin boundary layer of fluid flowing along the surface.

Conclusions on Air Resistance

The main conclusion of this elementary discussion is that aerodynamic drag force is proportional to the square of velocity V relative to the air. If a headwind V_w is present, the force involves the square of $(V + V_w)$; if there is instead a tailwind, V_w is negative. Figure 4.2 shows the power required by a cyclist on a normal bicycle in various head- and tailwinds. For example, cycling at 7.3 m/s (16.3 mph) in still air requires 100 W; in a 3 m/s headwind, the power required doubles to 200 W, and in a 3 m/s tailwind, it reduces to about 40 W. It becomes clear that wind is a vector, so a great enough tailwind generates not drag, but assistance for propulsion. If the wind comes from the side, the (true) wind vector must be added to the wind due to the forward motion, yielding an apparent wind vector

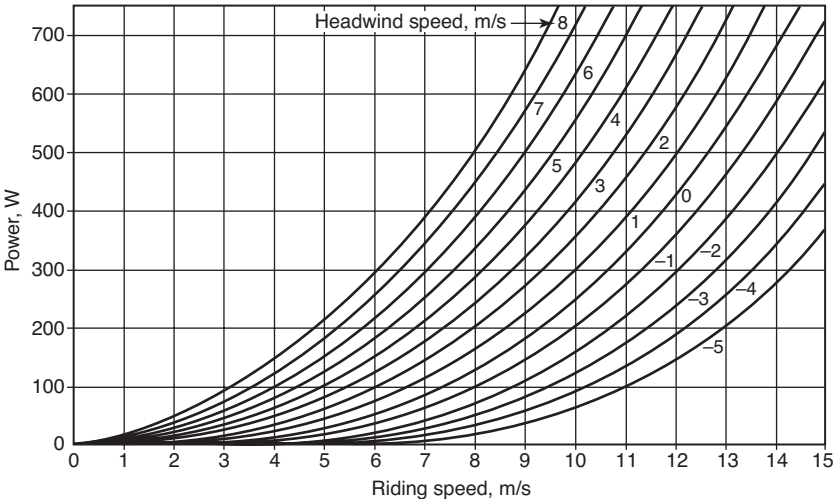


Figure 4.2 Air-drag power for a bicycle and rider with a drag area $C_D A = 0.42$ at various headwind speeds. The power assistance given by negative headwinds (tailwinds) greater than the riding speed is not shown.

coming from further forward than the true wind, as described in chapter 5.

Slope Resistance

In typical level-road riding, aerodynamic drag is the most important source of resistance that a rider encounters. However, when a rider is ascending noticeable hills, resistance from slope becomes the main factor, in part because the rider slows on hills, dramatically reducing the magnitude of the air drag.

Slope resistance (F_s) is based on the weight (mass \times gravitational acceleration) ($m g$) of a bicycle and rider and the slope of the hill up which they are traveling. F_s is in newtons if m is given in kilograms. Earth's gravitational acceleration g can be roughly estimated as 9.8 or 10 m/s^2 . The value of g is not constant but varies according to latitude and altitude and as a result of anomalies in the earth's crust. However, the variation is mostly less than 1 percent, and as a convention, the standard acceleration of gravity has been globally defined as $g_n = 9.80665 \text{ m/s}^2$. Online calculators such as that of the Physikalisch-Technische Bundesanstalt Braunschweig (ptb.de/cartoweb3/SISproject.php) can determine the actual gravity for any point on the earth. In Cambridge, Massachusetts, for example, it is 9.80387 m/s^2 ; in Cambridge, United Kingdom, 9.8125 m/s^2 ; at the North Pole, 9.8322 m/s^2 , in the vicinity of the equator 9.78 m/s^2 , and on the summit of Mount Everest, only 9.7643 m/s^2 .

Steepness can be defined either as an angle (e.g., α) or as a ratio of elevation increase (rise) per unit distance traveled *horizontally* (run), referred to as the *slope* (s), *grade*, or *gradient*. With respect to roads it is usually expressed as a percentage (s percent). As a rough approximation, each percentage point in grade is a little over half a degree in angle of inclination from horizontal. Whether distance traveled is measured horizontally, or along the slope, makes little difference for ordinary hills. For example, the old British designation of a slope as being "one in four" originally may have referred to a unit of height per four units distance traveled *along* the road. This would give a slope angle α of $\arcsin(1/4) \approx 14.5^\circ$. By the modern definition (rise/run) it would be $\arctan(1/4) \approx 14.0^\circ$. See figure 4.3 for the appearance of some grades.



Figure 4.3
Appearance of some grades.

Slope resistance depends on the vertical weight vector of the bicycle and rider, but this is not perpendicular to the road—what is relevant is its component parallel to the road surface: $m g \sin(\alpha)$. Therefore if the slope is (incorrectly) defined and measured using the distance traveled, for example, with a bicycle odometer, the arc-sine and sine terms cancel each other and $F_s = m g s$ for all slopes. However, if the horizontal run is (correctly) measured, for example, using a chart or a satellite navigation device, $F_s \approx m g s$ only for small slopes and angles. An exact solution for all angles is then given by

$$F_s = m g \sin(\arctan(s)) = m g s / (1 + s^2)^{-\frac{1}{2}}$$

Slope resistance F_s does not vary with speed. Hill-climbing power is therefore proportional to speed: $P_s = F_s V$. For example, a rider with a vehicle weighing in total 1,000 N climbing a 5 percent grade at 5 m/s will need to supply about 250 W to the wheels, in addition to a little bit for overcoming the air and rolling resistances.

Human senses can barely detect a slope of 0.001 (0.1 percent). Typical modest hills have slopes ranging up to 0.03 (3 percent). A hill with a slope of 0.06 (6 percent) is considered significant, one

with a slope of 12 percent is hard to ascend, and some roads have brief stretches on which slopes reach 20 or even 25 percent. The slope of rough terrain can exceed this, but tire-to-track friction must be good to permit climbing or braking on such terrain.

Two places in the United States that are infamous for the steepness of their slopes are Mt. Washington in New Hampshire, with an average slope of 11.5 percent over 12.2 km, and one block of Filbert Street in San Francisco, with a slope of 31.5 percent. We remember riding (or pushing!) our three-speed heavy bikes up hills in Devon, Cornwall, and Wales, United Kingdom, with slopes of 30 percent and greater. Indeed, the Ffordd Pen Llech in Harlech, Wales, is listed as the world's steepest road, at a slope of 37.5 percent.

Slope Assistance

If slope is downward, resistance becomes assistance, either decreasing the total resistance or even overcoming it and propelling the bicycle, which generally accelerates until a terminal velocity is reached in which resistance forces and the slope assistance force balance (= coasting). With steep downslopes this speed would be too high for safety and the brakes must be used, or regenerative braking (discussed in chapter 7) if available.

Any cyclist knows this, of course, but less noticed is the effect of gentle downslopes, especially with streamlined HPVs, which can coast at more than 10 m/s (22.4 mph, 36 km/h) even on a downgrade of only 0.5 percent, or pedaling with very leisurely 50 W, move along at 1.5 times this speed. Going up such a grade using 50 W, however, the speed is one-third of that going down it. The streamlined HPV thus acts as a sensitive "measuring instrument" for slopes that are so gradual as to be hardly noticeable to the eye. In contrast, if the same experiment is performed with an ordinary road bike, the down speed at 20 km/h is not very much higher than the up speed at 14.3 km/h.

If friction and air drag are neglected, the ground speed reached after descending from a given elevation h is easily calculated, as all potential energy at the top is converted to kinetic energy when $h = 0$. Thus the potential energy, given by $m g h$, must equal the kinetic energy, given by $\frac{1}{2} m V^2$. The mass m cancels out, leaving $V = (2 g h)^{1/2}$. This speed is the same whether one is jumping off a roof or rolling (frictionless) down a slope. In numbers, dropping

5 m gives a little less than 10 m/s, as g is a little less than 10 m/s^2 . A frictionless vehicle coasting from rest on a 1 percent slope will thus have reached this speed at 500 m distance. Surprisingly, a real vehicle (state-of-the-art faired tricycle) can be calculated to reach 7 m/s^2 at this distance.

The gravitational power supplied can be expressed the same way as in the expression for resistance. In numbers, a vehicle and rider weighing 1,000 N descending a 1 percent grade at 7 m/s “harvest” 70 W.

Measuring Slope

Measuring Slope on Vehicle

Cheap pendulum or bubble inclinometers are mostly designed for boats and viewing from the side, but at least two models are available for mounting on a bicycle’s top tube or handlebars and viewing from the top. Smartphones and solid-state electronic sensors can also be used, but first what exactly is measured needs to be established.

A pendulum or bubble inclinometer doesn’t just show a bicycle’s angle relative to downward but is really an accelerometer showing the direction of the bicycle’s total acceleration vector due to both gravity and change of velocity. On such an inclinometer, a change of velocity (acceleration or deceleration) physically has the same effect as acceleration due to gravity. Therefore a sensor for acceleration cannot distinguish between the two and shows the vector sum of both. A bubble inclinometer reading 10 percent can therefore mean a rider is cycling steadily up a 10 percent grade or cycling on the level but speeding up at a rate of $0.1 g \approx 1 \text{ m/s}^2$. Small angle values can be added; for example, a cyclist accelerating at 5 percent g ($\sim 0.5 \text{ m/s}^2$) up a 5 percent grade will also get a bubble inclinometer reading of just under 10 percent. Vehicle simulators (training or fair-ground) put this equivalence of acceleration vectors to good use, as tilting a cyclist wearing a virtual-reality headset can simulate the feel of both hills and forward acceleration or braking.

For measurement purposes or for very accurately controlling power-assist systems, the two vectors must be separated, which can be accomplished using a further input, for example, from a gyroscope or compass giving the bicycle’s true angle in space, or from calculating forward acceleration from the derivative of a speed

measurement at a wheel, or from a satellite navigation device. Modern smartphones or bicycle data systems often include sensors for all of these inputs but usually no consumer programs for separating and presenting the data.

Measuring the Slope of Roads Severe slopes can be measured with inclinometers or smartphones as previously described or derived from maps with elevation contours. Slight slopes are more difficult, as they are often obscured by local bumps and depressions. A survey with professional optical or satellite navigation instruments is always possible. Most of these are very expensive, but some low-cost devices are starting to appear. However, consumer-type satellite navigation or barometric devices are especially inaccurate in determining absolute elevations, though they often suffice for relative measurements.

To get slope data without actually visiting a site, as one sometimes wishes to do, one can use public and sometimes military data available in maps, databases, and online geographical information systems. Almost all of the earth's land surfaces have been mapped using various techniques, and those maps are publicly available. The accuracy varies from country to country and even regionally, as does the resolution. Satellites focus on a patch of a certain size. Data represented by a 100 m large focus patch appear to be available for all land surfaces and those represented by a 30 m large focus for many places. For roads in open planes this works quite well, but for roads adjacent to buildings and trees or on steep slopes, such data are of course rather ambiguous no matter how accurately the elevations are measured. Some topographical services sell prepared data specifically for roads.

Rolling Resistance

Tire rolling resistance on hard surfaces is never very great, so the only time it provides most of the drag acting on a rider is at low speeds on level surfaces, which is often the situation for casual low-power (50 W) pedalers, who also tend to have poorly inflated, high-resistance tires. Tire rolling resistance also predominates when one is riding with the wind or on stationary training rollers.

Whereas slope resistance is rooted in basic physical laws and can be calculated precisely, rolling resistance is founded on the

empirical observation that it takes a certain amount of force to roll a loaded wheel. Bicycle-wheel rolling resistance should probably be divided into tire resistance (which results from the tire's conforming to the much harder road) and ground resistance (which results from a hard tire's sinking into soft ground). The following is an overall view; chapter 6 discusses rolling resistance in detail.

Although ground resistance is less commonly encountered in most riding than tire resistance, in a way it is easier to understand. On soft ground or snow, rolling resistance arises from the work involved in pressing a bicycle's tires down into the surface, so the bicycle is continually climbing a slope of its own making, as shown in figure 6.10. Large-diameter or wide wheels reduce this resistance by sinking less to achieve a footprint for which the load-bearing pressure is low enough to stop any further penetration of the ground.

Tire rolling resistance is more mystifying. It is most conspicuous when one is riding on training rollers, in which, exacerbated by the small-diameter rollers, it accounts for virtually all of the drag. Even when one is riding on a road, it is far greater in magnitude than the bearing drag and the aerodynamic drag of the rotating spokes. It evidently arises from two factors.

1. Energy loss within the materials of construction. When a rubber inner tube, tread, or sidewall is bent or stretched through the application of a force, it doesn't spring back with the same force: some energy has been transformed into heat. This loss goes by names such as *hysteresis*, *viscoelasticity*, and *relaxation*. It usually depends strongly on the rate or frequency of deformation and on the tire temperature.
2. Energy loss due to rubbing of two materials (inner tube against tire at very low pressure, tire tread against road, or textile fibers against one another in the tire cords).

Both ground resistance and tire resistance increase when additional load is carried. As a rough empirical description of rolling resistance, it is usual to define the resisting force as weight supported times a coefficient of rolling resistance C_R . It is actually the force component of the weight normal to the surface; thus $F_R = C_R m g \cos(\alpha)$, or if the inclination angle α is small, $F_R \approx C_R m g$.

There is no particular reason to think that the force of rolling resistance should be exactly proportional to weight or normal force or that it should be independent of velocity, as the foregoing equation implies. Unfortunately this is an area in which too few careful measurements have been made, so there is no good basis for alternatives to the equation, though chapter 6 attempts to provide some. Tire resistance (i.e., rolling resistance on hard roads) is described by C_R values as low as 0.002 for high-quality racing tires at high pressure and as great as 0.008 for utility tires at low pressure. Even greater values may be experienced with especially small wheels.

Bump Resistance

Bumps, when encountered, unquestionably retard a cyclist's forward progress. Small-scale bumpiness, for example, as on a gravel road, is generally treated as part of rolling resistance even if much of the energy loss actually occurs in the bicycle's frame or suspension or even in the cyclist's body. This section, then, focuses on bumps large enough to cause the system's (cycle plus rider) center of mass to vary significantly.

Hitting a large bump can cause a vehicle to change direction, also upward, theoretically without energy loss through perfect elastic rebound, or stop it dead through perfect inelastic deformation. In practice both occur; for example, the vehicle is launched some distance into the air, but when it makes contact again with the ground, even if it bounces a few times, the energy associated with the vertical motion is lost, mainly by the relatively floppy human body, perhaps also by suspension dampers designed to do this. Only in very special situations, contrived, for example, by bicycle acrobats, can most of the energy be recovered by landing on a favorable ramp, allowing most of the energy to remain in the system. The same artists can also demonstrate perfect inelastic (nonbouncing) drops from some meters high, absorbing the "vertical" energy completely in their bodies.

In addition, hitting a bump induces rotation and a change of pitch or also of roll in multitrack vehicles. Assuming this rotational energy to be lost completely, the latter case is quantified for the example of wooden model gravity-powered cars rolling on bumpy surfaces (see Car Lecture 21 at pinewoodderbyphysics.com).

However, for bicycles it seems pointless to even try to calculate bump loss analytically because of the high proportion of the rider's mass that, voluntarily or not, absorbs large amounts of vibrational energy, leading to substantial energy loss.

Pradko, Lee, and Kaluzka (1966), writing on human vibration, correlate the rate of energy absorption in the human body (i.e., lost power) with a hard seat's vibration amplitude and frequency, as shown in figure 4.4. These authors also establish that energy absorption correlates well with the rider's perceived discomfort. This is a very important result, because it implies that improving vibration comfort will also reduce losses of energy that result from encountering bumps.

Based on Pradko, Lee, and Kaluzka's data, vibrational power P (in W) absorbed by their test subjects may be represented very approximately as a function of frequency ν (in hertz) and displacement amplitude A (in millimeters):

- For vibration frequencies between 1 Hz and 5.5 Hz,
$$P = (\nu^6/1,000) A^2.$$
- For vibration frequencies between 5.5 Hz and 9 Hz,
$$P = 28 A^2.$$
- For vibrational frequencies in the range of interest to bicyclists, between 9 Hz and 50 Hz,
$$P = (\nu^{2.6}/10.75) A^2.$$

Regrettably it is not possible to determine from Pradko, Lee, and Kaluzka's paper whether "displacement amplitude" refers to peak to peak, half that, or something else.

The highest power absorption charted by Pradko and colleagues is 2,000 W, and the lowest is 2.7 W. Evidently, intense bumpiness can dissipate thousands of watts and potentially slow a speeding bicycle in seconds. More widely relevant are roads on which bump losses are of a magnitude similar to those from tire rolling resistance. Of course, riding over most bumpy surfaces will not generate a single frequency of vertical movement. A spectrum of vibration frequencies is instead to be expected, perhaps with fairly distinct peaks at a few different frequencies. In such cases, the displacement amplitude of each frequency should be calculated (by treating it alone), and the results then added together. Pradko and colleagues' work

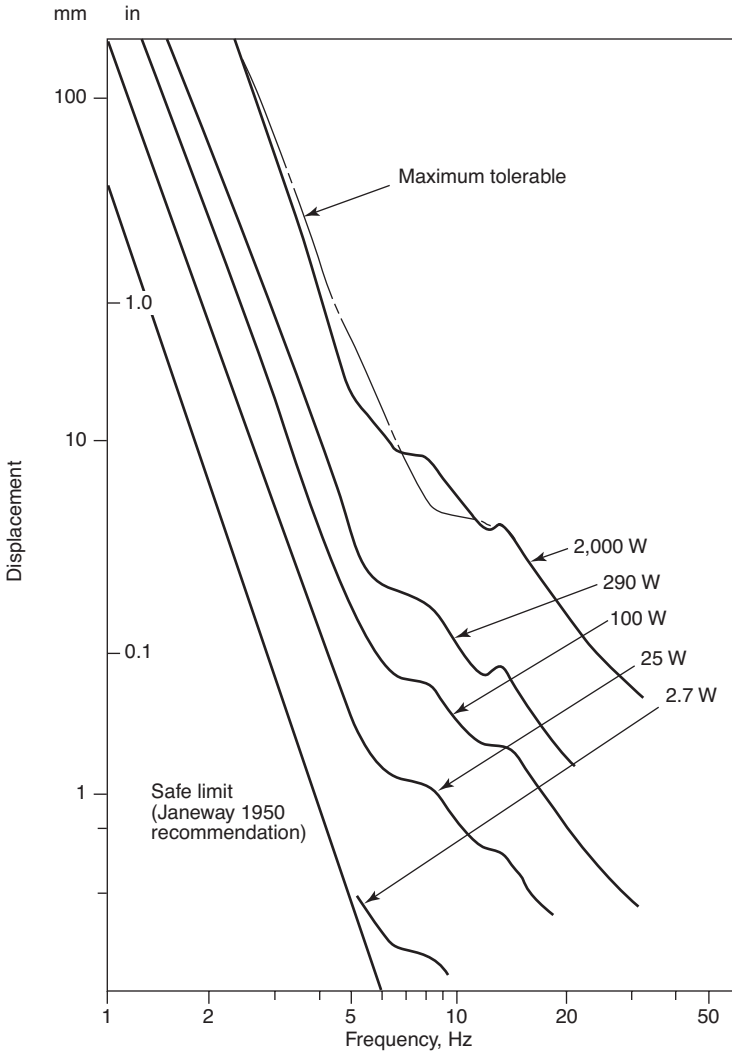


Figure 4.4 Power lost in vibration, as a function of amplitude and frequency. (From Pradko, Lee, and Kaluza 1966.)

implies that a computer can predict the energy loss of a rider on either a rigid or suspended bicycle by building a multipart mechanical model of the rider. Wang and Hull (1996) do exactly this and model losses due to the rider's action. (This is not really bump resistance, but a further form of resistance caused by propelling a suspended bicycle, even on a smooth road.)

Determining and Minimizing Bump Losses

There are no sensible, simple formulas for expressing bump resistance as a function of road condition, tire construction, inflation pressure, suspension details, and speed, and anyway, most roads are reasonably smooth, so this chapter's graphs and expressions for power leave out bump losses. The omission is admittedly a shortcoming, particularly for those whose riding is primarily on irregular surfaces.

The best way to measure bump losses is likely to be with an on-road power-measuring device, riding the same path with and without standardized bumps. Heine (2012) compared bicycles pedaled at 16 mph (≈ 7.2 m/s) on a smooth road and over *rumble strips*. These are transverse depressions milled into a road surface, not quantified in Heine's article, but common specifications show three or four depressions per meter, measuring 175 mm in the direction of travel, with a minimum depth of 13 mm. Heine used a PowerTap instrument (see "Measurement of On-Road Power" later in the chapter) to measure 183 W needed for the smooth road and 473 W for the part with the strips, an increase of 290 W. He was able to reduce the losses by one-third by using wider tires than usual and also a bit by using flexible steel forks or telescopic forks with springs and shock absorbers. The latter were, according to Heine, not especially efficient, but more comfortable in use.

The speed loss caused by a bump is minimized by reducing the force of a bump on the bicycle via tires, suspension when present, and most commonly intentional rider control of upper-body motion or stiffness. Tires and suspensions do not perform exactly the same functions in this regard. The most valuable attribute of tires is that they "swallow" small road irregularities such as pebbles; a rigid steel wheel with very low rolling resistance encountering the same small irregularities would be launched into the air or demolish the pebble (inelastic deformation). Enveloping a pebble with a tire,

on the other hand, produces very little extra force and so does not lift or jolt the rider. In addition, the slight retarding force produced when the tire is absorbing the pebble becomes a nearly equal propulsive force when the tire is leaving it (elastic deformation). It is thus plausible that wider, lower-pressure tires are superior for rough ground. Some proponents of wide tires even claim lower resistance on roads of ordinary roughness, and currently racing cyclists are moving away from the traditional very narrow, very high-pressure tires for somewhat wider ones.

When an obstacle encountered has a much bigger surface area, like a large step change in pavement height, tires are far less “soft.” Even low-pressure tires with wide cross sections are inferior to bicycle suspensions in this regard. The coauthor has test-ridden a small-wheeled bicycle with radical suspension that allowed it to be ridden at full speed up pavement steps with no feeling of discomfort and very little retardation.

Besides a means of allowing the bicycle’s wheel(s) to move relatively to the frame, a suspension needs in minimum an elastic spring element like a helical steel spring. Without an additional damping element (frictional or hydraulic), this element will, however, tend to oscillate, especially near the inherent resonant frequency of the mass spring system that the bicycle, rider, and spring constitute. Springing and damping are often provided by the same element made of rubber or another strongly damped material.

Although such suspensions improve comfort and often speed, they are designed to remove energy in the damping element, which is then wasted. *Regenerative* shock absorbers are, however, available for heavy vehicles. They produce electricity either directly from their movement or indirectly by hydraulic means. As up to several kilowatts are mentioned in various sources, if such shock absorbers could be developed for bicycles, they could at least power equipment or extend the range of e-bicycles.

The ultimate in suspension is an active system that senses bumps and adjusts springs and dampers automatically. With “massless” wheels and perfect control, smooth, efficient rides could be assured in many cases. Present systems of this type for expensive cars probably increase comfort, however, more than efficiency.

By far the greatest capability for traversing or absorbing bumps is that inherent in the human body. The body’s range of travel and

ability to absorb energy outstrips the hardware of any ordinary bicycle suspension. In addition, human adaptability or even active compensatory motion makes a huge difference. Jim Papadopoulos reports having had the experience of striking a bump in the dark unprepared and being thrown from his bicycle, whereas the same bump, traversed in the day, was barely felt. Part of the difference is simply a matter of “softening up” the arms and torso or even standing slightly, thereby unweighting the saddle, with the intention of allowing the bicycle to move up independently. A further strategy is to “lift” the bicycle over the obstruction, which involves far less of an energy change than having one’s entire body suddenly accelerated upward. Riders of long recumbent bicycles cannot do this, but recumbent seats are often flexible or padded.

Acceleration

So far this chapter has mainly considered forces corresponding to a steady cycling speed. If a cyclist is, however, accelerating or braking, another force component F_1 arises, equal to $m_{\text{eff}} a$, in which a is the change of velocity (dV/dt) and m_{eff} is the “effective” mass, which is slightly greater than total system mass m because it includes the inertial effect of the rotation of the bicycle’s wheels. Approximately, m_{eff} increases m by the mass of the tires and rims (these are thus counted twice) and one-third of the spokes. For most purposes, this slight difference is unimportant.

The equation $F_1 = m_{\text{eff}} a$ is not very useful in a manual calculation, because the acceleration a is generally not known. F_1 is the difference between the resistances so far described and the propulsive force the rider supplies (plus that from any downward gradient or strong tailwind). When a cyclist starts from rest, F_1 can initially be very high, if a medium-low gear and high peak power are employed, but soon becomes low at any appreciable speed. This is why a rider on a light bicycle in the right gear can beat most automobiles in moving away from stoplights but is overtaken after a few dozen meters. Therefore this rapidly changing force is not very amenable to manual calculations, but it can and must be used in spreadsheets and other programs that simulate time-dependent performance.

Power Required at a Given Speed

As a starting point for calculating the power required at a given speed, it can be assumed that—as an approximation, at least—of the forces of resistance that a cyclist encounters, only air drag is important. This is a fairly accurate assumption at airspeeds above about 7 m/s, if streamlining is poor and the road is level. Then the expression for drag power is $P_A = \frac{1}{2} \rho C_D A (V + V_W)^2 V$, in which V_W is headwind speed and V is bicycle speed, both relative to the ground and taken in the same direction.

Figure 4.2 shows air-drag power as a function of speed for a rider in a nonaerodynamic position ($C_D A = 0.42$) encountering various headwind speeds (including some tailwinds: these have a negative sign in the figure). Figure 4.5 shows total power as a function of speed for vehicles with various aerodynamic drag factors. (Rolling resistance's small contribution is not shown separately.) Achieving high speeds on a level road at any given power obviously requires a low value of $C_D A$. The figure assumes the following values:

- roadster (utility) bicycle (i.e., heavy utility bicycle with high-loss tires and an upright rider position): total mass including rider 93 kg, $C_R = 0.008$, $C_D A = 0.6 \text{ m}^2$
- sports bicycle: 86 kg, $C_R = 0.004$, $C_D A = 0.4 \text{ m}^2$
- road-racing bicycle: 84 kg, $C_R = 0.003$, $C_D A = 0.3 \text{ m}^2$
- commuting HPV (practical faired human-powered vehicle = velomobile): 97 kg, $C_R = 0.003$, $C_D A = 0.1 \text{ m}^2$
- ultimate HPV (i.e., “ultra” racing): 90 kg, $C_R = 0.002$, $C_D A = 0.048 \text{ m}^2$

For a complete solution, with all the force components of $F_p = F_A + F_S + F_R + F_B + F_I$ determined, the aerodynamic, slope, rolling, bump, and acceleration resistances can be used for calculating the real value of interest: the rider's required (foot) bicycling power P_F , which equals propulsive (wheel) power P_p divided by mechanical efficiency η :

$$P_F = F_p V / \eta = (F_A + F_S + F_R + F_B + F_I) V / \eta,$$

with V as the bicycle speed, and assuming no tire slip.

For steady-state riding at a given speed, that is, with $F_I = 0$, the calculation is straightforward and can easily be done manually or

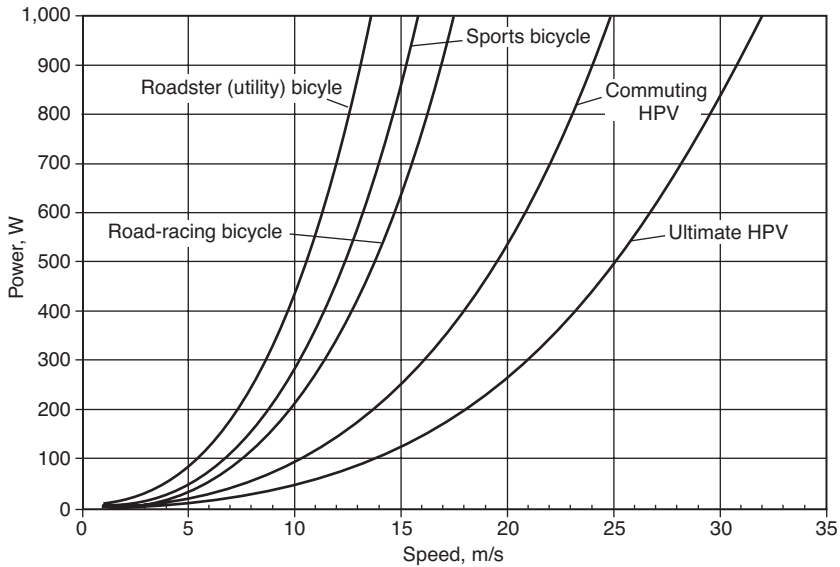


Figure 4.5

Power required to propel various bicycles in still air on the level, with the values given in the chapter text.

with a pocket calculator. A more advanced way to use this formula is to plot power as a function of speed with one’s own choice of parameters. This is easily achieved with a computer spreadsheet. One useful way to lay out the calculation is to let each row of the spreadsheet correspond to a different speed. Then within one row, the first column can be F_A , the second F_S , and so on. This makes it easy to see each term’s relative contribution, and the spreadsheet’s diagram function can be used to plot power curves as in figure 4.6. Or one can use one of the online calculators or other programs available; see “Online Tools and Simulations” later in the chapter.

Speed Achieved at a Given Power

Calculating the speed when the power is given is more difficult than vice versa. The simplest way is *graphical*: plot the power required as a function of speed as described in the preceding section and use the diagram in reverse to find the speed associated with a particular power.

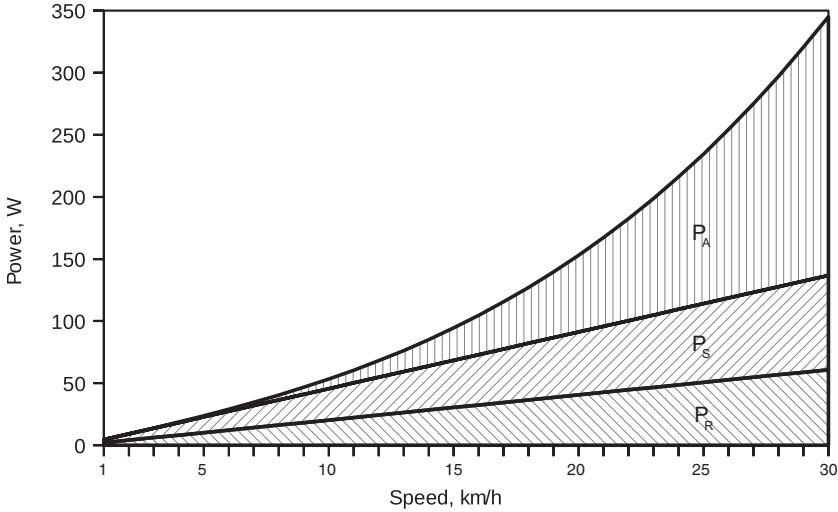


Figure 4.6

Power plot for a roadster bicycle (total mass including rider 93 kg, $C_R = 0.008$, $C_D A = 0.6 \text{ m}^2$) ascending a 1 percent slope. The powers for rolling resistance P_R , slope P_S , and air drag P_A are shown as areas, with the top line representing the total P_T .

The third edition of this book included a section explaining how to use a spreadsheet to produce *iterative* numerical solutions. Some spreadsheet programs can do this nearly by themselves by allowing iterative (circular) references: a cell containing a formula is allowed to refer to itself and recalculate itself over and over until all values (perhaps) match up. Often, however, no solution is found. Schmidt (2019) gives an example of such a spreadsheet and other more useful ones using the following methods.

An *analytic* solution is more elegant. Snyder (2004) shows that a depressed cubic equation must be solved and provides a formula and spreadsheet containing this. Lieh (2006) derives other equations, however, that give exactly the same results, and also provides a program for solving and plotting them, using a two-dimensional bicycle model.

A bicycle viewed from the side has two wheels and an elevated center of mass. If this is taken into account and the wheels are treated separately, even with sufficient power, there clearly will always be a maximum speed for every set of conditions, as above this the bicycle would start to flip over backward longitudinally.

Youngsters do this routinely; staying on one wheel under control is a maneuver known as a *wheelie*. Below this point, the maximum speed reached is determined by the power input. Lieh's equations are too extensive for a pocket calculator or to show here but are manageable with a spreadsheet.

The calculations and plots discussed so far do not include acceleration, even if it might look that way. They represent multiple steady-state solutions without acceleration, that is, for the power required to reach a given speed very slowly (theoretically infinitely slowly). Finding out how a cyclist and cycle perform over a stretch of time or distance with, for example, a constant power input involves performing a simulation. A spreadsheet can do this, but it does require some programming.

Lieh's (2006) analytical solution can also be used to plot simulations that consider inertia, in particular, speed as a function of time. Files are provided with Lieh's article that run in the Matlab and Scilab and (partially) Octave programming environments. Archibald (2016) also examines power equations in great detail in two and three dimensions and provides scripts for Matlab.

Online Tools and Computer Simulations

A number of online tools are available for calculating and plotting speed and power as discussed in foregoing sections—and more. A comprehensive website of such tools that has long been available is Compton 2001, which performs a wide variety of bicycling speed computations, including both variations of the power equation discussed earlier. In addition, it can run simulations and provide small plots.

A most useful site is Zorn 2008. Walter Zorn died in 2009, but his site is still being maintained. It uses the same equations discussed earlier, and they are presented in detail. Multiple speed-power diagrams are available, but no dynamic simulations.

Many other online power-versus-speed calculators can also be found online. A useful one is Gribble 2018, which also provides a nice plot of the different components of resistance.

The next advance in simulations is to model not just vehicle and perhaps rider, but also course, in two or three dimensions. One program that does this is Teufel's (2019) *Velocipedio*, a highly effective

program for personal computers that can take measured tracks as input in the form of Global Positioning System (GPS) data. The program uses the same equations discussed in previous sections, with parameter files modeling vehicles and riders and the altitude profile derived from a GPS track. A track's lateral curves are considered in the calculations, to limit vehicle speeds to values that are rideable without the vehicle's losing lateral traction.

Measurement of On-Road Resistance and Power

Determining the parameters of bicycle resistance is not a simple problem, partly because of the conditions in which cycling typically occurs: the air is rarely still or even constant in velocity (wind can gust or change direction within a few seconds). The road is rarely level, or even constant in slope, and even surfaces that appear smooth can vary in roughness. These considerations mean that casual outdoor coastdowns or terminal-velocity trials with an electronic speedometer yield only the crudest estimates of power. One is forced either to measure rapidly changing road conditions or to experiment in a large building.

The best data regarding the parameters that affect bicycle resistance are derived from wind tunnels and tire-drum testers. Of course, approaches based on these data still have some deficiencies. Wind tunnels generally lack a moving ground plane, and wheels of bicycles used in wind-tunnel tests often don't rotate (and rotational torque may not be measured when they do). Drum testers are not flat like the road, rarely are rough like the road, and may not be able to furnish temperature extremes.

In previous decades, some careful on-road drag tests were performed. In 1974 Chester Kyle conducted coastdown tests on corridors inside a large building between timing traps, and Kyle and Burke (1984) developed a heavy tricycle of especially low frontal area for coastdown studies with a minimal air drag ratio. Doug Miliken (personal communication, 1991) made aerodynamic comparisons by simultaneously coasting two bicycles (presumably with equal weights and tires) down a long hill. Such an approach subjects both vehicles to the same wind gusts and local slope variations. Since then experimenters have done a great many coastdown tests, usually to obtain resistance data for tires.



Figure 4.7
PowerTap measuring instrument. (Copyright Graber Products, 2001.)

In the 1990s practical on-bicycle power-measuring equipment became commercially available. If used carefully, it can allow bicycle resistance parameters to be determined with reasonable accuracy. An example is the original PowerTap system, shown in figure 4.7. A torque-sensing transducer and a speedometer are built into the rear hub, and data are wirelessly transmitted to a computer located on the bicycle. A competing system is the SRM, which is built into the bicycle's crankset. Since the first of these devices were introduced, more than a dozen manufacturers have developed a bewildering number of similar products measuring forces acting on components from the pedals to the wheel. They may measure before the chain (or other transmission) or after, and this must be kept in mind for calculations. Systems that measure directly at the pedals can, like the others, provide data on average forces and powers, but their value is mainly in examining the instantaneous magnitudes and directions of pedal forces.

Pedaling power is highly variable, so all instruments for measuring it require the ability to average data. For example, during each revolution of a bicycle's crank, the instantaneous power of a seated rider may vary from small values to several kilowatts (see figure 2.5). Also, a rider will occasionally ease off for a few pedal strokes, creating a significant variation in power level. On top of this, virtually

unnoticeable little rises or wind gusts can easily lead to a considerable variation in power. For testing purposes, it is best to seek out nominally constant conditions and then to determine the average power under those conditions, for several minutes, at least.

An instrument that measures and averages power can be used in two ways. One is to measure the power a rider can produce for various durations (i.e., the power-duration curves of chapter 2). The other is to evaluate the power required to ride in a certain fashion (e.g., at a certain speed or accelerating in a sprint). To achieve good results with such an instrument, careful protocols are needed. Increasingly a third method is used: the instrument records (highly variable) data during normal riding and training, which is then analyzed and presented using software provided by the instrument suppliers or specialized services.

On-Road Determination of Aerodynamic and Rolling Resistances

In the absence of a wind tunnel and a tire test stand, a reliable on-bicycle instrument measuring total power is the next-best method for deriving aerodynamic and rolling drag, provided speed and the effects from slope, acceleration, and drive train efficiency can be separated. Around a circuit, in particular, the average slope drag is zero. Acceleration and deceleration also cancel between instances of equal speed.

The approach for obtaining good measurements is to find a riding circuit on which it is safe to travel without any use of the bicycle's brakes, which would spoil the measurements. The circuit should be as level as possible, and unless totally shielded, preferably out in an open area, so that wind is not gusty or funneled at any location around the circuit. No wind at all is of course ideal, as from an indoor facility. However, chapter 5 describes possible corrections for wind.

The measurement scheme involves riding several laps at constant speed, with a flying start. There are several reasons for seeking to fix speed rather than power during a trial. Some are mathematical: for example, the effects of varied slope or headwind on power can be calculated easily for a fixed speed, but determining their effects on speed at fixed power requires the somewhat difficult power equation to be solved, as noted earlier. Furthermore, speed changes are slower than power changes because of the bicycle and rider's inertia,

and holding power constant seems considerably harder than holding speed constant.

Both average power and average speed should settle down to relatively constant numbers after a few laps around the circuit. Still, there may be visible variation within a particular lap due to wind or slope, so it is important to end the measurement by crossing the starting line at the same speed as when starting out. The data to be recorded are average speed and average power. Today's instruments are provided with software, or separate third-party data-analysis software is available to display these.

The essence of generating a drag curve is to repeat the test at a number of different speeds. It is essential that throughout the trial for a particular speed, and also for every different speed evaluated, body position and clothing should be identical. If wind cannot be avoided, it is preferable that its average velocity be the same for each trial.

However many different speeds are attempted, they should initially be plotted according to the value of V^2 . Therefore it is desirable to choose speeds with roughly equal intervals between their squares. (For example, speeds of 3, 6, 8, 9.6, and 11 m/s have squares of 9, 36, 64, 92, and 121.) The trials involving the various speeds should be conducted in a random order so that a progressive change in temperature, wind, or other factors will not introduce a variation that might otherwise appear correlated with speed.

Data for all speeds should be plotted on a graph as a function of speed squared, because as shown earlier in the chapter, propulsive force on the level is more or less the sum of air drag and rolling resistance: $F_P = \frac{1}{2} \rho C_D A V^2 + m g C_R$. In other words, if the theory holds and the data are of good quality, then the data points will fall on a more or less straight line and even with large variations can be evaluated using the linear-regression commands in most spreadsheets or through an eye fit. The slope of the line is $\frac{1}{2} \rho C_D A$, and the intercept at zero speed is $m g C_R$, thus separating the coefficients of air and rolling drag (see figure 4.8). Although this presumes that both coefficients are independent of speed, which is not exactly the case, any large deviations from a more or less straight line point to a change in conditions or a recording error, and a slight systematic deviation will indicate a speed effect, as shown in the figure by the

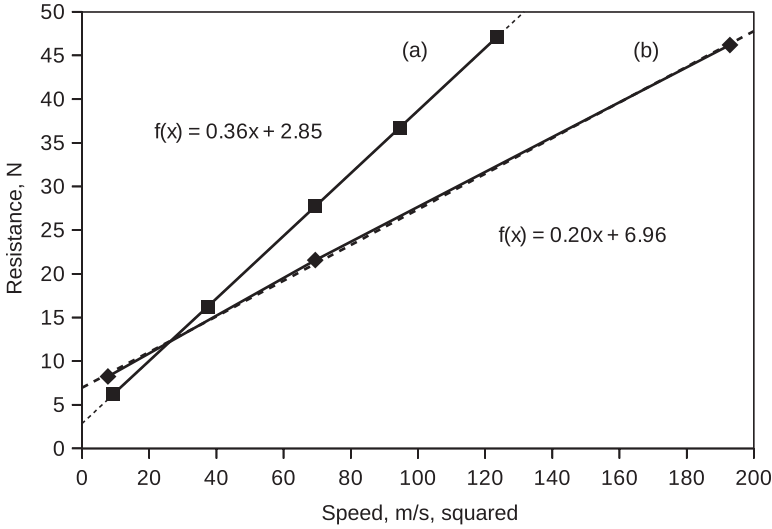


Figure 4.8

Drag versus speed-squared for two cyclists and bicycles: (a) $m = 85$ kg. Dividing the intercept of 2.85 by $m g$ yields a C_R value of about 0.0034. Dividing the slope of 0.36 by $\frac{1}{2} \rho$ gives a $C_D A$ value of about 0.6 m^2 . The straight line is perfect because all data are calculated, not real. (b) Aerodynamic bicycle and rider with separately measured wind-tunnel and rolling resistance data (from Shimano 1982) giving a value for $C_D A$ of about 0.33 m^2 . The value for C_R works out to be a surprisingly high 0.0083, and the small deviation in the curve shows a slight speed dependency.

slight curve in one plot. (The figure is provided only to illustrate the principle involved, in the absence of real on-road data sets.)

Comparing trials with different temperatures reveals that temperature can have a sizable effect on rolling resistance in addition to its effect on air drag through air pressure. In particular, rolling-resistance results in warm conditions are impressively low. (This suggests it may be important to control, or at least measure, *road surface temperature* when comparing the rolling resistance offered by two tires. Measurements on home exercisers, in which rolling has been found to get easier as the tires become warm to the touch, bolsters this hypothesis.) Comparing trials on the same day shows that $C_D A$ from shedding winter clothing reduces $C_D A$ more than crouching.

Once a linear regression is performed on the data obtained and the rolling resistance and aerodynamic drag coefficients obtained, it

is then appropriate to plot power curves based on those parameters in a similar manner as in figures 4.5 and 4.6.

Comparing Drag in Trials under Different Environmental Conditions

The preceding section alluded to the effect of temperature on rolling resistance. Determining which of two tires is better or worse obviously requires that they be compared at the same temperature. If that is for some reason not possible, some means for extrapolating to a reference temperature must be developed.

Similar concerns arise for measuring aerodynamic performance. If the drag of two setups is compared based on trials from different days, what has happened to the air density between the two days? One needs to know the air temperature and the barometric pressure to make this determination.

By far the greatest problem in this regard is wind. In most areas of the world, it will not reliably vanish at a convenient time. Even if the average wind speed during a trial can be determined, how can the data obtained be corrected to reflect windless conditions?

An often-made simplification is to assume that when a steady wind blows across a circular course, the effects of the upwind and the downwind parts cancel, and a lateral wind has no effect on an unfaired bicycle anyway. This simplification is tenable only for low wind-to-bicycle speed ratios, because in an average of quadratic terms, the unfavorable upwind part weighs more than the favorable downwind part. For example, if a constant wind speed is half of a constant bicycle speed, the associated upwind drag is about $1.5^2 = 2.25$ times the no-wind drag, and the downwind drag is $0.5^2 = 0.25$ of it. The average is then 1.25—that is, 25 percent more power is required around the circuit.

A second simplifying assumption is that the rider's shape acts roughly as if it were a circular cylinder (in an aerodynamic sense), so that wind approaching from any angle creates about the same force. Wind-tunnel measurements by Milliken and Milliken (1983) show, in our interpretation, that a 20 mph wind exerts more than twice the force on a standard bicycle with a crouched rider when it is coming from the side (10.8 lbf) than from ahead (4.9 lbf). However, as long as one is riding faster than the wind velocity, the wind always approaches one somewhat from the front. The Millikens' data show

that a cosine approximation to the retarding force offered by the wind is reasonable for an unfaired bicycle or one with a minimal front fairing. For a streamlined vehicle this is not valid, as the fairing acts like a wing and can provide a benefit on the crosswind parts of the circuit. Whether the overall effect of a steady wind is positive or negative depends on the exact characteristics and conditions (see chapter 5).

On-bicycle power instrumentation offers a relatively simple way to obtain reliable (but approximate) numbers for total drag parameters. Separating the parameters is complex because of the many irregular disruptions—primarily wind, but also slope. For a taste of the effort that can be required to achieve accuracy in such determinations, see Norrby 2012, which describes statistical methods used for coastdown tests of automobiles. See Papadopoulos 1999 and chapter 6 for more on coastdown tests for bicycles. Also, see Larry Oslund’s fascinating video (<https://www.youtube.com/watch?v=UW6dkT7TS6E>), recorded during the final event of the 2019 HPV World Championships in Nandax, France, which shows state-of-the-art onboard instrumentation within the camera view.

Insights Regarding Power and Drag

This chapter has been about the various forms of drag that act on a bicycle in motion and how in combination with available power they determine speed. Later chapters go into the specifics involving each type of drag, but at this juncture it is possible to outline some general conclusions and recommendations.

The Relationship between Power and Speed

Having reviewed the power-output capabilities of humans and the various power losses associated with bicycles and similar vehicles, it is now possible to assess these characteristics in combination to arrive at the power requirements for traveling at various speeds on different types of bicycles. Bicycling can also be placed along the entire range of muscle-powered movement on land and compared with other modes of wheeled transportation such as roller skating and walking.

It is easy to show that the bicycle is very energy efficient. However, it is unscientific to claim that it is the most efficient way of moving, a frequently heard statement. Resistance to motion, and

therefore overall energy efficiency, is a strong function of speed, for all modes of locomotion, and also of environmental conditions. The way in which resistances vary with speed is peculiar to each vehicle or mode. Therefore, comparisons among vehicles or modes are valid only if it is clear what exactly is being compared. Even with this proviso, however, the bicycle still comes out well.

Figure 4.9 shows the world-record speeds for different durations for the principal forms of human-powered propulsion. These speeds

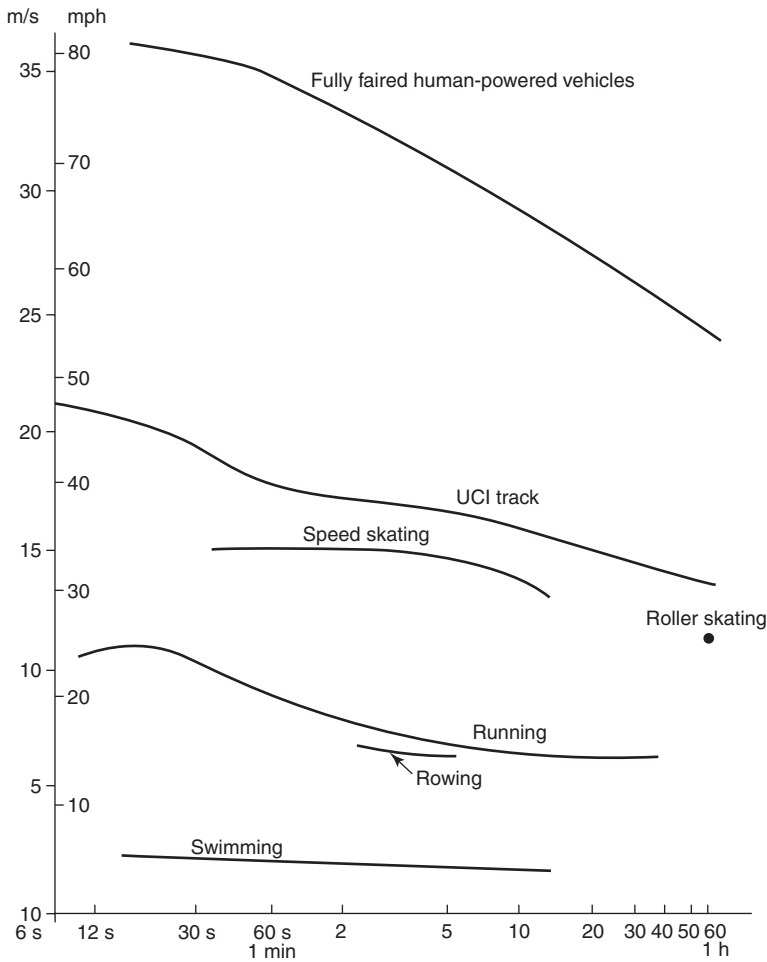


Figure 4.9

World-record speeds under human power employing various modes of transportation. (Data from various sources.)

may be derived reasonably accurately from the maximum power outputs of athletes for various durations (figure 2.4), the air-drag and rolling-friction-drag values of chapters 5 and 6, and estimates of the other frictional resistances in the transmission and the wheel bearings (chapters 6 and 9). As the figure shows, a cyclist on a standard lightweight track bicycle is 2–4 m/s (4.5–9 mph) faster than the best speed skater. The astonishing jump in record speeds from standard racing bicycles to machines using streamlined fairings adds another potential advantage to bicycling.

Energy Consumption as a Function of Distance

The specifications employed for figure 4.5 can be used to find the energy consumed in steady bicycling for various distances on level ground without wind. This is energy in addition to that required for living, the basal metabolism described in chapter 2. In the physical sciences, energy is measured in joules ($1 \text{ J} = 1 \text{ Ws}$), but in nutrition, kilocalories (kcal) or calories (cal) are often still used to measure food's energy content. A kilocalorie is the heat or work energy required to raise the temperature of a kilogram of water 1°C and is equal to 4.184 kilojoules. Unfortunately, in nutrition it is often abbreviated to "calorie," which confuses physicists even more than the mixing of different unit systems.

Figure 4.10 uses a value for muscular energy efficiency of 0.239, or 23.9 percent, because when multiplied by 4,184 J/kcal, this value gives a product of 1,000. For this value of net efficiency, very close to the 24–25 percent quoted in chapter 2, the consumption of one kilocalorie of food energy produces one kilojoule of work, allowing, for example, cycling at 100 W for 10 s. This is a useful rule of thumb to remember when confronted with literature or food packets giving energy values only in kcal.

The low-speed values are mainly given by the coefficient of rolling resistance of the tires, the high-speed values by the vehicle's aerodynamic drag areas. The solid curves do not include the food required just for living, the resting or basal metabolic rate described in chapter 2. If 20 cal/s (about 84 W) is allowed for this, approximately the dashed curve results for the roadster bicycle, with a minimal energy expenditure of about 15.5 kcal/km at around 3 m/s. Curves for the other bicycles would look similar, just shifted downward and to the right. For example, the ultimate (low-drag lightweight) HPV would

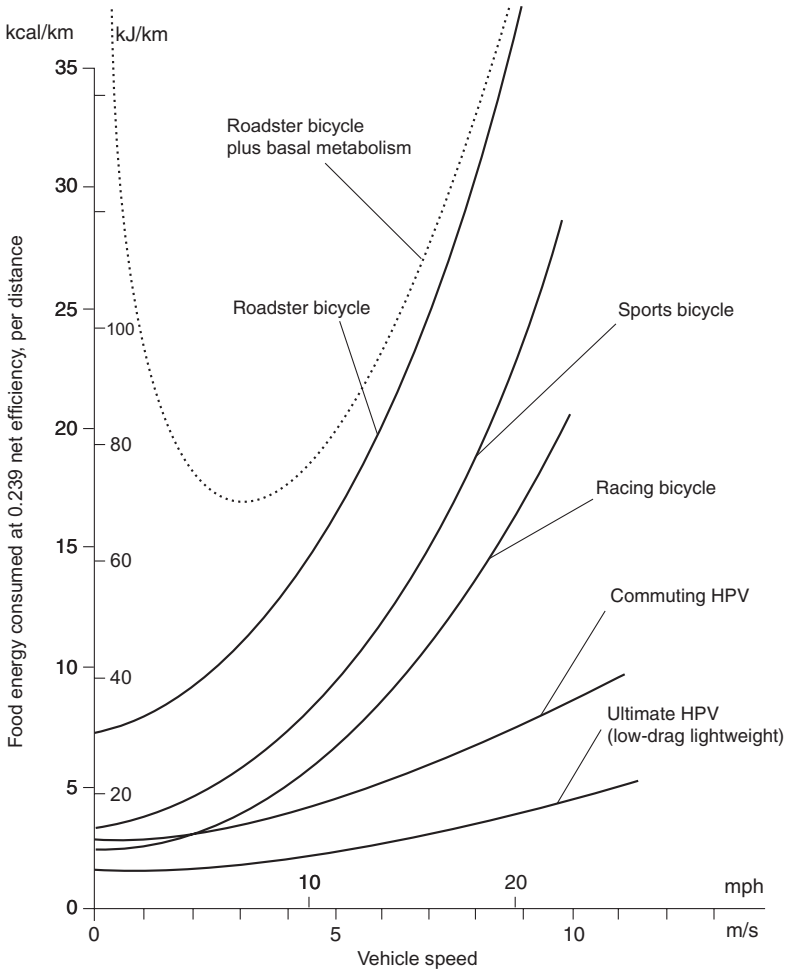


Figure 4.10

Energy consumption in bicycling over distances (for the same bicycles as figure 4.5), if net metabolic efficiency is 23.9 percent. Curves do not include basal metabolism (energy for living), except the dashed curve, which shows data for a roadster bicycle plus a basal-metabolism consumption of 20 cal/s.

be most efficient, at about 8 m/s with about 5.5 kcal/km. This is all rather approximate, as the basal metabolic rate is not really completely separable from the working metabolism, whose efficiency can furthermore vary considerably among individuals and the conditions to which they are subjected. Just the same, using the numbers just given for energy consumption, a cyclist in an ultimate HPV could theoretically travel about 1,500 mi/gal (US) of heavy cream, or a bit more realistically, about 1,000 mi/gal of rich ice cream. (Small cars achieve mileages of 40–50 mi/gal of gasoline.)

Power Needed for Land Locomotion

To survive, living species like animals and humans had to develop, early in their evolution, controllable movement, independent of gravitational and fluid forces that are the usual basis for movement of inanimate objects. The animal world developed systems involving levers that push against the ground in various ways like crawling, bounding, running, and walking, as practiced by man. In some ways bipedal walking is like the rolling of a spoked but rimless wheel. With the adoption of the wheel, yet another lever mechanism for movement, came the chance for moving creatures to use a separate, inanimate source of power besides that of their muscles. Building on the capacity the wheel created, vehicles powered by steam, internal-combustion engines, and electricity rapidly appeared once lightweight engines and motors of adequate power had been produced. Most wheeled vehicles have, in general, been fitted with driving units of progressively increasing power, just as the owners of carriages added real horsepower when they could afford it. The urge for more power and speed seems ever present in human activities.

As on such vehicles humans (that is, the passengers and maybe also the pilot) are considered part of the payload, their mass represents “dead weight,” and to improve the vehicle’s performance, the proportion of “live weight” (that is, that of the motor and energy supply) must be increased. This in turn means strengthening the structure, with the end result the technical absurdity of vehicles weighing a couple of tons and managing the power of hundreds of horses, all to transport mostly only one human for rather short distances.

With bicycles and other human-powered means of locomotion, the opposite is true. The payload is at the same time the motor and energy store, and hence it pays to increase the mass ratio of the human to the vehicle, with the latter therefore becoming as light-weight as feasible.

The bicycle is therefore the only vehicle in which hybridization can lead to an optimum mass ratio of a human to an extra energy source, and not to the extremes of overpowered automobiles or motorcycles, on the one hand, or racing bicycles or HPVs on the other. It is difficult to determine at what point this optimum might be, as so many other external factors are relevant, for example, range, costs, and regulations. However, it appears that for affluent people, the most popular bicycles (following standard nonelectric bicycles) are currently upright pedelec bicycles with batteries that weigh less than one's shopping or body fat stores, and motors with power capabilities rated a bit like those of a fit human, but less than those of an athlete. Why this type of vehicle and not one of the many other propositions? Later chapters look at this in more detail, but it seems to come mainly from the characteristics of the battery, which has a much poorer energy density than the rider's fat, but a much higher power density.

Bicycles versus Other Means of Locomotion

In common with most other wheeled vehicles and their passengers, bicycle and rider can move over hard smooth surfaces at speeds at which air resistance is significant. The sum total of wind resistance, ground movement resistance, and resistance from machinery friction decides the rate of progress for a given power input to a vehicle. These resistances have been studied carefully over a long period for commonly used machines, such as those using pneumatic tires on pavement and those using steel wheels on steel rails, as have the energy costs needed to propel them. Figure 4.11 offers an overview of these energy costs for bicycles and various other ways of moving, which are then explored in more detail in the following sections.

Human Power and Horsepower

For thousands of years—and even today in less-developed parts of the world—horses, cattle, dogs, and humans have been harnessed

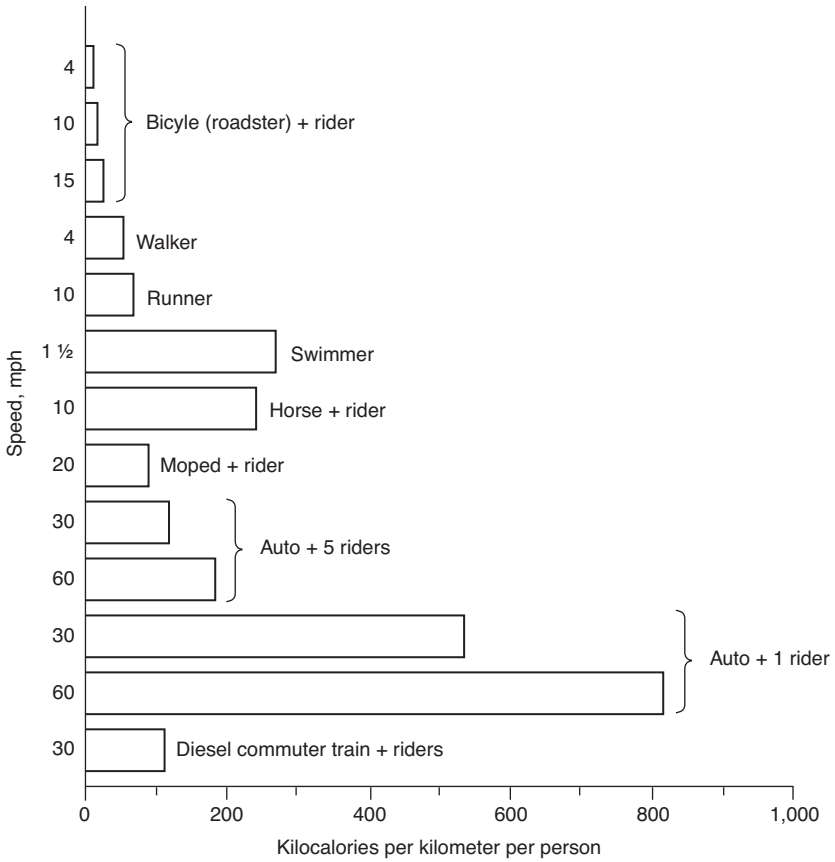


Figure 4.11

Energy cost of human movement and the propulsion of various vehicles.

to machines to turn mills, lift water buckets, and perform other tasks. When the steam engine was invented, it was necessary, for measurement purposes, to have handy a comparison between its power and that of a familiar source. Experiments showed that a large horse could maintain for long periods a power equal to that required to pull 33,000 lb one foot per minute, a quantity now known as one *horsepower* (hp). Ironically this figure was defined by James Watt, whose name was later given to the international unit of power, the watt (W). When defined as Watt did, 1 hp equates to about 745.7 W, but there exist several other types of horsepower that

deviate slightly from Watt's definition, such as metric horsepower, defined as 75 kg lifted at one meter per second. This equates to 735.5 W and implies the standard value for the earth's gravity, 9.0665 m/s^2 , in order to get 1 kg of force (kgf, a non-SI unit) from a mass of 1 kg. Because these other definitions of horsepower exist, it is best not to use horsepower in calculations, and if it must be used, to use Watt's original imperial one, now also referred to as *international horsepower*. Horses can in fact work at a greater rate than 1 hp, but only for brief periods. A human can achieve 1 hp briefly or 0.1 hp for long periods. The term *hup* is sometimes used for this, rounded to 75 W.

Humans, horses, and many other animals furthermore can develop large pulling forces, statically or moving slowly. This is a question of leverage: if a pulling or pushing person's center of gravity is displaced at an angle of 45° to the feet, the force is the same as the person's weight, and if a bumpy or uneven ground allows it, with a more horizontal angle the pulling force can even be increased to more than twice the weight. The record for a pair of horses is apparently four times their weight, but in popular horse-pulling contests, the forces are generally limited to about the horses' weight in order to avoid injury. As horses often weigh more than a ton, these are great forces produced by a "horsepower." Humans can also produce these forces, at a much slower rate, by using machines with a mechanical advantage, as is easy to understand for anybody who has ever raised an automobile using a jack.

Figure 2.4 gives other information relating power output to duration. An average human seems to adjust power output to rather less than 75 W (1 hup) if intending to work for other than short periods and not engaged in competition. Alexander (2005) offers information on the energy cost of locomotion in animals other than man, in particular relating to scale.

In a review of the energy used per ton-mile (or tonne-kilometer) and passenger mile (kilometer) for such varied means of transportation as the SS *Queen Mary*, the supersonic transport, a rapid-transit system, and oil pipelines, Rice (1972) points out that a bicycle and rider are by far the most efficient. He calculates that a modest effort by a bicyclist that results in 72 mi (116 km) being covered in 6 h could require an expenditure of about 1,800 kcal (7.54 MJ), which is in agreement with figure 4.10 for something between a roadster

and a sports bicycle. Assuming a mass of 200 lb (90.6 kg) for rider and machine, Rice stated that this figure is equivalent to 100 ton-mi (146 tonne-km) (or more than 1,000 passenger-mi) per gallon (3.785 L) of equivalent fuel. The *Queen Mary* managed, by contrast, 3–4 passenger-mi per gallon (1.27–1.70 passenger-km per liter). Physically all types of ships ought to scale favorably with respect to energy cost, as cargo ships do, because the volume usable for cargo increases in relation to the hull's wetted surface, which causes friction drag. Large passenger ships, however, scale unfavorably, as the increase in hull surface is needed for desirable outside cabins. The "leftover" volume inside is filled with luxury malls, theatres, and the like, all adding to the tonnage transported per passenger.

When the power requirements of cycling are compared with those of various other vehicles, the same relationships are observed: at low speeds nothing can beat the cyclist. At higher speeds automobiles and especially large public transport vehicles become more efficient, but only if compared according to gross weight. When net weights, that is, those of the transported riders, passengers, and luggage, are compared, cycling again reigns supreme.

Walking and Running

Every cyclist knows that when one encounters a steep uphill gradient, it is often easier to dismount and push one's bicycle. One reason is that there is a pause between each step in which almost no energy is used, as just standing involves no muscle contraction, even on an incline. In contrast cycling uphill requires holding some torque on the pedals all the time, especially during the cranks' dead centers, even in very low gears. Many people dismount even on lesser gradients (perhaps giving rise to the label *push bike* for an easily pushable standard bicycle). But what do measurements say?

The energy cost of walking and running has been well researched in the laboratory over the last 150 years, and more recently masses of data have been recorded by amateurs tracking their movements and pulse rates in the field. Minetti et al. (2002) conduct a series of measurements of young male athletes on treadmills at various speeds and slopes during 4 min tests. For uphill slopes steeper than 15 percent, they find mechanical efficiencies (defined by the virtual increase of the subjects' potential energy related to their oxygen consumption) of about 22 percent when running and 24 percent

when walking, with best results at a gradient of about 25 percent and a horizontal speed of around 1.2 m/s, which also correlates well with earlier laboratory and recent field measurements of mountain ascents. These efficiencies are very close to the maximal efficiency of muscle contraction and appear to include the basal metabolic rate, so it is difficult to imagine cycling being any better in this respect, especially considering the bicycle's additional weight. For gradients less than 15 percent, however, cycling is bound to become more efficient, especially as gradients decrease and speeds increase, and to be more efficient on level ground at any speed. Savage (2017) presents energy-cost equations and several dynamic tables comparing walking and running that can be set to any body weight. The energy cost of walking 1 km on the level at 1–1.3 m/s is 0.4–0.7 kilocalories per kilogram body mass (kcal/(kg km)), depending on the reference used. (Energy costs per distance are given here in units of kcal/(kg km): multiply by 4.184 for kJ/(kg km) and by 0.73 for kcal/(lb mi).)

The energy cost increases sharply above about 2 m/s, at which point running, which uses about 0.9 kcal/(kg km) at any normal speed, becomes more efficient. Both are much higher values than that for a cyclist on a roadster bicycle, as shown in figure 4.10, with a minimum of about 0.22 kcal/(kg km) (dotted line) at 3 m/s, assuming a cyclist weighing 77 kg.

For downslopes the picture changes even more. Even though a –10 percent gradient permits walking at the least energy cost (Minetti et al. 2002), about 0.25 kcal/kg/km, a rider on a roadster would then be coasting at more than 5 m/s without any energy cost other than the rider's basal metabolic rate, amounting to perhaps 0.05 kcal/(kg km) for this example. On steep downslopes, a cyclist must speed at breakneck pace or brake or can recuperate if riding an e-bicycle equipped with regenerative braking, whereas a walker's or runner's efficiency decreases to –125 percent or so. This means that not only is 100 percent of the walker's or runner's potential energy wasted, but the muscles must metabolize an additional 25 percent as “negative work.” This figure pertains to the laboratory treadmill; bounding down a real slope requires much less negative work depending on the surface and the walker's or runner's technique.

So far the discussion has assumed hard, even surfaces like a road. Most natural surfaces, however, are either hard and uneven, like a

rocky trail, or even and soft, like a beach or grassy plain. On such surfaces the energy costs of walking could become less than those for cycling.

The discussion here has considered only single trip segments. For round trips, it probably pays to use a bicycle even if it has to be pushed or carried on the way up. Only if a path is so poor that the bicycle has to be carried back down again, or carried for long level stretches, is its energy cost definitely greater than that of walking, and its use thus inferior.

Roller or In-Line Skates, Kickboards, and Microscooters

Roller skates (regardless of their wheel alignment), kickboards, and microscooters all imply a standing position for the wearer or rider and thus compare aerodynamically with a standard bicycle. They don't, however, allow drag reduction like low recumbents or faired HPVs. The use of such vehicles in any case involves a higher energy cost than cycling for several other reasons.

The substantial increase in rolling resistance between bicycle and skate wheels can be attributed to the use of very small wheels with solid polymer tires in the skates (about one-thirteenth the diameter of bicycle wheels). In the third edition of this book, calculations (using the value for roller skating shown in figure 4.9) and measurements by Frank Whitt of the pull required to keep a skater moving steadily show a rolling-resistance coefficient C_R of about 0.060 at low speeds. The hardest available rollers on extremely smooth surfaces generate somewhat less rolling resistance than this, but they could not be used safely at higher speeds, like the steel rollers formerly used. Microscooters today have somewhat larger wheels than they used to. Chapter 6 states that microscooter wheels of 100 mm diameter with a tire hardness of 90 Shore-A have a rolling-resistance coefficient of 0.0075–0.015, bordering on that of poor or poorly inflated bicycle wheels.

A second consideration is the drive system, or rather the lack of a mechanical one like that of a bicycle. Skating, although elegant and effective, involves producing large side forces that cause some sideways slip and friction losses. Kicking—that is, pushing on the road with one leg, as one does on a kickboard or microscooter—means varying the height of the body's center of gravity with each kick and can be done only at relatively low speeds.

On the other hand, kickboards and microscooters are lighter than bicycles and handy to take along. In practical use with trips also involving walking, stairs, or public transport, their total energy cost could be smaller than taking along a full-sized bicycle.

Ice Skating and Skiing

A comparison between bicycles and ice skates or skis doesn't seem very useful unless the various vehicles are used on the same surface. Presumably cycling on ice is not much different than on a track, in regard to energy use, but in practice it is hardly ever done.

Formenti (2014) reports coefficients of resistance for various skate runners of about 0.006 (modern steel) to 0.01–0.015 (prehistoric bone), thus comparable to those for medium to poor bicycle tires. A skater has an aerodynamic drag similar to that of a similarly clothed cyclist, but the former's method of propulsion involves large side forces that also increase the resistance of the skate runners. Ice skating therefore has a slightly higher energy cost than comparable cycling, but an elite ice skater is more efficient and faster than an ordinary cyclist or bicycle. Formenti and Minetti (2007) report an energy cost of about 0.3 kcal/kg/km for a skater moving at about 6.7 m/s. This is twice that of a racing cyclist or about the same as a cyclist on a roadster (see figure 4.10).

The coauthor's microscooter with the wheels replaced by skate runners feels at least as efficient as with the wheels but requires more effort because it is then 50 mm higher and requires bending the knee of the static leg for each kick of the propelling one. (This can be solved by using long crampons on one foot, but then it isn't possible to switch legs.)

There are two basic techniques for cross-country skiing, with many variations of the two. The skating style is faster and more efficient at speed but requires strength and hard snow, for example, a prepared piste. Such a piste would, however, seem soft to an all-terrain bicycle even with fat tires and allow only slow cycling. An energy cost of 0.8–0.9 kcal/(kg km) can be derived from Millet, Boissiere, and Candau 2003 for skating techniques, based on amateur skiers at a speed of about 4.7 m/s on a groomed oval track. No data are available for cycling on snow, but the resistance encountered is likely to vary more, depending on the exact hardness of the snow surface, than for the skis. Tires are also more susceptible to

unevenness, whereas skis, which are between one and two meters in length, tend to average it out.

The classic cross-country skiing style (with parallel skis) allows skiing or at least walking also in deep, quite uncyclable powder snow. Snow bikes with caterpillar tracks could also do this, but we've never tried one. Classic skiing becomes reasonably fast on hard, icy tracks, which would however be uncyclable for reasons of balance. Millet, Boissiere, and Candau (2003) provide no data for classic skiing but, quoting other references, suggest that skating is 10–20 percent more efficient except in low-speed, high-friction conditions. With all techniques, poles (and upper-body muscles) must be used to progress.

References

- Alexander, R. McNeill. 2005. "Review: Models and the Scaling of Energy Costs for Locomotion." *Journal of Experimental Biology* 208, no. 9: 1645–1652. <http://jeb.biologists.org/content/jexbio/208/9/1645.full.pdf>.
- Archibald, Mark. 2016. *Design of Human-Powered Vehicles*. New York: ASME Press.
- Compton, Tom. 2001. Online calculators and simulators. <https://analyticcycling.com>.
- Formenti, Federico. 2014. "A Review on the Physics of Ice Surface Friction and the Development of Ice Skating." *Research in Sports Medicine* 22, no. 3: 276–293. <http://dx.doi.org/10.1080/15438627.2014.915833>.
- Formenti, Federico, and Alberto E. Minetti. 2007. "Human Locomotion on Ice: The Evolution of Ice-Skating Energetics through History." *Journal of Experimental Biology* 210, pt. 10 (June): 1825–1833. <https://www.researchgate.net/publication/6342409>.
- Gribble, Steve. 2018. "Cycling Power and Speed." The Computational Cyclist (website). https://www.gribble.org/cycling/power_v_speed.html.
- Heine, Jan. 2012. "Suspension Losses." *Bicycle Quarterly* 29 (Autumn). <https://janheine.wordpress.com/2012/08/12/suspension-losses/>.
- Kyle, Chester R., and E. M. Burke. 1984. "Improving the Racing Bicycle." *Mechanical Engineering* 109, no. 6: 35–45.
- Lieh, Junghsen. 2006. "Determination of Cycling Speed Using a Closed-Form Solution from Nonlinear Dynamic Equations." *Human Power eJournal*, no. 3: art. 10. <http://www.hupi.org/HPeJ/0010/0010.htm>.

Millet, Gregoire P., Denis Boissiere, and Robin Candau. 2003. "Energy Cost of Different Skating Techniques in Cross-Country Skiing." *Journal of Sports Sciences* 21, no. 1 (January): 3–11. <https://www.researchgate.net/publication/10899114>.

Milliken, D. L., and W. F. Milliken. 1983. "Moulton Bicycle Aerodynamic Research Program." In *Proceedings of the Second International Human-Powered-Vehicle Scientific Symposium*, ed. Allan V. Abbott. San Luis Obispo, CA: International Human Powered Vehicle Association.

Minetti, Alberto E., Christian Moia, Giulio S. Roi, Davide Susta, and Guido Ferretti. 2002. "Energy Cost of Walking and Running at Extreme Uphill and Downhill Slopes." *Journal of Applied Physiology* 93, no. 3: 1039–1046. <https://doi.org/10.1152/jappphysiol.01177.2001>.

Norrby, Peter. 2012. "Prediction of Coast-Down Test Results—A Statistical Study of Environmental Influences." M.Sc. Thesis, Department of Product and Production Development, Chalmers University of Technology, Gothenburg, Sweden.

Papadopoulos, J. M. 1999. "Simple Approximations for the Effects of Tire Resistance, Wind, Weight and Slope." *Human Power*, no. 48 (Summer): 10–12.

Pradko, F., R. A. Lee, and V. Kaluza. 1966. "Theory of Human Vibration Response." Paper 66-WA/BHF-15 (1966 Winter Annual Meeting), American Society of Mechanical Engineers, New York. 1966 Winter Annual Meeting.

Rice, R. A. 1972. "System Energy and Future Transportation." *Technology Review* 74 (January): 31–48.

Savage, Jonathan. 2017. "Calories Burned Running and Walking." [Fellrnr.com](http://fellrnr.com/wiki/Calories_burned_running_and_walking). http://fellrnr.com/wiki/Calories_burned_running_and_walking.

Schmidt, Theodor. 2019. Spreadsheet supplements for *Bicycling Science*, 4th ed. <http://hupi.org/BS4/>.

Shimano. 1982. "Aerodynamics—And a New Era Is Upon Us." Document reproduced in *Proceedings of the First International HPV Scientific Symposium*, 92–93. San Luis Obispo, CA: International Human Powered Vehicle Association.

Snyder, John. 2004. "Algebraic Determination of Land HPV Velocity." *Human Power eJournal*, no. 1: art. 1. <http://www.hupi.org/HPeJ/0001/0001.htm>.

Teufel, Edgar. 2019. Velocipedio (computer program). <http://hupi.org/Velocipedio/>.

Wang, E. L., and M. L. Hull. 1996. "A Model for Determining Rider Induced Energy Losses in Bicycle Suspension Systems." *Vehicle System Dynamics* 25: 223–246. <https://www.researchgate.net/publication/245308958>.

Zorn, Walter. 2008. Speed and power calculator. www.kreuzotter.de. <http://kreuzotter.de/english/espeed.ht>.

5 Bicycle Aerodynamics

Introduction

This chapter is about aerodynamic drag and other aerodynamic phenomena such as the flow effects when people ride side by side and one behind another, wind buffeting from vehicles, and the effects of side winds. It is a large and complex subject: the chapter hopes to explain some (but a long way from all) of the complexities.

Air resistance is an everyday experience, particularly to cyclists: at normal biking speed it is the largest component of drag apart from that due to hills. Two main types of forces cause it: one normal to the frontal surface of the resisted body (which could be the human body or the body of a vehicle), felt as the pressure of the wind, and the other tangential to the surface (which is the true skin friction and is dissipated in immediate slight heating of the air) (figure 5.1, panel [a]). For a nonstreamlined body, such as a bicycle and its rider, the pressure effect is much the larger of the two, and chapter 4 gives a derivation of this effect. The dissipated pressure energy appears initially as kinetic energy in a wake that dissipates into heating of the air. Panel (b) of figure 5.1 shows this kinetic energy appearing as eddies at the rear of a cylinder. As panel (c) of the figure shows, a streamlined shape produces lower kinetic energy in the wake, because no large eddies are produced and there is pressure recovery from the still-attached flow along the aft (downstream) surfaces.

Vehicles intended for high speeds in air are almost always constructed to minimize pressure drag. Streamlined shapes incorporate gradual tapering from a rounded leading edge. The exact geometry of shapes that maximize the possibility of the airflow around the shape remaining attached (rather than separating in local jets and

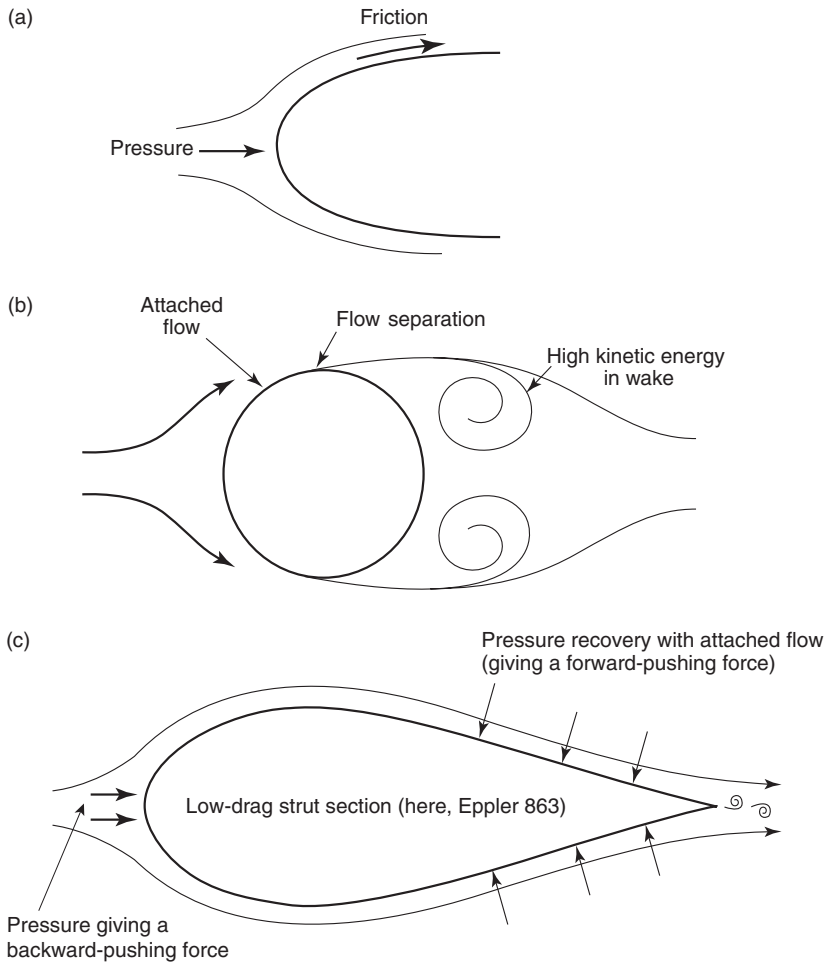


Figure 5.1

Flow around bodies: (a) Normal (pressure) forces and friction forces; (b) attached and separated flow around a cylinder; (c) attached flow and pressure recovery in a streamlined body.

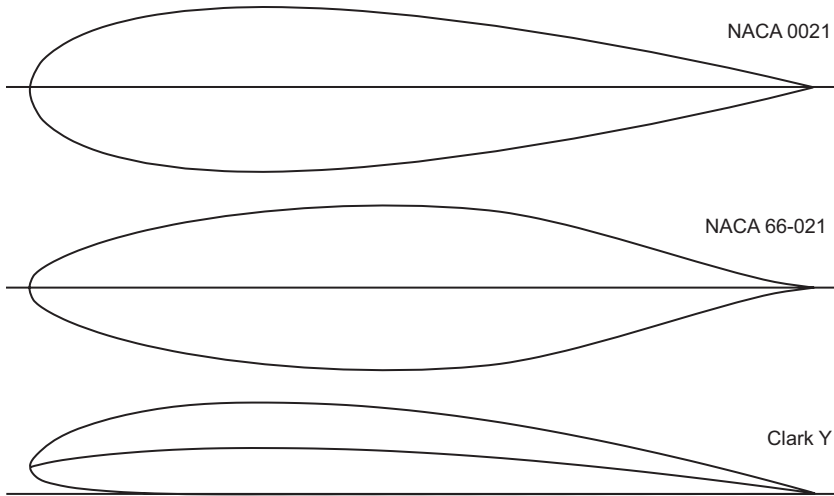


Figure 5.2

Low-drag shapes: National Advisory Committee for Aeronautics (NACA) profiles 0021 and 66-021, and wing profile Clark Y with camber.

eddies) and that minimize skin friction can be approximated using rather complex mathematics. Alternatively, it is usual in aeronautics either to refer to one of a family of published low-drag shapes or *wing sections* (as shown in figure 5.2) or to test models in a wind tunnel.

Although wind-tunnel experiments can yield solid data for components, faired vehicles, and even stationary cyclists, the interaction of the airflow surrounding a moving bicyclist with the stationary ground and with the usually whirling legs reduces the accuracy of wind-tunnel data for bicyclists on unfaired vehicles.

Drag and Drag Coefficient

One aim of aerodynamic experiments is to measure an object's drag coefficient C_D , defined as the nondimensional quantity $C_D \equiv \text{drag} / (\text{area} \times \text{dynamic pressure})$, in which the drag D is the force in the direction of the relative flow (the area A to be used in the formula is defined in "Definitions of Area and of Drag Coefficient" later in the chapter). However it is defined, the product $C_D A$ is very useful in studies of the drag on bodies, as it can be determined without

knowing or defining either C_D or A . The drag is simply $C_D A$ times the dynamic pressure. Table 5.1 later in this chapter shows values of $C_D A$ for various types of bicycles and other machines.

Dynamic Pressure and Air Density

Dynamic pressure is the maximum pressure that can be exerted by a flowing stream on a body that forces it to come to rest. At low airspeeds (say, below 45 m/s or 100 mph), $V^2 \rho/2$, (in which ρ is the air density in kilograms per cubic meter and V is the velocity of the air in meters per second) closely approximates the dynamic pressure (in the SI unit pascal [Pa] or newton per square meter [N/m^2]). Chapter 3 discusses the relationship between air density, air pressure P , and absolute temperature T in kelvin ($\rho = P/[287 T]$), and figure 5.6 provides values for P and temperature (in $^\circ\text{C}$) of the “standard US atmosphere.” For example, an HPV speed record of 35 m/s set at an altitude of 2,000 m would involve a dynamic pressure of about $600 \text{ N}/\text{m}^2$, 0.75 percent of the ambient air pressure of 80 kPa at the ambient temperature of 12°C . Further small pressure variations also arise as a result of weather and humidity (see Shelquist 2016 for detailed explanations and Gribble 2018 for an easily used calculator).

(A note here on units and values: 1 bar = 1,000 mb = 1,000 hPa = $10^5 \text{ Pa} \approx 0.987 \text{ atm} \approx 14.5 \text{ psi} \approx 750.1 \text{ Torr [mmHg]} \approx 29.53 \text{ inches Hg}$ [the height of a column of mercury that can be supported by one atmosphere]. The absolute temperature in kelvin (K) is the temperature in degrees Celsius ($^\circ\text{C}$) plus 273.15. Sea-level air density is about $1.2 \text{ kg}/\text{m}^3$ at 16°C [60°F] and about $1.14 \text{ kg}/\text{m}^3$ at 38°C [100°F] for dry conditions. If the humidity is 100 percent, the density *drops* by about 1 percent at the cooler of these temperatures and by about 2.5 percent at the hotter. The difference in pressure due to weather between strong high- and low-pressure areas is about 50 mb.)

Definitions of Area and of Drag Coefficient

The area to be used in the formula for the drag coefficient C_D given in the preceding section can be defined in several alternative ways, each one leading to a different definition and a different value of the coefficient. The most used definition is the frontal area, and unless otherwise stated, this book uses the form of drag coefficient that uses this definition of area: *drag* = $C_D \times \text{frontal area} \times \text{dynamic pressure}$.

Another form of drag coefficient is defined in terms of the surface area of the body on which the drag acts tangentially and is used only for slender or streamlined bodies (or plates or tubes), the drag on which primarily comes from skin or surface friction, rather than from the eddies coming off of bluff bodies. This is the entire surface area exposed to the airflow and is often called the *wetted area*; this book refers to this surface area as SA and its matching drag coefficient as $C_{D,SA}$. For a given body in a given condition, the surface-area coefficient of drag is smaller than the frontal-area coefficient because the surface area is larger than the frontal area. A sphere has a ratio of surface area to frontal area of 4.0. For a long cylinder of diameter d with spherical ends, the ratio is $4 \times (1 + l/d)$, in which l is the length of the cylinder's straight portion. The measured value of C_D for a rounded-end cylinder aligned with the airflow increases with l/d , whereas the value of $C_{D,SA}$ decreases with l/d to compensate for the increasing surface area (figure 5.3).

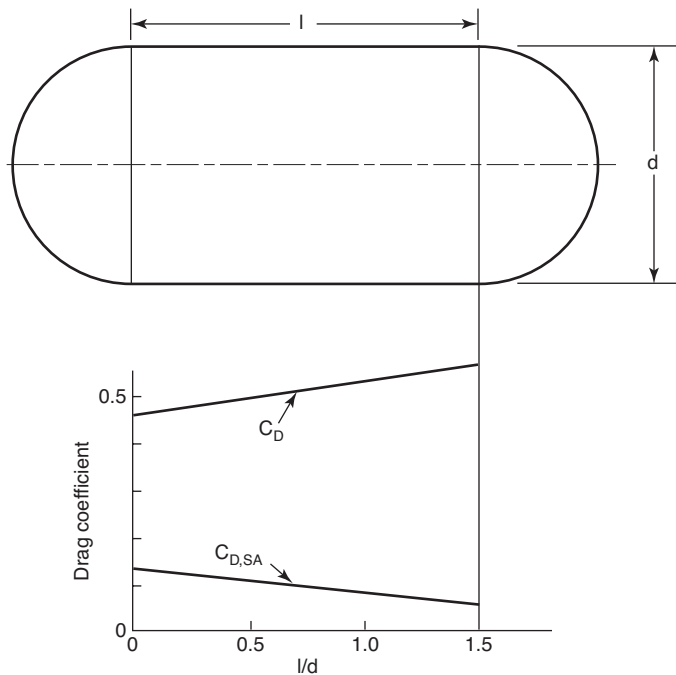


Figure 5.3

Frontal-area (C_D) and surface-area ($C_{D,SA}$) drag coefficients for a circular cylinder.

The following anecdote illustrates the significance of distinguishing between the two definitions of the area referred to in the drag coefficient. In the early days of the quest for a speed prize for the first HPV to reach 65 mph (~ 29 m/s), an MIT student decided that he could win the prize by assembling many pedalers in a line within the same frontal area as one pedaler. He had found that the drag coefficient for a reasonably streamlined single-rider recumbent vehicle was 0.15 and that the frontal area could be below 0.5 m^2 . He calculated the drag at 29 m/s to be about 38 N, leading to a power required to overcome air drag alone at greater than 1,100 W. He decided to build a vehicle carrying ten to fifteen riders in a line, reasoning that because the frontal area would be the same, the drag (he thought) would be the same, and the air-drag power required from each of ten riders would be an easily manageable 110 W. He confidently forecast reaching 80 mph or 36 m/s.

For various reasons that plagued development, the vehicle was quite slow. But the fallacy underlying the designer's reasoning was that the drag coefficient based on frontal area would not increase as the vehicle was made longer. It would and did, probably quadrupling the drag of a one-person faired body of the same frontal area. It is often preferable when calculating the drag for a streamlined body, therefore, to use the drag coefficient based on surface area. However, either form may be used with confidence so long as the value found experimentally for one configuration is not applied to the analysis of a completely different shape.

Specialized textbooks use further area-coefficient pairs. A common one, which will be used later in this chapter, is the plan area of an airfoil (*span* times average *chord*, a little less than half the wetted area) and its associated drag and *lift* (force normal to the direction of flow) coefficients, which are both highly dependent on the angle of incidence of the airflow. In particular, this form of drag coefficient starts out very low at zero angle of incidence, as it is in effect like the drag coefficient C_D for the foil's frontal area divided by its chord-to-thickness ratio. And at a 90° angle of incidence it is simply like the frontal drag coefficient C_D for the foil held sideways. But the purpose of airfoils is the region in between, where several interesting things happen that the chapter takes up later.

A skin-friction coefficient that clearly relates purely to a given surface area is often labeled C_F . Whatever coefficient is used, as long

as it is paired with the correct area, the product $C_D A$ will always be the same and be equal to that for a corresponding frontal area in which C_D is 1. Many vehicles have parts that experience pressure drag and parts that experience skin-friction drag. As long as the total $C_D A$ is known, it is unnecessary to separate these components, unless precise calculations are desired that include speed dependencies (as discussed later in the chapter).

Boundary-Layer Effects

The drag coefficients of bodies whose resistance is almost entirely due to pressure drag (e.g., thin plates set normal to the direction of flow) are virtually constant with airspeed, once this speed is higher than the “creeping flow” or laminar range (see the discussion of Reynolds number in the next section). But the drag coefficients of bodies with substantial contributions from the surface-friction drag of the so-called boundary layer can vary widely in different circumstances. In general, the flow in this boundary layer can exist in one of three forms:

1. Laminar, in which the layers of fluid slide smoothly over one another, as in the foreparts of the three bodies in figure 5.1
2. Turbulent, in which the boundary layer is largely composed of small, confined but intense vortices that greatly increase the surface friction, as will most likely be the case at the rearward end of the body shown in panel (c) of figure 5.1
3. Separated, in which the boundary layer, along with the main flow, leaves the surface and usually breaks up into large-scale unconfined jets or eddies, as in panel (b) of figure 5.1

Figure 5.4 shows skin-friction coefficients as a function of the Reynolds number (Re , explained in the next section). The lower slanting line in the figure is called the *Blasius line* ($C_F = 1.328/\sqrt{Re}$) and shows the theoretical limit for a laminar boundary layer, which corresponds closely to measurements of surfaces at about $Re = 10^3$ – 10^6 . Below $Re = 10^3$, the drag is purely viscous (like stirring in honey) and much higher, but of no consequence for bicycle parts, as either even small things like brake cables exhibit higher Reynolds numbers, or the airspeed is so low that the drag is negligible. The equation can be used in any case until $Re > 5 \times 10^5$, often until 10^6 , and exceptionally until 2×10^6 , at which point an extremely low coefficient of 0.001 would be reached.

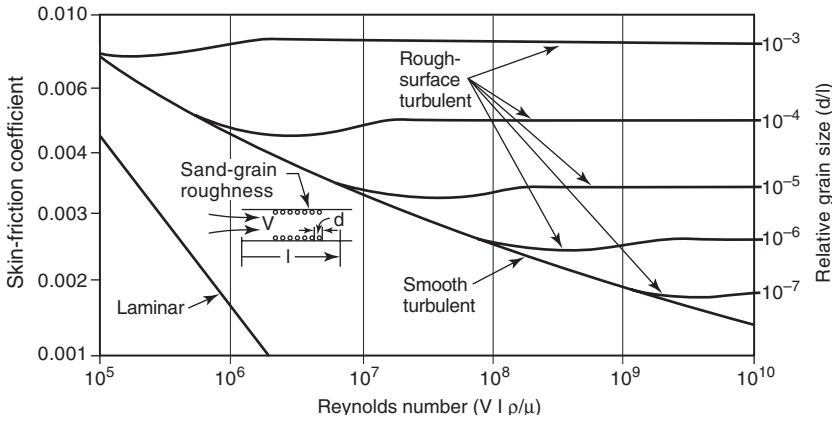


Figure 5.4

Laminar (Blasius) and turbulent (Schoenherr) limits for the skin-friction coefficient, along with roughness measurements. (Data from Hoerner 1965.)

The upper slanting line in the figure is called the *Schoenherr line* and shows the experimental limit for a turbulent boundary layer at a smooth surface. The textbook formula, $C_F = 4.27 / (\ln[Re] - 0.407)^{2.64}$ can be approximated by $C_F = 0.044 Re^{-1/6}$ in the usually valid range $Re > 10^6$. However, a turbulent boundary layer can easily occur at $Re = 10^6$ and exceptionally at a Reynolds number value as low as 5×10^5 . The figure also shows the (measured) effects of adding roughness.

If one wanted to produce a low-drag bicycle enclosure, it would be preferable that the boundary-layer flow be entirely laminar, but at the highest Reynolds number possible. Airplane designers have long strived to arrive at wings with the laminar flow extending as far rearward as possible, by moving the area of greatest thickness to about the middle of the chord, as seen in the National Advisory Committee for Aeronautics (NACA) 66-021 profile in figure 5.2. Conventional wing sections like that of the NACA 0021 have this at one-quarter to one-third from the front along the chord. Unfortunately, extended laminar-flow boundary layers are extremely sensitive to disturbances. Not only may they become turbulent, but they have a strong tendency to separate from the surface, producing especially high levels of drag, because flow separation prevents the recovery of most of the pressure along the downstream part

of a body. The further the boundary layer remains attached to the streamlined surface, the greater the pressure recovery, a forward-pushing force that, if there were no friction, would exactly balance the backward-pushing force at the front of the body.

Turbulent boundary layers in general produce higher surface friction than laminar boundary layers; however, they are less likely to separate from the associated surface than laminar boundary layers. At low Reynolds numbers, forcing the laminar boundary layer to become turbulent far enough forward to avoid the risk of separation further downstream often produces the lowest levels of integrated drag. At low speeds this may require either the roughening of the surface or the mounting of a trip wire at well before the location where separation might otherwise occur. A classic experiment by the aerodynamics genius Ludwig Prandtl showed this effect graphically (Prandtl and Tietjens 1934). Prandtl mounted a smooth sphere in an airstream, measured its drag, and observed the airflow using streams of smoke. In laminar separation, the flow separated even before the maximum diameter was reached (figure 5.5, top), with a high amount of drag. Prandtl then fastened a thin wire ring as a boundary-layer trip to force the boundary layer to become turbulent on the part of the sphere upstream of where laminar separation had previously occurred. The boundary layer did indeed become turbulent, and as a consequence the flow remained attached over a much larger proportion of the sphere's surface (figure 5.5, bottom), and the drag decreased greatly, as could be seen from the much smaller wake. Manufacturers of golf balls have learned from this and roughen the balls' surface with sharp-edged dimples, producing balls that can be driven faster and farther. (The dimples, combined with ball rotation known as *top spin*, also produce an aerodynamic lift force, which contributes to increasing the ball's range.) The section "Boundary-Layer Suction," later in the chapter, discusses another possibility for reducing drag: the use of surface suction to pull out the low-momentum inner part of a laminar boundary layer to force it to stay both laminar and stay attached.

The Reynolds Number

For any one shape of body, the variable that controls the drag coefficient is the dimensionless *Reynolds number* (Re), defined in general as $Re = V l \rho / \mu$, in which V is the relative velocity of a fluid (usually

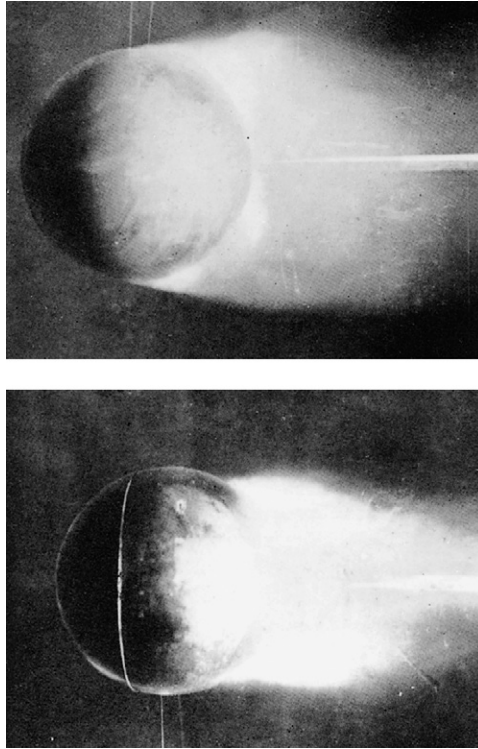


Figure 5.5
Effect of roughness on drag of a smooth sphere. (From Prandtl and Tietjens 1934.)

air or water) with respect to a shape's surface; ρ and μ are the fluid's density and viscosity, respectively; and l is a length or distance that has to be specified for the particular shape of body being considered. For a sphere or circular cylinder (in flow transverse to the cylinder axis), the specified length is the diameter. For streamlined bodies like fairings, the length of the body in the direction of the flow is usually specified as the actual length. For an aircraft wing, this dimension is the chord. For a sphere moving in air at sea-level pressure and room temperature, an approximate formula is $Re \approx \frac{2}{3}$ diameter (m) \times velocity (m/s) $\times 10^5$. A rule of thumb for any specified length l and speed V in such conditions is $Re \approx 66,666 l V$. The Reynolds number in air for any pressure and temperature can be determined using an approximation for viscosity as a function of temperature, referred to as *Sutherland's law*, and the ideal gas law,

described in chapter 3 and mentioned earlier in this chapter, for determining the air density as a function of pressure and temperature. The quantity μ/ρ is then called the *kinematic viscosity* (ν). Mixing the two functions together yields the following formula for the kinematic viscosity (in SI units):

$$\nu \approx 41.84 \times 10^{-5} T^{2.5}/(P [T + 110.4]),$$

in which ν is measured in square meters per second, air temperature (T) in kelvin, and air pressure (P) in pascals. Re is then Vl/ν . The air pressure P can be measured directly with a barometer or altimeter or determined as a function of altitude from figure 5.6, which also gives the temperature of the US standard atmosphere. Although for accuracy the actual temperature should then conform to this standard temperature, any deviation in pressure due to the weather is likely to be tolerable for most purposes. So for example, for a 2 m long faired bicycle moving at 10 m/s at 1,000 m altitude (which corresponds to a temperature of 18°C and a pressure of 90 kPa in figure 5.6 of the US standard atmosphere), the formula returns $\nu \approx 1.675 \times 10^5$, and thus $Re \approx 1.19 \times 10^6$.

One useful application of the Reynolds number is in model testing. Full-scale wind-tunnel tests, for example, of fairings, are very expensive. A smaller-scale model can be tested in a smaller wind tunnel; however, the wind speed must be scaled up by the same factor as the length is scaled down, so it may not be much easier to conduct such a test. The wind tunnel used for testing NACA airfoils (discussed in “Airfoil Sections for Struts and Fairings” later in the chapter) is even pressurized up to 10 bar to reach high values of Re . A model can, however, be tested fully submerged in water at the same Reynolds number at 10–15 times less speed, depending on temperature. Proper water tunnels are scarce, but natural streams can suffice for comparative drag measurements, or a buoyant shape can be released at a certain water depth in still water and its upward movement timed. This works only for shapes that keep a stable attitude, of course. The point is that a body’s frictional behavior in water is exactly the same as that in air at the same Reynolds number, provided that the body is deep enough in the water not to make waves at the surface and the speed is low enough for the airflow be considered incompressible. The viscosity of water is also temperature dependent, but in the opposite direction from that of air. The viscosity μ of water is about 0.0015 Pa·s at 5°C, 0.0013 at 10°, 0.001

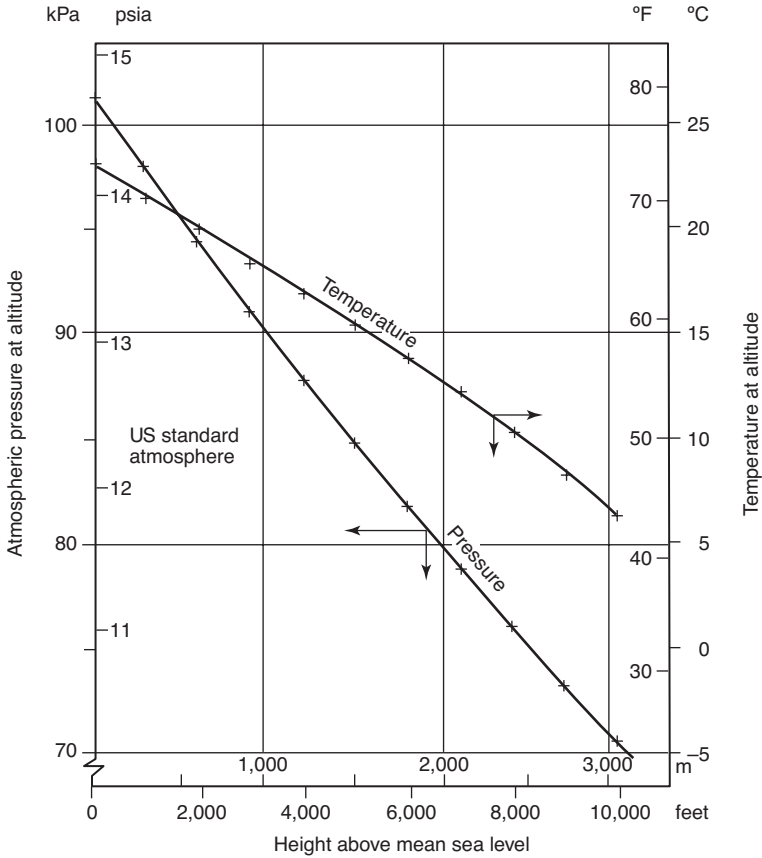


Figure 5.6
US standard atmosphere. (Data from US government.)

at 20°, and 0.0008 at 30°. In this temperature range, the density of water changes only slightly from 1,000 kg/m³, so v becomes 1.5×10^6 m²/s, and so on.

The form of Reynolds number discussed so far is a kind of average. The bit of fluid encountering the foremost part of a shape can of course not know the length of the shape further downstream. The instantaneous, local Re thus is very low at the beginning of the fluid's trip along the surface and increases with time and distance. Therefore most shapes have a laminar boundary layer at the beginning, and only when the local Re becomes large enough will the boundary layer become turbulent or separated.

Coefficient of Drag versus Reynolds Number for Various Bodies

Figure 5.7 plots the drag coefficient of various bodies versus their Reynolds numbers. As the figure shows, at $Re > 3 \times 10^5$, even smooth spheres do not need trip wires or rough surfaces to induce turbulence, because a laminar boundary layer will spontaneously become turbulent above that Reynolds number. When a boundary layer becomes turbulent at increased velocity and Reynolds number, the drag coefficient for a smooth sphere falls sharply, from 0.47 to 0.10. However, a golf ball about 40 mm in diameter driven at an initial velocity of 75 m/s has a Reynolds number of 2×10^5 at the start and would be in the high-drag-coefficient region of the figure if it were smooth. The ball's dimpling shifts the point at which there

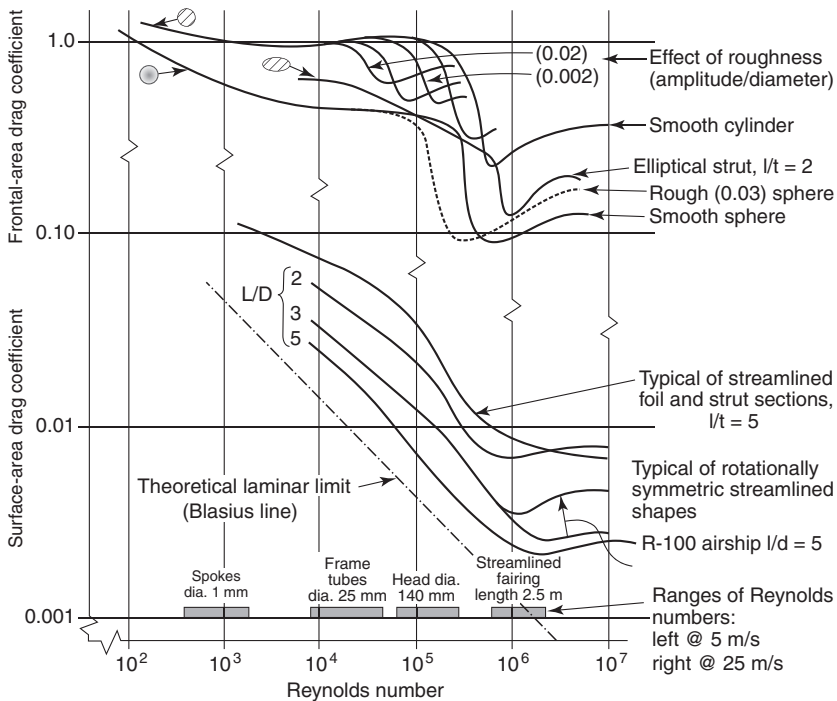


Figure 5.7

Frontal-area (C_D) (upper part of the figure) and surface-area ($C_{D,SA}$) (lower part) drag coefficients versus Reynolds number for useful shapes, and also the theoretical limit for $C_{D,SA}$. The quantity l/t refers to a body's length-to-thickness (or length-to-diameter) ratio. (Data from Hoerner 1965 and other sources.)

is a transition to lower Reynolds numbers and results in a low value for C_D . Thus, somewhat paradoxically, a rough surface can lead to low levels of drag.

Compared with a golf ball, a bicyclist travels much more slowly but has a larger equivalent diameter, so the two may have similar Reynolds numbers. A bicyclist using an upright posture may be considered for simplicity as a smooth circular cylinder normal to the flow, a curve for which is shown in figure 5.7. If a cylinder diameter of 600 mm is taken as representing an average person and a speed of 5 m/s is used, $Re = 2 \times 10^5$, which is less than Re at the transition region of about 4×10^5 . There may therefore be some advantage to wearing rough clothing for speeds in the transition region. Most bicyclists have become aware of the speed penalty that results from converting themselves into smooth but highly unstreamlined bodies (see figure 5.9 and “Partial and Full Fairings”) by donning a wet-weather cape or poncho, which usually greatly increases wind resistance without increasing cross-sectional area. Perhaps some trips woven into the cape material would be beneficial. Even better would be some type of frame that would convert the cape into a low-drag shape. Archibald Sharp proposed such a scheme in 1899, and capes with inflatable rims were for sale around that time. (See “Partial and Full Fairings” for modern variations.)

Most everyday bicycling takes place in the Reynolds number range of $1-4 \times 10^5$, at which the use of some form of practical low-drag shape as an enclosure or fairing can reduce air drag as much as nearly 90 percent. Special-purpose fairings for racing or setting speed records can produce an even greater reduction in drag.

Low-drag shapes do not generally exhibit a sharp transition from high drag (separated flow) to low drag (attached flow) as the Reynolds number increases. Rather, the boundary layer’s point of transition from laminar to turbulent tends to move upstream toward the leading edge of the body as the Reynolds number increases. Thus, the drag coefficients given for streamlined shapes (as would be represented by, for example, an airship) in figure 5.7 show a continuous decrease as the Reynolds number increases in the laminar-flow region, followed by a moderate rise to the fully turbulent conditions, and then a continued decrease. The Reynolds numbers of streamlined fairings for human-powered vehicles lie in the interesting region between 3×10^5 and 3×10^6 , where the transition from

high drag to low drag takes place, but also where the minimum possible $C_{D,SA}$ value of about 0.002 lies.

The drag coefficient usually does not drop rapidly enough with an increase of velocity or Reynolds number to counteract the need for greater propulsion power, which increases with the cube of velocity. However, hypothetically, certain bodies in certain conditions in which the drag coefficient decreases very rapidly as V increases could accelerate by 20–30 percent without any increase in power.

The curves in figure 5.8, taken from Hoerner 1965, show that for a drag coefficient based on maximum cross-sectional (or frontal) area, the minimum drag coefficient is given by streamlined shapes with a length-to-maximum thickness or diameter ratio of 3:1 to 4:1.

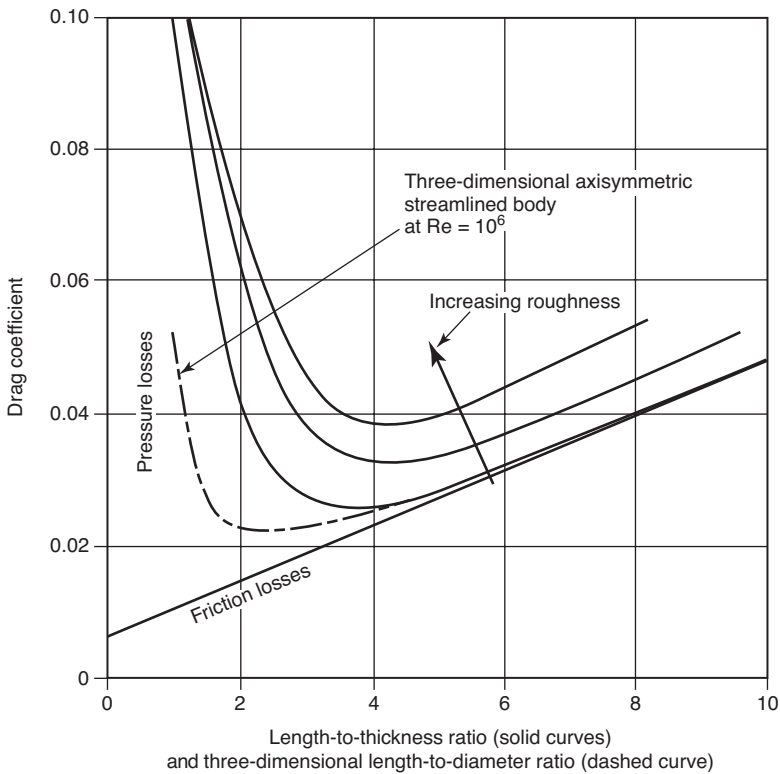


Figure 5.8
Optimum length-to-thickness ratios of wing and strut sections and of one three-dimensional streamlined body. (Data from Hoerner 1965 and other sources.)

Airfoil Sections for Struts and Fairings

Abbott and Doenhoff's (1959) *Theory of Wing Sections*, reprints of which are widely available, provides data on, among other things, NACA airfoils, which use a systematic scheme for naming wing sections; for example, one or two leading zeros in a name often identify a symmetrical section, and the name's last two digits generally give the maximum thickness in percent. The specifications for these wing sections (and many more) are also available from a large database available at Selig 2019. They were devised for airplane wings, propellers, and struts, but some of the symmetrical sections can be used for the main parts of low-drag fairings and canopies.

Abbott and Doenhoff's data are two-dimensional. Their model sections, about 1 m wide, were mounted between the walls of a wind tunnel, and the data were precisely measured at Reynolds numbers of 3, 6, and 9×10^6 . (For comparison, an HPV traveling at highway speeds just about reaches a Reynolds number of 3×10^6 .)

Interesting in regard to fairings is the symmetrical NACA 0024 (similar to the slightly thinner NACA 0021 shown in figure 5.2) section, which has its maximum thickness, 24 percent in relation to its chord, at 30 percent of the chord from the nose; the GOE 776 (Göttingen) is nearly identical. The minimal C_D value ranges from 0.0075 to 0.0085. The lower the Reynolds number, the higher the value of C_D , and for this section (calculated with values from Airfoiltools.com using Mark Drela's program XFOIL [see Drela and Youngren 2013]), at $Re = 10^6$, the C_D value increases to 0.01; at $Re = 10^5$, to 0.03; and at $Re = 50,000$, to 0.06. (Streamlined components of an aero-bicycle frame have a Reynolds number well below 50,000.) These C_D values are not directly applicable to fairings, as they relate to a wing area and thus do not represent the three-dimensional nature of fairings, but they are useful for comparisons and for showing the strong dependency of drag on the Reynolds number.

The NACA 00XX series and similar standard airfoils, with their greatest thicknesses at roughly one-third of the section's chord from the front, are designed to avoid sudden variations in the drag coefficient due to boundary-layer transition effects. By moving the greatest thickness further downstream from the front of the wing, laminar airfoils delay the transition of the airflow from laminar to turbulent, which potentially produces lower C_D values. For example, the NACA 66-021 section (21 percent thick at 45 percent chord;

see figure 5.2) has C_D values of 0.0035–0.0055 for the range of high Reynolds numbers given earlier (3 , 6 , and 9×10^6) and 0.009–0.05 for the low range (10^6 , 10^5 , and $50,000$). For $Re = 9 \times 10^6$ (which only extremely large and fast HPVs would ever reach), the improvement compared to standard airfoils is more than twofold, but for $Re = 50,000$ there is very little improvement, and the data also show a high sensitivity to the exact flow direction and surface roughness. Just a slight side wind could push C_D values up to 0.07 (at low Re), and a rough surface could treble the drag (at high values for Re). Imperfections, dust, vibrations, or a little side wind could ruin the improvement in the drag coefficient C_D and make C_D values higher than with the more tolerant standard shapes and their gentler tail angles. So although it is possible, in favorable conditions (e.g., dropping a test object into a still ocean), to reach extremely low C_D values through laminar flow at high Reynolds numbers, these values may not be possible for a bicycle fairing subjected to vibration, dirt, and turbulence, and thus it may be better to use more standard sections for such fairings.

Even thicker airfoil sections could reduce the minimal length and surface area required for a fairing. The Eppler 863 airfoil is designed for fairing struts (see figure 5.1). It is about 36 percent thick at 28 percent of the chord from the front. Values for C_D range from 0.015 to 0.15 with $Re = 10^6$ to $50,000$. This performance looks pretty poor compared to that of the thinner sections, but the airfoil's surface-area reduction can make up for it, at least when struts are faired at $Re = 10^6$.

Reducing the Aerodynamic Drag on Bicycles

To reduce the wind-induced drag on a bicycle and rider, two alternatives are to reduce either the frontal area of rider plus machine or the drag coefficient of the combined body. For years, bicyclists have adopted one or other of these alternatives, but only recently have there been concerted attempts to reduce frontal area and drag coefficient simultaneously. The results have been remarkable. Table 5.1 assembles a selection of interesting and typical data (from Gross, Kyle, and Malewicki 1983 and Wilson 1997). The table's first two columns list the drag coefficients and frontal areas, and the fourth column calculates the product of the two, $C_D A$; typical values for

Table 5.1

Bicycle drag coefficients and other data

Machine and rider	Drag coefficient on frontal area, C_D	Frontal area, A		Drag area, $C_D A$	Power to overcome air drag at 10 m/s (22 mph)	Power to overcome rolling resistance at 10 m/s for specified total mass and value of rolling-resistance coefficient, C_R		
	C_D	m ²	ft ²	m ²	W	kg	C_R	W
Upright commuting bike	1.15	0.55	5.92	0.63	345	90	0.0060	53
Road bike, touring position	1.0	0.40	4.30	0.40	220	95	0.0045	38
Racing bike, rider crouched, tight clothing	0.88	0.36	3.90	0.32	176	81	0.0030	24
Road bike with Zipper fairing	0.52	0.55	5.92	0.29	157	85	0.0045	38
Road bike with pneumatic Aeroshell and bottom skirt	0.21	0.68	7.32	0.14	78.5	90	0.0045	40
Unfaired long-wheelbase recumbent (Easy Racer)	0.77	0.35	3.80	0.27	148	90	0.0045	40
Faired long-wheelbase recumbent (Avatar Bluebell)	0.12	0.48	5.0	0.056	30.8	95	0.0045	42
Vector faired recumbent tricycle, single	0.11	0.42	4.56	0.047	25.8	105	0.0045	46
Road bike, Kyle fairing	0.10	0.71	7.64	0.071	39.0	90	0.0045	40
M5 faired low racer	0.13	0.35	3.77	0.044	24.2	90	0.003	26
Flux short wheelbase, rear fairing	0.55	0.35	3.77	0.194	107	90	0.004	35
Moser bicycle	0.51	0.42	4.52	0.21	118	80	0.003	24
Radius Peer Gynt, unfaired	0.74	0.56	6.03	0.42	228	90	0.0045	40
Peer Gynt, front fairing	0.75	0.58	6.24	0.44	240	93	0.0045	41

these three quantities for an upright commuting bike or roadster are 1.15, 0.55 m², and 0.63 m², respectively. Such a bicycle and rider and this set of values are usually regarded as the base case, to which improvements can be made. (The values include the rider and are a bit higher for very large people and lower for children or small people.)

Upright Cycling Positions

One obvious source of drag reduction is for the rider to switch from a completely upright position to one offering less frontal area. The so-called touring position, with the rider's hands on the top of the handlebars, is used when riding a road bike (one with dropped handlebars). This position reduces the drag coefficient from about 1.15 to 1.0 and the frontal area from 0.55 to 0.4 m², decreasing $C_D A$ values from 0.63 to 0.40 m². The fifth column of table 5.1 shows the power required at the driving wheel to overcome aerodynamic drag at 10 m/s (22 mph), the speed at which aerodynamic drag becomes dominant on unfaired bicycles. The data in this column show immediately why ordinary people do not commute on upright bikes at 10 m/s (except with power assistance): propelling the bicycle at that speed requires 345 W (approaching half a horsepower) just to overcome aerodynamic drag. A rider must also put power into the pedals to supply losses in the transmission, normally small, and to make up for the rolling friction of the tires on the roadway, for which some typical data are given in the last three columns. The total power required to propel the upright bicycle at 10 m/s is thus more than 400 W (including that required to offset transmission losses, not shown in the table), a level that NASA found "healthy men" could maintain for only 1 min (figure 2.4). Just switching to a road bike and using the touring position would reduce the total power required (on level ground in calm wind conditions) to about 275 W, which figure 2.4 shows a nominally healthy male could keep up for about 30 min, a typical commuting duration. (It would be atypical to be able to commute for 30 min at constant speed, but if the typical male could do that, the distance would be about 18 km or 11 mi.)

A further dramatic decrease in drag resistance results if a rider uses a racing bike. (A racing bike is actually little different from the road bike used in the preceding example, but the table specifies a

lighter weight and a frontal area that includes the effects of tight clothing and having the hands on the full-drop part of the handlebars; additionally, the figures for the rolling drag imply the use of high-pressure tires. Loose clothing can increase aerodynamic drag, at speeds greater than 10 m/s, by 30 percent.) On such a bike, the drag coefficient decreases to 0.88 (mainly because the head is down in front of the rider's rounded back), the frontal area is 0.36 m², and $C_D A$ drops to 0.32 m². The power required to ride at 10 m/s, including tire and transmission losses, is then about 210 W, which the typical healthy man can keep up, according to NASA, for almost 1 h. People who ride such bikes are more likely, however, to be more like NASA's "first-class athletes," whom figure 2.4 shows to be capable of riding at 10 m/s indefinitely—which might be translated as until the need for food, sleep, or other demands of the body must be answered.

An even more aerodynamic position is generally used in time trials: special handlebars called *tri-bars* allow the forearms to rest parallel to one another in front of the chest, further reducing $C_D A$ to 0.21 m² (see Blocken et al. 2013, which also reports $C_D A$ values of 0.25 m² for cyclists with dropped handlebars and 0.27 m² for upright cyclists). Between 1993 and 1996, several racing cyclists developed aerodynamically optimum positions for riders and set hour records that have never since been reached or exceeded, as the positions were banned afterward. Today's time-trial positions enable riders to achieve speeds for 1 h races that are 10–12 percent (or roughly 5–6 km/h) slower than the very best hour record of Chris Boardman, 56.375 km, using an arm position reminiscent of Superman.

Prone, Supine, and Recumbent Positions and Bikes

Only changing the pedaling position can reduce the frontal area presented by a bicycle and its rider below that required for a conventional racing bike. Speed records have been achieved on bicycles designed for head-first, face-down horizontal-body (prone) pedaling and for feet-first, face-up horizontal-body (supine) pedaling (in the strict forms of which a periscope or other device is needed to enable riders to see where they are going), and for a wide variety of what is known as *recumbent pedaling*. Purists would say that fully recumbent pedaling is supine and that strictly speaking the position used by the riders of recumbents is in fact *semirecumbent*. However, the form

of bicycle designed to be ridden in such a semirecumbent position has become known in the English-speaking world as recumbent, or “bent” (and in Europe, for example, as Liegerad, *vélo-couché*, or *ligfiets*). Table 5.1 shows one well-known successful recumbent, the Easy Racer, as having a drag coefficient of 0.77, a frontal area of 0.35 m², and a drag area of 0.27 m², considerably lower than that of the racing bike with the rider in a painful crouch. Therein lies a principal reason for the recumbent’s growing popularity at the turn of the millennium: it can be simultaneously fast and comfortable. (These data may not be typical: also given in the table are measurements on a Radius Peer Gynt recumbent, showing considerably higher drag values.)

Partial and Full Fairings

The organization that controls the rules for conventional bicycle racing, the UCI, has outlawed most measures aimed at reducing aerodynamic drag, including use of the recumbent position, and has even ruled inadmissible the form of racing crouch adopted by Graeme Obree, who beat the 1 h distance record twice in 1993, the second time reaching 52.7 km. However, this book is aimed at providing data helpful to people racing under all rules (including those of the IHPVA, WHPVA, and WRRRA), not just those of the UCI, and to those who simply want to use their muscles to travel either at the fastest possible speeds or with the least possible effort at a chosen speed. For these people, “going recumbent” or using methods of streamlining, including partial or total streamlined enclosures or fairings, offer attractive potential. A fairing also adds weight to a bicycle and makes it bulkier and more difficult to carry and to transport, and at the present stage of development, getting into and exiting a bicycle equipped with a fairing can take a rider considerable time. Accordingly, many people have devised partial fairings for the front or rear of bicycles, often more for practical than aerodynamic reasons.

Table 5.1 includes data for a bicycle with a partial front fairing, an early model known as Zipper. The Zipper’s configuration of bicycle and fairing is shown to produce a relatively low drag coefficient and an overall value of $C_D A$ lower than that for a racing bike with the rider in a full crouch. However, when a partial front fairing was fitted to a long-wheelbase Peer Gynt recumbent during



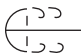
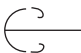
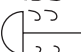
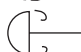
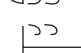
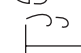

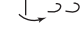




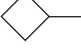

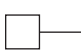
Three-dimensional		C_D	Two-dimensional		C_D
Sphere		0.47	Circular cylinder		1.17
Hollow half sphere		0.38	Open half cylinder		1.20
Closed half sphere		0.42	Closed half cylinder		1.16
Disk		1.17	Flat plate		1.98
Closed half sphere		1.17	Forward-curved half cylinder		2.30
Hollow half sphere		1.42	Square cylinder		1.55
Cube		0.80	Square cylinder		2.05
Cube		1.05	Triangular (90°) cylinder		1.55
Cone (60°)		0.50			

Figure 5.9

Drag coefficients of various shapes for $Re = 10^4$ – 10^6 . (Data from Hoerner 1965 and other sources.)

tests conducted for and published in the German bicycle magazine *Tour*, both the coefficient of drag and the frontal area *increased* by small amounts. The notes accompanying the article stated that small variations in the fairing’s positioning produce relatively large changes in drag. Figure 5.9 shows the drag coefficients of certain two- and three-dimensional shapes (from Hoerner 1965), including some that could be used as front fairings. The aerodynamic advantages conferred by front fairings have always been somewhat controversial, which seems to call for research into the flow patterns found with different settings and spacings between the fairing and the rider.

In 1899, Archibald Sharp suggested using inflatable tubes to form a poncho or cape or other piece of clothing into an aerodynamic shape. Paul van Valkenburgh developed this idea in the Aeroshell, with an inflatable “suit” plus a skirt to extend the shape to close to the ground, and as table 5.1 shows, reduced drag to less than half that of a racing bicycle.



Figure 5.10

Use of tail cone to reduce drag. (From Borge, *Le Vélo*, 116.)

The Swiss cyclist Oscar Egg, on a standard bicycle, set a 1 h distance record of 44.247 km in 1914 that lasted for nineteen years. In 1932 he was excited by the high speeds achieved by Francis Faure on the Velocar (see chapter 1) and started experimenting with tail cones to decrease his drag (Mochet 1999) (figure 5.10). Tests at the time showed no improvement in speed. However, it has become popular for the same purpose, particularly in Europe, to fit aerodynamic “tail boxes” behind the seats of recumbent bikes to achieve some pressure recovery. Table 5.1 includes data for a Flux short-wheelbase recumbent fitted with a rear fairing of this type, with a value for $C_D A$ considerably below that of the unfaired Easy Racer recumbent.

Table 5.1 also includes data for several machines with full fairings, which come as close to completely enclosing rider and machine as possible. Chester Kyle’s fairing of a road bike has a drag coefficient of 0.10 but a fairly large frontal area, as would be expected of a conventional bike, and the $C_D A$ value is found to be 0.071 m^2 . Recumbents tend to have higher drag coefficients when these coefficients are based on the frontal area, because the larger surface areas that



Figure 5.11

Bram Moens with his M5 Low Racer. (Courtesy of Bram Moens.)

result from riding in the recumbent position contribute drag, but the resulting $C_D A$ values can be very low: 0.056 m^2 for the Avatar Bluebell, 0.047 m^2 for the Vector recumbent tricycle, and 0.044 m^2 for Bram Moens's M5 Low Racer (figure 5.11). As table 5.1 shows, the estimated power required to overcome rolling drag at 10 m/s is higher in this last machine than that for aerodynamic drag.

Full fairings designed for record events must often be taped shut over the riders, who then must be released from the fairings at the end of their runs. There are many ways in which fairings can be compromised to make them easier to use in normal situations.

One way is to shorten the tail, taking a penalty in reduced pressure recovery, as shown in figure 5.12. Many riders prefer to have their heads out of fairings when using faired bicycles for commuting or recreation and to have gaps in the fairings for access. Such discontinuities will restrict the extent of laminar flow to the surfaces ahead of them; see Kyle 1995 for discussion of the relevant factors and how to interpolate among the data for relevant machines in table 5.1. Some equip their full fairings with foot flaps, so that the bicycles can be used on roads. Figure 3.5 shows such a machine with

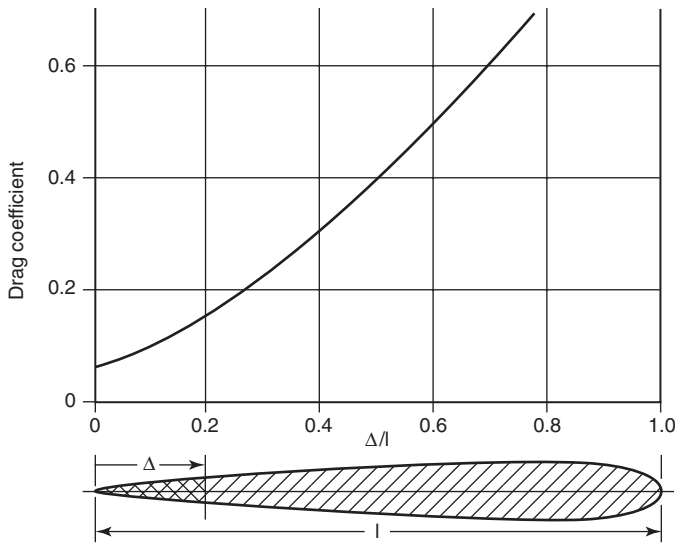


Figure 5.12

Effect on drag of cutoff trailing edges. (Data from Hoerner 1965.)

the foot flaps closed, and the rider of the Lightning shown in figure 5.13 also has slits in the fabric fairing for putting his feet through.

Partial fairings are more practical in traffic and can still be optimized for racing. Figure 5.14 shows a Birk Comet with the rear of the vehicle and the rider's helmet faired as much as possible, as well as the handlebars and fork.

Other Aerodynamic Phenomena

Boundary-Layer Suction

A separating flow leaves the surface of a fairing either because some fairly extreme form of roughness trips it or because the boundary layer becomes thick enough for an adverse pressure gradient to push the low-momentum inner layers (those against the fairing surface) backward (relatively). Therefore it is reasonable to expect that sucking these low-momentum layers away through holes or slits in the fairing surface could make a previously separating flow remain attached to the surface, enabling pressure recovery and greatly reducing drag.



Figure 5.13

Partially faired Lightning F40 with additional fabric. (Photo by Michael Amman.)

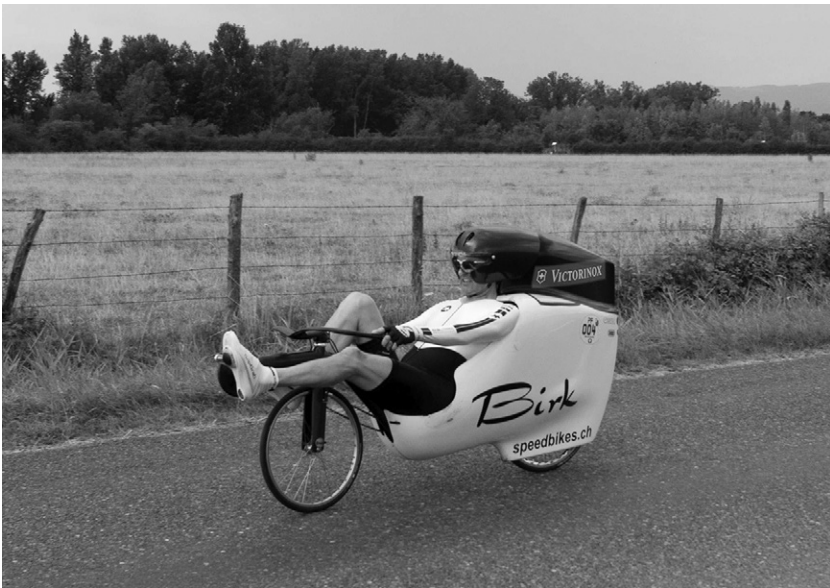


Figure 5.14

Partially faired Birk Comet in a road race at the 2019 HPV World Championship in Nandax, France. (Photo by Michael Amman.)

Sucking away the boundary layer requires some power, but it could be a small amount compared with the savings in propulsion power. For a typical human-powered fully faired vehicle traveling at 65 mph (~ 29 m/s), Bruce Holmes (of NASA Langley) calculates that the power required to overcome air drag, were there to be no laminar flow whatsoever, would be 225 W. However, normal natural laminar flow would be expected to cover about 50 percent of the vehicle's surface, resulting in 160 W drag power (see Wilson 1985). If suction were progressively applied until 95 percent of the vehicle's surface had an attached laminar boundary layer, the propulsion power required to overcome drag would be expected to be about 100 W, or even less depending on the actual Reynolds number. Figure 5.4 shows that at a Reynolds number of a few million, the skin-friction coefficient C_F would be reduced at least fourfold, from that for a fully turbulent to that for a fully laminar condition. In the example here, the drag would then be reduced to 65 W. Holmes estimates the power required to produce the required suction to be below 20 W, for a total power requirement of 85–120 W, much less than without suction.

This is a tantalizing prospect for anyone planning to break speed records, but caution in this area must be advised. In real conditions, more power than assumed might be necessary to suck away the boundary layer. Hoerner (1965) is not optimistic about suction and suggests that although the effective C_D of a 30 percent thick suction section could be reduced, using suction (at $Re = 10^6$), to reduce C_D from 0.025 to 0.01, this result is no better than that which can be achieved using other streamlined sections without suction.

The Effects of Surface Roughness on Streamlined Bodies

Although, as mentioned earlier in the chapter, a rough surface on a poorly streamlined body can provide advantages in promoting the transition of the boundary-layer flow from laminar to turbulent, which might permit more recovery of pressure on the aft portion of the body and thus a reduction in drag, with a streamlined body (which could be defined as one without flow separation), one should undoubtedly strive for as smooth a surface as possible. Nikuradse's classical experiments on flow in tubes (figure 5.4), discussed in Hoerner 1965, show the effect of simple sand-grain roughness on the skin-friction coefficient. Nikuradse's experiments use, for the

length in the Reynolds number, the length of the tube, and the lines of constant roughness are characterized as the sand-grain diameter divided by this length.

Hoerner (1965) also quotes the results of flight tests on the wing of a King Cobra airplane that had surface imperfections as received. Removing these imperfections reduced the drag at low-lift conditions (corresponding to the fairing of an HPV) by 65 percent.

Drafting, Tandems, and Side-by-Side Cycling

A bicyclist is *taking pace*, *drafting*, or *slipstreaming* when traveling close behind another moving body, using it to break the wind. The vortices behind a leading bluff body (see figure 5.1) may indeed even help to propel the trailing rider (see also chapter 3). Drafting is therefore an important part of strategy in massed-start races.

When streamlined fairings are used, riders find that there appears to be no benefit in drafting, because there are no trailing vortices or large masses of captured air behind an aerodynamically faired shape. In fact, some data reported later in the chapter indicate that drafting may impose a substantial penalty on a bicycle equipped with a fairing.

Graphs of the drag of pairs of bodies given in Hoerner 1965 and discussed by Papadopoulos and Drela (1998–1999), some of which are reproduced here, illustrate well the aerodynamic phenomena involved in drafting. A rough representation of two riders one behind the other is of two circular cylinders (figure 5.15). With a gap about two diameters between the two, the *lead* cylinder (or cyclist) experiences a drag reduction of about 15 percent. The *rear* cylinder encounters nearly zero drag. When the separation increases to four diameters or more, the lead loses any benefit, whereas the rear drag is reduced fourfold. Blocken and Toparlak (2015) investigate the “push” that a following car gives a leading cyclist.

Figure 5.16 offers treatment similar to that in figure 5.15 for streamlined cylinders (struts), which could be regarded as representing two-dimensional (vertical) fairings for HPVs. When two HPVs equipped with such fairings are within about one length of one another, the front one actually receives a push, whereas the drag on the drafting one quadruples. Presumably the wake from the first fairing causes flow separation over the second fairing. It is no wonder, then, that riders in (streamlined) HPV races do not try to draft one another.

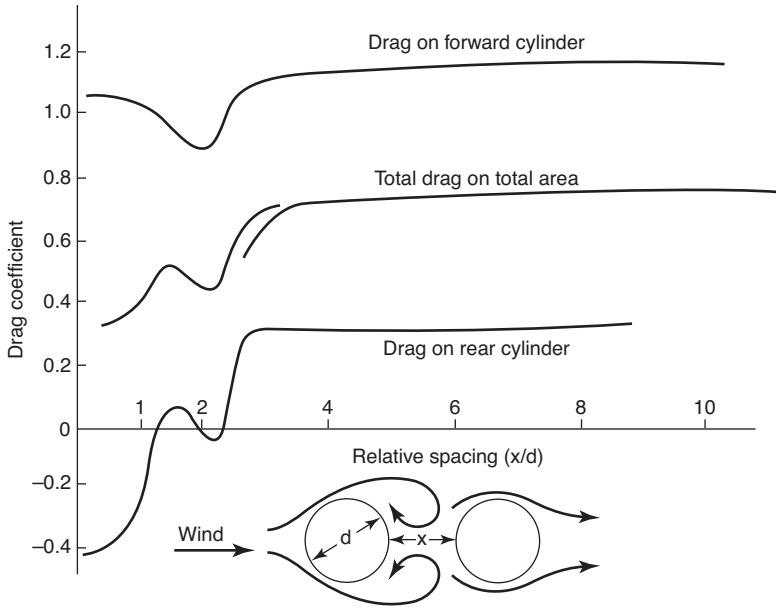


Figure 5.15
 Drag of a pair of circular cylinders, one behind the other, in tandem. (Data from Hoerner 1965.)

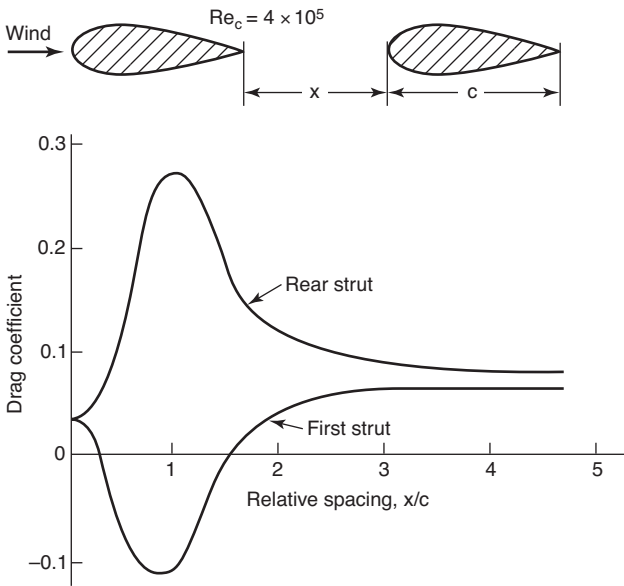


Figure 5.16
 Drag on a pair of strut sections, one behind the other, in tandem. (Data from Hoerner 1965.)

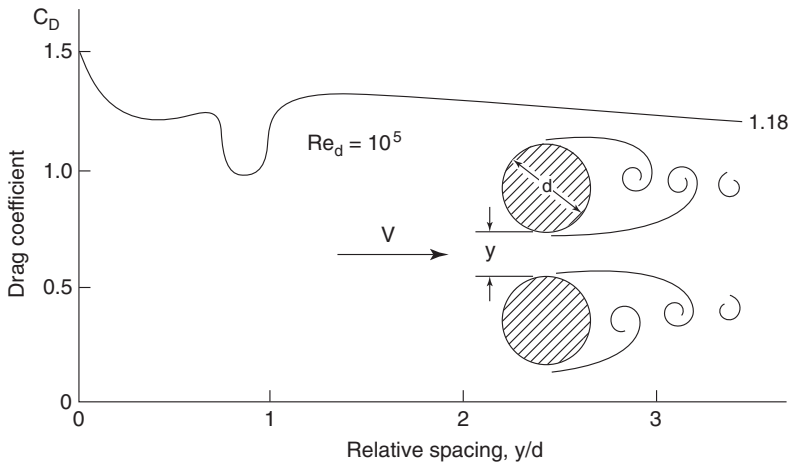


Figure 5.17

Drag of a pair of circular cylinders, one beside the other. (Data from Hoerner 1965.)

Figure 5.17 plots the drag on two circular cylinders side by side. When the cylinders are touching, this increases the drag about 25 percent over the solo value. One-diameter spacing reduces the drag about 15 percent over a small range, indicating a sensitive interaction related to the trailing vortices. When two streamlined cylinders (struts) are side by side (figure 5.18), the drag is greatly increased at small spacings and decreases to solo values only at relative spacings greater than four diameters.

When two streamlined cylinders (struts) are side by side (figure 5.18), the drag is greatly increased at small spacings and decreases to the solo values only at relative spacings greater than four diameters.

Two-person drafting has been explored in detail both experimentally and in simulations. Blocken et al. (2013) determine that $C_D A$ values may be reduced 15–30 percent for a following cyclist, depending on the type of position, from time trial to upright, at 15 m/s and with the bicycles almost touching. Not only the follower benefits, but also the leader slightly, by up to a couple of percent. The average benefit (determined by dividing the total benefit by the number of riders) is thus a bit more than 7.5–15 percent drag reduction in Blocken and colleagues' research.

If the number of closely following cyclists increases, as is usual for pelotons in road racing, this advantage remains or even increases to

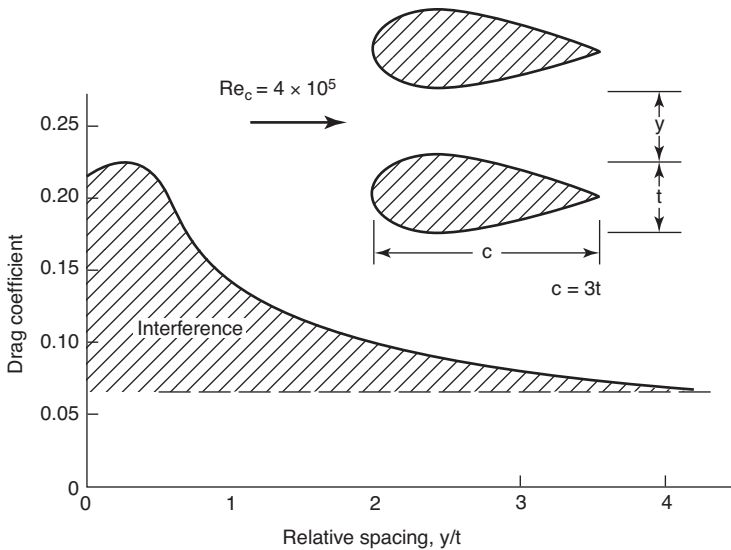


Figure 5.18

Drag on a pair of struts, one beside the other. (Data from Hoerner 1965.)

as much as 40 percent for following riders (see Defraeye et al. 2013 for data involving four riders). In theory it continues to increase even with a larger number of cyclists. Blocken et al. (2018) analyze pelotons of 121 riders and show that about half the riders experience only 5–10 percent of the drag of a single rider, and the other half also experience substantial reductions. Touring cyclists benefit a bit less than the figures above because larger gaps between riders are chosen, but the sources cited here suggest still large drag reductions when bicycles are a meter apart.

The best track time of four-man teams on 4 km course (2016 Olympic *team* pursuit), at 3 min 51 s, shows a speed advantage of 8 percent over the best individual times of 1996 and 2011 (men's *individual* pursuit), at 4 min 11 s. As power is proportional to speed cubed, if the power of each man is assumed the same and rolling resistance is neglected, the average drag reduction is $1 - (1.08 V)^3 \approx 20.6$ percent.

If drafting works, it should work even better in regard to unfaired, upright tandem bicycles, as the riders are closer together and there are fewer wheels and struts. The second rider (the *stoker*) is drafting

behind the leading rider and therefore incurs little additional drag beyond that which results from the first rider. Kyle (1979) estimates a 50 percent drag advantage for two-rider tandems, which would translate to about a 26 percent speed advantage. Seifert et al. (2003) verify this, at least approximately, by comparing physiological stresses (heart rate and lactic acid concentrations) of the same cyclists on tandems and individually at speeds from 19 to 29 km/h, finding a tandem speed advantage at about the same stress levels of 4.8–8 km/h. Tandems with up to five riders can gain even more of a speed advantage.

Wind Loads from Crosswinds and Passing Vehicles

All bicyclists who have ridden on roads frequented by large, fast-moving motor vehicles have experienced side-wind forces from the passing of those vehicles, but no experimental work concerning the magnitude of the lateral forces exerted on actual bicyclists seems to have been reported. However, the danger close-passing vehicles present to cyclists is evident not just because of the aerodynamic forces those vehicles put in play, but because slight steering errors or instabilities can lead to actual collisions, and a large and increasing proportion of cyclists' deaths result from being hit by motorists traveling in the same direction. Many countries and states therefore recommend or even require minimum passing distances between overtaking motor vehicles and cyclists. In Australia, New South Wales stipulates a minimum passing distance when overtaking a cyclist of 1.5 m, or 1 m in areas with speed limits of 60 km/h or lower. In the United States, 32 states require a minimum passing distance of 3 ft (see NCSL 2018).

Although the required passing distances (which are very often *not* observed) should mostly suffice in still air, windy conditions, especially those involving gusty crosswinds, are another matter entirely. There is little remarkable about the behavior of *unfaired* bicycles in crosswinds, except for the extraordinary stability they normally display (extraordinary because a non-bicycle-riding aerodynamicist, asked to predict the course of a bicycle hit by a sudden gust of wind at, say, 15 m/s or 34 mph, would estimate either that the bicycle would be unrideable in those conditions or that the rider would be forced into a wide swerving path to maintain stability). Most riders can ride fairly precisely (for instance, in traffic *or* in wind) in

such circumstances. Cycling starts to become dangerous with strong winds *and* traffic at the same time, especially when the cyclist is carrying out maneuvers such as looking backward, signaling, and turning.

It is quite another matter, however, to ride a *faired* bicycle in crosswinds. Even the use of front-wheel disks can make riding in crosswinds unpredictable. The large side area of a full fairing produces far greater transverse aerodynamic forces in crosswinds than those affecting an unfaired machine, as are quantified later in the chapter. How should a faired bicycle be designed to cope with these aerodynamic forces? And how a tricycle? A handful of developers have examined these questions in detail.

Milliken's (1989) simple and effective experiments showed that in most cases, the aerodynamic center of pressure of transverse flow on a fairing should be ahead of the center of mass to give good controllability in crosswinds. Matt Weaver (1991) constructed his faired bicycle Cutting Edge with the front wheel about in the middle of the fairing longitudinally, putting the center of pressure well ahead of the center of mass, with the explicit aim of good side-wind stabilization. Andreas Fuchs (1993) discusses this question in detail and reaches the same conclusion as Milliken and Weaver. Peter Sharp determined in a 1994 experiment that a bicycle pulled suddenly sideways by a cord could recover better if the cord was attached near the front of the frame than if it was attached near the saddle. Joachim Fuchs (1996) followed all of this advice in the construction of his faired bicycle Aeolos (figure 10.17) and reported that by virtue of its having its center of pressure well forward, it was easy and safe to handle in side gusts.

Gloger (1996) carried out intensive side-wind experiments using both a large fan and a small airplane to produce artificial side winds, through which he then rode his faired bicycle Desira in various configurations: unaltered, with lengthened nose, with lengthened tail, and with bottom skirt. He quantified the rides through video examination and qualified them by questionnaire, also involving a second, inexperienced test rider. Gloger found that the bicycle behaved in generally the same way in all configurations when it hit the gust: first a leeward displacement, then a lean to windward, enabling the steering to get back on course. The displacements were around 1 m for all configurations except that with the lengthened tail, with

which the displacement reached 2 m and in one case almost 3 m. The leans were mostly about 5°; those for the configuration with the extended tail were 9° and in one case 16°. The inexperienced rider also suffered a crash when using the extended nose. The subjective results were inconclusive, except that that Gloger much preferred his unaltered vehicle (similar in dimensions to Aeolos, but with a sharply truncated rear).

In an intensive study that included the Cornell bicycle equations of Ruina and Papadopoulos (see chapter 8) and the work of earlier researchers, Andreas Fuchs (1998) maintained that if a gust hit a bicycle from the side, “weathercock” behavior would tend to turn the bicycle into the wind, upset the lean angle and steering, and possibly put it into danger. He therefore recommended having the center of effort forward of the center of mass. However, Fuchs also acknowledged that such a configuration would obviously be aerodynamically unstable in situations in which the wheels were unloaded, for example, through a bump or hill at high speed, which would amplify any yawing moment even in the absence of any wind. Normally objects designed to fly free through the air, like rockets and arrows, have tail fins or feathers to make them fly straight.

The situation with tricycles is more difficult to assess visually because they don’t lean. The coauthor’s 1986 faired tricycle, with a huge rear tail fin and a center of mass very far forward, certainly felt very stable at speed and never had any problems with gusts. Sims (1998), in a series of road tests on his Greenspeed tricycles, found that steering stability improved the more lateral area was added *behind* the center of mass. He set up the test trike with reduced trail so that the steering would not move when the trike was pushed sideways. Then he tested it unfaired in strong gusting winds and found it to be completely stable. Then, with front-wheel disks fitted, its behavior was noticeably unstable, and with a 0.2 m² tail fin, it was stable again. Then he tried a full fairing, but without side windows, which resulted in a dramatic loss of straight-line capability in wind, until he mounted a large, 0.4 m² tail fin very far to the rear, which brought the handling back to almost entirely stable.

Assuming that both schools of thought are correct, a faired HPV cannot at the same time have the desired type of crosswind stability or controllability and high-speed aerodynamic straight-line

stability. Fuchs (1993) discussed this and recommended that the riders of well-controllable velomobiles such as the Leitra (see figure 10.17) that have their center of pressure very far forward should limit their downhill speeds if there is any chance of losing wheel contact.

Sailing Bicycles and Faired HPVs

There are several ways a bicycle can sail. Traditional cloth sails and small self-adjusting wing sails have been tried. Although they work well in favorable conditions, such conditions are rare in most places. And even where ideal moderate crosswinds blow, unencumbered by buildings, trees, or traffic, a sailing bicycle is rarely if ever seen. Perhaps the undertaking is just too adventurous, as there will be some other traffic, too much slope, or severe headwinds or gusts sometimes—or more likely just too little wind and the sail will have to be furled or otherwise packed up. Tailwinds are also not very useful with most sails. They are either too weak, or if strong enough, exploitable just as well without a sail. Isvan (1984) gives an extensive analysis of “sailing” bicycles on which the rider is considered to be an object like a cylinder with the same drag in all airflow directions. He concludes that

- crosswinds from 90° will slow the rider down;
- winds between 90° and 105° may provide or require extra power depending on bike speed;
- a circular course will always take longer compared to the no-wind time by approximately 30 percent $(V_T/V)^2 - 5$ percent (V_T/V) , in which V_T is the true wind speed and V the bicycle speed (not valid for very large or small ratios).

The above characterizations are in contrast to the performance of the land or ice yachts popular in some places, which on beaches or frozen lakes sail well even in light winds. The former tend to be tricycles unsuitable for use on roads, none of which have additional pedals for practical use, although kickboards with windsurf sails are versatile enough to be used in a wide range of environments. Prolonged hybrid operation, using both power sources available on the vehicle at the same time, would be unlikely anyway, as if there is enough wind to accelerate at all, these vehicles go fast, often at several times the wind speed.

With fully faired HPVs, any sailing is more likely to go unnoticed or in gusting wind be more of a detriment than an asset. However, the remainder of this chapter tries to quantify what is possible in a steady wind.

Two-Sheet Analogy

A short excursion here in the discussion: How does sailing work in principle? On its most basic level, it involves a vehicle that couples to two sheets or planes (mechanical surfaces) that move relative to it and to each other. If the coupling were perfect (such as with rack-and-pinion gears) and everything frictionless, it would be possible to move at any speed in any direction using mechanical gearing, and it is easy to build small geared models that move at several times the speed of their inputs. When, however, one or even both of the planes are actually fluids, perfect coupling is no longer possible, and there will be limiting speeds apart from those that arise through friction anyway.

Land or ice yachts can easily move several times as fast as the wind if it comes from the side, and they can tack (that is, zigzag) downwind fast enough to reach a point directly downwind before the wind (original air parcel) arrives. And of course they can tack upwind, but more slowly. After several decades of spirited discussion, it has also finally been proven in practice that a land yacht can sail *directly* downwind faster than the wind (the record is at nearly three times wind speed), if it is fitted with an efficient air propeller connected to the wheels. (The propeller size makes the vehicle impractical for most purposes other than setting records.) It is difficult to understand how this is possible, but Cavallaro (2008, 2011) and Simanek (2017) offer explanations.

Here the discussion comes back to the sailing bicycle. In following winds it is generally easy to pedal up to the wind speed, unhampered by anything but rolling resistance. A normal sail is no good in this situation, as mentioned previously, as the force of the sail decreases to zero as the cyclist approaches wind speed. But with an air propeller connected to the pedals (which doesn't need to be as large as that needed for a record-breaking vehicle), it is easy to go faster than the wind. The cyclist is in effect coupling propulsive power to the wind sheet rather than the road sheet and is harvesting

power from the following true wind, although the apparent wind is then coming from ahead.

In the same way, but connecting a wind turbine instead of a wind propeller to the wheels, a bicycle, or more likely a tricycle, can travel straight upwind more efficiently than without. The relevant forces go through the required mechanical (or electrical) mechanism in the opposite direction from the downwind case, but wind energy can still be extracted. What has changed is that the apparent wind speed is now much higher, and every little bit of parasitic air drag from vehicle and body components counts more than before. However, it is possible to go upwind at twice wind speed (see Cavallaro 2012). Because of the way the forces couple, any bicycle or tricycle fitted with even a small wind turbine can work its way upwind, provided the gearing between the turbine and the pedals is correct. It could be a practical vehicle: the coauthor would immediately build and use one if he lived on a windswept island rather than in a sheltered inland country!

A more usual way for a bicycle or HPV to sail is with a fairing that has been mounted for other reasons such as drag reduction or weather protection. Weaver (1999–2000) shows that over a wide range of angles of the apparent wind to the direction of motion, the wind acts on a bicycle fairing in much the same way as it does on a sailboat: it provides forward thrust (see figure 5.19). The fairing can take flow at a considerable range of incidence angles and can even provide forward thrust from wind coming somewhat forward of exactly sideways. Wind therefore has an important effect on records involving bicycling, even if a record-setting ride is made on a circular or oval track. Howell and Hughes (1984) show in wind tunnel tests that even if there is not enough thrust to support actual sailing, a 25 m/s wind speed reduces a vehicle's effective frontal-area drag coefficient C_D from 1.2 to 0.6 if the apparent wind deviates 15° from the longitudinal axis. The action of wind on a bicycle's fairing can reduce thrust or drag even though the fairing has no camber or asymmetrical curvature; is not rotatable, as with sails; and has no flaps or control surfaces, as with airplanes. The next section attempts to quantify the conditions necessary for sailing partially or fully.

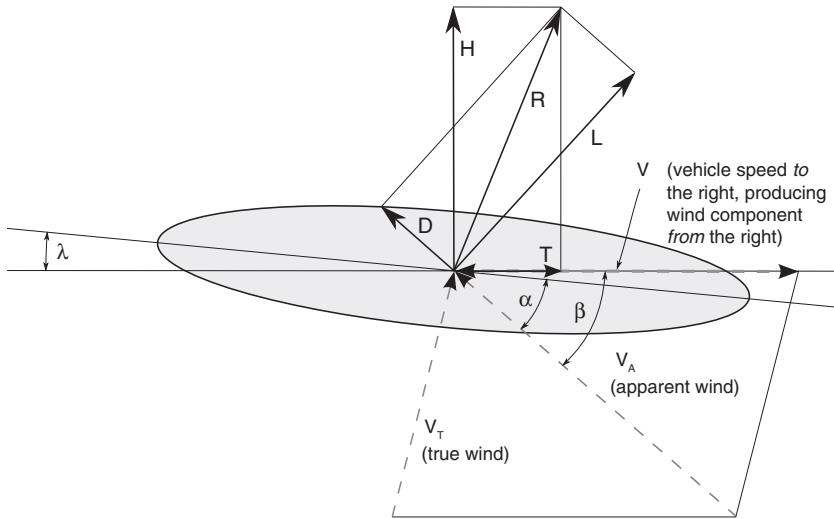


Figure 5.19

Resultant force R and its components arising from the apparent wind V_A (vector sum of V [here from 90°] and true wind V_T [here from $\sim 190^\circ$]) acting on a fairing. L is lift, D is drag, H is heel or sideways force, T is thrust; α refers to angle of incidence relative to the fairing, β to the angle of the apparent wind relative to the vehicle's axis of movement, and λ to the difference between α and β .

Calculating Sailing Forces

The first task in calculating forces operating on any type of sailing bicycle is to calculate the magnitude and direction of the *apparent wind* V_A relative to the bicycle, which is simply the vector sum of the *true wind* V_T relative to the ground and the wind V arising from the bicycle's movement. This is easily done graphically on paper or using standard formulas, in which case great care must be taken with the signs or directions of the magnitudes and angles, as there are several different conventions. Most use the non-SI unit degree instead of radians ($1 \text{ rad} \approx 57.3^\circ$), so that every equation must include conversion factors where needed. The following discussion uses the meteorological definition of the wind direction and the traditional compass rose. A north wind is defined as blowing *from* the north, which is 0° on the compass rose and points upward on maps; a northeast wind has an azimuthal angle of 45° , and so on. A bicycle moving at speed V *toward* a certain direction in still air produces wind of the same magnitude *from* this direction, so we can

use V also for this wind, rather than $-V$. Adding V and V_T as vectors thus gives V_A , which always comes from a forward direction as long as V is larger than V_T .

The angle of V_A relative to the vehicle's axis of movement is represented by the symbol β . It is not in general the same as the angle of attack or angle of incidence α relative to the fairing, because of lateral tire slip due to the sideways force H (which is described in chapter 6 and is on the order of a few degrees). The difference between α and β is in sailing terminology called leeway (λ). The following discussion ignores it (that is, it assumes $\alpha = \beta$). It also assumes no air drag from anything but the fairing itself, which is treated like a short wing or airfoil, and also assumes that the fairing is fixed and symmetrical. (A pure sailing vehicle would probably be able to rotate the wing or steer all wheels and use an asymmetrical foil section, flaps, or other means of steering the airflow.)

A faired HPV in wind is in principle like the Windmobile (windmobile.net) designed and described by James Amick (1979). Using a fixed, symmetrical, arch-shaped solid wingsail, this (electric) tri-cycle is in ideal conditions able to travel without the motor at up to 4.5 times the wind speed, 1.5 times the wind speed to windward, and 2.5 times that to leeward in good conditions, or with regenerative braking to harvest 1–2 kW electrically while moving at several times wind speed, when the true wind comes from about 100° relative to the heading. Like this Windmobile or the related Darrieus wind turbine, a faired HPV cannot normally start sailing itself but must first be powered up to a speed that causes the apparent wind to come from a direction enabling it to sail. In a personal communication with the coauthor in 2018, James Amick's son, Douglas Amick, said that the original Windmobile could steer all wheels in order to influence the angle of attack but that this was shown to be unnecessary, as the Windmobile can accelerate with the motor until the angle of attack becomes favorable, which then allows the wind to provide the power. A faired HPV can do the same thing.

As shown in figure 5.19, the apparent wind V_A acting on a vehicle's fairing produces a predominantly sideways resultant force R , the calculation of which requires its orthogonal components *lift* (L , exactly at right angles to V_A) and *drag* (D , in the direction of V_A). As forces, lift and drag operate under the same formulas as those for pure air drag, described previously in the chapter, and are

represented with the coefficients C_L and C_D . Those coefficients relate to a specific surface area, and for wings (and thus fairings in their role as sails), neither the frontal area nor the wetted surface area as previously described is used, but the projected lateral area, as seen when looking at the fairing from the side. The coefficients C_L and C_D can be calculated using various formulas or looked up in graphs or tables for particular shapes or their sections as a function of the Reynolds number (described earlier) and α .

However, such tabulated data can't just be used as presented, as they are two-dimensional. Airplane wings and the like usually have a high *aspect ratio* (AR), that is, they are many times longer than they are wide. Or in aeronautical terminology, a wing's span (b) is much larger than its chord (c), and $AR \approx b/c$. The airflow around a slender wing or similar structure is two-dimensional except at the ends, where it "leaks" around from the high-pressure to the low-pressure side. However, there is an approximate proportionality between α and C_L for values of α up to about 10° . The function is simply linear up to $C_L \approx 1$ at $\alpha = 10^\circ$ (see the leftmost curve in figure 5.20). Most wing sections go on a bit further, less than linearly, with C_L values reaching 1.2–1.5 at 15 – 20° , then they *stall*—they rapidly lose a great deal of lift with greatly increased drag. But below a maximum of 10 – 15° , C_L values are easy to calculate, and values of C_D can be looked up. There is a further drag component to be added: the *induced drag*, given by $C_{Di} = C_L^2/(\pi AR)$. The real quantity of interest here, however, is the lift-to-drag ratio (L/D), which can be as high as 50 – 100 for sailplane wings. The wingsail even for a specifically designed practical sailing tricycle would be less efficient than such wings, but still pretty effective, as the example of the Windmobile described earlier shows.

A normal fairing is much lower to the ground than a sail, and because it has an aspect ratio of 1 or less, the lift is smaller and the drag is larger, as can be seen by calculating the induced drag. Most of the air "leaks" around the fairing, greatly reducing lift. Therefore the precise value of AR becomes more important and must be defined exactly, and b^2/A is used instead of b/c . (A is the fairing's projected lateral area here. Fuchs 1993 discusses the subject.) Data for low-aspect-ratio wings are rare, but Hoerner and Borst (1975) give a relationship for $AR \lesssim 1$: $C_L = \alpha AR \pi/2$ (α in radians), or $C_L \approx 0.0274 \alpha AR$ (α in degrees). Measurements provided by Hoerner

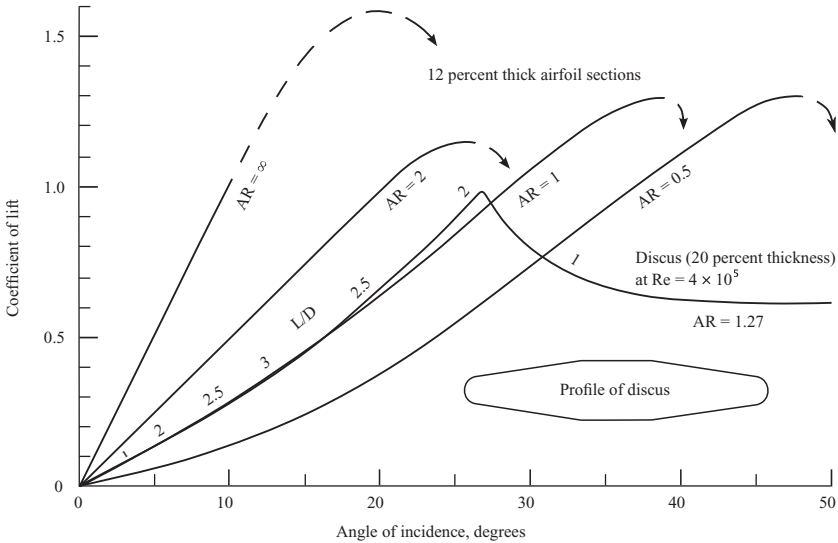


Figure 5.20 Lift coefficients for low-aspect-ratio airfoils and Olympic discus, with lift-to-drag ratio L/D . (Data from Hoerner and Borst 1975.)

and Borst (see figure 5.20) (at unknown Reynolds numbers) agree well with this up to $\alpha \approx 15^\circ$, as do data offered by O'Neill (2006). Unlike high-aspect-ratio wings, these shapes do not stall until α exceeds 40° . Unfortunately, Hoerner and Borst include no complete C_D values except in the case of one specific object: a discus (as thrown in sport) at several Re values around 400,000 (see figure 5.20). This discus has an aspect ratio of $\pi/4 = 1.27$ but follows the curve for $AR = 1$ rather well for α values up to about 27° , then it stalls with a sharp peak at $C_L = 1$. Figure 5.20 does not plot the drag data for the discus (which follow the curve-fit polynomial $C_D \approx 0.09 - 0.1 C_L + 0.54 C_L^2$ [for $C_L \leq 1$]), but its C_L curve is marked with a number of values for the lift-to-drag ratio, the best being 3 at $C_L = 0.4$ and $\alpha = 13^\circ$.

A discus is similar to an oblate spheroid (like a lentil) with a thickness of 20 percent of its diameter, roughly like the shape in figures 5.19 and 5.20. If this shape is halved, a possible shape emerges for a fairing mounted close to the road, for example, at 2.5 m long, 1.25 m high, and 0.5 m wide. As little air can pass between such a fairing and the ground, its aspect ratio is effectively doubled, that is,

it becomes the same as the full discus in free air. The force R can now be calculated as a function of V_A and the C_L/C_D data. A simplification is introduced in neglecting the negative effects of the ground: drag of the ground plane itself, interference drag, and wind shear. The results are thus optimistic rather than conservative. To obtain the *thrust* (T) in the direction of movement, R must be resolved into orthogonal components H and T using standard sailing formulas. The *heeling* force H (a sailing expression) at right angles to the direction of movement is given by $H = L \cos(\alpha) + D \sin(\alpha)$, and $T = L \sin(\alpha) - D \cos(\alpha)$ is the force that is of interest here (see figure 5.19). If T points opposite the direction of movement, it causes extra drag and must be added to the drag forces (rolling resistance and slope) acting on the vehicle that the rider must oppose at speed V . If instead T acts in the direction of movement, it is subtracted from the other drag forces. If it is then smaller than the other drag forces, the total drag is reduced, and the rider may produce less power for the same speed than would be needed without the wind. If it is larger than the other drag forces, however, the vehicle is truly sailing and speeds up until the forces balance.

Figure 5.21 calculates and plots an example for a vehicle equipped with the fairing described in the previous paragraph and moving at 10 m/s with a 5 m/s true wind. The horizontal line in the figure represents the power required to propel the vehicle at the same speed with no wind. The curve, plotted from a headwind (0°) through to a tailwind (180°) relative to the vehicle, can represent either a vehicle on a fixed course with the true wind changing direction or, more realistically, a vehicle on a circular course in a steady fixed true wind. As the figure shows, until the true wind deviates more than 30° from straight ahead, more power must be supplied to reach a speed of 10 m/s than if there were no wind at all. For all other angles (beyond 30° from straight ahead) the required power is reduced, and between 60° and 145° the vehicle is truly sailing, with the power shown negative—that is, it must be braked away to avoid speeding up. Not shown in the figure is the lateral force H , which in this example approaches 200 N, and as chapter 6 shows, could produce a tire slip angle of almost 2° (which has been neglected in the figure).

Figure 5.21 is relatively straightforward to plot by means of a spreadsheet (see Schmidt 2019), because the speed is taken as

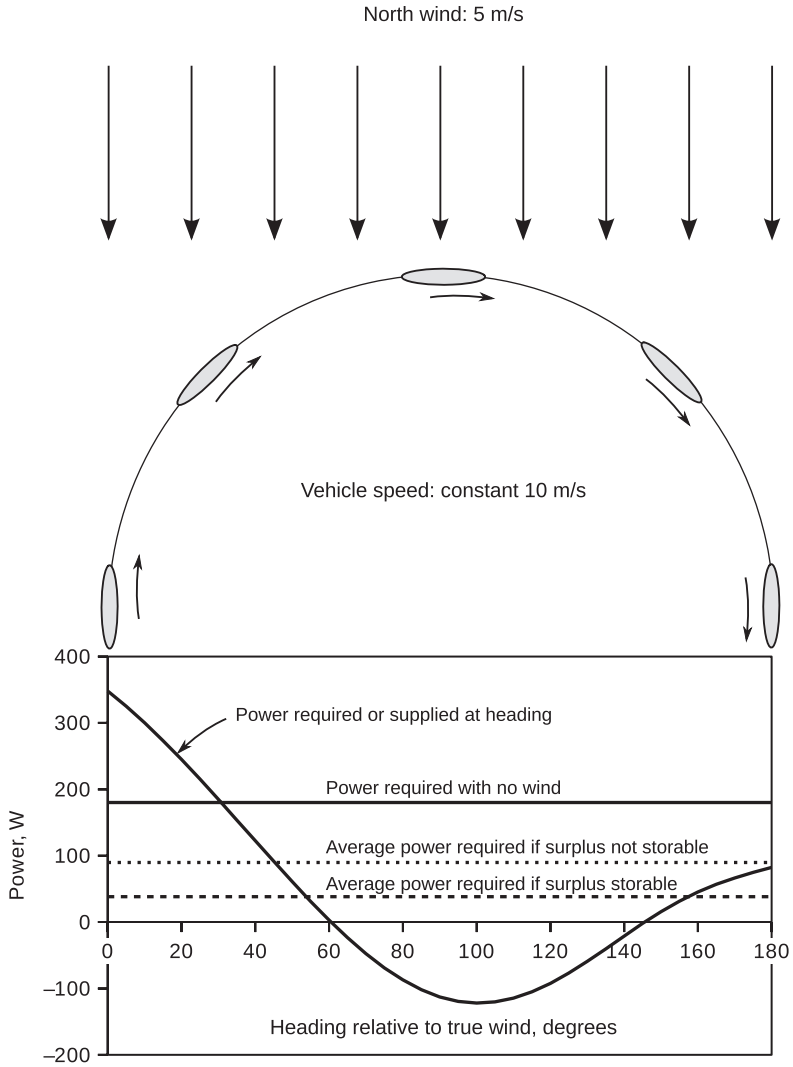


Figure 5.21

Power plotted as a function of the heading of a vehicle on a circular course, from a headwind (0°) to a tailwind (180°). Wind speed is 5 m/s; vehicle speed is 10 m/s; mass is 100 kg, including rider; coefficient of rolling resistance is 0.005. The fairing is a halved lentil or discus shape as described in the text, close to the ground, with an aspect ratio of 1 assumed. Other ground-drag effects are neglected. The solid horizontal line is the no-wind power. The dashed line shows the average power (if the “negative” power could be stored).

constant. This is not a very realistic assumption, but constant speed is much easier to calculate than constant power, as explained in chapter 4. The figure shows data for the vehicle with discus-type fairing traveling halfway around a circular course, and the second half would be a mirror image. If the sailing power (represented here as being negative) could be stored, the average for the whole course would be at the level of the dashed line. Without such storage capability, the average power needed would be higher, but still much less than the power required without wind. In this example, the rider must still provide about 40 W, averaged around the whole course, but with a higher ratio of wind speed to vehicle speed, the power required would be less or even negative. (Any reader who tries out the spreadsheet will see that this is the case if the wind speed is raised only from 5 to 6 m/s.) In the case of very little wind, there is no true sailing regardless of the wind direction, but still an overall advantage around the course. For example, a wind of 1 m/s will on average provide over 20 W assistance in this example.

The method used here can also be applied to other courses, for example, oval ones. As expected, the wind's power is more advantageous if the wind blows across an oval's long axis and less so if it blows along it. The greater the ovality, the greater the difference. An extreme oval, representing almost exclusively headwinds and tailwinds, is in any case disadvantageous for this type of vehicle, as shown in chapter 4. (This is not the case for vehicles with propellers and turbines, as explained earlier in the chapter.)

The values calculated in the preceding paragraphs and in the figure can seldom be realized in practice, because most available courses are lined with structures and plants that modify the wind a great deal. Velodromes have raised banks, as do parts of large circuits. Racers maintain that the winds experienced in velodromes and on large circuits are gusty and that the resulting fight for control usually more than compensates for any theoretical advantage arising from wind assistance. The best courses for wind assistance, other than flat coastal roads, would be on the grounds of airports. A further thing to consider is wind shear, the decrease of wind speed near the ground, that occurs even with smooth, unobstructed winds. Because of the wind shear factor, unlike sailing boats with their tall sails, the fairings of low racers experience lower wind speeds than those at the official measuring height of 2 m.

As noted earlier, the calculations presented neglect the 1–2° tire slip and leeway angle produced by the heeling force H . Furthermore, if H becomes too strong, an HPV of normal width will capsize, or in the case of a bicycle, have to lean into the wind at an extreme angle and slide away. If there is enough room, the HPV can make a turn away from the wind, which generally increases thrust (and speed) but decreases heel, and then brake safely. Turning toward the wind would decrease both thrust and heel, but the turn itself would strengthen the capsizing moment, and such a maneuver would probably come too late when a wheel is already in the air—and unlike in a real sailing craft, the sail cannot be released to feather in the wind. On a road, especially with other vehicles, the room to maneuver is very limited. For all these reasons, HPV sailing is so far almost unknown and probably likely to remain so, outside of some specialty applications or fortuitous circumstances experienced during long-distance touring.

References

- Abbott, I. H., and A. E. Doenhoff. 1959. *Theory of Wing Sections*. New York: Dover.
- Amick, James L. 1979. "The Windmobile." In *Power from the Wind* (Booklet 91), 55–62. Essex, UK: Amateur Yacht Research Societ. <https://www.ayrs.org/booklets/>.
- Blocken, Bert J. E., and Yasin Toparlar. 2015. Cycling Aerodynamics Research (web-site). <http://www.urbanphysics.net/Cycling%20aerodynamics%20research.htm>.
- Blocken, Bert J. E., T. W. J. Defraeye, E. Koninckx, J. E. Carmeliet, and P. Hespel. 2013. "CFD Simulations of the Aerodynamic Drag of Two Drafting Cyclists." *Computers and Fluids* 71 (January 30): 435–445. <https://doi.org/10.1016/j.compfluid.2012.11.012>.
- Blocken, Bert J. E., T. van Druenen, Y. Toparlar, F. Malizia, P. Mannion, T. Andrienne, T. Marchal, G. J. Mass, and J. Diepens. 2018. "Aerodynamic Drag in Cycling Pelotons: New Insights by CFD Simulation and Wind Tunnel Testing." *Journal of Wind Engineering and Industrial Aerodynamics* 179 (August): 319–337. <https://doi.org/10.1016/j.jweia.2018.06.011>.
- Cavallaro, Rick. 2008. "Downwind Faster Than the Wind (DWFTTW) Myth Challenge." Published November 15, 2008. YouTube.com. <https://www.youtube.com/watch?v=xHsXcHoJu-A>.
- Cavallaro, Rick. 2011. "Ride Like the Wind (Only Faster)." FasterThantheWind.org. <http://web.archive.org/web/20110904002520/http://www.fasterthanthewind.org:80/>.

Cavallaro, Rick. 2012. "Wind Powered Direct Upwind Vehicle—DUWFTTW." Published June 26, 2012. <https://www.youtube.com/watch?v=F7PNSyAfcjk&t=43s>.

Defraeye, Thijs, Bert Blocken, Erwin Koninckx, Peter Hespel, Pieter Verboven, Bart Nicolai, and Jan Carmeliet. 2013. "Cyclist Drag in Team Pursuit: Influence of Cyclist Sequence, Stature, and Arm Spacing." *Journal of Biomechanical Engineering* 136, no. 1 (January): 011005. <https://www.ncbi.nlm.nih.gov/pubmed/24149940>.

Drela, Mark, and Harold Youngren. 2013. XFOIL Subsonic Airfoil Development System, version 6.99 (computer program). <http://web.mit.edu/drela/Public/web/xfoil/>.

Fuchs, Andreas. 1993. "Dynamic Stability of Velomobiles: Forces, Distributions Torques." Paper presented at the First European Seminar on Velomobiles, Technical University of Denmark, Kongens Lyngby, July 8. <https://velomobileseminars.online/>.

Fuchs, Joachim. 1996. "Aeolos-Verkleidung" [A-Fairing]. *Pro Velo [The Bicycle Magazine]* 44.

Fuchs, Andreas. 1998. "Trim of Aerodynamically Faired Single-Track Vehicles in Crosswinds." Paper presented at the Third European Seminar on Velomobiles, Roskilde, Denmark, August 5. <https://velomobileseminars.online/>.

Gloger, Stefan. 1996. "Entwicklung muskelkraft-getriebener Leichtfahrzeuge" [Development of Human-Powered Light Vehicles]. *Fortschritt-Berichte VDI* [VDI Progress Reports], no. 263. VDI-Verlag Düsseldorf.

Gribble, Steve. 2018. "Air Density Calculator." The Computational Cyclist (website). https://www.gribble.org/cycling/air_density.html.

Gross, Albert C., Chester R. Kyle, and Douglas J. Malewicki. 1983. "The Aerodynamics of Human-Powered Land Vehicles." *Scientific American* 249, no. 6 (December): 142–152.

Hoerner, S. F. 1965. *Fluid Dynamic Drag*. Bricktown, NJ: Hoerner.

Hoerner, S. F., and H. V. Borst. 1975. *Fluid Dynamic Lift*. Bricktown, NJ: Hoerner.

Howell, J., and D. Hughes. 1984. "Aerodynamic Characteristics and Performance of the 'Dark Horse' Tandem HPV." In *Proceedings of the Second International HPV Scientific Symposium*, ed. Allan Abbott, 60–84. San Luis Obispo, CA: International Human Powered Vehicle Association.

Isvan, Osman. 1984. "The Effect of Winds on a Bicyclist's Speed." *Bike Tech* 3, no. 3 (June): 1–6. <https://docs.google.com/file/d/0B-pZ1ubTOGTtNjjMTM3NWitZDRkMi00YmJiLWEzM2EtNTUzZDM4YzY3YmRl>.

- Kyle, Chester R. 1979. "Reduction of Wind Resistance and Power Output of Racing Cyclists and Runners Travelling in Groups." *Ergonomics* 22, no. 4: 387–397.
- Kyle, Chester R. 1995. "Bicycle Aerodynamics." In *Human-Powered Vehicles*, ed. Allan Abbott and David Wilson, 141–156. Champaign, IL: Human Kinetics.
- Milliken, Doug. 1989. "Stability? Or control?" *Human Power* 7, no. 3 (Spring): 9–11. <http://www.ihpva.org/HParchive/PDF/24-v7n3-1989.pdf>.
- Mochet, Georges. 1999. "Charles Mochet and the Velocar." *Recumbent Cyclist News*, no. 52 (July/August).
- NCSL (National Conference of State Legislatures). 2018. "State Safe Bicycle Passing Laws." *Legis Brief* 26, no. 32. National Conference of State Legislatures, Washington, DC. <http://www.ncsl.org/research/transportation/state-safe-bicycle-passing-laws.aspx>.
- O'Neill, Charles. 2006. "Wing Configuration Study." AeroFluids Answers: Aeronautical Physics, Math, and Engineering with Dr. Charles O'Neill (website). <https://charles-oneill.com/blog/low-aspect-ratio-wings/>.
- Papadopoulos, Jim, and Mark Drela. 1998–1999. "Some Comments on the Effects of Interference Drag on Two Bodies in Tandem and Side-by-Side." *Human Power*, no. 46 (Winter): 19–20. <http://www.ihpva.org/HParchive/PDF/hp47-n46-1998.pdf>.
- Prandtl, L., and O. G. Tietjens. 1934. *Applied Hydro- and Aeromechanics*. New York: Dover.
- Schmidt, Theodor. 2019. Supplemental material for *Bicycling Science*, 4th ed. <http://hupi.org/BS4/>.
- Seifert, J. G., D. W. Bacharach, and E. R. Burke. 2003. "The Physiological Effects of Cycling on Tandem and Single Bicycles." *British Journal of Sports Medicine* 37: 50–53. <https://bjsm.bmj.com/content/37/1/50>.
- Selig, Michael. 2019. UIUC Applied Aerodynamics Group, Department of Aerospace Engineering, University of Illinois (website). <https://m-selig.ae.illinois.edu>.
- Sharp, Archibald. 1899. *CTC Gazette*, no. 11 (January).
- Shelquist, Richard. 2016. "An Introduction to Air Density and Density Altitude Calculations." Updated January 14, 2016. Shelquist Engineering (website). https://wahiduddin.net/calc/density_altitude.htm.
- Simanek, Donald. 2017. "DDWFTTW Vehicle Analysis: Dead Downwind Faster Than the Wind; A Conceptual Conundrum." Unpublished manuscript, Lock Haven University, Lock Haven University. Online. <https://www.lockhaven.edu/~dsimanek/museum/ddwfttw.htm>.

Sims, Ian. 1998. "Stability of Faired Recumbent Tricycles." Paper presented at the Third European Seminar on Velomobile Design, Roskilde, Denmark, August 5. <https://velomobileseminars.online/>.

Weaver, Matt. 1991. "The Cutting Edge Streamlined Bicycle." *Cycling Science* (September–December).

Weaver, Matt. 1999–2000. "Body Shapes and Influence of the Wind." *Human Power*, no. 49 (Winter): 21–24. <http://www.ihpva.org/HParchive/PDF/hp49-1999.pdf>.

Wilson, David Gordon. 1985. "Report on Address by Bruce Holmes to the Second IHPVA Builder's Workshop." *Human Power* 5, no. 1 (Winter): 7. <http://www.ihpva.org/HParchive/PDF/15-v5n1-1985.pdf>.

Wilson, David Gordon. 1997. "Wind-Tunnel Tests: Review of Tour, das Radmagazin, Article." *Human Power* 12, no. 4 (Spring): 7–9. <http://www.ihpva.org/HParchive/PDF/43-v12n4-1997.pdf>.

6 Rolling: Tires and Bearings

Introduction

Wheels surely count among the greatest of human inventions. But their ability to convey a load with low resistance depends on their size, the smoothness and firmness of the surface on which they travel, and the properties of tires and suspensions. As discussed in chapter 4, road irregularities retard motion, by shaking the rider, compressing the bicycle's suspension, or accelerating the bicycle upward. However, such retardation is primarily a question of suspension and is not discussed in this chapter, which delves into the friction and drag of smoothly rolling wheels and turning bearings.

Some Historical Notes

A wheel's resistance to rolling can increase fifty- to one hundredfold from pavement to soft soil, far more than resistance increases in walking on those same surfaces. Hence, there was a real incentive to develop paved roads when wheels were adopted for horse-drawn vehicles (figure 6.1). The Roman Empire was the first civilization to put a system of paved roads into use, and it took less time to travel across various European routes to Rome in the Roman era than a thousand years later in the Middle Ages, when the Roman road system had almost vanished through lack of maintenance.

After the Middle Ages, inventions to improve everyday life appeared rapidly. Among these were iron-covered wooden railways, followed after 1767 by iron wheels and cast-iron rails. These gave rise to the steam railways of Victorian times, which were paralleled by the reappearance of a fair number of paved roads. Thomson in

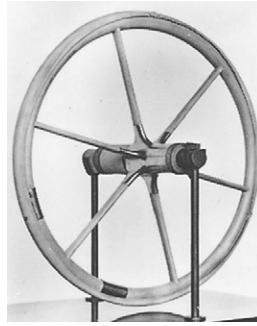


Figure 6.1

Replica of Egyptian war-chariot wheel of 1400 BC. Note the rawhide wrapping to make the tire resilient. See Joukowsky Institute for Archaeology 2010 for the construction of a working replica. The earliest evidence of vehicular wheel usage and some discoveries of wooden disk wheels in the Near East and Europe date to 3200–3400 BC. (Courtesy of Science Museum, London; reproduced with permission.)

1845 and Dunlop in 1888 introduced pneumatic tires that dramatically decreased the impact of forces on riders due to bumps and thereby made the energy losses smaller, introducing a degree of comfort for those traveling on common roads.

Though magnetically levitated and air-supported transportation vehicles experience essentially zero friction from the ground at normal speeds, they require power to supply and control the lift needed to enable the vehicles to move. Consequently, hard steel wheels on smooth steel rails require the least power of all systems used to support practical vehicles on land, as the intrinsic rigidity of the contacting components minimizes the energy lost due to material deformation as the wheels roll. In relationship to the carried load, the average automobile wheel on the best surfaces generally available has ten or more times the resistance to motion of a train wheel on its track, and bicycle tires are somewhere in between. The difference in resistances is in part due to the intentional deformability various types of tires have in order to reduce the forces of bumps and vibration. Bicycle tires have lower resistance than automobile tires because the parts deformed when they carry weight are thinner and give rise to smaller hysteresis and scrubbing losses from the repeated deformations. The resulting susceptibility to punctures and damage is accepted because the greater resistance or hardness

of very robust tires, for example, some available solid ones, is immediately felt when riding.

Basic Rolling Resistance

The power needed to move loaded wheels over a smooth surface depends on the physical properties of both. A great deal of empirical information is available concerning the power requirement for moving all types of wheels on harder surfaces. Wheel-movement requirements under soft-ground conditions have until recently been significant mostly to agricultural engineers and designers of military vehicles but are now of concern also to designers and users of mountain or all-terrain bicycles. Some information on soft-ground rolling resistance is given later in the chapter.

The term *rolling resistance* as used in this book refers to the resistance to a wheel's steady motion caused by power absorption in the materials of the wheel and of the road, rail, or soil on which it rolls. Rolling resistance does not include bearing friction or the power needed to accelerate or slow the wheel because of its inertia. Nor does it include *suspension losses*: energy losses in the wheel, suspension, or rider due to impact and vibration, described in chapter 4.

In what follows, the force of rolling resistance is usually represented as the *coefficient of rolling resistance* (C_R , introduced in chapter 4) times the load carried, just as sliding friction is represented as a friction coefficient times load. This empirical approximation is useful, but measurements and sophisticated analyses do not always bear out its validity. Readers interested in rolling-friction theory may wish to consult Trautwine and Trautwine 1937, Reynolds 1876, and Evans 1954 for details about a subject not frequently discussed in textbooks on basic physics. Table 6.1 lists some early empirical rolling-resistance coefficients.

Bicycle Wheels

A conspicuous characteristic of most bicycles is the relatively large-diameter wheels (about 20 percent larger than those of a typical passenger car) turning on ball bearings and shod with tires inflated to two to four times the pressures of passenger-car tires. Even the word *bicycle* (from Latin *bis* [twice] and Ancient Greek κύκλος [circle])

Table 6.1
 “Historic” low-speed rolling-resistance coefficients

Surface	Coefficient of rolling resistance (C_R)	Speed	Vehicle
Railway	0.0012 (CB&Q) 0.0016 (Schmidt)	5 mph	60 ton railway car, including journal bearings
Railway	0.0031 (CB&Q) 0.0038 (Schmidt)	5 mph	15 ton railway car, including journal bearings
Cubical block pavement or planks	0.014–0.022	“slow pace”	Four-wheeled wagon
Small broken stone in macadam (or cement concrete)	0.02 (0.028)–0.033	“slow pace”	Four-wheeled wagon
“A fine road”	0.034–0.04	4–10 mph	1.5 ton stagecoach with steel tires
Gravel	0.062	“slow pace”	Four-wheeled wagon
Common earth road	0.089–0.13	“slow pace”	Four-wheeled wagon
Asphalt pavement	0.015–0.0155	4 mph	Tricycle with pneumatic tires
Flint	0.015–0.0185	4 mph	Tricycle with pneumatic tires
Flint, flag pavement	0.03	4 mph	Tricycle with solid tires
Heavy mud	0.0365	4 mph	Tricycle with pneumatic tires

Sources: Trautwine and Trautwine 1937, 683 (four-wheeled wagon and 1.5 ton stagecoach with steel tires); Trautwine and Trautwine 1937, 417, 1060 (railway cars); and Sharp 1896 (tricycles).

Note: The rolling resistance coefficients in Trautwine and Trautwine 1937 are given in pounds per ton. Both short (American) tons of 2,000 lb and long (imperial) tons of 2,240 lb are specified, sometimes for the same measurements on different pages. For converting to the C_R values in the table, long tons have been used unless otherwise specified. CB&Q (Chicago, Burlington, and Quincy) and Schmidt refer to entries within Trautwine and Trautwine 1937. (This very detailed 1,608-page book was written and maintained by three generations of J. C. Trautwines from 1882 to 1937.)

acknowledges the importance of wheels to the vehicle it names. Bicycles' large wheel size benefits bicycle performance in several ways:

- The angle from a wheel's axle to the point of impact of a vertical discontinuity (e.g., pebble, bump, depression, curb edge) is more nearly vertical in a large wheel than in a smaller one, so a large wheel can roll over holes or bumps that might completely stop a small wheel. Obviously if a front wheel meets a vertical or nearly vertical curb higher than the wheel's radius, this will completely stop a bicycle and throw the rider off forward or bend the fork (or both), unless the bicycle is fitted with a very elaborate suspension or pulled up actively by the rider. Greater horizontal travel is required before a large wheel crests a bump, so vertical accelerations are gentler. Forces acting to jar the rider are smaller for large wheels, as are vertical velocities, whose associated kinetic energy is largely unrecoverable.
- Smooth rolling on large wheels causes less tire energy loss than on otherwise identical small ones. At the same tire pressure and width, a large wheel develops a load-supporting *contact patch* with less tire flattening and flexing, so less energy is dissipated in the tire structure, the resistance being about inversely proportional to the diameter in *otherwise identical conditions* (see figure 6.2).
- A larger wheel allows the wheel's bearings to turn more slowly, enabling them to last longer and contribute less friction.
- Large wheels reduce the degree of sinkage in soft ground compared to small ones, and the angle of the tilted contact patch (that is, the part of the wheel or tire in contact with the ground, described later in the chapter) is less unfavorable.
- A large wheel improves the feel and stability of steering and balancing.

On the other hand, there is greater aerodynamic drag on a large wheel than on a small wheel at a comparable speed, and it is difficult to make large, light, slender structures such as large bicycle wheels laterally stiff for precision in steering and strong enough so that they don't collapse when subjected to more than light side loads. Conventional bicycle wheels must be considered marginal in strength when used with nonleaning vehicles such as tricycles,

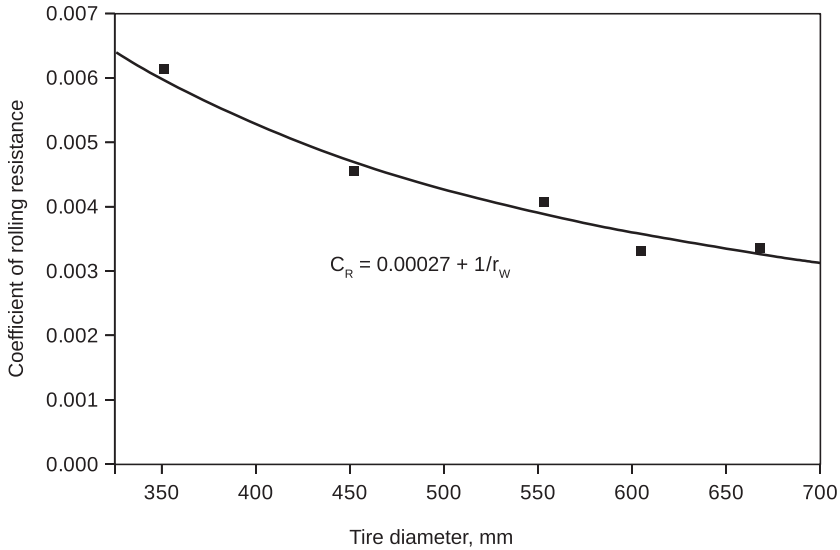


Figure 6.2

The coefficient of rolling resistance C_R as a function of wheel diameter ($2 r_W$) with a series of Schwalbe Standard GW tires, all having the same width (47 mm), construction (Profile HS159), pressure (3 bar), and load (540 N). On the fitted curve, C_R is equal to $1/r_W$, plus an offset of 0.00027 (only for these tires, units, and pressures, and a curve fit of $1.06/r_W$ is nearly the same). The data come from low-speed rollout tests on a laminate-covered concrete floor. (Data from Senkel 1992.)

unless care is taken to avoid excessive side forces. Weak wheels don't usually cause bicycling accidents, but when such accidents do occur, the bicycles are often destroyed. (However, the rim of a bicycle wheel can act as a "crush zone" that lessens severe impacts, e.g., when a cyclist hits a vehicle or wall.)

Comparing the Friction of Tires and Bearings

When a bicycle rolls forward, the tires as well as the wheel bearings resist the motion to some extent. But whereas the drag of the tires can be measured or even felt while riding, the drag of ordinary ball bearings is mostly negligible, as long as they are not adjusted far too tightly (see the calculation in the section "Bearing Friction" later in the chapter).

Tires

The amount of rolling resistance a vehicle's tires exert depends on their dimensions, construction, and material parameters (e.g., hardness for solid tires or maximum inflation pressure for pneumatic ones), as well as on the load carried, on any lateral load imposed, on the temperature, and on the speed at which they are rolling, although the effects of temperature and speed on resistance are not ordinarily acknowledged. Tire rolling resistance is usually tested by pressing a vehicle's wheel with a known amount of force against a turning drum and measuring the power required to keep the wheel turning at a specified speed. Ideally, the drum should be of considerably greater diameter than the wheel, or else the resulting contact patch is rather different from that of the wheel with a flat road surface (i.e., the drum penetrates deeper into the tire) and the drag is greater, as with competition-training rollers. Unfortunately most available data are from drums smaller than the wheels being tested. However, Schuring (1977) offers a correction formula:

$$C_R [\text{flat surface}] = C_R [\text{measured on drum}] / (1 + r_w/r_D)^{1/2},$$

in which r_w is the radius of the wheel and r_D that of the drum. This correction formula has been derived under the assumption that the area of a curved contact patch is the same as that of a flat one and that there is no force contribution from the tire sidewalls. S. K. Clark presented the same equation written slightly differently a bit later (see Unrau 2013), and it was also used in the old International Organization for Standardization (ISO) 18164 and ISO 28580 standards on "methods of measuring rolling resistance for passenger-car, truck and bus tyres." Although automotive tires are quite different and the standards for those tires require drums of at least 1.7 m diameter operated at 60 or 80 km/h, the formula appears to work quite well also for bicycle tires, as shown in figure 6.3. Freudenmann, Unrau, and El-Haji (2009) and Sandberg (2011) offer adaptations of the formula that fit car tires better, but they appear to give completely wrong data for bicycle tires and are therefore not included here.

The drum diameter would be less of an issue for a pair of identical and identically inflated tires pressed together for drag measurements: the contact region would then be planar and the deformation-based drag precisely twice that of one tire (see also US Patent application US20080115563). However, the friction due to the motion of the tire against the road within the contact patch

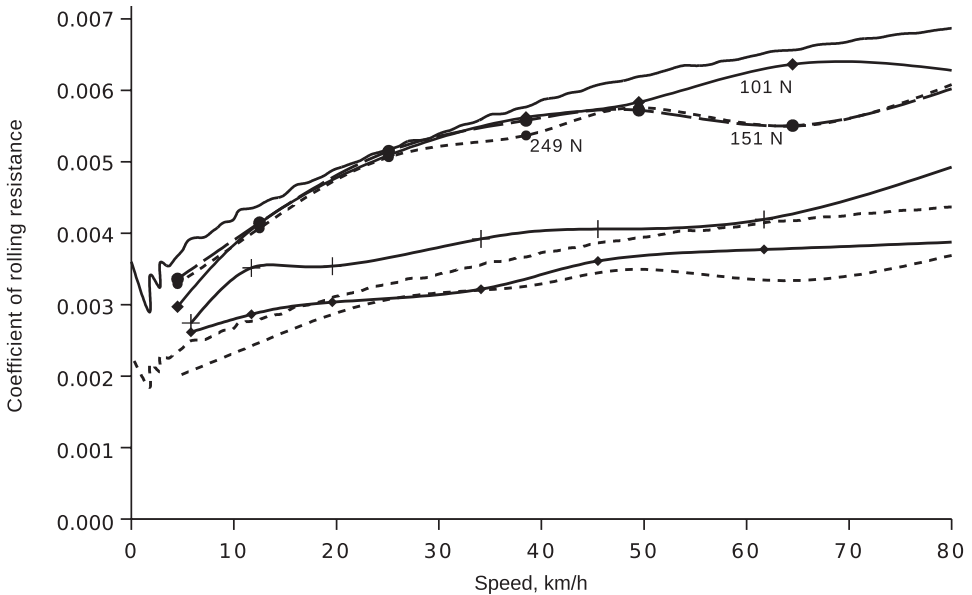


Figure 6.3

Data plots of the coefficient of rolling resistance of the same tire model (Schwalbe 20-inch Ultramo ZX) as a function of speed, with pressure and load as parameters. The bottom two solid-line plots show tire-to-tire measurements, the upper lines, tire-to-drum measurements. The bottom dashed lines show two of the curves transposed according to Schuring 1977 and ISO 28580 (2009). As an average of all measurements and calculations, this tire model, warm and at around 9 bar, has on a flat surface a static coefficient of rolling resistance of 0.002, which rises to 0.003 at slow to medium speeds and to 0.004 at high speeds. (Data from Datza 2015 and Henry 2015.)

would also be reduced, so the rolling resistance measured might then be artificially low. Leonardi Datza constructed a test apparatus in 2015 that measured two identical tires in this way and also one tire from the pair against a 266 mm diameter drum. Under otherwise identical conditions, the tire-on-tire drag was 55–75 percent of the tire-on-drum drag, depending on speed. The data in figure 6.3 suggest that this method represents tire-on-road drag well and that the drum correction formula works well. But they are slightly on the optimistic side, as the *corrected* tire-on-drum curve should not, as it does, give lower values than the tire-on-tire curve. The figure also shows the (usually neglected) speed dependency of rolling resistance, which is discussed later in the chapter.

An imperfect wheel, misaligned mounting, or uneven tire construction also may play a role in the amount of drag from the attached tire, depending on whether the wheel is free to tilt or move vertically while the bicycle is being ridden and whether or not that motion dissipates energy. Alignment is especially important with double-track wheel pairs, such as with trailers or tricycles. Any deviation from parallelism in the direction of motion gives rise to sideways forces, forced slippage, and hence extra resistance. Vander Wiel et al. (2016) measure wheelchair wheels with solid tires: a wheel with a 1° misalignment in yaw (“toe-in” or “toe-out,” i.e., 2° between a pair) generates 25 percent more drag; for 2° (i.e., 4°) it generates 96 percent more! Differences in roll, for example, from a cambered road or a soft suspension, can also lead to increased drag, but according to the Vander Wiel et al. tests, it is little, and sometimes wheels are purposely tilted from vertical, for example, for more stability or to fit into a narrow fairing better.

Under typical test conditions, the force of rolling resistance F_R is measured via either the vehicle’s operating power or its coasting (unpowered) deceleration (*coastdown* or *rollout* test) and then is represented as C_R times F_V (average vertical force supported). The force to use is actually the component perpendicular to the road (normal force), as explained in chapter 4, but for the slight gradients that might be used in testing, the difference is very slight, and this chapter uses F_V throughout. For bicycle tires on a smooth, hard surface, C_R values are usually considered to be between 0.002 and 0.010, depending on inflation pressure, wheel diameter, and tire construction. Then for a bicycle-plus-rider mass of 80 kg, the weight is 785 N and the rolling drag between 1.5 N and 7.8 N (0.3 lbf to 1.75 lbf). For comparison, aerodynamic drag in low-wind conditions typically ranges between 5 N and 30 N in level riding at usual speeds. Grappe et al. (1999) discuss some mathematical methods for coast-down testing, and Tetz 2005 is an invaluable resource with practical advice on such testing.

Tire rolling resistance can also be measured directly, by rolling a tire along flat surfaces pulled by a spring scale or falling weight, with the following caveats:

- Slope is highly important. Nominally level indoor surfaces can easily slope 0.001 in places, altering the apparent value of C_R by

as much as 10–50 percent. Outdoor variations in slope can be far greater.

- Wind is also a concern. Unless the test vehicle has much less frontal area than a normal rider, any perceptible wind will substantially alter the force being measured. In fact, even in windless conditions, air drag must often be determined and subtracted.
- If the rig on which tests are conducted is not a special guided test device or a bicycle skillfully controlled by its rider, outrigger wheels, a pair of wheels, or a tricycle are required to maintain low-speed balance. Any wheel misalignment will add considerably to the drag.
- Although it seems attractive to evaluate drag from the force required to restrain or tow the wheel on a powered treadmill, such a technique must account for the effect of the treadmill's soft belt, which will create added resistance.

Two additional methods can be used for measuring low-speed rolling resistance. A road sloped just enough for a bicycle to roll, but not accelerate, immediately gives a C_R value, but such a slope is difficult to ride on a bicycle, is hardly measurable by ordinary means, and may be quite variable. For a tricycle or special rig, a large stiff board can be placed on a horizontal surface and one end raised in a precisely measured way until rolling just starts, with the slope at that point then providing the value for C_R .

A similar but more accurate method is the pendulum test as used by Wim Schermer (2013). Two wheels are rigidly connected coaxially by a stiff axle. A large weight (Schermer uses a mass of 80 kg) is solidly attached to the axle somewhat off center, so that a pendulum is formed and rolling the tire a fraction of a revolution raises the center of mass. If the wheel pair is rotated away from the stable position and released, it rocks back and forth with a slowly diminishing amplitude, like a rocking chair. The smaller the value of C_R is, the longer this oscillation carries on. Schermer mounts a laser pointer on the device that shows the slightest movement, measures the time it takes for the oscillation to decay from a measured position, and calculates the value of C_R from this. For example, in tests Schermer conducted (each six times, always at 19°C), a Schwalbe Shredda (2015) 40–406 at 5 bar rocked for 50 s, which corresponds to $C_R = 0.0057$. Then his best tire, an experimental Michelin radial

(2011) 40–406 (with latex inner tube) at 7 bar rocked for 218 s for an astonishing $C_R = 0.0013$. The type of test Schermer conducted has the advantage that it can be done almost anywhere on any surface and the disadvantage that it is an almost static test, yielding lower resistance values than at a higher speed.

An appealing measurement possibility is with an on-bicycle instrument as described in chapter 4. Measurement using this method makes it possible to ride multiple circuits of a flat course at several constant speeds, determine the average powers required, and separate the proportions of air drag and rolling resistance, as explained in that chapter. For this separation, testing needs to be conducted at both low and high riding speeds, but a low-speed test alone will give a good indication of rolling resistance. One problem, however, is that a steady wind adds to the average drag around the circuit and could possibly lead to very variable measurements with faired vehicles if sailing occurs (see chapter 5). Indoor riding in a large building would eliminate this problem, but then exploring the effects of a range of temperatures and road surfaces would be more difficult.

The aerodynamic drag coefficient C_D of faired vehicles is likely to *decrease* with increasing speed (see chapter 5). The coefficient of rolling resistance C_R , on the other hand, increases slightly with speed, so the two dependencies may sometimes cancel. However, going faster also increases tire temperature and hence also tire pressure, both leading to a reduction in the value of C_R . Preliminary on-road measurements suggest that C_R values drop roughly 1 percent for each degree Celsius of temperature increase, and Tetz (2005) in numerous coastdown tests even measures C_R as dropping by 0.002 for every 10°C increase, starting from 0.0085 and 0°C or above. Because of their short duration, coastdown tests mainly reflect the ambient temperature, and because of their low speeds, mainly rolling resistance.

In road tests tires are subjected to strong ambient temperature airflow, road temperature, and sunlight. In drum tests, most testing of tires is conducted at room temperature with measurements after longer warm-up periods, so that the tires can reach considerably elevated temperatures. Unless both temperature and pressure are held constant or at least monitored closely and known, measurements from these different kinds of tests, and even from similar tests in different conditions, cannot be accurately compared.

Bearings

Rolling-element bearings use many small balls or rollers to reduce friction and wear. The first widespread use of ball bearings was in bicycles, although the concept of ball bearings was understood prior to their use in bicycles.

Although the rolling-element approach seems obviously superior, bearings are highly sophisticated devices, and how well they work depends on various subtle factors. Bearings made of strong materials, properly manufactured and finished with high precision, positioned with the proper configuration, and kept clean and lubricated can last for many millions (small ones even a few billions) of revolutions (depending on the load they are required to carry). For bicycle use, the temptation is usually to adopt bearings made of lighter or cheaper materials, reducing the life of the bearings to a tolerable minimum: less than 1 million wheel revolutions for a bicycle that is not ridden much and perhaps 10 million revolutions for a “serious” bicycle.

A most authoritative reference on ball and roller bearings is *Rolling Bearing Analysis*, by Tedric Harris (1991). Bearing manufacturers also present basic information in the engineering pages of their catalogs. Danh et al. (1991) measure standard bicycle cup-and-cone bearings and industrial sealed bearings.

Bearing Friction

If a bicycle wheel is removed from the bicycle’s frame and its axle is turned with the fingers, a small resistance may be felt. This resistance typically is due to the use of a thick grease or of bearing seals. Bearings adjusted too tightly (preloaded) may give a better idea of their friction under load. Low-precision bearings will turn roughly, and with high-quality bearings, it will feel more as if an extra-heavy grease has been added.

A bicycle wheel’s quick-release skewer (the through-axle tension rod used to secure most modern wheels) applies considerable compressive force to the wheel’s axle, shortening it by 0.02–0.04 mm and thereby “tightening” the bearing adjustment. The effect of this shortening and the resultant tightening can be felt by placing some washers on the axle to take the place of the bicycle frame and squeezing them with the skewer as if the wheel were installed. (This experiment will not simulate any bearing load that might arise from

axle bending due to operating loads or preexisting frame misalignment, however.)

Manufacturers sometimes publish approximate friction coefficients (defined at the radius of the circle of rolling elements) for well-aligned, properly lubricated bearings, but Harris (1991) presents a more complete treatment. Besides pure rolling, the rolling elements in most bearings also undergo a certain amount of scrubbing motion within their tiny contact areas. Angular-contact (i.e., cup-and-cone) ball bearings like those shown in figure 6.4 have a friction coefficient of $0.001 \times (\text{service load}/\text{static load rating})^{1/3}$. Needle-roller bearings or radial-contact ball bearings can have friction coefficients that are smaller by as much as a factor of five.

A ball bearing's static load rating is the highest load that will produce a specified, minuscule, permanent indentation by the ball in the ball race. For bicycle-sized bearings, service catalogs show that the static load rating is typically half of the basic dynamic load rating, which ISO 281 defines as the load at which 90 percent of a group of bearings will last at least 1 million revolutions. If actual bearing life is taken as 8 million revolutions, a conventional bearing-life calculation implies that the service load is also approximately half of the basic dynamic load. Therefore, by the relationship in the last paragraph, the friction coefficient should be close to 0.001.

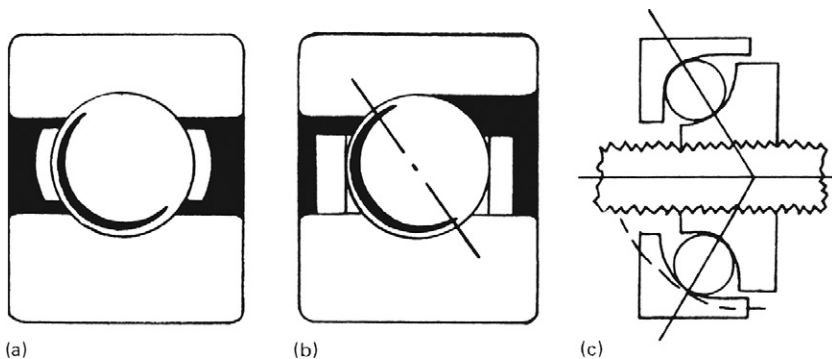


Figure 6.4

Types of ball bearings: (a) annular or radial; (b) 1893 "magneto" (the Raleigh version had a threaded inner race); (c) cup-and-cone (the bearing is self-aligning and can accommodate a bent spindle).

What this means is that a wheel carrying 450 N (100 lbf) would develop a tangential friction force (at the ball bearing) of about 0.45 N (0.1 lbf), in addition to any friction from seals, preload friction, and other friction that may be present. The finger feel of this friction could be simulated by winding a thread around the axle where its diameter is 16 mm, with a 0.55 N force or equivalent weight at its end, to create 0.004 Nm torque. As this force of 0.45 N acts at the small radius of 10 mm, it causes a far smaller force at the wheel radius of perhaps 330 mm. Therefore, the drag force due to the bearing friction of one wheel is in the neighborhood of $0.45 \text{ N} \times 10 \text{ mm}/330 \text{ mm} = 0.014 \text{ N}$ at the circumference of the wheel, yielding a drag power of 0.14 W at 10 m/s speed, and is quite negligible compared with a typical tire rolling resistance of 1–3 N. In a long race, however, using the lowest-drag bearings with a fractional percent advantage could make a difference. Clearly, bearings benefit tremendously when the wheel's own radius is much greater than theirs: the ratio of the wheel radius to the bearing radius reduces both drag and wear rate per unit distance traveled.

The approach just outlined suggests a linear dependence between load and bearing torque and little dependence on speed. Measurements by Danh et al. (1991) suggest nearly the opposite: "It can be concluded from these tests, that for most common bicycle applications, bearing drag increases somewhat with increasing speed and is approximately independent of load" (32). These authors measured bearing torques from 0.0001 Nm (cup-and-cone bearings lubricated with "20 weight" oil at 60 rpm) to 0.05 Nm (cartridge bearings lubricated with "typical automotive chassis" grease at 600 rpm). At medium speeds (300 rpm), the cup-and-cone bearings measured less than 0.001 Nm with oil and typically 0.003 Nm with grease and the cartridge bearings 0.0075 with oil and 0.03 with grease. Typically the torque values for the cup-and-cone bearings were five (oil) to ten times (grease) *better* than those for the cartridge bearings, although the latter had no lip seals. With seals, the cartridge bearings produced 0.03–0.05 Nm additional torque. The authors assumed that the friction of the new cartridge bearings would decrease after the bearings became worn with use. They unfortunately don't give the size or type of the cartridge bearings, apart from calling them "roller bearings" (that is, not ball bearings). However, it is clear from the paper that traditional cup-and-cone bearings generate minimal

torque drag if they are well adjusted and that the main source of drag from bearings is likely to come from using heavy grease instead of light oil or special lubricants.

The exact calculation of bearing resistance is more complex (for example, see SKF Group 2018a), as the balls or rollers have microscopic irregularities and roll partly on these and partly on a film of lubricant that itself causes viscous drag. For popular industrial bearings, resistance can be calculated online using the SKF bearing calculator (SKF Group 2018b). Taking, for example, a typical steel, grease-lubricated radial ball bearing of the size needed—that is, four required for two bicycle wheels—at 250 N radial load per bearing and 600 rpm speed yields about 0.25 W power loss per bearing, excluding any seals. Radial ball bearings are also available with ceramic (silicon nitride) instead of steel balls. They are much more expensive but can have a lower resistance and longer lifetime in clean conditions (their tighter tolerances make them less tolerant to contamination from particles such as road dust).

Since wheel bearings contribute so little to overall drag, could more economical plain bearings—close-fitting bushings of low-friction metal or plastic—be used? The bearing radius of such bearings might be as small as 5 mm, providing a wheel mechanical advantage of 0.33/0.005 or 66. To add less than 0.001 to the apparent rolling-resistance coefficient C_R (effectively, the difference between an excellent tire and a good one), the plain bearing would have to have a sliding friction coefficient less than 0.07. This is achievable with a modern dry-film lubricant coating. For example, fluoroplastics like polytetrafluoroethylene paired with metals can exhibit friction coefficients of 0.05–0.10 or even lower in certain conditions: at relatively high pressures, with a slight degree of roughness present, and after a certain amount of rubbing (break-in) has built up a film of lubricious material on the mating bearing part. Truly low friction coefficients in plain bearings from 0.01 to 0.07 can be achieved with the addition of a liquid lubricant, but this achievement is highly dependent on speed and load.

Appropriate plain bearings therefore offer sufficiently low friction for use in bicycles. However, they are susceptible to weeping of lubricant and to abrasive wear from road dust, unless perfectly sealed, as well as to damage if overloaded. For bicycle wheels, traditional or industrial ball bearings offer more robustness for a

similar cost. Plain bearings *are* used for lightly loaded derailleur jockey pulleys and for the pinions of very well-lubricated internally geared hubs. On its cheaper models, Raleigh used plain bearings in pedals and in the lightly loaded upper headset bearings for a short time around 1970; the coefficient of friction was noticeably and annoyingly high. Wear and contamination probably resulted in much worse performance than discussed here. Therefore, the major advantages of rolling bearings compared to plain bearings are their relative durability and low friction even when poorly lubricated.

Rolling Resistance: Observations, Theory, and Correlations

For typical bicycles and tires, rolling resistance on smooth surfaces is the second-most-important contributor, after air resistance, to overall resistance in level-road riding. There is considerable uncertainty about precise values of rolling-resistance coefficients in particular cases, and the general effects of factors such as wheel diameter, tire pressure, temperature, speed, and load pressure on rolling resistance have not yet been fully explored.

The entire subject of rolling resistance has been treated primarily empirically from a variety of perspectives, and further study is needed. For these reasons, the chapter mainly summarizes a wide range of published results. Chapters 8–9 of Johnson's *Contact Mechanics* (1996) provide one of the most comprehensive available theoretical treatments.

Sliding and Internal Friction

Osborne Reynolds (1876, also in Sharp 1896) proposed *sliding* friction as a component of rolling resistance. He experimented with a machined cast-iron cylinder with a 6-inch diameter, 2 inches wide (~14 lb, 6.35 kg), rolling on various surfaces, including soft india (natural) rubber, a kind of reverse model to a soft wheel rolling on a hard surface. By marking the edges of the cylinder and rubber block, Reynolds was able to observe the rubber's distortion and the behavior of the two contact surfaces. Figure 6.5 depicts a cylinder rolling from left to right and in contact with the rubber from point A to point D. As the figure shows, between points B and C, the surface of

the rubber is distended and does not slide relative to the cylinder. Therefore, it must be compressed in front of B and after C, which generates sliding friction between A and B as well as between C and D. Reynolds measured a rolling-resistance coefficient of 0.0067 for his roller on rubber and surprisingly found that lubrication with oil or blacklead (graphite) made little difference. He also used other hard and smooth surfaces, finding rolling-resistance coefficients of 0.0008 to about 0.001 whether the roller was lubricated or not. His apparatus consisted of a very precise tiltable table able to detect rolling starting at an angle (or rolling-resistance coefficient) of 0.0002. This is also the best experimental value given by Kumar, Sarkar, and Gupta (1988) for steel rollers on steel. Although a hard wheel rolling on a soft elastic surface is not the usual configuration for a bicycle or indeed any vehicle, the type of sliding friction described in Reynolds's experiments is bound to occur also with the contacting surfaces of elastic tires on hard roads and even steel wheels on steel rails, as the circumferential segment of the round member is longer than the corresponding flat support patch and must be shortened during rolling.

Figure 6.5 also shows that the rubber in Reynolds's experiments would experience compression, distortion, and shear stress. If it were perfectly elastic, it would rebound completely and give back all energy absorbed, and the pressure in the trailing part would be exactly the same as that in the forward part. There would be no rolling resistance from this. However, rubber is by no means a perfect

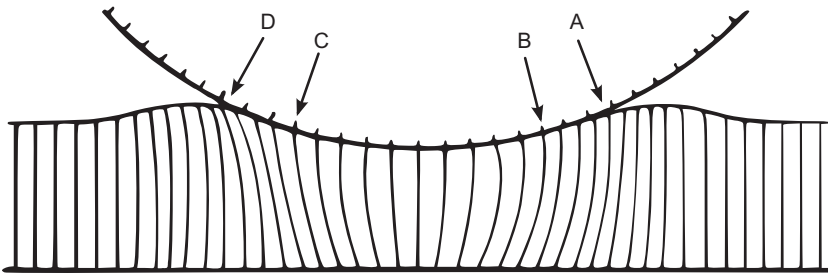


Figure 6.5

Sliding friction between A and B as well as C and D with a cylinder rolling on a rubber sheet from left to right. (From Reynolds 1876.)

spring material and does not return stored energy completely, the difference being lost as heat. This is called *internal friction* or *elastic hysteresis*.

Similar effects occur with wheels made of rubber or synthetic elastomers (rubbery materials), and even with steel wheels and rails. In the physical sense steel is more elastic than rubber, and particularly hard materials like quartz and ceramics are even more so—contrary to the intuitive concept of elasticity. Presumably a tiny ceramic bicycle wheel rolling on a smooth ceramic tile would have less resistance than one made of steel.

Most bicycle tires are pneumatic, more or less a thin-walled torus filled with pressurized air. For rolling on a smooth surface, the air can be considered to be a practically lossless support, as its pressure does not change, and the tiny bit of internal displacement due to the flattening of the contact patch is negligible. This flattening does, however, cause bending around the edges of the contact patch and flexing of the tires' sidewalls, as is evident in figure 6.11. Whereas the sidewalls can be made as thin as their function of a "pressure vessel" allows and constructed of strong materials such as polyamide or aramid fibers, the tires' tread must be of sufficiently thick material to protect the pressurized skin and allow a certain amount of wear. Thus the same type of elastic hysteresis loss is incurred as with a solid rubber or elastomer tire, but there is less of it, as less material is involved. Decreasing the size of the contact patch, by increasing the air pressure, clearly decreases both the sliding and the internal friction.

Representation of Rolling Resistance by a Tilted Ground-Force Vector

As wheels and the surfaces they roll on can be hard or soft and more elastic or inelastic, this gives rise to a number of possible combinations of wheel and surface. Additionally, wheels can be smooth or rough, homogenous or layered, and surfaces cohesive or granular. It is plausible that hard and smooth wheels and surfaces, such as steel wheels rolling on steel rails, generate the least resistance, as is borne out in practice, with C_R values of only a few thousandths (see table 6.1) and even less for cylinders rolled very slowly in the lab. If a wheel made only point or line contact with a geometrically flat surface, the force between the wheel and the surface would have

to be at an exactly right angle to the surface, and there would be no rolling resistance. However, a loaded wheel or ball never makes true line or point contact with a flat surface: if it did, the contact pressure (force divided by area) would be infinite, and materials failure would occur. In reality, some deformation takes place to create a nonzero area of contact. For steel, this area is very small, and because it is elastic, very little energy is lost through the temporary deformation.

Assuming a wheel's bearing friction to be negligible, the force of the ground must act on a line directed through the center of the wheel, so the wheel's rolling drag is equivalent to that presented by the ground force's being located ahead of the axis and tipped back from vertical to aim at the axle.

When a wheel is moving, the pressure from contact with the underlying surface is generally not uniform within a particular contact area. Forward rolling causes the pressure to be greater in the leading part of the contact patch than in the trailing part (figure 6.6), which leads to rolling resistance, as a result of the previously

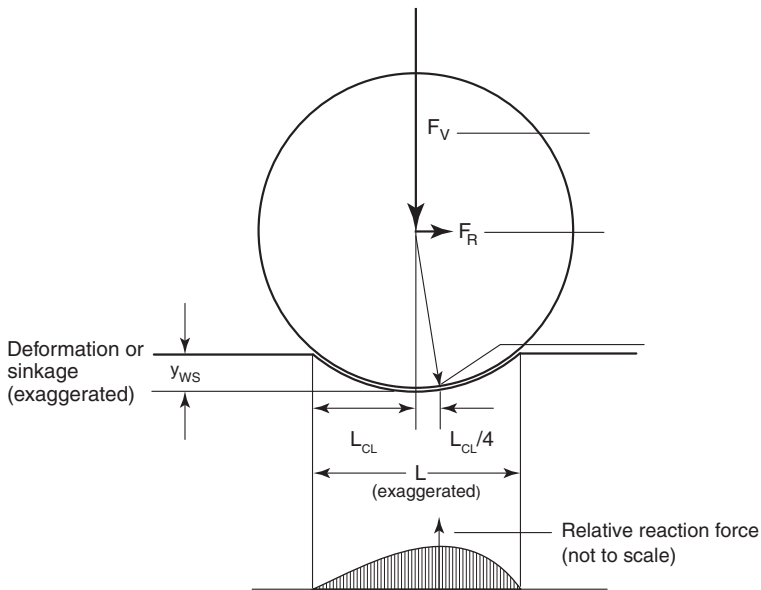


Figure 6.6

Resistance of a hard wheel on a soft, largely elastic surface, rolling left to right.

mentioned sliding and internal friction. Therefore the center of pressure and the line of ground force are forward of the center of the contact patch.

The angle through which the support force is tipped is bound to be considerably less than the angle from the wheel's axle to the foremost point of the contact patch. Thus, in otherwise comparable situations, the wheel whose contact patch subtends the smallest angle is likely to generate the least drag. This implies that wider tires should give rise to less drag, and this is indeed the case, if tires *inflated to the same pressure and of otherwise identical construction*, or solid tires, are compared (see the discussion near the end of this chapter). If the contact length forward of the wheel's axle (i.e., half of the smooth-road contact-patch length L) is denoted L_{CL} (the *contact half-length*), then the maximum possible support-force tilt angle (in radians) is closely approximated by the ratio L_{CL}/r_w , in which r_w is the radius of the wheel.

Form of Resistance Equation

The reasoning outlined in the previous section (combined with some dimensional analysis) suggests a likely form for the force (F_R) that resists rolling of a wheel-supporting force (F_V): $F_R/F_V = f(L_{CL}/r_w)$, in which f represents an unknown function increasing from zero. This ratio, F_R/F_V , is defined as the coefficient of rolling resistance, C_R . It is often considered to be independent of the load F_V (i.e., F_R is considered to be a constant fraction of any F_V) even though it is not completely (since L_{CL} is affected by F_V). When the literature provides a single number for the value of C_R , it should be assumed to apply only to specific loading conditions, which unfortunately are not always described.

The following section gives examples of simple rolling-resistance analyses or measurements. All contact half-length (L_{CL}) calculations involve vertical load (F_V), wheel radius (r_w), and a quantity with dimensions of stress, such as modulus (E), inflation pressure (p), or the yield stress of the soil. Vertical wheel sinkage (y_{ws}) is related to L_{CL} through $y_{ws} \approx L_{CL}^2/(2r_w)$. This value is also related to the wheel's *effective* rolling radius, which must be smaller than r_w but larger than $r_w - y_{ws}$. This effective radius can be determined from the setting of an accurately calibrated bicycle speedometer (or used to calibrate this in the first place), or calculated. (See also Wright 2019 for further well-presented contact patch and tire information.)

In addition, ancillary geometrical factors may affect the calculation of contact half-length, such as wheel width (L_{WW}) and radius (r_{T}) in the case of a round tire cross section. The drag itself is caused by material energy-loss parameters that are not often tabulated. In the simplest case the energy loss would appear as a multiplicative loss factor, possibly dependent on speed.

Examples of Correlations for Different Conditions

Firm Wheel and Firm Ground

“Firm wheel and firm ground” means here that both the wheel and the material on which it rolls are simultaneously stiff and elastic, as most metals are, and also many other materials to some extent. In practice firm ground for a firm wheel is almost always a steel rail, as even the smoothest roads are so rough that the use of really stiff wheels generates a great deal of vibration and noise—which is why iron-clad carriage wheels and steel skate wheels are no longer used (as well as because of their limited traction). Even solid wheels for indoor vehicles are rarely made of the hardest materials for these reasons, as well as to avoid scoring the floors.

The equations of classical contact mechanics developed by Heinrich Hertz describe the stresses and deformations of the various curved surfaces (e.g., solid wheels and surfaces), for example, the depth and area of the contact patch of a sphere or cylinder pressed into a plane or of two crossed cylinders. The latter is what actually describes the contact of unworn railway wheels and rails. (The radius of a rounded rail profile, which the [actually conical] wheel contacts, is a bit smaller [e.g., 300 mm] than that of a railway wheel [for example, 450 mm], but with a bit of wear it can become the same, in which case the contact patch of the two crossed cylinders is the same as that of a sphere with the same radius that contacts a plane.) These equations have nothing to do with rolling and the subsequent location of the force vector but should indicate a maximum possible value for $L_{\text{CL}}/r_{\text{W}}$ and hence an upper limit for C_{R} values. The Hertzian contact formula for two identical crossed cylinders or the equivalent sphere on a plane is $L_{\text{CL}}/r_{\text{W}} = (1.5 F_{\text{V}} [1 - \nu^2] / [r_{\text{W}}^2 E])^{1/3}$, in which ν is Poisson’s ratio for the material (~ 0.3 for steel) and E is Young’s modulus (~ 200 GPa for steel). Mesys (2019) provides an online calculator for this formula and more general cases.

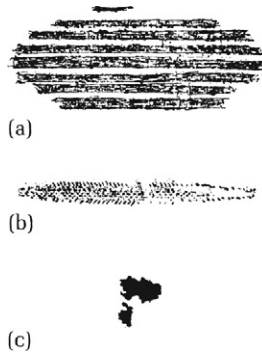


Figure 6.7

Contact prints of bicycle tires on a hard surface and a steel train wheel on a steel track: (a) 12.5 × 2.25-inch bicycle tire inflated to 1.8 bar (26 psi), with a 400 N (90 lbf) load (actual length of impression: 100 mm [4 inches]); (b) 27 × 1.25-inch bicycle tire inflated to 2.8 bar (40 psi), with a 400 N (90 lbf) load (actual length of impression: 97 mm [3.8 inches]); (c) 890 mm (35-inch) diameter steel train wheel on steel track with 27 kN (6,075 lbf) load (actual length of impression: 19 mm [~0.75 inch]). (From Whitt 1977.)

For an 890 mm steel wheel, this formula yields a value for L_{CL}/r_W of ~0.01 and an L_{CL} value of ~4.3 mm, considerably smaller than the contact print shown in panel (c) of figure 6.7, with an L_{CL} value of about 8.5 mm. Presumably this is because the carbon paper that may have been used to make the print is thicker than the depth of impression.

For a railroad wheel on its track, Koffman (1964) indicates that C_R is proportional to L_{CL}/r_W and introduces a constant of proportionality K_1 so that $F_R/F_V = K_1 (L_{CL}/r_W)$, and he quantifies K_1 as 0.25. If the example from figure 6.7 ($F_V = 27$ kN, $r_W = 445$ mm) is taken with the calculated contact patch half-length L_{CL} of 4.3 mm (rather than the 8.5 mm from the contact print), and the constant K_1 from above, $C_R = 0.25 \times L_{CL}/r_W \approx 0.0025$, which fits in well with the railway data of table 6.1 and would correspond to a railcar of about 24 short tons, assuming eight wheels.

As this book is about bicycles and not heavy trains, wheels that could be useful for rail bikes, that is human-powered rail vehicles (see chapter 10), are more the topic of interest here. In this field all manner of things have been tried: bicycle rims without tires, railway

wheels of small diameter, thin steel or plastic disks, roller-skate wheels, and even ball bearings running directly on the rails. None of the experimenters appears to have recorded C_R values, and none has beaten the speed records of comparable road vehicles, as was the initial hope in conducting the experiments. Applying the Hertzian formula for a cylinder of width L_{WW} contacting a plane, $L_{CL}/r_W = (8 F_V [1 - \nu^2] / \pi r_W L_{WW} E)^{1/2}$, that is, with the length of the contact patch $2 L_{CL}$, to an aluminum-alloy (assumed $E = 70$ GPa) bicycle wheel loaded with 400 N running on a steel rail, but without its tire, yields an L_{CL} value of 0.5–1 mm (depending on the total contacting-rim width chosen) and a value for L_{CL}/r_W of ~ 0.0015 – 0.003 , which is less than when the wheel is operated with most tires, even before the factor K_1 is applied. So why not simply take the tires off of bicycles to go faster? Apart from the obvious practical issues like traction, noise, and wear, the vibration from the smallest roughness probably makes C_R values higher than expected from the contact-patch calculations. Although the operators of touristic human-powered rail draisines (see chapter 10) use steel wheels for robustness and perhaps sound, serious rail-bike racers and tourers use standard pneumatic bicycle tires for the loaded wheels. The examples in this section assume perfect smoothness. However, the depth of impression y_{WS} for a metallic rail-bike wheel is a few micrometers or less. Thus the slightest bit of unevenness, even dust or rust, is bound to have a great effect, as the wheel has to climb, impact, or crush these particles or other microelevations.

Effect of Wheel Diameter For a 10 mm wide steel wheel with 1 m diameter rolling on a steel rail and loaded with 10 kN, the Hertzian formula gives an L_{CL} value of about 2.5 mm and a value for L_{CL}/r_W of about 0.005. If the diameter is reduced to 100 mm and nothing else is changed, the L_{CL} value decreases to about 0.75 mm and that for L_{CL}/r_W increases to about 0.015. For a further tenfold reduction in diameter, the formula yields values of ~ 0.25 mm for L_{CL} and ~ 0.05 for L_{CL}/r_W , the latter value being ten times greater than that for a 100-times-larger wheel. Thus, other things being equal, C_R is proportional to $r_W^{-1/2}$, a relationship also reported, approximately, by Kumar, Sarkar, and Gupta (1988): they find $C_R \propto r_W^{-0.48}$ for cylinders of Teflon, nylon, and steel. Jules Dupuit (1837) performed extensive tests with iron cylinders and proposed that $C_R = 0.001 (2 r_W)^{-1/2}$.

Effect of Wheel Load The railroad data from Trautwine and Trautwine (1937) included in table 6.1 clearly show a *decrease* in C_R values with higher loadings. Indeed, A. K. Shurtleff in the same publication advances a formula for railway cars that, under an assumption of eight wheels per car, amounts to $C_R = 0.05/F_V + 0.0005$ [in kN per wheel]. This fits the value of $C_R = 0.0025$ worked out for the 27 kN example in figure 6.7) but contradicts the idea that higher loadings mean a longer contact patch, and other things being equal, should lead to an *increase* in values for C_R , and the opposite for a shorter contact patch. Indeed, taking the example from the preceding section and reducing the load hundredfold from 10 kN to 100 N results in values for L_{CL} of about 0.25 mm and for L_{CL}/r_W of about 0.0005, the latter being ten times less than that for a wheel bearing a load 100 times greater. An increase in load in the opposite direction has the opposite effect: 1 MN gives an L_{CL}/r_W value of ~ 0.05 . Therefore $C_R \propto F_V^{0.5}$. Kumar, Sarkar, and Gupta (1988) report $C_R \propto F_V^{0.48}$ for cylinders, a very nearly identical result.

The preceding observations are now completely at odds with the measured railway data and Shurtleff's formula. Even though for the example in figure 6.7 ($F_V = 27$ kN, $C_R = 0.25 \times L_{CL}/r_W = 0.0025$), the values obtained using both methods agree perfectly, at any other load, the two formulas predict quite different results. For example, with a load of 1 kN, the Shurtleff formula gives $C_R = \sim 0.05$, but for the Hertzian formula together with Koffman's proposal, $C_R = \sim 0.0008$, using $K_1 = 0.25$.

There could be several explanations for the discrepancy:

- The "constant" K_1 given by Koffman for railway wheels is actually a highly load-dependent variable.
- In regard to the rolling resistance of complete railway cars, other effects (including the bearings and the "self-steering" of a pair of conical wheels on a common axle) dominate over the rolling resistance of the pure wheel taken by itself, so that the two types of rolling resistance coefficients are not comparable.
- The rails are not as smooth as assumed and the higher loadings are less sensitive to roughness.

Intuition tells us, for the preceding example, that both calculated values must be wrong, the first too high, and the second too low. As shown later in the chapter, and also for pneumatic tires,

measurements hardly bear out the predicted effect of load, but at least they don't go the "wrong way"!

Effect of Wheel Width The contact-patch model also implies that wider is better. As noted previously, Kumar, Sarkar, and Gupta (1988) find $C_R \propto r_T^{-0.48}$ for cylinders. This proportionality is, however, of little use in practice in regard to hard wheels and rails, especially rounded rails, which rail bikes probably come into contact with only for a few millimeters, as even a precise cylinder would be susceptible to the slightest mismatch or misalignment.

What Should Rail Cyclists Do in Practice? Certainly it is a bad idea to reduce excessively both the diameter and width of steel wheels, as several rail bike racers have done in the past (and replacing the steel with nylon, as the coauthor has tried, is a particularly bad choice). However, multiple individually suspended thin disks could be an option for reducing drag. Dupuit (1837) states that distributing load across many wheels reduces drag (again in contradiction to the conventional railcar measurements and Shurtleff formula!), which suggests using many wheels on railcars, if the object is to transport many passengers or loads on rails with size-limited wheels. However, the coefficient of rolling resistance does not appear to be the main problem in regard to rail-bike record attempts in comparison to reducing the drag of the guides required to keep the wheels on the rails.

Soft Wheel and Soft Ground

Mountain bikes and more recently "fat bikes" have renewed interest in all-terrain riding, including on very soft surfaces such as dry sand and snow. In many countries of the world, dirt roads are hard when dry but become soft when wet. Rural roads and cycle paths are often constructed of hard, compacted gravel, but the very top surface is loose unless binding agents are used. For all three environments it is important to know how bicycle tires behave and how to minimize rolling resistance. Although in soft ground a pneumatic tire might be considered "hard" and most of the resistance to be coming from the plastic deformation of the soil, a flattened contact patch still occurs, especially at the low inflation pressures that are advantageous for traction. This is especially the case when only the top layer is soft and the tire plows through this, mainly supported by

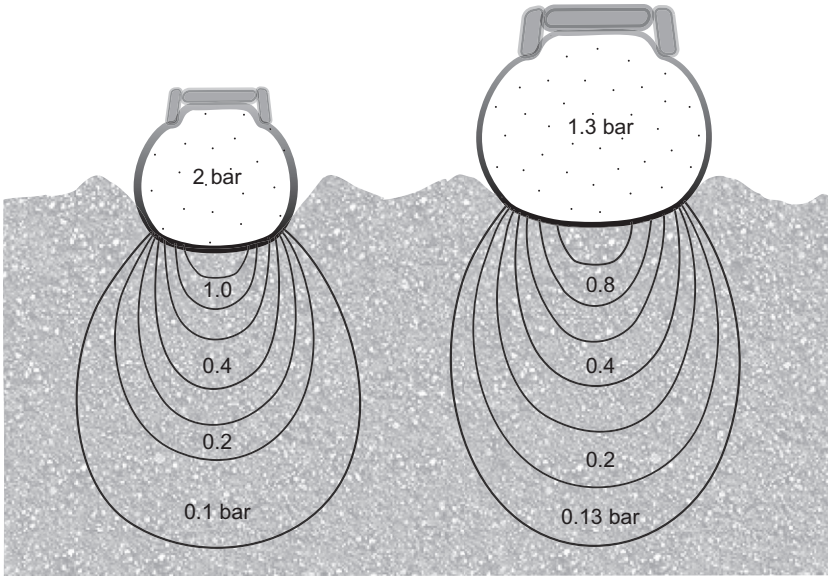


Figure 6.8

Sketch of the *pressure bulbs* of a mountain bike (left) and a fat tire (right) (shown only as skin cross sections), at different pressures but the same (unspecified) load, on loose soil. The pressure underneath the tire is a function not just of the pressure of the contact patch, but also of the tire's width. The fat tire has a lower pressure at the surface and therefore sinks less but exerts a greater pressure farther down. Soil is also pushed up sideways.

firmer layers below (see figure 6.8). Further environments for which soft tires may present an advantage are cobbled streets or potholed roads, both of which are hard but structured—and dreaded by riders of vehicles with hard, thin, or small wheels.

There are therefore a great many types of surfaces, both natural and constructed, that can be considered soft, and for many of these it is better to measure rolling resistances than to calculate them. The following sections, however, attempt to present some basic understanding on how these resistances come about.

Soil Most natural surfaces and many constructed ones are made of soil, which basically consists of rocky grains of various sizes, possibly with some living or decaying matter, such as turf, leaves, or humus, on the very top. The grains cover a wide range in size,

from (in increasing order) the extremely fine, referred to as *clay*, to the fine, called *silt*, through grain sizes of *sand* from fine to coarse, and then to *gravel* and *stones*. Apart from the grain size, the grain shape (rounded or sharp-edged), the composition (e.g., gravel with sand, or sand with silt and clay [called *loam*]), and the degree of compaction and water content are all also important. Clay and silt are *cohesive* (the grains stick together) and extremely sensitive to water. Loam can be a firm cyclable surface when dry or slippery mud when wet. Noncohesive, purely frictional soils like gravel are not affected much by water, but sand is, by the surface tension of the water between the grains. Anyone who has cycled along the waterline of a sand beach knows the narrow region where the waves have just drained away, which is firm and a pleasure to cycle on, but becomes much softer a few seconds later, when much of the water has drained away, or a little farther up the beach.

Although soil grains are made up of hard and often extremely elastic (in the physical sense) material, such as quartz, soil itself is not elastic in this sense, but has both solid- and liquid-like properties. Under low stress, many soils behave as solids yet will deform if an applied shear stress τ exceeds the material's shear strength governed mainly by its *angle of internal friction* ϕ (see figure 6.9) and its *cohesion* c . Cohesive, fine-grained soils are more or less plastic, depending on water content, meaning they tend to deform irreversibly under stress. Except for dry sand or freshly deposited layers of gravel, both roads and natural surfaces are more or less compacted, with a surface that can be loose or cohesive. The behavior of a loose layer is closely governed by ϕ , whereas that of a cohesive layer depends on c , itself highly dependent on moisture content. In 1773, Coulomb (mentioned in chapter 2) formulated the basic equation of soil mechanics: $\tau = c + \sigma \tan \phi$, in which σ is the normal stress. Therefore, the larger c and ϕ , the more stress the soil can withstand without deforming.

For consistent calculations and experiments involving loose soil (and thus avoiding an unknown, fickle, or difficult-to-measure value of c), it should at best be coarse grained and uncompacted, like sand or purchased gravel with defined properties, and dry. The main property to know is the angle of internal friction ϕ , which can be approximately visualized by its angle of repose, the maximum slope that a heap or bank of the material can maintain. For the most

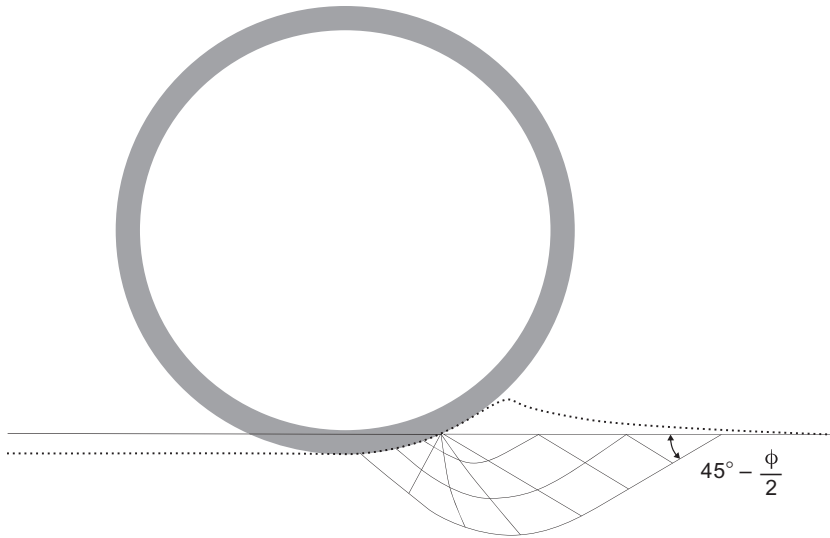


Figure 6.9

A hard cylindrical wheel rolling from left to right through dry sand with $\phi = 30^\circ$. The solid lines show the initially undisturbed ground and shell-like surfaces along which the soil slips, forming a hill ahead and a rut behind. This representation is an abstraction of a three-dimensional situation in which the material emerging from below is also pushed sideways.

unstable material imaginable, uniform hard and smooth spheres, this is about 22° , for normal sands it is $25\text{--}35^\circ$ depending on the roundness of the grains, and for the most stable material, crushed rock with sharp edges, it can approach 45° . Pressure and vibration can compact mixtures of gravel and sand in particular by causing the finer grains to migrate into the spaces between the larger ones, making a stable, hard base surface. *Mature soil* that has been undisturbed for thousands of years is naturally compacted and also firm. Therefore many natural paths are easily firm enough for bicycling. However, they are often uneven, with protruding larger stones or roots, accumulated loose stones, or holes where water or frost has been active. Even well-compacted gravel roads cannot maintain a solid upper surface when subjected to the pressures of wheels and shoes. If a natural binding agent is used that itself consists of cohesive grains (i.e., does not set hard like cement), it can form a fine, smooth, firm surface when dry but may become soft when

waterlogged, and it is then quickly removed by the next few tires: a pothole develops.

Theory and Measurements M. G. Bekker provides comprehensive, mathematically based references on soft-ground support and traction. In particular, Bekker's *Theory of Land Locomotion* (1956, chapters 5 and 6) applies the classical theories of soil mechanics to the real-world problem of wheel loadings and includes plentiful references.

As cited in Bekker 1956, one possible power-law fit to results by Grandvoinet for cylindrical wheels on unspecified soil (214) could be $F_R \propto F_V^{4/3} r_W^{-2/3} L_{WW}^{-1/3}$. This relationship, attributed to Gerstner, means that if the diameter of the wheel is increased 35 percent, the rolling resistance decreases 18 percent (Grandvoinet: 20 percent). A similar increase in width decreases the rolling resistance by only 10 percent. Bekker examines other power laws that show similar tendencies. He is therefore adamant that a large, narrow wheel has less rolling resistance than a small, wide one for the same load. As F_V is raised to a power greater than one, an additional, properly aligned wheel sharing the load with another wheel should always reduce the total soft-ground rolling resistance.

A plausible analogy exists here with cross-country skis, which are long (often about 2 m) and narrow (often about 50 mm), rather than wide, because this way the cross section of snow to be compressed or thrown aside is reduced. (The friction of skis on snow is treated by Bekker [1956], who quotes data by Gorubonov. These amount to values of friction coefficient μ as a function of snow density ρ (in units of tonnes per cubic meters): $\mu = 0.12 - 0.17 \rho$, for ρ between 0.1 and 0.55 t/m³.)

More recently, finite-element analysis has been used for computer modeling at least for automobile tires and sand (for example, Grujic et al. 2010). Once carried out and validated by experiments, such methods can help establish power-law formulas. Unfortunately, however, most work in this area is on automobile tires.

Various sources give the coefficient of rolling resistance for tires for cars and agriculture as ranging from 0.012 on hard-packed surfaces to 0.04 on loose sand or loamy soil and as high as 0.06 on wet, loose gravel. The values increase with loading. For wheels on agricultural vehicles loaded with 4.4 kN (1,000 lbf), values of C_R can reach 0.05–0.09 on sod and even 0.2–0.5 on tilled loam or loose

sand. The huge variations show that without knowledge of the soil properties, measurements cannot be compared or values predicted. For loose soil, at least the angle of internal friction is required. However, most testing is for agricultural or military purposes, on layered cohesive soils that may be described by up to six different values. A single number used in some formulas is the *cone index*, a measure for soil penetration resistance.

For any given shape of wheel-periphery cross section and load, reducing the amount of sinkage that occurs minimizes soft-ground resistance. Increasing a wheel's radius or width always reduces drag, as the support area is increased. An increase in the radius additionally reduces the virtual upslope formed because of the rut (figures 6.9 and 6.10).

Akande et al. (2010) measured the resistance of 16-, 20-, 24-, and 26-inch \times 1.9-inch bicycle tires on various surfaces (asphalt, hard grass, and tilled sandy loam with a mean cone index of 1.1 MPa) at 4 vertical loads from 313 to 810 N and 3 inflation pressures, 40,

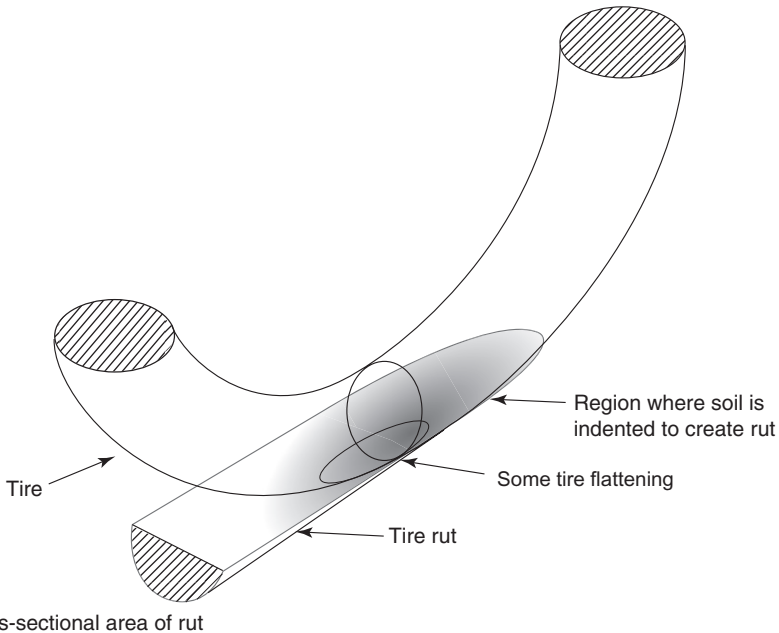


Figure 6.10

Rolling resistance in soft soil through creation of a rut and a continuous upslope.

50, and 60 psi (276, 345, and 414 kPa). They used a single-wheel trailer connected to a tractor traveling at 4.4 km/h. The best values of C_R that they measured for the grass surface were slightly more than 0.015 at 613 N load for the largest tire with the highest pressure or for the 24-inch tire inflated to 50 psi at 810 N load. The best values for asphalt paving were only slightly lower and not achieved with the highest inflation pressure; they were surprisingly high and rather at odds with the data in the next section. For the tilled soil, the best value of C_R reached was 0.064 with the largest wheel at the highest pressure and the lowest load of 313 N, easily doubling with higher loads and smaller wheels, and with a worst value of 0.21 with the smallest wheel at the highest load, as expected, but at the lowest pressure. Akande and his colleagues later also tested with wetted soil, solid wheels, and higher towing speeds, all of which increased the rolling resistance. Their main objective for using relatively narrow tires was to enable low-cost agricultural equipment that compacted the soil as little as possible (see figure 6.8) and of course also gave a smaller rut between crops.

Users of off-road vehicles generally already employ the largest-diameter wheels feasible and try to reduce sinkage by increasing the width or the number of wheels. They refer to many wheels or a large flat support area as *flotation*, the extreme example being a “caterpillar” track. Among serious cyclists, perhaps the best examples of flotation with a given maximum tire diameter are the doubled rims and tires of bicycles previously used in races on snow and more recently the fat-bike tires that have become popular. These tires range in width from 3.0 inches (76 mm) to more than 5.0 inches (130 mm) and allow bicycling on soft terrain like snow and sand with low inflation pressures of about 0.35–0.7 bar (~5–10 psi), as well as on roads at 0.7 to 1.4 bar (~10–20 psi).

Soft Wheel and Firm Ground

Solid Tires Although bicycles are mainly fitted with pneumatic tires, there are always uses for “soft” solid wheels, such as when the total freedom from punctures or lack of air makes such wheels’ somewhat higher rolling resistance worthwhile or when tiny wheels are for some reason required. In the latter case, on a smooth surface, solid wheels generally generate less rolling drag than equally small inflated tires. Wheelchairs are one such case in particular, because

those who use them are often not easily able to mend or pump tires, and because they may stand unused for long periods but must be ready for emergencies. In such cases reliability is often more important than minimal resistance or comfortable rolling.

Manufacturers of solid industrial wheels provide vague data on the wheels' associated rolling resistances; for example, for a polyurethane wheel of 0.2 m diameter rolling at walking speed (3 mph), $C_R = 0.004$ to 0.007, depending on the exact material, and is inversely proportional to the wheel's diameter, thus making the values 0.0075 to 0.015 for a polyurethane wheel of 0.1 m diameter. The resistance of rubber is given as ten times higher than that of the best polyurethane (see Lippert and Spektor 2013 for all the above data), but unfortunately no manufacturer of solid wheels seems to publish actual rolling-resistance measurements for its wheels, not even for skate wheels and the like.

Kauzlarich and Thacker (1985), on the other hand, give far more detailed information for solid wheelchair wheels. These wheels are made either of *gray rubber*, which is natural rubber filled with 50 percent clay particles, or polyurethane. For a wheel of 2 ft (0.61 m) diameter equipped with a tire 22.4 mm wide, Kauzlarich and Thacker specify the coefficient of rolling resistance for gray rubber (in both theory and measurement) at about 0.015, at walking speed and room temperature, almost independent of load. For a wheel of the same diameter but with a 150 mm wide polyurethane tire (with Young's modulus E stated as 9.6 MPa), the same authors measure and calculate the value of C_R to be about 0.0035 at low loads, 0.006 at typical wheelchair (or bicycle) loads, and up to 0.0067 for heavier loads. These authors give a general formula based on Hertzian contact (discussed earlier in the chapter), with complicated material and geometric parameters:

$$C_R = 0.07 m (F_V^{3/2} / r_W) (1.5 [r_W r_T / \{r_W + r_T\}] [1 - \nu^2] / E)^{1/3},$$

in which m is the result of a sixth-order polynomial fit that depends on the ratio of wheel radius r_W to tire radius r_T (half the tire width). For the example with the ratio $r_W / r_T = 610 / 150 \approx 4$, m is 1.67; for a ratio of 10, it would be 2.37. The quantity 0.07 in the equation represents a hysteresis factor that combines a value of 0.15 for polyurethane (the useable range is 0.10–0.15) and a value several times higher for rubber, and it includes a value of 0.5 for Poisson's ratio ν . Kauzlarich

and Thacker include all of this information, but predictions are still difficult because of the sensitivity of C_R values to Young's modulus E , which is often not known. Young's modulus E varies considerably depending on material and also on stress and temperature. Values for it are generally not available even for specific tire materials, but Shore (hardness) values offer a more readily available proxy. The hardness of skate wheels is mostly designated according to the Shore-A scale, with values typically from 70 (medium soft) to 100 (extremely hard), easily measured using a spring-loaded indenting device called a *durometer*; there are also Shore B and D scales for harder materials. There is no defined relationship between the Shore scales and Young's modulus, but a number of approximate correlations have been published. Kunz and Studer (2006) provide an equation, validated through experiments, in which 75 Shore-A (ShA) corresponds to about 10 MPa, 85 ShA to about 16 MPa, and 90 ShA to about 24 MPa. Shore-A values above this become inaccurate, however, as a value of 100 ShA means no indentation at all, that is, the durometer cannot distinguish between the rubber wheel and a high-modulus metal (see also Larson 2016).

Using both the Kauzlarich and Thacker Hertzian contact formula and the Kunz and Studer equation relating Shore-A to E , for a skate wheel with a 100 mm diameter and 25 mm width (implying $r_T = 12.5$ mm), a hardness of 75 ShA results in a C_R value of 0.01–0.02 depending on load; 90 ShA reduces this to 0.0075–0.015, better than the values for ordinary pneumatic tires of the same diameter. Presumably 100 ShA wheels yield values similar to those of larger pneumatic bicycle wheels, at least on very smooth and hard surfaces. Certainly it feels that way when one is skating on polished stone (such hard wheels must then be used with care, as the static friction needed for safe steering and braking is minimal). However, the Kauzlarich and Thacker formula was developed for wheelchair wheels at walking speed; skate wheels turn much faster, so they warm up more quickly, which decreases E values and hence increases C_R values as well.

For full-size bicycle tires, solid polyurethane would be rather heavy, although such tires are available for 22- to 24-inch wheelchair wheels, and there are also polyurethane inserts for rubber tires to be used instead of pneumatic inner tubes. Mounting solid tires requires split wheels or special tools to stretch the tires onto the

rim. Solid tires for bicycles are generally made of dense, closed foam and are comparable to pneumatic tires in terms of weight and ease of mounting, but not in regard to removal. They generate slightly more rolling resistance than hard-pumped pneumatic tires (but presumably less than poorly inflated ones) and less static friction on smooth surfaces. Some users like them; others complain of a hard ride. Presumably they last longer than rubber tires, especially when not used for many years, which tends to cause rubber to disintegrate. They wear out less quickly in use, as polyurethane has particularly good abrasion resistance, at least an order of magnitude better than that of rubber, and there is more material in the tire.

Pneumatic Tires Thin-walled air-filled tires develop a contact patch with the road or other surface on which they roll as do solid tires, but instead of those described by the Hertzian formulas given earlier, other relationships must be found. A slender pneumatic bicycle tire on a hard road can be analyzed approximately under the assumption of a contact-patch length ($2 L_{CL}$) considerably longer than the tire width ($2 r_T$). The approach is to calculate the amount of sinkage at each position along the contact patch and use it to determine contact width at that position. The total calculated contact area multiplied by inflation pressure p is then related to load F_V and wheel radius r_w . The resulting equation is $L_{CL}/r_w = (3 F_V/4 K_2 p r_w^2)^{1/3}$. The coefficient K_2 in the equation represents the ratio of the contact half-width to the sinkage of the tire cross section (figure 6.11), which is approximately constant for well-inflated tires in normal use, that is, when sinkage is not extreme. Tire width per se doesn't enter the equation, but K_2 does depend on the ratio of tire width to rim width (i.e., rim-flange separation). For an often-used rim-to-tire width ratio like that shown at the top of figure 6.11, the equation simplifies to $L_{CL}/r_w \approx 0.75 (F_V/[p r_w^2])^{1/3}$.

In 1977, Frank Whitt carried out tests in which he pressed an inked wheel with known loads against paper, then measured the rim's sinkage. Whitt's experiments showed that the behavior of real tires departs from that predicted by the simple model for several reasons. Perhaps the most important is tread pattern and thickness: only when a tire has unpatterned tread of uniform thickness does pavement pressure equal inflation pressure and contact area equal F_V/p . A variable-thickness tread permits contact zones in which the taut tire fabric at the zone edges is not perfectly horizontal. A band

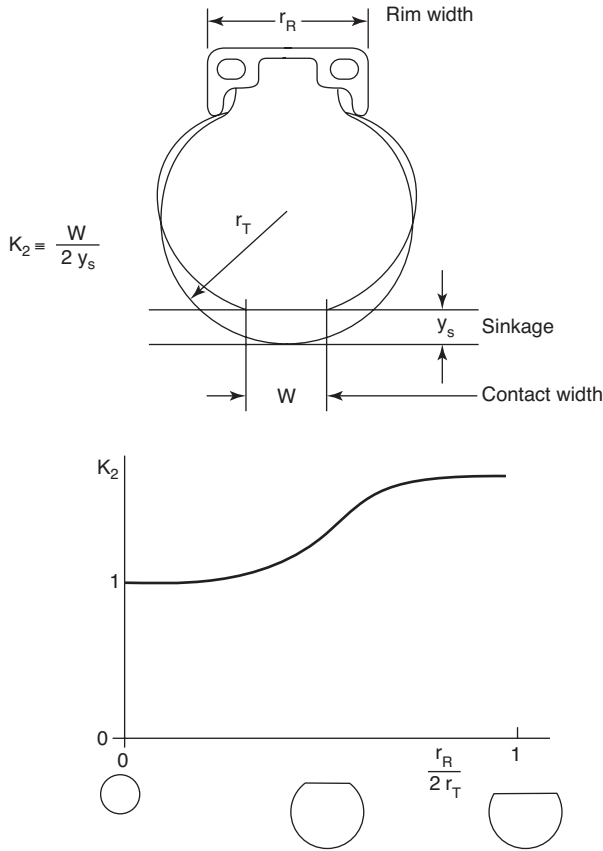


Figure 6.11
Contact mechanics for a slender, thin-tread tire.

on the tire in which its tread is worn flat increases the tire’s contact area without increasing supporting force. On the other hand, a raised tire rib is pressed to the ground not only by the tire’s inflation pressure, but also by tension in the tire fabric, which can bulge downward toward the ground without quite meeting it.

Whitt measured 97 mm for the length of the contact patch in panel (b) of figure 6.7, a tire with a nominal r_w value of 344 mm. The measured value for L_{Cl}/r_w is thus 0.14. If the simplified equation just discussed is used, L_{Cl}/r_w is 0.165 for the data given for figure 6.7. The measured length of the contact patch is thus 85 percent of that calculated, which is the same as the factor of 85 percent

found by Smiley and Horne (as cited in Clark 1981). Of course this information still doesn't provide a value for C_R , in the absence of a function or factor relating C_R and L_{CL}/r_W . Earlier in the chapter, $C_R = 0.25 L_{CL}/r_W$ was used for steel train wheels and rails, but it isn't at all applicable to pneumatic wheels. If $C_R = 0.04 L_{CL}/r_W$ were employed for the relationship, the C_R value in Whitt's example would be roughly 0.007.

More recently, toroidal contact-patch calculations have been examined very thoroughly, first by Thomas Senkel (1994), then Andrew Dressel (2013), and then Leonardi Datza (2015), who provides a spreadsheet (Latsch.zip) that draws a contact patch when provided with values for r_W , r_T , F_V , and p as inputs. Using the data from panel (b) of figure 6.7, Datza's spreadsheet outputs 70 mm for the length of the contact patch instead of the measured 97 mm. MontyPythagoras (2014) presents exhaustive mathematical solutions for rolling resistance far too complicated to give here that suggest that C_R is approximately proportional to $(F_V/p)^{2/3}$ if a tire with a zero-thickness skin is assumed, which implies that the only source of drag is the sliding friction between the tire and the road. Although this assumption may seem an oversimplification, the examples provided do seem realistic for thin-walled high-pressure bicycle tires and answer questions regarding changing loads and pressures. For panel (b) of figure 6.7, MontyPythagoras's expression calculates the C_R value as 0.005, if it is assumed that the coefficient of sliding friction of the tire on the road is 1.

The drag force acting on a tire is due to the energy dissipated, with three likely contributions to this dissipation. If MontyPythagoras (2014) is correct, the main loss, especially at low speeds, is due to the tire tread's continually undergoing a slight slippage or rubbing in a manner analogous to that shown in figure 6.5. Additionally, there is the viscoelastic bending loss (elastic hysteresis) in the rubber of the tire, affected by time of deformation (L_{CL}/V , in which V is the bicycle velocity), by load, and also by temperature. A further contribution is from friction loss between the fibers of the tire cords.

Clark (1981) presents a great deal of information about pneumatic tires, but not much drag data. Even today it is difficult to find systematically measured drag data for variations in wheel diameter, width, load, speed, temperature, and roughness, but a

few correlations are available and are summarized in this section. The best-documented relationship is that of the coefficient of rolling resistance as a function of inflation pressure for different types of tires.

Pressure and Type Tire manufacturer Avocet commissioned Inoue Rubber Company tire-testing data (Brandt 1998) (see figure 6.12) representing fourteen sew-up and clincher tire models of sizes $700 \times 20C$ to $700 \times 28C$, from two tire suppliers, Avocet and Specialized, tested over a range of pressures. (More accurate names for these tire types are *tubular* for the former, for the sewn-up casing containing an inner tube that is glued to a special rim, and *wired-on* for the latter, for the open casing containing wire or cord beads that sit on the rim and usually having a separate inner tube.) For the testing, the wheel housing the tire was loaded by a force of 490 N and rolled against a smooth drum of unknown diameter at unspecified speed and temperature. The rolling-resistance coefficient values obtained

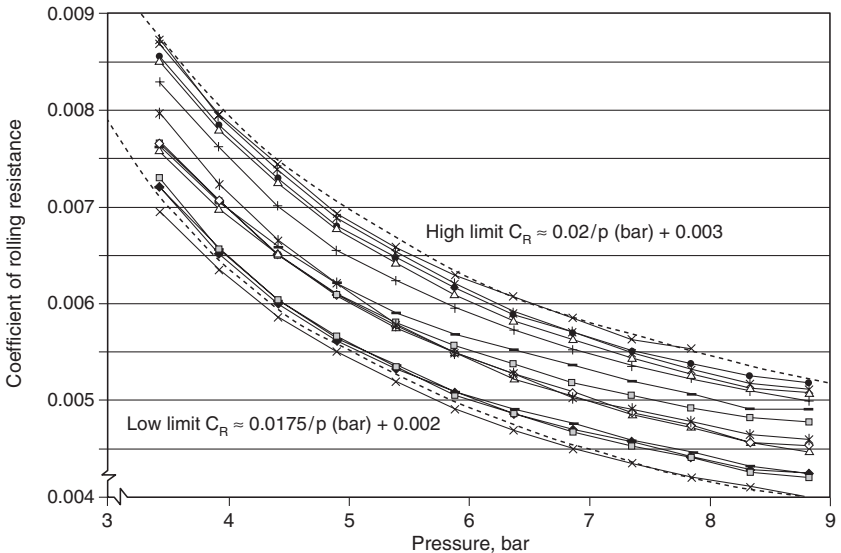


Figure 6.12

Tests of miscellaneous tires against a drum, showing effects of inflation pressure, including curve fits for the highest- and lowest-resistance tires. (Data from Brandt 1998.)

seem a little high, perhaps because a drum was used, which is equivalent to testing a wheel of smaller diameter.

Brandt's (1998) very clean data are significant in showing that the coefficient of rolling resistance does not approach zero as tire pressure increases (one way to see this is to plot C_R versus $1/p$), so a purely power-law theory regarding rolling resistance cannot hold. It is easy to find rather simple curve fits that match the data for individual tires quite well. For the best (i.e., lowest-resistance) tire, $C_R = 0.0175/p$ (bar) + 0.002 fits well, and for the tire with the highest resistance, $C_R = 0.02/p$ (bar) + 0.003 fits very well, up to a p value of 8 bar. This does not mean that the value of C_R for infinite pressure would necessarily be 0.002 or 0.003, however, as very similar curves can be found with completely different polynomials and values, for example, $C_R = 0.155/p^{1/2}$ (bar) for the high limit in figure 6.12.

Brandt (1998) observes that the curves for the sew-up tire models in figure 6.12 cross those for the clincher-tire models and attributes this to the rim adhesive's adding a constant offset. Such adhesive can be permanent setting for track use or reusable sticky for road use. For the sew-up tires in the testing, road adhesive was used and presumably created extra resistance through viscous drag.

Figure 6.13 shows similar but newer measurements of the same type as shown in figure 6.12, providing more information and including data for additional types of tires (touring, mountain bike, and fat tires). The tires for which data are presented in the figure were selected as follows: from the large amount of data available, the best and worst tire (in terms of drag) of each type was chosen, along with one in between (for road tires, two more). The figure shows two curve fits for the lowest drag: $C_R = 0.006/p$ [in bar] + 0.0012 approximately covers the whole range from the best road to the best fat tire, and $C_R = 0.0055/p^{1/2}$ [in bar]—quite a different formula—yields practically the same curve for p values from 3 to 9 bar. The point of this comparison is not to find the best fit (which is easy to do by trial and error using a spreadsheet or with a curve-fitting program), but to show how empirical the correlations are. Simple “cut and try” curves often fit as well as or better than those based on higher-order polynomials or other functions that try to conform to theoretical relationships. These measured data, it should be recalled, are from a *drum* and not the road. The data, all at the

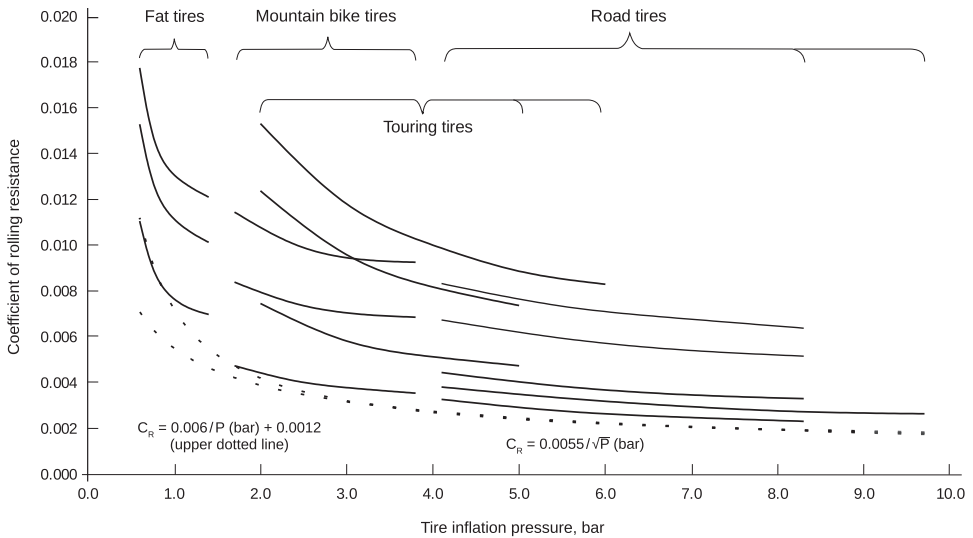


Figure 6.13

Data for various tires, all tested on the same 0.77 m diameter drum with a structured metallic surface, at room temperature, after a 30 min warm-up. The load is 417 N and the speed 29 km/h (18 mph, ~ 8.1 m/s). The values for the coefficient of rolling resistance are directly calculated from the drum forces. Data for four groups of tires are shown, from the best to worst per group. Two possible lower-limiting lines are also shown. (Data from Jarno Biermann's website [see Biermann 2014].)

same speed (8.1 m/s), the same load (417 N), and the same drum diameter (0.77 m), show, in addition to the plotted effect of pressure, the large variation due to tire construction, for example, thickness of tread and sides. And they show that the best fat tire inflated hard experiences the same drag as the worst road tire!

Senkel (1992) conducts a low-speed (rollout) test of a single tire (Continental Top Touring 37–622) at a pressure range of 1 to 6 bar. The result can be described very well by $C_R = 0.009/p \text{ [bar]} + 0.0015$ or approximately by $C_R = 0.01/p^{0.7} \text{ [bar]}$. This indicates many possible mathematical models, with the best describing the coefficient of rolling resistance as inversely proportional to pressure, plus an offset representing a minimal value for the coefficient at infinite pressure. It would be interesting to test this by measuring C_R values for a tire filled with a hard material instead of air.

Effect of Diameter The section “Bicycle Wheels” earlier in the chapter describes the effect of wheel diameter on rolling resistance (see figure 6.2). The data presented in that section show that, in otherwise equal conditions and at low speeds, the coefficient of rolling resistance is almost exactly inversely proportional to wheel diameter. Tires for smaller wheels are often constructed differently from those for the more usual large wheels, however, creating some difficulty in evaluating wheel diameter’s effect on rolling resistance. Small tires are often made for children’s sidewalk bicycles, for which puncture resistance and low cost are primary considerations. For recumbent bicycles, tricycles and faired HPVs that require smaller wheels, especially front wheel(s), such tires are a poor option, but these vehicles need wheels of two-thirds to three-quarters the usual diameter. Racers of these types of vehicles especially are keen to still have low tire drag and therefore take care to inflate the tires until hard and buy known low-drag types. Amateur resistance measurements, published and discussed exhaustively on internet forums, quickly identify exceptional tires. For example, the late designer and engineer Alex Moulton was able to develop a smaller-diameter tire (Wolber 17 inch) whose rolling resistance rivals that of tires of normal size. Many of these tires were bought also by the builders of HPVs and record-breaking solar vehicles (see Hadland 2012). Today a number of tires with exceptional rolling resistance values are available, and some can even be ordered in experimental versions, for example, with thinner tread or sidewalls but still usable at high pressures. The combination of small size and high pressure gives a hard ride except on the very smoothest surfaces, so some form of suspension is employed whenever possible, even for road use.

Effect of Width The effect of width on rolling resistance is an old but still ongoing discussion. The contact-patch relationship implies that between two tires of differing widths but bearing the same load and inflated to the same pressure, the wider one will have a shorter contact patch and hence experience less drag, as figure 6.14 illustrates for varying widths of two tires. But tire pressure exerts stress on the tire: if a tire is viewed as a cylindrical pressure vessel, the hoop stress due to air pressure is proportional to its width, that is, its radius r_T . Thus a tire twice as wide as another with the same construction and material thickness can be inflated only to *half* the

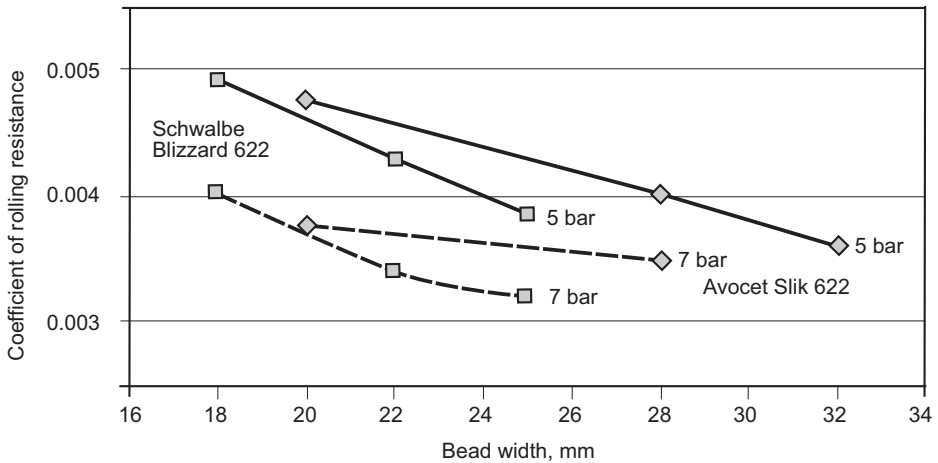


Figure 6.14

Comparison of two types of tires, Schwalbe Blizzard 622 (solid lines) and Avocet Slik 622 (dashed lines), which were each available in three widths, at 5 and 7 bar pressure, 540 N load, in low-speed rollout tests. The results show that, all other factors equal, wide tires experience less drag than narrow ones (however, all factors cannot remain equal: see the chapter text). (Data from Senkel 1992.)

pressure of the other with the same margin of safety. For the two tires to be inflated with the *same* pressure with the same margin of safety, the skin of the wider tire must either be thicker or made of a stronger material; otherwise the margin of safety is necessarily smaller. Only under the latter condition, however, is there a clear advantage for the wider tire in regard to reduction of rolling resistance. All other cases involve an optimization between the amount of flexing the length of the contact patch imposes and the thickness of material that is flexed, along with other effects. Therefore a definite answer for optimal tire width with respect to rolling resistance requires some careful experiments and analysis or numerical computing.

Apart from this not-completely-resolved question, tires for traditional racing cycles are quite narrow for additional reasons beyond rolling-resistance reduction:

- **Comfort:** For racing tires comfort is not a primary goal, so their narrowness and hardness are more tolerable, especially on the smooth surfaces of velodromes, than when tires are for other

uses. However, recently there seems to be a trend toward increasing width from 23 mm to 25 mm in tires for road-racing use.

- **Weight and mass:** A twice-as-wide tire would have twice the weight and inertia (both linear and rotational), or if constructed to withstand the same pressure, four times as much.
- **Air drag:** A twice-as-wide tire would have about twice the air resistance.

For everyday use, tires may be wider for practical reasons that may be more important than weight and drag, including greater loads, for example, with tandems and cargo bikes.

Especially heavily loaded small tires on special vehicles may need to be somewhat wider in any case to avoid excessively high pressures or too much sinking. The tire company Continental made a series of small, wide tires in the mold of child-bicycle tires but with very thin and careful laminations. These tires resulted in much lower drag values for solar racing cars than if they had used automobile or motorcycle tires, but they were also more fragile.

Effect of Load and Number of Wheels According to the contact-patch relationships given earlier, the drag coefficient should increase with load at the same rate it decreases with pressure. Gordon, Kauzlarich, and Thacker (1989) are responsible for one of the few available measurements that test this theory. Gordon and his coauthors measured the rolling resistance of pairs of various types of 24-inch tires on a treadmill operated at speeds of 1.5, 2, and 3 mph with loads of 85 to 205 lbf per pair. Whereas for the object of the test, foam tires, the coefficient of rolling resistance did increase with load, for pneumatic tires, that coefficient was about 0.01 for all loads and all speeds and even decreased slightly with load (see figure 6.15), contrary to what would be expected. A similar behavior is indicated in figure 6.3, in which several different loads do not change the coefficient of rolling resistance much except at speeds around 60 km/h, and then also in the opposite direction from what would be expected. Two possible explanations for this can be advanced:

- The few available measurements of the coefficient of rolling resistance as a function of load involve a small range of contact-patch sizes from normal to small (high pressure-to-load ratios). For these contact-patch sizes, the change in the value of C_R as the

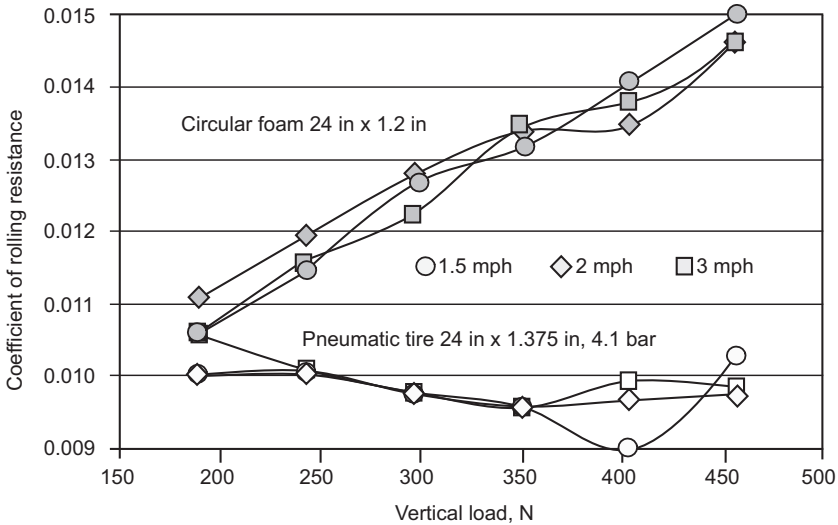


Figure 6.15

Coefficient of rolling resistance versus load of 24-inch solid foam polyurethane (upper curve) and pneumatic (~4 bar) (lower curve) tires. (Data from Gordon, Kauzlarich, and Thacker 1989.)

load changes is slight, as it is already near the minimum possible. In contrast, the many measurements of this coefficient as a function of pressure are conducted on a wide range of contact-patch sizes from small to large (low pressure-to-load ratios) and show both the flat and the steep parts of the function.

- For pneumatic tires, greater loads produce loss-induced higher temperatures, which then increase the air pressure and work in the direction of steepening the C_R -versus-pressure function but of flattening the C_R -versus-load function. In the case of foam tires, in contrast, it is the other way around, as a higher temperature softens the elastomers used and increases the coefficient of rolling resistance.

Experiments by Grappe et al. (1999) do show the expected relationship between load and rolling resistance within a narrow range. These authors tested a bicycle, with a rider (76 kg), equipped with Vittoria Techno Kevlar clincher tires (23 mm, 250 g) inflated to 10 bar. They measured, indoors, in coastdown tests, a coefficient of rolling resistance of 0.0035. If the bicycle carried an additional 5 kg

mass, the coefficient increased to 0.0036; with a second additional 5 kg load, it increased to 0.0037; and with a third additional 5 kg load, it increased to 0.004. The authors do not report temperatures and loaded pressures.

Closely related to the load question is that of the number of wheels. McConica (1985) argues that total rolling drag decreases with the square root of the number of wheels; that is, a quadracycle should have 71 percent of the drag of a bicycle—under the assumption that all other things are equal. They aren't, of course: air drag and weight increase with the addition of tires. Baldissera and Delprete (2016) also see the coefficient of rolling resistance decreasing with decreasing load, so that without increasing air drag and weight, the optimal number of wheels would be infinite. They then carefully model rolling resistance and the effect of additional weight from additional wheels. For example, even for 10 kg wheels equally loaded, they find the optimum number would be 5–6, and for lighter wheels, even more. When aerodynamic drag is also considered, they report, the number of tracks becomes important, so a tricycle might have more drag than a bicycle or a quadracycle.

Effect of Speed Although rolling resistance is usually conveniently assumed to be independent of speed, other than through the heating up of the tires that is greater at higher speeds (which would tend to increase pressure), many sources list a definite increase in rolling resistance with speed and offer prediction formulas with speed-dependent linear or quadratic terms.

Kyle and Edelman (1974) report an effect of speed on rolling resistance in some of their tests of bicycle tires. Their tests found the coefficient of rolling resistance doubled from low speeds to speeds around 17 m/s; for example, in one tubular tire inflated to greater than 7 bar, it increased from 0.0029 to 0.0058 at 17.6 m/s, and in another, also inflated to greater than 7 bar, it rose from 0.0039 to 0.0078 at 22.7 m/s. In a third clincher tire inflated to 4 bar, the coefficient rose from 0.0047 to 0.0094 at 16.1 m/s. Bekker (1956, 208) and Ogorkiewicz (1959) offer the following correlation (for automobile tires): $C_R = 0.0051 (1 + [1.09/p] [(1 + F_V/3) + \{1 + F_V/30\} \{V/39\}^2])$, with p in bar, F_V in kilonewtons, and V in meters per second. Engineering Toolbox (2008) also diagrams the coefficient of rolling resistance versus speed for automobile tires conforming to

$C_R = 0.005 + (1/p) (0.01 + 0.0095 [V/100]^2)$, with p in bar and V in kilometers per hour.

Henry (2015) conducts his own on-bike and drum measurements (one of which is shown in figure 6.3, along with several from Datza 2015) and compares them to one another and to predictions from a formula by Goro Tamai that has the form of a zero-speed constant for the coefficient of rolling resistance (e.g., 0.0025) plus a linear increase of about 0.00015 m/s in speed (yielding, for example, 0.004 at 10 m/s = 36 km/h). At 3 m/s = 10.8 km/h, all of Henry's measurements and the formula as well yield values for C_R of about 0.003, and at 10 m/s, the measurements (on a concrete velodrome) give 0.0045 and the drum 0.0043. Above this speed, the drum values continue to rise, but a bit more slowly, and the velodrome measurements level off and then drop. Henry uses a fully faired recumbent bicycle (figure 3.5) with an assumed constant aerodynamic drag area $C_D A$ of 0.135 m². Henry (2015) (incorporating Tamai's formula) and Kyle and Edelman (1974) propose C_R -versus-speed relationships that have remarkably similar slopes, even though the researchers are comparing dissimilar tires (tubulars and smaller, wider tires) and methods (drum, rollout, velodrome).

Summary The theory and correlations discussed in the foregoing show that there is more to the rolling-resistance coefficient than the speed- and load-independent constant usually assumed. The effects of diameter, width, and tire pressure are well researched, and temperature effects are at least acknowledged. The proportions of losses from sliding friction and hysteresis seem to be unknown. A single empirical formula for the coefficient of rolling resistance as a function of *all* the described variables remains to be developed.

Increase in Speed Due to a Reduction in the Coefficient of Rolling Resistance

Using the equations and methods of chapter 4, it is not hard to analyze a specific situation to determine how a given change in rolling resistance or slope will alter speed at a fixed power level. What is more difficult is to develop simple, generally applicable conclusions.

The approach taken here is to assume a base value for the coefficient of rolling resistance of 0.004, with a system weight of 1,000 N (225 lbf) for a fully faired HPV and 932 N for a road bike with rider, and present the effect of reducing the value of C_R to 0.002. The

assumed values for the aerodynamic drag area $C_D A$ are 0.015 m^2 for the HPV and 0.5 m^2 for the rider and road bike.

Figure 6.16 presents the results of a simulation. The road bike using tires with $C_R = 0.004$, powered by a constant 235 W, reaches its maximum speed of 30.5 km/h within 500 m; with tires with $C_R = 0.002$, it reaches a speed 0.7 km/h faster at a slightly farther distance. The HPV with tires with $C_R = 0.004$, however, is still accelerating at 9 km distance and at that point has a speed of 88 km/h; equipped with $C_R = 0.002$ tires, it has a speed at the same point of 96 km/h, which is 8 km/h faster than with the other tires.

For the road bike, then, the difference in speed is minimal, although it would still help win races, but for the aerodynamic HPV, the speed difference is considerable. The simulation does not take the speed dependencies of the rolling-resistance and drag coefficients into account.

Tire Construction to Minimize Energy Loss

Tires have a variety of features that reduce energy loss in smooth-surface rolling (i.e., that decrease rolling resistance). Clark (1981)

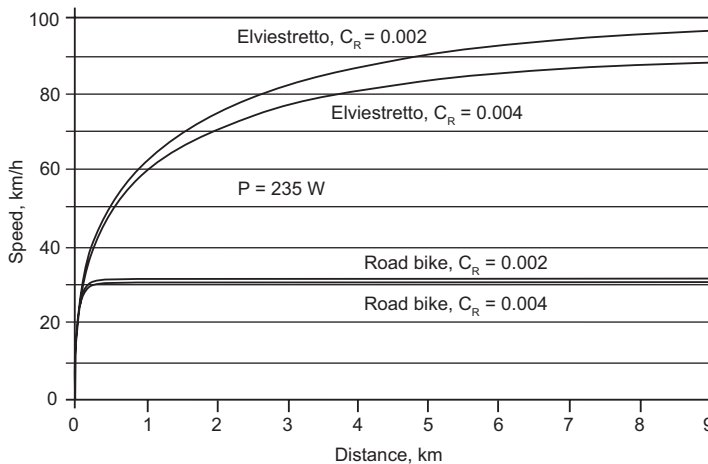


Figure 6.16

Plots of speed and distance for a simulated streamlined human-powered vehicle (Elviestretto) and road bike accelerating with a constant power of 235 W, each with two values for C_R , 0.004 and 0.002.

discusses tire construction in detail, and Schwalbe North America (2019) provides information specifically for bicycle tires.

Although a solid-steel tire generates less rolling resistance than any pneumatic tire on a smooth surface, on a normal road it would have to leap over or smash every little pebble it encountered. The great superiority of pneumatic tires when no steel rails are available is that, as noted earlier in the chapter, they simply swallow minor bumps, with almost no change in force. Therefore, small bumps apply no shocks to the rider, and suspension losses occur only when roughness is severe.

A wheel with many small steel springs around the circumference in place of a rubber tire (examples of which have been developed in the past) might also have very low loss of power over bumps, but at considerably greater complexity. A modern variation is Michelin's Tweel, which isn't available, however, in bicycle sizes.

The following salient points apply to pneumatic-tire construction only:

- The special fabric of which a tire is composed is generally not interwoven, as interweaving results in thread rubbing during tire deformation. Instead, one layer of parallel threads is placed over another layer of differently oriented parallel threads. For bicycle tires specifically, the fabric is almost universally used on the bias (diagonally), instead of having radial and circumferential threads. Positive and negative helix angles are employed, making it easy for the fabric to undergo circumferential stretching or compressing when it is formed into a torus and also when the tread is pressed close to the rim. Bias-ply construction increases lateral stability because of the greater length of rim supporting the contact patch and because of triangulation of support for the contact patch, but it also increases scuffing when loaded. Radial bicycle tires do generate particularly low levels of rolling drag. Senkel (1994) lists experimental radial tires by Paul Rinkowski with a rolling-drag coefficient as low as 0.0016. National/Panasonic offered some radial bicycle tires in the 1980s, but they were not accepted in the market—probably because of poor lateral stability—and today are made only to special order, for example, for HPV record attempts.
- Thin thread layers bend and spring back more easily than thicker ones, so the very thinnest possible threads are used, glued

together in the thinnest possible layer. Thread thickness may be characterized by “thread count” (number of threads per inch). Higher-strength fibers are ideal for bicycle tires, as long as they resist abrasion. A thin tread and inner tube are also desirable, consistent with the desired length of tire life. Inner tubes made of latex instead of butyl rubber reduce rolling resistance but are more fragile and less airtight. Tubeless tires are even better in this regard: Biermann (2014) shows a rolling-resistance reduction of 10 percent for tubeless mountain bike tires at high pressures and of up to 30 percent at low pressures, compared to those using butyl inner tubes. Using latex instead of butyl inner tubes offers a reduction of up to 20 percent. (A further advantage of tubeless tires: they need an internal gooey sealant to stay airtight at the rim contact, and this can double as a sealant when the tires are punctured by thorns or nails.)

- The strength of pneumatic bicycle tires is maximized to allow inflation to high pressure. Hard tires deform less than softer ones but still have a long enough contact region to swallow small pebbles. However, they are more susceptible than softer tires to minor changes in road level, which lead to large bump forces.
- Interior layers such as thorn deflectors are avoided in bicycle tires or constructed integrally (rather than constituting a separate, slidable layer).
- The materials from which bicycle tires are constructed, especially the rubber, are selected for good rebound (i.e., low energy loss due to deformation). Air is ideal for rebound, as its pressure hardly varies. However, low energy loss in a tire’s tread can sometimes mean poorer traction in slippery conditions.

Lateral Properties of Tires

Tires are generally considered to be somewhat flexible vertically for obstruction swallowing, but rigid otherwise. For many purposes this approximation is good enough. But in actuality, when tires are supporting a side load, they do not travel exactly in the direction they are pointed. Also, the length of tires’ contact with the surface on which they are traveling gives rise to unexpected torques: of greatest interest are those that tend to reorient the steering, namely, a

rearward shift of any side force, called *pneumatic trail*, and a resistance to twisting motions, referred to as *scrub torque*. In some circumstances, these phenomena can significantly affect vehicle handling and even add to the drag acting on the vehicle.

Pneumatic tires differ from rigid disks in that the primary load creates a longer contact patch, which obviously resists yawing (i.e., twisting around a vertical axis). But other unexpected behavior arises when a pneumatic tire is rolling forward simultaneously with a slight amount of yawing, crabbing, or leaned motion. An element of tread that is laid down at the front edge of the contact patch experiences essentially no lateral force or torque from the road or surface, but as the tire's rim moves forward, this element, which is effectively locked to the ground, ends up laterally offset and possibly twisted relative to the rim before being picked up again. Therefore, side force or twisting moment (or both) build up toward the rear of the contact patch.

The lateral properties of tires have largely been ignored in discussions of bicycle handling. For those attempting to dig into the tire literature, it is important to realize that bicycle tires are fairly similar in construction to motorcycle and aircraft tires, which are of bias-ply construction and quite different from modern car tires, which typically have radial cords and a circumferential belt.

Sideslip

To understand so-called sideslip, imagine a wheel being rolled forward while at the same time being forced by a lateral force to crab rightward 10 mm for every meter it moves forward (that is, a 1 percent rightward lateral drift). The contact patch in such a case might be 150 mm long. A bit of tread that is laid down on center at the leading edge of the contact patch will, by the time it comes to the rear of the contact patch, be 1.5 mm off center. The tire is thus increasingly deformed to the left from front to back of the contact patch. As each bit of tire is picked back up off the ground, it slides back to center, in some cases with an audible squeaking. The result is a net side force from the tire that opposes the wheel's sideslip (figure 6.17). In the case of a leaning bicycle, side force refers to a force component perpendicular to the plane of the wheel, which is not the same as a force component parallel to the surface on which the bicycle is traveling.

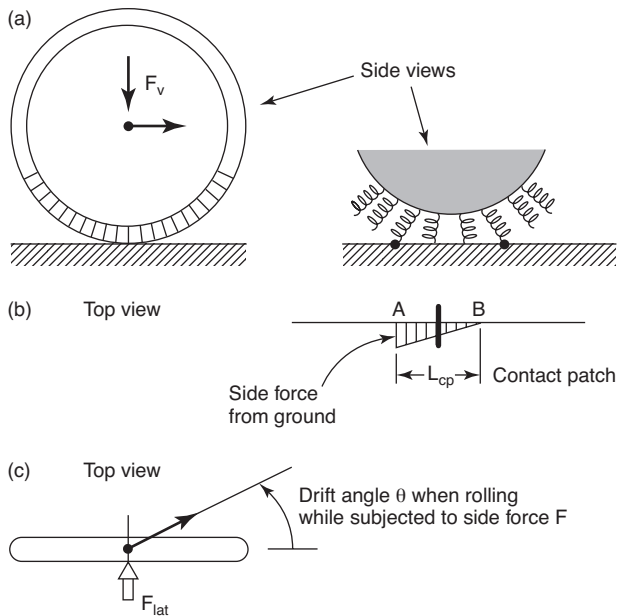


Figure 6.17

Tire cornering-stiffness model: (a) approximate pneumatic tire as a sequence of radially and laterally springy “fingers” or “spokes” (brush model); (b) a finger touches down at A, and because of the drift angle, builds up side force until picked up at B, and the sum of spring forces equals F ; (c) top view of a simpler model.

The ratio of an upright wheel’s side force to its drift slope (or angle in radians) is called its *cornering stiffness* (K_{CS}). Ordinary variations in the coefficient of friction do not affect cornering stiffness much, since most of the contact patch is not actually slipping. Rather, the primary factor is the lateral stiffness of the tire cross section, defined largely by pressure and somewhat by whether the wheel’s rim is narrow or wide; a secondary factor is the contact-patch length, determined by wheel radius, vertical load, and inflation pressure.

Since the lateral-force intensity builds up toward the rear of the contact patch, the net force should be considered to act at a point somewhat behind the lowest point of the wheel. Theoretically, this point is about one-sixth the contact-patch length behind the midpoint of the contact patch, a distance known as *pneumatic trail*, since it acts just like trail (or caster) in tending to align a steerable wheel with the direction of travel (figure 6.18). For example, when

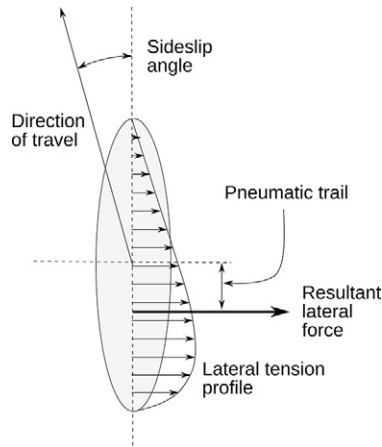


Figure 6.18

Pneumatic trail. (Visualization by Andrew Dressel.)

subjected to a sideways push *while rolling forward*, a wheel with a vertical steering axis and no fork offset (and so no trail) will still experience a steering moment tending to reorient the wheel toward the direction in which it is drifting. Any contact-force component perpendicular to the wheel plane is shifted rearward in this way.

When does tire side force occur in normal riding? The answer to this question depends partly on a given rider's maneuvering style. In a steady turn a bicycle's wheels virtually line up with the balance plane, so whereas *horizontal road forces* are large, *wheel side forces* can be small. In ordinary riding, the main origin of wheel side forces is sudden maneuvers in which the rider's body inertia resists rolling or yawing. It is best to avoid this kind of maneuver with especially lightly built bicycle wheels, which are laterally weak. In the case of tricycles and other (nonleaning) multitrack HPVs, there are of course large side forces when cornering, so stronger wheels must be used in order to avoid collapse. HPVs often use smaller wheels, which are much stronger and not at risk.

Examples of Flexible-Tire Behavior

Tire lateral flexibility has a number of surprising theoretical consequences that lead to side forces or yawing moments in response to drift angles, lean angles, or yawing rates (see Dressel and Rahman

2010 and Dressel 2013 for a great deal of information on these matters):

- A nonsteered, nonleaning multitrack vehicle on a side slope has a side force acting on each wheel and will drift down the slope. It must be pointed slightly upslope to follow a horizontal line as it drifts. However, if its rear wheels drift more than its front ones, it will tend to aim increasingly upslope and will eventually travel uphill.
- Whenever a wheel experiences sideslip, extra propulsive power is required. Given a forward velocity V , side force F , and cornering stiffness K_{CS} , the dissipated power is $V F^2 / K_{CS}$.
- The tires of a bicycle ridden vertically on a side slope experience *camber thrust*, the force acting on a leaned wheel carrying a vertical load and rolled while preventing sideways motion. In motorcycle tires, camber thrust is approximately proportional to camber angle for small angles (see Cossalter 2006, 47–48, and Foale 2006; see also Foale 1997). The exact nature of camber thrust in bicycle tires is still being debated.
- A bicycle in a steady turn approximates the previous case, because the contact force is nearly in the plane of the wheel. Therefore the bicycle's lateral drift should be minimal, an important consideration, because lateral drift absorbs power in the amount of drift velocity times lateral force.
- A bicycle ridden straight forward with the rider leaning out of the frame plane engenders purely vertical forces on the ground, which can be divided into components parallel and perpendicular to the wheel plane. The bicycle should creep in the direction of the side toward which the wheels lean. Riding with such a tilt should cause an increase in rolling drag and also a wheel scrub torque tending to steer toward the side of leaning.
- A cart with its wheels on either side tilted inward at their tops (like the letter A) acts differently. The wheels can't creep together, so they build up side force (camber thrust) until the ground force is roughly in the plane of the wheels. In a sense they are trying to move together and "squeeze" the cart. They should be toed out for minimum rolling resistance, an important finding, as it applies to racing wheelchairs.

- A vertical wheel traveling slowly in a counterclockwise turn twists its rim counterclockwise above the contact patch, that is, scrubbing occurs in the contact patch, leading to a clockwise torque (scrub torque) tending to straighten the path. Only when the wheel forms the base of an imaginary cone, lying on the ground with its vertex at the center of the turn, is there no scrub torque.
- In general, drag resulting from bicycle-wheel alignment should not become an issue, unless the wheels are substantially canted, leading to scrubbing. But for a tricycle, even vertical wheels can fight one another, especially when the tricycle's frame is deformed by load. Confirming proper alignment of tricycle wheels, however, is difficult. Tricycles cannot benefit from camber thrust when cornering and therefore should show considerable energy loss in hard turns, and even some on cambered roads.

References

- Akande, Fatai, D. Ahmad, O. B. Jamarie, Shamsuddin Sulaiman, and A. B. Fashina. 2010. "Empirical Determination of the Motion Resistance of Pneumatic Bicycle Wheels for On- and Off-Road performance." *African Journal of Agricultural Research* 5, no. 23: 3322–3332. <https://doi.org/10.5897/AJAR10.427>.
- Baldissera, Paolo, and Cristiana Delprete. 2016. "Rolling Resistance, Vertical Load and Optimal Number of Wheels in HPV Design." *Proceedings of the Institution of Mechanical Engineers, Part P: Journal of Sports Engineering and Technology* 231, no. 1 (February). <https://www.researchgate.net/publication/293015309>.
- Bekker, M. G. 1956. *Theory of Land Locomotion*. Ann Arbor: University of Michigan Press. <https://babel.hathitrust.org/cgi/pt?id=mdp.49015002826726>.
- Biermann, Jarno. 2014. "Tubeless vs Latex Tube vs Butyl Tube, Rolling Resistance Compared." Bicycle Rolling Resistance (website). <https://www.bicyclerollingresistance.com/specials/tubeless-latex-butyl-tubes>.
- Brandt, Jobst. 1998. Post to the internet newsgroup rec.bicycles.tech, March 3. Linked from <http://terrormorse.com/bike/rolres.html> and http://yarchive.net/bike/rolling_resistance.html.
- Clark, S. K., ed. 1981. *Mechanics of Pneumatic Tires*. DOT HS 805 952. Washington, DC: US Government Printing Office, for US Department of Transportation, National Highway Traffic Safety Administration. <https://www.worldcat.org/title/mechanics-of-pneumatic-tires/oclc/560250787>.

Cossalter, Vittore. 2006. *Motorcycle Dynamics*. 2d ed. Lulu.com. <https://books.google.ch/books?id=rJTQxITnkgC&pg>.

Danh, Kohi, L. Mai, J. Poland, and C. Jenkins. 1991. "Frictional Resistance in Bicycle Wheel Bearings." *Cycling Science* 3 (September and December).

Datza, Leonardi. 2015. "Reifenlatsch rein theoretisch genau berechnen" [Theoretical Calculation of Contact Patch]. Velomobil Forum (website). <https://www.velomobilforum.de/forum/index.php?threads/reifenlatsch-rein-theoretisch-genau-berechnen.42777/>.

Dressel, Andrew E. 2013. "Measuring and Modeling the Mechanical Properties of Bicycle Tires." PhD diss., University of Wisconsin-Milwaukee. <http://dc.uwm.edu/etd/386/>.

Dressel, Andrew E., and A. Rahman. 2010. "Measuring Dynamic Properties of Bicycle Tires." In *Proceedings, Bicycle and Motorcycle Dynamics 2010: Symposium on the Dynamics and Control of Single Track Vehicles, 20–22 October 2010, Delft, The Netherlands*. <http://www.bicycle.tudelft.nl/ProceedingsBMD2010/papers/dressel2010measuring.pdf>.

Dupuit, Jules. 1837. *Essai et expériences sur le tirage des voitures* [Experiments and Experiences on the Traction of Carriages]. <https://archive.org/download/essaietexprienc00dupugoog/essaietexprienc00dupugoog.pdf>.

Engineering Toolbox. 2008. "Rolling Resistance." The Engineering Toolbox (website). https://www.engineeringtoolbox.com/rolling-friction-resistance-d_1303.html.

Evans, I. 1954. "The Rolling Resistance of a Wheel with a Solid Rubber Tire." *British Journal of Applied Physics* 5: 187–188.

Foale, Tony. 1997. "Camber Thrust." Motochassis (website). <https://motochassis.com/Articles/Tyres/TYRES.htm>.

Foale, Tony. 2006. *Motorcycle Handling and Chassis Design: The Art and Science*. Tony Foale Designs.

Freudenmann, T., H. J. Unrau, and M. El-Haji. 2009. "Experimental Determination of the Effect of the Surface Curvature on Rolling Resistance Measurements." *Tire Science and Technology* 37, no. 4 (December): 254–278.

Gordon, John, James J. Kauzlarich, and John G. Thacker. 1989. "A Technical Note: Tests of Two New Polyurethane Foam Wheelchair Tires." *Journal of Rehabilitation Research and Development* 26, no. 1 (Winter): 33–46. <https://www.rehab.research.va.gov/jour/89/26/1/pdf/Gordon.pdf>.

Grappe, F., R. Candau, B. Barbier, M. D. Hoffman, A. Belli, and J.-D. Rouillon. 1999. "Influence of Tyre Pressure and Vertical Load on Coefficient of Rolling Resistance

and Simulated Cycling Performance." *Ergonomics* 42, no. 10: 1361–1371. <https://www.doi.org/10.1080/001401399185009>.

Grujicic, M., H. Marvi, G. Arakere, and I. Haque. 2010. "A Finite Element Analysis of Pneumatic-Tire/Sand Interactions during Off-Road Vehicle Travel." *Multidiscipline Modeling in Materials and Structures* 6, no. 2: 284–308. <https://www.scribd.com/document/359559935/FEM-Analysis-of-Pneumatic-tire-sand-Interactions>.

Hadland, Tony. 2012. "Small Wheels for Adult Bicycles." *Hadland's Blog*. June 25, 2012. <https://hadland.wordpress.com/2012/06/25/small-wheels-for-adult-bicycles/>.

Harris, Tedric A. 1991. *Rolling Bearing Analysis*. New York: Wiley.

Henry, Charles. 2015. "Fahrwiderstände beim Birk Comet im Vergleich zu Rollwiderstandsmessungen auf Rollenprüfstand" [Birk Comet Resistances Compared to Drum-Measured Rolling Resistance]. <http://www.velomobil.ch/ch/en/node/477>.

Johnson, K. 1996. *Contact Mechanics*. Cambridge, UK: Cambridge University Press.

Joukowsky Institute for Archaeology. 2010. "Building an Egyptian Chariot." *Fighting Pharaohs: Ancient Egyptian Warfare* (online course). https://www.brown.edu/Departments/Joukowsky_Institute/courses/fightingpharaohs10/9985.html.

Kauzlarich, James, and John Thacker. 1985. "Wheelchair Tire Rolling Resistance and Fatigue." *Journal of Rehabilitation Research and Development* 22, no. 3: 25–41.

Koffman, J. L. 1964. "Tractive Resistance of Rolling Stock." *Railway Gazette* (November): 889–902.

Kumar, Prashant, D. K. Sarkar, and Sharad Chandra Gupta. 1988. "Rolling Resistance of Elastic Wheels on Flat Surfaces." *Wear* 126, no. 2 (September 1): 117–129. [https://doi.org/10.1016/0043-1648\(88\)90133-0](https://doi.org/10.1016/0043-1648(88)90133-0).

Kunz, Johannes, and Mario Studer. 2006. "Component Design: Determining the Modulus of Elasticity in Compression via the Shore A Hardness." *Kunststoffe International* 2006/06. <https://www.kunststoffe.de/en/journal/archive/article/component-design-determining-the-modulus-of-elasticity-in-compression-via-the-shore-a-hardness-588533.html>.

Kyle, Chester R., and W. E. Edelman. 1974. "Man Powered Vehicle Design Criteria." Paper presented at the Third International Conference on Vehicle System Dynamics, Blacksburg, VA.

Larson, Kent. 2016. "Can You Estimate Modulus from Durometer Hardness for Silicones?" Dow Corning. http://web.archive.org/web/20170713183219/http://www.dowcorning.com/content/publishedlit/11-3716-01_durometer-hardness-for-silicones.pdf.

Lippert, Dave, and Jeff Spektor. 2013. "Rolling Resistance and Industrial Wheels." Hamilton White Paper No. 11, Hamilton, Hamilton, OH. <http://www.hamiltoncaster.com/Portals/0/blog/White%20Paper%20Rolling%20Resistance.pdf>.

McConica, Chuck. 1985. "Rolling Drag: Three Is Less Than Two?" *Human Power* 5, no. 1: 12–13.

Mesys. 2019. "Contact Stress: Calculation of Contact Stress" (Universal Hertzian online calculator). Mesys AG, Zurich. https://www.mesys.ag/?page_id=1220.

MontyPythagoras. 2014. "Rollwiderstand von Fahrradreifen" [Rolling Resistance of Bicycle Tires]. *Mathroids Matheplanet* [Mathroid's Maths Planet], May 29. <https://matheplanet.com/matheplanet/nuke/html/print.php?sid=1620>.

Ogorkiewicz, R. M. 1959. "Rolling Resistance." *Automobile Engineer* 49: 177–179.

Reynolds, Osborne. 1876. "Rolling Friction." *Philosophical Transactions* 166: 155–156. <http://www.pdftitles.com/download/4936>.

Sandberg, Ulf, ed. 2011. *Rolling Resistance—Basic Information and State-of-the-Art on Measurement Methods*. Report MIRIAM SP1. MIRIAM (Models for Rolling Resistance in Road Infrastructure Asset Management Systems). http://miriam-co2.net/Publications/MIRIAM_SoA_Report_Final_110601.pdf.

Schermer, Wim. 2013. "Bandentesten deel 1" [Tire Testing Part 1]. <https://www.ligfiets.net/news/4584/bandentesten-deel-1.html>.

Schuring, D. J. 1977. "The Energy Loss of Tires on Twin Rolls, Drum, and Flat Roadway: A Uniform Approach." SAE Technical Paper 770875, Society of Automotive Engineers, Warrendale, PA. <https://doi.org/10.4271/770875>.

Senkel, Thomas. 1992. "Plädoyer für einen guten Reifen" [A Plea for a Good Tire]. *Pro Velo* 32. http://www.forschungsbuero.de/PV32_S15_19.pdf.

Senkel, Thomas. 1994. "Federungseigenschaften von Fahrradreifen" [Springing Characteristics of Bicycle Tires]. *Pro Velo* 38. http://www.forschungsbuero.de/PV38_S6_8.pdf.

Sharp, Archibald. 1896. *Bicycles and Tricycles*. London: Longmans, Green. Reprint, Cambridge, MA: MIT Press, 1977.

Schwalbe North America. 2019. "Rolling Resistance: Why Do Wide Tires Roll Better Than Narrow Ones?" Schwalbe North America, Ferndale, WA. https://www.schwalbetires.com/tech_info/rolling_resistance.

SKF Group. 2018a. "Bearing Friction, Power Loss and Starting Torque." SKF Group, Gothenburg, Sweden. <http://www.skf.com/group/products/bearings-units-housings/principles/bearing-selection-process/operating-temperature-and-speed/friction-powerloss-startingtorque/index.html>.

SKF Group. 2018b. "SKF Bearing Select—New." SKF Group, Gothenburg, Sweden. <http://www.skf.com/group/knowledge-centre/engineering-tools/skfbearingcalculator.html>.

Tetz, John. 2005. "Crr vs Temperature." Metro Area Recumbent Society. Recumbents.com. <http://www.recumbents.com/mars/pages/proj/tetz/other/Crr.html>.

Trautwine, John C., and John C. Trautwine, Jr. 1937. *The Civil Engineer's Reference Book*. 21st ed., ed. John C. Trautwine 3rd. Philadelphia: National. <https://babel.hathitrust.org/cgi/pt?id=coo.31924004585646&view=1up&seq=6>.

Unrau, Hans-Joachim. 2013. *Der Einfluss der Fahrbahnoberflächenkrümmung* [The Influence of the Road Curvature]. Karlsruhe: KIT Scientific Publishing. <https://books.google.de/books?id=KSS9Ls-rv2IC>.

Vander Wiel, Jonathan, Boice Harris, Carl Jackson, and Norman Reese. 2016. "Exploring the Relationship of Rolling Resistance and Misalignment Angle in Wheelchair Rear Wheels." Paper presented at RESNA (Rehabilitation Engineering and Assistive Technology Society of North America)/NCART (National Coalition for Assistive and Rehab Technology) 2016, Arlington, VA, July 12–14. http://www.resna.org/sites/default/files/conference/2016/wheelchair_seating/wiel.html.

Whitt, Frank R. 1977. "Tyre and Road Contact." *Cycle Touring* (February–March): 61.

Wright, Chris. 2019. "Chapter 2020: The Contact Patch." The Contact Patch (website). <http://the-contact-patch.com/book/road/c2020-the-contact-patch>.

7 Braking

Introduction

The task of braking bicycles can be broken down into several aspects: providing sufficient braking force in all conditions, transmitting this force to the road or other surface without losing control, and removing the braking energy. These aspects are briefly introduced here and then discussed further in later sections. Other considerations are safe and ergonomic operation, weight, and cost.

Frictional Braking Force

Two places where solid-surface friction occurs must be considered in normal bicycle braking: the brake surfaces and the wheel-to-road contact. Experiments have shown that when two surfaces are pressed together with a normal force F_N , there is a limiting (maximum) value F_F of the frictional resistance to motion. This limiting value is a definite fraction of F_N , and the ratio F_F/F_N is called the *coefficient of friction* μ . Therefore, $F_F = \mu F_N$. For dry, rigid surfaces, neither the area of the surfaces in contact nor the magnitude of F_N affects the value of μ much, provided that the surfaces can actually slide past each other and are not blocked by edges or other macroscopic features.

When the surfaces don't move in relation to one another, the accompanying friction is called *static* friction. If one surface moves relative to the other, such as rotating brake surfaces with respect to friction pads, the coefficient of friction is then designated *kinetic*, falls in value, and is somewhat dependent on the speed of the relative movement. The friction coefficients of various metal-to-metal contacts are 0.5–1.0 when the surfaces are static and 0.25–0.5 when

they are sliding. When the contacts are lubricated, the friction coefficients reduce to 0.1–0.2 when the surfaces are static and again often half this when they are sliding. Leather-to-metal contacts have friction coefficients of 0.3–0.5, also decreasing with movement. Brake-lining materials against cast iron or steel have a static friction coefficient of about 0.7, and this value decreases less with movement than it does for other materials. Elastomers deform under load, which causes their friction to be highly variable. Some “sticky” materials have coefficients well above unity but cannot be used for brakes or tires.

For typical tires on asphalt, the static friction coefficient is about 0.6 (dry) or 0.4 (wet). There is initially no true kinetic coefficient, as the material can creep along a surface, reaching a frictional maximum at a relative movement of 1–10 mm/s (for asphalt) (see Persson et al. 2005 regarding this and also for the following rubber-asphalt values derived theoretically and also measured). Rubber tires that roll must therefore *slip* to provide braking force, the force being at first proportional to this slipping. Typically, on asphalt or concrete roads, up to $\mu = 0.5$, the slip is 5 percent of μ , whether the roads are wet or dry. For more slippery surfaces like cobblestones, it is more like 10 percent of μ . Only with respect to dry surfaces can μ values increase further, up to 1.0 or so, and here the slip approximately doubles. If the braking force increases further, so does the slip, but now μ decreases, with increasing relative velocity, to typically 0.5 (dry) or 0.4 (wet) above 10 m/s. However, all these values depend not only on the type of rubber and the roughness of the road, but also on the temperature. Friction *is highest within an optimal temperature range and decreases with both warmer and colder temperatures.*

The maximum braking force therefore occurs at slips of 10 percent or less. This makes little difference to the braking process and may even improve it, as some of the braking heat is dissipated by the tires instead of the braking surfaces. In the case of propulsion, this slipping loss of course decreases propulsive efficiency, but as normal propulsion in cycling occurs mostly at low values of μ , this loss is small and therefore is not included in the calculations in chapter 4.

As rules of thumb, dry tires on good roads are often assumed to have friction coefficients of 0.5–1 with 5–10 percent slipping and

three-quarters of this when wet. Tires on snow have friction coefficients of at most 0.2 and on ice 0.05–0.1 (without spikes).

Wet weather also reduces the friction of exposed brake surfaces, sometimes dramatically (more on this in the section “Wet-Weather Braking” later in the chapter). The variability of friction with contact area and relative motion, coupled with the flexibility of brake mechanisms, often leads to a stick-slip sequence that, occurring repeatedly and rapidly, gives rise to brake squeal.

The adequacy of a vehicle’s braking surface is, of course, only one factor in determining the distance required to stop the vehicle. It is necessary in addition to be able to apply an adequate force to the brake system. Bicycle brakes are often deficient in this respect, especially with thin (flexible) or rusty (high-friction) wire cables.

Control

Many motor vehicles and some low HPVs can be stopped by slamming on the brakes, completely blocking the wheels. On a clear, straight road, when the brakes are blocked, such vehicles will slide in the direction they were going until standstill. But as described in the preceding section, the coefficient of friction is then reduced, control is lost, and bicycle tires are quickly ruined. Advanced control systems or skilled manual braking can minimize the stopping distance and allow braking and steering at the same time. Most bicycles, on the other hand, have a high center of mass, so that only slower decelerations are possible than the tire-road friction would otherwise allow. Also, most cyclists hesitate to brake as strongly as possible for fear of losing control or pitching forward over the handlebars. Two-wheelers need at least one steerable wheel to stay upright for any length of time and, lacking antiblocking or antiskid systems, eventually crash when steering is lost.

Therefore, where deceleration is regulated at all, smaller deceleration values are legally required for bicycles (e.g., in Switzerland 2 m/s² [each wheel alone] and 3 m/s² [both wheels]) than for fast motor vehicles (5–6 m/s²), but the following also apply:

- The consequences of a bicycle crash are often worse for the cyclist (internal safety), but less severe for others (external safety), than those from the crash of a motor vehicle, where it is often the other way around.

- Bicycle speeds are often quite low, and in these cases adequate physical stopping distances are possible even with poor brakes, most of the total stopping distance then being due to the human reaction time.
- Most cyclists are aware of their instability, their vulnerability, and other traffic. They are, in addition, loath to lose useful kinetic energy. The inherent aerodynamic braking is also rather large. For all these reasons cyclists in normal riding tend to use the brakes sparingly and lightly and compensate for known deficiencies in their braking systems.

Braking control problems therefore mainly have to do with unexpected situations such as emergency stops. In addition, many bicycle brakes, through poor design or lack of maintenance, tend to fail exactly when they are needed most, such as when a brake-cable connection breaks when the brake lever is pulled really hard.

A second general problem area is the unsuitability of many bicycle brakes for prolonged heavy use on long and steep hills. What is the best braking strategy?

Cooling

The task of braking, that is, reducing speed, requires the removal of kinetic energy ($E_K = \frac{1}{2} m V^2$) from the moving bicycle and rider and either converting this to something useful (e.g., energy storage for later propulsion) or, more often, releasing it as heat into the environment. In the second case this means into the surrounding air, or the heat can also be radiated away. Fluid (or heat-pipe)-cooled radiators like those in motor vehicles (or computers) have, as far as can be determined, so far not been used for bicycles, as they add complexity and weight. And weight is crucial in regard to bicycles: this is the reason that the removal of the energies involved, though rather small compared to those that build up in motor vehicles, is not such a trivial task as might first be thought.

Bicycle Brakes

At least five types of brakes have been fitted to regular bicycles for ordinary road use. (Track bicycles are braked by resisting the motion of the pedals, the rear cog being fixed to the wheel hub without a

freewheel, and brakes that act directly on the ground are ignored here.)

The *plunger brake* was formerly used on some children's bicycles and tricycles and was the main form of brake on early bicycles such as the ordinary or high-wheeler and on pneumatic-tired safeties up to about 1900. On a bicycle equipped with such a brake, pulling a lever on the handlebars presses a metal shoe (sometimes rubber-faced) against the outer surface of the tire. Plunger brakes were and are used on solid and pneumatic tires; their performance is affected by the amount of grit the tire takes up from the surface on which it is riding, which fortunately increases braking effectiveness and wears the metal shoe rather than the tire. A modern form is the simple metal shoe pressed by foot onto the solid polyurethane rear wheel of microscooters. Such brakes perform very poorly in wet weather because in those conditions, the tire is being continuously wetted and thus the pressure of the shoe against its surface exerts less stopping force than when the tire is dry (see "Wet-Weather Braking" for the effects of water on braking).

The internal expanding *drum brake* is a hub brake similar to former automotive ones. Drum brakes used to be popular on medium-weight roadsters in the 1930s, but they lost favor mostly because they weighed a great deal compared to rim brakes. They were reintroduced a number of years ago in a lighter form by Sturmey-Archer (figure 7.1). Drum brakes are popular on the rear wheels of tandems and on various other human-powered vehicles to eliminate the rim and tire heating that rim brakes produce.

The *backpedaling* or *coaster brake* brings multiple disks or cones together when rotation of the cranks is reversed by backpedaling (figure 7.2). These brakes operate in oil and are entirely unaffected by weather conditions. They are very effective on a bicycle's rear wheel; they cannot be fitted to the front wheel because the actuating force required is too great to be applied by hand. (However, see the Calderazzo patent described later in the chapter [figure 7.10] for a possible way of using coaster brakes on a bicycle's front wheel.) They cannot be used with derailleur gears, and if the bicycle's chain breaks or comes off the sprockets, this braking is lost. Coaster brakes are compact, without much thermal mass or surface area for radiating heat, so they quickly reach high temperatures in prolonged or heavy use. These temperatures can become high enough to change

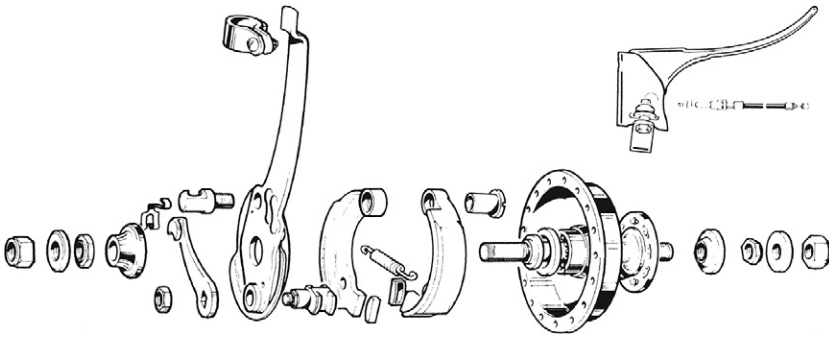


Figure 7.1

Magnified view of Sturmev-Archer internal expanding drum brake, also available for wheelchairs. The body, formerly made of steel, is today constructed of an aluminum alloy, with a thin steel liner where the friction pads make contact. (Courtesy of Sturmev-Archer Ltd.)

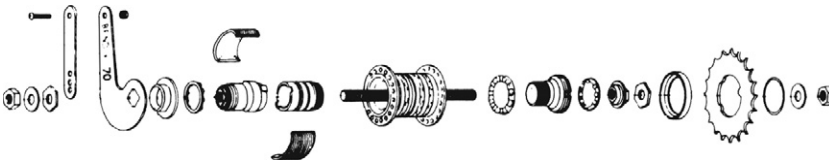


Figure 7.2

Magnified view of Bendix backpedaling coaster brake. (Courtesy of Bendix Corp.)

the properties of the steel used, reducing effectiveness or ruining the hub. They are therefore unsuitable for prolonged mountain use unless additionally cooled, which in an emergency can be done using a water spray. The coauthor was able to safely and slowly brake his way down a steep 1,000 m descent using only a coaster brake and a total of about 1 kg of water applied in small amounts during frequent stops. The heat of vaporization of water is 2.26 MJ/kg, and the total potential energy of the undertaking was about 1 MJ.

The *disk brake*, having become the preferred form of brake in motorcycles, automobiles, race cars, and aircraft, is becoming accepted as the most effective system for most types of bicycles, when they can be fitted with them and such a system can be afforded. Figure 7.3 shows the required components: a disk segment



Figure 7.3

Magura hydraulic disk-brake system, including an integrated reservoir. (Photo in public domain.)

connected to a wheel hub, a caliper fitted with friction pads (also called *disk pads* or *brake pads*) normally not touching the disk, and a method of forcing the pads to grip the disk when braking. Good-quality disk brakes of sufficient size more or less solve many of the problems associated with other types of brakes for bicycles. This type of brake can be operated either by cable or hydraulically from normal hand levers. The effective braking diameter is normally less than half the wheel diameter, which requires a higher braking force than for rim brakes but keeps the braking surfaces away from the wheel spray in wet weather, so disk brakes normally have good wet-weather performance. Those found in cars are generally made of cast iron, and those on bikes are usually of steel. They often have holes, mainly to reduce weight, and this may also improve cooling.

Hydraulic disk brakes for vehicles are generally of the *open* type. This means that they have a reservoir for brake fluid, which automatically replenishes any lost through leakage and compensates

for temperature changes. Most hydraulic bicycle brakes are of this type, but *closed* systems are also available (and for rim brakes [discussed later in the section] as well); there is then no special brake-fluid reservoir, and the system is often supplied prefilled. Provided there is no leakage, hydraulic systems are maintenance free except for occasional replacement of the disk pads. Because the precisely machined and mounted disks normally run true with little clearance necessary and the calipers are compact and stiff, relatively little friction pad travel is required, so that a high degree of force amplification between the hand lever and the friction pads is possible. Oertel, Neuberger, and Sabo (2010) measure an amplification of 40–50 times from the brake lever to the friction pad, so that the disk is pressed together with up to 5 kN using a hand force of 100 N. For a disk with an effective radius at the location of the friction pads of one-fourth of the wheel diameter and with a friction coefficient of 0.5 assumed, a disk brake provides an actual retarding force (F_R) of 625 N, minus the losses, which are very small for static hydraulic systems. As acceleration $a = F/m$, for a 100 kg bicycle and rider, the braking deceleration is 6.25 m/s^2 or about 0.64 g. Oertel, Neuberger, and Sabo perform their measurements both on a test rig using an actuator and on a bicycle with riders using one or two fingers to pull the brake lever.

The *rim brake* is the most popular type of bicycle brake around the world. With such a brake, a pad or block, usually of rubber-composition material, is forced against the inner or the side surfaces of a bicycle's wheel rims, front and rear, usually by a cable acting on calipers directly or through a roller-cam mechanism (see figure 7.4). Because the braking force is applied at a large radius to the existing rim, and because the braking torque does not have to be transmitted through the hub and spokes, the brake parts are intrinsically very light. Rim brakes are, however, very sensitive to water. The coefficient of friction with regular combinations of brake pads and steel wheel rims has been found to decrease, when the brakes are wet, to below a tenth of the dry value. Rim brakes require continual adjustment (provided automatically in a very few designs) and relatively frequent pad replacement.

Bicycle manufacturers in many countries have solved the wet-weather-braking problem of rim brakes by switching from steel to aluminum wheel rims, the friction coefficient of which does not



Figure 7.4

Rim brake in a roller-cam configuration. In principle, any type of leverage could be made available through the choice of cam geometry. (Adaptation of photo by Jeff Archer, licensed CC-BY-SA 3.0.)

fall nearly as much when the rims are wet as does that for steel. However, the aluminum alloys used in such rims are much softer and wear much faster than does steel. Particles of grit can become embedded in brake pads, thereby scoring the rim surface with potentially deep grooves, or the rims can just become generally thinner because of overall wear. The high pressures used in modern tires can then cause the rims to explode outward, with a high likelihood of locking the wheel (Juden 1997). (This has happened, with relatively low-pressure tires, four times to the senior author and three times to a friend of the coauthor.) This is a very serious event if it occurs at the front wheel. Some aluminum-alloy rims can be supplied with a flame-sprayed ceramic coating that greatly reduces the rate at which they wear. Users of small-wheeled bicycles in hilly regions especially learn to replace their rims in time or to have it done by mechanics able to measure the remaining rim thickness. (This is rarely possible

by eye or with standard vernier calipers, although placing a straight-edge against the side of the rim will show the amount of wear.)

Because of the proximity of a bicycle's tire and inner tube, bicycle wheel rims should not be allowed to get as hot as would be necessary for prolonged hard braking of heavy bicycles. This topic is examined in detail later in the chapter.

Major design and maintenance problems with rim brakes have to do with the possibility of wheels becoming untrue or shoddy ones being bent or wobbly even when new. The brake pads will jam, snatch, or at least touch when this happens or must be adjusted to have enough clearance. This in turn requires so much travel of the pads on the calipers that little mechanical advantage is available from the hand lever, limiting the braking force. Ways of solving this are discussed later in the chapter, but otherwise, great braking forces require precise calipers paired with well-maintained wheels.

On the positive side, no braking system is more universally serviceable than one employing rim brakes. Spare parts are widely available or can be improvised.

Electric brakes are available only with some types of e-bicycles, those having a direct-drive motor, usually in the hub (in addition to the bicycle's mechanical brakes). Modern hub motors are usually brushless and gearless, so the permanent mechanical connection to a wheel incurs little friction. With other types of electric motors this isn't the case, and they mostly operate through a freewheel, so they are not available for braking. Electric bicycle brakes often offer *regenerative braking*, whereby the bicycle's battery is charged using the motor as a generator. Direct charging of the battery occurs at speeds high enough for generator voltage to exceed battery voltage, but the electronic controllers needed for operating most hub motors can step the voltage up and provide regenerative braking almost down to standstill. Usually there is a choice of several braking levels that can be manually set for downslopes, and additionally a medium level is automatically activated whenever a lever of one of the bicycle's mechanical brakes is pulled. With careful use and slow descents, an e-bicycle's regenerative brake can significantly extend the bicycle's range per battery charge, but in normal use regenerative braking doesn't have a very large effect, say about 10 percent more range on routes with slopes and stops. Their greater importance comes from decreasing the use of the bicycle's

mechanical brakes, which saves on maintenance costs and increases safety.

Unfortunately regenerative braking is least useful exactly to those people who could potentially benefit most: those living at higher elevations and commuting down into areas of lower elevation. The reason is that one often charges an e-bicycle battery overnight, so that it is fully charged in the morning. When a cyclist starts downhill, the battery can take almost no additional charge, and either it will sustain damage, or more likely, the motor's controller will refuse to brake with any useful power. The use of *resistive braking*, whereby the electric power created through braking is dissipated in an air-cooled resistor or semiconductor, can in theory resolve this problem. In principle resistive braking is a simple form of electric braking for ordinary direct-current motors, as all that is required is a rheostat (variable resistance) or several resistors. Simple does not mean cheap, however, as in a form that would work on an e-bicycle, these items would have to be fairly large and cooled by fans. We know of no e-bicycles sold with resistive braking or equipped to implement the ideal solution of both charging the battery and automatically diverting excess electricity to a cooled resistor.

Magnetic (eddy-current) or *aerodynamic* (fan) brakes are fitted to many stationary exercise bikes, but not to bicycles for road use. *Hydrodynamic* brakes, which heat a fluid, are a theoretical possibility, but we know of no experiments in the direction of equipping bicycles with such brakes, not even water-cooled friction brakes. Larger drag devices such as propellers or parachutes would be highly effective for bicycle braking but impractical except for specialist or emergency use. Small parachutes have been fitted to bicycles and even deployed by adventurous mountain bikers. Drag parachutes of about 1.5 m² area, designed for training runners, are available very cheaply.

Effective friction brakes have been developed for bicycles, but not the various dynamic brakes described, for a number of reasons:

- Regulations in place in many countries require bicycles to be equipped with at least one, and usually two, reliable brakes with specified deceleration, right down to zero speed, or specified stopping distances. This requirement is relatively easy to meet with conventional friction brakes, but dynamic brakes become less powerful the lower the speed is.

- Once the legal requirement is fulfilled, there is little incentive to fit additional braking systems to a bicycle unless the additional costs are small, as with the described regenerative braking for hub motors.
- Conventional (unfaired) bicycles don't usually require constant heavy braking on descents because of the rider's high aerodynamic drag. Low-drag velomobiles, which would benefit greatly from electric brakes of the sort described in the foregoing, are sold only in relatively small numbers, so the market for bicycle versions of such brakes is limited.

Power and Energy Absorption of Brake Surfaces

Brakes can be designed to allow a certain *constant power* to be dissipated. Such a scheme is useful for calculating the effects of constant downhill braking (long enough for the parts to reach a stable temperature). The limiting factor here is the permissible temperature of the bicycle rim, hub or disk, and friction pads, which must be kept at a low enough level to avoid damaging associated materials in close contact. Determining this temperature requires a rather complicated calculation, as both the convective and the radiative cooling of these parts must be determined, as well as conduction between them. Bicycle rims, for example, should not get any hotter than the tire mounted on them or its inner tube will stand and are cooled predominantly by convection, which depends on the ambient temperature and airspeed. A calculation model is discussed in "Rim Temperatures Reached during Downhill Braking" later in the chapter. Disks or hubs, however, can become as hot as the brake pad material and the associated parts, including any seals and brake fluid, can tolerate. At these elevated temperatures much of the cooling is through radiation, which depends on the emissivity of the part's surface at the range of (infrared) wavelengths corresponding to the temperature. The principle is the same as the cooling of the human body given in chapter 2, but with quite different numbers. Because, according to the Stefan-Boltzmann law, the power radiated away from a surface is proportional to the fourth power of the (absolute) temperature, increasing the braking power by a large amount will increase the disk temperature only by a smaller amount. For example, a brake disk with a total surface area of 0.02 m^2 would

need to reach a temperature of about 280°C to radiate away 50 W, assuming an emissivity of 0.5; for 100 W it would be about 380°C. In practice the amount of power radiated away is less, as the disk and other brake parts are also cooled by convection. Disks with holes in them may have less total surface area but also more edges and may cool better. The amount of power that actually needs to be continuously dissipated by the brake in order to maintain a desired speed is examined later in the chapter.

Another way to characterize a brake is by the *energy* that its thermal mass can absorb in a single strong braking action. If the heat capacity and the thermally relevant mass of the brake—for example, a bicycle rim or brake disk—are known, a brake's temperature rise resulting from such a braking action is easily calculated, assuming no heat is dissipated during this short period of time. As an example, it is possible to determine, for an 85 kg bicycle and rider, the energy absorbed at the brake pads for braking from 9 m/s (~20 mph) to a full stop and the temperature rise in the associated metallic parts. The kinetic energy E_k to be absorbed by the brake parts, assuming no other sources of drag and no slope, is $\frac{1}{2}mv^2$, which for this example yields a value of ~3,443 J.

If a single rim brake is acting on the front wheel with a 500 g aluminum rim, the temperature rise can be calculated as E_k divided by the heat capacity 920 J/(kg K) and mass, yielding 7.5 K or 7.5°C for this example. This temperature increase isn't large, but through repeated braking, the total can add up to something substantial. Many riders in mountainous country have learned, to their dismay, that the thermal mass of and the heat transfer from a wheel rim are small. Rim brakes can cause the rim's temperature to rise quickly to the point at which the rubber cement holding tire patches, or even the tire itself, softens, and the tires deflate or (in the case of stick-on tubular tires) come off the rim. When these failures occur on the front wheel, as they are likely to, they can cause serious accidents. If the same calculation as previously is performed for the 75 g active part of a steel disk (heat capacity 470 J/[kg K]), the temperature increase is found to be roughly 100 K.

Minimum Braking Distances for Stable Vehicles

If it is assumed that air resistance and rolling resistance have negligible slowing effects in braking, a relatively simple formula can be

used to estimate the approximate minimum braking distance S of a vehicle fitted with adequate braking capacity and having a center of gravity sufficiently low or rearward in relation to the wheelbase for there to be no danger of the rear wheel(s) lifting during braking: $S = \frac{1}{2} V^2/a$ (if the deceleration a is known) or $S = \frac{1}{2} V t$ (if the braking time t is known). Because a is the gravitational acceleration g times the achievable coefficient of friction μ , the first of the two equations can also be written as $S = \frac{1}{2} V^2/(\mu g)$, or roughly in SI units: $S = 0.05 V^2/\mu$. Thus a rule of thumb for bicycle braking distance could be $S = V^2/10$, for S in meters and V in meters per second. A more exact formula would be $S = \frac{1}{2} V^2/(g [\mu + s + C_R])$, in which s is the slope expressed as a fraction, which is taken to be negative in the case of a downslope. However, if the slope is large, $(\mu + s)$ should be replaced with $(\mu \cos(\theta) + \sin(\theta))$, in which θ is the slope as an angle (see the discussion earlier in this chapter for values of μ and chapter 6 for values of C_R). The latter is relatively unimportant here, being much smaller than μ ; s is always important, as a total brake failure even on a small downslope will often result in a crash.

Note that a vehicle's braking distance is not the same thing as its stopping distance, as the latter includes the distance traveled during the human reaction time (about 1–3 s).

Longitudinal Stability during Braking

The weight of a bicycle and its rider does not divide itself equally between the bicycle's two wheels. On a road bicycle, about 40 percent of this weight is typically distributed (on level ground, when the bicycle is either at rest or is moving at constant velocity) to the front and 60 percent to the rear. This distribution can change dramatically, particularly during strong acceleration (for example, doing a wheelie) and braking (possibly leading to "taking a header").

As an example, here the changes in wheel reactions are estimated when a typical bicycle and rider with total mass 89 kg brakes at half the acceleration of gravity. If the bicycle has a wheelbase of 1,067 mm (42 inches) and the center of gravity of rider and machine is 432 mm (17 inches) in front of the rear-wheel center and 1,143 mm (45 inches) above the ground (figure 7.5), the front-wheel reaction $F_{V,f}$ when the bicycle is stationary or when the rider is riding at

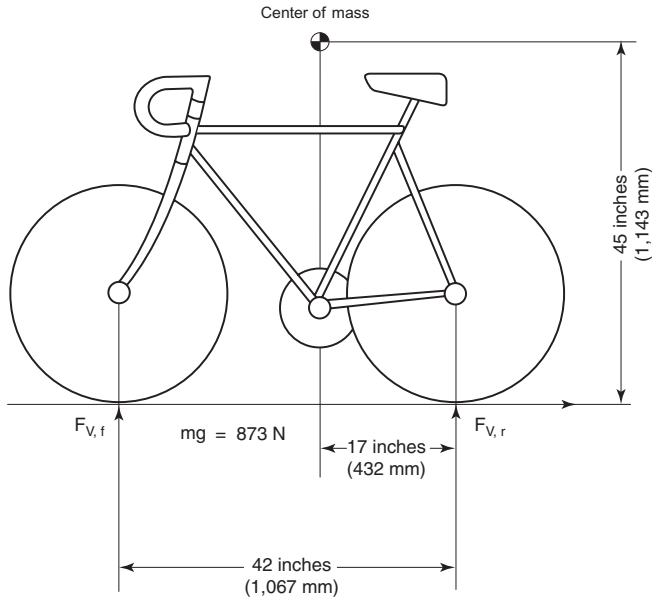


Figure 7.5

Configuration specified for braking calculations in the text.

constant speed can be calculated. The total weight is $89 \text{ kg} \times 9.81 \text{ m/s}^2 = 873 \text{ N}$; $17/42$ of this, $\sim 353.5 \text{ N}$, acts on the front wheel, and $42/17 \times 873 \text{ N} \approx 519.5 \text{ N}$ on the rear wheel.

During 0.5 g braking, a total braking force of $89 \text{ kg} \times 0.5 \times 9.81 \text{ m/s}^2 = 436.5 \text{ N}$ acts forward at the center of mass and backward at the tire contact patches, producing a forward pitching moment of $436.5 \text{ N} \times 1.143 \text{ m} = 499 \text{ Nm}$. If this moment is taken around the contact patches, it produces a force there of $\Delta Fv = 499 \text{ Nm}/1.067 \text{ m} \approx 467.5 \text{ N}$, which is added to $F_{v,f}$, giving 821 N vertical force at the front wheel, and subtracted from the rear-wheel reaction $F_{v,r}$, 52 N at the rear wheel. Thus, in braking at 0.5 g , the bicycle's rear wheel is in only light contact with the ground, so only a slight pressure on the rear brake will cause the rear wheel to lock and skid. The front brake therefore has to provide well over 90 percent of the total retarding force.

Another conclusion for the configuration specified here is that a deceleration of 0.5 g ($\sim 4.9 \text{ m/s}^2$) is almost the maximum that a crouched rider on level ground can risk before going over the

handlebars. Riders of tandems and low recumbent bicycles and drivers of cars do not have this limitation on deceleration: if their brakes are adequate, they can theoretically brake to the limit of tire-to-road adhesion. If the vehicle's tire-to-road coefficient of friction is 0.8, for example, they are theoretically, with optimal braking, capable of a deceleration of 0.8 g, which is about 40 percent greater than that of a bicyclist with the best possible brakes. For this reason (and many others) bicyclists should never tailgate motor vehicles.

If, in the foregoing upright bicycle example, only the rear brake is used, with a coefficient of friction μ of 0.8, a retardation of only 0.26 g is achievable, which translates into more than twice the stopping distance required with the front brake (at $\mu = 0.5$).

Skilled mountain-bike riders increase their deceleration capability when descending steep slopes by crouching as low and as far behind the bicycle's saddle as possible. Beck (2004) describes braking techniques for mountain biking and conducts a series of measurements on dirt and pavement. Using only the rear brake (which can be locked, giving a permanent skid that is continuously compensated for by front steering), mountain bikers can, he finds, achieve retardations of 0.24–0.32 g (on dirt). Using only the front brake, 0.26–0.46 g can be achieved, and with both brakes, 0.31–0.54 g. On pavement, he finds, the achievable retardations are only slightly higher.

Lieh (2013) has developed an analytical solution for problems like the last one presented, including air and rolling resistances and slope, and also provides a program that plots braking performance values for front, rear, and full braking. Figure 7.6 shows one such plot for an upright bicycle, similar but not equal to the one in the configuration depicted in figure 7.5, braking with a friction coefficient of 0.7 (tire to road, front and rear). Lieh's program sets the resulting braking forces automatically. It draws lines (which have a slight curvature because of air drag) separately for the rear wheel only and the front wheel only, as well as for both together. In the example shown in figure 7.6, the latter two are very close together, which shows, as in the last example discussed, that in maximum braking, the front brake is providing practically all of the braking force, and with any stronger braking (setting a larger μ), the bicycle would pitch forward. Using only the rear brake more than doubles the stopping time t (from less than 2 s to more than 4 s) as

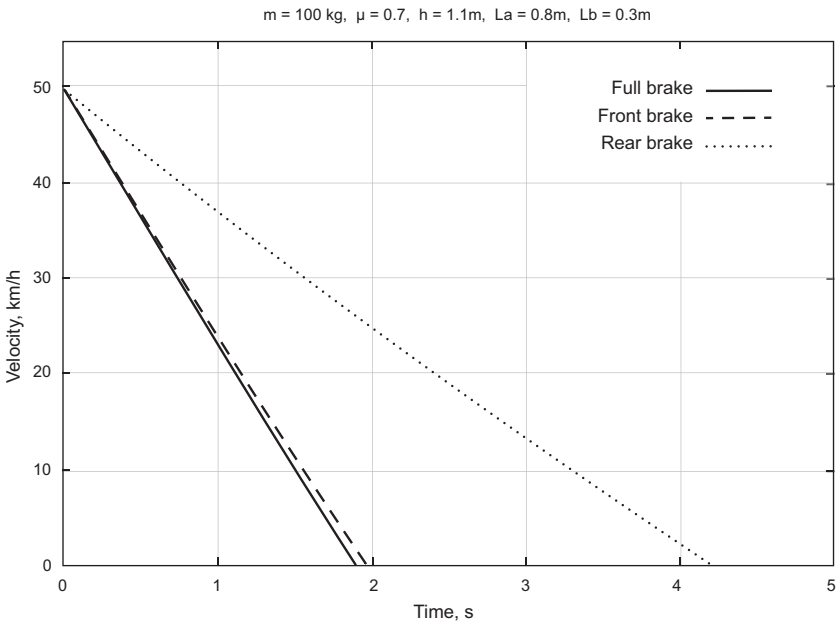


Figure 7.6

Plot from Junghsen Lieh's braking program, showing speed versus time when an upright bicycle is braked from 50 km/h with $\mu = 0.7$. L_a is the horizontal distance from the front contact patch to the center of mass, L_b the distance from the center of mass to the rear contact patch.

well as the stopping distance ($V t/2$) (from 13.2 m to 29.2 m) from $V = 50 \text{ km/h}$. Both could be reduced somewhat with a higher friction coefficient at the rear tire, but not by very much, as a μ value around 1 is a likely maximum.

For a long-wheelbase recumbent the situation is quite different. Figure 7.7 shows a plot for a Fateba braking with $\mu = 1.2$ front and rear, which is only just conceivable (and normally not achieved), and still no stability limit is reached. Braking with the *front* wheel only results in the poorest stopping time of $\sim 2.3 \text{ s}$. Braking with the rear wheel only is not much better with $\sim 2.2 \text{ s}$, and both times are worse than that for the upright bicycle with $\mu = 0.7$. But when both brakes are used together, the minimum braking time of $\sim 1.2 \text{ s}$ achievable. If a more realistic smaller μ is assumed, the minimum braking time is still better than with the upright bicycle.

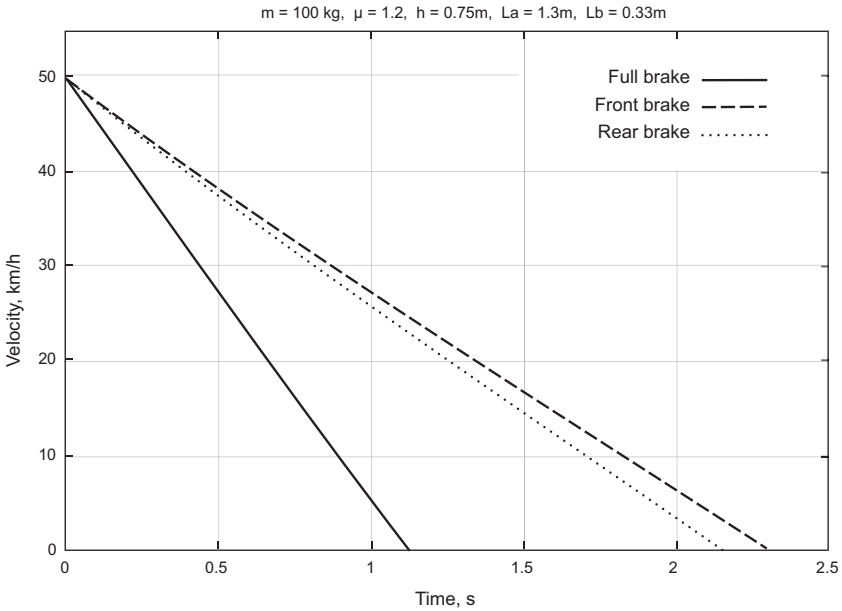


Figure 7.7

Plot from Junghsen Lieh's braking program for a Fateba long-wheelbase recumbent bicycle with $\mu = 1.2$.

In a comparison between the two bicycles, an emergency stop with a long-wheelbase recumbent is easier and quicker than the same maneuver with an upright bicycle, provided both brakes are working, because for stopping the recumbent, both hand levers can be pulled evenly. Stopping an upright bicycle quickly involves light or no rear braking and certainly releasing the rear brake the moment the rear wheel skids, and the front brake must be pulled hard and partially released when the rear wheel begins to lift. This can be done in practice, but most people either are wary of taking a header and won't use the front brake hard enough, or don't know which hand control governs the front brake, or confuse the brake levers, as the configuration is different from country to country. On the long-wheelbase recumbent, on the other hand, overbraking is likely to result in an unrecoverable skid, dumping the rider sideways, with injuries to the leg and arm, rather than the head. Short-wheelbase recumbents tend to behave more like upright bicycles, unless the rider position is extremely low.

Wet-Weather Braking

Wet conditions affect, usually adversely and often to a considerable extent, both adhesion of bicycle tires to the road on which they are riding and the grip of rim brakes on the rim of bicycle wheels. As is shown later in the chapter, stopping distance can in some cases increase in wet weather to more than ten times the dry value. On the other hand, wet weather barely affects disk or shielded drum brakes unless the brake is for some reason temporarily submerged in water.

Wet weather approximately quadruples braking distances for bicycles equipped with conventional rim brakes on steel rims. Hanson (1971) and Allen Armstrong (1977; personal communication, 2000) used laboratory equipment to simulate wet-weather braking of a bicycle wheel and learned a number of significant things. For brake pads of normal size and composition running on a regular 26-inch (equivalent to 650 mm) plated steel wheel, Hanson's tests at MIT (see figure 7.8) showed that the coefficient of friction when the pads were wet was less than a tenth of the dry value. Moreover, the wet wheel turned an average of thirty times with full brake pressure applied before the coefficient of friction began to increase, and a further twenty turns were necessary to attain the full dry coefficient of friction, which did not happen at all if water was being added to the brake pads or rims after brake application, as might occur during actual riding in very wet conditions.

The MIT tests were conducted in the 1970s on wheels with steel rims then popular. Several different brake-block materials were investigated. What were at that time (and still are in most of the world) standard bicycle brake pads (*B rubber*) had the highest dry coefficient (0.95) and the lowest wet coefficient (0.05) of friction of all materials tested. Attempts to improve the wet friction by cutting grooves of various types in the pads or by using "dimpled" steel rims were unsuccessful. (Others have reported similar findings.) Two cork pads were tested, with μ_{dry} values from 0.6 to 0.8 and μ_{wet} values from 0.2 to 0.25 obtained. Other high-performance aircraft brake pads were also tested, with μ_{dry} values from 0.3 to 0.4 and μ_{wet} values up to one-half the dry values. As some of these pads contained asbestos, they are no longer usable today.

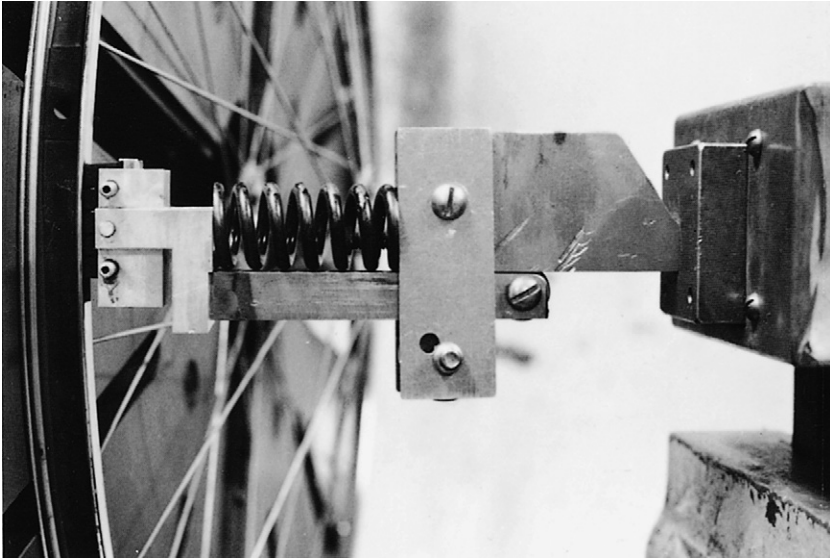


Figure 7.8

Test setup (at MIT) for brake-pad materials in Hanson's (1971) experiments. Just visible: the rim was rigidly mounted on a large lathe. The spring allowed the test pad to follow an inevitably uneven rim without substantial variations in force. Strain gauges in the support allowed measurement of normal and tangential forces. (Courtesy of Allen Armstrong.)

One consequence of the MIT work with steel rims was the development of a brake that could use aircraft brake-pad materials found to suffer little drop in friction coefficient in going from dry to wet conditions. These materials had a friction coefficient that was too low to permit them to be used in a regular caliper brake, because it would require too great a squeeze force. It was not possible to strengthen a regular caliper brake and then to increase the leverage, because one consequence of increased leverage is decreased brake-pad motion. (Bicycle wheels of present construction cannot be relied upon to run true, so a considerable brake-pad gap must be allowed.)

Therefore, a brake with two leverages was developed. When the brake lever is initially squeezed, the pads are moved under low leverage (low force, large movement). As soon as the pads contact the rim, a slider in the brake mechanism locks up, and further

movement has to take place through a high-leverage, high-force action. The brake therefore has the additional advantage that it automatically compensates for pad wear without further adjustment. This dual-leverage brake was subsequently redesigned by Positech, Inc., and tested. Used on the front wheel only, with a regular caliper brake on the rear, it regularly achieved stopping distances more than four times shorter than those achieved by regular brakes on steel rims in wet conditions (3.5 m from 6.7 m/s, instead of the usual 15–20 m). However, the Positech brake (described a little more fully in the second edition of this book) was never taken up commercially.

Transmission of Braking Force

The forces generated by hand-operated brakes in early bicycles were transmitted along rods and levers. The invention of *Bowden cables* (flexible steel tension cables inside flexible steel compression housings) in 1902 offered simultaneously a saving in weight and in manufacturing cost coupled with freedom to design both the bicycle's frame and its brakes in different ways. Unfortunately, designers apparently forgot that the laws of sliding friction apply inside a Bowden cable just as they do on braking surfaces. The force transmitted by the inner cable is continuously reduced, particularly around bends, according to the formula $(F_1/F_2) = e^{\mu\theta}$, in which $e = 2.718$ and μ is the coefficient of sliding friction. The total angle θ (in radians; divide by π and multiply by 180 for degrees) through which a brake cable is bent along its whole length should be used in calculations involving this formula (figure 7.9). The tubular housing's cradling or squeezing action on the inner cable increases the apparent coefficient of friction by a small amount, in the same way as the friction of a V-belt is increased by the squeezing action of its pulley.

Fortunately, perhaps, the front brake cable on regular bicycles has a smaller total bend angle than does the rear, and it is easy to get a greater braking force at the front, where it is needed. (Riders must develop the requisite skill to apply the brake in such a way that they don't precipitate a header.) Additional friction in the large total bending angles of the rear cable can decrease the force applied to the rear pads by 20–60 percent compared to that applied at the

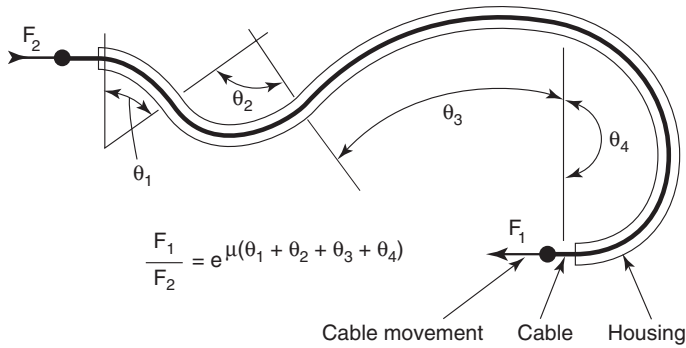


Figure 7.9

Attenuation in a braking force that is transmitted through cable bends. μ = coefficient of friction between the cable and housing; θ = angle (in radians).

front by the same braking action. Unlubricated brake cables often rust internally, reducing the transmitted brake forces even further, especially when the ends are mounted pointing upward, so that rain can enter the cable housing but not leave it. For all the reasons given, brake-cable linings of low-friction plastic, such as polytetrafluoroethylene, have been developed and have become standard for high-quality bicycles.

Although bicycle brakes with automatic wear-adjusting mechanisms have been offered commercially, they have not been successful. Virtually no brakes currently available allow adjustment through the whole range of brake-block wear without the use of wrenches, which can lead to extremely dangerous conditions in bicycles ridden by less mechanically able or observant persons.

Hydraulic actuation of rim and disk brakes has become popular. It allows high force amplification through the choice of the relative areas of the pistons in the hand levers and those at the brake pads. Force transmitted hydraulically is entirely unaffected by bends in the hydraulic tubing, and the amount of friction generated is negligible and moreover stays low during the life of the brake. The brake pads in some hydraulic rim brakes are attached to the pistons of the “slave” cylinders and so move linearly in toward the wheel rims during braking. Such linear motion offers the significant advantage that, as the pad wears, there is no danger of its going into either the tire sidewall or the spokes, as can happen with the pads on

some rim brakes as they wear. Some hydraulic systems adjust the volume of brake fluid automatically, to compensate for wear and temperature changes; some have a manually adjustable reservoir for this, and some require manual adjustments of the brake blocks themselves.

Other Developments in Bicycle Braking

In the past, brakes have been developed in which the braking forces themselves supply part of the actuating force. One example is over-run brakes as used on trailers, even some bicycle trailers, in which a sliding mechanism between the trailer and the tow vehicle operates the trailer brakes when the tow vehicle brakes. Other examples are drum brakes in which the brake shoes' geometry amplifies the forces on the brake shoes and rim brake calipers mounted toe-in so that the brake blocks automatically increase braking force when they start to engage by pulling themselves forward and inward. However, if the mechanism acts in such a way that excessive positive feedback can lock the brake or prevent its release, such an arrangement is dangerous. The coauthor had a serious accident this way, when his front brake seized too fiercely and wouldn't release, even bending the fork and instantly locking the wheel.

In addition, such brakes with self-actuating amplification might either not work at all in wet conditions or be too effective when dry. What is needed is an added negative feedback stage to limit braking force in dry conditions to less than the amount that would result in the rider's being projected over the bicycle's handlebars. Franklin Calderazzo developed a braking system incorporating such a combination of positive and negative feedback (figure 7.10). In Calderazzo's system, the rider actuates only the rear-wheel brake, which is mounted on a lever pivoted near the wheel axis so that the brake is carried forward during braking. In moving forward, the rear brake axis actuates (through a cable or hydraulic line) the front brake, with any reasonable desired degree of force multiplication. Accordingly, strong braking can be accomplished with little effort. At the point at which the rear wheel would otherwise start skidding, braking at the front wheel is automatically limited. In hundreds of tests with this system, in which testers made "panic stops" from high speeds on different surfaces, never did a rider even begin to

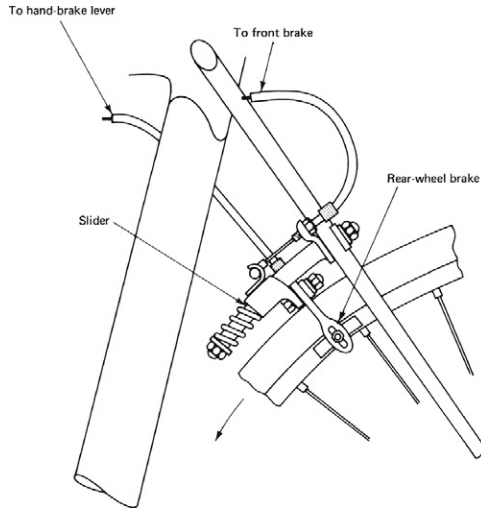


Figure 7.10

Franklin Calderazzo's feedback brake system (US Patent 4102439A). When the hand brake is operated, the rear brake is carried forward on a slider against a spring, actuating the front brake through the cable simultaneously. If the bicycle starts to pitch forward, the road surface no longer rotates the rear wheel, and the front brake is released.

go over the handlebars. (The front forks of the test bicycle eventually failed through fatigue, testimony to braking effectiveness and to the inadequacy of the fork design.) This promising system apparently died in patent litigation (R. C. Hopgood, personal communication, 1979). As noted, it could well be used to actuate other types of brakes (e.g., a coaster brake) on the front wheel.

Braking Power and Rim Temperatures Reached during Downhill Braking

Wilson (1993) studies rim temperatures attained during steady downhill braking of the type required in cycling on mountain roads. His results show that the rims of standard road bicycles that rely on rim brakes alone are likely to reach dangerously high temperatures, and those of bicycles with smaller front wheels and for tandems may reach even higher temperatures. Among other effects,

heated rims increase the air pressure inside the tire, making failures even more likely. It is therefore highly desirable that all tandems be equipped with at least one brake that does not heat the wheel rim, such as a drum or disk brake. But even standard bicycles with two rim brakes can be at risk.

Using the methods discussed in chapter 4 and depicted in panel (a) of figure 7.11, it can be determined that a bicycle of 12 kg (26.5 lb) and rider of 73 kg (161 lb), with an aerodynamic drag area $C_D A$ of 0.5 m² and a rolling-resistance coefficient C_R of 0.0033, would coast down a 10 percent grade without braking at around 16 m/s, with mostly air drag balancing the slope power of about 1.35 kW. If this speed can be safely maintained, there is no braking power.

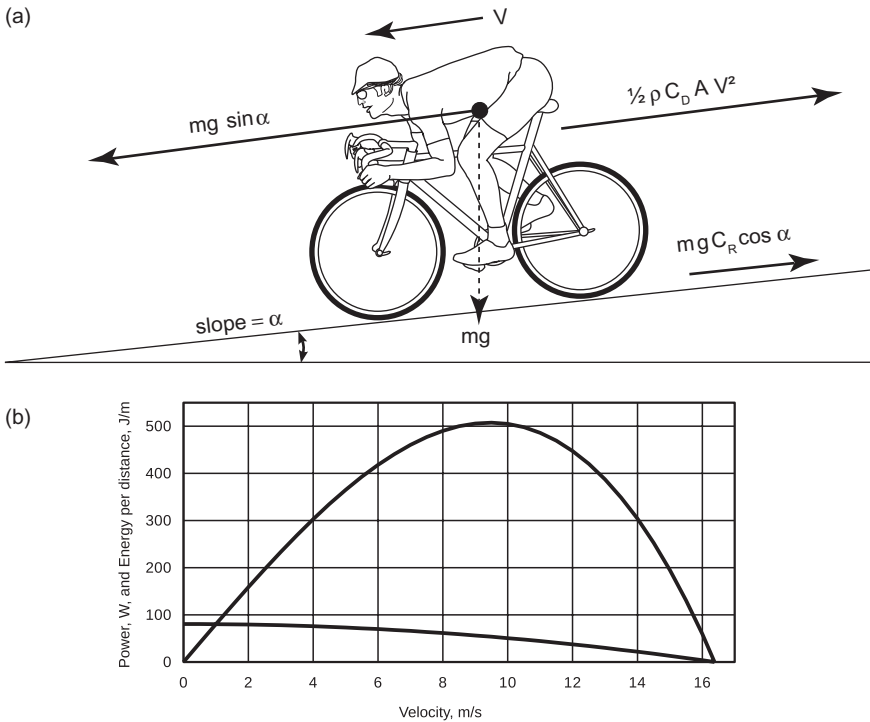


Figure 7.11

(a) Forces on a slope (angle α). The power dissipated in the brakes is the net downslope force ($m g [\sin \alpha - C_R \cos \alpha] - \frac{1}{2} \rho C_D A V^2$) multiplied by V , or for small slopes $V (m g [s - C_R] - \frac{1}{2} \rho C_D A V^2)$. (b) Plotted example for the values given in the chapter text.

If the rider wanted or needed to reduce the speed to 9 m/s, however, the slope power would then be only about 750 W, but the air-drag power would be reduced much more, to less than 250 W, so (including the small amount of rolling resistance also involved) about 500 W would have to be braked away. As shown in panel (b) of figure 7.11, this is the very speed that taxes the brakes most. Going either faster or slower reduces the required braking power. The figure also shows the braking energy per distance, which is the same as the braking force. It starts at 80 J/m or 80 N and reduces to zero at the terminal velocity. This curve is interesting for those who want to get the best regenerative braking on their e-bicycles. Going as slowly as possible maximizes the energy but is not pleasant riding, and the bicycle's motor-generator and charging system won't be working at their best efficiency. Depending on these two components, a good speed could be somewhere between 3 and 7 m/s.

Figure 7.12 shows, for three types of bicycles, the terminal velocities for which the net downslope force is zero, together with their specifications. The figure shows that tandems and faired HPVs in particular can travel at their terminal speeds safely only on rather gentle downslopes; for steeper ones they must brake strongly. Figure 7.13 presents a thermal model showing, principally, the area from which rim heat can be dissipated in convection heat transfer. In the figure, radiation and conduction of heat through the spokes and tire have been ignored to err on the conservative side. The heat-transfer model depicted uses one developed for turbine disks by F. J. Bayley and J. M. Owen in 1970 (see Wilson 1993) to show general trends rather than to predict absolute values.

The equation resulting from the heat-transfer model for the difference in temperature between the rim and the air is, for typical sea-level values of properties for air:

$$\Delta T = F / (100 r L_{\text{WW}} [0.6 + 1.125 \{1 - 0.0632 r V\}]),$$

in which F is the net downslope force (N) (figure 7.11), V is the speed of the bicycle (m/s); r is the mean radius of the rim (m); and L_{WW} is the effective width of the rim (m) (figure 7.13). (See Wilson 1993 for an equation incorporating values of properties of air at other than sea level.)

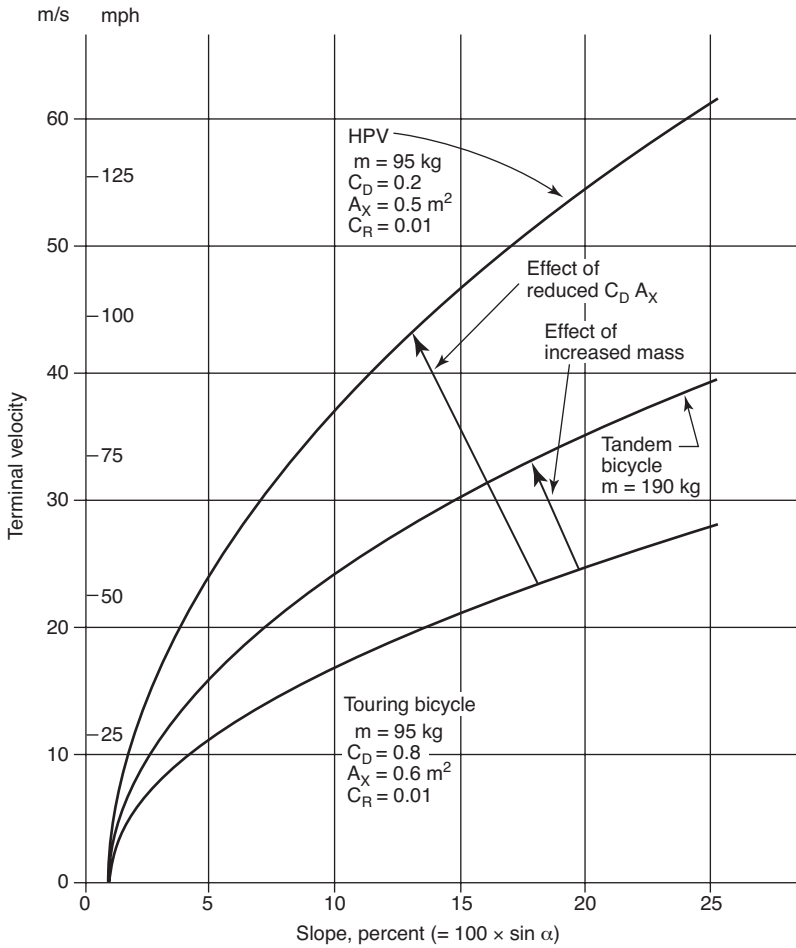


Figure 7.12
Terminal velocity versus slope. (From Wilson 1993.)

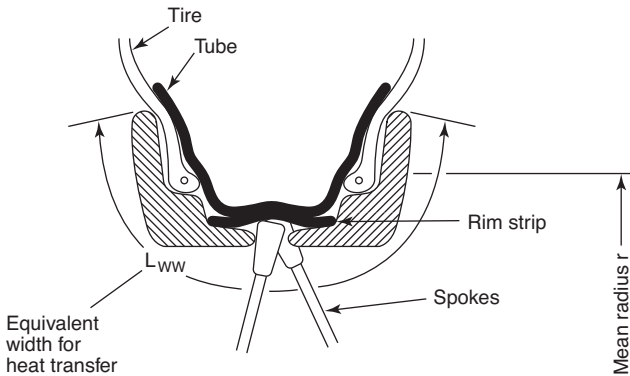


Figure 7.13
Thermal model. (From Wilson 1993.)

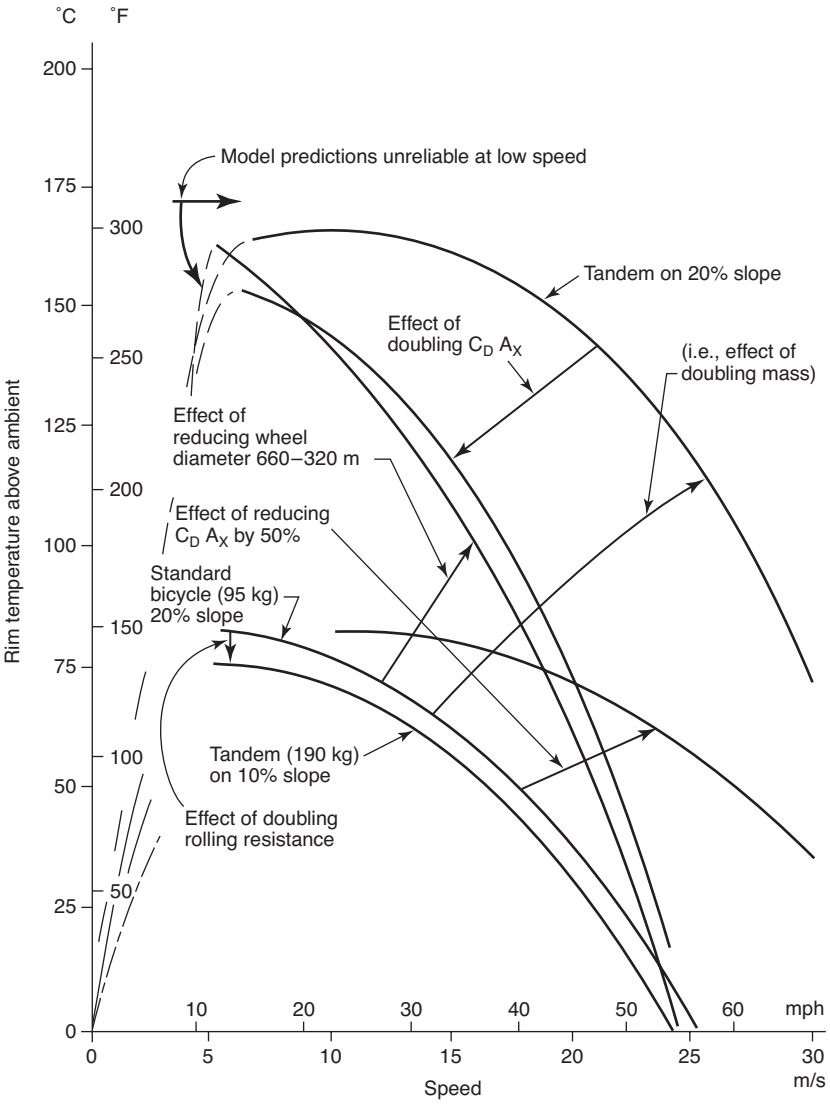


Figure 7.14
Temperature rise of rims during long braking on hills.

Figure 7.14 shows rim-temperature increments above ambient temperature for various machines. The increments are zero at zero speed and at terminal speed. Between zero and terminal speed, there is a speed at which the incremental rim temperature will be at a maximum. The thermal model is unreliable at low speed, so the estimation of the speed at which maximum rim temperature will be reached is particularly imprecise. However, the overall shape of the curves must mirror reality closely. The graphs indicate that it is better, in regard to rim temperature, to go either slower or faster than about 10 m/s, which makes the dilemma of downhill racers very clear: going fast avoids heating the rim unless emergency braking has to be applied, in which case the danger of overheating the rim is sudden and serious.

Wheels with deep-section, streamlined rims run cooler than those with narrow, unstreamlined rims that produce separated airflow, which has little cooling effect. Wide rim strips used under a bicycle's tires and tubes can insulate the tubes somewhat from the heated rims. It is also important in downhill cycling that braking be applied to both wheels fairly evenly, but with a bias in favor of the rear wheel, because of the extreme danger of a front-tire blowout at speed.

References

- Armstrong, Allen E. 1977. "Dynamometer Tests of Brake-Pad Materials." Positech, Inc., Lexington, MA.
- Beck, Roman F. 2004. "Mountain Bicycle Acceleration and Braking Tests." Beck Forensics, Inc., San Diego, CA. <http://www.beckforensics.com/mtbtesting.html>.
- Hanson, B. D. 1971. "Wet-Weather-Effective Bicycle Rim Brake: An Exercise in Product Development." MS thesis, Massachusetts Institute of Technology, Cambridge, MA. <http://hdl.handle.net/1721.1/12572>.
- Juden, Chris. 1997. "How Thin May the Braking Rim of My Wheel Get?" Technical Note. *Human Power* 13, no. 1 (Fall): 20. <http://ihpva.org/HParchive/PDF/44-v13n1-1997.pdf>.
- Lieh, Junghsen. 2013. "Closed-Form Method to Evaluate Bike Braking Performance." *Human Power eJournal*, no. 19: art. 7. <http://hupi.org/HPEJ/0019/0019.html>.

Oertel, Clemens, H. Neuburger, and A. Sabo. 2010. "Construction of a Test Bench for Bicycle Rim and Disc Brakes." *Procedia Engineering* 2, no. 2 (June): 2943–2948. <https://doi.org/10.1016/j.proeng.2010.04.092>.

Persson, B. N. J., U. Tartaglino, O. Albohr, and E. Toasatti. 2005. "Rubber Friction on Wet and Dry Road Surfaces: The Sealing Effect." *Physical Review B* 71, no. 3 (January 15): 035428. <https://arxiv.org/pdf/cond-mat/0502495.pdf>.

Wilson, David Gordon. 1993. "Rim Temperatures during Downhill Braking." *Human Power* 10, no. 3 (Spring/Summer): 15–18. <http://ihpva.org/HParchive/PDF/34-v10n3-1993.pdf>.

8 Steering, Balancing, and Stability

Introduction

Balancing a bicycle when it is at rest is normally possible only using a special technique known as a *track stand*, but it is easy when the bicycle is moving forward. Like walking on stilts, balancing a bicycle derives from an ability to steer the support points to a position “under” the center of mass. Many bicycles are capable, at medium speeds, of making the necessary steering adjustments for balancing automatically, without any rider input.

A more direct way by which a rider could balance a bicycle would be to exert righting torque manually on a suitable object with large moment of inertia. The long pole tightrope walkers often carry is such an object, but hardly feasible for balancing a bicycle. If that pole is shrunk, allowed to rotate freely parallel to the bicycle’s roll axis, and geared up, it becomes a *reaction wheel*. As a reaction wheel rotates only when needed, it does not require much power. Balancing a bicycle manually using a reaction wheel way is just conceivable, but highly marginal. As a rough example: if while sitting on a bicycle one had a spare bicycle wheel mounted vertically in front of one like a nautical steering wheel, one would need to spin the wheel up from zero to at least 1,000 rpm within 0.1 s to correct a 5° lean. Therefore a step-up gear of about 20:1 would be required or a much heavier wheel. And once the bicycle was balanced, one would then have a spinning wheel on one’s hands, good for correcting a lean in the opposite direction to before, by braking it, but otherwise imposing a huge control problem. Balancing a bicycle with a reaction wheel is better suited for an electrical system, as demonstrated

by the auto-balanced robotic bicycle of Almujaheed et al. (2009) and a few existing smaller models.

A rotating mass can, however, be used also as a stabilizing gyroscope, as was done more than one hundred years ago with the two-wheeled Gyrocar and has been done many times since with various robotic bicycles. Several configurations are possible. A popular design for existing self-balancing bicycle models uses a top-heavy gyroscope with its nominal spin axis vertical, mounted in a gimbal with its horizontal axis parallel to the rear-wheel axle. Such gyroscopes must be relatively massive or spin very fast, giving considerable frictional losses and safety problems.

Neither of the systems described up to this point for bicycle balancing seem useful for purely human-powered or even hybrid bicycles, for which the conventional bicycle balancing system has now been in use for more than two hundred years, on probably billions of bicycles, and combines balancing and steering in a most elegant manner without the use of external power.

Unfortunately, the mathematics purporting to describe bicycle motion and self-stability is neither complete nor easily understandable, so design guidance remains empirical, especially as the conditions needed for self-stability and for good human handling and steering are not identical. Questions regarding the stability of tricycles and related vehicles, compared with bicycles, seem trivial, which they are at slow speeds. However, this chapter looks at some of the basic problems in regard to tricycle steering, balancing, and stability that arise at higher speeds. It also makes some simple steering-related observations and discusses the rapid steering oscillation known as *shimmy*.

The most visible wonder in balancing a bicycle is that the bicycle can be balanced on just two points of support. Indeed, above a minimum speed, it appears impossible to fall down even if one were to try! This is of course not so; it would be easy to crash a fast-moving bicycle, but riders obey an unconscious compulsion not to do so.

Many bicycles can self-balance or be ridden free-handed within a certain speed range. At very low or very high speeds, however, those same bicycles fall over. When a bicycle is controlled by a rider, the usable speed range is very wide, from below walking speed to well over legal speed limits.

Special Characteristics Affecting Bicycle Steering

The geometry and mass distribution of a bicycle's steering mechanism play a significant role in the bicycle's handling, but scientific study of such matters has been relatively elusive. Part of the reason for this is that the concepts involved in a largely self-balancing vehicle are fairly subtle, and the relevant equations are complex (i.e., difficult both to derive and to interpret). But far more important is the central role of the bicycle's "pilot": unlike the pilot of an airplane or even the rider of a motorcycle, the rider is by far the heaviest part of the system in bicycling and is able to use all kinds of body motions, largely unconsciously, as control inputs. Furthermore, the handling behavior that feels good to a rider is always changing, conditioned by adaptation and affected by fatigue.

There is a comprehensive received wisdom about the design features that supposedly make for good bicycle handling in a given situation (e.g., high-speed cornering or negotiating a slippery trail), and for all anyone knows, the prescriptions offered by this received wisdom may often hold true. At this juncture, what science can prescribe remains more limited in spite of ongoing progress in the field.

Wheeled-Vehicle Configurations

A wide variety of human-powered vehicles have been built. Among them are those with one wheel: *unicycles* (with the total center of mass higher than the wheel axle, as also with circus balls on which one can walk), large-wheel *monocycles* (with a lower center of mass giving slight longitudinal stability, as also with amphibious inflatable spheres or rollers with persons inside them), and the acrobatic *monowheels* that consist only of a hoop held by a person gyrating within. Figure 8.1 shows examples of the first two types.

Then there are *dicycles*, with two wheels side by side. Pedaled dicycles maintain a slight longitudinal stability by keeping the total center of mass beneath the axis of rotation. There are also *gymnastics wheels* for one or two persons, who are positioned inside them. Except for one type of balancing toy, there are no human powered dicycles with a high total center of mass; they are available only with electrical auto-stabilization (far easier than the auto-stabilization of a *bicycle*) and electrically powered.

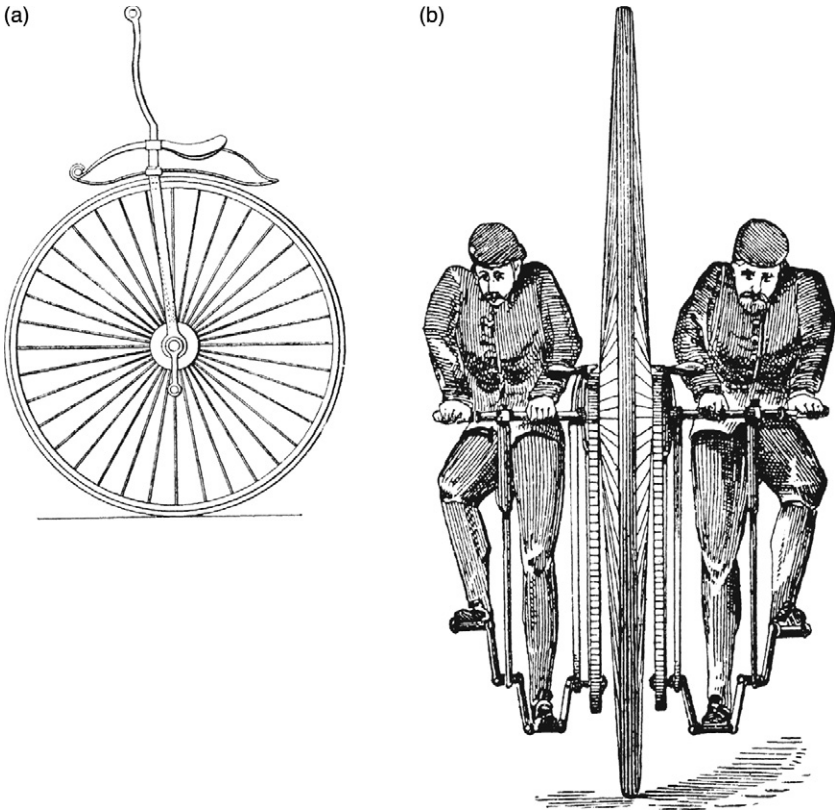


Figure 8.1

(a) Historic unicycle and (b) sociable monocycle. (From Sharp 1896 and Harter 1984.)

By far the most popular configuration is the main subject of this book, the *bicycle*, for two wheels and one or more riders in line. Very rarely seen is also the bicycle for a side-by-side couple called a *sociable*.

Finally, there are *tricycles* and *quadracycles*. (The term *quadracycle* is also used, especially for motorized four-wheelers, but *quadracycle* seems to be favored increasingly by the manufacturers of four-wheeled HPVs.)

Besides wheeled vehicles, there are also some without wheels but with balancing characteristics at least as complex as those of wheeled ones. They can have tracks, runners or skis, feet, or rimless wheels. With very few exceptions, these vehicles are not part of this

book. It does, however, devote some space to water “bicycles,” some of which balance in a manner similar to that of true bicycles.

Though modern upright bicycles and tricycles appear very similar when viewed from the side, they have distinctly different characteristics:

- Bicycles must be balanced, requiring some skill, especially to mount them and get them moving. Tricycles and quadracycles, in contrast, are innately stable at rest.
- When traction (adhesive friction) is good, bicycles can easily corner at high speed. Balance is maintained by leaning. Side forces on the wheels are relatively small, so the wheels need only small amounts of stiffness and strength against lateral forces. Most tricycles cannot lean, so fast cornering is possible only by “hiking” one’s body to the inside of a turn to avoid rollover (figure 8.2). Wheel side loads are then large, except in the case of special leaning tricycles that tilt the wheels in the direction of the center of the turn. Recumbent tricycles are at an advantage here, having both a lower center of mass and mostly smaller, stronger wheels.
- When traction is poor, bicycle balance can easily be lost, often resulting in a crash. Tricycles are less affected by slippery conditions.
- A bicycle’s single track makes it far easier to avoid or pass obstacles such as potholes or stationary cars and to negotiate very narrow paths than it is to do so on a tricycle with its three tracks.
- A bicycle’s narrow width makes it easier than a tricycle to carry up stairs and over or around obstacles.
- Even though a bicycle must operate in a state of balance, this balance is easily achieved even with offset mass, because the lean angle can always be adjusted to place the center of mass over the support line. An extreme case of such an adjustment is found in a sociable two-person bicycle with one rider heavier than the other. Rather than the heavy side’s sinking down, balance is attained by raising that side comically higher!
- A side slope or cambered road has an effect on both types of vehicle that is quite similar to that of a steady turn. It has almost no effect on a bicycle but gives rise to an annoying steering torque on a tricycle and side force on its rider—or in extreme cases, the risk of rolling over.

(a)



(b)

**Figure 8.2**

Cornering tricycles. (From *Cycling and Sporting Cyclist*, September 14, 1968.)

- On a tricycle that has two coaxial wheels like a dicycle or a bicycle trailer, misalignment may cause one wheel to direct the vehicle slightly to one side, against the resistance of one or more others, with the potential for substantial rolling resistance and wear. Very accurate alignment, optimum steering alignment in turns, or a self-aligning caster arrangement may prevent these ill effects.

Broomstick Analogy

A bicycle balances when its center of mass (CM) is over its support. At rest or in steady horizontal motion, “over” means vertically above. But in horizontally accelerated motion, such as a steady turn (imagine sitting in a fast-turning merry-go-round), “over”

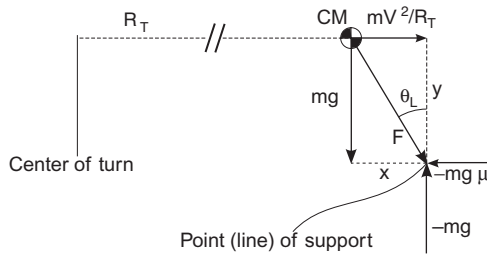


Figure 8.3

Definition of “the center of mass being over the support” when a bicycle travels around a curve. The cross-sectional diagram shows the center of mass CM traveling in a circle of radius R_T at speed V (at a right angle to the cross section, here “into the paper”). The virtual point of support is on a line between the two tire contact patches. The movement imposes an apparent outward centrifugal force of $m V^2/R_T$ on the center of mass and can be added as a vector to the weight $m g$ (mass $m \times \sim 9.81 \text{ m/s}^2$) to give the resultant force $F = m g/\cos \theta_L$ (the lean angle). The real force is that provided by the tires, which causes an inward centripetal acceleration V^2/R_T . The radius to use is that at the center of mass and not that at the tires. However, this radius is initially unknown, so an exact analytical solution is more complicated than that given here. For the bicycle to be in balance, F must go through the point of support, and the clockwise torque $y m V^2/R_T$ around this point must be counteracted by a counterclockwise torque $x m g$ of the same magnitude, which is achieved when $x/y = \tan \theta_L$. On a horizontal surface, the reacting ground force must be composed of a vertical component $-m g$ supporting the weight and a lateral component $-m g \mu$, in which μ is the minimum required coefficient of friction for the tire not to slide laterally on the surface and is therefore equal to $\tan \theta_L$.

means at an angle, such that the combination of downward gravitational pull and horizontal centrifugal force aims directly from the bicycle’s center of mass to the point at which it is supported, as in figure 8.3.

An examination of the simple exercise of balancing a broomstick upright in the palm of the hand can elucidate many important aspects of bicycle balancing. The key rule is that *unstable balance of an unstable rigid body requires an accelerated support*. Whether its support point is at rest or moving steadily, a broomstick inverted and placed on the palm of the hand is unstable and will simply fall over. (A gyroscopically stabilized top is a quite different case.) Balancing a broomstick (or a bicycle) consists in making the small support motions necessary to counter each fall as soon as it starts,

by accelerating the base horizontally in the direction in which the broomstick is leaning, enough so that the acceleration reaction (the tendency of the center of mass to get left behind) overcomes the tipping effect of lack of balance. The base must be accelerated with proper timing to ensure that the rate of tipping vanishes just when the balanced condition is reached. Even more sophisticated control is needed to maintain balance near a specified position or while moving along a specified path. Taller broomsticks fall less quickly than shorter ones, the time it takes being proportional to the square root of the height above the support. Therefore, high-wheeled bicycles are actually rather easy to ride, but getting on and off is another matter!

How Bicycles Balance

A rider balances a bicycle in the left-right direction by *steering it while rolling forward* so as to accelerate the support of the bicycle laterally. Restraining a bicycle's steering makes it unrideable, a fact that is put to good use in steering locks for deterring bicycle theft. Surprisingly, the small steering motions necessary to right a bicycle after a disturbance can take place *automatically*, even with no rider, as releasing a riderless bicycle to roll down a gentle hill and then bumping it can demonstrate.

It was and often still is widely believed that the angular (gyroscopic) momentum of a bicycle's spinning wheels somehow supports it in the manner of a spinning top. This belief is absolutely inaccurate. *Gyroscopes can react against (i.e., resist) a tipping torque only by continuously changing heading.* For example, a tilted top can resist falling only by continuously reorienting its spin axis around an imaginary cone. Locked steering on a forward-rolling bicycle does not permit any wheel reorientation, and the bicycle will fall over exactly like a bicycle at rest, no matter how fast it travels or how much mass is in the wheels. To be sure, bicycle wheels actually are changing heading continuously whenever the steering is turned, but their mass is small compared to the "mass times acceleration times center of mass height" moment that predominantly governs bicycle balancing.

Still, there is an extremely interesting gyroscopic aspect to bicycle balance: the angular momentum of a bicycle's front wheel urges it

to steer (i.e., to precess) *toward the side on which the bicycle leans*, as can be demonstrated by lifting a bicycle off the ground, spinning the front wheel, and briefly tilting the frame. In other words, the gyroscopic action of the front wheel is *one part of a system that automatically assists the rider in balancing the bicycle*. If the angular momentum of this gyroscopic action is canceled, as Jones (1970) did with an additional counterrotating front wheel, considerably more skill and effort are needed for no-hands riding.

The broomstick analogy presented in the preceding section is actually only partly applicable to a bicycle, as a bicycle is supported at two distinct points that generally accelerate somewhat differently. A low-speed slalom maneuver after riding through a puddle demonstrates that the front wheel travels a much wavier path than the rear, which also lags in phase (figure 8.4). Only in a steady turn do the contacts of both wheels with the ground follow paths of comparable curvature, yet the front wheel's turning radius (R_F) is greater than that of the rear (R_R) by the amount ($\frac{1}{2} R_F^2 R_R$). Therefore, lateral acceleration (equal to V^2/R or equivalently to V times the rate of change of the wheel heading [e.g., in radians per second]) is generally greater for the front contact than for the rear. In fact, only at the front of the bicycle frame can lateral acceleration be brought about relatively rapidly, by accelerating the steering angle and by maintaining a rate of increase of steering angle. The steering angle must settle to a steady value before the front acceleration reduces to match the rear.

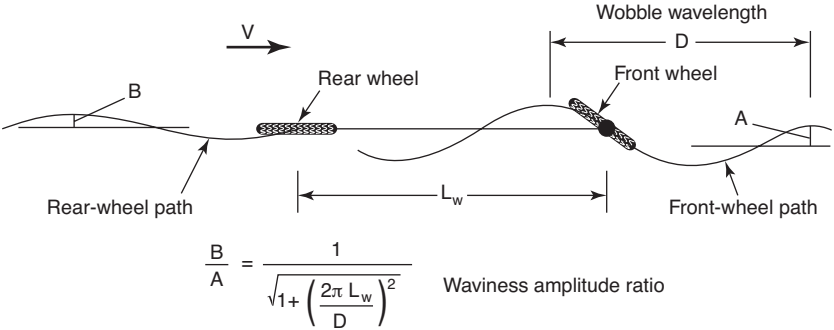


Figure 8.4 Front-wheel track compared to that of the rear. Note that the front-wheel track is wavier.

One implication of the delayed and reduced lateral acceleration of a bicycle's rear contact is that, when the bicycle is moving, mass over the front contact is more easily balanced than that over the rear. If mass is to be carried over both contacts, keeping that in the rear lower than that in the front will allow the front-support acceleration to exert more control over balance. (Rear steering would make the rear contact the more controllable one, but a rear-steering bicycle is difficult to ride fast.)

The basic means by which bicycles are balanced and controlled involves *vehicle supports that travel only in the direction in which they are pointed* (implying that they can support loads perpendicular to that direction). For this, at least one wheel must be steerable, usually the front one. This balancing-by-steering function can be performed not only by conventional large-diameter bicycle wheels (or their equivalent as shown in figure 8.5), but also by small-diameter wheels, as on a foldable scooter, by skates on ice, by skis or runners on snow, and by fins or foils in water. It is even possible to tip a three- or four-wheeled vehicle up on the wheels of one side and to balance and steer it like a bicycle or motorcycle for as long as desired. In each of these cases, the required steering torque may differ, and the particular sideslip, inertia, or flex may affect the feel, but with regard to steering, all are essentially bicycles.

Countersteering to Generate Lean

An unstable balanced object like a broomstick or bicycle must have the appropriate (say) leftward lean to maintain significant acceleration leftward of the center of mass. In other words, *the support point must first move to the right of the system center of mass to create a leftward lean*. The motion of the support point can be hard to observe while riding, because it happens so quickly and unconsciously. To see it most clearly, one can ride a bicycle along a painted line and watch the front wheel's position while making a quick maneuver to change lanes rightward. One will notice a brief leftward deviation of the front wheel's path, caused by briefly steering leftward before settling into a sustained rightward steer angle (figure 8.6).

But in fact every cyclist knows so-called countersteering very well, unconsciously: it is the only possible way to maneuver a bicycle or to stop with the right degree of lean to allow whichever foot the cyclist chooses to touch the ground. That everyone who knows how



Figure 8.5

Bicycle with booted spokes. Bicycles can be perfectly adequately balanced and steered not just with the use of large wheels, but also using very small wheels, skis, or as shown here, spokes with boots on them! (Photo by Jean Gerber.)

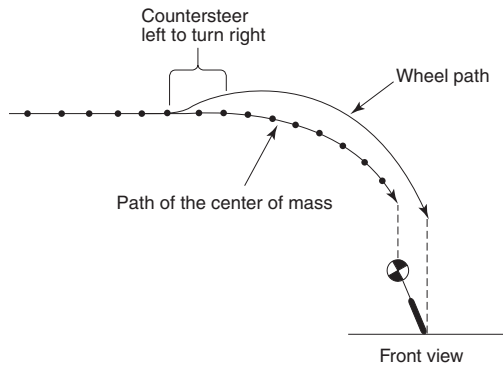


Figure 8.6

Brief leftward “countersteering” to generate the rightward lean necessary for rightward turning.

to ride a bicycle already unconsciously understands the method becomes clear when one is riding close to the edge of a curb or a slight drop-off. Riding closer to either of these than about a hand-span makes one feel nervous and “trapped”: one knows that it will be necessary to turn toward the danger in order to steer away from it. If there’s no room, one senses that trying to escape will take one over the edge. Nonetheless, it is useful to practice (obviously completely separated from other traffic) abrupt, forced countersteering, for use in emergency maneuvering (see, e.g., Forester 2012).

Countersteering is also required when one encounters a side-wind gust or when one is pushed by a neighboring rider. Whenever any force pushes one to the right, one must briefly turn right to generate leftward lean, so as to counter that force steadily.

Incidentally, all principles of unstable balance apply to runners too. To accelerate, runners lean forward, and to decelerate quickly, they lean back, by getting their feet out in front. Running straight and then suddenly turning leftward requires a step to the right in order to generate lean.

Basic Bicycle-Riding Skills

At the height of the 1890s bicycle boom, bicycle-riding schools sprang up in major cities. But for most reading this book, who acquired bicycling skills at a later time, learning to ride was typically a trial-and-error process conducted near home. Does the study of bicycle balance offer any insight into the process?

- The common advice to “turn toward the lean” is good. US Patent 5,887,883, to Joules, describes a quick method for teaching this.
- It’s hard to see how training wheels can inculcate any of the desired balancing habits, unless the training wheels are off the ground (i.e., used only when at rest). This has largely been realized as time has gone on, and nowadays, instead of training wheels, young children are often given simple foot-propelled bicycles without pedals, in order to build up their balancing skills before their pedaling skills, which tend to come more easily.

Beyond these thoughts, the commonsense idea of having those learning to ride a bicycle adjust the bicycle’s seat low enough to plant their feet on the ground and practice by coasting down gentle, grassy slopes is indeed an attractive one. Also, a scooter is an

excellent tool for learning to balance, almost free of the risk of a fall, as stepping off onto the ground is easy.

Once basic balancing of a bicycle has been mastered, important cornering techniques can be developed:

- Paying attention to surface conditions that provide poor traction or influence the steering (e.g., loose gravel, wet leaves, snow and ice, railway or tramline crossings). As these cannot always be avoided, practicing their negotiation at slow speeds and suitably protected is recommended.
- Adopting the gentlest possible turn radius (i.e., starting wide then grazing the apex of the curve). Riders must be prepared to brake hard before entering a turn if their speed seems to be too high to enable them to complete the turn safely.
- Gripping the bicycle's handlebars more tightly when cornering hard at high speed, to stiffen the arms and to reduce instability, and also when negotiating uneven surfaces.
- Holding the inside pedal in a raised position during hard cornering, so that it does not strike the pavement. The limit of cornering traction on good dry pavement is typically at 40° lean or greater, but a bicycle's inside pedal held low or moving typically strikes the pavement at 30–35°. Holding the bicycle more upright than the upper body places more stress on the wheels but may allow continued pedaling through a corner without slowing. (On a bicycle equipped with a freewheel, this technique is optional; on a fixed-gear bicycle, it is essential.)

Cyclists often extend the inside knee in executing a turn, like hard-cornering motorcyclists. This practice offers the seemingly marginal benefits of making the bicycle's frame slightly more upright, keeps a little more of the tire central tread on the pavement, and counters the tendency of a steered wheel's *mechanical trail* (defined in figure 8.8 and later in the chapter) to shrink because of lean. Snapping the leg inward momentarily decreases side force and may enable recovery if the rider loses traction during the turn. However, many skilled riders do the opposite when coasting: they “lean the bike” more than the body and put weight on the outside pedal, which automatically puts it into a safe position for cornering. As the tires' camber is increased, this technique could provide extra cornering force and permit a tighter turn. Other skilled riders suggest keeping

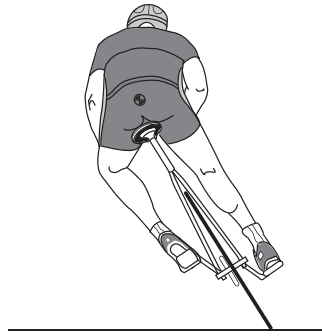


Figure 8.7

Typical high-speed cornering attitude of a champion racer, with approximate center of mass. On lesser curves the inside leg may be tucked in.

everything in line as much as possible, and yet others that it doesn't matter. Videos of champion racers show that in a way all three techniques can be applied at the same time: outside foot down, extended inside knee, twisted torso with head more outside, and center of mass nearly in line with contact patches (figure 8.7).

History of Balancing and Stability Research

The foregoing observations should make the basic way bicycles balance clear, as it already was to Karl von Drais two centuries ago. Since then and until this day many researchers have tried to determine the exact mechanisms through which bicycle balancing is accomplished, as well as mathematical expressions for describing them. Most have had the right ideas but have also made mistaken assumptions or errors in trying to find elegant solutions. Arend Schwab's (2009) bicycle dynamics history page lists most of these attempts up to 2005 and his main page (2017) those until recently. For a long time gyroscopic action was considered essential, if not for skilled riders, at least for the automatic balancing of riderless bicycles. Front-wheel steering with mechanical trail was regarded similarly. In 1970 D. E. H. Jones tried to find answers by building unrideable bicycles to disprove preliminary assumptions. He installed an off-ground counterrotating front wheel as an "antigyro." Not only was the resulting vehicle still rideable, but it also still balanced automatically when given a push, and thus it disproved the myth that gyroscopic action is necessary for a bicycle's front wheel to self-steer.

In 1985, research on bicycle balancing and stability began at Cornell University, with Jim Papadopoulos in Andy Ruina's lab. Papadopoulos 1987 represents the state of research then and Olsen and Papadopoulos 1988 is a well-presented short summary. In 1988 Richard Hand published his thesis with further research, confirming much of the previous work, but still hadn't found a complete and error-free solution to describe bicycle balancing. With few exceptions, not much more research emerged over the subsequent decade and a half, until renewed interest in 2002 commencing with Arend Schwab of Delft University visiting Andy Ruina's lab and later undertaking bicycle research in his own lab. In 2004, the third edition of this book included an introduction to many equations regarding bicycle dynamics that are still in use today. In 2005 Åström, Klein, and Lennartsson of Lund University published a very nice article, but still apparently with errors or contradictions of previous and later work. The next years saw frequent student research, and in 2011 the US-Dutch team of Kooijman, Meijaard, Papadopoulos, Ruina, and Schwab managed to build a riderless bicycle with no trail and tiny, nongyroscopic wheels, demonstrating conclusively that a bicycle's mechanism for balancing and self-steering does not need wheels with trail or gyroscopic action, given the right mass distribution causing the bicycle to automatically steer into a fall. Schwab and Meijaard (2013) review the group's and others' work up to this date. The team also built a rear-steering bicycle, which worked both with and without a rider. Videos of the models and further papers are available at Schwab 2017. An important resource is Ruina 2014, with copies of many papers up to this date.

Thanks to all this research work, it is clear today that certain aspects of bicycle geometry, including trail, mass distribution, and gyroscopic action, all play a part in bicycle stability. None of these aspects is uniquely important, but with the right combinations, auto-stable bicycles are possible, and the wrong combinations will result in unstable, perhaps even unrideable bicycles. For bicycle designers, this information is still not very useful, as the equations involved remain complicated and do not lend themselves to "bicycle-cookbook"-type design formulas. A computer-program, JBike6, accessible through Dressel 2015, is, however, available for determining the speed range within which a particular bicycle is self-stable.

Effect of Bicycle Configuration on Steering and Balancing

Some of a bicycle's steering and balancing behavior can be explained in terms of basic geometry: the placement of the wheels, possibly of differing radii, the line of the steering axis, and the centers of masses of the front (steerable) and rear assemblies. In figure 8.8, a horizontal distance called the *wheelbase* (L_W) separates the bicycle's two wheels. The bicycle's steering axis, shown as a dashed line, forms an angle with the horizontal surface on which the bicycle rides that is known as the *head angle* (λ) and typically intersects with the ground just ahead of the front-wheel contact. (In some calculations, λ is instead measured from the vertical, as in figure 8.11.) The line of the steering axis commonly passes below the front-wheel axle, that is, the bicycle's fork is bent forward.

The bicycle's front axle is ahead of the steering axis by a perpendicular distance referred to as the *fork offset* (L_{FO}). This distance is sometimes also called *rake*, an unfortunate usage, as in motorcycling this term is used for the angle of the steering axis from the vertical. The horizontal distance by which the front-wheel contact is behind the imaginary point where the steering axis intersects the ground

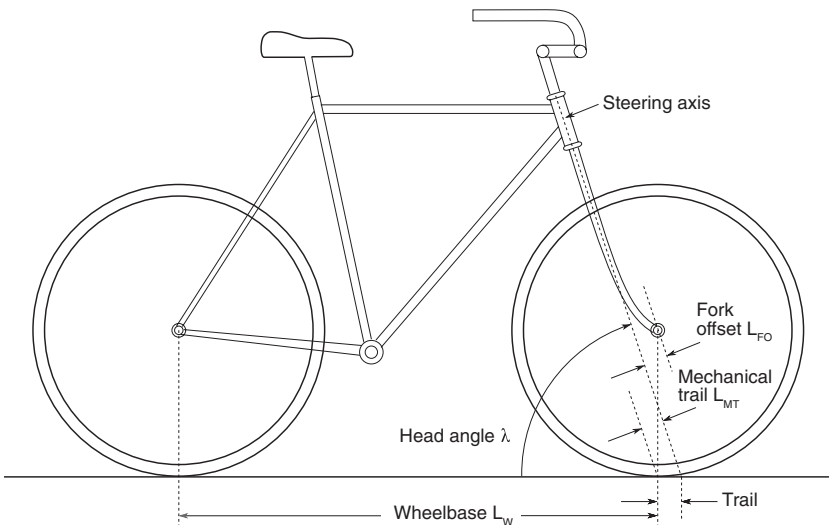


Figure 8.8

Bicycling parameters related to handling and stability.

is called *trail* (similar to automotive caster). A related quantity is the shortest (perpendicular) distance from the front-wheel contact to the steering axis (positive when the axis is ahead of the contact point), which is called *mechanical trail* (L_{MT}). A further relevant quantity, shown in figure 8.11, is the *wheel flop* (sometimes *wheel-flop factor*), the distance by which the front assembly is lowered if the front wheel is rotated 90° about the steering axis (or raised, in the case of negative trail).

The various geometric features described in the last two paragraphs are difficult to measure, but they have such a great effect on handling and stability that we have tabulated some values for a number of different large-wheeled bicycles in table 8.1. It is apparent that as one moves from (particularly stable) touring bicycles to road-racing and finally track bicycles, the head angle becomes steeper and the amounts of trail and wheel flop decrease. Note that a bicycle's fork offset is *increased* to *reduce* its trail. Various online calculators are available that allow quick comparisons between the parameters; Jim G. provides a nice one at yojimg.net/bike/web_tools/trailcalc.php that provides values for trail, mechanical trail, and wheel flop. These quantities are also easy to work out manually; the formulas are given, for example, at en.wikipedia.org/wiki/Bicycle_and_motorcycle_geometry.

Table 8.1

Mechanical trail and wheel flop for the angles and offsets of typical bicycles

Bicycle type	Head angle to road, degrees	Fork offset, mm	Mechanical trail, mm	Wheel flop, mm
Touring	72	47.5	58.5	18
Touring	72	50.7	55.2	17
Touring	73	57.9	42.3	12
Road racing	74	50.0	44.5	12
Road racing	74.5	55.1	36.5	10
Road racing	74	66.9	27.6	8
Track racing	75	52.1	36.7	9
Track racing	75	65.4	23.4	6

Note: All bicycles included in the table have a wheel radius of 343 mm.

The values shown in table 8.1 represent the results of the fine-tuning of conventional bicycles to obtain the greatest suitability and handling for their intended purpose. These are more general qualities than stability in balancing and steering, but they are related. The process of bicycle design must satisfy different requirements, starting with riders' ability to put at least one foot down on the road when the bicycle is stationary, their being able to pedal without hitting the front wheel in turns (track racers can tolerate this to some extent), or the bicycle's ability to carry cargo. Thus special-purpose bicycles, even with conventional large wheels, may have different angles and offsets from other bicycles. Many e-bicycles, for example, place the battery between the seat tube and the rear wheel, thus lengthening the bicycle. However, the geometrical parameters for most large-wheeled bicycles are rather similar. Vehicles with small wheels, recumbents, and those with unusual designs can have completely different configurations from the typical one. For bicycles with suspension, possible changes in geometry must also be kept in mind, for example, when braking.

Small Wheels and Special Configurations

Whereas the design of conventional bicycles with large wheels has for generations been in the hands of large companies and also countless frame builders, HPVs, including recumbents, velomobiles, and cargo bikes, mostly have at least one smaller wheel and, being relatively new and few, are the subject of avid research and experimentation by small companies, universities, and individuals. Accordingly there has been a great evolution in design, and there is much variability among type and models in the parameters that influence balance, steering, and handling. Unfortunately, there are few design tools or published guidelines to assist builders in achieving optimum designs right from the beginning.

The Basic Design Problem for Recumbents The basic design problem for recumbents, in particular, is a bit different from that for upright bicycles. Putting the feet (or sometimes even the hands) on the ground for balancing at rest is no problem in recumbents (except for ultralow ones), but to avoid, in a turn, a collision between the steered front wheel and the pedaling feet, this wheel must either be well in front, resulting in a long wheelbase, or somewhere under the knees, yielding a short wheelbase. Normally a smaller wheel is

required in either case, say, one nominally 0.4 m in diameter. Long-wheelbase recumbents are delightfully stable at speed, but difficult to maneuver when moving slowly in tight places like city traffic. Short-wheelbase recumbents, on the other hand, are more maneuverable but can seem a bit skittish at speed, as only tiny steering motions and little torque are required (as also with many upright small-wheeled and short folding bicycles). Between long-wheelbase and short-wheelbase recumbents are *compact long-wheelbase recumbents*, described in chapter 10, which are both easy to ride and stable because of their especially small front wheels and high seating positions. For all configurations, achieving optimum angles and offsets can make the difference between “just rideable” and “enjoyable” or “safe.”

One Systematic Research Project The adjustable recumbent Multilab test vehicle of Rohmert and Gloger (1993) at the University of Darmstadt systematically explored balance and steering in recumbents. Multilab was a short-wheelbase recumbent with two 400 mm wheels and an adjustable wheelbase (but nominally about 1 m), head angle, and track. It also featured a special “mirror-symmetrical” front-wheel geometry with the head angle pointing *backward* but a large negative fork offset in order to achieve a normal trail. Such a geometry results in “reverse wheel flop,” that is, the wheel doesn’t flop at all, but is stable in a neutral position.

Two components essentially determine whether and how strongly a wheel actually wants to flop:

1. The *load* on the front assembly, which tries to find its lowest potential energy, that is, lowest point of the *total center of mass*.
2. The center of mass of the *front assembly itself*, which becomes noticeable when the cyclist is dismounted and holding the unloaded bicycle by the seat.

Because of the way Multilab is designed with respect to these two components, its required steering torque as a function of the steering angle is greater than for the conventional geometry (see figure 8.9). Rohmert and Gloger (1994) evaluated six different configurations with nineteen test subjects who ranked them on six points of handling quality. All were able to ride the Multilab within minutes, and the best-rated configuration, with a head angle of 89° (i.e., 91° measured in the conventional direction) and a trail of 59.5 mm

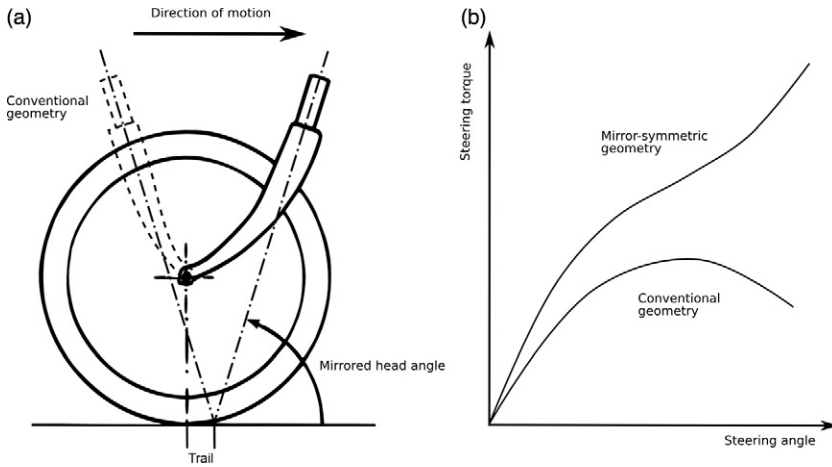


Figure 8.9

(a) Mirror-symmetric fork geometry (from Rohmert and Gloger 1993) and conventional geometry (dotted lines). Note the larger fork offset required. (b) Conventionally the steering torque increases as a result of trail and decreases with large angles because of wheel flop. In the mirror-symmetric geometry, both trail and wheel flop work in the same direction.

(requiring a negative fork offset of 62 mm and resulting in only -1 mm wheel flop), got an average of 7 out of 10 possible points (“somewhat good”). Rohmert and Gloger gave the advantages of this configuration as a larger possible collision-free steering angle with the pedaling feet and a longish wheelbase without an excessive overall length and thus more stability in braking and with obstacles and crosswinds. They subsequently used this concept in their DESIRA-2 single-track velomobile with a wheelbase of 1,080 mm, a head angle of 88° (i.e., 92°), and a track of 40–50 mm (for a 16-inch \times 1.75-inch tire), but we know of no other implementations since.

Some Other Configurations There are a number of other very different configurations for short-wheelbase recumbents that are rear or center steered. A good reason for rear steering is to have the front wheel fixed so that it can be a bit larger and still fit between the cyclist’s swinging legs and also be driven, avoiding a long chain (some designs even put the pedal axis *through* the front wheel axis using special hub gears). Schnieders and Senkel (1994) provide an

overview of rear-steering recumbents and interesting numerical stability plots. They conclude that rear-steered recumbents are rideable but not self-stable. Indeed, quite a few videos of various rear-steered recumbents can be found, in which they appear to be rideable but do not seem very stable. However, a video of a talk by Arend Schwab at TEDxDelft2012, “Why Bicycles Do Not Fall” (linked from Schwab 2017), shows a student-designed rear-steered bicycle in action, both with a rider and also self-stabilized. Schwab and Kooijman presented a rear-steered high-speed racer at a 2014 conference, and in 2017 P. H. De Jong completed a master’s thesis on rear-wheel steered bicycles at Delft University of Technology.

Some bicycles pivot from the center. Perhaps the most famous is the original Flevobike, which is steered by leaning and with the legs via the pedals, which are attached to the front assembly. This arrangement can leave the hands free, and the Flevobike is extremely maneuverable once mastered (but can otherwise be “self-folding”—even while riding!). An internet video, “Flevobike Crashtest,” shows a dozen consecutive test falls on gravel. (More remarkable than this extreme example of instability is the passive safety shown: the totally unprotected crash rider—in shorts—seems to suffer a single minor elbow scrape.) A further remarkable video, “Flevobike & Difficult Riding Situations,” shows advanced riding, including track stands and slow, hands-free maneuvering. This Flevobike model is no longer in production, but it still has many enthusiasts, who are united at flevofan.ligfiets.net, with links there also to various home-built variants. (A similar Flevotrike was also produced.) Figure 8.10 shows a side view of the Flevobike and its dimensions, as well as the similar, large-wheeled, center-steered Airbike. (There even exists a center-steered [vertical-axis] upright bicycle, the Snaix, that is advertised as a training device.) Also shown in figure 8.10 is the center-steered Python (2018) tricycle with a unique, huge *negative* trail. Python-lowracer.de/geometry.html describes the advantages of the Python’s geometry, which gives a large negative (self-centering) wheel flop, referred to as *seat rising* here.

Patterson (1998; see also calpoly.edu/~wpatters/lords.html) attempted to provide guidelines for standard front-steered recumbents, which he used for some years in his class on single-track dynamics at California Polytechnic State University. (This class was later continued; see Davol and Owen 2007.) His approach was to

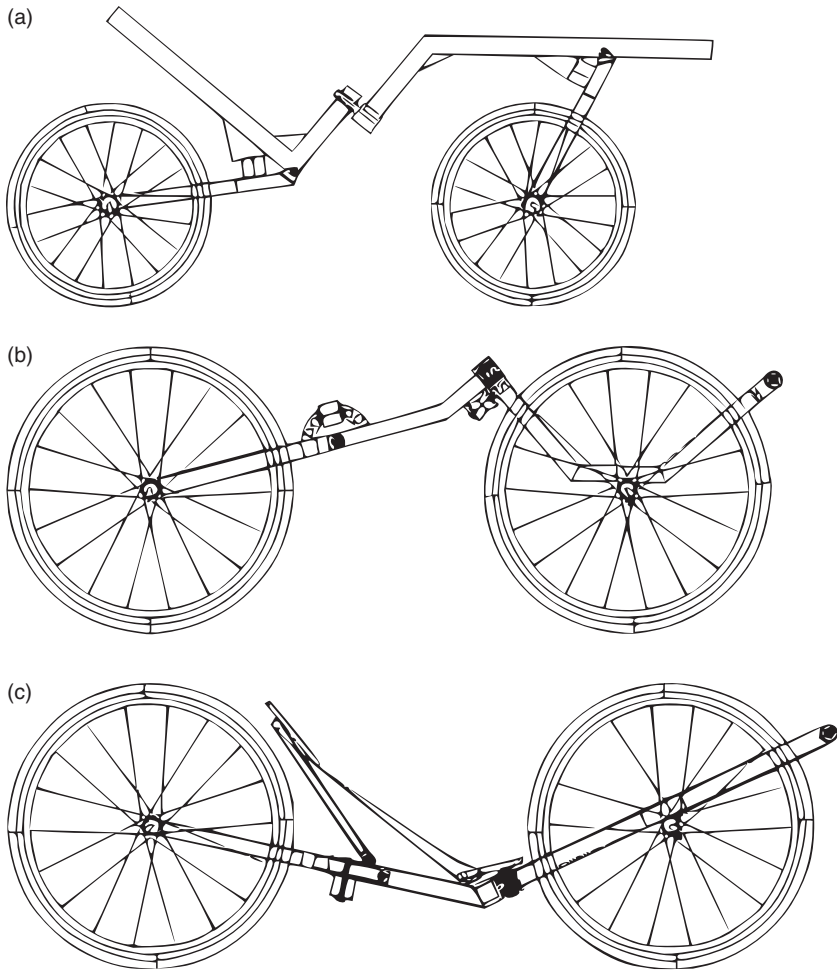


Figure 8.10

(a) Flevobike with pivot angle 40° , trail 130 mm, and wheelbase 950 mm; (b) Airbike with pivot angle 50° , trail 190 mm, and wheelbase 1,070 mm; (c) Python with pivot angle 65° , trail -300 mm, and wheelbase 1,290 mm. (Drawing by Jürgen Mages, licensed CC-BY-SA-3.0.)

find simplified equations describing good handling, meaning optimum parameters for steering movement and torque. He devised six parameters and a value he called *sensitivity*, meaning the rate of a recumbent's frame roll (rear assembly) in relation to the control motion at its handlebars. Patterson gives recommended minimum and maximum values for these seven parameters, plus trail and fork-flop force, based on practical experience. They are not very complicated and readily entered into a programmable calculator or spreadsheet. The idea is to enter an initial bicycle geometry, then vary aspects of it until the all parameters fit into the recommended ranges.

Patterson's goal was to enable anybody with a calculator to predict the handling qualities of front-steered recumbents, but at least college-level mathematics and considerable motivation to grapple with the method are still required. Archibald (2016) has since presented Patterson's method in a more accessible manner with examples and in addition makes a Matlab script available.

Zero-Radius Wheels

For many analytical purposes, the radii of a bicycle's wheels are not significant. A simple model with the same contact points and steering axis as real wheels involves just tiny "zero-radius" wheels (see figure 8.11). Such a model effectively freezes the mechanical trail L_{MT} at a fixed value, whereas on an actual bicycle, L_{MT} is somewhat reduced during hard cornering.

A variety of observations based on this simple model can easily be understood:

- Riding straight while bending the torso to the right side of a bicycle's frame requires the frame to lean leftward to maintain balance (i.e., center of mass over the line joining the contact points). The vertical support force on the front contact then has a component perpendicular to the wheel; this component acts through the lever arm of the mechanical trail and tends to turn the handlebars to the right, as can easily be felt. The small effect of handlebar weight simply adds to this torque (see figure 8.12).
- When riding a bicycle at low speed (e.g., 2.5 m/s) in a circle, being careful to keep one's torso in the plane of the frame, and controlling the handlebar position with just one finger, it is

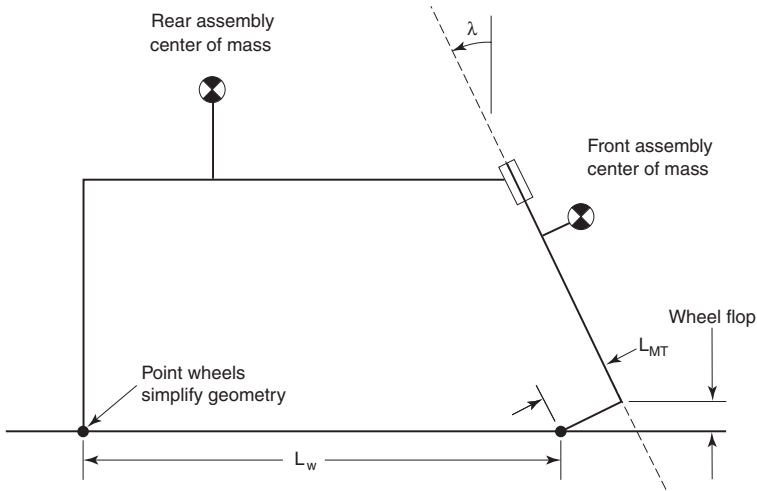


Figure 8.11

Model of a bicycle with point (i.e., zero-radius) wheels. If the bicycle is held level and the steering is turned, the front wheel will lift off the ground. If it is free in pitch and the steering is turned 90° , the front assembly will fall by the distance labeled *Wheel flop*. The figure shows, therefore, that the front wheel of a stationary but loaded and unbraked bicycle (or tricycle) will tend to flop to one side, usually in addition to a small torque produced by the location of the front assembly's center of mass.

clearly necessary to restrain the bicycle from sharpening the turn. This characteristic is primarily a reflection of *the system's potential energy being at a maximum in the upright, straight configuration*. When the handlebars are turned, the center of mass falls by an amount proportional to the mechanical trail (equivalently, with the mass center at a fixed height, turning the handlebars would lift the front contact off the ground). The resulting torque cannot be demonstrated at rest because of tire friction. As is discussed later in the chapter, the tendency to sharpen a turn is part of bicycle self-stability.

- Low-speed turns to the right place the front contact to the left of the frame plane; to retain balance the frame must therefore lean left. In low-speed turns, therefore, *the frame leans to the outside*. Only above a certain minimum speed (defined approximately by $V = [g L_{MT} \tan \Theta_L]^{1/2}$) does the bicycle frame actually lean toward the center of the turn.

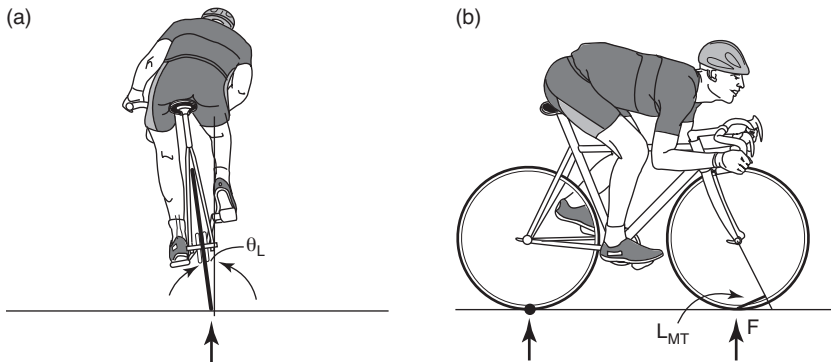


Figure 8.12

Steering torque from frame tilt when riding straight: (a) rear view; (b) side view. The center of mass will be over the support line connecting the wheel contacts. The vertical force at each wheel can be resolved into two components parallel and perpendicular, respectively, to the wheel plane. The ground force (F) supporting the front wheel tends to turn it leftward, with moment $F L_{MT} \sin \theta_L$. In addition, the scrub torque at the front contact and the handlebar weight also promote leftward steering.

In no-hands riding, and if gyroscopic torques and special tire contact-patch torques are ignored, the bicycle's center of mass is at its maximum height in the *balance plane* defined by the center of mass and the two ground contacts. The handlebar torque is zero (i.e., the steering is in the balanced orientation). The tendency of the bicycle to turn to one side, or equivalently the need for torso lean to keep it traveling straight, is in this case a sensitive indicator of various asymmetries. At moderate speeds, the principle that the steering can achieve equilibrium only by turning against any disturbing torque can predict no-hands handlebar orientation qualitatively. Here are some examples:

- Applying a clockwise (rightward) torque bias to a bicycle's steering (e.g., with a taut rubber band from the seat post pulling on a string wrapped around the steering axis) ultimately leads to the steering's being turned counterclockwise (i.e., a leftward turn). Alternatively, the rider's torso must lean to the right of the frame, so frame lean creates a countering leftward torque.
- Intentionally misaligning a bicycle's front wheel relative to the forks (say, bottom displaced to the left of the rider and top to

the right) also creates a steering torque initially tending to turn the handlebars (rightward, in this case). In equilibrium they are therefore turned leftward: the bicycle curves to the left. Misaligning the rear wheel so that its forward edge is moved rightward also generates leftward steering.

- Torso lean to the left of a bicycle's frame tilts the frame to the right, generating a torque tending to turn the steering right. The equilibrium configuration therefore involves steering to the left. Relative to the frame's midplane, the cyclist leans in the direction of the intended turn and then straightens the torso to return the bicycle upright.

However, all these zero-radius-wheel models (and also those assuming three-dimensional but rigid tires) leave out the potentially important contribution of tire scrub torque: because of the finite size of its contact patch, a vertical wheel traveling in a circle requires a steering torque to keep it going around a turn. Scrub torque arises as a result of this turning, because an element of the tire at the front of the contact patch is moving inward relative to its path of travel, and an element at the rear of the patch is moving outward.

Correcting the Straight-Line Steering Torque of an Imperfect Bicycle

A bicycle that is not perfectly symmetrical generally requires an annoying steering torque, or an upper body lean, to travel straight when ridden with no hands. (A bicycle may of course be constructed asymmetrically on purpose, as was a bicycle for ladies sitting sideways, made by Ariel in 1872.) It is conventional to check a bicycle's wheel alignment by placing a straightedge at two points of the rear wheel near ground level (i.e., parallel to the intersection of the wheel plane and ground plane) and determining whether the front wheel grazes the same straight-edge when turned parallel to it. But this test alone cannot indicate whether straight-line riding on the bicycle will require a steering torque.

Straight-line riding requires only that the ground traces of the bicycle's wheels (i.e., the line of intersection of each wheel plane and the ground plane) be parallel. In that condition, with the bicycle in balance, steering torque arises whenever the steering axis does not pass directly above the front contact or does not pass directly below the front-assembly center of mass. Any of a number of factors (load

imbalance, wheel tilt or offset, steering-axis misplacement) can give rise to steering torque, and any other of those same factors can be altered to reduce or cancel that torque. It's probably simplest just to make every component of the bicycle symmetric in the usual sense.

Stability

One of the questions related to bicycling that can be studied via equations involves a bicycle's intrinsic stability: When does an *uncontrolled* bicycle automatically tend to ride straight and upright?

In the field of dynamics, *stability* has a precise meaning. For the purposes of the discussion here, a steady motion (such as rolling straight and upright) is stable if, after it is disturbed, it eventually settles down to being steady again. In the technical sense, a well-aligned riderless conventional bicycle with freely turning steering bearings is stable over a range of speed that depends on its design (say, 3–6 m/s). If it is bumped while it is in motion, it will soon return to straight upright running. The nature of its stability is defined by a settling time (how quickly the disturbance dies away) and possibly a frequency, if the system (e.g., the steering) tends to oscillate while settling down to steady motion. Note that nothing in this entire section addresses the question of suspension, which of course can further change bicycle (or vehicle) behavior.

Unfortunately, hands-off stability with no rider input of any kind does not seem to have much to do with a bicycle that feels stable. For example, all standard (uncontrolled) bicycles and motorcycles lose stability both at low speeds (when they execute greater and greater weaving oscillations) and also theoretically at high speeds (when they fail to recover from a turn and instead progressively increase their lean and turn angles in a spiraling crash). But no competent rider has much cause for complaint when riding a typical bicycle at speeds between 2 and 15 m/s.

Experienced cyclists actually seem to redefine the technical term *instability* to mean “oversensitivity to small input torques.” That is, a bicycle could be perfectly stable at a certain speed with a no-hands rigid rider and yet might seem too skittish, or even unsafe, if each little shift of body weight or hand pressure caused a large steering deviation, as has been suggested by Andy Ruina; this idea also forms the basis of Patterson's method.

Having offered some caveats about the limited significance of technical stability studies, we still find it interesting to ask when an uncontrolled bicycle is stable. It's an intriguing scientific question and may help in identifying more important issues regarding bicycle handling (see Society of Automotive Engineers 1978 and 1979, two important collections of papers on motorcycle-related stability).

Bicycle-dynamics equations can reveal no-hands and uncontrolled stability by any of several routes:

- By direct simulation (i.e., instant-by-instant numerical solution of the involved differential equations) to calculate the motion of a bicycle starting from a small initial lean. Inspection of the simulations results can reveal whether the bicycle straightens up or crashes. It doesn't really matter what the small initial disturbance is (e.g., a lean, bump, or wind gust): an unstable bicycle will almost always wobble or fall, and a stable one will always straighten up. The disadvantage of this approach is that it is hard to determine general rules from specific cases (see Roland 1973).
- If constant-coefficient equations are solved exactly by standard algebraic methods, stability is revealed by the resulting eigenvalues (exponential growth factors). These are generally complex numbers, their real parts (x -coordinates) reflecting growth tendency, and their imaginary parts (y -coordinates) indicating oscillation frequency. If their real parts are all negative, then steering disturbances decrease over time, whereas if any one eigenvalue has a positive real part, then its corresponding pattern of disturbance is predicted to grow infinitely. This approach has disadvantages similar to those of the previous one: the algebraic eigenvalue formulas are too complex to use, so eigenvalues are generally determined numerically for specific cases of interest.
- If the main interest is in identifying a simple criterion of stability, and not the details of a bicycle's motion as it either straightens up or crashes, then the *Routh-Hurwitz stability criteria* may be employed. According to these criteria, if four specific algebraic quantities (functions of velocity and bicycle parameters) are all positive, a given bicycle will be stable. If a bicycle is stable at a certain speed, then altering the design or the speed may destroy that stability. Loss of stability is revealed by monitoring just two of the four quantities. Some conclusions of this approach follow.

Nonoscillatory Instability

The simplest criterion for establishing a bicycle's stability is just the condition that in a steady turn, it should try to sharpen its steering angle. In other words, the steady-turn handlebar torque required of the rider must be such that it restrains the steering from turning further. If an uncontrolled bicycle lacks this property, it never pulls itself out of a turn but gradually increases its lean and steering angles while following a tighter and tighter spiral, a phenomenon referred to in the motorcycle-stability literature as *capsizing*.

In a conventional bicycle, the steering geometry and the front-assembly center of mass position, which together tend to increase any steering angle if the bicycle is balanced, afford turn-sharpening behavior at low speeds. But at high speeds, gyroscopic "stiffening" effects reduce the steering's geometry-based turn-sharpening tendency. Because a bicycle's steering axis is not vertical, some of the "tipping" torque needed to overcome the front wheel's gyroscopic resistance to continually changing its heading must be supplied through the handlebars. At low speeds, the required steering torque is minuscule, but when the bicycle is traveling faster, it significantly reduces the geometry-based tendency of the steering to sharpen the turn. Finally, at a critical "inversion" speed, there is theoretically no need for steering torque or upper-body lean to hold any turn. Above the inversion speed, the bicycle's steering will tend to self-center, thus reversing the ordinary sense of required handlebar torque or torso lean.

In principle, all conventional bicycles and motorcycles possess a steering-torque inversion speed, and above this speed they will display the mild nonoscillatory instability described earlier (i.e., they will capsize). For typical ridden bicycles, this speed is in the range of 5–8 m/s. But in actual bicycle riding, torque reversal and instability are not very apparent.

The tendency of an uncontrolled bicycle to capsize at high speed is not a matter for concern to most riders. The instability that results from this tendency is so slight that it takes many seconds to develop, and riders' slight unconscious upper-body motions probably suffice to compensate for it.

However, at low speeds, violation of the turn-sharpening criterion for stability through poor design causes an uncontrolled bicycle to capsize far more quickly. Since gyroscopic effects are then

negligible, the requirement is for maintaining stability in a poorly designed bicycle essentially static and may be stated in either of two equivalent ways:

- The upright, straight bicycle must be at an absolute maximum of potential energy with regard to any combination of reasonable steering and lean angles.
- A stationary, balanced bicycle, if its handlebars are turned *while balance is maintained*, must lower its center of mass, or equivalently, must generate a steering torque that tends to increase the steering angle.

A bicycle with a vertical steering axis and negative fork offset to produce a trailing front contact does not satisfy these requirements. With the bicycle at rest, steering the front wheel to the left, and tilting the entire bicycle to the right to bring it into balance, *raises* the center of mass.

The turn-sharpening stability criterion can be given as a simple design formula if the normally small front-assembly mass offset forward of the steering axis, which tends to turn the steering if the stationary bicycle is held in balance with its steering turned (see Papadopoulos 1987), is ignored. The criterion for automatically straightening up is then

$$0 < (x_{CM}/y_{CM})(L_{MT}/L_W) < \sin \lambda,$$

in which L_W refers to the wheel base. That is to say, the mechanical trail and the rearward tilt of the steering axis must be positive. This last relation can be shown geometrically (figure 8.13):

- draw a line from the rear contact through the system center of mass;
- call the point on this line vertically above the front contact (P in the figure); and then
- the steering axis must intersect the ground ahead of the front contact and pass below P and above the front contact. In fact, with normally large bicycle wheels, it is usual for the steering axis to pass below the front-wheel center, which is to say that the front fork has a positive offset.

Who was the genius who thought of tilting a bicycle's steering axis, as was done with some very early bicycles, and why was it originally done? The development of a tilted steering axis is one of

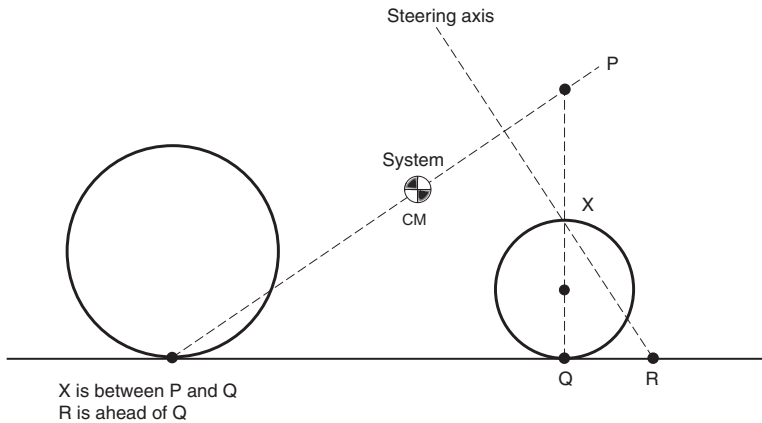


Figure 8.13

Geometric stability requirement for negative turns (which restricts the position of the steering axis).

the major mysteries of bicycle evolution. John Allen (personal communication, 2001) writes:

In the early days of the safety bicycle, the handlebars were placed close to the cyclist, as had been traditional and necessary with high-wheelers, with their very serious pitchover problem. High-wheelers had little or no forward angling of the front fork: it would not have been practical because it would have prevented the cyclist from standing over the pedals, and would have placed the force vector from pedaling too far from the steering axis, making steering difficult. Bicycle evolution involved innumerable experiments, but the answer is most likely mundane: the fork was angled forward in order to keep the handlebars close to the cyclist, and for the front wheel to clear the feet, in spite of what intuitively would seem to be a stability reduction.

A bicycle can also exhibit *oscillatory* instability. (By this we do not mean *shimmy*, which is described later in the chapter).

Stability of Tricycles and Related Vehicles

As outlined at the beginning of this chapter, tricycles and other multitrack vehicles act very differently from bicycles in numerous ways. In fact, when bicyclists ride an upright tricycle the first time, it feels very odd, and the countersteering bicyclists unconsciously use to create lean for in-balance cornering poses additional risk on an upright tricycle of rolling over or collapsing a wheel. (Recumbent

tricycles, on the other hand, do not have this problem and are easier to ride than bicycles at low speeds and when stopped or starting.) Some of the conditions for bicycle stability stated in the preceding sections no longer apply to tricycles or are reversed, as there is no lean angle to worry about, just the steering angle. For normal bicycle geometry, the wheel-flop factor tends to decenter the steering. For tricycles, however, this decentering is a cause of instability and no advantage. It becomes possible to use the wheel-flop factor to center the steering at slow speeds, as is done with the Python center-steered low racer (see panel [c] of figure 8.10).

Although stability and steering appear unproblematic for tricycles at low speeds, this is no longer the case for higher speeds, at which rollover stability and tire-related and aerodynamic yaw stabilities are not always assured. Whereas a bicycle can adjust somewhat to the rider's swinging legs by rolling, a tricycle is not free to roll, so that the outside wheels experience periodic changes of load. In addition, poor wheel alignment and sloppy steering mechanisms are more readily apparent in riding tricycles rather than bicycles.

We cannot, for space reasons, give more than an overview of the extensive field of multitrack-vehicle stability, for which there is extensive literature, but we raise a few of the most important points in the following sections.

Rollover Stability If the point (line) of support in figure 8.3 is taken to represent the line between contact patches of the *outside* wheels of a turning quadracycle, this shows the limit just when the inside wheels (not shown in the figure) become completely unweighted and the vehicle begins to roll over, when traveling at a critical speed $V = (R_T g \mu)^{1/2}$. However, if the height of the center of mass (y in the figure) is smaller than half the width between tires (x in the figure) divided by the tire coefficient of friction μ , the vehicle will slide laterally instead of capsizing. Of course this applies only to a quadracycle with two equidistant tracks. For other configurations and tricycles, the longitudinal location of the center of mass is important, the rollover stability obviously being reduced the nearer the center of mass is to the single wheel. The criterion given is only a rough guide anyway, especially for high-center-of-mass vehicles going around sharp corners, which are easy to tip onto two

wheels or to capsize completely. However, going fast on country roads rarely approaches the lateral acceleration needed to slide or capsize, and other steering instabilities may occur first. Note that μ values approaching 1.0 are achievable (doing so requires sideslip, described in chapter 6) but imply a lateral acceleration of 1 g (about 9.8 m/s^2), which few riders could manage, even if they weren't flung away first. In addition, the discussion here does not take into account beneficial road banking or adverse camber, either of which may contribute to tipping a tricycle, as may even small obstructions in the road surface. However, the coauthor extensively rode and even raced his two short-wheelbase, high-center-of-mass tricycles with very limited stability and never came even near a rollover situation or saw one occur in numerous HPV races during curves. Both authors have, however, seen several HPVs roll over after going out of control during straight-line riding.

In spite of its unlikelihood in most situations, many people riding tricycles feel a real fear of rollover in curves, and various projects feature leaning tricycles, either automatically or imitating the behavior of a bicycle, and only locking the normally free roll axis at very slow speeds. The coauthor's 1986 tricycle, with this in mind, was designed to lean, but after a single very tottering ride, he decided to lock its roll axis permanently. As the mechanism doubled as a suspension, it rolled the wrong way in curves, but the tricycle was still perfectly rideable. Dong et al. (2014) show, especially in a very illustrative video showing their Bricycle, what may additionally be involved when trying to get a tricycle to behave as a bicycle. The student HPV Mjölfnir (see Bamford et al. 2011) was a leaner, and in spite of very extensive design work, came to grief on its first run, influenced by a gust of wind. From this anecdotal evidence, it seems in practice that for tricycle riding, stability during straight-line riding and controllability in wind are more important than great rollover stability.

Tire-Related Yaw Stability Huston, Graves, and Johnson (1983) examine straight-line tricycle stability, giving detailed calculations for what they call the "lateral stability" of tricycles and quadracycles: their ability to correct for yaw in the right direction when disturbed, and thus a prerequisite for stable straight-line riding. This ability has to do with tire properties (slip angle and cornering stiffness) and the

longitudinal location of the vehicle's center of mass. Below rather high critical speeds (starting at 25 m/s in the examples they give) nothing happens; the vehicle rolls straight. If the vehicle's center of mass is located enough forward that the front tires are loaded more than the rear ones (i.e., forward > 50 percent of the wheelbase L_{WB} for a quadracycle, $> \frac{1}{3} L_{WB}$ for a tricycle with one front wheel, and $> \frac{2}{3} L_{WB}$ for a tricycle with two front wheels), the critical speed is infinite, that is, the vehicle's stability (in this respect) is always assured. If, however, the center of mass is further back, the vehicle's stability isn't assured, and it could spin out of control above the critical speed, which nonetheless seems high enough so as to be of minor concern for practical HPVs.

Huston, Graves, and Johnson (1983) also examine tricycle roll-over stability in turns. When braking in a curve, they find it is better to have two wheels in front, because of the direction of the total force vector. For accelerating in a curve it is the opposite: two rear wheels are better.

Stability of Rear-Steered Vehicles With the feasibility of even rear-steered bicycles having been mentioned earlier in the chapter, the design of rear-steered tricycles should be easy. Indeed, the coauthor has seen at least one design with a single steered rear wheel work perfectly from the start. The advantage of this configuration for an HPV is the possibility of a simpler, narrower fairing. Of course, as with most boats, which are almost all rear-steered, care must be taken to always keep enough lateral distance to accommodate the stern, which swings out sideways during turns.

However, rear steering involves instabilities in yaw (oscillations) that are not a problem in front steering. John Whitehead (1990) discusses these and presents some solutions, such as adding a steering damper or active control elements. He lists numerous previous articles on rear steering.

Aerodynamic Roll and Yaw Stability While steady winds are no great danger to bicycles and many HPVs, which indeed can be sailed, such winds are rare on most roads, which are lined with buildings or plants, giving rise to turbulence. Even on clear roads with steady winds, other vehicles, notably trucks, can cause severe gusting. It is thus a clear design goal for bicycles and HPVs, as discussed in chapter 5, to minimize their sensitivity to gusting.

Shimmy

Shimmy is an unnerving bicycle instability that can sometimes cause an inexperienced rider to crash. When a bicycle undergoes shimmy, the steering oscillates right and left several times per second, with growing amplitude. Similar wheel vibrations are well known in airplane nose wheels, wheelchair and shopping-cart casters (castor flutter), and motorcycles (in which a violent occurrence of shimmy has been called a “tank slapper”). Wikipedia refers to all of these phenomena as “speed wobble.” A similar “trailer-wobble” effect can occur with trailers and also with two-wheeled cycle trailers, at a lower frequency. Particularly bad wobble is incurred in strings of trailers, although it is brought about by *weaving* (repeated yawing), described in chapter 10.

Before outlining an explanation for shimmy, it is worth considering what to do if it happens. Shimmy presents a danger when a cyclist panics and attempts actively to fight the shimmy by applying countertorque to the bicycle’s handlebars. Because the shimmy frequency is so high, the muscular response occurs too late, possibly accelerating the handlebars when they are already well on their way to the other side and increasing the oscillation. As long as the cyclist does not compound the problem through active intervention, any of several different methods seems to stop the oscillation at once:

- Reducing weight on the saddle (by standing slightly) deprives the vibrating system of a key restraint and adds considerable damping.
- Clamping the top tube of the frame between the rider’s knees tremendously alters the vibrating mass and also adds damping.
- Lightly using the hands in a passive “resisting” or “motion-reducing” mode also increases damping.

Shimmy Theory

No-hands shimmy appears at a critical speed and grows to a final steady amplitude at any higher speed, with greater amplitudes for greater speeds. The frequency of shimmy is relatively unaffected by speed, as it is mainly a resonance effect. The frame of a bicycle, its fork, its wheels and its tires together with their “connections” to

the ground, through their spring rates and masses and the large but loosely connected mass of the rider, form a strongly damped oscillator. Even before the shimmy is noticeable at the bicycle's handlebars, strong oscillations can be initiated and felt by striking the front of the bicycle laterally while moving. The higher the riding speed, the longer these oscillations take to disappear, and eventually they may not disappear and may develop into a severe shimmy.

Contributing causes of bicycle shimmy can include an untrue wheel, a flexible frame or fork, loose bearings, or gyroscopic effects. Although these factors can help initiate or worsen shimmy, they are clearly not essential to the phenomenon. A key bit of evidence for this conclusion is the constancy of shimmy frequency at different bicycle speeds. In contrast to this constancy, an untrue wheel will create a steering disturbance once each wheel revolution, and the gyroscopic precession of a rotating wheel involves wobbling twice per revolution. Loose bearings, on the other hand, can induce shimmy even in wheels that are supposed to be fixed, for example, in shoddily manufactured three-wheeled microscooters.

Shimmy is a self-excited oscillation: there is no alternating force turning the bicycle's handlebars back and forth except that generated by their motion. In instances of shimmy, the equation of motion shows a negative number for vibration damping, causing vibrations to grow rather than decay. The vibration energy is provided by the moving bicycle.

It is not our intention here to present a detailed dynamic analysis of shimmy, and indeed many aspects of the phenomenon remain in question. But it is both appropriate and feasible to present a simple system with bicycle-like features and explain how shimmy arises in the case of that system.

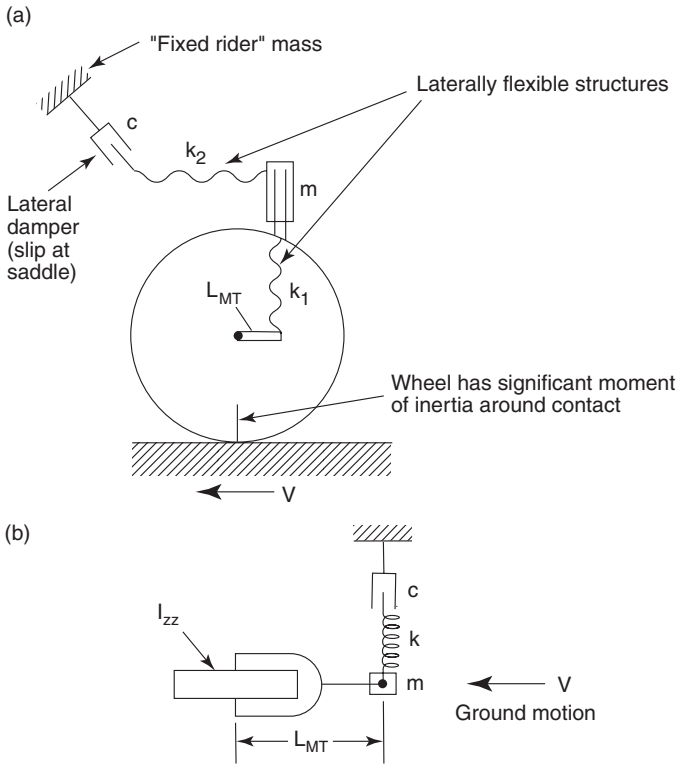
A castered wheel (like the front wheel of a bicycle, which is physically being towed if it has positive trail), or more generally, any rolling system with trail, such as a trailer, is capable of surprising energy interchanges with the unit that is towing it. In a situation in which the connecting hitch (or pivot axis) oscillates back and forth laterally, details of the distribution of its mass affect the side force it imposes on the ground. Because of the trailer's angular deviation from the straight-line path of the towing vehicle, the trailer wheel's side force on the ground has a fore-aft component that will either propel the towing vehicle (as does the tail of a fish) or retard it.

Imagine a person sitting at the back of a pickup truck that drives along a straight road, and imagine that the person is holding a trailer hitch and swinging it side to side to make the trailer follow a sinusoidal path. If the result is to propel the truck forward (i.e., do work on the truck), then the side-to-side motion will require effort (power) from the person moving it. On the other hand, if the result is to retard the truck, power from the truck's engine will flow into the person's hand, and the hitch will try to "run away" to either side.

A very simple distribution of mass that is seen to pump energy into a vehicle hitch can be represented by a large polar moment of inertia centered at the hitch's pivot axis. If the system is traveling forward fast enough that the hitch length is far smaller than a wavelength of the oscillation on the road surface, then the angle of the trailer towbar is essentially aligned with the path of the wheels. It can be seen that the rotation rate of the trailer is maximum rightward at the far left crest of the oscillation and maximum leftward at the far right crest. Maximum angular acceleration occurs as the trailer crosses the center line of the oscillation. What is important is that the force required to cause angular acceleration is opposite to the hitch velocity: as the hitch moves from left to right, the force of the hand holding the hitch is directed to the left. In other words, the trailer pumps power into the arm of the person holding it, trying to increase the speed of its lateral motion in both directions, right and left.

Given that a towed wheel (or trailer) with appropriate inertial properties is capable of pumping energy into lateral oscillation, such oscillations are to be expected. When energy-absorbing devices (dampers) are present, it is to be expected that a higher speed must be attained before the power delivered at the hitch can overcome the damping tendencies. Figure 8.14 shows a simple system analogous in several ways to a bicycle's front end viewed from the side and from above. The system has the following elements:

- A wheel or contact point towed a trailing distance (L_{MT}) behind a hitch point (analogous to the front-wheel contact point's being towed behind a "hitch point" low on the steering axis).
- A significant polar moment of inertia (I_{ZZ}) of the towed wheel: a conventional bicycle wheel has much of its mass quite far away in comparison to the trail.



Simpler one-dimensional model (ignoring tire flex and scrub)

Figure 8.14

Simple shimmy model (trailer oscillates because of motion of ground): (a) side view; (b) top view of simpler model.

- The mass (m) of the bicycle head-tube area, whose lateral inertia force is transmitted simultaneously to the steering axis (or hitch) through a spring with stiffness (k_1) and to the rider through a spring with stiffness (k_2).
- The rider's mass, much greater than that of the head-tube area, is assumed not to move laterally during the vibration. If the head-tube-area mass is moved laterally while the wheel is not permitted to steer, k_1 and k_2 can be represented by a composite stiffness (k), derived mainly from the torsional flexibility of the frame, including forks.

- A damper c in series with k to represent the energy-absorbing connection between the frame and rider (i.e., slip at the bicycle's saddle). A firm connection is modeled by a large value of c .

In this basic system, shimmy is predicted when velocity exceeds $V = k L_{MT}/c (1 + I_{ZZ}/m L_{MT}^2)$, or approximately $V > k I_{ZZ}/(m c L_{MT})$.

This relationship implies that it is important to keep stiffness high, damping constant low, head-area mass low, and mechanical trail either much less, or much greater, than $(I_{ZZ}/m)^{1/2}$. The great surprise in the relationship is the apparent value of increasing I_{ZZ} , which presumably helps by reducing the amplitude of steering excursion. The frequency (in radians per second) is $\omega = (k/m[1 + \{m L_{MT}^2/I_{ZZ}\}])^{1/2}$, identical to the oscillation frequency of the system at rest, as long as the energy dissipation is not too great (i.e., as long as the value for c is large—see later discussion).

This model fails to include tire sideslip or such known problems as flexibly mounted rear luggage. But it agrees with the following observations and research by Jim Papadopoulos and others:

- If a bicycle's saddle is restrained by pressing it against a door jamb, the head tube has a clearly defined lateral resonance at several cycles per second.
- Experimental data by Magnani et al. (2013) support the conjecture that shimmy while riding occurs essentially at this same frequency, which is usually between 5 and 10 Hz and at accelerations of 5–10 g.
- Shimmy can be sustained at widely different speeds depending on the firmness of the rider's connection to the saddle (denoted by c in the foregoing discussion). By reducing saddle pressure, shimmy onset speed can be raised above 17 m/s. Conversely, by increasing pressure and lateral firmness (by exerting upward pedal forces and contracting the muscles of the buttocks), it is possible to sustain shimmy at 5.5 m/s.

No-hands shimmy experiments have found that slightly exceeding the speed at which the onset of shimmy occurs brings about sustained oscillations at a medium amplitude. Higher speeds clearly increase the steady amplitude, but not dramatically. Unfortunately, it is not possible to use this model to predict the speed at which the onset of shimmy will occur, because c is an unknown quantity. The best that can be done is to use the onset observations

given earlier to determine the range of c . Taking m as 1 kg and k as 1,000 N/m to yield a reasonable static frequency, guessing that L_{MT} was 40 mm for the bicycle ridden in the experiments, and taking I_{zz} for the wheel as half of mass times radius squared, or $(1 \text{ kg})(0.35 \text{ m})^2/2$, suggests c values from 260 kg/s (sitting firmly) to 70 kg/s (sitting very relaxedly).

The latest work by Tomiati et al. (2017) includes computer simulations that do include tire sideslip and support the foregoing analysis. They show that the main elements that contribute to the rise of oscillations are the lateral compliance of the bicycle's frame and the tires' deformation.

To summarize, bicycle shimmy vibrations depend on the combination of elastic flexibility with inadequate damping. With foreknowledge of the shimmy phenomenon, a rider can generally learn to provide adequate damping to prevent shimmy or arrest it when it occurs.

References

Almujahed, Aamer, Jason Deweese, Linh Duong, and Joel Potter. 2009. "Auto-Balanced Robotic Bicycle (ABRB)." ECE-492/3 Senior Design Project. Electrical and Computer Engineering Department, Volgenau School of Engineering, George Mason University, Fairfax, VA. https://ece.gmu.edu/sites/ece/files/S-09-ABRB_0.pdf.

Archibald, Mark. 2016. *Design of Human-Powered Vehicles*. New York: ASME Press.

Åström, K. J., R. E. Klein, and A. Lennartsson. 2005. "Bicycle Dynamics and Control." *IEEE Control Systems Magazine* 25, no. 4: 26–47. <http://lucris.lub.lu.se/ws/files/4692388/625565.pdf>.

Bamford, Tad, Ben Higgins, Neal Pang, Chris Schultz, and Aaron Stanton. 2011. "2011 Human Powered Vehicle: Mjölnir." ME 493 Final Report, Portland State University Mechanical Engineering Department, Portland, OR. [http://web.cecs.pdx.edu/~far/Past Capstone Projects/2011/HPV/2011 ME 493 Human Powered Vehicle Design Report.pdf](http://web.cecs.pdx.edu/~far/Past%20Capstone%20Projects/2011/HPV/2011%20ME%20493%20Human%20Powered%20Vehicle%20Design%20Report.pdf).

Davol, A., and F. Owen. 2007. "Model of a Bicycle from Handling Qualities Considerations." *ME 441—Single-Track Design* (course web page). California Polytechnic State University, San Luis Obispo. <https://www.calpoly.edu/~fowen/me441/index.html>.

De Jong, P. H. 2017. "Rear Wheel Steer Bikes: Unconventional Stable Bicycle." Master's thesis, Delft University of Technology, Delft, Netherlands. <http://resolver>

.tudelft.nl/uuid:76f67586-ab15-4c85-9841-544259b3be82 (embargoed until February 24, 2022).

Dong, O., C. Graham, A. Grewal, C. Parrucci, and A. Ruina. 2014. "The Bricycle: A Bicycle in Zero Gravity Can Be Balanced or Steered but Not Both." *Vehicle System Dynamics* 52, no. 12: 1681–1694. http://ruina.tam.cornell.edu/research/topics/bicycle_mechanics/brike_paper23-proof_corrections.pdf and <https://www.youtube.com/watch?v=rNQdSfgJDNM>.

Dressel, Andrew. 2015. "Benchmarking a Fully Non-Linear Bicycle Model with JBike6." Cornell University, Ithaca, NY. http://ruina.tam.cornell.edu/research/topics/bicycle_mechanics/JBike6_web_folder/JBike6_Benchmarking.htm.

Forester, John. 2012. *Effective Cycling*. 7th ed. Cambridge, MA: MIT Press.

Hand, Richard Scott. 1988. "Comparisons and Stability Analysis of Linearized Equations of Motion for a Basic Bicycle Model." MS thesis, Cornell University, Ithaca, NY. http://ruina.tam.cornell.edu/research/topics/bicycle_mechanics/comparisons_stability_analysis.pdf.

Harter, Jim. 1984. *Transportation: A Pictorial Archive from Nineteenth-Century Sources; 525 Copyright-Free Illustrations Selected by Jim Harter*. New York: Dover.

Huston, J. C., B. J. Graves, and D. B. Johnson. 1983. "Three Wheeled Vehicle Dynamics." In *Proceedings of the Second International HPV Scientific Symposium*, ed. Allan Abbott, 123–135. San Luis Obispo, CA: International Human Powered Vehicle Association.

Jones, D. E. H. 1970. "The Stability of the Bicycle." *Physics Today* (April): 34–40. http://www.phys.lsu.edu/faculty/gonzalez/Teaching/Phys7221/vol59no9p51_56.pdf.

Kooijman, J. D. G., J. P. Meijaard, Jim M. Papadopoulos, Andy Ruina, and A. L. Schwab. 2011. "A Bicycle Can Be Self-Stable without Gyroscopic or Caster Effects." *Science* 332, no. 6027: 339–342. <http://bicycle.tudelft.nl/stablebicycle/StableBicycleV34Revised.pdf>.

Magnani, Gianantonio, Nicola Maria Ceriani, and Jim Papadopoulos. 2013. "On-Road Measurements of High Speed Bicycle Shimmy, and Comparison to Structural Resonance." In *2013 International Conference on Mechatronics (ICM)*, 400–405. <https://www.doi.org/10.1109/ICMECH.2013.6518570>.

Olsen, John, and Jim Papadopoulos. 1988. "Bicycle Dynamics—The Meaning behind the Math." *Bike Tech* (December). http://ruina.tam.cornell.edu/research/topics/bicycle_mechanics/bicycle_dynamics.pdf.

Papadopoulos, Jim. 1987. "Bicycle Steering Dynamics and Self-Stability: A Summary Report of Work in Progress." Cornell Bicycle Project report, December 15. http://ruina.tam.cornell.edu/research/topics/bicycle_mechanics/bicycle_steering.pdf.

Patterson, William B. 1998. "Single-Track Vehicle Dynamics." In *Proceedings of the Third European Seminar on Velomobile Design, Roskilde, Denmark, August 5*. <https://velomobileseminars.online>.

Python. 2018. "Frame Geometry." python (website). <http://www.python-lowracer.de/geometry.html>.

Rohmert, Walter, and Stefan Gloger. 1993. "The Test-Vehicle MULTILAB and Its New Front-Wheel Geometry: Less Interference of Hells and Front Wheel." In *Proceedings of the First European Seminar on Velomobile Design, Technical University of Denmark, Kongens Lyngby, July 8*. <https://velomobileseminars.online>.

Rohmert, Walter, and Stefan Gloger. 1994. "Evaluation of the Handling Characteristics of a Human Powered Vehicle with a Mirror-Symmetric Front-Wheel Geometry."

Roland, R. D. 1973. "Computer Simulation of Bicycle Dynamics." In *ASME Conference on Mechanics and Sports*, 35–83. New York: American Society of Mechanical Engineers.

Ruina, Andy. 2014. "Bicycle Mechanics and Dynamics—Papers." Cornell University, Ithaca, NY. http://ruina.tam.cornell.edu/research/topics/bicycle_mechanics/papers.html.

Schnieders, Jürgen, and Thomas Senkel. 1994. "Recumbents with Rear Wheel Steering." In *Safety and Design: Second European Seminar on Velomobiles/HPV, Laupen Castle, Switzerland, August 25, 1994*. <https://velomobileseminars.online>.

Schwab, Arend L. 2009. "History of Bicycle Steer and Dynamics Equations Delft University of Technology, Delft, Netherlands. <http://bicycle.tudelft.nl/schwab/Bicycle/BicycleHistoryReview/>.

Schwab, Arend L. 2017. "Bicycle Dynamics." Delft University of Technology, Delft, Netherlands. <http://bicycle.tudelft.nl/schwab/Bicycle/>.

Schwab, Arend L., and J. D. G. Kooijman. 2014. "Balance and Control of a Rear-Wheel Steered Speed-Record Recumbent Bicycle" (paper presented at the 10th Conference of the International Sports Engineering Association, Sheffield, UK). *Procedia Engineering* 72: 459–464. <https://repository.tudelft.nl/islandora/object/uuid:57f85414-fe2d-4e83-a683-142f011ede96/datastream/OBJ/download>.

Schwab, Arend, and J. P. Meijaard. 2013. "A Review on Bicycle Dynamics and Rider Control." *Vehicle System Dynamics* 51, no. 7 (July). https://www.researchgate.net/publication/263686076_A_review_on_bicycle_dynamics_and_rider_control.

Sharp, Archibald. 1896. *Bicycles and Tricycles*. London: Longmans, Green. Reprint, Cambridge, MA: MIT Press, 1977.

Society of Automotive Engineers, International Automotive Engineering Congress and Exposition. 1978. "Motorcycle Dynamics and Rider Control." Paper no. SP-428, Society of Automotive Engineers, Warrendale, PA.

Society of Automotive Engineers, International Automotive Engineering Congress and Exposition. 1979. "Dynamics of Wheeled Recreational Vehicles." Paper no. SP-443, Society of Automotive Engineers, Warrendale, PA.

Tomati, Nicolò, Gianantonio Magnani, Bruno Scaglioni, and Gianne Ferretti. 2018. "Model Based Analysis of Shimmy in a Racing Bicycle." Paper presented at the 12th International Modelica Conference, Prague, May. https://www.researchgate.net/publication/316990951_Model_Based_Analysis_of_Shimmy_in_a_Racing_Bicycle.

Whitehead, John C. 1990. "Rear-Wheel-Steering Basics." *Human Power* 8, no. 4 (Winter): 9–12. <http://www.ihpva.org/HParchive/PDF/28-v8n4-1990.pdf>.

9 Power Transmission and Hybrid Systems

Introduction

A transmission is the connection between a vehicle's power source and the driving wheel(s). Its purpose is to transmit power with as little loss as possible, and (in the case of bicycles) to transmit it in a way that enables the rider's limbs to move in as near optimum a manner as possible. A bicycle's transmission therefore encompasses two basic functions: to transmit power from the rider's feet or possibly hands (or both) to its wheels, and to do so in such a way that at one favored speed, at least, and perhaps over a range of speeds, the rider either is exerting maximum possible power or is producing a lesser amount of power in maximum comfort.

In spite of countless measurements, efficiency curves as a function of both pedaling speed and torque are rare. Figure 9.1 offers one presentation of measurements by Sergio Savaresi and members of the mOve research team at the Politecnico di Milano (see Savaresi 2014), for a "normal" (not sporty) subject. This interesting diagram allows us to make a number of observations. For the data set used here, it appears optimal to pedal at 65–70 rpm at low powers, decreasing to about 40 rpm at 200 W, then rapidly increasing to 90 rpm at 500 W. However, a linear increase from 70 to 90 rpm results in only 1 percentage point less efficiency at medium power. A good transmission should therefore provide for gear ratios that allow pedaling a bicycle at least within this range from steeply uphill to slightly downhill.

Important secondary aims for a bicycle's transmission include little flexibility or play, no undue jerking, enabling the rider's down-moving leg to lift the rider's up-moving leg, absence of large variations in the leg's kinetic energy, and perhaps enabling the bicycle

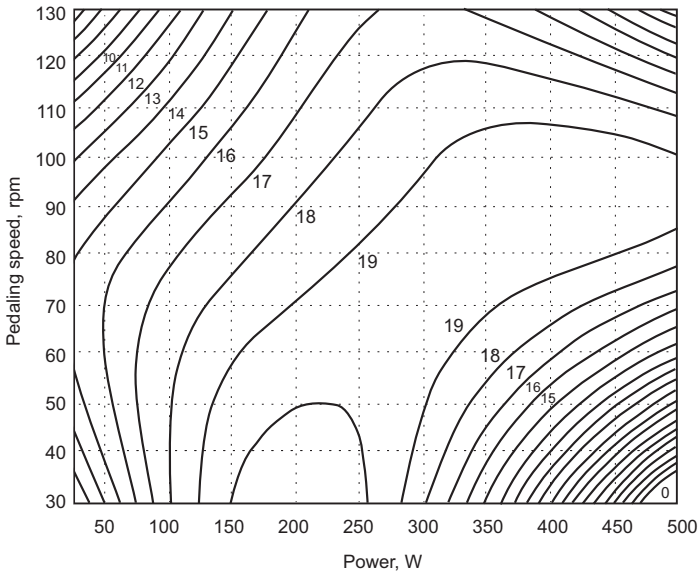


Figure 9.1

Contour lines of human gross efficiency (mechanical power output / metabolic power input, in percent) as function of power output and pedaling speed. (Redrawn, with permission, from Savaresi 2014.)

to be wheeled backward. A third function is permitting the optimal mixing in of additional hybrid power sources in power-assisted vehicles. This chapter reviews the principles of the standard form and of alternative means of power transmission in bicycles, examines some examples, and discusses some past and present developments in the area of e-bicycle power transmission.

One starting point for this examination is existing knowledge about the generation of human power, which is limited to the circular or linear foot and hand motions used in existing bicycles, rowing boats, and ergometers. With the exception of the speed variations given by elliptical chainwheels or similar mechanisms, the foot velocity in rotary pedaling is a constant proportion of the wheel velocity. Therefore, although it may seem, instinctively, that there are other foot, hand, or body motions (or combinations of these) that could enable humans to produce higher levels of maximum power (higher than the upper curves in figures 2.4 and 2.9) or equal levels of power at greater levels of comfort, scientific knowledge

confines the discussion to rotary or roughly linear motions as inputs to power transmissions. The more basic transmission of force when a vehicle is pushed with the feet, as with the first Draisines, and before that with carts, or today with kick scooters, is more difficult to describe and quantify. For this reason the discussion here will involve, principally, transmissions connecting rotary pedal motions to rotary wheel motions, typified by the familiar pedals and cranks of a bicycle, and also some linear mechanisms. First, however, comes a brief review of the historical development of transmissions to indicate how advances resulted from perceived needs.

Transmission History

Power has been transmitted in machinery driven by water, wind, and animal (including human) power since very early times. Human-powered vehicles that preceded the bicycle were mostly various types of pushed or pulled carts, sleds, or wheelbarrows, but cranks or handles of some type were probably also used early on, even if only for turning the spokes of wheels, which, for example, can provide a mechanical advantage of nearly two, or much more in the form of a windlass. McGurn (1987) shows an old print of Stephan Farffler, apparently legless, on a hand-cranked three-wheeled chair that he had made to get himself to church near Nuremberg in the 1680s. He also shows how some important (self-important?) people circa 1760 had themselves transported in developments of horse-drawn traps driven by a servant operating foot cranks on the rear axle. Karl von Drais also constructed such vehicles before demonstrating his Draisine in 1817.

The first bicycle “transmission” was linear: to ride a Draisine (figure 1.4), one pushed one’s foot backward on the ground to propel the vehicle forward. The motion was similar to walking and running. However, in walking, the legs act as spokes of partial wheels, with the body rolling over the feet, being given both support and forward motion. The essence of von Drais’s machine was that it relieved the legs of the need to provide support for the body’s weight and they could just give thrust. Some downward push was still necessary to provide enough friction and to help with maintaining balance.

The next two developments in bicycling transmissions were true transmissions that were approximately linear. Lewis Gompertz in

1821 added a sector-gear hand drive connected to the front wheel of a Draisine by a one-way clutch (figure 1.5). This hand drive was, no doubt, meant to supplement a rider's foot thrusts, as he provided no footrests. The relatively small amount of power the arms could deliver, coupled with the need to steer, the vehicle's evident weight, its solid-rimmed wheels, and the poor road surfaces of the time, must have doomed this design to failure. We have found no reports of its use. The velocipede shown in figure 1.6 also used an approximately linear (actually arcuate) drive, with the feet pushing forward on swinging levers. This was the first true bicycle transmission, and it enabled riders to travel long distances with their feet off the ground. Although the rear (driving) wheel was larger than the front, it was only about a meter in diameter, and the feet had to move back and forth with each rotation, resulting in a low gear. However, this arrangement probably suited the road conditions of the day. If one stopped with the cranks aligned with the pull rods (at dead center), the machine would have to be moved a little by pushing on the ground before the pedals would provide torque. No thread of development followed from these pioneering efforts.

Pierre Michaux, Pierre Lallement, and other early developers of rotary crank drives for bicycles attached the cranks directly to the front wheel. This was a somewhat simpler arrangement than the Macmillan one and afforded the bicycle's front wheel more freedom to steer, but the wheel diameter was also close to one meter, so a similar low gear was the result.

Imitators and other developers followed, and the bicycle's driving wheel was gradually increased in diameter to provide a better coupling, or speed match, between the human body and the machine during level riding. The high-wheeler (figure 1.10) offered the first combination of a comfortable riding position and an easy rate of pedaling on a two-wheeled vehicle (Sharp 1896). The gear ratio of the high-wheeler was preserved when the chain drive was developed to the extent that a step-up drive between the machine's (separate) cranks and its (rear) driving wheel could be used. The resulting safety bicycle, equipped with such a chain drive, was so successful that it is still, in its essentials, the standard bicycle of today.

Thus, by 1885 the principal requirements of a bicycle transmission had been met—superbly—by the chain drive: to provide a foot

motion and a pedaling frequency well suited in average conditions to the capability of the human body to produce power and to transmit this power from the body (in this case from the feet) to the driving wheel with as little energy loss as possible. Developments to cover nonaverage conditions followed rapidly. A simple approach to low-torque requirements (for downhill travel or level running with a strong tailwind) was to fit a one-way clutch or freewheel (figure 9.2) to the bicycle's chain drive, thus permitting coasting with the feet on the pedals. This removed one possibility for braking but otherwise made cycling easier.

In high-torque conditions, such as starting, hill climbing, or riding in headwinds or on soft ground, riders of single-gear bicycles have to strain at the pedals, often standing on them and pulling up on the handlebars, while pedaling at a very low rate and low power, with mostly poor efficiency. In the twenty years following the introduction of the chain-driven safety bicycle, many different gear-change mechanisms were developed to extend the range of conditions in which a cyclist could pedal effectively and in reasonable comfort. The two most successful types, the multispeed hub gear and the derailleur gear, were developed to cover a wide range of conditions and are the predominant types today. In light of their success, it is perhaps surprising that there seems to be more innovation and development in the area of variable-ratio transmissions than in any of the bicycle's other aspects. So much development is occurring in this area today that to examine more than a few prominent examples of different types would be beyond the bounds of

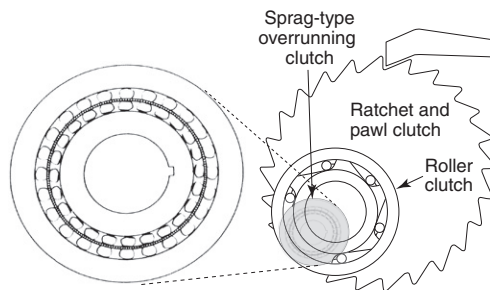


Figure 9.2

One-way clutches (sprag type shown magnified, ratchet and pawl schematically).

the discussion here. Rather, the chapter looks at some fundamental principles and reviews alternative possibilities, drawing conclusions where warranted.

Transmission Types and Their Losses

Transmission or mechanical efficiency η is defined in bicycling as the energy output at the driving wheel divided by the mechanical energy input from the human body, usually via the feet. Both can be measured as the product of force and distance. At a wheel or crank, this product can also be expressed as the product of an average torque T (the tangential force times the radius from the center of rotation at which it acts) and the angle through which it acts (θ , measured in radians). Thus, $\eta = (T_{\text{wheel}} \times \theta_{\text{wheel}})/(T_{\text{crank}} \times \theta_{\text{crank}})$.

The ratio $(\theta_{\text{wheel}}/\theta_{\text{crank}})$ is also known as the *speed ratio* or *gear ratio*. A perfect transmission, with an efficiency of 100 percent, therefore has an average torque ratio $(T_{\text{wheel}}/T_{\text{crank}})$ that is exactly the inverse of the gear ratio. In practice—meaning with an efficiency of less than 100 percent—the torque ratio is less than the inverse of the gear ratio.

Energy loss in a transmission can occur in two ways. One is through friction in bearings and in other components such as the chain. This is the only significant form of loss in “positive-drive” (chain-and-gear) transmissions operating at slow speed. (At high speeds, impact losses become increasingly important.) The other is slip loss, which can occur in transmissions in which the drive is not positive (such as those that use a smooth belt, or some other form of friction or “traction” drive, or an electrical or hydraulic coupling). An insidious form of slip loss arises from belt stretch, even when no obvious slippage is occurring. A stretched belt shrinks as it travels from the taut side to the looser side, and the driving sheave seems to rotate faster than expected, by the ratio (taut length)/(slack length).

From this categorization of the forms of energy loss possible within them, we can divide transmissions into two broad types: those with and those without positive drive.

Positive Drives

Chain Drives

The steel *roller chain*, in which a freely rotating lubricated roller surrounds each bushing (figure 9.3), invented by Hans Renold in 1880 and subsequently used in safety bicycles, can, together with a front chainwheel and a rear-wheel cog or sprocket, constitute a complete transmission for track bicycles that are used principally on velodromes, for circus and special sports purposes, or increasingly also as puristic urban bicycles. The Wikipedia article on *fixed-gear bicycles* includes many references and suggests that a commonly used gear ratio is 2.75:1. In the 1950s Sturmey-Archer manufactured a special three-speed hub gear for such bicycles (see Brown 2008), and in 2009 it introduced a new version, the S3X.

More commonly, however, the rear sprocket is attached instead to a one-way clutch or *freewheel* (figure 9.2) or to multiratio gears (usually enclosed in the rear-wheel hub and incorporating a one-way clutch, as shown in figure 9.4). Or an overlong chain can be used with guiding-plus-tensioner sprockets or pulleys that can force the chain to run on one of many in a nest or cluster of sprockets on the wheel and on the chainwheel (the *derailleur* gear, figure 9.5).

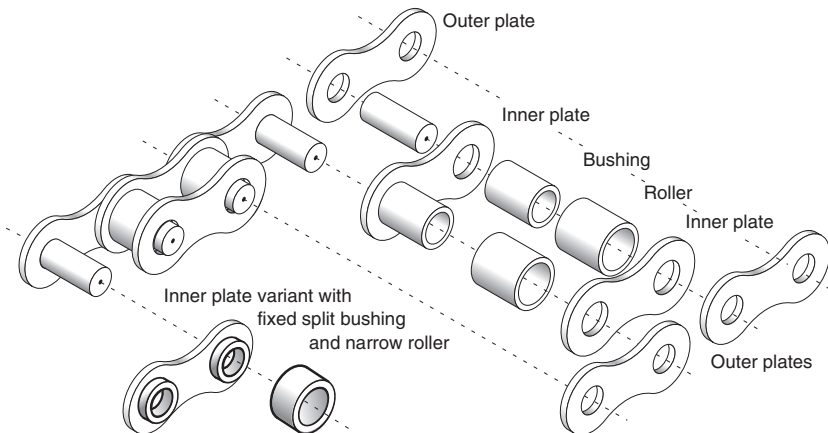


Figure 9.3

Roller-chain components, including a modern “bushing-less” design (from 1981; see Berto, Shepherd, and Henry 2000) with one-piece inner plate and half-bushings. (Adapted, with permission, from a drawing by Markus Roeder.)

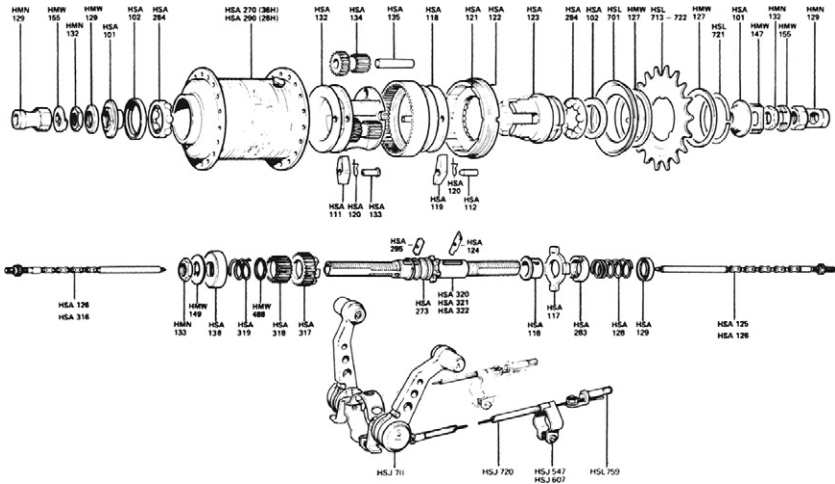


Figure 9.4
Exploded view of Sturmey-Archer five-speed hub gear. (Courtesy of Sturmey-Archer Ltd.)

Despite the chain drive's importance to bicycles and especially to industrial equipment, published research on it has been spotty. Some of the best work is secreted in manufacturers' vaults or stored in the minds of retired engineers, because there is no present commercial value to applying or disseminating it. Matthew Kidd's (2000) doctoral dissertation at Heriot Watt University offers a relatively complete compilation of the (then) available literature on efficiency and examines by theory and measurement the various sources of friction in the bicycle chain and derailleur drives. Studying US patents can provide an idea of the level of sophistication that has been reached in shaping the teeth of multiple chainwheels and sprockets to provide smooth chain shifting; of particular interest are US Patents 4,889,521 (1989), 5,192,249 (1991), 5,188,569 (1993), 5,162,022 (1992), 5,133,695 (1992), 5,514,042 (1995), 5,545,096 (1995), 5,569,107 (1995), and 5,632,699 (1997), all from Japanese or Taiwanese inventors.

When new, clean, and well-lubricated, and when its sprockets have a minimum of twenty or so teeth, a bicycle-chain transmission is highly efficient (at a level of maybe 99 percent or even higher) and very strong (capable of withstanding the tension from maximum

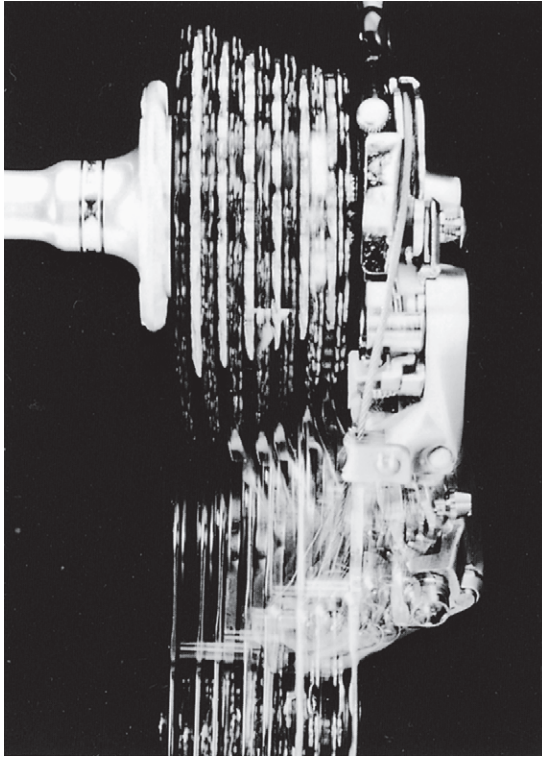


Figure 9.5

Multiexposure photo of a rear derailleur during the changing sequence. The photo shows a closely spaced gear ratio, such as that used on racing bicycles. (Courtesy of Shimano Corp.)

force exerted by a strong, heavy rider on the pedals, which may produce torque fifteen times the normal operating torque). Some bicycles have enclosed chains (so-called gear cases), and their transmissions (as well as trousers and dresses!) stay in good condition, often for many years of hard use. (Figure 9.6 shows a roadster bicycle with enclosed chain drive.) There is a clear trade-off between the increase in bicycle weight and cost incurred in using an enclosure and obtaining the benefits mentioned. Unfortunately (in the opinion of many), chain enclosures are nowadays seldom available on standard bicycles, and as a result, chains, which tend to be in the path of water thrown up by the front tire or carried over by the



Figure 9.6
Raleigh Roadster bicycle with a gear case.

rear tire, often operate in a mixture of old grease, sand and grit, and salt water. Under these conditions, wear is more rapid and is seen as “stretch”: the chain becomes longer as the effective spacing between pins increases, and the chain therefore rides up the teeth at a larger-than-normal radius (figure 9.7). A remarkable feature of chain drives is that unless the wear becomes so great that the chain skips, they continue to operate, usually reliably and relatively efficiently, although their efficiency does decrease.

Chains used in multispeed derailleur transmissions wear even more rapidly. Operation of such chains may become unreliable as the teeth develop hollows, forming hooks that can prevent the entering chain from seating, periodically carrying links over and producing a slipping effect. (An excellent reference on derailleur mechanisms is Berto, Shepherd, and Henry 2000).

Full chain enclosures would have to be very large for derailleur systems, but partial protection, usually made from resilient plastic, is available. Recumbents’ long chains are often threaded through a “floating” plastic tube. But Clemens Bucher (1998) went further: he encapsulated, within the main frame tube of his recumbent bicycle, the chains, a hub gear on a countershaft, and a derailleur, all protected from the weather and safeguarding the clothing of the rider

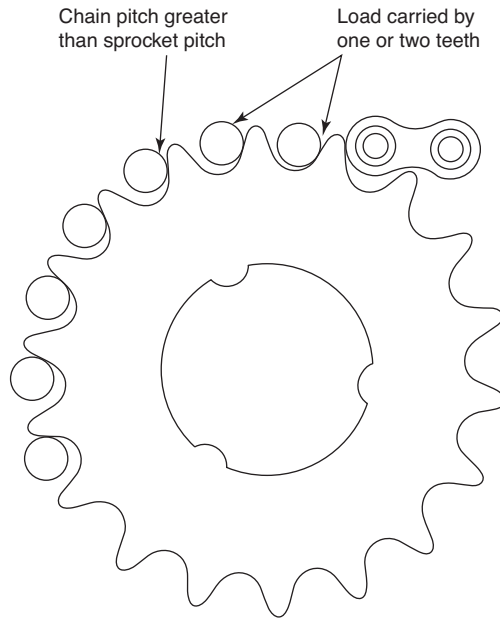


Figure 9.7

Tooth wear from stretched chain.

from oil and dirt. Today this system is commercially available on the Flevobike Green Machine.

Derailleur chains have a further “unofficial” use. Because they have to be fairly flexible, many such chains can be twisted 90° within a short distance, say, 0.7 m. This makes them very useful for chain-driven propeller drives in which the pedal and propeller axes are at right angles.

Small-Pitch Chains

Standard bicycle chain has a $\frac{1}{2}$ -inch pitch between links (actually called *half-links* in the usual type of chain). A smaller pitch seems desirable to give a wider choice of gear ratios and to reduce the chain’s weight. In 1909 the Coventry Cycle Chain Company introduced the Chainette, a small-pitch (8 mm) chain weighing 177 g/m (1.9 oz/ft), which when tested by *Cycling* was found to run over sprockets “more like a silken cord” than a chain. The British racing cyclist F. H. Grubb broke road records on a bicycle fitted with this

chain. A chain of 6 mm pitch works well for the propeller drives of boats but would tear on bicycles and is even marginal with larger propellers, in which case two parallel such chains, or a double chain with three instead of two plates (per half-link), can be used. Of course the strength of a chain is defined primarily not by the pitch, but by the tensile strength of the plates and the shear strength of the pins. Chains for go-karts and similar small motor vehicles often use chains with a pitch of $\frac{3}{8}$ inch, and these are actually stronger than bicycle chains with a $\frac{1}{2}$ -inch pitch.

As becomes clear in later sections of this chapter, smaller-diameter chain sprockets lead to lesser efficiencies, as both relative chain-link rotation and the rate thereof increase. Smaller sprockets also have a fewer number of teeth. Kyle and Berto (2001) find unusually low efficiencies with twelve-tooth sprockets (meaning, presumably, that smaller sprockets would have even lower efficiencies). This has to do with a sprocket's *polygon effect* or chordal action, which causes vibration and speed variation in the chain by the amount $1 - 180^\circ/N$, in which N is the number of teeth. This already exceeds 4 percent with an eleven-tooth sprocket and rises sharply with fewer teeth (see Kanehira 1995). Because of the inertia in the system, having mainly to do with the mass of the rider, this results in high, short-acting forces between chain and sprocket, which increase friction. However, obtaining the gear ratios that the data in chapter 2 confirm as being most desirable does not offer much freedom of choice for the diameters of a bicycle's chainwheel and sprocket. The size of the chainwheel is limited by practical considerations, so that rear sprockets of twelve teeth must be used for the highest gears, or even eleven teeth for small-wheeled bicycles. A small-pitch chain increases the number of teeth for the same diameter and thus allows higher gear ratios or reduces the polygon effect for the same ratio. Such a chain also has smaller-diameter pins and bushings, which increases efficiency, as explained later in the chapter.

Whether or not chains of smaller pitch than those currently employed are used, using jockey pulleys of larger diameter than that of those presently fitted can slightly reduce friction and wear in derailleur gears. Not only does this decrease the polygon effect, but it reduces the rotation rate of the pulleys, which nowadays usually incorporate plain plastic-to-steel (rather than ball) bearings,

in an inverse ratio to the increase in pulley diameter. Of much greater import are idler sprockets or rollers in the taut section of chain drives, such as those some recumbent bicycles have in order to avoid front-wheel interference. Such idlers subjected to the maximum chain tension, when unavoidable, should be as large as conveniently possible.

Adjustable Chainwheels

There have been many designs of geared transmissions for bicycles in which the chain maintains its alignment in one plane. Patents for such designs go back to 1894 (US Patent 524,830). There have also been many designs in which the size or number of teeth in the chainwheel or the rear sprocket or both is changed during bicycle operation. Nothing of this type is presently available on the market so far as we know. In honor of the senior author of the first two editions of this book, Frank Rowland Whitt, figure 9.8 shows his expanding-chainwheel gear, which is circular in the lowest gear and increases in ovality as one shifts to higher gears. At the time Whitt developed his gear, oval chainwheels were generally believed to allow a rider to produce either greater power or the same level of power in greater comfort. The transmission efficiency of such a gear should be slightly higher than that of derailleurs, because it eliminates the small effects of chain misalignment. The range of expanding-chainwheel diameters is less, in general, than can be obtained for wide-spaced derailleur gears. In 1985, however, Royce Husted patented an expanding chainwheel (see figure 9.9) with a wider range, and it was on sale for a few years under the name Excel Cambiogear, with most parts made of injection-molded glass-fiber-reinforced and graphite-loaded nylon. The coauthor used it on one of his tricycles. To change the gear of the Cambiogear, one has to operate a toggle and then backpedal slightly, choosing one of 16 indexed positions that offer the equivalent of 24–54 teeth. Six thousand of these chainwheels were made, but many less were sold. Brooks (2016) describes and offers video links for this and several other expanding chainwheels, including the drive by Michael Deal (US Patent 4,618,331, 1986), which won widespread acclaim but no commercial success.

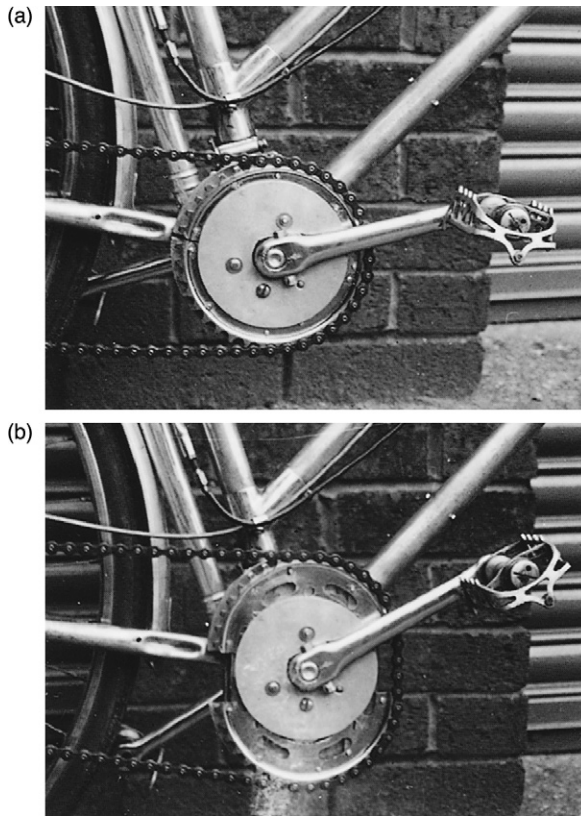


Figure 9.8
Whitt's expanding oval chainwheel.

Innovative Bicycle Transmissions and the Patent System

The US and European patent systems have enormous research value for studies in any field, including that of innovative bicycle transmissions. To encourage innovation, patents (which are limited-term monopolies) are granted to help inventors profit from their creations, in exchange for making complete descriptions available to the public. To make this information most accessible, patent offices attempt to categorize inventions into classes and subclasses and to call attention to related work. Although they inevitably fall short in this task, exploration of a relevant subclass is likely to expose a cataract of useful illustrated ideas.

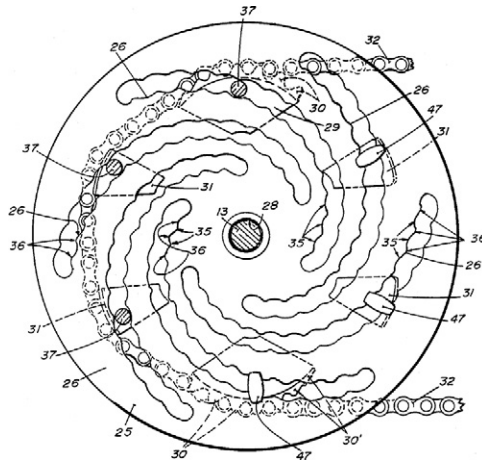


Figure 9.9

Husted's Expandible Sprocket and later Excel Cambiogear. The tooth segments (30 in the diagram) are held in position by pins (37) in spiral grooves. The hollow locations in these grooves (35) hold the pins in position without any other fixation. (From US Patent 4,493,678.)

The internet has dramatically reduced the effort required to search patents, at least for recent patents (e.g., since 1976 for US patents). Several official and commercial databases exist, and a typical internet search will also find patents. Each patent will furthermore list earlier patents relevant to the subject.

Herzog 1991 includes figures from older patents for bicycle transmissions (and other components), partly for amusement.

Flexible Chains

The W. M. Berg Company manufactures a lightweight chainlike belt with flexing articulation, the SpeedE flexible drive, for use in vehicle transmissions. This drive uses stranded steel cables to take the chain tension, and polyurethane "buttons" take the place of the rollers in a steel chain (figure 9.10). This drive has achieved brilliant successes and considerable weight savings in the Gossamer Condor, Gossamer Albatross, and Chrysalis human-powered airplanes, as well as a few others. According to Winfred M. Berg (personal communication, 1981), however, there has been no successful application to bicycle transmissions because the small diameters of the

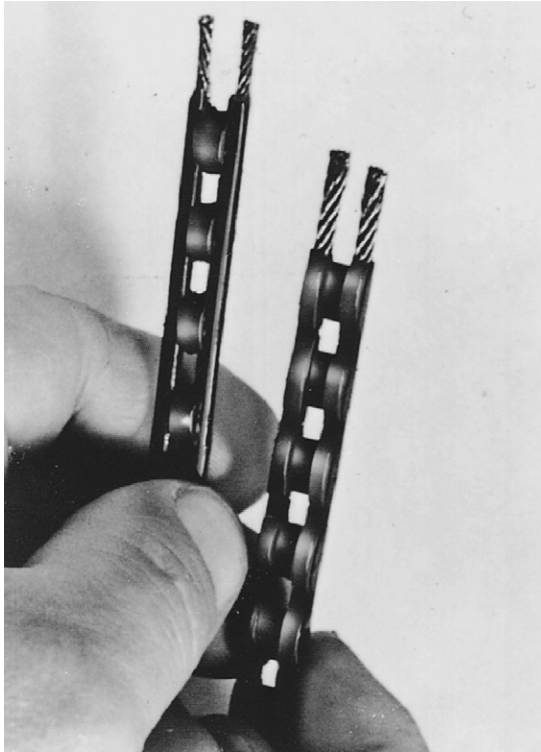


Figure 9.10
SpeedE flexible drive. (Courtesy of W. M. Berg, Inc.)

rear-wheel sprocket and derailleur pulleys in bicycles have led to fatigue failures of the metal cables and especially of the cable joints. Bicycling occasionally creates much higher pedaling torques (e.g., when accelerating from rest) than human-powered airplanes, and unlike such airplanes, it virtually demands a ratio-changing gear system to produce these high torques. The same applies to many similar flexible drives offered by Berg and others, but not to toothed belts, which are available in very robust sizes.

Toothed Belts

The cable-reinforced toothed belts used to such a large extent for industrial and automotive purposes are also good candidates for bicycles, at least those with hub gears. They have been around

for a long time, mostly with trapezoidal teeth, but had specifications that made them marginal for use in bicycles, with their requirements of light weight, high efficiency, and high torque. This began to change with the availability of new materials and tooth profiles. Tension cords in such belts can be steel, aramid, or glass or carbon fiber, the base rubber or polyurethane, the teeth involute or rounded, usually faced with polyamide fabric. Izzy Urieli designed his own bicycle using Gates Poly Chain components (polyurethane belts with carbon-fiber tension cords) and reported total satisfaction with it. A belt of 8 mm pitch and 12 mm width suffices for typical bicycle applications (see figures 9.11 and 9.12). The coauthor uses Gates PowerGrip HTD and similar Continental belts (round-toothed rubber belts with mostly glass-fiber tension members) of 3 and 5 mm pitch for a variety of boat and intermediate HPV drives, as these belts are claimed to offer the highest efficiency. Continental developed a 8 mm bicycle drive but now discourages its use (Continental Bicycle Systems 2018). It is not clear from its website whether the company now encourages the use of 14 mm toothed belts, or no toothed belts at all, for bicycle use. Gates, on the other hand, has launched an 11 mm system especially for bicycles.

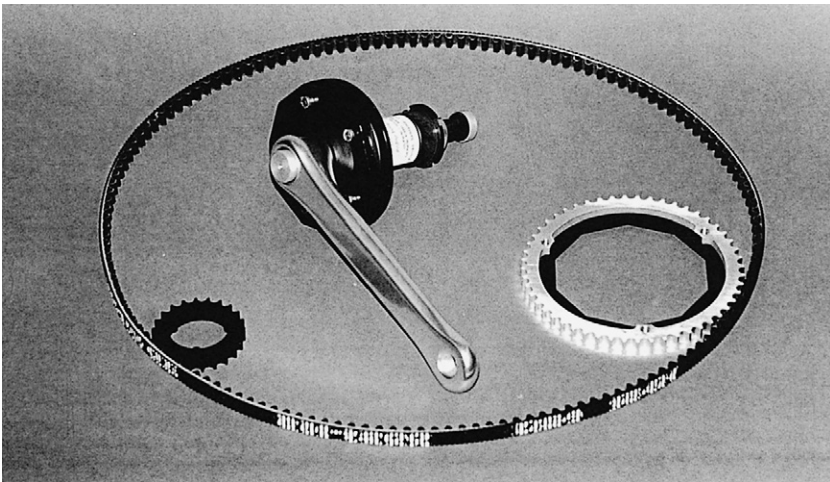


Figure 9.11

Components of Poly Chain drive. (Courtesy of Izzy Urieli.)

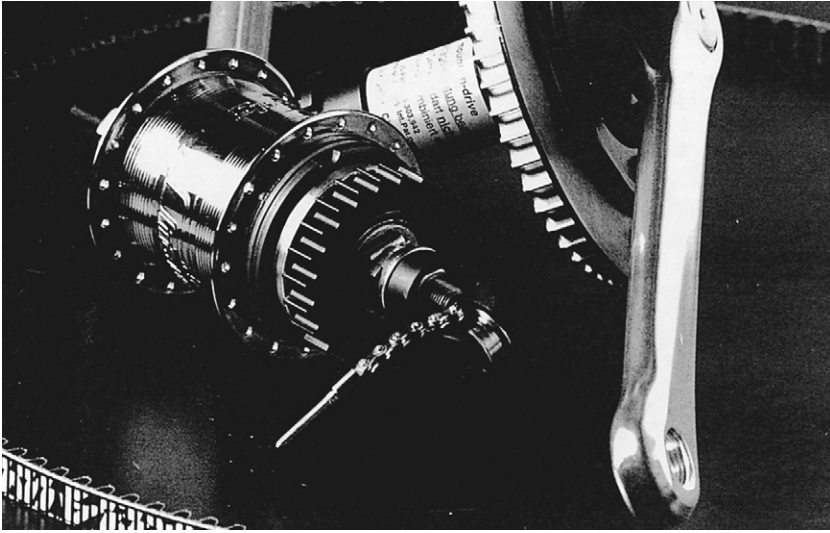


Figure 9.12

Three-speed hub and Mountain Drive bracket gear equipped for Poly Chain drive. (Courtesy of Izzy Urieli.)

As with chain drives, the critical area in such belts is the smallest cogwheel available in the belt. The belt's width and pre-tension must be carefully chosen, calculated (from tables or online calculators), and adjusted (which can be done "by ear," using the sound produced when plucked). The example in figures 9.11 and 9.12, with about sixty and twenty-two teeth, employed on a bicycle with the rider pedaling at 60 rpm with 100 W, might involve, according to the Gates data, a pre-tension of about 150 N (~35 lbf) in each leg of the belt (sounding at ~185 Hz when plucked), increasing linearly to about 750 N (~170 lbf) for a power input of 500 W (~400 Hz). Such adjustments are made to maintain enough tension at all times in the slack belt leg to avoid tooth jump. The belt pre-tension is thus a compromise between too much (a little extra friction at low power) and too little (teeth skipping at high power).

Unlike traditional flat belts, toothed belts must be laterally guided, usually with a flange each on the chainwheel and the cog. The Gates Carbon Drive toothed belts made especially for bicycles have central longitudinal grooves and the sprockets matching central guiding ridges, which is a neat solution but hinders the use of

industrial or self-constructed cogs. Carbon Drive belts are 11 mm pitch belts with carbon-fiber cords and rounded teeth. The recommended pre-tension—between 125 and 235 N (28–53 lbf) depending on the application—is lower than that employed in smaller pitched belts. However, the correct setting is still important, and five types of tensiometers are available for determining it!

Numerous comparisons can be made between bicycles equipped with chain and those with toothed belt drives. The most obvious difference is that belt-drive bicycles usually need a detachable stay, in order to thread in the continuous belt, or a special belt-compatible frame geometry, as most belts are endless. An exception is the Veer belt system, which allows a split belt to be joined with rivets, much like a chain.

Belts don't need lubrication and are therefore mostly cleaner than chains, as well as impervious to water and salt. A major difference is the aforementioned need for pre-tension in order to avoid skipping teeth, whereas chains do not have such a need. And there is obviously some hysteresis loss when the belt's polymer material is bent. Accordingly, belt drives appear to be slightly less efficient than chains at low power but can become similar in efficiency to chains at the designed power.

Spur-Gear Systems

Although the word *gear* is used in several different ways in connection with bicycling, in mechanical engineering it refers to a toothed spur gear that meshes directly with another spur gear rather than via a chain or toothed belt. When a set of gears is to be designed to yield a particular speed (or torque) ratio between input and output shafts, two alternative approaches to the design are possible. In one, all the axes around which the individual gears rotate are fixed relative to the gearbox or casing (figure 9.13); in the other, some of the gear axes themselves rotate around a center (figure 9.14). The latter are called *epicyclic* or *planetary* gears. Most bicycle spur-gear systems used at present are epicyclic, principally because of the compact arrangement that is possible. Though at different times gear-change systems have been developed to fit the bottom-bracket or crank position on a bicycle, these systems have tended to be large, because they must withstand the full cranking torque exerted when the bicycle is in operation. In the rear-wheel hub,

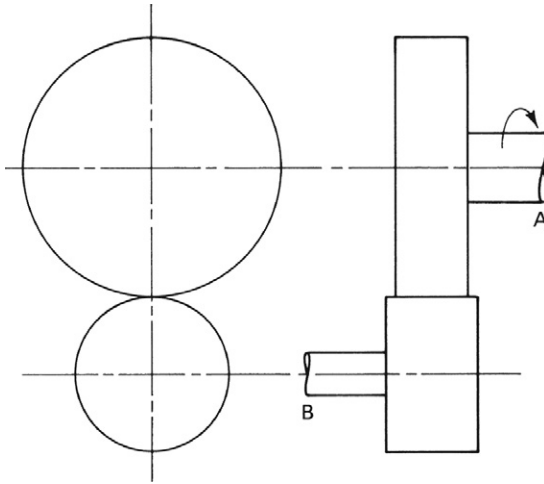


Figure 9.13

Fixed-axis gears. If the gear on shaft A has N_A teeth and that on shaft B has N_B teeth, then one turn clockwise of shaft A will turn shaft B counterclockwise by the quantity N_A/N_B , and the output torque will be the input torque times N_B/N_A .

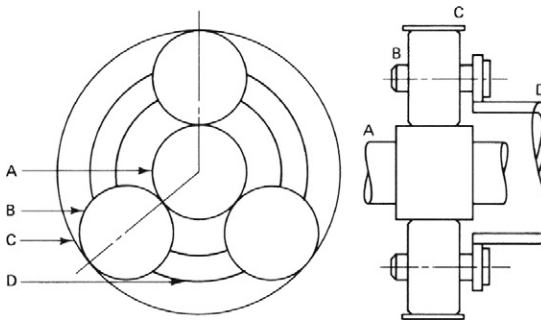


Figure 9.14

Moving-axis (epicyclic) gears. Inputs and outputs can be connected to A, C, and D. In a three-speed bicycle hub gear, A is on a stationary shaft. In the lowest gear, the chain-sprocket input is connected to C and the output (D) is connected to the wheel hub. In the highest gear, these connections are reversed. The gear set is bypassed in the middle gear, with the sprocket connected via the freewheel to the wheel hub. If the central “sun” pinion is the same size as the “planet” pinions, then the highest gear ratio is 4:3 and the lowest is 3:4.

connected to the chainwheel by a conventional chain, the torque is reduced by the chainwheel-to-sprocket ratio (usually about 3:1), so a hub gear can be designed to withstand one-third the peak torque of a bottom-bracket gear. However, the two-speed Schlumpf Mountain Drive gear, an external view of which is shown in figure 9.12, has been used successfully in the bottom-bracket location. It is operated by the cyclist's heel hitting a central button (just visible in the figure), which in one position engages the 250 percent step-down ratio. A Speed Drive is also available in which the gear, when engaged, gives a 165 percent step-up ratio. When not engaged, both drives are locked at 100 percent.

A relative newcomer is the Pinion gearbox, located in the bottom-bracket position and requiring frames made especially for this location. The operation of this spur-gear system is superbly explained at pinion.eu/en/technology/. A number of gear ratios—9, 12, or 18—are available in a range 364–636 percent and, depending on version, weighing 2.2–2.7 kg.

At the time of writing, hub gears for bicycles are undergoing a renaissance. For many decades in the twentieth century, the Sturmey-Archer three-speed hub gear and a few similar hub gears were almost universal in many parts of the world, at least on utilitarian bicycles. Around midcentury Sturmey-Archer introduced a model incorporating two epicyclic gear sets, giving four- and five-speed hubs. Although the company advertised that British cycling champions trained on bikes equipped with its four-speed hubs, the bicycling public perceived the advent of reasonably low-cost “ten-speed” derailleurs as giving more choices, even if the advertised ten speeds more usually produced six or seven actually useful ratios. The two chainwheels and five rear sprockets, giving ten derailleur speeds, then grew by increments year after year to three chainwheels and nine rear sprockets offering nominally twenty-seven speeds. These require a bicycle equipped with them to have a more widely splayed set of rear forks, more “dished” (asymmetric) rear wheels, and narrower chains. Established manufacturers of hub gears have also added more internal epicyclic gear trains to give seven-, eleven-, and twelve-speed versions. A fourteen-speed hub gear, the Rohloff Speedhub (figure 9.15), is being used increasingly, even with e-bicycles, putting the combined motor and human power through the hub. The spacing of the gears on the hub is almost uniform,

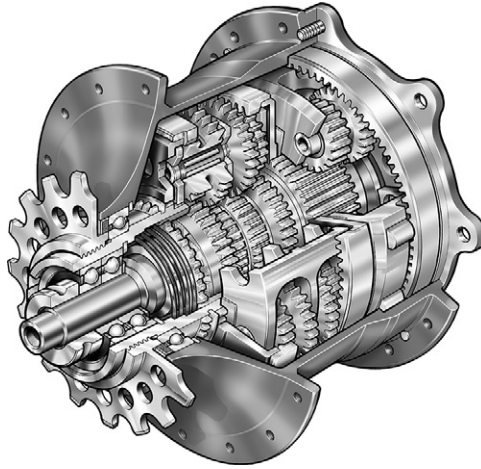


Figure 9.15

Rohloff fourteen-speed Speedhub gear. (Courtesy of Rohloff AG.)

with about 13.5 percent difference between adjacent gears. The overall speed-ratio range of greater than 500 percent is equivalent to that of all but the most extreme derailleurs on all-terrain bicycles, and the system mass at slightly under 2 kg is comparable to that of comparable derailleur systems. The coauthor has used one daily for more than three years with thousands of perfect gear changes via the single twist-grip shifter.

Despite the increasing effectiveness of derailleur shifting mechanisms, shifting a hub gear can be easier and faster, and the shift can be made when the bicycle is stationary. (A derailleur-equipped bicycle must be moving for a gear shift to be made.) A good hub gear and its chain, if enclosed, also last longer than derailleur gears, which generally need new cogs, chainwheel sprockets, and chains every year if they are in daily use.

However, there are additional factors that determine the choice between derailleur and hub gear: cost, weight, and efficiency. While the weights of comparable systems are similar, the prices of the best hub gears are higher. With regard to efficiency of gears, considerable uncertainty exists. This is the subject of a later section, “Transmission Efficiencies of Chain Drives and Gear Systems.”

Open-Wire or Rope Transmission

An endless wire or rope used in the manner of a chain is light, in comparison to the chain, but slips. However, if a wire (aramid line, etc.) is simply unwound from one spool to another, the only slip is virtual, caused by stretching. A drive based on this type of arrangement has been successfully used for power transmission for a duration limited by the line length, in particular in human-powered helicopters.

Direct Drive

A wheel driven directly by pedals, as in the first bicycles, is referred to as *direct drive*. In order to achieve a desirable gear ratio in a direct-drive system with standard-size wheels and optionally several speeds, a special hub gear must be used, the central axle of which is free and strong enough to accommodate the pedal cranks. With such a transmission, the direct-drive bicycle offers many advantages and a few disadvantages, all described by Kretschmer (1999–2000), who furthermore devised an eleven-speed hub for such a bicycle, shown in figure 9.16. Garnet (2008) thoroughly explored the effects from different geometrical parameters of such a bicycle, built and used an adjustable test bicycle, and in conclusion recommends the design shown in figure 9.17, which returns only a calculated 12 percent of the peak applied pedal force to each hand of the rider. Nurse (2019) reviews bicycles with intermediate and direct-drive hub gears, including a range of recumbents recently developed by Kervelo (Kervelo.com).

Shaft Drives

Some early safety bicycles used a shaft drive in place of a chain, with one right-angle bevel gear set at the crank spindle and another at the rear wheel (figure 9.18). Such drives had a neat, compact appearance but were heavier, less efficient, and much more expensive than chain drives. Their fundamental problem is plain: drive torque is transmitted with a moment arm (shaft or gear radius) of about 12 mm, which leads to far higher forces and distortions than the 50 to 100 mm radius of chain drives.

In the waning years of the nineteenth century, most US bicycle manufacturers produced at least one shaft-drive model. Tests by R. C. Carpenter in 1898 (cited by Kidd [2000]) report a best efficiency

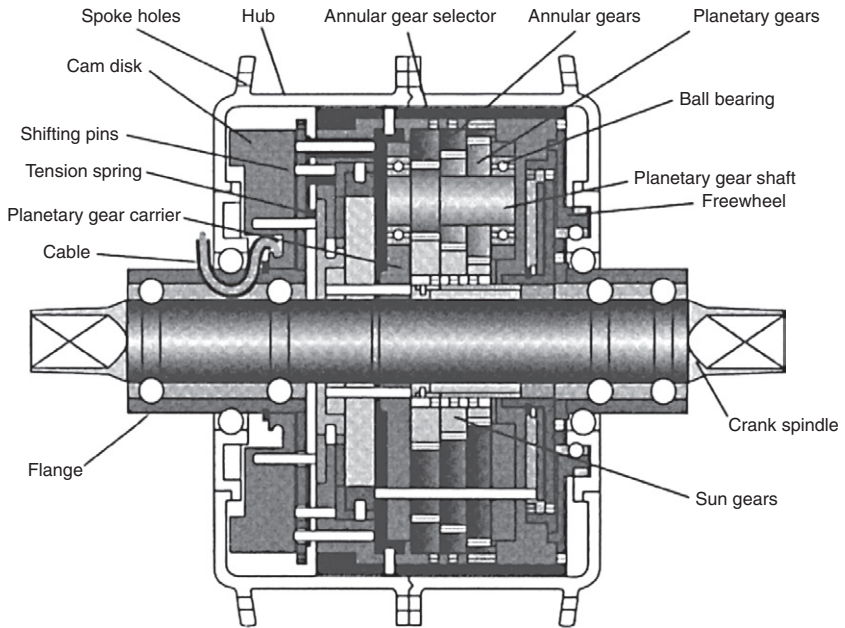


Figure 9.16
Hub for direct-drive bicycle. (From Kretschmer 1999–2000.)

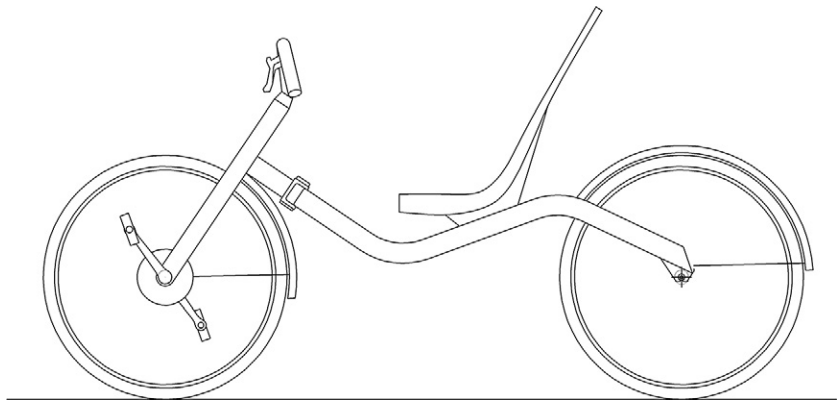


Figure 9.17
Recommendation for a direct-drive bicycle (from Garnet 2008). Wheel size: 700C, front and rear; wheelbase: 1,300–1,550 mm (51–61 inches); head angle: 56° from horizontal; centering spring rate: 18 Nm/rad, adjusted for particular rider; front wheel trail: 25 mm (1 inch); seat height: 560 mm (22 inches) for 1.83 m (6 ft) rider; recumbent angle: 53° ; tread: 297 mm (11.7 inches) between pedal centers; handlebar position: over seat, arms outstretched; handlebar type: inverted-U or inverted-W; handlebar width: 560 mm (22 inches) between handlebar grip centers.

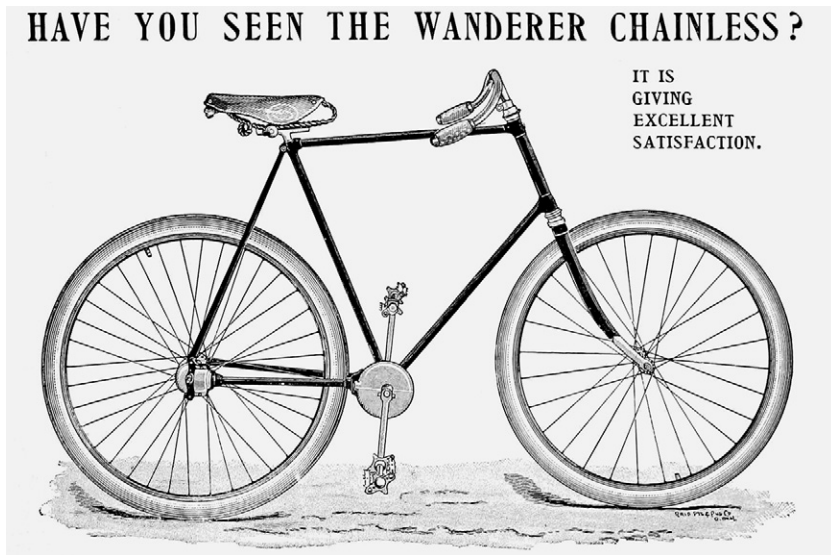


Figure 9.18

Advertisement for the Wanderer shaft-drive bicycle, 1895. (From *Wheel Outings* [Canada].)

of 97 percent for shaft drives, compared to 99 percent for chain. The Waltham Orient pattern using roller pins instead of machined teeth performed well, however, and Major Taylor broke many records using this type of transmission (Ritchie 1996). Keller (1983) compares an unspecified shaft drive with a $\frac{1}{2}$ in \times $\frac{1}{8}$ in chain and finds a 7 percentage-point difference in efficiency between 50 and 200 W at 50 rpm and a 17 percentage-point difference at 25 W. At the time of writing, CeramicSpeed (2018) had introduced a shaft-driven prototype bicycle with a new roller-pinion shaft drive Driven, with thirteen gears, which it claimed to be “the world’s most efficient drive train,” at 99 percent efficiency at 400 W.

Linear and Oscillating Transmissions

Figure 9.19 illustrates an early form of linear transmission, an oscillating drive with spring return. Such a drive can be used independently left and right, for example, in a normal out-of-phase motion, or with both feet pushing together. Figure 2.21 shows a more sophisticated, shiftable version of this oscillating drive from 1905.

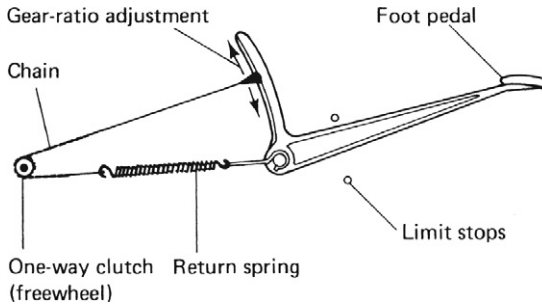


Figure 9.19
Oscillating drive.

In the version depicted in figure 2.21, the slack part of the oscillating chain appears to return the opposite pedal back to a starting position; the rider is free to choose the most effective or pleasant pedaling amplitude. The coauthor constructed a similar system for a boat, using sliding pedals and thin aramid lines wound around pulleys on sprag clutches (figure 9.2). It worked, but he no longer remembers how well.

The linear or oscillating drive has attracted many because it can provide a transmission with a continuously variable ratio that is apparently well matched to a natural ladder-climbing action of the legs. However, above very low “pedaling” speeds, bringing the legs and feet up to the speed of the wheel requires considerable energy, and this energy will be lost (with the additional metabolic costs of eccentric contraction) if muscles are also used to decelerate the legs and feet at the end of the stroke. Increasing the gear ratio at the end of the power stroke to decelerate the limb can reduce such a loss of energy. One method for doing this is to incorporate a *fusee*, a grooved cone used in some spring-wound timepieces, which was employed in a modified form in the tricycle *Dragonfly II*, designed by Steve Ball. Two photographs and a short description are given in the second edition of this book (Whitt and Wilson 1982).

The mechanisms discussed in the preceding paragraphs, as well as the one shown in figure 1.5, and also the rowing ones described later in this section, are *unconstrained* within their limits. Linear or oscillating transmissions can also be *constrained*, rather like the pistons of an engine connected to a crankshaft or the treadle of a

historic sewing machine. Examples are shown in figures 1.6, 1.7, and 1.16. These transmissions work more like circular pedals and if designed and used properly *should* work very efficiently, but in practice they have two problems: if they are connected through a freewheel, it is possible to “catch” a dead center, preventing further movement; if they are connected in the manner of a fixed-gear bicycle, the unstoppable pedals pose the same problems and risks, precluding fast coasting.

Looking for a good bicycle rowing drive, Bert and Derk Thijs started developing their Snek cable drive in 1992 as a clever extension of the fusee principle just mentioned (see Thijs 2018). The length of the path on the Snek’s fusee is substantially longer than the stroke of the steel cable that wraps and unwraps around it (figure 9.20). The Thijses devised a derailleur shifting mechanism to allow the cable to start its stroke on different parts of the fusee, thus providing several effective gears. The fusee itself is mounted on a vehicle’s rear wheel, connected to it by a sprag or other one-way clutch, and contains a rotary spring that rewinds the fusee as the cable is released at the end of a stroke. The cable is pulled by a combination of a sliding carriage to which the pedals are attached and pivoting handlebars, which are pulled toward the chest as the feet are pushed forward. It would be interesting and useful to know the power-duration curves, similar to those that have been mapped for conventional drives, for the form of power production involved in this design, but some educated guessing can fill the void in the absence of such curves and the data behind them. The motion required is similar to rowing, as the name of the bicycle that employs the Snek cable drive, the Rowbike, implies, and according to the data in chapter 2, top athletes produce amounts of power in rowing that are similar to those produced in rotary pedaling. A solid guess might be that the contribution of the arms, which can add 20 percent more power to rotary pedaling, at least for short durations, compensates for the losses to be expected from a rowing motion that does not conserve the kinetic energy of the limbs and mechanism at the end of the stroke. The motion of the modification produced by the fusee might also be expected to increase the power output to some extent over that produced in constant-velocity rowing.

Enthusiasts for human-powered vehicles of any description have in any case preferred the judgment of race results to laboratory

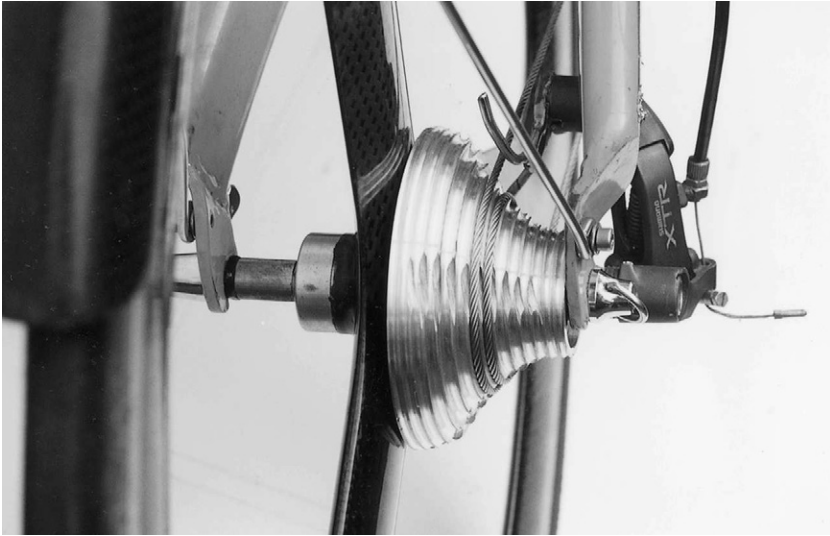


Figure 9.20
Snek cable transmission.

data. Derk Thijs has won races and broken several records on his Rowbike, which can be purchased in several models and has now become popular enough in the Netherlands for one-design races to be held.

Hydrostatic Drives

Heavy earth-moving equipment (for example) often uses a type of transmission in which the engine drives a positive-displacement hydraulic pump and high-pressure oil is piped to hydraulic motors in the wheels. A major advantage of such a transmission is that a type of variable-angle swash-plate axial-piston pump permits the output to be varied over a wide range from positive to negative flow, resulting in a continuous variation in speed ratio. There have been many attempts to apply this type of transmission to passenger automobiles and to bicycles. The peak efficiencies of hydraulic pumps and motor can exceed 90 percent, which would give a total efficiency of about 80 percent, comparable to the lower range of efficiencies in chain-based systems. Many patents for hydraulic bicycle drives can be found in a search; why is there (to our knowledge) not yet a single model in commercial production?

We can think of several partial answers. Most available components for such transmissions operate at higher power levels than needed for a bicycle and are either relatively heavy or operate at high speeds, so that mechanical gears are additionally needed. The efficiency of hydraulic parts is very dependent on minimizing leakage, and because of scaling laws, such minimization is more of a problem for small components. Or if zero-leakage seals are used, it is friction that scales poorly. However, thinking in terms of pistons and bellows, instead of rotary pumps and motors, could yield zero-leak configurations without excessive friction that are at the same time reasonably simple and affordable. The coauthor constructed a pedalable and well-working 200-bar compressor using near-zero-leak seals and pistons from cheap gas springs. The difficult task of optimizing, for example, weight versus cost remains, however.

Hydraulic bicycles have become a popular design challenge for students and colleges, leading to dozens of working vehicles. From about 2006 to 2016, the Parker Group organized nine Chainless Challenges, which then became the Fluid Power Vehicle Challenge (see Parker Hannafin 2016). The goal is (hydraulics) education and competition, but unfortunately no results seem available apart from ranking lists and some videos, as well as the information given by the teams themselves (see Fluid Power Vehicle Challenge 2018). All we can say here is that the presented vehicles appear to work well but look heavy and complex. They include some energy storage, as is usual for traditional hydraulic machines, and this is even required in the rules of the competition. In HPV competition rules it is mostly the other way around: energy storage is prohibited, in spite of repeated calls for allowing it.

For larger human-powered vehicles with several distributed humans and wheels, hydraulic solutions would give similar advantages as the electrical ones described in “Electrical Transmissions” later in the chapter, compared to purely mechanical systems.

Nonpositive Drives

Flat belts without teeth slip a little bit when loaded. V-belts and multi-V-belts increase traction, but also friction and hysteresis losses. However, V-belts do lend themselves to continuously variable-ratio transmissions (CVTs).

Continuously Variable Transmissions and Traction Drives

A popular type of CVT employed in industry, small automobiles, and motor scooters uses wide V-belts or even V-chains that run between pulleys whose side sheaves can be pushed apart or together, causing the V-belt to run at a larger or smaller radius. However, the efficiency, weight, and appropriate speed range of this type of transmission are probably not suited for bicycles.

Metallic traction drives promise less weight and higher efficiency. Figure 9.21 shows some well-known types. These might deserve examination, despite having been tried repeatedly and rejected over many years by the major automobile manufacturers, because of the discovery of lubricants that, under high-pressure contact

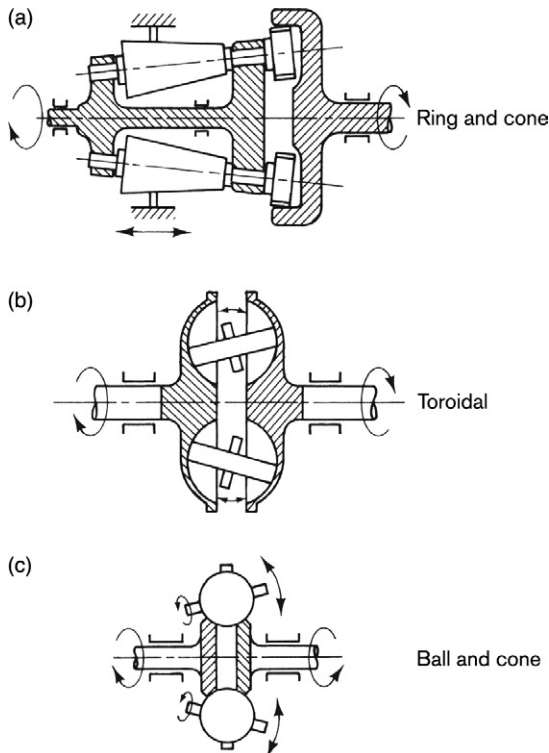


Figure 9.21

Continuously variable transmission drives. (From Loewenthal, Rohn, and Anderson 1983.)

between two hard surfaces, undergo a reversible change in viscosity that enables them to transmit a high shear force (see, e.g., Idemitsu Kosan Company 2018). These lubricants have extended the range of usefulness of traction drives even to sizes suitable for bicycles.

Several CVT prototypes have been proposed, but one that has become a commercial success is the widely publicized and discussed NuVinci, now called Eviolo. It is of the tilting-ball type, has a 380 percent gear width ratio (0.5 underdrive to 1.9 overdrive), and is available with a manual twist-grip shifter or automatic. Only one set of efficiency measurements for the NuVinci appears to be available, carried out by Andreas Oehler in 2014 and archived in issue 17 of Oehler 2019. For the NuVinci he found a highest efficiency of 86 percent at 200 W and 84 percent at 50 W, both at the drive's middle setting, which is more or less direct drive. At both its step-up and step-down extremes, efficiency becomes 81 percent (200 W) and 79 percent (50 W). Oehler also reported a 10 percent slip at 200 W, but it is not clear whether this is part of the efficiency calculation. To put this measurement into perspective, Oehler's setup measured 97 percent for a single-speed chain, 60 rpm input at a 42:21 sprocket-to-tooth ratio.

It would be easy to dismiss other forms of transmission involving nonpositive drives from further consideration, because the additional slip losses incurred in such drives present a considerable penalty for bicycle application. To forestall frictional slip, nonpositive transmissions often resort to elevated contact pressures, which lead to unnecessarily large losses when the amount of torque is small. To get around this, some such drives employ pressure increasers that operate only when high amounts of torque are applied and can minimize losses over a large torque range. For example, the coauthor used a Deltamat CVT on an HPV and an e-bicycle. The Deltamat consists of a large-diameter steel output disk onto which is pressed a smaller tilted ring of clutch material that is free to move along the disk, yielding different gear ratios. (Matthias Wegmann fitted the Deltamat system to an e-bicycle in such a way that it pressed directly onto the bicycle's aluminum rear disk wheel, resulting in an extremely wide ratio.) One of the key parts of the Deltamat is a cam under the high-speed ring that increases its pressure in proportion to torque.

Electrical Transmissions

An electrical transmission in its simplest form consists of a generator connected to (in the case of a bicycle) the pedals and a motor connected to the drive wheel, with two wires transmitting the electric power from one to the other. A patent for such a transmission (US Patent 3,884,317 to Augustus Kinzel) was issued as far back as 1975. In 1995–1996 further patents and publications appeared, and at least one working model (see Kutzke, Fuchs, and Neupert 2012). Figure 9.22 shows an early prototype of a pedal generator.

Ordinary generators and motors in the required power range for bicycles need to rotate with several thousand rpm and thus must have both step-up gearing at the generator and step-down gearing at the motor. The speed of permanent-magnet direct-current motors and generators is, in a wide range, nearly proportional to voltage, and their torque proportional to current. Because of Ohm's law (current = voltage / resistance), the power they generate increases with the square of speed when a cyclist is pedaling into a constant load. This suits a bicycle drive well, at least when only rolling

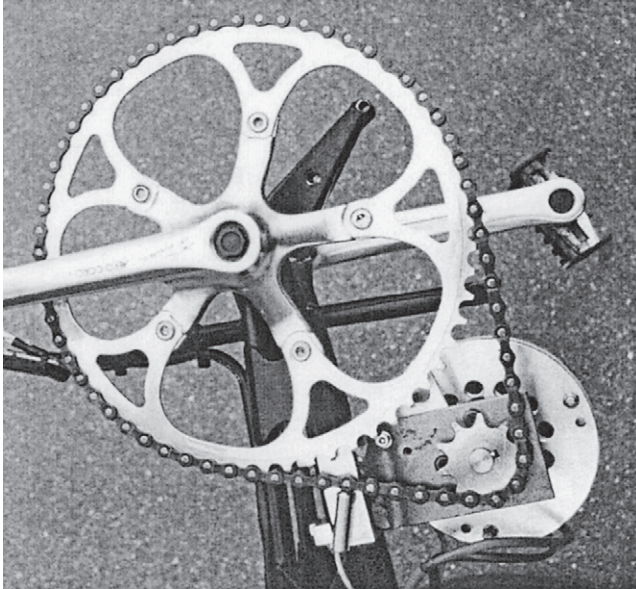


Figure 9.22

Transmission to pancake generator. (Courtesy of Andreas Fuchs.)

resistance and any light upslope, where the power also increases with the square of speed, are considered.

In contrast to the very high efficiencies over a large range of torque and speed in the positive transmissions described earlier in the chapter, the efficiency of an electric motor (output power/input power = torque × speed / [current × voltage]) follows the sort of curve shown in figure 9.23. Motor data are usually presented with various values, as a function of torque, for a *fixed* constant voltage. For a motor with permanent magnets (the usual type of magnets for e-bicycles), the current required is nearly proportional to torque except near zero torque. In figure 9.23 both current and input power follow the rising line, and with a real motor they would start with a small offset (not shown). A lossless motor would, at a fixed voltage, run at the same speed right up to its maximum current and torque and be 100 percent efficient at all torques. In a real motor, the

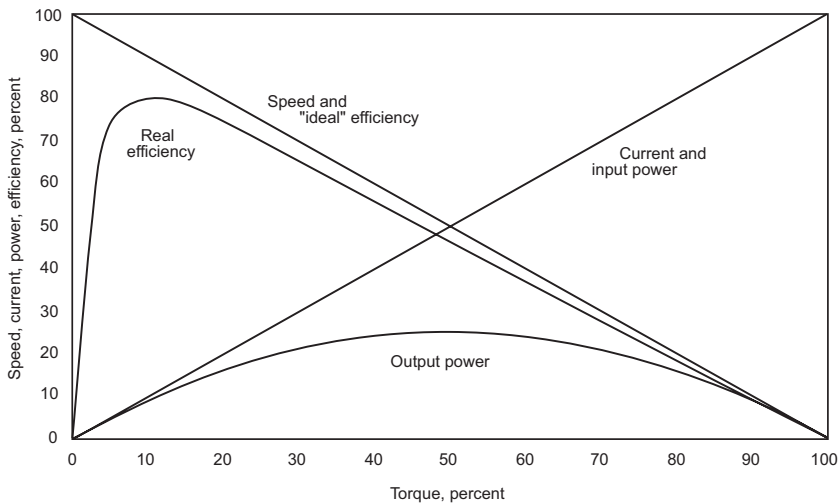


Figure 9.23

Ideal and real properties of a permanent-magnet motor, expressed as percentages of maximum values at a fixed constant voltage. As the figure shows, a motor that absorbs 1,000 W electrical power when stalled would absorb 500 W at half-speed and half-torque and at that point furnish a maximum of 250 W, yielding an efficiency of slightly less than 50 percent. Normally such a motor would be used at between 5 and 25 percent of maximum torque (50–180 W) at more than 70 percent efficiency, with a peak of 80 percent at 10 percent torque.

speed decreases nearly linearly with torque, and the output power, being the product of the torque (rising line) and the speed (declining line), forms a parabola with its maximum at half the maximum torque and half the maximum speed; in the figure it is 50 percent \times 50 percent = 25 percent of the input power, but this is only a relative value with little physical meaning. The highest possible efficiency of such a motor at maximum output power would be 50 percent, zero at zero speed (maximum torque), and 100 percent at zero torque and maximum speed. However, a real motor must have zero efficiency at zero torque and experiences various losses, with an efficiency curve like the one shown in the figure as a result. In the example shown in the figure, real efficiency has a maximum of 80 percent at around 10 percent of maximum torque—for another motor it might be 90 percent at 5 percent—and the efficiency at maximum power is below 50 percent. This is not as bad as it looks, as motors are generally rated and used well below their maximum power. Indeed it is an advantage: they have huge power and torque reserves when used briefly or well cooled, which is why an e-bicycle rated at 500 W can outperform a gasoline-powered moped rated at 1 kW—until the electric motor gets too hot.

Now the efficiency picture painted in the preceding paragraph is misleading for this e-bicycle application, as a *controlled* motor is *not* used at constant voltage, but rather the voltage and current increase together, just as pedaling speed and torque increase together when a bicycle is accelerating gradually. A different set of curves for a number of voltages or a corresponding 3D map, like the one in figure 9.24, must therefore be drawn, showing that after reaching a minimum power, the bicycle can operate at the top of the efficiency curves across a wide range of operation.

However, when air resistance or slope increase too much, the equivalent of a gear change is required, or the motor's efficiency drops. With a large enough motor, or one with multiple windings, this can be handled electronically, and hence Harald Kutzke coined the term *electronic bike*. The great advantage of such an arrangement is that the rider need not change gears mechanically but can just keep pedaling. The controller can be programmed to yield any desired function of load versus speed and thus separate the two distinct functions of a pedal drive: power and control. This also allows tailoring of the pedal *feeling*. Positive transmissions couple

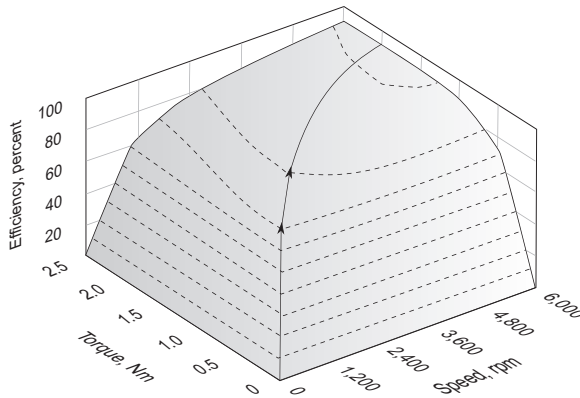


Figure 9.24

Three-dimensional motor efficiency map. When the motor is starting from rest at point (0,0) and linearly increasing speed and torque (or voltage and current) at the same time, there is initially a steep increase in efficiency, which reaches 70 percent at about 1,200 rpm and 0.5 Nm, then a gradual increase to 80 percent and 90 percent. Even if more torque or more speed is required, efficiency doesn't change much having reached the plateau. The map doesn't show the maximum torque area. (Courtesy of CuroCon GmbH Germany.)

the pedals directly and relatively firmly to the road. Pedaling acts against the inertia of the whole mass of bicycle and rider even during fractions of a pedal revolution, that is, with constant speed and highly variable torque. A generator is more loosely connected to the inertia of the bicycle, and pedaling a generator takes place at a more constant torque than pedaling a mechanical bicycle. However, a fast electronic controller can simulate constant speed, if desired, or instead allow instant acceleration peaks that a mechanical system cannot normally match. That is, it can furnish any desired pedaling characteristic.

We sense the reader thinking: What about the total efficiency? Is it sufficient? In principle large electrical machines can have efficiencies near unity, as can special smaller ones, for example, some without iron, a source of magnetic hysteresis loss. But the latter rotate extremely fast, and even with ordinary generators, step-up gearing is required as in figure 9.22. Such gearing generates more losses than the bicycle chain that the electrical system replaces. The unit shown in the figure has a chain ratio of 6:1 and a further planetary gear;

a pedal generator planned and used by the coauthor had a two-stage chain ratio of 30:1. The same sort of ratio is needed again at the motor end, unless a many-poled direct-drive hub motor is used. Ordinary direct-current motors have a peak efficiency of about 80 percent, superior ones around 90 percent. Generator data are difficult to find, but permanent-magnet motors make good generators. Using a popular 24 V motor (MY1020) rated at 500 W, with a peak efficiency of 80 percent at 300 W, as a generator (without gearing), the coauthor obtained very flat efficiency curves around 80 percent between 25 and 175 W, with an uncertainty of 10 percentage points. So with everything included, the transmission efficiency will be between 40 and 60 percent; if the best components are used, this efficiency could increase to about 80 percent. For example, using a computer, González (2014) designed a 200 W, twenty-pole generator with a peak efficiency of more than 88 percent.

A complete system at 80 percent still wouldn't be much fun to pedal, and therefore all contemporary schemes with pedal generators include a small storage battery, in order to cover the (20 percent) losses and also keep the electronics running. If charged only by regenerative braking and surplus pedaling, such a system can still be used as and considered a net pure human-powered transmission.

However, as such a system already has all the components of an e-bicycle, it makes sense to make the battery a bit larger to arrive at a kind of superior e-bicycle that can be called a *series hybrid pedelec*. And this is exactly what Andreas Fuchs and Jürg Blatter at the Bern University of Applied Sciences developed from 1996 to 1998. Fuchs emphasizes that the efficiencies of just the transmission components should not be compared, but instead complete series hybrid pedelecs with parallel hybrid pedelecs. Therefore the section "Classification: Series and Parallel Hybrids" later in the chapter takes just such an approach, and the section "Hybrid Power-Assist Systems" describes further developments.

Even if used purely as a transmission, a pedal-generator system has a special advantage compared with many mechanical systems: the ease with which it enables many people to contribute, entirely flexibly, to powering an HPV, from a tandem to a human-powered ship, such as one planned for 154 pedalers for the Swiss National Exhibition Expo 02 in 2002. In the end, the ship wasn't built, but

a twelve-person solar boat was fitted with stylish pedal generators. Pedal generators—or *pedal-pods* as they are often called—can be used anywhere and just have to be plugged in, which makes them much more flexible than fixed mechanical drives or even hydraulic ones.

Other Transmissions

The foregoing review of alternative transmissions probably omits more transmission types than it includes, among them several interesting types shown in earlier editions of this book. A fascinating but far-from-comprehensive summary of bicycle patents by Herzog (1991) includes many more that are worthy of examination. It is not clear that the best designs for alternative transmissions are those that have succeeded in the marketplace. However, space considerations preclude showing all potentially interesting transmissions here, and stating principles and reporting data on transmissions in general use must be sufficient (see Kyle 1991 for a comprehensive overview).

Transmission Efficiencies of Chain Drives and Gear Systems

The power loss due to mechanical friction is proportional to the product of force and the rate of movement between components in contact. As is evident in figure 9.3, there are two potential internal friction surfaces: between a fixed pin and bushing (or pair of half-bushings), which is in turn fixed to the next link, and between a bushing and roller. In addition there is some friction between a roller and the flank of a sprocket tooth and between a side plate and the side of a sprocket tooth. Kidd (2000) derives equations for all of these frictions and concludes that the friction between pins and bushings is the most important (75 percent of the total). This friction is intrinsically unavoidable, as two links each have to rotate relative to one another when they articulate onto and off of a sprocket, which they do with an angle equal to $360^\circ/N$, in which N is the total number of teeth on the sprocket or chainwheel.

Kidd's equations are too long for presentation here, but a simpler approach, perhaps, involves considering a chain as a special form of linkage or connecting rod under tension. Imagine a single-bar linkage as the simplest way of connecting two longitudinally displaced

wheels, as is done with a coupling or side rod in a steam locomotive. When it is 90° from dead center, such a rod behaves momentarily like a chain with one (half-)link. Imagine the link moving a short distance and (in thought) jumping back to the original position over and over again. Regarding total pin rotation, there is in principle no difference between this single link and a chain, in which a rotation of a link around a pin starts exactly when that of its predecessor stops. If such a link is connected to a wheel or sprocket at radius R with a pin of radius r , there is, as regards friction, a mechanical advantage of R/r because the relative movement between pin and bushing is that much slower than the chain speed. If r were equal to R (which is sometimes the case in steam engines for rods that operate valves), the power lost at speed V and force F would be $F V \mu$, in which μ is the coefficient of friction, typically 0.1 for lubricated steel. The efficiency would be $\eta = 1 - \mu$, typically 90 percent. However, with the mechanical advantage, and for *two* pins and sprockets (taken here to be the same), the efficiency is $\eta = 1 - 2 \mu r/R$.

The pin of a bicycle chain has a diameter of 3.6 mm and the effective diameter of a thirty-six-tooth sprocket is about 72 mm. With $\mu = 0.1$, an efficiency of 99 percent results. This is less than the best efficiency—99.5 percent—that Kidd (2000) measures for well-lubricated bicycle chains, including the friction between bushings, rollers, and sprocket teeth and that in the slack part of the chain, so μ must then be less. Kidd measures pin friction coefficients with pendulum tests (load 44 N) and obtains a very best value of $\mu \approx 0.001 R/(\pi r)$. R is not given in Kidd's dissertation, but a photo sent by Matt Kidd in 2019 shows it to be about 285 mm, yielding $\mu = 0.05$ or $\eta = 99.5$ percent by the simple formula given in the last paragraph, for the 72 mm sprocket. The results thus seem in agreement, but this could be coincidental. Kidd also obtains several higher values of μ for half the load, and more again for misaligned, unlubricated, or worn chains, right up to $\mu = 0.75$. The coauthor reproduced one of Kidd's tests with a 4 kg pendulum and with a new "nine-speed" chain, measuring $\mu = 0.35$ – 0.4 (Schmidt 2019). Thus there can be great variation in a chain's coefficient of friction, which, however, costs only a few percentage points in efficiency. This loss in efficiency isn't felt much by ordinary cyclists but can of course win or lose races.

A full knowledge of the losses occurring in current bicycle transmissions would focus attention on whether these losses indicate problems and, if so, how to correct them. Unfortunately, there is no universal consensus on either of these matters. We therefore report data with cautions and comments.

In 1983, Keller published some rather remarkable measurements of various Fichtel & Sachs components of the time, with 50 rpm input at the driving chainwheel and the driven bicycle wheel bearing loaded normally with 600 N (the bottom-bracket resistance was not measured). The best drive, with a single-speed hub and integrated coaster brake, reached 99 percent efficiency at greater than 400 W, 98.2 percent at 200 W, 97.3 percent at 100 W, 96 percent at 50 W, and 94 percent at 25 W. A three-speed hub, in second gear (direct drive), achieved 1 percentage point less at higher power levels, 2 percentage points less at 100 W, 3 percentage points less at 50 W, and 5 percentage points less at 25 W. In first gear, the values were 3 percentage points less than in second and 1–2 percentage points less than in third. These were the “best of class”; other hardware was slightly less efficient at high power levels and considerably so at low power levels. A six-speed derailleur with the larger driven sprockets produced practically the same values as the three-speed hub in second gear and 1–2 percentage points less with the smallest (thirteen-tooth) sprocket and its required misalignment. Keller observed a small effect (0.5–1 percentage point) of changing the derailleur pulley geometry by lengthening or shortening the chain, but he could not explain the effect in any logical way.

Cameron (1998–1999) measured *static* chain efficiencies of greater than 99 percent (greater than 60 N chain tension) on a forty-two-tooth cog and 97–98 percent on complete systems (at greater than 255 N). Figure 9.25 plots data from various sources (Wilson 1999). The highest efficiencies for the hub gears examined are lower than the highest efficiencies for the derailleur gears considered and considerably lower than those measured by Keller, described earlier.

Spicer et al. (2000) measure efficiencies from 81 to 98 percent on a derailleur system at 60–175 W and find linear relationships between efficiency and the reciprocal of the chain tension as well as the number of the driven sprocket (see figure 9.26). Kyle and Berto (2001), in a very comprehensive article, report 87–97

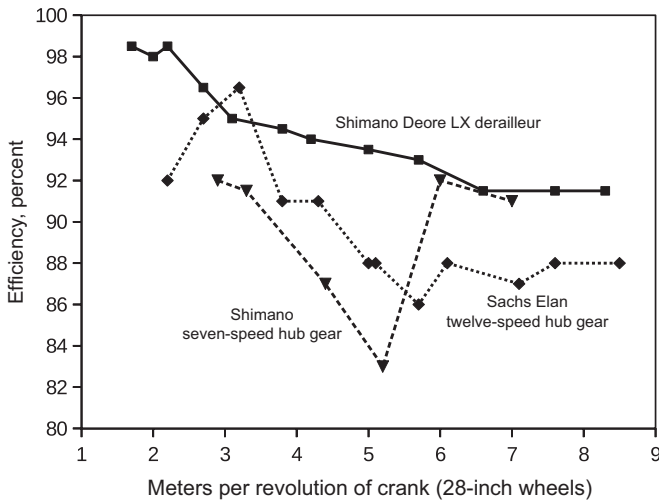


Figure 9.25

Transmission efficiencies for a derailleur chain drive and two gear hubs as a function of gear expressed as a relative distance per crank revolution, all at 200 W input power. (Data from various sources reported in Wilson 1999.)

percent for derailleurs and 86–96 percent for gear hubs, at power inputs of 80–200 W. If the friction of the Monark-style ergometer used is accounted for, 1–2 percentage points can be added to these results. Rohloff and Greb (2004) measure 95–98.5 percent, both for a twenty-four-speed derailleur system and for their fourteen-speed Speedhub, at 60 rpm and 300–400 W input and including all components. Andreas Oehler also measured the Speedhub in 2013 and archived the results in issue 16 of Oehler 2019. He measured 87–94 percent (and a year later 93–97 percent) for the Rohloff Speedhub, 86–90 percent for a Shimano Alpine eleven-speed hub (86–94 percent in 2014), and 94 percent (95.5 percent) for a derailleur, all at 200 W and nominally 60 rpm input. He also measured 96 percent (97 percent) at 200 W for a single chain without any other components and 86 percent (96.5 percent) at 50 W. The components also measured at 50 W had 10–20 percent percentage points lower efficiencies, showing even more than the expected drop-off at low power levels. (Speed-independent losses of 1–2 W translate to 2–4 percentage points less efficiency at 50 W, but only 0.25–0.5 percentage points less at 400 W.)

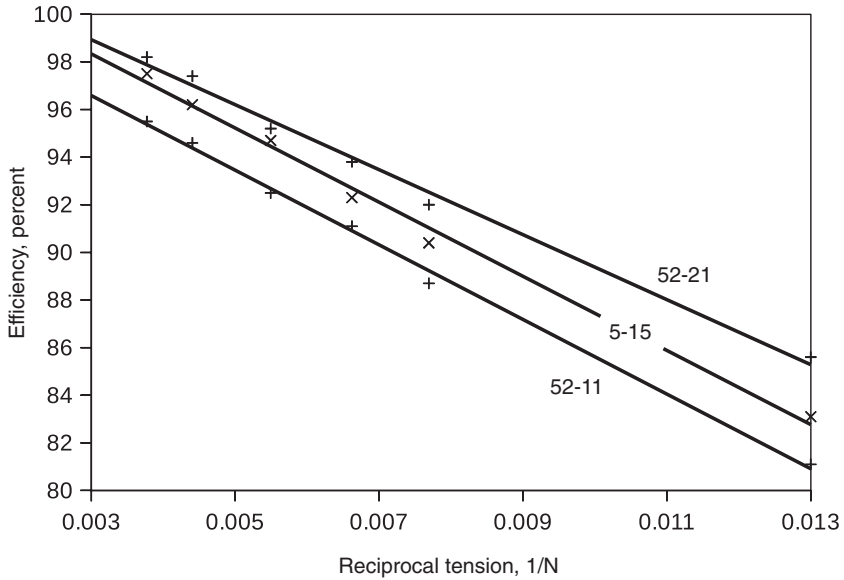


Figure 9.26

Transmission efficiencies for chain drives as a function of (reciprocal) chain tension and number of teeth driven. A similar figure is shown in Walton and Walton 2000. (Data from Spicer et al. 2000).

Bolen and Archibald (2017) measure the efficiency of the Pinion P1 twelve-speed pedal-crank gear using a flywheel and a complete drive train with chain. The method they employ, developed by Casteel and Archibald in 2013, involves speeding up the flywheel with a variety of speed and torque combinations at power levels of mostly 200–400 W. They find a maximum efficiency of ~91 percent in twelfth gear, with efficiency rising to an average of 97.5 percent in first gear. Andreas Oehler, in 2015, for the Pinion P1 eighteen-speed gear at 200 W, measured relatively constant efficiency values around 90–91 percent for most of the gear ratios, with a drop to 89 percent in seventh gear and a rise to 92 percent in tenth (Denham 2017).

The ceramic-bearing company CeramicSpeed has published on its website the results of a number of very detailed tests of all moving components of a derailleur drive, with results expressed in watts lost, apparently with a constant 250 W input at 95 rpm. The very best chain is found to be CeramicSpeed's own brand, lubricated

with a product having a *slack wax* (mixture of paraffin wax and oil) base, in the very best conditions, with a 4–4.5 W loss (from 98.6 to 98.2 percent efficiency). For various other makes, the company finds a 5–7 W loss (from 98.0 to 97.2 percent). A later test by the company using its own Teflon-based lubricant on various chains resulted in an average of 3.8 W loss (98.5 percent) It then examines the effects of sprocket combinations using the following components: eleven-speed Shimano CS-9000 11–28T cassette, Shimano FC-9000 53T big ring and 39T small ring; average of two chains, a Shimano Dura-Ace CN9000 and a SRAM PC Red 22, with unspecified derailleur pulleys. For the big chainwheel at a gear ratio of 1.9, it finds a 5.6 W loss, with this rising almost exactly linearly to 7.9 W loss at a gear ratio of 4.8. With the small chainwheel, the results also graph in an almost straight line from a 6.1 W loss at a gear ratio of 1.4 to a loss of 8.2 W at a gear ratio of 3.5. These data are roughly comparable to those of Spicer et al. (2000), but the latter have about twice the slope, that is, twice as much drop-off with smaller driven sprockets.

The measurements discussed up to this point apply to perfectly aligned sprockets. In an actual crossover setup, only the ratios 2.3 and 3.8 are achievable with such an alignment, or approximately 7 W loss from ratios of 1.8 to 3.8 *if the right combination is chosen*. At other ratios or with wrong (strongly misaligned) combinations, the losses increase to 8.5 W (for a large chainwheel) and 10 W (for a small chainwheel). So this translates to efficiencies from 96 percent (very worst combination and greatest misalignment), to 97 percent (mid-range gear ratios), to 97.3 percent (largest chainwheel and sprocket with ratio ~2), to 98.5 percent (best lubricant and conditions).

When all the data in the preceding paragraphs are compared, some show remarkable agreement, but others differ by significant amounts. Measurements conducted by firms result in the highest efficiencies, especially for their own products, and those by amateurs the lowest, with those by scientists somewhere in between. Transmission efficiency is difficult to measure accurately, because it involves subtracting two imperfectly known large quantities (input and output power) to find a much smaller quantity. Average torques must be known to within 0.1 percent to determine losses with accuracy. Rohloff and Greb (2004) point out that measurements at constant torque do not accurately represent actual cycling conditions,

as a cyclist's torque is highly variable. In spite of their differences, all the measurements presented show very nicely the large effect of power, that is, torque, that is, chain tension, on efficiency, and also of the size of the driven sprocket. The effect of using hubs in their directly driven gear (e.g., eleventh for the Speedhub) is noticeable, but not always as expected. Which type of gearing is the best overall depends on which measurements are the most correct. A derailleur system appears to be the most efficient for hill climbing, but at high speed and high power levels, it could well be the Speedhub or another hub gear, and in the middle range, the time-honored three- or five-speed in direct drive.

Hybrid Power-Assist Systems

The electrical "chainless transmission" described earlier becomes a hybrid power-assist system as soon as a battery is used for more than just covering the transmission losses, as there are then two distinct power sources: the human body and the battery. The following discussion is about hybrid drives as used for e-bicycles such as those introduced in chapter 1.

Almost all e-bicycles have functional pedals for a number of reasons (the first three mentioned here applied mainly to early models, the latter two to present-day ones):

- With limited battery capacity, speed and range are improved.
- It is possible to complete a trip even if the battery is exhausted.
- Initial acceleration is better, allows simple motor control, for example, with switches, or both.
- It is often more pleasant and fun.
- Powered bicycles without pedals are classed as motorcycles (or sometimes mopeds) in many countries, requiring more expensive insurance and licensing.

Classification: Series and Parallel Hybrids

Most e-bicycles are *parallel hybrids*. That is, their motor and pedal drives act independently on one or both wheels (or additional wheels) either directly or through transmissions. Assuming no gear changing or slipping, both drives are thus constrained to act at the same speed, but their torques can each vary from zero to maximum.

The speeds (or their ratio) are equal and torques are added. The simplest parallel hybrids are not pedelecs, as both drives are normally completely independent of one another, the motor just turned on with a switch or relay or controlled via a twist-grip “throttle.” In a pedelec, pedal-speed or torque sensors or both control the motor, either switching it on at a certain speed or offering a sophisticated human-power amplifier characteristic. Most parallel hybrids require changeable gears at least for the pedals and often also for the motor.

In a *mechanical series hybrid*, the motor and pedal drives act through a differential gear with a single output to a wheel. Assuming no gear changing or slipping, both drives are thus constrained to act at the same torque (or torque ratio), but their speeds can each vary from zero to maximum. *The torques (or their ratio) are equal and speeds are added.* This automatically results in a wide speed range in which no gear shifting is required, a kind of virtual CVT, and also a very low gear when either the pedals or the motor are used by themselves. The system then requires one-way clutches to prevent the motor from turning backward or unproductive static pedal pressure. Although a bicycle equipped with such a system is not intrinsically a pedelec, its low motor-only speed encourages pedaling. If the motor controller additionally sets the motor speed about proportional to the pedal speed (plus a minimum offset), a wide speed range in true pedelec human-amplifier mode is realized. Additional gears in the pedal drive are required for gradients, but not normally for the motor, which should be able to furnish the required torque in every situation. Probably the only mechanical series hybrids are the Velocity by Michael Kutter and its quasi clones, described in chapter 1.

In such a mechanical series hybrid pedelec, a sensor measures the rider’s pedaling speed and controls the battery-powered electric motor according to a programmable function. This determines the feel of the ride, from “economical” to “Wow!” Because of the predictable relationship between speed and power, a torque sensor is not required. The Velocity has a high-resolution crankshaft sensor, and motor-voltage output was a simple linear function of the speed input plus an offset. The system allows smooth acceleration while pedaling from a standing start to about 30 km/h without changing gears.

An *electrical series hybrid* consists of a pedal generator powering a motor, as described in the section on electrical transmissions earlier in the chapter, with an additional battery large enough not just to cover the transmission losses, but to give actual power-assist. Whether the bicycle is a pedelec or not is determined entirely by the programming of the controller, a digital processor that can produce any desired voltage or current ratio, that is, speed or torque ratio, for both the motor output and the pedal input. Provided the motor is strong enough, no gears are required and the full speed range can be realized without shifting, even for changing gradients.

Andreas Fuchs and Jürg Blatter (Blatter and Fuchs 1998) developed several electrical series hybrid bicycles and tricycles. A schematic for an electrical series hybrid is shown in figure 9.27 and an early pedal generator prototype in figure 9.22. Fuchs (2008) developed further vehicles and components, as did others; an excellent overview is given in Kutzke, Fuchs, and Neupert 2012. Sergio Savaresi (2014) researched series hybrids with his students at Politecnico di Milano, with an emphasis on sensors and control (see also Corno, Berretta, and Savaresi 2015). Several companies have tried to start production of series hybrids, but most have failed. The Mando Footloose made it into mass production in 2015; a review was published in *Electric Bike Review* (electricbikereview.com/mando/footloose-im/).

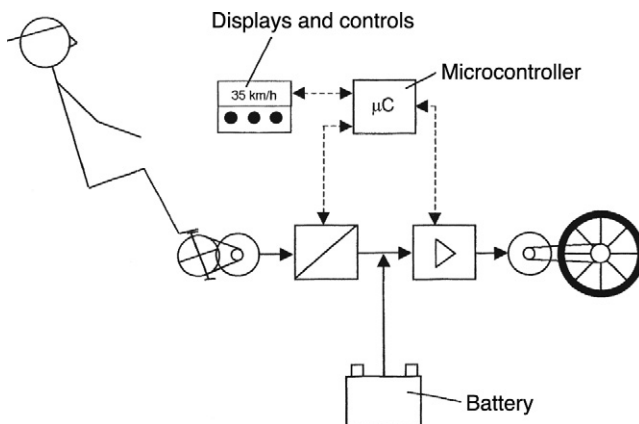


Figure 9.27

Complete system of an electrical series hybrid. (Courtesy of Andreas Fuchs.)

The many advantages of the electrical series hybrid system include reliability and maintenance: there is little to degrade or get dirty or worn out, and the built-in and virtual continuously variable transmission can be programmed so that riders are always pedaling close to their optimum cadence and never have to pause to change gears. Regenerative braking is assured, and even charging while stationary. It offers particular advantages for folding bicycles, in which the oily chain of the typical chain drive is a significant problem; for tandems, on which both riders can pedal at their optimum speed; and for recumbents, which normally must necessarily have a long chain that must be routed around pulleys to pass under the rider to reach the rear wheel—because for all three, only electrical wires need connect the generator at the pedals with the motor at the wheel or wheels.

The motor in an electrical series hybrid must always supply the full propulsive power and torque needed, including when the vehicle is traveling uphill. As there is generally no mechanical gearing, this leads to a good midrange efficiency and poorer efficiencies when cycling with low torque (slowly on the level) and high torque (steeply uphill).

Configuration

In its simplest form, an e-bicycle is a standard bicycle retrofitted with either a motor that can mechanically engage a wheel with a freewheel, centrifugal clutch, or roller pushing onto a tire or a low-friction hub motor that rotates continuously even when not being used. Some such drive systems are available as add-on kits. Many motors are gearless and brushless and therefore exhibit no mechanical friction. Chapter 1 briefly described the BionX pedelec kit, and figure 9.29 later in this chapter shows part of its latest motor. Unfortunately the company went into liquidation in late 2018, and the coauthor is left with some systems that are now irreparable. Still around and hopefully expanding is a similar and mechanically even simpler concept: the Italian-funded Copenhagen Wheel was developed at MIT (see Outram, Ratti, and Biderman 2010), with prototypes available from 2013 and production models since 2017 through superpedestrian.com (see figure 9.28). Its red casing houses all components, including a thirty-six-pole motor, 280 Wh battery, and torque and speed sensors. Proper use of this



Figure 9.28

Bicycle fitted with Copenhagen Wheel hub motor and battery, a project by the MIT Senseable City Lab (senseable.mit.edu/copenhagenwheel/). (Photo by Max Tomasinelli [maxtomasinelli.com].)

and similar products requires a smartphone app. This arrangement saves on mechanical and electrical components and provides powerful electronic functions, but on the other hand it can also give rise to new problems, for example, when one's wireless connection doesn't work well or doesn't support Apple or Google stores.

The most widespread configuration for manufactured e-bicycles appears to be having the motor act on the bicycle's pedal-crank chainwheel or its axle. In such an arrangement, the motor also uses the pedal gearing; the chainwheel is, however, usually a single one. The motor can be packaged unobtrusively around the bicycle's bottom bracket—the ideal location for the additional mass. The disadvantage of this solution is that it results in a great deal of wear and tear on the bicycle's chain and cogwheels, which aren't engineered for the combined electro-human torque. The coauthor knows a fast

commuter who changes his chain every month. Popular pedelec drives manufactured by Panasonic and Bosch are of this type and are used in many bicycle brands.

The mechanical series hybrid Velocity, described in chapter 1 and earlier in this chapter, uses a planetary differential gear accepting a standard derailleur pedal drive on one side and a small toothed belt from the motor on the other side. A number of e-bicycle drives look the same, but their hubs have no differential, and they are parallel hybrids that rely on a motor sufficiently powerful to work with such a fixed single-stage gearing.

In most e-bicycles the power-assist provided by the motor goes to the rear wheel together with the pedal drive. This results in maximum traction, especially when going uphill. A hub motor or roller push-on motor, in contrast, can also be mounted on the front wheel. This arrangement yields a lower maximum traction, especially in slippery conditions, because of the longitudinal moments involved. However, as in such an arrangement both wheels are driven, the *total* traction can be superior. But as any slipping of a bicycle wheel can lead to falls, powerful motors in front wheels must be used with special caution, and also in case they brake suddenly as a result of an electrical fault.

A further possible e-bicycle configuration is for its power-assist to be integrated in a trailer. This can be a “phantom trailer” that powers only itself and its payload and keeps up with the speed imposed by the pedaled bicycle (see Könekamp 1998–1999) or a pushing trailer.

Motors and Gears

Most bicycle motors are of the conventional, high-speed permanent-magnet direct-current type. Such motors are small and light but require a great amount of reduction gearing. The use of permanent magnets results in slightly more efficiency than copper-wound electromagnets, which are typically found in household appliances, for both the rotating (rotor) and the stationary (stator) motor parts. Both types of motors require moving contacts (brushes and commutator) that give rise to sparking and wear. Brushless alternating-current asynchronous induction motors (such as those used in washing machines) with appropriate power processing are possible on bicycles, but hardly ever used. Electronically commutated direct-current

motors, which can be considered synchronous alternating-current motors, are being used more and more in high-torque direct-drive hub motors. Instead of the two or four poles found in standard motors, these motors have many more poles formed by small windings (usually on the stator) and magnets (usually on the rotor, that is, the wheel itself). With other things being equal, the speed of a motor is inversely proportional to the number of poles, and therefore using enough poles eliminates the need for reduction gearing.

These direct-drive hub motors are therefore especially efficient and quiet and inherently available also for regenerative or electronic braking. The latter feature is very valuable not so much for actually extending the range per battery charge, but for reducing wear on the bicycle's mechanical brakes. The disadvantage of such motors is the extremely wide variation in the torque-to-speed ratio imposed by the lack of gearing. If optimized for steep climbing, they are less efficient at high speeds, and vice versa. Even the rather extreme bicycle motor whose stator is shown in figure 9.29 could, by itself, power a normal bicycle and rider only up a 10–15 percent grade. Employed on a pedelec with the pedal drive acting in parallel, however, such a motor does not suffer from such a limit in practice.

The sustainable power of an electric motor is highly dependent on how well it is cooled. The nominal rated power used for legal classification is therefore little more than a defined value measured in certain conditions. Common legal limits are 250, 500, 750 and 1,000 W and 4 kW (for pedicabs and the like). The maximum power available for short periods is often several times the rated power and the maximum torque twice the torque at the maximum power (see figure 9.23). Many high-performance fast pedelecs, although allowed 1 kW, therefore often have 250–350 W motors, because these motors provide enough power to reach legal limits of 45 km/h or 28 mph on the level. It is about the same as riding a tandem together with an athlete weighing only 10–20 kg!

Motors (and batteries) these days often operate between 24 and 48 V. This is about the limit at which dry skin feels no tingling or shock if exposed. Often the same motor unit can be used in different e-bicycle configurations and its performance adjusted electronically.

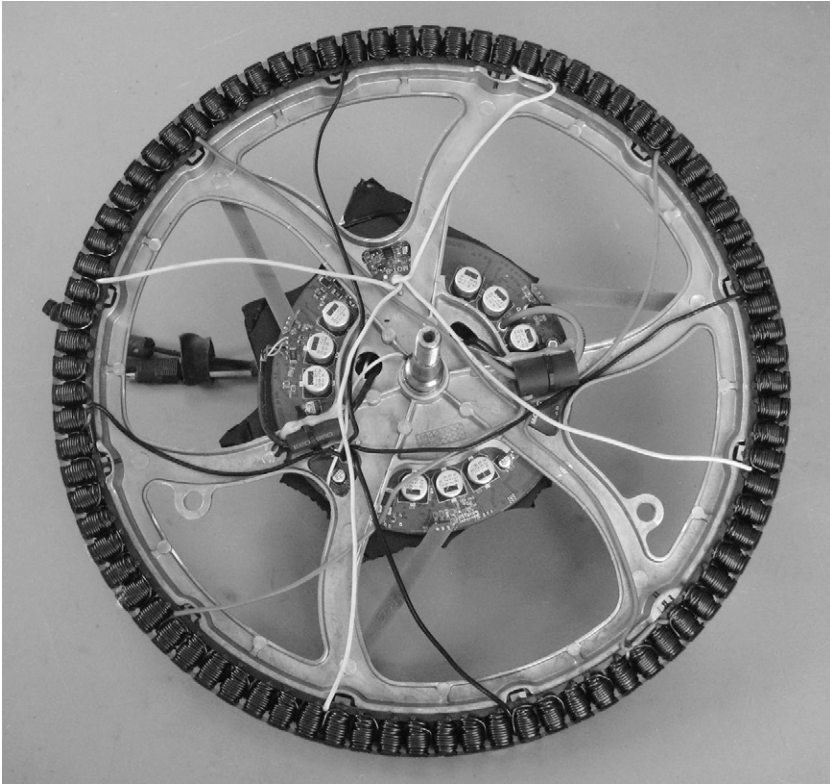


Figure 9.29

Stator of a brushless, gearless BionX D hub-motor system with eighty-four electro-magnets and controller. The rotor (not shown) consists of thin magnets attached to the casing inside the spokes of a wheel. At ~ 0.34 m diameter, it will just fit into a 20-inch wheel. The 3.9 kg motor is rated at 500 W and 25 Nm (50 Nm peak). See Ron/Spinningmagnets 2018 for details.

Control

In Europe, as influenced by legislation, most e-bicycles are *pedelecs*, and this is increasingly the case in the United States. This term is used for electrically assisted bicycles on which the pedals *must* be used to get the motor to operate, except when the bicycle is in a low-speed “push mode” intended for walking it uphill. But the discussion here starts with controls that can be employed on all e-bicycles, pedelecs or not.

The simplest controller for an e-bicycle is an on-off switch, but this is not the cheapest solution, because the large electric current involved with the usual low-voltage setups requires large, heavy-duty contacts. Electromechanical or electronic relays can be used instead, controlled by a small switch on the bicycle's handlebars. The next-higher degree in sophistication would be a multiple-stage switch giving the rider a choice of motor speeds via multiple motor windings or resistances. Today such methods of controlling motor speed have become practically obsolete because electronic controllers using pulse-width switching have become universal for conventional motors. Such controllers are also called *choppers*, because the electric current is chopped into many pieces (usually above 20,000 times per second, to prevent audible noise) and the average power controlled by varying the length of the pulses. As the electronic switches used for this chopping are either on or off, there are hardly any losses, as there are with controllers using resistances. Early experimental e-bicycles and vehicles did use variable resistors called *rheostats*, but mostly only for starting, as prolonged use would be quite wasteful and require the rheostats used to be large and expensive.

Simple e-bicycles have a spring-loaded twist grip for choosing power, like motorcycles. In many countries, however, the pedelec control system has become much more popular. This system involves using the bicycle's pedal speed or torque (or both) to control the electric motor. In its simplest form the controller is just a switch, and in its most sophisticated, it is fully programmable and can take any combination of inputs: pedal speed and torque, motor and bicycle speed and torque, slope, and acceleration, as well as user and body inputs, to give any desired relationship between human and motor power.

Some of these inputs are redundant or can be calculated from other values. We are unaware of any vehicles using an acceleration input, although many controllers offer an acceleration output *ramp*, that is, a limit to how fast motor current can increase. A bicycle's momentary slope on a road could be calculated from the total acceleration vector measured by an accelerometer and the purely longitudinal acceleration derived from the speed sensor. The result could be used to adjust the gears and the motor power accordingly, or gyroscopic-type sensors could be used instead. Many e-bicycles

have both speed and torque sensors somewhere in the drive train and work out a motor output depending on programmed curves. The popular BionX hub-motor system measures the bending strain of a bicycle's rear axle, more or less proportional to the total drive torque. This can lead to positive feedback, with the motor applying more and more torque, which is interpreted as more pedal torque, until the bicycle runs by itself. To avoid this, a dozen or so parameters can be programmed by computer, or even using the display console itself, to accommodate different bicycles and riders. Other motor-system makes use similar methods but guard them more closely, so less is publicly known about them.

An e-bicycle's rider is interested in two things: usability and a good feel. Today's quality pedelecs all achieve both, and the differences are slight even when radically different technologies are used. Most people like (unnecessary, but attractive and easily achieved) strong acceleration, fine controllability during normal riding, and acceleration reserves at all speeds, all of which can be achieved with proper controller programming tailored to give an attractive human-power amplifier feel.

An increasing trend is the pairing of e-bicycles with smartphone apps. As noted earlier in the chapter, the Copenhagen Wheel even requires a smartphone app to use it at all, with the app available only to those registered with Apple or Google. The app is used for unlocking the drive, displaying statistics, and choosing the degree of assistance, which is claimed to be fast (varying within each pedal revolution) and "self-learning."

Bad Battery ⇔ Good Battery

The first e-bicycles used lead-(sulfuric)-acid batteries (by "batteries" here we mean rechargeable accumulators). With a specific energy density of about 20–50 Wh/kg, batteries of this type are quite heavy. They also don't last very long, especially if discharged rapidly or deeply (or both). But for a long time they were the only affordable batteries, and they still have a lot to recommend them: easy to charge; no shortage of materials, although toxic; readily recyclable; and no immediate hazards as long as the hydrogen and oxygen that is produced during charging is vented. The coauthor's first e-bicycle used a single 12 V battery of this type weighing about 20 kg, his Tour de Sol hybrid solar tricycles two of these, later replaced by four

smaller sealed units, in which the acid is contained within fleeces or gels. Later vastly more expensive nickel-cadmium batteries and cells, in which hundreds of small cells are connected to form a formidable battery with a very high power density, became popular for high-performance solar vehicles and the Twike. Cadmium is toxic and nickel scarce, but the batteries can last a very long time and are worthwhile to recycle. Their energy density, at 30–80 Wh/kg, is somewhat higher than that of lead batteries, but they are more robust and can supply large currents and be fully discharged. They have now mostly been replaced by less toxic nickel-metal-hydride batteries (70–130 Wh/kg), which are in a way self-contained hydrogen stores and fuel cells. Nickel-based batteries have degraded capacities at low temperatures and when regularly partially discharged (the so-called memory effect). Modern lithium batteries don't exhibit this effect, but they need very close cell-by-cell charge monitoring to avoid overheating and even catching fire.

Because early batteries were relatively heavy, the bicycles and vehicles they were used in had to be light and efficient to be at all useful. Probably the most efficient pederlecs and microcars were devised in the late 1990s. They could be relatively objectively tested by measuring the achievable distance per charge on defined routes and with 100 W human input. For a long time, ExtraEnergy.org tested every available model this way. The ranges achievable with these batteries were enough for commuting, but not enough for longer tours, unless extra battery packs were carried, exchanged, or recharged at stops.

The arrival of today's lithium-based batteries has changed all that. Their energy densities of 130–200 Wh/kg coupled with very high potential discharge rates and no memory effect now allow light-weight e-bicycles with sufficient ranges for touring and mountain biking. In spite of initial quality-control problems and the possibility of fire when damaged, they have become the standard battery system for anything portable. Cell-wise charge control is mandatory, but this also allows high charging rates. The batteries are non-toxic, and lithium is more plentiful than nickel.

Although these “good batteries” have really made e-bicycles popular, there are of course a few associated *rebound effects*. Lighter batteries allow heavier vehicles and more powerful motors. The power density of modern batteries is so much higher than that of humans

that the human power input in hybrid vehicles hardly counts any more, even for pedelecs, except as a means of controlling the motor. Formerly assist ratios of 1–3 or less were common; now there are ratios up to 10 and more. Bicycles built with conventional technology, especially a complete pedal chain drive with gearing, for the moment continue to retain a bicycle-type character and design, in order to retain bicycle-typical privileges, but the boundary conditions have been shifted. Electrical series hybrid bicycles especially need a large motor anyway, and with a potent battery it doesn't matter very much for the energy balance what happens to the power from the pedal generator. The pedelec becomes a motorcycle, with the pedals being used more as control devices than as power devices.

The eROCKIT (eRockit.de) is such a pedelec motorcycle, weighing 120 kg with an 8 kW motor controlled exclusively by a pedal generator, presumably with a maximum assist ratio approaching 100. According to the manufacturer, there are no gears or multiple settings, and it is technically a series hybrid, with the pedal feeling entirely up to the characteristics of the electronic controller. Henshaw (2018) describes a near clone by the original designer of the eROCKIT called the Gulas (gulas.bike). It can be operated only by using the pedals, but apparently they act solely as a speed controller, not furnishing any power themselves, and motors are available rated at up to 28 kW.

Most cyclists would probably frown upon such large degrees of motorization. In the opinion of the coauthor, there are three answers to objections of this type:

- It depends what one compares these high levels of motorization with. Even highly overmotorized pedelecs are better in environmental respects than conventional, far heavier, or more polluting nonhybrid motor vehicles.
- From a health perspective, as presented by Allan Abbott (chapter 1), even some exercise is better than none.
- Conventional motor vehicles are usually driven just a little too fast for comfort and safety, as very safe speeds give rise to boredom. Experiments by the coauthor show that the use of pedals increases *subjectively* felt speed and therefore decreases actual speed, with all associated safety and energy advantages.

The Future of Pedelecs?

Pedelecs both slow and fast are becoming ever more popular, especially in affluent and hilly regions, because they combine often the fastest trip with fun and health benefits that far compensate for the greater risk posed by cycling faster. Their additional financial and environmental costs compared to conventional bicycles are nonetheless small compared to those involved in the production and use of pure motor vehicles, and it looks as though cycling as a whole can benefit from their existence. Electrical-series hybrids in particular appeal to automobile and motorcycle companies, as they may be successful in attracting new customers with easy-to-use pedelecs without the traditional bicycle image. In addition, assisted-delivery and family vehicles, as well as pedicabs, can now be used in places other than the flat terrains where they first appeared.

Although the future of pedelecs as a “species” appears rosy, the future of individual vehicles is likely to be short. In contrast to mechanical bicycles or even early power-assisted ones, which last a long time and can mostly be repaired even without original parts, modern pedelecs are “black boxes” full of undisclosed proprietary electronic systems, and they frequently fail after a few years. Even if the manufacturer is still in business once the period of guarantee is over, repairs are often not possible, not done, or too expensive. (This is an increasing problem also with other ever more electronically controlled bicycle components such as electric gear shifters and even lights.) Only a few years ago, it was still easy to exchange battery cell packs separately; now they are so heavily integrated within the battery module, both electronically and mechanically, that a complete new unit must be purchased when the cells lose capacity or an electronic component fails. Battery modules include a casing and part of the electronic system and are considerably more expensive than the battery cells themselves. Keen-skilled individuals can sometimes find instructions for replacing batteries (e.g., see kmpres 2016), but most people will find they have to discard their pedelecs when they no longer work well. For heavy users like commuters, replacing batteries and bicycles isn’t much of a problem, as the benefits far outweigh the costs. However, occasional users are well advised to rent or share e-bicycles instead of purchasing them, as batteries degrade even when they are not being used.

References

Berto, Frank, Ron Shepherd, and Raymond Henry. 2000. *The Dancing Chain—History and Development of the Derailleur Bicycle*. <http://web.archive.org/web/20190113222335/http://www.thedancingchain.com/>.

Blatter, Jürg, and Andreas Fuchs. 1998. “Fully Electrical Human-Power Transmission for Ultra-lightweight Vehicles.” Paper presented at the Extra-Energy Symposium, IFMass, Koln, Germany.

Bolen, Rachel, and Mark Archibald. 2017. “An Experimental Study on the Efficiency of Bicycle Transmissions.” Paper presented at the American Society for Engineering Education Zone 2 Spring Conference, “Engineering Everywhere for Everyone,” San Juan, Puerto Rico, March 2–5. <http://zone2.asee.org/papers/proceedings/3/78.pdf>.

Brooks “Retrogrouch.” 2016. “New Is Old Again: Expanding Chaining Cranks.” *The Retrogrouch* (blog). January 11, 2016. <http://bikeretrogrouch.blogspot.com/2016/01/new-is-old-again-expanding-chaining.html>.

Brown, Sheldon. 2008. “The Sturmey-Archer ASC Fixed-Gear Three-Speed Hub.” Harris Cyclery (website). <https://www.sheldonbrown.com/asc.html>.

Bucher, Clemens. 1998. “Recumbent with Encapsulated Drive Train.” Paper presented at the Third European Seminar on Velomobile Design, Roskilde, Denmark.

Cameron, Angus. 1998–1999. “Measuring Drive-Train Efficiency.” *Human Power*, no. 46 (Winter): 5–7. <http://www.ihpva.org/HParchive/PDF/hp47-n46-1998.pdf>.

CeramicSpeed. 2018. “Driven—The World’s Most Efficient Drivetrain.” Ceramic Speed, Holstebro, Denmark. https://www.ceramicspeed.com/media/2979/driven_brochure.pdf.

Continental Bicycle Systems. 2018. “Belt Drive.” Continental Bicycle Systems, Eschborn, Germany. <http://www.continental-bicycle-systems.com/Ebikes/Belt-Drive>.

Corno, Matteo, Daniele Berretta, and Sergio M. Savaresi. 2015. “Human Machine Interfacing Issues in SeNZA, a Series Hybrid Electric Bicycle.” *Proceedings of the American Control Conference 2015*: 1149–1154. <https://www.researchgate.net/publication/283439648>.

Denham, Alee. 2017. “What’s the Difference in Speed between Gearbox Systems?” *Cycling About* (website). <https://www.cyclingabout.com/speed-difference-testing-gearbox-systems/>.

Fluid Power Vehicle Challenge. 2018. “Meet the Teams.” National Fluid Power Association, Milwaukee, WI. <http://nfpahub.com/fpc/vehicle-challenge/meet-the-teams-fpvc/>.

Fuchs, Andreas. 2008. "Series Hybrid Drive-System: Advantages for Velomobiles." *Human Power eJournal*, no. 5: art. 15. <http://hupi.org/HPeJ/0015/0015.htm>.

Garnet, Jeremy. 2008. "Ergonomics of Direct-Drive Recumbent Bicycles." *Human Power eJournal*, no. 5: art. 17. <http://hupi.org/HPeJ/0017/0017.htm>.

González, Fernando Álvarez. 2014. "High Efficiency Electric Generator for Chain-Less Bicycle." Thesis, Universidad de Oviedo, Asturias, Spain. <https://core.ac.uk/display/71868094>.

Henshaw, Peter. 2018. "Tested—The Amazing Super-power Gulas." *A to B magazine*, no. 119. <http://www.atob.org.uk/product/atob-119-digital/>.

Herzog, Ulrich. 1991. *Fahrradpatente* [Bicycle patents]. Kiel, Germany: Moby Dick Verlag.

Idemitsu Kosan Company. 2018. "TDF (Traction Drive Fluid)." Idemitsu Kosan Company, Tokyo, Japan. <http://www.idemitsu.com/products/lubricants/tdf/>.

Kanehira, Makoto. 1995. "The Complete Guide to Chain." Tsubaki Inc. US, Wheeling, IL. <http://chain-guide.com/basics/2-2-1-chordal-action.html> and http://tsubaki.ca/pdf/library/the_Complete_guide_to_chain.pdf.

Keller, Josef. 1983. "Comparative Efficiencies of Shaft Drive and Clean and Used Chains" [in German]. *Radmarkt*, no. 2: 71–75. Reprinted in *Pro Velo* 5 (1986).

Kidd, Matthew D. 2000. "Bicycle-Chain Efficiency." Ph.D. diss., Department of Mechanical Engineering, Heriot-Watt University, Edinburgh, Scotland. <https://ethos.bl.uk/OrderDetails.do?uin=uk.bl.ethos.313628>.

kmpres. 2016. "How to Rebuild a BionX E-Bike Lithium-Ion Battery Pack." Instructables (website). <https://www.instructables.com/id/How-to-Rebuild-a-BionX-E-Bike-Battery-Pack/>.

Könekamp, Andreas. 1998–1999. "The Phantom Trailer." *Human Power*, no. 46 (Winter): 3–4. <http://www.ihpva.org/HParchive/PDF/hp47-n46-1998.pdf>.

Kretschmer, Thomas. 1999–2000. "Direct-Drive (Chainless) Recumbent Bicycles." *Human Power*, no. 49 (Winter): 11–14. <http://www.ihpva.org/HParchive/PDF/hp49-1999.pdf>.

Kyle, Chester R. 1991. "Alternative Bicycle Transmissions." *Cycling Science* (September and December): 33–38.

Kyle, Chester R., and Frank Berto. 2001. "The Mechanical Efficiency of Bicycle Derailleur and Hub-Gear Transmissions." *Human Power*, no. 52 (Summer): 3–11. <http://www.ihpva.org/HParchive/PDF/hp52-2001.pdf>.

- Kutzke, Harald, A. Fuchs, and H. Neupert. 2012. "An Overview of the Most Significant Milestones for Series Hybrid Pedelects." *ExtraEnergy Pedelec and E-Bike Magazine*, no. 12: 33–42. <http://extraenergy.org/main.php?id=79314>.
- Loewenthal, S. H., D. A. Rohn, and N. E. Anderson. 1983. "Advances in Traction-Drive Technology." Technical Memorandum 83397, National Aeronautics and Space Administration, Washington, DC. <http://hdl.handle.net/2060/19830020184>.
- McGurn, James. 1987. *On Your Bicycle: An Illustrated History of Bicycling*. London: Murray.
- Nurse, Stephen. 2019. "In-Hub Gearbox Front Wheel Drive Cycles." *Human Power eJournal*, no. 11: art. 26. <http://hupi.org/HPeJ/0026/0026.htm>.
- Oehler, Andreas. 2019. *Fahrradzukunft* [Bicycle Future] (online). <https://fahrradzukunft.de/archiv/>.
- Outram, Chrisine, Carlo Ratti, and Assaf Biderman. 2010. "The Copenhagen Wheel: An Innovative Electric Bicycle System That Harnesses the Power of Real-Time Information and Crowd Sourcing." Paper presented at "Ecologic Vehicles, Renewable Energies," Monaco, March 25. http://senseable.mit.edu/papers/pdf/20100325_Outram_et_al_CopenhagenWheel_EcologicVehicles.pdf.
- Parker Hannafin. 2016. "9th Annual Chainless Challenge Puts Students to the Test." Parker Hannafin, Cleveland, OH. <http://blog.parker.com/9th-annual-chainless-challenge-puts-students-to-the-test>.
- Ritchie, Andrew. 1975. *King of the Road*. Berkeley, CA: Ten Speed.
- Ritchie, Andrew. 1996. *Major Taylor: The Extraordinary Career of a Champion Bicycle Racer*. Baltimore: Johns Hopkins University Press. <https://archive.org/details/majortaylorextra00ritc>.
- Rohloff, Bernhard, and Peter Greb. 2004. "Efficiency Measurements of Bicycle Transmission—A Neverending Story?" *Human Power*, no. 55: 11–14.
- Ron/Spinningmagnets. 2018. "BionX Reorganization? (They're NOT Calling It a 'Bankruptcy')." *ElectricBike*, March 27. <https://www.electricbike.com/bionx-reorganization/>.
- Savaresi, Sergio. 2014. "E-Bikes: Present and Future of High-Tech Solutions." Paper presented at the International Li-Ion E-Bike Industry Summit, Shanghai, April 13. http://www.datei.de/public/extraenergy/2014-EnergyBus/savaresi_china-cycle_2014.pdf.
- Schmidt, Theo. 2019. "Maximum Chain Efficiency." *Human Power eJournal*, no. 11: art. 27. <http://hupi.org/HPeJ/0027/0027.htm>.

Sharp, Archibald. 1896. *Bicycles and Tricycles*. London: Longmans, Green. Reprint, Cambridge, MA: MIT Press, 1977.

Spicer, James B., C. J. K. Richardson, M. J. Ehrlich, and J. R. Bernstein. 2000. "On the Efficiency of Bicycle Chain Drives." *Human Power*, no. 50 (Spring): 3–9. <http://www.ihpva.org/HParchive/PDF/hp50-2000.pdf>.

Thijs, Derk. 2018. "Rowingbike over the Years." RowingBike.com. <https://rowingbike.com/en/modellen/historie/>.

Walton, Claire L., and John C. Walton. 2000. "Efficiency of Bicycle Chain Drives: Results at Constant Velocity and Supplied Power." *Human Power*, no. 51 (Fall): 14–15. <http://www.ihpva.org/HParchive/PDF/hp51-2001.pdf>.

Whitt, Frank Rowland, and David Gordon Wilson. 1982. *Bicycling Science*. 2d ed. Cambridge, MA: MIT Press.

Wilson, Dave. 1999. "Transmission Efficiencies." *Human Power*, no. 48 (Summer): 20–22. <http://www.ihpva.org/HParchive/PDF/hp48-1999.pdf>.

10 Special Human-Powered Machines

Introduction

Human-powered vehicles include not just bicycles and vehicles with more or fewer than two wheels, but also boats, airplanes, amphibious vehicles, and so forth. It is doubtful whether devices such as sleds, skis, or even shoes can be called HPVs, but the wider term *human-powered mobility* surely covers these, and “human powered” can also be applied to machines and even tools in everyday use.

This chapter includes examples of human-powered machines from the last edition of this book that would seem outdated given the progress expected then. Although some of these examples no longer exist, we found ourselves still impressed with the range of devices that we had reviewed then and simultaneously disappointed at the few significant developments that have been produced since then. Therefore we have retained some that are still “best of class” or unique, either leaving material as previously described or by making comments to indicate those changes about which we have information. Our aim is to expand readers’ experience and perhaps to make them want to use, or even to design and make, some interesting human-powered devices in addition to bicycles.

People in the developed world who choose to bicycle generally do so for reasons connected with their own health and well-being and that of the region in which they live and perhaps out of concern for the earth as a whole. There are rather similar, but more limited, choices that such people can make for mowing grass and clearing snow, for example, and for recreational boating. The role of human power in the modern world of electric pepper grinders and soap dispensers is, alas, declining. Although we are engaged in

some advocacy for human power in this chapter, we are not recommending that everybody cycle long distances or that human power should be used to clear snow from a supermarket parking lot or to cut the grass of a golf course. However, even in large countries like the United States, more than half the daily person-trips by automobile are of less than 8 km (5 mi), a distance most people can easily cover on a bicycle. Likewise, most lawns and driveways are of sizes that can easily be handled by human-powered devices. The past enthusiasm for reducing what has been characterized as “back-breaking” labor through the incorporation of gasoline-engine- and electric-motor-powered devices has led to an almost total neglect of efforts to improve human-powered tools. In consequence, there is today an unfair competition between highly developed modern electric devices, for example, and manual ones that have not been sensibly improved for a hundred years. Perhaps we need a new series of prizes like the Kremer (see discussion later in the chapter) for specific achievements in human-powered tools. For example, we have never heard of a human-powered leaf blower, but surely one could be developed, as the efficiency of the usual motorized and very noisy devices is extremely low.

We have chosen to discuss in this chapter two examples of human-powered tools and a series of interesting vehicles (other than standard bicycles) for use on land, on and under water, and in the air. Each example deserves several pages of description and discussion, but the available space will not permit such an extensive treatment. We have selected some interesting features in each case and hope that readers wanting more information will examine the references cited to find out all they want to know.

Human-Powered Lawn Mowers

The first three editions of this book included descriptions of various pedaled lawn mowers. Since then many more have been built, including an attractive one by Herslow (2011) as a degree project in design. However, we suspect that there will be no breakthrough in this field for a simple reason: except on very hard turf, overcoming the rolling resistance of a person on a pedal mower requires greater effort than walking, and this is additional to the effort needed to operate the cutting device. The energy required to pedal a machine

across soft ground is so great that the only way in which pedaling a mower would be superior to pushing it would be for the pedaler to be either stationary or moving slowly, while the cutter covers a wide swath area at a higher rate of speed (in fact, rather like scything described in the next section). Also, some conventional reel-type push mowers have become very efficient through the use of extremely accurately made reels, which can be adjusted so as not to contact the mower's fixed knife edge at all (typical gap: 0.1 mm) and still cut grass. The effort needed to cut most lawns with such mowers is initially very small. (Unfortunately, the precision parts get worn or damaged eventually and without refurbishment or replacement either no longer cut well or cause more resistance.) For long grass, a so-called sickle bar has to be used. We suspect that those sold in the early twentieth century (see figure 10.1) had a relatively high degree of friction and are therefore no longer sold.

However, human-powered grass cutting with the traditional scythe has undergone a minor revival, and so we mention it here.

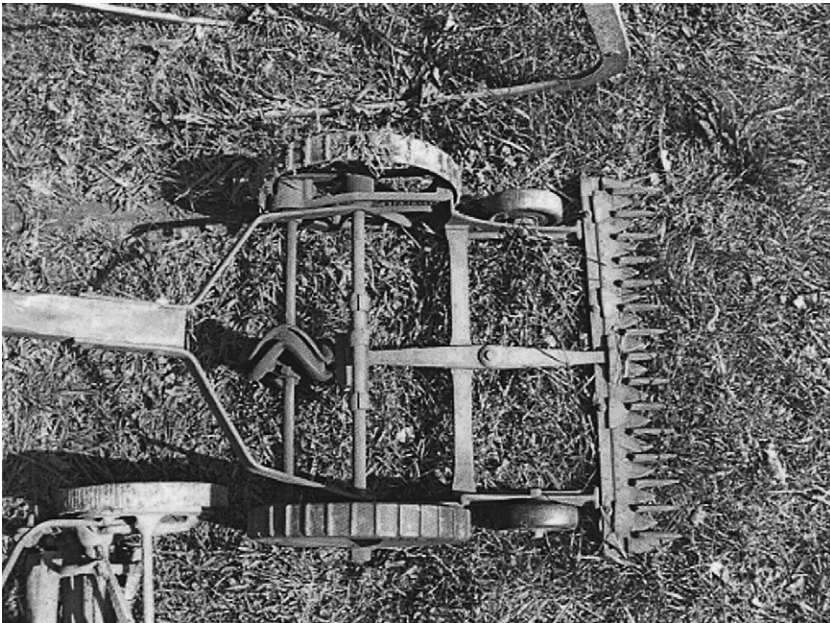


Figure 10.1

Sickle-bar push lawn mower. (Photo by Ora E. Smith.)

The website of the Scythe Association (scytheassociation.org) offers an enormous number of recent resources. Scything is effective for cutting grass if at least two of the following three are available:

1. A sharp blade set at the correct angle
2. Skill or experience
3. Strength or good physique

The main point is the first one, and the main problem from a technical perspective is the sharp blade. Scythers generally hone their blades every few minutes and regularly have to peen them, say, after 12 h of use. If science could find a suitable ever-sharp material or at least a handy peening machine, scything could be more widespread. However, if the first two points can be satisfied, scything is quite efficient, and if all three points, fast as well. Champion scythers take less than 2 min to mow 25 m²; those less strong and skillful typically need 8 min.

Human-Powered Snow Removers

The use of snow shovels at the first snowfall of the winter always seems to produce reports of heart attacks. Shoveling snow is a heavy task involving the use of the muscles of the arms and back and of having the back bent uncomfortably. It would be more efficacious and put less stress on the body to use instead the big muscles of the legs and to have a more natural posture. More than that, it would be delightful to have a small, lightweight device that, from leg operation alone, scooped up a quantity of snow and projected it in a desired direction, as one does with considerable effort using a snow shovel. Nothing like that has been on the market, or even in the patent literature, unfortunately, judging from searches carried out by the senior author and his students. Figure 10.2 shows his favorite tool for clearing snow: an old push plow purchased at a garage sale. He made and installed on the push-plow a fiberglass “blade” with a mild-steel cutting edge. He liked to demonstrate that, on the asphalt surface of his driveway (about 50 m²), he could clear snow in about half the time it took his neighbors with similar driveway areas, using their engine-powered snowblowers.

Another very useful device in this regard is a snow sled shovel, a very wide curved shovel with a double handle. Pushing this forward



Figure 10.2

Dave Wilson's push snow plow. (Photo by Ellen Wilson.)

and adjusting it vertically, the snow is scooped up, transported, and dumped, but never needs to be lifted. Using this device, it is easy to push heavy, wet snow (too heavy for the snow plow) a considerable distance over snow, which can be built into a long ramp, before dumping it.

More recently a device called Snow Wolf Shovel has come on the market that more or less combines the two devices just discussed. However, the senior author still preferred his, and the coauthor likes to keep the snow in place for skis and sleds!

Kick Scooters

Whereas the evolution of the Draisine into the bicycle is well-known, both being vehicles for normally *saddle-supported* persons, the evolutionary branch toward two-wheelers for *standing* persons is less documented. However, the US Patent Office lists hundreds of patents related to scooters (often also called *coasters* and rarely *pedicycles*) from 1920 through 1940 and beyond. The German Bundesarchiv has photographs of children using foot-propelled (kick-)



Figure 10.3

Small-wheeled children's scooters in Berlin, 1948. (Photo from Bundesarchiv, Bild 183-19000-2205, licensed CC-BY-SA 3.0.)

scooters in Paris, Berlin, and Leipzig between 1930 and 1951 (see figure 10.3). Wikimedia Commons 2018a shows some of these and a few others, along with later scooters with relatively wide pneumatic tires from the mid-1950s onward.

We remember as children such kick scooters. Their medium-sized, relatively low-pressure pneumatic tires had too much rolling resistance to make them much fun, especially after we were introduced to “real” bicycles, capable of long-distance excursions and travel in traffic, even by children. The scooters with tiny, solid-tired wheels that are common today had then already come and gone, perhaps because most road surfaces then were likely to be too rough for them to be used comfortably. In the 1980s, *kickbikes* were developed with almost full-sized pneumatic bicycle wheels, or at least a large front wheel. With bicycle-like rolling characteristics, they can be used off road and on many roads, can carry luggage, and today are popular for touring purposes and for exercising dogs.

A specialty was developed in the 1970s in the Democratic Republic of the Congo: long, wooden scooters called *chukudus* (figure 10.4).



Figure 10.4

Man using a *chukudu* in North Kivu, Democratic Republic of the Congo. (Photo by Neil Palmer [CIAT], licensed CC-BY-SA-2.0.)

They are a widely used form of cargo transport around the city of Goma and are among the most efficient and ecological forms of land transport possible, given the situation: goods are mainly transported from the hills downward into the city, up to half a ton or so at a time, with employment for local pushers on uphill stretches. Empty, *chukudus* can be propelled by foot, the body supported on the nonpropulsion knee. An online search readily provides information, pictures, and videos.

The children's scooters and large-wheeled kickbikes described in the preceding paragraphs are not very suitable for urban transportation. They are not as vehicular as bicycles on busy main roads, not very maneuverable on sidewalks and hardly unobtrusive there, and not very suitable to take easily on public transport or inside buildings. Therefore in the late 1990s, compact tiny-wheeled scooters were reintroduced and also made foldable. Unlike their predecessors with rubber tires, they had extremely hard-wearing polyurethane skate wheels, and by then riders had a wide choice of smooth

sidewalks and roads on which to use them. Their quick foldability, small size and weight, high maneuverability, and low rolling resistance on smooth surfaces made them immediately popular not just with children, but also with adults, including the coauthor and his wife. This revival and the modern aluminum design is credited to Wim Ouboter, first as personal practical transport, and later as the basis of the company Micro-Mobility. Around the year 2000, sales exploded, and the scooters became quite fashionable with young urbanites. The ensuing fad was helped along by countless plagiarized copies that worked reasonably well even in cases of cheap or even shoddy designs and both helped and hindered sales of the more expensive quality brands. Recognizing this, Ouboter didn't waste time in legal conflicts but instead kept ahead of the competition by producing new models for different user groups, as well as tricycle scooters and toys, today producing more than fifty different models. Interestingly, evolution repeats itself: from tiny solid-tired wheels, to larger solid wheels (greater usability on rougher surfaces), to small, high-resistance pneumatic and wide solid wheels (neither much fun except downhill), to medium-sized pneumatic wheels like those in the 1950s (and to saddles and power; more about these later).

Most of these two-wheelers steer, balance, and handle in a manner roughly similar to bicycles and seem even easier to use, except that the handlebars and standing platform take over the role of the saddle in allowing the rider mass to apply roll to the dynamic system. Like bicycles they work well even if distorted, loose, or otherwise decrepit. However, some alternative designs exist with certain advantages, once they are mastered. One is the Plankalkül developed by Bernhard Kirsch and Christian Marx (figure 10.5) as the ultimate street scooter suitable for "extreme shopping," as they say, and steerable with one hand or no hands, as they show. This is achieved with a mirror-image (negative) head angle α , which makes the wheel-flop factor (described in chapter 8) center the front wheel. The Plankalkül has a joystick for holding on during kicking but can also be propelled by *wedeln* (oscillation) in a manner rather like what can be done with *caster boards*. Unfortunately, Kirsch and Marx's project hasn't made it to production yet, but it is well described on the Plankalkül website (bodenstaendig.de/strassensurfbrett/).

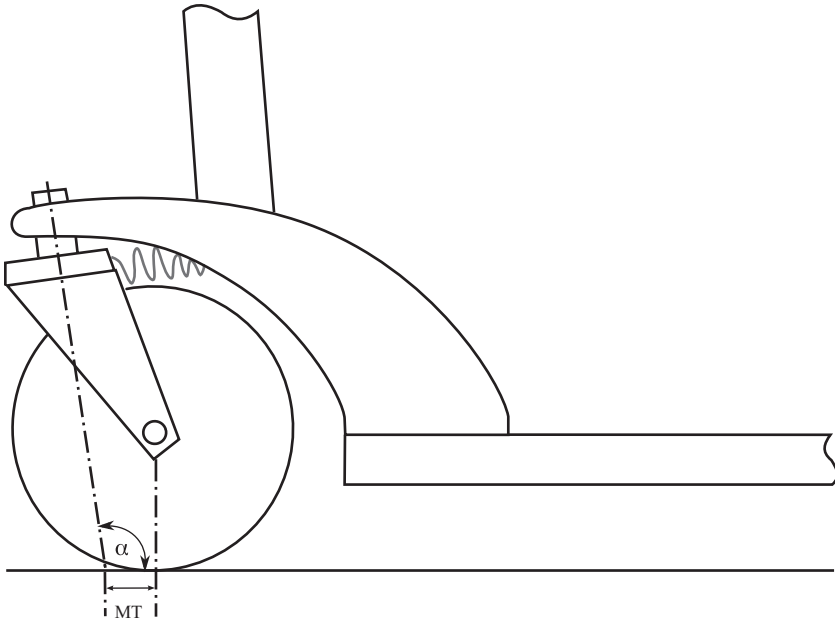


Figure 10.5

Drawing, showing head angle (α) and mechanical trail (MT), of an early model of the Plankalkül street surfer, which can be ridden with no hands by virtue of a wheel-flop-centered, castering front wheel.

Three Wheels and More

Most of the two-wheeled scooters described in the foregoing steer somewhat like bicycles, even though leaning the body works in a different way and free-handed riding is normally not possible. With the addition of a third wheel or more, steering and balancing are radically different from that of a bicycle, especially as many different configurations are possible, for example, modifications of the four-wheeled skateboard, in which putting pressure on one side of the board causes it to roll and the wheel axes to yaw, producing a turn. A single four-wheeled roller skate works much the same way, and so do many three-wheeled kickboards. Instead of the *turntable* of a traditional cart or cargo trike, which has a vertical axis and is directly yawed with some lever or handle, skateboards and the like have *trucks* on slanted axes, centered by elastomers and operated by weight shift. Theoretically their steering can be improved with Ackermann-type linkages, as discussed in Downs 2011.

Unlike countless historic designs with a single steered front wheel, newer tricycle scooters mostly have two wheels in front, with Ackermann-type linkages like those on larger vehicles, but operated by the scooter platform's roll angle and not by a steering wheel or bar (see figure 10.6). The models for adults originally had a handle with a knob, suggesting that it was not for yawing, but rather for one-handed rolling, or simply holding on to. Models for children and even newer adult models now have a handle for holding with two hands but still work the same way.

Although they are somewhat stable at rest, steering and balancing these tricycles is less intuitive, to cyclists at least, than the same operations on two-wheelers, even for well-designed models.

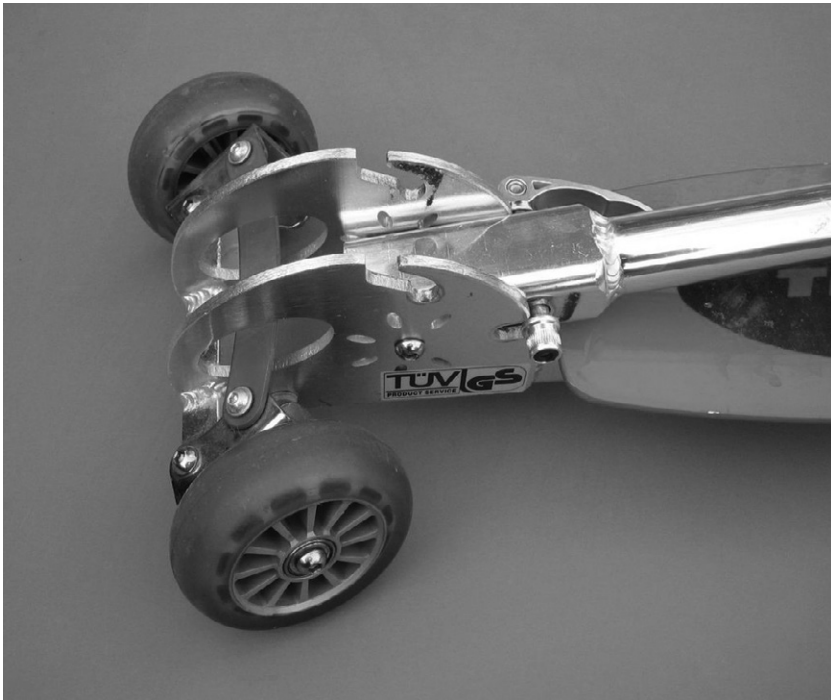


Figure 10.6

One of the coauthor's three-wheeled kickboards, unrideable at greater than walking speed even when new, probably because of excessive play in the linkages, in spite of TÜV—"tested" sticker and the logo of a reputable brand (not shown) (both may be forged)!

Unfortunately there are many ways to make these devices nearly unrideable at anything above walking speed. All that is required is a flawed geometry or too much play in linkages and bearings, which can also happen through wear even in better models. This is perhaps one reason they haven't caught on as much as two-wheelers and four-wheelers.

Many variants with peculiar geometries can also be found, for example, three-wheeled *carving* scooters with two pivoting trailing arms and rear wheels, one for each leg. This allows a strong leaning effect, small turn radii, and propulsion through properly phased weight shifting and steering movements. The word *carving* in this context probably comes from modern types of skis and snowboards that, in turning, are strongly inclined and “carve” through the snow on their edges, in contrast to traditional skis, which are inclined less and “slide” sideways.

Loads and Luggage

Most scooters don't have luggage racks or a provision for attaching a trailer, although both are possible. In an attempt to achieve at least a small percentage of the carrying capability of the African *chukudus* mentioned earlier in the chapter, two other approaches have been tried: industrial cargo scooters for warehouses and the like and trolley-type suitcases fitted out with an additional kickboard that can be folded up.

Models of the first type are, for example, designed for loads additional to the rider of about 50 kg and 70 L (Nimble two-wheeler), 90 kg and 150 L (Monark three-wheeled transport scooter, one front wheel steered, one front wheel castering, rear wheel fixed), or 120 kg and 190 L (Nimble five-wheeler = two middle fixed, two castering front, one steering rear).

The second type are typically for about 25 kg or 25 L and can be used not just in airports and railway stations, but also on sidewalks and minor roads. There are several makes. The coauthor bought two of the first ones available. A pioneer was the nicely named and designed Scootcase in 2001 by Robert Wohlfahrt, who has since gone out of business. Wohlfahrt found a clever solution for the requirement that such scooter suitcases must be able to roll in the opposite direction when scooted to that when trailed by the handle, like any two-wheeler suitcase trolley or hand-trailer. When

the suitcase is used in the tricycle-scooter mode, the two front wheels have axle journals freed for steering by weight shift. When the platform is folded up, it automatically fixes the two wheels so that they don't shimmy when the suitcase is used as a trolley (with reversed trail). Unfortunately the Scootcase was very difficult to ride in a straight line, the mechanism not technically mature or well engineered.

About ten years later, the much larger companies Micro-Mobility and Samsonite introduced their Micro Luggage (see figure 10.7), which today still gets good press and customer reviews and is produced in several similar variants. The coauthor's model came with four wheels. Two are on a front turntable-like axle, but attached with an angled axle to the case with just enough flexibility to yaw a bit when the device is forced to roll, like a very stiff skateboard truck, and two as a fixed double on the rider's rear folding platform. The Micro Luggage rides nicely in a straight line, but only under about 3 m/s, above which it starts to shimmy. The owner's manual states, often with double exclamation marks: "Maximum speed: 10 km/h. Not a toy, not for children. Not for down slopes (braking not assured). Not for both feet on the board. Not for wet surfaces." Also, only a very large turning radius is possible. After the coauthor inquired about this, Micro sent him a "carving" wheel as replacement for the double rear wheel. This has a clever castering axle inside, held elastically but very stiffly, that produces about 40 mm trail when mounted with the caster axis at -45° . This improves the maneuverability at the cost of a considerably higher rolling resistance. As a suitcase the Micro Luggage is of good quality, but rather small, only 10 L for rectangular things like file folders and 25 L for deformable things like clothes or small items. The coauthor pretested a new model now on sale. It has a larger capacity (33 L) and a very small turning radius but in the test started to shimmy severely at about running speed. This problem needed to be solved and no doubt has been.

Interestingly, the first concept for such a design was probably the Caseboard, proposed by two Swiss design students, Christof Hindermann and Jérôme Gesaga, in 1999. They offered it to Samsonite without success, but this may have caused Samsonite to contact Micro-Mobility ten years later in order to develop the Micro Luggage, according to Glanzmann (2011), after the Caseboard trademark had



Figure 10.7

Micro Luggage in typical environment, with special rear “carving” wheel.

expired. The coauthor, inspired by Scootcase, has also experimented with suitcase scooters, which he calls TranSportIV(e) (Schmidt 2008).

A newer make of luggage scooter is the Olaf-Scooter, which on video appears to handle well and is available with cases up to 40 L.

Saddles and Power

In China there have been many millions of slow electric scooters on the road for years, equipped with saddles. In the United States and

Europe, e-scooters are available that look almost like unmotorized kick scooters, although they are much heavier. They are becoming popular as a result of new legislation allowing legal use, and huge quantities are today available for rent (see chapter 11). Many are cheap and shoddy, but some are more expensive, of good quality and equipped with lights, disk brakes, lithium-based batteries, and a powerful multipole motor inside the rear wheel. Whether they can be legally used on public roads depends on local legislation and the scooter's configuration and speed. In Switzerland and Germany, for example, legal models can be used as a "bicycle," at least on cycle paths and minor roads at speeds up to 20 km/h using only the motor (Federal Ministry of Justice 2019). Although many models require an initial foot-kick to be able to switch on the motor (6 km/h minimal speed in Germany), they aren't hybrid vehicles like the pedelecs described in this book and keep going without further human power.

The coauthor includes in Schmidt 2008 the idea for an assist system controlled by sensors measuring the true acceleration (derivative of speed) and the apparent acceleration, allowing the calculation of slope and controlling the motor with any desired kick-augmentation characteristic. In 2018 he was able to ride such a kick-controlled e-scooter prototype at Micro Mobility and is convinced that a forced deceleration of about 0.05 m/s^2 , thus requiring regular kicks to keep going, would be much superior in regard to fun and safety to the fully powered e-scooter models that authorities have now allowed. Micro Mobility (2019) now sells such models fitted with what it calls "motion-control steering." A short video explains the function. Slope is compensated for, and after 10 s of operation, a renewed kick or a sharp hip movement is required to keep the motor going. This raises the legally permissible motorized speed in Switzerland to 25 km/h, a strong incentive for the use of at least some human power.

We haven't seen any nonmotorized scooters with saddles, but Paul Schöndorf, who formerly conducted HPV research at Cologne University, fitted a folding scooter with a saddle in such a way that it can still fold (figure 10.8). He says he can scoot much more easily and farther while seated than while standing. (Kick-scooting involves moving one's entire body weight unproductively a few inches up and down for every push.) Schöndorf's device is in effect



Figure 10.8

Paul Schöndorf's scooter with saddle (still foldable).

a very short and maneuverable Draisine. He finds it better to use only one leg for propulsion as if still standing and suspects that early Draisine riders did this also, as it results in a better connection from the rider's body to the vehicle without the rider's having to grip tightly with the hands. The unobtrusive vehicle with saddle can also be taken into crowded places and offers a weary person a seat almost anywhere.

Safety

Although kick scooters seem dangerous and generate a large number of accidents, fatalities involving such scooters appear rare (although increasing in the United States; see the injury statistics in CPSC 2019), and at least in Switzerland, the home of the modern kick scooters, a great many children are allowed to use them, even

on (minor) roads with traffic, to get to school before they are old enough to bicycle.

The quality of many kick scooter models is questionable, in spite of “tested” stickers. Some of their marginal features are inherent, especially the poor braking and steering capability in wet weather. (It is still possible, but requires practice, to brake adequately [briefly] by putting one’s full weight on the rear brake shoe.) It may be that specifically the *perceived insecurity* involved in riding a kick scooter leads most people to go no faster than they are willing to hit the road and motorists to take more care than with cyclists and pedestrians. Nonfolding robust models with more ground clearance are also available for sporting use in half-pipes and the like.

Human-Powered Vehicles for People with Disabilities

A great many special HPVs have been constructed to allow humans with disabilities to participate in cycle racing and general sports and to facilitate everyday transport. The adaptations include slight adaptations and hand cranks in lieu of foot pedals, and there are in addition completely custom-made constructions. Figure 10.9 shows a tricycle (Varna I) designed by George Georgiev especially for Daniel Wesley, a world skiing champion and Olympic gold medalist and a double amputee. Figure 10.10 shows an arm-powered, unfaired low recumbent being used in a road race. Amphibious boats are available that allow fit paraplegics to transfer from a wheelchair and enter the water safely. Hand-crank or hybrid add-ons or even half-bicycles (for a second person) can be fitted to wheelchairs.

A related field is that of electrical-assist devices. One method, uniquely for people with spinal-cord injuries, uses *functional electrical stimulation* to get paralyzed muscles to contract and enable, for example, paraplegics to power tricycles with their legs (see Technical University Berlin 2009 and Inria 2018). (Others are working on powered exoskeletons for rehabilitation and even for able-bodied people; see Marinov 2016.) A more frequent usage is assist-motors fitted to wheelchairs and special-needs bikes or trikes. Some firms specialize in fitting these as human-power assist instead of simple fingertip-controlled traction (see, e.g., Van Raam 2018 and Rio Mobility 2018).

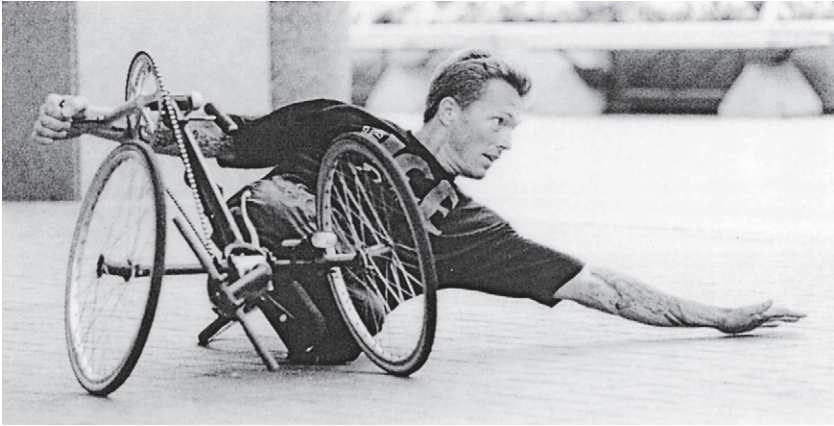


Figure 10.9
Varna I tricycle, designed by George Georgiev for Daniel Wesley. (Courtesy of George Georgiev.)



Figure 10.10
Arm-powered recumbent in a paracycling race circa 2013. (Photo by Pixabay user Mzter.)

Human-Powered Snow and Ice Vehicles

Skis and sleds may have been the first practical human-powered land vehicles. Today, the most versatile skis from a locomotion point of view are classic cross-country types: narrow and long enough to offer minimal resistance even in deep snow, a small “one-way” traction surface (skins, scales, or sticky wax) for resistance in the backward direction, boots free to pivot at the toe, and poles for aiding propulsion and balance. More modern skate-skis are faster but require a wide, smooth snow surface that generally must be prepared by machines. Skis and boots for mountain use are heavier and require the fitting of skins for going uphill. A new invention, Crossblades, functions like snowshoes uphill yet can be quickly transformed into miniskis for skiing downhill.

Leaving aside fat-tired or studded bicycles on snow or ice, there are a number of other types of snow and ice bikes available. Fitting skis instead of wheels on a bicycle-type frame results in a *ski bob*, which is generally used with tiny skis and claws on the feet for additional balance and braking. A ski bob is more or less a pure downhill device and is often fitted with suspension to avoid excessively jarring the rider’s spine. More bicycle-like and transportation oriented is a Swiss specialty called a Velogemel (figure 10.11), invented in



Figure 10.11

Velogemel “bicycle sled” with pivoting runners, static and leaning in curve. (Courtesy of Holzcreation Schmid AG [velogemel.ch].)

1911 by the carpenter Christian Bühlmann for getting around more easily with his slight handicap. Made almost entirely of wood except for the steel surfaces under the roughly 20 mm wide, slightly concave runners, it steers like a coasting bicycle downhill, with the feet resting on stubs or used for braking. On flat surfaces, they can also be used for propulsion as with a Draisine. On steep uphill ground, the narrow and light (~7 kg) Velogemel is easily pushed or shouldered. As today even ski resorts tend to remove all snow from roads, Velogemels (like sleds and skis as well) can often no longer be used for local transport, only for sport and tourism. They can be rented (at the railway station), raced, and purchased in Grindelwald, Switzerland, where they are still manufactured.

Human-Powered Speed Machines

A great many speed records have been set in HPVs (some recent ones are noted in chapter 3), and space is insufficient here to pay tribute to them. However, we would like to make space for a commercial of sorts. In the second edition of this book, the senior author applied the methods recommended in earlier chapters to forecast that the maximum speed of a streamlined HPV pedaled by a top athlete through a measured 200 m would be 65.4 mph (29.25 m/s) (Whitt and Wilson 1982). He was subsequently very proud that this transpired with the Easy Racer Gold Rush (designed and built by Gardner Martin), at 65.5 mph in 1986. This apparently accurate forecast held for six years, when it was proven pessimistic, as the Cheetah fully faired recumbent bicycle (figure 10.12), designed and built by a team from the University of California, Berkeley, achieved 30.7 m/s (68.7 mph) on a high-altitude desert highway in Colorado. Nine years after the Cheetah set its record, in 2001, the Varna Diablo recumbent bicycle sped along at 36.0 m/s (80.6 mph) on a long, nearly flat asphalt road near Battle Mountain, Nevada. Second in speed at the same venue was Matt Weaver's Kyle Edge (figure 10.13). By having the vehicle's rider lie on his back, looking at a small monitor connected to a television camera in the vehicle's nose, Weaver was able to design a fairing with a flow that was predominantly laminar and therefore with a low drag (see chapter 5). Panel (b) of figure 10.13 shows his speed and power versus distance. Not shown in the figure is the effect of gravity at this site: the slightly sloping run-up

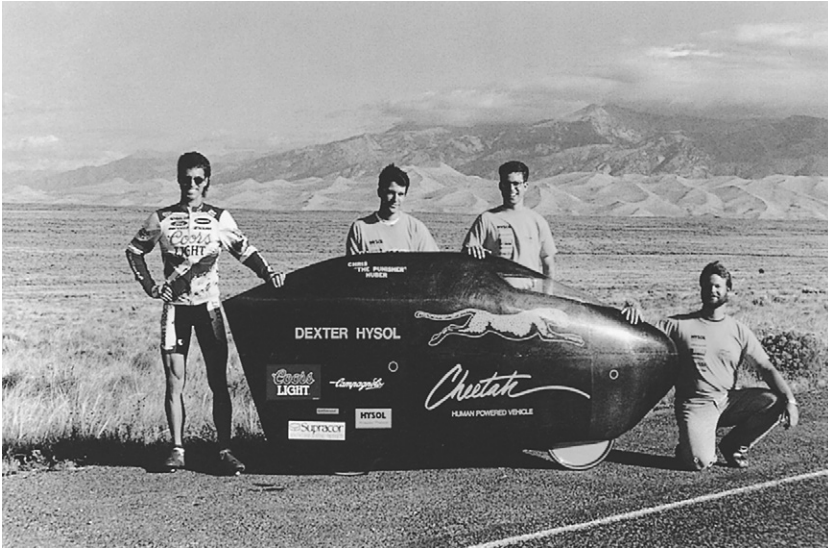


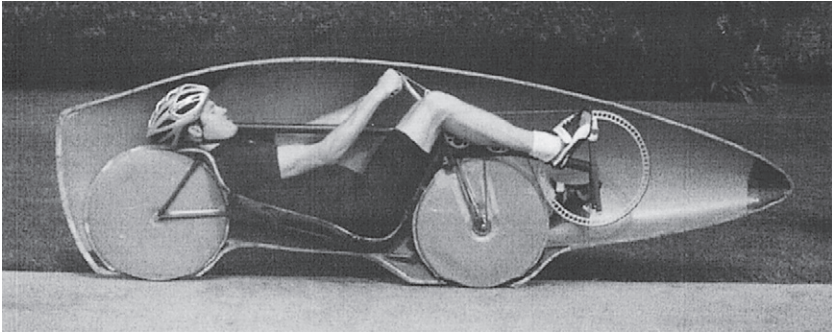
Figure 10.12
Cheetah fully faired recumbent bicycle.

allowed “harvesting” of about 30 kJ potential energy, and the slope contributed up to 200 W power at maximum speed (see chapters 3 and 4). Of particular interest is the planned power level, starting at 350 W and reaching 600 W in the timed section. A successful speed record of this type has as much to do with the continuous optimization of the human power level during the run-up as with the technical optimization of the vehicle. The higher speeds achieved today at the Battle Mountain site reflect not only vehicular improvement, but also experience and practice in this human-power-level optimization. The present record at this site, by the Aerovelo Eta, is over 40 m/s (89.6 mph, 144 km/h).

Human-Powered Rail Cycles

During and after the time when railroads were being built, railcars—generally worked by hand levers (pump trolleys)—were used to take workers along the rails and to inspect the track. Some rail inspection continued into modern times using especially light single-person pedaled vehicles. In some Asian countries railcars and even small

(a)



(b)

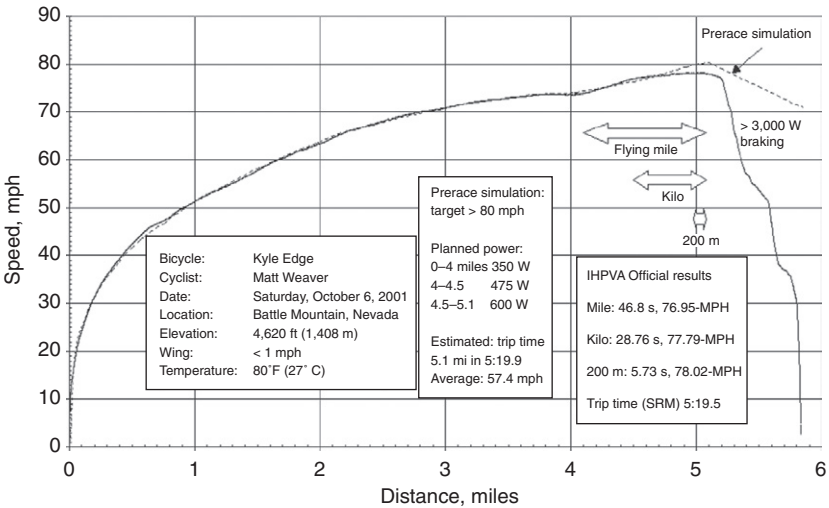


Figure 10.13

(a) Matt Weaver in half of the fairing of the Kyle Edge HPV; (b) Matt Weaver's speed and power versus distance in his October 6, 2001, run, Battle Mountain, Nevada. (Courtesy of Matt Weaver.)

trams with passengers were hand pushed, as were small mining carts everywhere. See Wikimedia Commons 2018c and its subcategories for many photos of both historic and modern vehicles and Wikimedia Commons 2018b for many more.

Today many tracks are in heavy use by high-speed trains and no longer suitable for such vehicles. Others are being abandoned, leaving priceless rights-of-way connecting towns across (usually) picturesque rural routes having low maximum gradients and ideal for cycling. The rails are removed from many such trails, and some are made into cycle paths. In many other cases, however, the rails remain and are available for either officially organized or clandestine (mostly illegal) sport and tourism. Traditional small rail vehicles are called *handcars* or *draisines*, even though they are technically quite different from the Draisines described in chapter 1. However, a draisine in both senses of the word was patented in 1897 and is now preserved in the Mulhouse (France) railway museum. Restricted to a single rail, it must be balanced as well as propelled with the legs, requiring special skills.

Today human-powered draisines are offered mostly for touristic use by track owners themselves. The website Railbike.de lists over a dozen sites, mainly in Germany and France, where such vehicles are available (figure 10.14). They are generally moderately heavy, with four steel wheels, and usually pedal powered by two persons, but with room for more passengers. As the lines are mostly single-track, passing involves one party lifting the vehicle entirely off the track in order to let the other one pass. Speeds are usually under 4 m/s or so, because of friction or gearing, and this is often desirable from a safety point of view. Compared to road vehicles, there is the danger of derailment and injuries from the track's rough, sharp-edged gravel ballast. Also, the tracks sometimes cross roads, and the draisines must be able to stop in order to give way. At least one resident of the Hallig Nordstrandischmoor (a special type of North Sea island off the coast of Germany) is seen regularly using the track connecting to the mainland at Lüttmoorsiel in order to go shopping with his rail bike.

An unofficial type of adventure sport or tourism is rail biking: cycling on one rail, balanced by an outrigger to the other rail. A true single-rail bicycle without outrigger would be practical for passing other rail bikers. No easy way of balancing seems yet to have been



Figure 10.14

Typical tourist rail draisines at Saint-Thibéry, France, one of three Pedalorail sites (pedalorail.com). (Photo by Didier Duforest, licensed CC-BY-SA 3.0.)

conceived, but it would be possible by using (powered) flywheels as gyroscopes or reaction wheels (see chapter 8).

Rail bikes are used mostly on remote, hardly used, or abandoned railroad tracks in North America (see Mellin 1996). Figure 10.15 shows Richard Smart's Railcycle apparatus for converting a bicycle to a rail cycle. It steers the bicycle's front wheel (and consequently also the rear wheel) to stay exactly on the rail and uses a lightly loaded outrigger to keep the bicycle upright, as the normal weaving motion for balancing is no longer possible (see chapter 8). The steering apparatus uses a magnet to locate itself against the inside of the rail, as the outside edge is often unavailable or clogged up. Similar devices can be built at home; plans are available on Richard Bentley's comprehensive railbiking website (rrbike.freesevers.com), which also includes pictures, travel reports, and links to many other projects.

Human-Powered Rail Vehicle Technology

Typical rails offer a 2–3 inch (~50–75 mm) wide steel surface that is, however, slightly rounded on top and generously rounded on



Figure 10.15

One of ten Railcycles purchased by the London Underground, used here by an engineer. (Courtesy of Richard Smart.)

the edges and is often canted inward at a 1:40 angle. Typical steel wheels are conical at 1:20. Thus in normal operation there is a “point” contact, and the wheel flanges do not touch the rails. If two wheels are fixed on a common axle, they will steer themselves without using the flanges, as any lateral displacement causes a difference in the wheels’ radii and a resulting corrective torque and movement. This results in smooth steering but also, depending on the degree of freedom in yaw, some scrubbing and friction. In turns the flanges come more and more into play. In practice, however, most human-powered draisines don’t use such a common-axle system anyway and instead allow the wheels to turn independently. Some use lightweight cylindrical wheels with attached conical or vertical inside flanges that then cause friction when they touch the edge of the rail. A square inch or so (25×25 mm) is generally free at the rail’s inside edge for flanges or other guidance, but the rail’s outside edge is often not usable, notably at level crossings and points. This is a problem for asymmetric rail bikes with lightly

built outriggers, especially as the width between tracks (e.g., 1,435 mm standard) varies, being greater in curves. Some rail bikes use guides on the outside edge that can flip up or are very short. Most rail bikes, including those used for racing, separate the vertical-load-carrying and the lateral-guidance functions completely. For the former, bicycle wheels with tires are often used or thin machined disks; for the latter, thin inclined skate wheels or even just small ball bearings, inclined or vertical. Single outriggers generally don't need lateral guides.

A further type of rail vehicle uses a recumbent position and a full fairing. See chapter 3 for a description and picture of Charles Henry's record-breaking faired machine Snapper (figure 3.8), which was built for officially organized 200 m rail speed trials in Laupen, Switzerland. These speed events came about because the local railway company closed the line between Laupen and Gümmenen, serving commuters with buses instead, and the coauthor wanted to "rescue" the rail connection with solar- or human-powered draisines for travelers. Of course this option was of no interest to the rail company, but its director, Erich Scheidegger, knew the line's leisure potential and helped organize the speed events and purchased touristic draisines himself. Unfortunately, a small part of the track has been ripped up, severing the Gümmenen connection, but most of the length is still available for booked parties using the draisines. Scheidegger bought the remaining track and since his retirement runs the family business (Schienenvelo.ch) and organizes trips for up to 8,000 persons per year.

A page on the Future Bike website (futurebike.ch/page.asp?dh=2058) shows the results of the four events on the Laupen track from 1997 to 2001, along with some pictures. (The coauthor managed the slowest recorded time at 18.5 km/h with his ScootRail, a four-wheeled rail kneeboard.) At just over 70 km/h (19.46 m/s), Charles Henry achieved the fastest rail speed during the 1999 HPV World Championship (Interlaken Festival of Human Power). He and his cobuilders based Snapper's design on that of a road machine with a 17-inch front wheel and a 20-inch rear wheel driven by a 2 × 7 transmission. Skate wheels are used on the sides of the rail under the cockpit to keep the vehicle's wheels centered. The layout has a compact long wheelbase (1.5 m) with a single-tube chassis, on which the fairing is mounted.

The track in Laupen was, as noted previously, out of regular service, but it was well-maintained, straight, and relatively flat. The last speed trials on rail took place there in 2001. Charles Henry was a bit slower in those trials, but another rider achieved a speed of more than 70.5 km/h in Snapper, and another team led by Romeo Gridelli achieved 74.53 km/h with a rather similar vehicle and a champion rider. This may be still be the 200 m speed record—at least we are unaware of any similar events since. It could easily be bettered at another site, as the available run-up at the Laupen site is only about 1.5 km.

It has generally been believed that streamlined (faired) rail cycles should be the fastest possible HPVs. However, to achieve top speed they would probably need to have a special narrow-gauge track, perhaps of 200–300 mm, which, for a record attempt, would probably be a banked circular track of, say, 200 m diameter. This would confer on rail cycles using such a track the following advantages over pneumatic-tired bicycles on a highway:

1. Wheels made of steel (or of other hard material) used on steel rails would have very low rolling resistance.
2. The wheels would not have to be steered, so they would be mostly inside the fairing and could run in narrow gaps (thus avoiding large “pumping” losses).
3. Not being needed for steering, the rider’s arms could be used to add power to that delivered by the legs. An increase of 20 percent in power output could be expected for a short-duration effort. Also, the rider would not have to see ahead, if the track were circular and well protected, so that the air drag associated with a window and a heads-up position could be eliminated.
4. The streamlined enclosure would be better aligned with the relative airflow and steadier than that on a typical road machine, so that boundary-layer suction might be used to extend laminar flow and thereby to reduce the aerodynamic drag (see chapter 5).

This is the theory, but so far rail vehicles have been slower, not faster, than similar road vehicles. A good example is Charles Henry and his Snapper, just described. During the same week in 1999, with a similar run-up of about 1.5 km and a 200 m timed section, he achieved 81.6 km/h with Snapper as a road vehicle (on the runway

of the Interlaken airport) and more than 11 km/h less as a rail vehicle in Laupen. Part of the difference is due to unequal slopes (about -0.33 percent in Laupen and -0.45 percent in Interlaken) and part to the vehicle's outrigger and its wheel. A further reason may be that a road bicycle is free to weave very slightly with the periodic yawing moment caused by the rider's swinging legs, but a rail cycle experiences periodic side forces that are taken up only by guides—skate wheels in this case. The similar Gridelli vehicle was also ridden by the same champion in both 1999 speed events: 72.5 km/h road and 69.0 km/h rail. This rather smaller difference is a bit surprising, as the vehicle's rail outrigger consisted of four unfaired tubes generating considerable air drag. An unknown factor was the wind, which, although slight, wasn't monitored closely enough to estimate its actual effect.

To sum up, human-powered rail vehicles could theoretically be faster than similar road vehicles, but only with careful optimization of all components. Up to today they have always in practice been slower.

Human-Powered All-Terrain Vehicles

All-terrain bicycles (ATBs or *mountain bikes*) are well known and fall outside the topic of this chapter, as do the multitrack, often artistic human-powered all-terrain vehicles that can traverse sand, mud, and water. The former are still undergoing development, spurred by competition for a still-large market and by the desire on the part of component and bicycle manufacturers to win races, in order to increase market share. The rapid developments in suspensions, gear-shifting mechanisms, disk brakes, wheels, and tires for ATBs have been beneficial to the rest of the bicycle industry, including HPVs. Derailleur transmissions and exposed chainwheels are weak points in present ATBs, and it seems probable that some of the alternative transmissions described in chapter 9 will be adopted for these bicycles. Electrically assisted ATBs have extended their attractiveness to new user groups, fat tires to new terrains. Organized downhill ATB racing is a growing activity. Improved reliability of all components is a probable outcome of further competition and development.

Human-Powered Recumbent Vehicles

Recumbent bicycles are those in which most of the rider's weight is carried in a seat; a little on the pedals, which are out in front of the body; and virtually none on the handlebars. (On a diamond-frame [i.e., upright] bicycle, the weight is ideally divided equally among saddle, handlebars, and pedals.) Enthusiasts for recumbents (as we are) believe in this type of bicycle for commuting, touring, and its own form of racing. Only in dense city traffic does the upright bicycle seem superior with respect to overall vision and maneuverability.

As observed in chapter 8, recumbents are produced in many configurations. Some have the front wheel behind the cranks and bottom bracket, producing a short wheelbase (SWB). Others have the front wheel ahead of the bottom bracket, resulting in a long wheelbase (LWB). A growing proportion have the bottom bracket over the front wheel (for a high pedaling position), sometimes referred to as a *compact long wheelbase* (panel [c] of figure 10.16).

Another variation among recumbents is in the position of the handlebars, for steering either under or over the seat (USS or OSS). LWB recumbents tend to use USS handlebars with a single or two linkage rods (panel [a] of figure 10.16). The LWB-OSS combination is possible, but the handlebars and stem of the bicycle can be quite long, and if the handlebars are directly mounted, there can be a pronounced "tiller effect": the handlebars must be swung in a wide arc to steer. An alternative arrangement is to use some form of gearing or universal joint at the head tube. The handlebars can then be twisted and become something like a steering wheel or a joystick. USS handlebars are also often configured as short single joysticks. We prefer USS handlebars because in the event of the rider's being ejected in an accident, there are fewer bicycle parts that might cause injury.

However, OSS systems (panel [b] of figure 10.16) are more popular, probably for psychological reasons: there is something to hold onto, the arrangement is familiar to car drivers, and the soft belly that creatures are normally loath to present to the hostile environment seems protected. SWB and compact LWB recumbents are also more easily fitted out with direct OSS handlebars than with the additional parts that USS systems usually require.

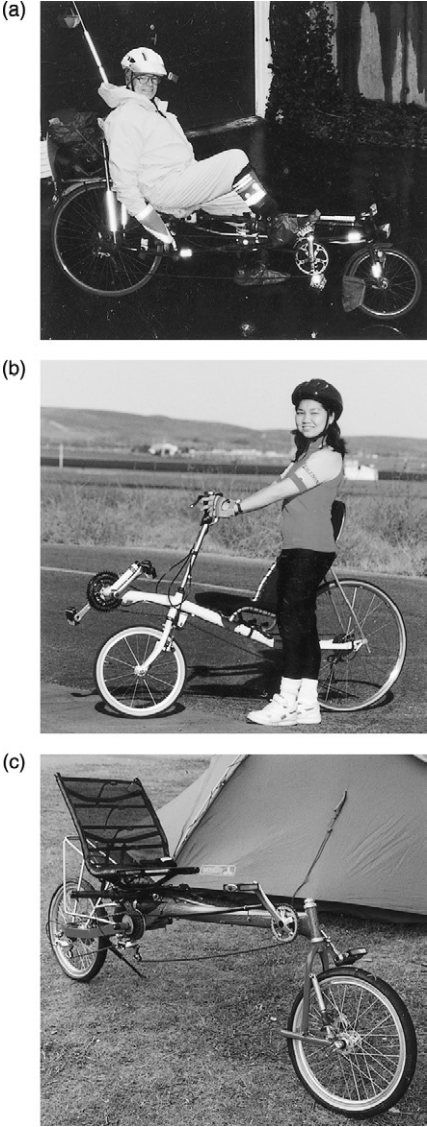


Figure 10.16 Recumbent-bicycle wheelbase types: (a) long, (b) short, and (c) compact long. (Photos (a) by Ellen Wilson, (b) courtesy of Lighting Cycle Dynamics, and (c) by Dave Wilson.)

Finally, many recumbents are center or pivot steered by the rider's propelling legs, with fixed handlebars on the rear assembly mainly to hold brake levers and shifters.

Recumbents can be unfaired, as in the examples in figure 10.16, or partially (figure 5.14) or fully (figures 3.5 and 10.12) faired. They can be driven through the rear wheel, again as in the examples in figure 10.16, requiring particularly long chains, or through the front wheel. They often have a rear wheel of conventional size and a smaller front wheel, as in the examples in panels (a) and (b) of the figure, or two wheels of the same size, usually smaller than conventional wheels, as the example in panel (c). Variations in the height of the bottom bracket are associated with variations in the angle of the seat back. Either the seat or the chainwheel position must be adjustable to accommodate riders of different sizes.

A number of advantages are claimed for recumbent bicycles over the traditional diamond-frame, upright pattern:

1. Greater safety because of the smaller possibility of taking a header over the front wheel or of catching a pedal or foot on the ground when cornering. We have experienced numerous such mishaps with conventional bicycles, but only leg scrapes with recumbents. The senior author had a chain break in early 2016 on an upright bicycle, causing a chest impact and long-lasting traumatic brain injuries, with associated health problems. Presumably these would have been avoided had he used his usual recumbent.
2. Greater comfort in an almost complete absence of pain or trauma in the rider's hands and wrists, back, neck, or crotch, including nearby internal and external organs.
3. Improved braking mainly in LWB models.
4. Better visibility forward and to the side for the rider compared with that for a diamond-framed road bike with dropped handlebars.
5. Lower aerodynamic resistance for some configurations.

Some disadvantages are also noted:

1. Rear vision is more difficult than for conventional bicycles, so that good rearview mirrors are essential for safety.
2. Recumbents are generally not good on rough terrain and in snow, because one cannot use changes in body position to improve balance.

3. For the same reason, one cannot attack a hill, for instance, by jumping up on the pedals, which can give some muscle relief for riders of conventional bicycles. A wider range of gears is therefore desirable on recumbents.
4. Most recumbents are heavier and more expensive than their diamond-frame counterparts.

Sales figures, at least in the United States, of recumbent bicycles at the turn of the millennium exceeded those of tandems. However, most bicyclists in most regions of the world have not seen or even heard of recumbents, and even in the Western world, they remain a niche.

There will be some who question the use of the word *innovation* in respect to ongoing work on recumbents. Bicycles and cycling have a rich history, and it sometimes seems that a precedent can be found for every “new” development. The senior author’s involvement with recumbents started with his organization (1967–1969) of an international design competition in which he encouraged recumbency, entirely unaware of the existence of earlier recumbents. Subsequently, friends constructed prototypes of five of his designs, and each one could later be said to bear at least some resemblance to earlier machines.

There is, however, a fundamental difference between recumbent design today and that in earlier periods: there are now technical publications and symposiums, including their online archives on the internet, that, along with other routes, such as forums, allow information to be disseminated at a speed orders of magnitude greater than was previously possible. These faster dissemination channels should ensure that future innovators will spend less time repeating earlier developments and more time making advances.

Tricycles and Quadracycles

Classic and historic multitrack cycles are described (briefly) in other chapters of this book. Modern recumbent tricycles and quadracycles are perhaps the most “natural” vehicles for humans that there are: almost anybody can get going on one without any instruction or experience, and very safely, at least as long as no other traffic or gradients are involved—and with a bit of experience these too can be mastered. They then offer relaxed rolling, especially when going

slowly from necessity or choice; stopping is always easy and comfortable. Many of the characteristics of the vehicles described in the next section also apply.

Velomobiles

HPVs with full fairings are often called *velomobiles*, mainly if they are meant for practical use. The first probably appeared in 1925. The many types are too numerous for discussion here (for this see Dovyđenas 1990, Rasmussen 2015, and Lohmeyer 2018), but the following subsections describe some of their properties according to the number of wheels.

Two Wheels

Two-wheeled (single-track) velomobiles have many of the advantages of unfaired bicycles, and in addition, less air drag and greater rider protection. The fastest speed records for faired HPVs are achieved by two-wheelers. However, practical two-wheeled velomobiles are very rare, and none appear to be commercially available today, unless partially faired models are counted. The reasons are fairly obvious. Although their medium-speed stability is good:

- Stability at rest is zero. The fairing must be open to the road, have flaps for putting the legs through, or have retractable balancing wheels.
- Low-speed stability is poor. Weaving in traffic or uphill requires a fair amount of room and looks odd.
- High-speed travel looks odd if the vehicle weaves because of the rider's (not visible) reciprotating legs and can be unsafe in gusting wind.

Therefore, these presumably safest and certainly fastest of all vehicles *appear* to be the least safe. In 1985 Vytas Dovyđenas constructed his 30 kg V-11 two-wheeled velomobile with retractable side wheels. A Belgian model called Velerique was sold around this same time. Today no models with full fairings are commercially available. Stefan Gloger has extensively researched most aspects of two-wheeled velomobiles, in particular with his 33 kg Desira-2 with bottom foot openings. He has examined the usability and handling problems, also in crosswinds (Rohmert and Gloger 1994 and Gloger



(a)



(b)



(c)



(d)

Figure 10.17

Velomobiles: (a) Leitra enclosed tricycle, with Mr. and Mrs. Georg Rasmussen; (b) Aeolos enclosed recumbent bicycle, with its constructor, Joachim Fuchs; (c) Cab-Bike; (d) Alleweder semienclosed tricycle. (Photos by Dave Wilson.)

1996). Another constructor of a practical two-wheeled velomobile is Joachim Fuchs (1996) with his Aeolos (figure 10.17, panel [b]). The rear part of Aeolos's two-part fairing slides rearward for entry and riding in hot conditions. Fuchs reports good handling in crosswinds as the result of a well-forward lateral center of pressure (see chapter 5).

Three Wheels

Almost all velomobiles are tricycles (mostly tadpole models—that is, those equipped with two front wheels and one rear wheel), for good reasons:

- At the cost of just one more wheel, good static and low-speed stability is achieved, practical for loading and pleasant for puttering, even in traffic.
- All three wheels make contact on any surface; that is, they all touch, even without suspension.
- The disadvantage of poor dynamic lateral stability is not severe in normal riding.
- The disadvantage of (normally) three tracks is not severe on the well-surfaced roads mostly available.
- Highly aerodynamic fairings are possible in tadpole and some delta (that is, one front wheel and two rear wheels) configurations.
- Fairings are adaptable for different environmental conditions.
- Space for luggage is reduced, but any items carried are well protected from the environment and from loss. The rare delta models can provide considerable space for luggage or even cargo or passengers (the coauthor was even able to sleep full length in his faired tricycle).

Conversely most tricycle velomobiles are unsuitable for rocky, slippery, or highly cambered roads, narrow or obstructed paths, fast cornering, and emergency braking. A few tilting models are available. These combine good static stability (with the tilting mechanism locked) with high-speed cornering stability.

Georg Rasmussen, a Danish physicist, developed the Leitra enclosed tricycle (figure 10.17, panel [a]), which has hundreds of enthusiastic users, almost entirely in Europe. His pioneering work has been followed by the development of the Alleweder (figure 10.17, panel [d]), the Twike, and the Cab-Bike (incorporating battery-electric power assist) (figure 10.17, panel [c]). Many similar (but generally cruder) carlike HPVs had also been developed previously. Some flourished for a few years, for instance, in the years after World War I, and for shorter periods after World War II and during the energy crises of the 1970s. It could be said that they were overcome by affluence: as people earned more money, they tended to

“trade up” to vehicles of increasing size, power requirements, and speed.

Four Wheels

The HPV designers Paul Schöndorf, Ingo Kolibay, and Juliane Neuss (junik-hpv.de) all point out the advantages of going to four wheels:

- Lateral and longitudinal stability are simultaneously good, as are braking and traction.
- Short models are possible, and some can be parked vertically.
- Ample space for luggage or cargo is assured.
- Two tracks allow driving over central obstacles.

The disadvantages of four-wheeled velomobiles include higher weight and cost, especially as suspension is required to keep all wheels in even contact on all surfaces. A major sticking point in the acceptance of four-wheel velomobiles appears to be the way they are perceived: two-wheelers are “cool” as racing machines, and three-wheelers are seen as something exotic and superior to wobbly bicycles, whereas four-wheelers are in danger of being regarded as tiny cars, for example, for children, poor people, or pedal-car or soapbox racers, and compared unfavorably to standard automobiles, also with respect to internal passive safety.

Prospects for Velomobiles

The skewed perception mentioned in regard to two- and four-wheeled velomobiles applies to some extent to all HPVs: instead of recognizing the enormous gains in *external* safety compared to standard cars and considerable gains in *internal* safety compared to standard bicycles, people dwell on relatively rare situations like being rolled over by a truck or a head-on collision. In 1985 Sir Clive Sinclair produced an electrically assisted, partially faired recumbent tricycle, the C5. In spite of being pronounced particularly safe in a government study, it was ridiculed by the press as a dangerous toy. Its price was also much too low, giving rise to a number of ergonomic design faults (short pedals, no gears, no seat adjustment), so it is remembered more as a flop than the partial breakthrough it was (see Henshaw and Peace 2010).

Similar perceptions regarding speed and status mean that velomobile usage is far lower than that of other vehicles. The relatively

new development of light and effective electric-assist drives may help to improve this low usage rate. Two major disadvantages of velomobiles compared to open HPVs are greater noise (generated or amplified by the fairings) and less effective cooling. Noise can be reduced by constructing the fairings from high-density foam plastic instead of hard materials or through careful sound design, and cooling can be improved with fans and also with power-assist, which can reduce the amount of rider sweating, especially when riding uphill.

We think it is important, however, to retain the element of human power. Pure motor vehicles have a tendency to become faster, heavier, and larger. Only if some element of human power is retained is the human scale also retained. The relatively powerful and expensive Twike, for example, with a few exceptions was always sold as a hybrid vehicle and kept its original dimensions from its inception as a pure HPV. Indeed, the developers around Ralph Schnyder tried to make it a pedelec using Kutter's Velocity drive (see chapters 1 and 9). They didn't succeed, but they managed to retain functioning parallel pedal drives.

Not just their aforementioned former demise, but also recent interest in velomobiles and HPVs, comes as a result of affluence. Too many people, in our opinion, use motor vehicles too much and—as has been well established by the medical community—are getting too little exercise. City centers and beyond in many parts of the world are clogged with internal-combustion-engined vehicles that can move only very slowly because of the congestion their sheer numbers create. Worldwide the air is extremely dirty, with people dying prematurely by the millions as a result. The climate is warming and the planet is changing, with potentially catastrophic results. It would be logical, therefore, to predict that HPVs have a rosy future ahead of them. We hope they do! On the other hand, there are large flows of tax moneys and other funds aimed at developing larger battery-electric and fuel-cell vehicles that seem unlikely to sufficiently solve these problems, although lower local noise and pollution levels are of course to be welcomed. However, they could also lead to even more cars on the roads, because of a rebound effect, and because the existing cars won't just go away. As rich nations electrify their fleets, many discarded cars end up in Southern cities, intent on repeating Western and Eastern automobility disasters.

Velomobiles are Northern creatures, and it is difficult to see how they can achieve any status in equatorial regions, given the increasingly extreme climate—maybe open or power-assisted ones will be able to, or closed ones if they can be fitted with air conditioning.

Partial Fairings

Fully faired velomobiles can be very fast, or practical, but seldom both at the same time. A major consideration is getting in and out of the vehicle. The fairing bottom in front of the seat must be strong enough to stand on, retractable, or protected by strong load-bearing members. Easier to accomplish are an open bottom, an open front, or open sides. In racing, partially faired HPVs are defined as those with either a front fairing or a rear fairing, but not both (see figure 5.14). Partially faired velomobiles generally have both, but large enough side or top openings for easy access. Many are convertible, with a closed top for racing or rain, which can be removed for greater cooling but less speed. Good compromises between usability and speed can often be identified by observing which models arrive at HPV meetings or races powered by the racers themselves, rather than transported by motor vehicles.

Human-Powered Multirider Machines and Road Trains

Bicycles for two riders *in tandem* (one behind the other) are well known, and versions for three to five riders are occasionally also used. Tandems for ten to twenty riders have been demonstrated but are not very practical. More useful human-powered “buses” for up to a dozen riders are usually *sociables* with side-by-side seating and at least three heavy-duty wheels. In some the riders face each other, as with the Conference Bike for seven riders sitting in a circle (conferencebike.com). More riders are possible with *road trains* formed by connecting great numbers of trailers or tricycles. One of the first was the Thuner Trampelwurm (figure 10.18), or “Thun City Centipedal” in a loose translation, a brainchild of the Swiss artist Albert Levice in 1994, which is still in use in 2019. Ten two-wheeled trailers, each for carrying one person, are hooked up behind a LWB recumbent tricycle in such a way that they follow the leader nearly perfectly—almost as if on rails defined by the path of the leading trike. It was a difficult task for a group of students at the Engineering

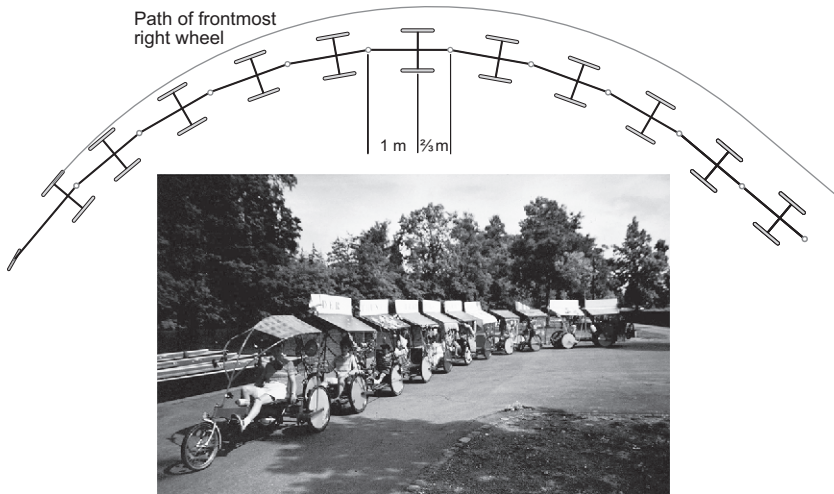


Figure 10.18

Thuner Trampelwurm: photo and path of the complete road train turning left 90°. The shown displacement to the inside is purely geometrical without regard to tire or dynamic forces and is less in practice, when it is possible to form a 360° merry-go-round with only slightly more displacement than one trailer width.

College of the Canton of Bern in Biel, Switzerland, to come up with a usable system. They designed a good compromise with almost perfect following (tracking) and enough stability to drive up to about 15 km/h without the train's beginning to snake back and forth. Even so, hydraulic yaw dampers are required at half of the connecting links. A similar pitch-stability problem was solved by using the trailer units in pairs, with each pair having one fixed pinned and one detachable vertically sliding coupling. This also allows the train to be shortened easily, which comes in very handy if only a few people want to use it. Each unit has a seat and pedals or a linear drive or rowing mechanism, as well as a roof made of canvas on a tubular frame.

Four complete Trampelwurms were built by unemployed persons in the Swiss city of Thun and extravagantly decorated by local schoolchildren. The ownership and management of what has become a local tourist attraction has changed several times since the start. For many years a group of about ten part-time drivers were employed and trips organized for several thousand persons per year.

Now twenty-five years later, nearly half the units have been used up for spare parts, but the others are still going. Although as heavy as an automobile and as long as any legal road vehicle, the Trampelwurm can negotiate the most crowded and narrow pedestrian areas in safety and can also travel on typical roads as long as they are not too steep. Parties enjoy the tricks the drivers perform, like catching up with their train's own tail, forming a temporary human-powered merry-go-round, or diving into a particular steep narrow tunnel in roller-coaster fashion.

All of the technical difficulties of road trains—tracking or stability, braking, and a high empty weight (i.e., the pilot has to shift nearly a half-ton unaided when pedaling to a pickup point)—could be solved by using motors in some of the wheels, a rather expensive solution for which it would probably be difficult to get official approval. The (unmotorized) Thuner Trampelwurm brakes through a combination of (not very effective) mechanical overrun brakes, (very effective) hydraulic brakes on the front six wheels, an occasional manual “hill brake” in the middle, and an “emergency brake” at the end.

A most interesting problem is faithfulness of tracking. A moment's reflection will show that for a large number of two-wheeled trailers to track perfectly, they must be constructed symmetrically, that is, the distances from the wheel axis to the hitch points must be the same in the front and in the rear. If all hitch points were ball joints, there would obviously be zero stability in both yaw and pitch, and the whole train could fold completely. The only thing preventing this is the most forward hitch connected to the tractor vehicle, which defines all joint positions for the entire train, but as play accumulates to the rear, they would in practice oscillate, sway, and jackknife. At the other extreme, if the rear hitching distance is zero, that is, each trailer is hitched at the wheel axis of the front trailer, the stability is high, but the tracking in curves is poor, each trailer to the rear moving more and more to the inside. The Thuner Trampelwurm is a compromise: the ratio of forward to rearward hitch distances is 3:2. The tracking is not perfect, but adequate. Figure 10.18 shows the displacement due to the actual geometry. The exact situation at the beginning and end of the curve is unclear and would need a mathematical analysis. In practice there are opposing forces due to tire slip, hydraulic dampers, and centrifugal pseudoforce, so

the tracking is better than shown. The speed is, however, limited, as above about 15 km/h swaying oscillations and jackknifing start (in the case of deformed frames or unevenly pedaling riders, even at half this speed). The ratio of hitch distances should therefore probably be increased.

This type of train can also be formed with commercial delta tricycles. The front wheel of a tricycle is connected with a second, pivoting fork to the tricycle in front of it, or more often the wheel is removed and its fork connected directly via a pivoting pin (see Mary 2010 for an account of delta tandem touring). Trains of many more delta tricycles are occasionally formed for fun and records. The longest appears to be a train of ninety-three Hase Kettwiesel trikes demonstrated in 2007. Lateral stability and tracking seems not to have been a problem, but rather the control of pedaling and braking, which was accomplished with “Pedal!” and “Brake!” placards held up at appropriate times. More recent trains of twenty-three to twenty-seven trikes in the United States were more roadworthy but still too long to be really practical. By using sociable trikes the number of passengers per length of train can be increased. Figure 10.19 shows three coupled Gem sociable tricycles made by HPV pioneer Peter Ross. The value of such trains is not technical, but rather in allowing a single guide to pilot a group of people, who can then concentrate on activities such as sightseeing and talking instead of driving.

Cargo Bicycles

Cargo bikes, or *freight bicycles* as listed in the so-named Wikipedia entry, have been around for a long time, for example, tradesmen’s



Figure 10.19

Train of three recumbent sociable Gem tricycles. (Photo by Jason Patient.)

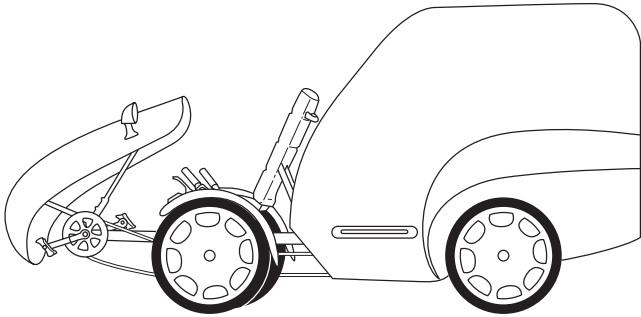


Figure 10.20

Freight-carrying recumbent quadracycle.

bicycles with sturdy luggage racks front and rear, various designs from the Netherlands and Denmark, and especially strengthened bicycles for load carrying in Africa. At the time of writing, cargo bikes are starting to become popular, with attractive designs, electrical assist, and trailers with enormous capacity—greater than that of small cars. Many of the many types of vehicles are tricycles or quadracycles (see figure 10.20), but the following subsections mention just two concepts: “long” bicycles and bicycle trailers. Wood (2013) provides an illustrated history of cargo bicycles and tricycles.

There are many cargo trike manufacturers. One making modular delta-configuration cargo trikes and pedicabs is Cycles Maximus (cyclesmaximus.com) in Bath, England. Tadpole-design cargo trikes are sold by Haley Tricycles (haleytricycles.com) in Philadelphia and Icicle Tricycles (icetrikes.com) in Portland, Oregon. Worksmen Cycles (Worksmencycles.com) in Ozone Park, New York, makes traditional bikes, quads, and trikes of both types.

Long Cargo Bicycles

In order to create a generous space for cargo, a bicycle can be lengthened. If the length is added at the rear (as can be done to a standard bicycle, for example; see instructables.com/id/How-to-Build-a-Longtail-Cargo-Bike/), the resulting vehicle is called a *long-tail bike*.

If a bicycle is instead extended in front, it becomes a Long John, a type first produced about a century ago in Denmark. A low platform is added between the bicycle’s front wheel and steering post, and

the handlebars steer the front wheel via a linkage. The wheelbase can be up to 2 m in length, so that slow riding and turns are more difficult than with a standard bicycle, especially without a load, as there is then little weight on the steered wheel. Today many firms produce similar designs under various names for the transport of children or goods. Since electrical assist systems have become popular, Long John-type bicycles so fitted are frequently seen even in nonflat areas. The website Larryvsharry.com shows a popular modular cargo bike, the Bullitt (figure 10.21). A total weight of 180 kg is permissible, including the 24 kg weight of the basic model and that of the rider.

Another website, 8freight.com, shows a different configuration of a long bicycle by HPV pioneer Mike Burrows. On this model, the cargo basket is located behind the rider, so that riding it is more like riding a standard bicycle.



Figure 10.21
Modern Long John-type delivery bicycle.

Trailers

Standard two-wheel, single-axis bicycle trailers can carry large and bulky loads but become dangerous or unusable on steep gradients or when braked sharply. Although the mass, which is usually higher than the wheel axis, then tends to load the bicycle's rear wheel, giving some extra road friction, it needs only a slight lateral imbalance to create a yawing couple, and if the resulting force is greater than the bicycle can handle, it jackknifes or crashes. An additional problem of long trailers is the severe cutting of corners in tight curves. An Open Source Hardware project called Carla Cargo (werkstatt-lastenrad.de/index.php?title=Bauanleitung_Carla_Cargo_Crowd) addresses both problems using a third wheel that is steered by a long connecting bar containing an integrated mechanical overrun brake for the rear wheels and an electrical brake sensor. A maximum cargo of 150 kg and 1.5 m³ can be transported. For hills, the third wheel can be fitted with a hub motor that is controlled by a pedal sensor on the bicycle and a braking sensor. A commercial version is also available (carlacargo.de/en/) that is not only legal (at least in Europe) but at the time of writing is supported by the German government, which will subsidize 30 percent of the purchase price. It can also be used as a powered hand cart. The control system does not seem as sophisticated as that in the "phantom trailer" concept by Andreas Könekamp (see chapter 9), in which one would ride the leading bicycle as if the trailer weren't there. However, some "feedback" from the trailer is useful, as caution is in any case required in curves.

Human-Powered Water Vehicles

Almost all water vehicles at rest are supported in or upon the water by *buoyancy*. This is created by a lighter-than-water hull displacing a volume of water and allowing the water pressure to press the hull upward with the same total force as the weight of the displaced water. For most craft this applies also when moving; they are thus referred to as *displacement* craft. For reasons given later in this discussion, large human-powered boats and utility craft are of this type, whereas the fastest human-powered racing boats are *hydrofoil* craft, supported in the water by dynamic lift in the same manner as birds and airplanes in the air.

Water Drag

If other things are equal, the drag of a vehicle is proportional to the density of the fluid in which it operates and to the square of its speed, as described in chapters 4 and 5. Water drag is thus about one thousand times air drag, and speed (for the same power) is ten times less in water than in air. Although other things are not all equal, this ten-to-one rule does apply approximately to comparable vehicles: swimmers to runners, canoes to partially faired bicycles, and rowing shells to fully faired HPVs.

The majority of water-vehicle hulls operate on the interface between water and air, giving rise to sources of drag not experienced by land or air vehicles or fully submerged vehicles. The water pushed away by the moving hull produces surface waves, and struts piercing the surface create spray. Both remove energy and create additional resistance to movement. The wave drag can be relatively small for very large hulls (ships), very slim hulls (rowing shells, multihulls), or very flat hulls (stand-up paddling [SUP] boards). For others, including canoes and pedaled boats wide enough for reasonable stability, it tends to become especially large just at the bicycle-like speeds at which one would like to travel, in effect creating a kind of limiting speed called the *hull speed*, about 1.3 m/s times the square root of the waterline length in meters (e.g., under 2.3 m/s for a 3 m long boat). High-powered motorboats or sailboats can exceed the hull speed by dynamically lifting the hull when it *planes* on the water's surface. This reduces both wave making and the hull's wetted surface. Complete planing does not appear achievable with human power (just as running on the water's surface is also not achievable by ordinary humans, even though some lizards are able to do it!). However, other forms of dynamic lift are possible with human power, notably using hydrofoils or underwater wings. Once moving, hydrofoils can lift a boat and rider out of the water. Julius Schuck demonstrated his unique Wasserläufer in 1953, traveling sideways and relatively slowly on top of two large hydrofoils. Nobody else appears to have experimented with large hydrofoils for human-powered boats because there is no advantage: the water drag generated by such hydrofoils is greater than for a fine displacement hull. However, if the hydrofoils are made small enough to generate just the required lift at maximum human power, they

allow the highest purely human-powered speeds currently achievable on water.

Speed Vehicles

Sailing hydrofoil pioneer James Grogono fitted his rowing shell with hydrofoils and in 1975 was able to fly briefly using the oars, but the first human-powered hydrofoil to demonstrate sustainable flight was Flying Fish (figure 10.22) in 1983 (see Abbott and Brooks 2013 for a description, including spectacular videos, and Brooks 1987 for technical background). The above-water configuration is much like that of a bicycle, with the handlebars connected to a front assembly employing a rudder and a small horizontal hydrofoil. A surface follower maintains the proper depth a little below the water surface, which indirectly also sets the depth of the main weight-bearing horizontal hydrofoil located on a strut below the rider. The pedals are connected by a thin twisted chain to a propeller mounted on this strut.

For the first experiments in which it was involved, Flying Fish was launched from a kind of catapult, as it could not start to fly



Figure 10.22

Flying Fish propeller-driven hydrofoil by Allan Abbott (shown) and Alec Brooks.

from the water. With only the frame and rider visible, this gave it a spectacular “water bicycle” appearance, which has since been duplicated by a slower craft called Waterbike (see the website human-powered-hydrofoils.com for this as well as a dozen other craft). In order to allow repeated flights away from the shore, Flying Fish was fitted with two lightweight inflatable pontoons developed by the coauthor using methods of his employer, Keith Stewart. With three or four strong pedal strokes, the hydrofoils lift the pontoons out of the water, and flying begins. Abbott likens the riding and balancing of Flying Fish to riding a bicycle on a very smooth road. In 1987 he set a record for 100 m at 12.94 knots (kn).

Flying Fish was immediately faster than rowing shells. With a run of 11.15 kn (5.74 m/s) in 1987, it holds the single-rider speed record for 2,000 m (standing start), somewhat faster than the best single-sculd rowing shell even today. Shells for eight rowers are nominally faster over this distance (the 2017 world record is 12.21 kn, 6.28 m/s), but the wind conditions for rowing records are not closely controlled or in many cases even published.

In 1989 a chemical firm offered a prize of \$25,000 for the first single-person human-powered water vehicle to reach a speed of 20 kn (10.3 m/s) for 100 m (flying start) before the end of 1992, or in the event no vehicle of that type achieved such a speed, for the vehicle that had reached the highest tested speed (under strict rules) by that date. The competition for this prize stimulated much activity. The Flying Fish team intended to try, and several others, including the MIT group that had successfully mounted the Dædalus human-powered airplane effort (see discussion later in the chapter). They decided to enter with a craft using an air propeller, as employed in their aircraft. This gave the team an advantage, unforeseen by those who set the rules used for this competition, which allowed a maximum wind speed of 6 km/h (1.67 m/s). (The relevant IHPVA and WHPVA water rules have since changed and now allow no vehicle speed advantage greater than 1 percent compared to a no-wind situation.)

A water vehicle using air to generate thrust has a bonus when traveling with a tailwind. For example, if it is traveling at 10 m/s with a propulsive power of 800 W (= 1 kW input times 80 percent efficiency), the thrust is 80 N, and a 1.5 m/s tailwind contributes $80 \times 1.5 = 120$ W of this (at 100 percent efficiency), 12 percent of

the total input power (in practice a bit less). The MIT team's use of an air propeller (much larger than a water propeller) also meant having to cope with its high pitching moment. Wall, Drela, and Finberg (1995) superbly document the craft's development. The team also designed a unique laddered hydrofoil with a large foil for initially lifting the craft (initially supported by catamaran hulls) out of the water and a smaller foil below this for full speed, with the large foil then pivoted out of the water. Their craft Decavitator (figure 10.23) didn't quite reach 20 kn, but it won the prize with a speed of 18.5 kn (9.5 m/s). In 2000 the tandem hydrofoil boat Super Phoenix, with a water propeller, achieved 18.67 kn (9.6 m/s).

Why are the top speeds of even hydrofoil-equipped boats so low compared to those of land vehicles? It isn't the propulsion, as the best propellers can exceed 90 percent peak efficiency (see later discussion); it has to do with the energy cost of supporting any weight, which can be expressed as a lift-to-drag or weight-to-resistance ratio. For a displacement hull, this ratio increases to very high values at low speeds and large sizes (see later discussion). Such a hull is useful for



Figure 10.23

Decavitator world-record-setting pedaled hydrofoil. (Courtesy of Mark Drela.)

moving cargo, but not for small racing boats, for which hydrofoils are superior. The best hydrofoils could be expected to have a lift-to-drag ratio of about 50:1, like sailplanes, but this doesn't include the considerable drag of one or more surface-piercing struts needed to connect the underwater parts with the rider and above-water parts, nor does it include the slight wave-making drag of the foils, which cause a slight depression in the water surface unless very deeply submerged. Therefore the flights of hydrofoil boats are less efficient than those of airplanes and are mostly slower and shorter.

In contrast the lift-to-drag ratio of wheels (including tires and bearings) on hard surfaces, or runners on ice, can be several hundred to one. With this in mind, inventors have experimented with boats rolling over the water on buoyant tracks. Long, well-shaped tracks synchronized to the forward movement could nearly eliminate wave-making and water-friction resistance at the same time, replaced by the drag of wheels and their bearings. But here theory and practice are very far apart. The tracks splash or at least throw about clinging water, as shown in figure 10.24. They must be large,



Figure 10.24

Thusnelda human-powered boat with tracks, during the 1991 European Human-Powered Boats Championships in Gdansk, Poland. (Photo by Christian Meier.)

and then they generate considerable air drag, especially as the top parts of synchronized tracks are moving forward at twice the vehicle speed.

One way to go faster over water would be with a flying boat. Considering that human-powered airplanes can exceed 20 kn (see later discussion), one flying very low over the water surface should be faster, as the lift-to-drag ratio is greater the closer the wing is to the surface below, in what is known as *ground effect*. Of course such a vehicle might not be considered to be a water vehicle, unless perhaps if it were able to take off from the water, which is more difficult than taking off from a runway. A more practical and possibly even faster proposition could be a true human-powered *wing-in-ground-effect* flying boat. Such a craft has a lower-aspect-ratio wing than an airplane, but the wing's tips or endplates almost touch the surface, minimizing induced drag. A diagram in Hoerner and Borst (1975) suggests a 100 percent increase in the lift-to-drag ratio (relative to free flying) for *ram wings* with aspect ratios from 1:1 to 4:1, with end plates almost touching the surface, and maximum lift-to-drag ratios from 25:1 to 60:1. Flying closely over the water, however, creates additional wave drag, from the shallow impression in the water surface under the craft. Many large wing-in-ground-effect craft have been built, but we don't know of any human-powered ones. However, Steve Ball built a human-powered *hovercraft* with sidewalls, fan, and air propeller, the fan absorbing about one-third of the total power (Hostetter 1990–1991). His craft Dragonfly III is reported to have reached 7 m/s (13.6 kn) and was officially timed at 5.9 m/s (11.47 kn) over 100 m.

Submerged Buoyancy: A Warning Some fast industrial and military craft are constructed as small-waterplane-area single-hulls. These are trimarans or even monohulls with most buoyancy concentrated in a submerged torpedo-like hull with minimal wave drag (see Bluebird Marine Systems 2014 for an overview). This hull is connected to the craft's above-water parts by a thin strut. Obviously this creates an unstable inverted pendulum, like a bicycle or unicycle, and must be balanced both statically with adjustable buoyancy chambers and dynamically by actively controlled fins. The coauthor built a human-powered one and naively hoped to balance it like Flying Fish (described earlier in the chapter) and to achieve very low drag because of both minimal wave making and minimal

surface area. However, unlike hydrofoil craft, which permit gentle transition from static buoyancy to dynamic lifting as they speed up, this craft had really vicious capsizing and pitching moments at rest, acting much faster than the rider could react (Schmidt 1985), and it only ever worked once—and then very slowly—with four additional draggy stabilizing outriggers. Although such a craft might work better with a fast-acting automatic control system, only partial buoyancy, or both, the reader is forewarned, and we urge anyone tempted to try this to go straight to a triangular arrangement of three such hulls, for the same reasons that a tricycle is much easier to ride than a unicycle.

Recreational and Utility Watercraft

Human-powered marine vehicles have been in use since prehistoric times, mainly paddled, canoe-like monohulls and multihulls, later also rowed craft, even quite large ones (see figure 1.1). In quite a few places around the world, marine vehicles are the main means for transporting goods, often worked by paddles, oars, or a single “sculling” oar often called a *yuloh* (see Groves 2008 and Hawley 2014). In the city of Venice, the famous *gondolas* are today only for special events and tourists, but the seven *traghetto* are public ferries in constant use, for up to a dozen standing passengers, powered by two standing rowers (see Venipedia 2012). The discussion here could include a great many other interesting human-powered transport boats, but reasons of space restrict it to a few observations and very few special examples.

Hull Efficiency In the absence of wind, waves, or currents, a person can shift great loads on a barge by pulling from land with a rope, pushing with a pole, or with a large hydrodynamic propulsor. This is not only because there is no slope resistance, but also because the frictional drag of a displacement hull decreases with about the third power of the speed decrease, that is, it gets arbitrarily small as the craft goes slower. This can be expressed as a lift-to-drag ratio, which is the same as weight times speed divided by power, the inverse of what is called the *specific resistance*. If we assume a high propulsive efficiency, a single person can shift any load by going slowly enough, and the lift-to-drag ratio can become very high. As resistance increases only by a power of two-thirds of weight, making a water vehicle bigger and going slower increases the efficiency of

transportation to any value. Even if only the load is counted, not the weight of the person driving the craft, and assuming 20 percent muscular efficiency and subtracting the basal metabolic rate (see chapter 2), this still holds true, although the increase is less. However, at some point increasing the size further will become impractical. A great deal of effort will be needed to accelerate the load, and any wind will begin to dominate, so that transporting more than 50 tonnes (1 t = 1,000 kg) per person is rarely feasible. With this 50 t displacement and a propulsive power of 500 W, a hypothetical optimal hull would move at about 1.5 m/s and achieve a lift-to-drag ratio well over 1,000:1. Or if the human “engine” is treated as a fuel cell with 20 percent efficiency and a basic metabolic rate of 450 W (food) input is subtracted, an energy-cost lift-to-drag ratio greater than 200:1 is still attained (see figure 10.25).

From the foregoing it is clear that hydrofoils (or planing hulls) are not suitable for human-powered utility craft because the high lift-to-drag ratios available from displacement hulls are not achievable. Even recreational human-powered hydrofoils (other than hybrids)

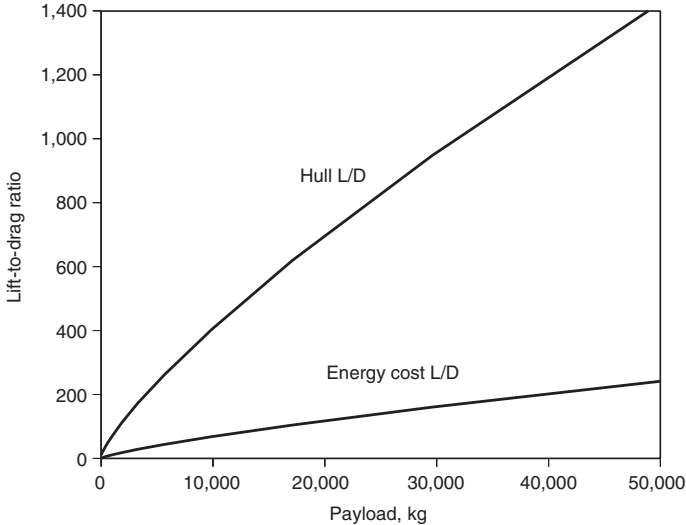


Figure 10.25

Lift-to-drag ratios of hypothetical hulls with negligible wave drag being propelled by human power (pulled from land with a rope or winched) at 500 W (2,500 W food input).

are only marginally suitable, as fast flight is sustainable only for a limited time. For practical boats, a single hull is usually optimal, provided it is either operated at a speed at which wave-making drag is not excessive, or slim enough (rowing shell) or flat enough (SUP board) for the same aim. However, a rowing shell, very narrow and round, is really a trimaran, as it relies on oars for maintaining stability, just as racing kayaks and canoes depend on paddles for this. Boardlike hulls, on the other hand, are very stable but have a large proportion of wetted surface area relative to their volume. Narrow-hulled boats with pedal drives get stability by adding a single outrigger (proa) or two outriggers (trimaran). The latter can be particularly efficient with the floats just touching the surface but are impractical for disembarking at a jetty. More practical and frequent is the catamaran configuration with two same-sized slim hulls. These are stable, fast, and practical but have $\sqrt{2}$ more wetted surface area than a geometrically similar single hull with the same volume.

Optimal Propulsion A propulsor can approach 100 percent efficiency by accelerating a huge body of fluid by an imperceptible amount. This is expressed by the *Froude efficiency* and the *actuator-disk theory* (the projected area swept by a propeller blade more or less describes the actuator disk area). In essence, if the *slip* is defined as the ratio of the fluid velocity increase through the actuator disk to the vehicle velocity, the Froude efficiency can be expressed as $1/(\text{slip} + 1)$. Therefore, paddle wheels or other very large drag-producing devices theoretically tend toward 100 percent efficiency if they are large enough. However, as in the case of the tracked boat (discussed earlier in the chapter), clinging water, splashing, air drag, and fragility limit the efficiency that can be obtained, and practical, robust paddle wheels are too small for really high efficiency. Even lower efficiencies are realized by the jet drives sometimes proposed for human-powered boats. The relatively small cross sections of water jets (i.e. small actuator disks) mean that the water ejected backward carries with it considerable kinetic energy, which is then lost to the system.

The highest-efficiency embodiment of an actuator disk (here an actuator rectangle) would be a high-aspect-ratio foil or a pair of such foils moving at an angle of approximately 45° to the direction of travel at such a speed that the angle of attack to the apparent flow is at the optimal lift-to-drag ratio, usually a few degrees. Fast fish like

sharks and mammals like whales and dolphins move their tail fins this way to some degree. An efficient mechanical embodiment it is, however, difficult to construct, even though the efficiency of a pair of *opposing* foils is limited only by their lift-to-drag ratio (including induced drag). The coauthor developed both horizontal and vertical foils with theoretical high efficiency, but they were pretty useless in practice. More successful have been Harry Bryan, Cal Gongwer, and others (see Bryan 1994 and Langenfeld 2009). Several “hopping” hydrofoils that combine propulsion and support in the same hydrofoil have also been built and even sold. These haven’t been a commercial success so far, probably because water starts are not possible: once back in the water after a short ride, the rider has to swim back with the device. More successful are modern embodiments based on SUP boards, which allow buoyant slow-speed operation and momentary (very brief) flights through simultaneous hopping and paddling. They are, however, not sold for such operation, but rather for foil-borne *surfing* even in very low-amplitude waves.

If propulsive foils can pivot like birds’ wings, it makes their functioning easier. Anybody who has watched videos of penguins swimming underwater has no doubts about this obviously effective and apparently efficient mode of propulsion. A most successful technical embodiment is Hobie’s Mirage drive, which since 1997 has been used on many Hobie craft and is also available for use on other boats. In a boat equipped with the Mirage drive, a pair of opposed flexible foils both swing through nearly 180° under the boat, sweeping a larger area than most propellers (resulting in a large actuator half-disk). Although the device will not win races against optimized propellers and cannot propel a boat backward, it is otherwise highly practical, being able to operate in both deep and very shallow water, and is easily cleared of weeds.

For completeness, we mention low-aspect-ratio flexible fins as used very successfully by most fish and by human swimmers, but we know of no other human-powered technical usage.

Finally, there are propellers, which are not used in nature other than in a sense by bacteria at extremely low Reynolds numbers but are extremely successful in human-powered boats. Their propellers are more efficient than motorboat or ship propellers, which are highly restricted by draft and changing water lines. Human-powered boat propellers can be large enough to achieve a high

Froude efficiency (see foregoing discussion). The more resistance a boat has, and therefore the slower it travels with a given amount of power, the larger the propeller must be. Propeller blades are limited by their local lift-to-drag ratios and losses due to tip vortices, resulting in overall best efficiencies from about 85 percent (practical boats) to 90 percent (extreme boats) to ~95 percent (structural limit). Propellers for human-powered racing boats are designed rather like aircraft propellers, with slightly wider blades for practical boats. Here an overall good efficiency over a wide speed range and high thrust in adverse winds is more important than a peak efficiency that exceeds 90 percent at a single operating point. The coauthor's "standard" propeller has a diameter of 0.5–0.6 m, about the same amount of pitch, and two blades about 90 mm at their widest. A "racing" version is similar, but a bit smaller and with blades half as wide. A simulation program shows that such propellers operate most efficiently at a Froude efficiency between 95 and 98 percent (see Larrabee 1984, 2003, and Schmidt 1988, 1999).

Most nontraditional human-powered boats employ propellers, and at least one manufacturer (Sea-Cycle) sells complete pedal drives, which can also be used on other boats. Sea-Cycle's drive and similar drives (like that of Flying Fish described earlier) employ a chain, with the chainwheel and driven cog twisted 90°. Some recreational boats are offered with air propellers, even though at the speeds achievable, the propellers are too small to achieve a high Froude efficiency, and they are more expensive than water propellers. Advantages include zero draft, weed-free operation, and often variable-pitch blades for always optimal adjustment.

Hybrid Boats The combination of wind and human power is age old, that of human and electric or even solar power relatively recent. A new development is an aquatic pedelec with a design similar to Flying Fish described earlier in the chapter but able to do water starts without pontoon floats. It is also slower than Flying Fish, with cruising speeds of 6–9 kn. The coauthor managed a very short hybrid flight with his own catamaran and hydrofoils supplied by David Owers, but normally used the solar- and human-powered boat in displacement mode. In the years around the turn of the millennium, there were numerous races for such boats. The advantages of hybrid operation include slightly better performance, better

reliability, and adjustability to the operator's body and mental state: if cold or bored, pedal faster; if tired or hot, pedal slower.

Escargot The late Philip Thiel (1991) had produced plans for a range of utility boats, including a tiny pedal-powered houseboat for cruising canals, propelled by one or two people using Sea-Cycle drives, with sleeping berths for up to four, toilet, and kitchen. This craft, Escargot (figure 10.26), had a rather unique design and was quite popular, with quite a few having been built. Unfortunately, the original plans have been replaced by a version with an outboard engine. The Sea-Cycle drives were designed for lighter, faster craft

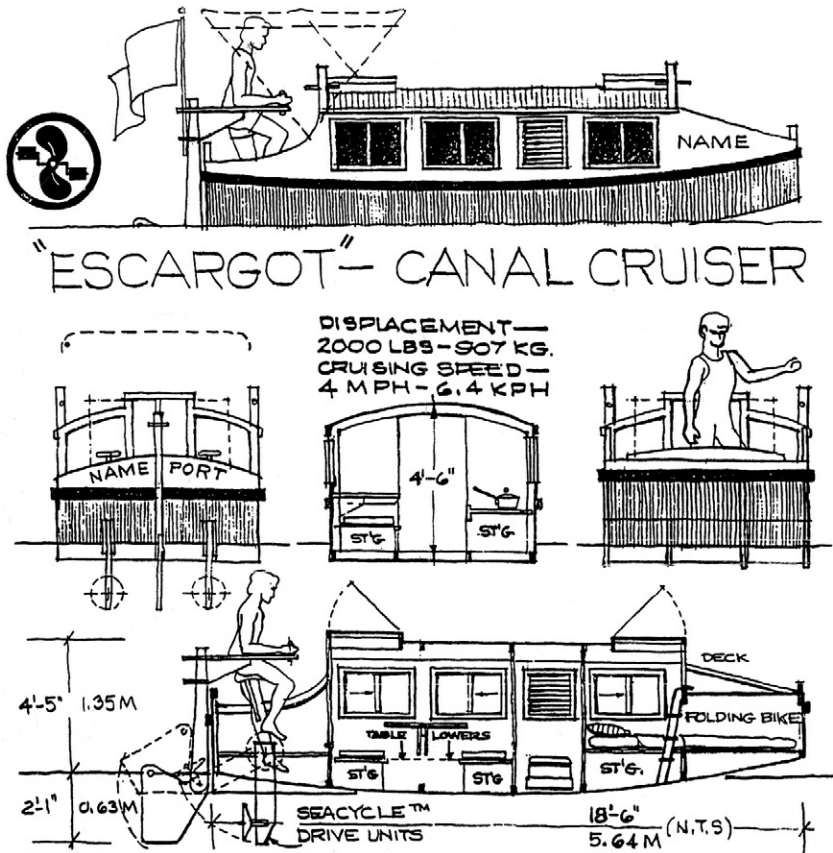


Figure 10.26
Escargot pedal-powered "Pénichette" by Philip Thiel.

and not ideal for the Escargot's displacement, as the coauthor found out himself. The original Escargots, still available for hire in Germany, have modified propellers and a cruising speed of 3.5 kn (see whpva.org/HParchive/hp55p22-23.pdf). Instead of optimizing the human-powered drive, perhaps also with a solar-assisted hybrid, the Escargot plans now call for at least a 1.5 kW (2 HP) outboard motor for a speed of 4–4.5 kn. This great decrease in efficiency is mainly due to a smaller propeller area.

Human-Powered Submarines

The IHPVA organized the first international human-powered submarine race in 1989, and since then a dozen others have been conducted by other organizations. An entire issue of *Human Power* edited by P. K. Poole (1993) offers guidance on design parameters for human-powered submarines and describes five submarines by teams competing in the 1993 race. Since then the greatest success in submarine competitions has been achieved by the Omer series of submarines, designed and built by students at the École de Technologie Supérieure in Montreal (see also the discussion of this school's helicopter project later in the chapter). The hull of the one-person Omer 3 (with a variable-pitch propeller) has at its widest point a diameter of 610 mm and at its longest point a length of 2.75 m. The maximum speed reached (in 1999) was nearly 7 kn, which was very high for this type of vehicle, almost all others having top speeds of less than 5 kn. Omer 8 in 2013 achieved 7¼ kn. The Omer 5 two-person submarine even reached 8 kn in 2007, the current world record (the records for both one- and two-person submarines are with a flying start and timed over 10 m). The very productive Omer project has a Wikipedia page and its own website, with descriptions of, but no data on, its eleven submarines (clubomerets.com).

The current (2018) record speed for a one-person submarine, at just over 7.4 kn, was achieved in 2016 by students of the Delft University of Technology forming the WASUB team (wasub.nl). The impressive design report for their WASUB V submarine is available from a page on the International Submarine Race website (internationalsubmarineraces.org/13th-isr/). The WASUB V's hull is roughly 2.5 m long, 0.5 m wide, and 0.6 m high, with 3.7 m² surface area, and was modeled on a NACA 0020–44 laminar profile. It has counterrotating two-bladed propellers 0.36 and 0.43 m in diameter, with

a design speed of 350 rpm at 7.5 kn and the pilot furnishing 800 W at 100 rpm.

The European competition website (subrace.eu) has further general information and links to extensive video material on human-powered submarines.

Modern human-powered submarines are flooded, that is, piloted by divers with breathing equipment. The energy needed to compress the air in a diver's air tank is greater than that used for propulsion (e.g., compressing 1 m³ of ambient air into a 200 bar tank requires well over 0.5 MJ). However, dry submarines are much more complicated and dangerous (the *Hunley*, noted later in this paragraph, sank and killed its crew three times). Historically, human-powered naval submarines were built as pressure vessels containing air. The very first such submersible, the famous *Turtle* of 1775, was powered by one man. The US Navy's first submarine, *Alligator*, was launched in 1862 (at the time of the Civil War). The 14 m long, 1.4 m wide iron vessel initially had 16 or 18 pairs of underwater paddles for a crew of 17, achieving a speed of 2 kn with these, and a year later 4 kn with a 1.6 m propeller (see navsource.org/archives/08/08444.htm). The well-documented 7 ton Confederate submarine *L. H. Hunley* attained a speed of 4 kn with a propeller cranked by eight men.

Human-Powered Aircraft

The Kremer Prizes

Human beings have tried to imitate birds for at least two millennia. Leonardo da Vinci sketched a helicopter, and many nineteenth-century experimentalists dedicated themselves, and sometimes their lives, to demonstrating human-powered flight, without success. Some short "hops" were achieved in the 1920–1960 period. In 1959 Henry Kremer, a British industrialist, was persuaded in a moment of weakness to offer a prize of £5,000 (then equivalent to about \$20,000) for the first human-powered aircraft to fly a figure-eight course at least 10 ft from the ground around two pylons 0.5 mi apart. Nearly two decades later, in 1977, Paul MacCready's *Gossamer Condor* won the prize. Kremer was delighted and agreed to offer a series of prizes, starting with one for a human-powered crossing of the English Channel (La Manche). This prize (£100,000, then worth \$180,000) was won by another MacCready plane, the

Gossamer Albatross, in June 1979. (The prize money awarded in this case seems a substantial sum. However, if a government commissioned the development of a human-powered plane to cross the Channel, it would cost many times this. Kremer's generous prizes stimulated an enormous amount of interest and activity, out of proportion to the amounts involved.)

The Gossamer aircraft have been given a great deal of well-deserved publicity. The discussion here illustrates human-powered flight with two other remarkable aircraft series: the Musculair and the Daedalus. It also mentions some helicopter and dirigible projects. A full description of human-powered aircraft is given by Roper (1995).

The Musculair Aircraft

Musculair I was built by the late Gunter Rochelt and his son Holger, supposedly a compromise design to win two different Kremer prizes. The younger Rochelt, characterized by Roper (1995) as "not particularly athletic," was designated as the pilot. However, he won the non-US figure-eight prize in June 1984, shortly after the Musculair I's first flight. He also took his younger sister Katrina up for a short trip: the first passenger flight of a human-powered aircraft. In August of that year he won a second Kremer prize, for speed around a circuit. The rules governing the Kremer prize allowed energy storage to be used; the energy had to be generated by the pilot during the 10 minutes preceding the flight and stored on board the aircraft. The Rochelts decided that they could do better without energy storage and proved themselves right. The wings of their aircraft also had a quarter of the wing area of the Gossamer Condor and no wing bracing. The flight was a remarkable achievement, technically, and also physically for someone "not particularly athletic"!

The Musculair I was unfortunately destroyed in 1985 in a traffic accident while being towed in its trailer. The Rochelts built a new version, Musculair II (figure 10.27), aimed at winning another speed prize. (Successive Kremer prizes could be awarded for a 5 percent improvement in speed over the previous record.) Holger Rochelt won a third Kremer prize for what had earlier been regarded as an unbelievable speed of about 12.5 m/s (23.9 kn, 44.3 km/h, 27.5 mph) on October 2, 1985, around a triangular 1.5 km course. Roper (1995) reports that the Royal Aeronautical Society, the prize



Figure 10.27

Musculair II at the Basel Air Show, 1985; a DC-3 (left) and a Concorde (right) can be seen in the background. (Courtesy of Ernst Schoberl.)

administrators, closed the Kremer speed prizes shortly afterward because it was considered impossible to exceed Rochelt's speed by another 5 percent.

Daedalus

Students at MIT, along with faculty members and other advisors, designed and built a biplane, Chrysalis, as preparation for an attempt to win the cross-Channel Kremer prize. (The senior author was one of the many permitted to power and pilot it.) Later they built the monoplanes Monarch A and Monarch B and won a Kremer speed prize. They could not hope to surpass the Rochelts' speed, however, and in 1985 they began considering a remarkable flight that had no monetary prize: a re-creation of the mythic flight of Daedalus, from

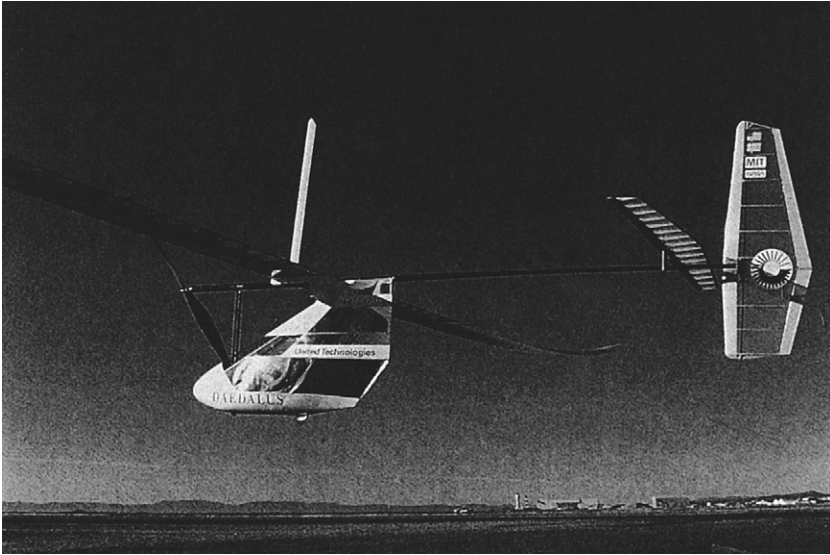


Figure 10.28

Daedalus world-record-distance human-powered airplane. (Courtesy of Mark Drela.)

Crete to Greece. The destination chosen was actually the island of Santorini, 119 km from the launching site on Crete. The aircraft they created for this endeavor, the Daedalus (figure 10.28), and its Greek pilot Kanellos Kanellopoulos were successful on the first attempt, even though the aircraft broke up at the very end as it was hit by a rather violent crosswind just as it was coming in to the beach on Santorini.

The crossing of the Daedalus was possible only as the result of a great deal of preparation that is described by Nadel (1991) and in chapter 2. For example, the team devised and tested an energy drink containing 10 percent glucose and 0.4 g sodium per liter, to be consumed at the rate of 1 L/h during the 4 h duration.

Most human-powered aircraft before the Daedalus had used a lightweight steel-cable chain substitute (see chapter 9) to transfer the pilot's power from the pedaled shaft to the overhead propeller shaft at right angles. In the Daedalus, power was instead transmitted by means of two sets of bevel gears and a torque tube. The design was a remarkable accomplishment, simultaneously saving weight, achieving greater reliability, and producing a higher transmission

efficiency with a drive that, when applied to bicycles, has up to now generally been heavier and less efficient than the chain drive it has replaced.

Recent Human-Powered Airplanes

Today about a hundred human-powered airplanes have been built. A more recent focus for new craft and prizes is practical usage in normal weather and over long distances. An example is Pennsylvania State University's PSU Zephyrus, based on the Muscular II, which is used for classes and in competing for a new Kremer Sports Prize (see Royal Aeronautical Society 2018 for details of this and also a new Marathon Prize). One of the newest ongoing projects is Alec Proudfoot's brainchild Dead Simple HPA (see dashpa.blogspot.com). The Japan International Birdman Rally has an event for long-distance human-powered airplanes, and in 2019 the Team Birdman House Iga won the first prize with a flight of 60 km in 2 h 36 min. The next-best team achieved 38 km, and the fifteen Japanese teams totaled 135 km (see <https://japanesehpa.wordpress.com>).

Human-Powered Helicopters

In 1980 the American Helicopter Society offered a prize, named after the helicopter pioneer Igor I. Sikorsky, for the first human-powered helicopter to hover for 1 minute and to reach a minimum height of 3 m for at least a moment. The winning helicopter also had to remain over a 10 m square, support at least one (nonrotating) member of the crew, and obtain lift solely through rotating elements. Figure 10.29 shows some of the concepts developed to attempt this. The prize was won three decades later, in 2013, by the AeroVelo team with their human-powered helicopter Atlas (see vtol.org/hph/ and figure 10.30). This is the largest helicopter ever constructed, with an overall width of 58 m (190 ft) and four 20.4 m (67 ft) diameter rotors, but weighing only 52 kg (115 lb)!

Human-Powered Blimp: The White Dwarf

Piloted by its designer, Bill Watson, the nearly 15 m long White Dwarf human-powered airship (figure 10.31), conceived and owned by the popular comedian Gallagher, is filled with approximately 170 m³ (6,000 cu ft) of helium. Its 1.6 m diameter propeller, mounted on a pylon behind the pilot, can have its thrust angle

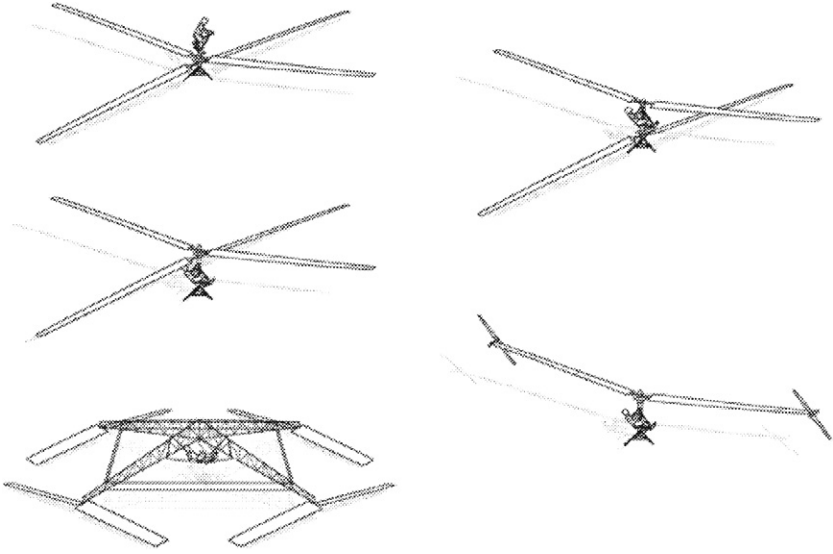


Figure 10.29

Conceptual designs for a number of human-powered helicopters from Doug Furton (2000), the supervisor of Project Helios at the École de Technologie Supérieure, Montreal. Those in the left-hand column were developed under the direction of Akira Naito (1991) at Nihon University in Japan. The lowermost of these, the Yuri I, and the Da Vinci III, at the lower right, were the first human-powered helicopters to fly. Helios, upper right, is most similar to the early two-rotor Naito designs. The AeroVelo Atlas is also of the Yuri I type. (Courtesy of Doug Furton.)



Figure 10.30

AeroVelo Atlas a year before achieving its record flight. The four rotors counterrotate pairwise. They each completed nine revolutions during a 1 min hover during the record flight. The seat with pedals and the single rider are (not discernable) in the middle, the lattice structure practically invisible. Eight yellow markers show the 10 m square. (Courtesy of AHS International.)

altered through nearly 100° to allow altitude control via a hand lever. Two triangular tanks, under and behind the pilot, carry water ballast up to a total of 114 kg (Allen 1985). Using the methods and data presented in chapters 4 and 5, a blimp of this shape and size should move at about 12 kn with 100 W propulsive power, that is, before the external structure and rider and the losses from the propeller and drive train are considered.

The Kremer Prize cross-Channel pilot Bryan Allen (1985) says that human-powered blimps seem to be the only type of human-powered aircraft that can provide recreation and possibly utility with reasonable availability. Successful flights by winged heavier-than-air human-powered airplanes are typically preceded by long periods of waiting for light winds, and they must be stored disassembled or indoors. The White Dwarf, although slower with its 7–9 kn cruising and 12 kn top speed, is smaller and stronger than these airplanes, with their large and fragile wings. Two persons can ground-handle the White Dwarf in winds up to 14 kn, and it can be tethered in stronger winds. Allen describes a trip he took over the California countryside on a lazy summer day, requiring little power input, floating over communities in relative silence, and able to greet and talk with people below him (often to their considerable surprise). He thinks human-powered blimps are a way for almost any person to fly and have fun, but the loss of valuable and expensive helium (roughly 0.25 percent per day for the White Dwarf) sensibly requires group use and organization. (Cheaper and renewable hydrogen could be used if the required precautions are taken.)

A less optimistic picture appears from following the experiences of Stéphane Rousson (2014) with his beautiful pedaled blimp Zeppy. He used his 190 m^3 aircraft successfully in many events indoors or in very calm conditions but never achieved his aim of crossing the English Channel. An award-winning short film by Loic Tanant (2009) shows Rousson's two attempts in 2008. In spite of relatively good low-wind conditions, Rousson is seen plagued by control and safety problems, fatigue, and wind from unfavorable directions. The blimp's two propellers don't just provide propulsion but are needed to constantly adjust altitude and attitude, which they do with a relatively low efficiency when fighting gusts. Rousson had to give up both times he tried. (The coauthor is full of sympathy, also having had to give up two Channel crossings: once with a

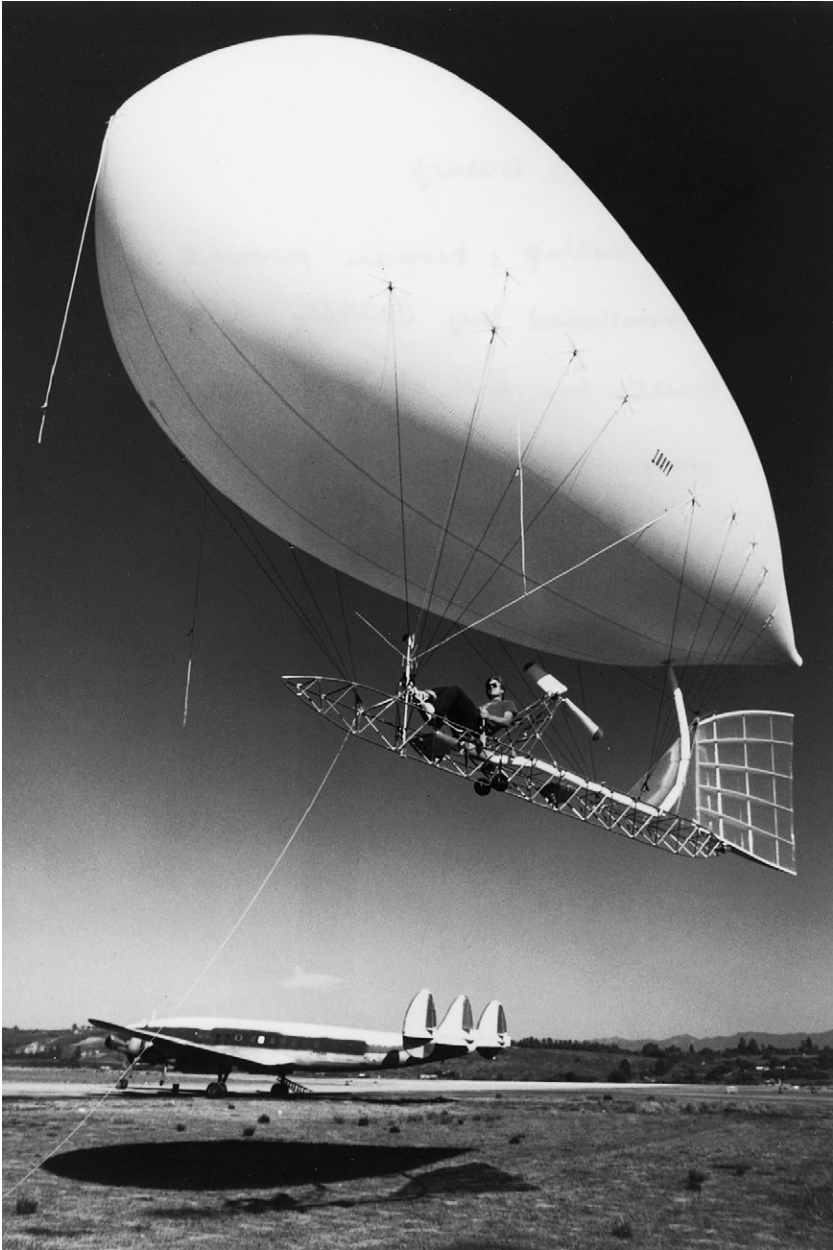


Figure 10.31
Human-powered blimp White Dwarf. (Photo by Bryan Allen.)

semiamphibious pedaled tricycle and once with a purely solar powered catamaran.) A much longer television film by James Woodroffe in 2016 (<https://www.youtube.com/watch?v=8Fve2Stn1II>) shows the television adventurer Guy Martin thoroughly training for a further cross-Channel attempt with Rousson's Zeppy. The exceedingly fine balance of bouyancy required is shown (already disturbed by a brief moment of sunshine heating the gas or clinging moisture), as well as the skill needed to maneuver even indoors. On the day of the intended crossing, conditions are marginal, but Martin is fit. However, he is blown off course and after a few miles Rousson stops the attempt. Martin is able to return to the start, with a more favorable wind direction reaching 13.7 kn. (Rousson can achieve higher speeds when *sailing* his Zeppy [now called Aerosail] by means of an attached "water kite" known as Seaglider or Hapa, a system also applicable to larger blimps.)

Exercise Bicycles and Virtual Cycling

Chapter 2 briefly described stationary bicycles used as ergometers. Many people have similar devices at home and use them for exercise or rehabilitation instead of cycling outdoors. For some people or situations this is important—for example, if going outdoors is especially unpleasant or overwhelming or presents special risks. Less necessary and often a bit absurd is the trend of fit and strong people driving cars to central fitness centers and then cycling on exercise bicycles there. This often happens partly because exercise bicycles and related machines have become sophisticated, large, and expensive devices that are best shared and not owned. They not only act as ergometers but can be programmed to monitor and achieve fitness goals. Motivation is improved through "gamification" and virtual environments presented using screens, virtual-reality headsets, and even physical feedback. Connections to the internet permit virtual racing against real people doing the same anywhere in the world, represented by onscreen avatars—this is also available to those who train at home, so long as they have a computer connection. Athletes who use such systems in addition to normal training report the danger of addiction and overexercise. Others enjoy "cycling" in interesting virtual environments, even in groups. Some dystopian science fiction films have described future human beings as nearly immovable creatures firmly connected to machines providing every

satisfaction. Maybe such virtual-cycling programs will at least keep them human in the physiological sense.

References

Abbott, Allan, and Alec Brooks. 2013. Flying Fish: The First Human-Powered Hydrofoil to Maintain Flight (website). <http://flyingfishhydrofoil.com>.

Allen, Bryan L. 1985. "Blimps and Human-Powered Flight." *Human Power* 3, no. 3 (Spring): 1. <http://www.ihpva.org/HParchive/PDF/12-v3n3-1985.pdf>.

Bluebird Marine Systems. 2014. "SWASH—Submerged Single Hull with Active Stabilization." http://bluebird-electric.net/SWASH_Submerged_Single_Hull_Active_Surface_Stabilization.htm.

Brooks, Alec. 1987. "20-Knot Hydrofoil." *Human Power* 6, no. 1 (Spring): 1, 8–14. <http://www.ihpva.org/HParchive/PDF/19-v6n1-1987.pdf>.

Bryan, Harry. 1994. "Fin Power—Success Comes from Copying Nature." *Human Power* 11, no. 1 (Winter-Spring): 6–9. <http://www.ihpva.org/HParchive/PDF/36-v11n1-1994.pdf>.

CPSC (Consumer Product Safety Commission). 2019. "Toys & Children Products." CPSC, Washington, DC. <https://www.cpsc.gov/Research--Statistics/Toys-and-Childrens-Products>.

Dovydenas, Vytas. 1990. "Velomobile." Verlag Technik GmbH, Berlin.

Downs, Daniel. 2011. "Ackermann Steering Geometry Applied to a Skateboard Truck." Digital Commons, California Polytechnic State University, San Luis Obispo, CA. <https://digitalcommons.calpoly.edu/imesp/94/>.

Federal Ministry of Justice. 2019. "Elektrokleinstfahrzeuge-Verordnung—eKFV" [Miniature Electric Vehicles Regulation]. <https://www.gesetze-im-internet.de/ekfv/>.

Fuchs, Joachim. 1996. "Aeolos-Verkleidung" [Aeolos-Fairing]. *Pro Velo* 44: v.

Furton, Doug. 2000. "Helios: A Helicopter with Legs." *Rotor & Wing* (April).

Glanzmann, Lilia. 2011. "Design-Piraten" *Hochparterre*, nos. 1–2.

Gloger, Stefan. 1996. "Entwicklung muskelkraft-getriebener Leichtfahrzeuge" [Development of Muscle-Powered Light Vehicles]. *Fortschritt-Berichte VDI* [VDI Progress Reports], no. 263. VDI-Verlag Düsseldorf.

Groves, Robert. 2008. "Some Thoughts on the Yuloh." *Junk Rig Association Newsletter*, no. 54. <https://junkrigassociation.org/Resources/Documents/Slieve%27s%20Files/Yuloh%20efficiency.pdf>.

Hawley, Jim. 2014. "Physics of a Stern-Fixed Single-Blade Sculling Oar like a Yuloh." Article 36. JimHawley.ca. http://jimhawley.ca/downloads/Physics_of_a_stern_sculling_oar_like_a_yuloh.pdf.

Henshaw, David and Richard Peace. 2010. *Electric Bicycles*. Dorset, UK: Excellent Books. ExcellentBooks.Co.UK.

Herslow, Joel. 2011. "Hybrid Mower." Joel Herslow Industrial Design (website). <https://cargocollective.com/joelherslow/Hybrid-Mower>.

Hoerner, S. F., and H. V. Borst. 1975. "Fluid-Dynamic Lift." Hoerner Fluid Dynamics, Brick Town, NJ.

Hostetter, Daniel. 1990–1991. "Dragonfly III." *Human Power* 8, no. 4 (Winter): 5–6. <http://www.ihpva.org/HParchive/PDF/28-v8n4-1990.pdf>.

Inria. 2018. "FREEwheels." Inria, Rocquencourt, France. <https://freewheels.inria.fr/>.

Langenfeld, Christopher. 2009. "PowerSwim" (compilation). Rex Research (website). <http://www.rexresearch.com/powerswim/powerswim.html>.

Larrabee, E. Eugene. 1984. "Propellers for human-powered vehicles." *Human Power* 3, no. 2 (Winter): 9–11. <http://www.ihpva.org/HParchive/PDF/11-v3n2-1984.pdf>.

Larrabee, E. Eugene. 2003. "Minimum Induced Loss Wings and Propellers for Human-Powered Vehicles (May 1985)." *Human Power*, no. 54 (Spring): 17–20. <http://www.ihpva.org/HParchive/PDF/hp54-2003.pdf>.

Lohmeyer, Dietrich. 2018. *Velomobile*. LD-Verlag.

Marinov, Bobby. 2016. "Electrical Muscle Stimulation in Rehabilitation, Cybernetic Bicycles and Exoskeletons." Exoskeleton Report (website). <https://exoskeletonreport.com/2016/08/electrical-muscle-stimulation-rehabilitation-cybernetic-bicycles-exoskeletons/>.

Mary. 2010. "Why Tour by Trike Tandem?" *Velomobiling* (blog). <http://velomobiling.blogspot.ch/2010/08/>.

Mellin, Bob. 1996. *Railbike: Cycling on Abandoned Railroads*. San Anselmo, CA: Balboa.

Micro Mobility. 2019. "Motion-Control Steering." Micro Mobility, Küsnacht, Switzerland. <https://www.micro-mobility.com/en/glossar/motion-control-steuerung>.

Nadel, Ethan. 1991. "The Daedalus—The Physiological Problems of Human Powered Flight across the Sea of Crete." *Cycling Science* 3, no. 2 (June): 22–26.

Naito, Akira. 1991. "Review of Developments in Human-Powered Helicopters." *Human Power* 9, no. 2 (Summer): 1, 7–9. <http://www.ihpva.org/HParchive/PDF/30-v9n2-1991.pdf>.

Poole, P. K. 1993. "H.P. Submarines: Design Parameters." *Human Power* 10, no. 4 (Fall): 24–26. <http://www.ihpva.org/HParchive/PDF/35-v10n4-1993.pdf>.

Rasmussen, Carl Georg. 2015. "An Overview of a Hundred Years Velomobiles." Paper presented at the Eighth European Velomobile Design Seminar, Dornbirn, Austria, October 30–November 1. <http://www.velomobileseminars.online/>.

Rio Mobility. 2018. "eDragonfly Attachable Power Assist Handcycle." Rio Mobility, Berkeley, CA. <https://riomobility.com/edragonfly/>.

Rohmert, W., and S. Gloger. 1994. "Typical Design-Problems of Velomobiles—Solutions for the DESIRA-2." In *Safety and Design: Second European Seminar on Velomobiles/HPV, Laupen Castle, Switzerland, August 25, 1994*. <https://velomobileseminars.online/>.

Roper, Chris. 1995. "History and Present Status of Human-Powered Flight." In *Human-Powered Vehicles*, ed. Allan Abbott and David Wilson, 217–238. Champaign, IL: Human Kinetics.

Rousson, Stéphane. 2014. "The Pedal Balloon" (photos). http://www.rousson.org/Stephane_Rousson/Le_ballon_a_pedales.html.

Royal Aeronautical Society. 2018. "What Is Human Powered Flight?" Royal Aeronautical Society, London. <https://www.aerosociety.com/get-involved/specialist-groups/business-general-aviation/human-powered-flight/>.

Schauer, Thomas and N. O. Negård. 2009. "Development of Mobile and Stationery FES-Cycling Systems with Motor Assist." Technical University Berlin. http://www.control.tu-berlin.de/Development_of_Mobile_and_Stationary_FES-cycling_Systems_with_Motor_Assist.

Schmidt, Theodor. 1985. "A Submerged-Buoyancy Human-Powered Boat." *Human Power* 3, no. 3 (Spring): 6–9. <http://www.ihpva.org/HParchive/PDF/12-v3n3-1985.pdf>.

Schmidt, Theodor. 1988. "A Simple Program for Propeller Performance Prediction." *Human Power* 7, no. 2 (Fall/Winter): 8–9. <http://www.ihpva.org/HParchive/PDF/23-v7n2-1988.pdf>.

Schmidt, Theodor. 1999. "Propeller Simulation with PropSim." *Human Power*, no. 48 (Summer): 3–7. <http://www.ihpva.org/HParchive/PDF/hp48-1999.pdf>.

Schmidt, Theodor. 2008. "Projekt TranSportIV." Entry for the Future Bike Idea Competition "Car Dinghy." <http://hupi.org/BS4/Articles/TranSportiv.pdf>.

Tanant, Loïc. 2009. *Voyage à la lisière de l'utopie* [Journey to the Edge of Utopia]. <https://www.youtube.com/watch?v=vzjV-fiDGM0>.

Thiel, Philip. 1991. "Pedal-Power on the French Canals." *Human Power* 9, no. 1 (Spring): 4. <http://www.ihpva.org/HParchive/PDF/29-v9n1-1991.pdf>.

- Van Raam. 2018. "Special-Needs Bikes Van Raam." <https://www.vanraam.com/en-gb/our-bikes>. Van Raam, Varsseveld, the Netherlands.
- Venipedia. 2012. "Traghetti." <http://www.venipedia.org/wiki/index.php?title=Traghetti>.
- Wall, Matthew, Mark Drela, and Steve Finberg. 1995. "Decavitator Human-Powered Hydrofoil." Massachusetts Institute of Technology, Cambridge, MA. <http://lancet.mit.edu/decavitator/>.
- Whitt, F. R., and D. G. Wilson. 1982. *Bicycling Science*. 2d ed. Cambridge, MA: MIT Press.
- Wikimedia Commons. 2018a. "Category: Black and White Photographs of Scooters." Photographs. https://commons.wikimedia.org/wiki/Category:Black_and_white_photographs_of_scooters.
- Wikimedia Commons. 2018b. "Category: Draisines by Country." https://commons.wikimedia.org/wiki/Category:Draisines_by_country.
- Wikimedia Commons. 2018c. "Category: Human-Powered Rolling Stock." Photographs. https://commons.wikimedia.org/wiki/Category:Human-powered_rolling_stock.
- Woodroffe, James. 2016. "Speed With Guy Martin—Season 3 Episode 2—Pedal-Powered Airship." <https://www.youtube.com/watch?v=8Fve2Stn1II>.
- Wood, Gavin. 2013. "Short History of Cargo Cycling." http://one.cyclelogistics.eu/docs/111/D2_1_Analysis_of_Cargo_Cycling_v_2_Sept2013.pdf.

11 Human-Powered Vehicles for Transportation

Introduction

The bicycles and HPVs described in this book so far have mostly been vehicles for racing or recreation. This chapter tries to show the important role of standard bicycles and some special vehicles in transporting people and goods from one place to another.

Government Regulations and Incentives

We have lived both in Britain and in the United States. On one hand, the very different nature of bicycling in the two countries could be taken to be representative of their different cultures. On the other hand, a major component of national behavior comes from laws and regulations and the degree to which these are enforced. While it could be stated that these laws and regulations in turn come from the people of their respective countries, the “law of unintended consequences” applies to laws themselves in addition to regulations and customs, and thereby laws shape communities in ways that those who proposed them or voted for them might not originally have foreseen.

For example, in the nineteenth century in the United States, the federal government saw an overwhelming need to connect the various parts of the country and to “open up the West,” and it gave generous inducements to railroad companies to build westward lines. For this and many other reasons was born an era of railroad barons such as Cornelius Vanderbilt: people with great wealth and power.

The arrival of automobiles and the empires associated with them changed things. The regulatory bodies seemed to have opposite

effects on railroads and highways: railroads began losing money and merging or going out of business, while truckers began taking over freight hauling, even over long distances along the same routes covered apparently more efficiently by the railroads. Similarly, differential taxation and regulation made it far less expensive for a family and even an individual to drive an automobile or to take a bus or airplane between two cities than to take a train, and passenger railroads have died out except when highly subsidized.

Costs and Benefits

Economists show that trucks and automobiles are also subsidized, in fact, subsidized to a far greater extent than are passenger railroads; however, the subsidies are of a totally different character. Subsidies for passenger railroads and subway systems are generally funded from tax monies that are handed over to the railroads' or subways' management. Subsidies for highway users take the form of costs that are imposed on general taxpayers and on many others (for instance, the costs of highway maintenance, snow clearing, bridge repair, accident services, police, delay, and urban sprawl that are not charged directly to highway users). If external costs are included in the calculations—that is, those associated with damages like pollution, noise, climate warming, injuries, and loss of health and life—the subsidies contributed by the population in general and the taxpayers in particular are, in most countries, much higher. It is politically very difficult to correct this anomaly, because lobbyists connected with all the powerful groups that would be affected by the changes that would be required are very active in advancing legislation favorable to the industries they represent and vice versa. There are virtually no potent lobbyists looking out for the interests of the weaker groups, including poor people, pedestrians, and bicyclists, who would benefit from the correction of this anomaly and the promotion of fairness. Litman (2009, 8) gives an example: “Francis owns a bike. Her neighbors benefit when she cycles rather than drives because it reduces congestion, crash risk and pollution. These external impacts are economically inefficient if Francis does not receive an incentive to cycle equal to the benefits her neighbors enjoy when she shifts mode. With such an incentive everybody could be better off because Francis would choose to bicycle whenever her neighbors' benefits are sufficient to induce a shift.”

In summary, users of large automobiles in particular are highly subsidized. In the United States, the quantifiable costs alone were assessed by some economists as, on average, \$0.67 per mile in 2002. Lemp and Kockelman (2008) studied different car models and arrived at figures of \$0.18 per mile for the best small cars to \$0.41 per mile for the worst pickups. (However, their research results did not include the costs of noise and end disposal.) Model for model, these costs were one-and-a-half to ten times higher than the sum of the Corporate Average Fuel Economy (CAFE) fine and gas-guzzler tax imposed on new cars that do not meet required federal fuel economy levels. Therefore, the users of other forms of transportation, including bicyclists, are competing with this and other enormous motor-vehicle subsidies.

In other countries with higher fuel and other taxes, the subsidies are lower than those in the United States, but they are still significant. Becker, Becker, and Gerlach (2012, 39) put the external costs for cars in Germany in 2008 at €0.15 per vehicle-kilometer or ~\$0.35 per mile. A recent Swiss study (Federal Office for Spatial Development 2018) found that passenger cars in Switzerland caused on average almost \$0.08 per passenger-kilometer in external costs but provided no external benefits. Surprisingly, the external costs of a bicycle was found to be similar to that of a car (assuming one passenger per bicycle and 1.6 per car), at nearly \$0.13 per passenger-kilometer, in spite of less pollution, as a result of higher costs of injury per distance traveled. However, as average cycle trips are shorter than average car trips, cycling is safer than driving when the risks are calculated per *trip*, and the external costs are less per trip (Schmidt 1994). More important, the external *benefits* of cycling are higher, the Swiss study found, at more than \$0.18 per passenger-kilometer, and outweigh the external costs. These are mainly health benefits, so it is no surprise that also the *internal* (health and time) benefits of cycling outweigh the costs due to accidents. The study also said that numbers like those presented here are comparable only if exactly the same conditions apply, which is seldom the case. Costs associated with automobile ownership and operation can also be highly dependent on location. A 2006 US study by Edlin and Karaca-Mandic, summarized by Varian (2006), puts the annual extra insurance cost of driving due to congestion-caused accidents at \$1,725 to \$3,239 in California, but only \$10 in North Dakota.

Börjesson and Eliasson (2012) suggest that the main monetary benefit of cycling is saved time: “Cyclists’ value of travel-time savings turns out to be high, considerably higher than the value of time savings on alternative modes. ... Cyclists’ value of time is estimated to be 16 €/h (street) and 11 €/h (bike lane). Only 17% of responding cyclists would go by car if they did not cycle.”

Health-related costs and benefits associated with bicycling are very difficult to assess, that is, the costs incurred by breathing polluted air and the benefits of exercise. Mortality statistics can be interpreted in widely different ways, however, all references we have seen say that the benefits of cycling outweigh the costs (see, e.g., Royal College of Physicians 2016). The relationship is not a linear one and depends on level of exposure, so the higher the air pollution in a particular location, the shorter the beneficial period for cycling: for example, seven hours per day in average urban areas. This means, for example, that professional bicycle delivery in a city with heavy pollution largely benefits the population (that is, the external benefit is higher) but not the delivery person (the internal cost is higher).

A fuel tax is an obvious method of recovering some of the external costs of using motor vehicles but is overly simplistic and doesn’t focus on the areas of greatest external cost. It imposes a relatively high penalty on those in areas where the external costs are relatively low, mileages are high, and alternative transport options are minimal, such as rural areas, and a relatively low penalty on those in congested urban areas where mileage is low but the external costs are high. To produce greater fairness in road use, three complementary forms of taxation are needed: electronically collected per-distance road-use taxes and parking taxes, varying with both place and time of day, in addition to fuel taxes. Preferably, proposers of this kind of taxation should also stipulate the destination of the monies collected. It is our opinion that such levies should be deposited in a trust fund that is reduced to near zero regularly by a uniform distribution to all citizens through a “negative” income tax—that is, a refund or rebate. In this way, poor people would receive a guaranteed small income. Rich people would receive the same rebate income, but their additional expenditures would likely be higher than this rebate if they used automobiles. The senior author advocated this policy so stridently through nearly four decades, beginning in the

early 1970s, that his friends dubbed it “Wilsonomics.” In Switzerland it is called “Oekobonus.” Had France’s president, Emmanuel Macron, proposed such a policy in 2018 instead of simply trying to increase gasoline *taxes*, he might have escaped the ensuing huge protest that resulted.

The vital relevance of this policy to our mission in this book is that most bicycling occurs in urban and suburban areas, the same locations where there is increasing traffic accompanied by gridlock and road rage, apparently all over the world. If all three forms of taxes suggested in the preceding paragraph were introduced or increased gradually, there would be a gradual reduction in motor-vehicle use, starting with those people whose use of motor vehicles is a daily choice between two level-value alternatives and who would happily decide not to drive if it were made a little less attractive.

There have been many movements in many countries to introduce road-use taxes, sometimes referred to as *congestion taxes*, and in some places tolls on high-speed roads parallel to heavily used roads are collected electronically. However, the region-wide introduction of road-use taxes for a large nation or group of associated nations involves so great a complexity that such taxes have been introduced only in a few places and cities. A form of congestion charge was introduced in London in 2003 and has won high praise for its early success. Although not a pure congestion charge (low-emission vehicles are exempt from the £11.50 daily charge), it has reduced traffic levels by more than 10 percent within the covered area and vehicles entering the area by 27 percent, with bicycle usage having increased by 66 percent (Transport for London 2018).

In addition to taxing or tinkering with incentives, governments can also regulate. Motor vehicles can be prohibited in city centers, parks, and other recreational areas or curbed and slowed in residential areas. (Unfortunately this often leads to higher rents or property prices in a process referred to as *gentrification*.) Things also work the other way: highways are generally off limits for bicyclists. There have been several campaigns in Asian countries to banish rickshaws and to restrict bicycles in cities, even in China. In most of the world’s democracies, motor-vehicle and oil-producer lobbies are very powerful, and bicyclists need to have lobbyists to counteract what would otherwise be absolute power, lest their interests be overridden entirely. “Power corrupts, and absolute power corrupts

absolutely,” as nineteenth-century British historian Lord Acton has been credited with saying. In Switzerland, a small country with neither oil nor automobile producers, voters in 2018 at least passed an amendment to the constitution giving bicycles the same legal status as pedestrian traffic and public transport, thus making bicycle infrastructure, for example, eligible for federal subsidies.

Because of the many complicated factors discussed in the foregoing, forecasting the future use of bicycles and other human-powered vehicles is an impossible task, dependent on government actions that might be directed at one set of problems unrelated to bicycles but then have unintended effects on bicycle usage (we refrain from discussing the controversial effects of helmet laws in this book). As the famous maxim—attributed to many different sources—goes, “Eternal vigilance is the price of liberty.”

Bicycle Usage and Infrastructure

We know of no comprehensive set of data on bicycle usage over time and across regions. However, the International Bicycle Fund (2018) has put together a collection of various relevant statistics showing, for example, that the number of bicycles manufactured is relatively stable or slowly increasing in many countries, including the United Kingdom, but decreasing in the United States, where it went from more than 10 million units per year in the 1990s to under 1 million by 2000. According to other sources, this number continued to fall to an extreme low in 2015 but is now slowly picking up again. Worldwide about 100 million units per year are being produced.

Usage doesn't seem to follow production, however. According to the Royal College of Physicians (2016), in the United Kingdom, “in contrast to the growth in motorized traffic, active transport such as walking and cycling has declined progressively since the 1950s. The total distance walked each year declined by 30% between 1995 and 2013, and the distance cycled in England and Wales in 2012 was just 20% of that in 1952. However, there are some signs of a reversal; trends over the last decade show a slow return to cycling” (9). The League of American Bicyclists on its page for bicycle commuting data (bikeleague.org/commutingdata) reports that in the United States, “the number of bicyclists is growing rapidly from

coast to coast. The National Household Travel Survey showed that the number of trips made by bicycle in the U.S. more than doubled from 1.7 billion in 2001 to 4 billion in 2009.” The league also offers usage reports based on the US. Census Bureau’s American Community Survey. From 2000 to 2017, bicycle *commuting* grew 43 percent. In 2017, in four cities, more than 10 percent of commuters biked: Boulder in Colorado and Davis, Santa Cruz, and Palo Alto, all in California. The senior author’s hometown Cambridge was nearly in this group and also had a record number of walking commuters: more than 23 percent; Berkeley, California, had a similar statistic, as did Somerville, Massachusetts. Half a dozen more cities made it into the 5 percent group, but almost all other US cities had very low percentages or none reported.

Bicycle usage is heavily influenced by authorities’ and taxpayers’ willingness to implement cycling infrastructure. Although experienced vehicular cyclists (and especially users of fast bicycles, HPVs, and e-bicycles) often prefer to use roads and therefore frown on any legislation forcing them to use narrow or winding cycle paths, there is no doubt that separate cycle paths are more pleasant for slower and inexperienced cyclists, especially children, people who cycle infrequently, and some tourists or elderly people. The cycling community as a whole is thus best served by having three freely choosable possibilities: attractive, slower cycle paths segregated from car traffic (figure 11.1); faster on-road cycle lanes (figure 11.2); and roads themselves for maximum speed. Even a fourth choice is gaining popularity: separated, fast *cycle highways* for fast bicycle commuters and e-bicycles. Transport for London has already built six such highways and is planning four more. In spite of their name, *Cycle Superhighways* may not be laid out for really high speeds, but they are certainly faster than what are called *Quietways*. Transport for London (2017) plans to complete 90 kilometers of the former and 250 kilometers of the latter by 2022, as well as something it calls *Mini-Hollands*—features to make cycling feel safer and more convenient. The planners estimate 250,000 potential bicycle trips to London’s main railway stations each day and 1.2 million additional longer multimodal trips. Transport for London (2016) has also published its very comprehensive and attractive *London Cycling Design Standards*. Its eighty-three-page chapter 4, “Cycle Lanes and Tracks,” includes material that will spark enthusiasm in bicycle planners and



Figure 11.1

An ideal scenic cycle path (in Copenhagen), as can be found in many places, with separated space for medium-speed cyclists and pedestrians. (Photo by Kristoffer Trolle, licensed CC-BY.)



Figure 11.2

Typical urban bicycle lane in Switzerland, colored red. (Photo by Andrew Bossi, licensed CC-BY-SA.)

likely disgust *bicycle drivers* (outspoken vehicular cyclists). Forrester (2012) explains the philosophy of “driving” bicycles. He recognizes that most authorities put cyclists into an inferior status, and into conflicts with pedestrians, if they force cyclists to use unsuitable infrastructure in order to keep them off the roads. However, the beauty of the bicycle is that it can fill two widely divergent roles: often the very fastest vehicle, and often the means to slow and relaxing locomotion. The key is choice.

The London design standards recommend minimal cycle lane widths of 2 meters, with 1.5 meters being acceptable on slow roads with few trucks. On-carriageway segregated cycle tracks should be 1.5–2.5 meters wide (or more), for very low to very high traffic flow conditions, and 2–4 meters wide (or more) for two-way tracks. (Earlier very detailed recommendations developed by the Canton of Bern in Switzerland also take slope, speed, and roadside environment into consideration, suggesting lanes from 1 meter [slow, flat, open] to 2.1 meters [fast, steep], with up to an extra meter for curves or adjacent retaining walls.) Regarding roads and lanes, an important finding is the “rule of thumb to avoid situations where motorized vehicles and cyclists are expected to move together through a width between 3.2 m and 4 m. Where lane widths are between these two dimensions, there is uncertainty about space for overtaking and a high risk that other vehicles will seek to pass cyclists too closely thereby putting the more vulnerable road user at risk.” Unfortunately “this includes the typical lane width adopted in much UK practice of 3.65 m. Use of this lane width should be avoided” (Transport for London 2016, 55).

Such recommendations often differ strongly from reality. The coauthor has seen on-road marked cycle lanes under 0.2 meters in width!

Infrastructure intended for bicycles is implemented in many different combinations in different places. Throughout the world’s top cycling nation, the Netherlands, complete “medium-speed” cycling networks are implemented (figure 11.3 shows a typical example), as well as bicycle parking facilities. This is partially the case as well in other Scandinavian countries, and the capital of Denmark, Copenhagen, is world famous for its cycling quality and quantity. This didn’t just happen by chance but is instead the result of decades of cycle-friendly policy, described, for example, in Wikipedia 2019b.

The process even has its own word, “to *copenhagenize*(.com),” and blog, *copenhagenizeindex*(.eu). (This wording has spawned more -izes and blogs, for example, *portlandize*[.com]). Cycling on such infrastructure is not necessarily especially safe and sometimes even increases the number of accidents at intersections (see, e.g., Jensen 2007). However, it *feels* safer and is more pleasant, so bicycle usage increases, which in turn increases the *relative* safety of each cyclist, as a strong function of the increase in usage (see figure 11.4). Some cities, for example, many large German ones, copy the Scandinavians to some extent, but only partly, with cycle tracks mainly on sidewalks, subject to pedestrian-type crossings at intersections (see figure 11.5). The previous on-road conflicts with cars are thus transferred to conflicts with pedestrians and increasingly e-microscooters. Cycle tracks of this type let people cycle who otherwise wouldn’t, but they don’t allow fast commuting; for that, cyclists must keep to the roads. It is mandatory for bicyclists to use available marked bicycle paths in many northern European countries, including



Figure 11.3

Typical cycle path in the Netherlands, between road and sidewalk, also used by mopeds. (Photo in public domain.)

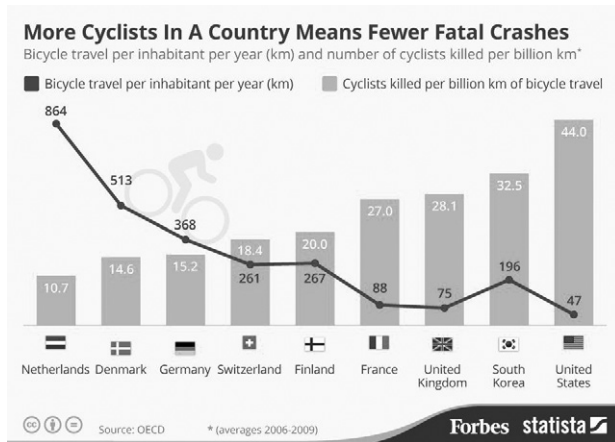


Figure 11.4

Safety in numbers. Cycling in the Netherlands was, according to the 2006–2009 average, about four times safer per distance traveled than in the United States. (Graphic from Forbes Statista, licensed CC-BY-SA, using data from International Transport Forum 2013.)



Figure 11.5

Typical on-sidewalk cycle path in Germany. Useful for casual and medium-speed cyclists, but not fast cyclists. Frequent intersections and narrow substandard parts further diminish the average speed.

Germany and Switzerland, and in some US states, but not in the United Kingdom.

In the United States, a number of cities have introduced cycling infrastructures:

- New York City has *greenways* along the Hudson, East, and Harlem Rivers around Manhattan, totaling 51 kilometers, and several shorter bike ways. Ambitious new projects are planned. The well-known High Line is not a bicycle path, but the High Line Network's website (network.thehighline.org/projects/) lists similar projects in North America that do reserve space for cycling.
- Portland, Oregon, has numerous bike ways, such as the 9-mile 20s bike way link. Many of these bike ways use quiet residential streets, but the 20s bike way provides a seamless cycling path connecting them across previous obstacles.
- The 606, a four-kilometer-long "linear park" in Chicago along a converted railway (the606.org) includes the Bloomingdale trail, a 10-foot-wide path open to cyclists, with 2-foot-wide running tracks along both sides.
- The Lafitte Greenway runs 2.6 miles through New Orleans.
- The Minuteman Bikeway is a 10-mile paved multiuse path in the greater Boston area. As is typical of converted rail trails, most parts of it are flat and straight, enabling the bikeway to be both fast and idyllic.

Transportation Systems Based on Human-Powered Vehicles

The Mount Holley and Smithville Bicycle Railroad (figure 11.6) opened in 1892 (Stockinger 1992). Two similar copies were built and three more with a suspended design (figure 11.7). Wilson (1992) reviews this and several other attempts at producing safer, faster, or more enjoyable conditions for bicyclists. Some of these systems provided a complete separate right-of-way or "guideway" that took either special vehicles, as in figures 11.6 and 11.7, or regular bicycles, human-powered or totally externally powered or having power assistance when needed.

There has been no shortage of more modern proposals, such as Jim Kor's skyway project called Solos Personal Transit (see Kor 1994), and some are even operational. The Shweeb is a kind of individual transparent pod for a recumbent cyclist suspended under

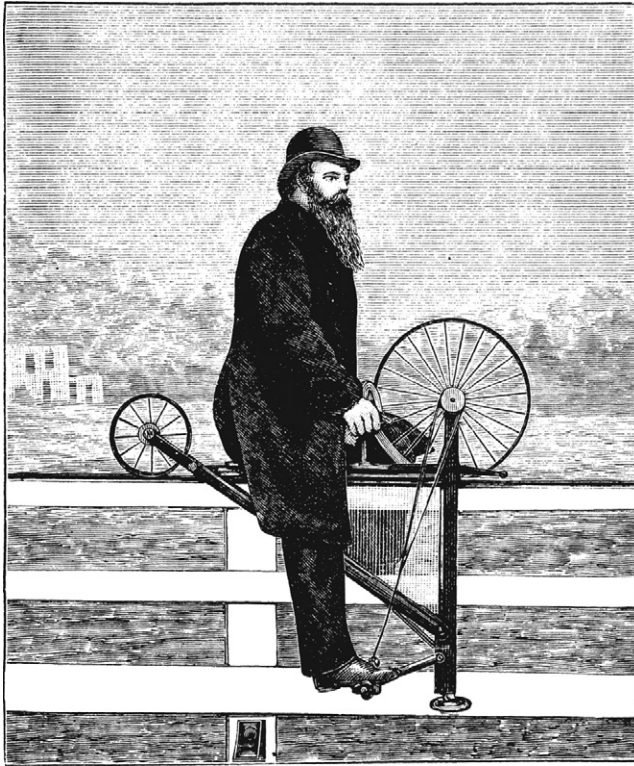


Figure 11.6

Mt. Holley and Smithfield Bicycle Railroad. (From Harter 1984.)

a monorail. Two 200-meter stretches supporting the Shweeb were built in New Zealand in 2010. Strong riders take about one minute for three laps, a speed of 10 meters per second. Scott Olsen's SkyRide (skyridetechnology.com) was built in Waconia, Minnesota, in 2012; here the cycle involved is also a suspended semirecumbent, but half-open and with a hybrid propulsion system. Like their historical fore-runners, the systems have not yet been successful as transportation systems, except in amusement parks (and on a ship!). An internet search for "skycycle roller coaster" finds a further remarkable Japanese example. However, the goal of using the Shweeb system for serious transportation in the Netherlands is studied in detail in several theses by students of the Eindhoven University of Technology and the University of Applied Sciences Utrecht from 2013 to 2017, available at the IntroVation website (introvation.nl/projects/shweeb).

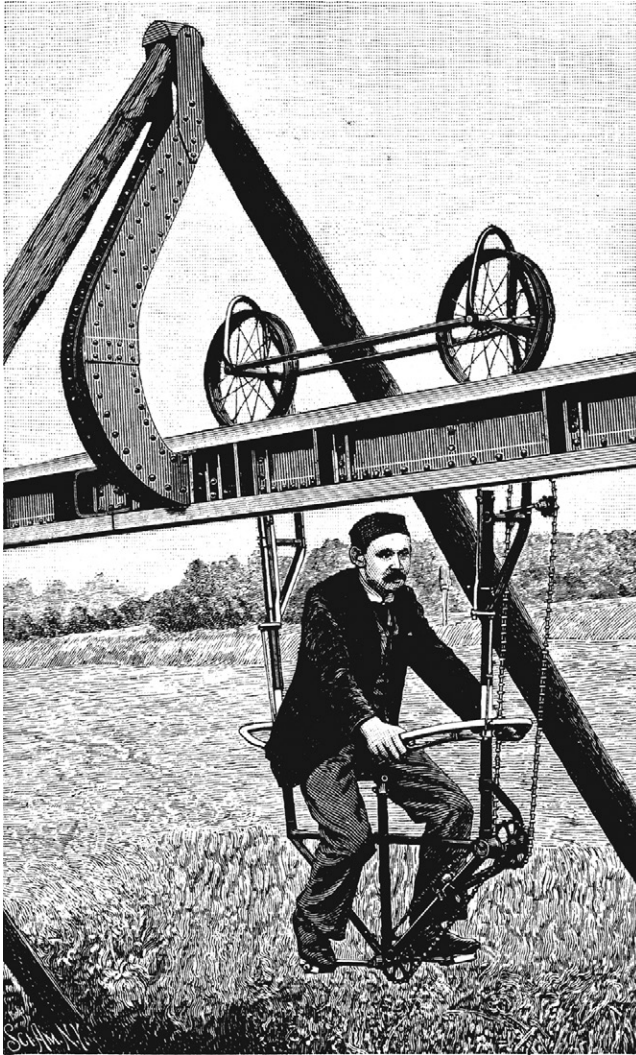


Figure 11.7
Suspended human-powered monorail. (From Harter 1984.)

One disadvantage of such systems compared to cycling on roads is obvious: there is no overtaking. If the speeds of individual pods or carriages vary, as is the case with those propelled by human power, large safety distances, elaborate control systems, or both may be required. The SkyRide system maintains a minimum distance of 20 feet. Obviously this limits the speed of all following vehicles to that of the slowest in front, unless there is a kind of collective power distribution, as in a mechanical train of coupled cars.

For this reason, the coauthor wanted to use gravity for a human-powered rail system—like a mild roller coaster—planned for the Swiss national exhibition Expo 02. (His proposal wasn't accepted.) A gravity system would ensure an almost exactly predictable speed, minimizing the necessary safety distances and control measures. The passengers would, however, have been required to pull or push their vehicles up ramps at the system's stations, in order to gain elevation. As most people are relatively powerful anaerobically, a few seconds' work would then allow a long, relaxing coasting session.

Cargo Bicycles

Already described in chapter 10, cargo bikes and cargo HPVs have represented a great success story over the last few years, in many more places than previously. Ever more businesses and services have begun to realize their advantages, especially in crowded city centers. Goods up to a few hundred kilograms and few thousand liters can be transported more quickly than by any other means, as the vehicles are generally allowed to park on sidewalks for unloading and use cycle paths if they are not too wide. Low-speed assist-motors of up to four kilowatts are allowed in many countries, so hills are manageable. Most loads are not particularly large, so that single-track cargo bikes often suffice, as shown in figure 11.8. With a width of typically sixty centimeters, they can also negotiate the narrowest cycle-ways. The Long John type is popular for fast runs carrying children, whereas some models of three- and four-wheelers can also take adults.

In recent years various urban initiatives have been undertaken to promote the use of cargo cycles. One is CycleLogistics (CycleLogistics.eu), founded by representatives of several cities and delivery companies. This in turn spawned the European Cycle Logistics Federation (eclf.bike) and the Register of Initiatives of Pedal Powered



Figure 11.8

Postal delivery bicycle. (Photo by Mikael Colville-Andersen.)

Logistics (rippl.bike), both with websites providing a great deal of information and images. A study by CycleLogistics reckons that on average more than half of all motorized trips in European cities that involve the transport of goods could be shifted to bicycles or cargo bikes. The benefits to society are much less environmental impact than conventional motor vehicles, even electric ones; less congestion; and practically no noise.

The advantages for both the operator and the customer in an urban environment are obvious: cargo bikes are usually faster and more reliable than services involving cars or vans, and they generally cost several times less. However, cargo bikes' speeds on main roads are lower, and hence their ranges are smaller, so they are not suited for widely sprawled areas. And they need more pickup points, as they cannot carry a whole day's worth of packages at once. Without

good organization, their operational costs can be high. However, parcel delivery firms like UPS are testing electric “phantom” bicycle trailers large enough to carry 200- or even 500-kilogram loads at a time.

Off-Vehicle Power Assist

The last two editions of this book described several ways of helping cyclists up hills using stationary installations such as lifts or moving handrails. They remain a niche and are today even less likely to become common, because increasingly effective e-bicycles are becoming more popular and can to a large extent effectively “flatten” even the steepest and longest hills.

Still in widespread use, and increasingly in some places, are facilities for taking one’s bicycle on public transport vehicles, mainly trains and ferries. In this mixed mode of traveling, cyclists are often the fastest in going from one point to another, even over long distances. Increasingly buses and subways also take bicycles outside of peak commuting periods. And even these peak hours are open to users of folding bicycles, covered if necessary or disguised as other luggage.

Additionally, long tours and holiday trips can be undertaken in mixed mode using public transport, but careful or minimal packing is called for, and maybe also a trailer. Train companies are increasingly making it easy to self-load bicycles on the same train or even in the same compartment as the cyclist passengers, without their having to send them in advance or place them in baggage cars. Figure 11.9 shows a typical facility. The disadvantage of such arrangements compared to the old baggage cars is that increasingly, only bicycles with standard dimensions are transported, as baggage cars have disappeared. The Swiss national railway company recently banned previously allowed long vehicles such as tandems, recumbents, and cargo bikes. Paradoxically, because platforms are higher, it would now be possible to wheel such vehicles directly onto railway cars without having to lift them as previously, but they are no longer allowed. This nips in the bud a car-free long-distance self-transportation system, for example, for voluminous shopping or goods. At least bicycle-messenger services can still use trains between cities, knowing exactly which facilities to use or trains to take.

As the railway companies are mainly worried about obstruction from large objects, and not about the weight or number of items,



Figure 11.9

Modern bicycle compartment of Swiss railways.

the use of large bicycles that are disassembled into parts and packed is still possible. This can be done with the use of bicycle torque couplings such as those made by S and S Machine (Sandmaschine.com). And compact HPVs or even velomobiles such as the Leitra can often find a space at least on local trains, if one is prepared to take a chance, or perhaps the next train, in case of stern guards. The father of the Leitra, Carl Georg Rasmussen, has described techniques for persuading guards, with polite arguments and demonstrations, but even he is not always successful!

Public Bicycle Systems

Public bicycles or bike-share systems started as experiments in the 1960s in an attempt to promote cycling and help visitors as well as local people. The first bicycles for such systems were donated as a public good and often simply distinctly painted or designed and released unlocked for free use. Not surprisingly, many were stolen

or damaged. Coin-operated locks were introduced as a deposit or payment system. Some systems are highly successful; the Vélib', which debuted in 2007, is believed to have greatly promoted the use of bicycles in Paris, making more than 20,000 bicycles available at 1,450 stations to 3 million subscribers (see streetfilms.org/velib'/). Many similar projects have far fewer bicycles and then never get going. Vélib' experts suggest that the bike-share system requires at least one bicycle per two hundred city inhabitants to work. (The coauthor has never seen one of his hometown's public bicycles used, as there are only a fraction of the number specified in the Vélib' recommendation.) Much more information and lists of services are available in a comprehensive Wikipedia article (Wikipedia 2019a). Fishman (2013) provides a literature review.

Today's systems (figure 11.10 shows a typical one) are electronic (software-controlled locks, monitored by GPS, the internet, or both),



Figure 11.10

Early public bicycle system with dock at the Milan main railway station.

and many are not really public anymore, as they require smart-phones, software, and accounts managed by one of the two market leaders, credit cards, preregistration, or even all of these. Unlike public transport, which can generally be used by anybody able to buy a ticket at a counter or ticket machine, the current bike-sharing systems are more restricted and difficult to use. Some allow the purchase of a smart card from a counter or machine, as do the systems in the authors' cities: Velospot (Velospot.ch) and BLUEbikes (Bluebikes.com), the latter requiring at least a credit card.

Some systems use fixed stations called *docks*, where the bicycles are stored; others allow the system's bicycles to be deposited anywhere within certain limits (what is known as a *free-floating system*). The latter systems in particular sometimes get out of hand, with literally piles of bicycles deposited at popular "targets." Well-managed systems can be expensive if employees have to continually shift bicycles around. All systems seem to record every single ride and store these data for years, with some operators even selling personalized data to third parties. Data-conscious users should study the fine print and avoid suspect operators. To sum up, public bike sharing is in some places very successful, in others less so, or even a nuisance. For people either well versed in modern technology or able to preregister, the systems can be useful.

An alternative to the new bike-share systems are conventional bicycle rental, where available, and newer bicycle leasing systems, often attractive for company bicycles. Both give users more responsibility for the bicycles involved, but the latter are returned after an agreed duration and are generally insured against mishaps and often maintained by the operator.

E-Scooter Sharing Systems

Increasingly, companies are offering e-bicycles, e-scooters (by which is meant here e-microscooters), or even larger motor scooters in sharing systems in addition to or instead of bicycles. This can either help or defeat the objective of better mobility with fewer disadvantages. Advantages will accrue only if mainly users of cars use the powered vehicles instead of driving, rather than people who would otherwise walk, cycle, or use public transport, and if the e-scooters actually used are environmentally better than cars. Hollingsworth, Copeland, and Johnson (2019) study the environmental impacts of

shared dockless e-scooters in detail and suggest that more e-scooter trips would need to replace trips by car (say, 50 percent) than is presently the case according to surveys (34–36 percent in this study). Obviously this depends on placement, and much lower percentages result if the e-scooters are placed within large pedestrian zones. For good usability, there need to be many e-scooters available (just as with shared bicycles), but too many such vehicles will be perceived as a (new) nuisance by pedestrians and users of conventional vehicles.

Ever more cities are implementing fleets of such free-floating e-scooters in public spaces. Louisville, Kentucky, is documenting its scheme on an open-data website (data.louisvilleky.gov/dataset/dockless-vehicles). For example, in the very first month of the Louisville project, in August 2018, roughly 4,000 riders completed 10,000 trips of nearly two miles each at an average speed of seven miles per hour, with no reported accidents. Using the available data, Alison Griswold in a widely publized March 2019 article (qz.com/1561654) in the online publication *Quartz* suggests that that the average e-scooter in Louisville's first batch lasted less than twenty-nine days and traveled 163 miles in ninety-two trips before disappearing from the database. Although these figures have no doubt improved (various German media list average lifetimes of three to six months), unless they continue to do so by a much greater margin, they are financially and ecologically counterproductive. Problems for the operators include vandalism and misuse, problems for traditional road users the encroachment of space and plenty of near-collisions. In addition, dockless e-scooters have to be regularly collected and recharged, at present defeating the energy benefits of substituting for inner-city car trips. How the collection is handled is a key factor in regard to the environmental impact. Collecting by cargo bikes over short distances and only when really required is obviously desirable to the alternatives.

While microscooters can represent the fastest way of getting from one point to another for short distances in city centers, the legal status of the various unpowered and powered models is often doubtful—for example, some are legal on sidewalks, some on cyclepaths, some on roads, and some on no public spaces at all. The shared ones are also quite expensive, costing at least a dollar per mile or even per kilometer to use, and require the use of a

smartphone and payment system. And while some authorities mandate a minimal speed, by initial foot-kick, to switch on the motor, the scooters may then continue as pure motor vehicles, unlike pedelecs, which require at least minimal human power input all the time that the motor is running. (A “kickelec” solution is proposed in chapter 10.)

References

- Becker, Udo J., Thilo Becker, and Julia Gerlach. 2012. “The True Costs of Automobility: External Costs of Cars.” Institute of Transport Planning and Road Traffic, Technical University of Dresden, Dresden, Germany. https://www.greens-efa.eu//legacy/fileadmin/dam/Documents/Studies/Costs_of_cars/The_true_costs_of_cars_EN.pdf.
- Börjesson, Maria, and Jonas Eliasson. 2012. “The Value of Time and External Benefits in Bicycle Appraisal.” *Transportation Research Part A: Policy and Practice* 46, no. 4 (May): 673–683. <https://doi.org/10.1016/j.tra.2012.01.006>.
- Federal Office for Spatial Development. 2018. “Costs and Benefits of Transport.” Federal Office for Spatial Development, Federal Department of the Environment, Transport, Energy and Communications, Bern, Switzerland. <https://www.are.admin.ch/are/en/home/transport-and-infrastructure/data/costs-and-benefits-of-transport.html>.
- Fishman, Elliot. 2013. “Bikeshare: A Review of Recent Literature.” *Transport Reviews* 36, no. 1: 92–113. <https://www.doi.org/10.1080/01441647.2015.1033036>.
- Forrester, John. 2012. *Effective Cycling*. 7th ed. Cambridge, MA: MIT Press.
- Harter, Jim. 1984. *Transportation: A Pictorial Archive from Nineteenth-Century Sources; 525 Copyright-Free Illustrations Selected by Jim Harter*. New York: Dover.
- Hollingsworth, Joseph, Brenna Copeland, and Jeremiah X. Johnson. 2019. “Are e-Scooters Polluters? The Environmental Impacts of Shared Dockless Electric Scooters.” *Environmental Research Letters* 14, no. 8. <https://doi.org/10.1088/1748-9326/ab2da8>.
- International Bicycle Fund. 2018. “Bicycle Statistics: Usage, Production, Sales, Import, Export.” International Bicycle Fund, Seattle, WA. <http://www.ibike.org/library/statistics-data.htm>.
- International Transport Forum. 2013. *Cycling, Health and Safety*. ITF Research Reports. Paris: OECD Publishing. <https://doi.org/10.1787/9789282105955-en>.
- Jensen, Søren Underlien. 2007. “Bicycle Tracks and Lanes: A Before-After Study.” Trafitec ApS, Lyngby, Denmark. https://www.researchgate.net/publication/237524182_Bicycle_Tracks_and_Lanes_a_Before-After_Study/citation/download.

Kor, Jim. 1994. "Solos Personal Transit." In *Proceedings of the Second European Seminar on Velomobiles/HPV: 85-101, Laupen Castle, Switzerland, August 25, 1994*. <http://velomobileseminar.online>.

Lemp, Jason, and Kara Kockelmann. 2008. "Quantifying the External Costs of Vehicle Use: Evidence from America's Top Selling Light-Duty Models." *Transportation Research* 13D, no. 8: 491–504. <https://www.researchgate.net/publication/222398495>.

Litman, Todd A. 2009. "Transportation Cost and Benefit Analysis." Victoria Transport Policy Institute, British Columbia. <http://vtpi.org/tca/tca01.pdf>.

Royal College of Physicians. 2016. *Every Breath We Take: The Lifelong Impact of Air Pollution*. London: Royal College of Physicians. <http://bit.ly/1Nv4ClA>.

Schmidt, Theodor. 1994. "What Is HPV Safety?" In *Safety and Design: Second European Seminar on Velomobiles/HPV, Laupen Castle, Switzerland, August 25, 1994*, 21–27. <http://velomobileseminar.online>.

Stockinger, Herbert H. 1992. "The Bicycle Railroad." *American Heritage of Invention & Technology* 8, no. 2. <http://www.inventionandtech.com/content/bicycle-railroad-1>.

Transport for London. 2016. *London Cycling Design Standards*. London: Transport for London. <https://tfl.gov.uk/corporate/publications-and-reports/streets-toolkit#on-this-page-2>.

Transport for London. 2017. "Strategic Cycling Analysis: Identifying Future Cycling Demand in London." Transport for London, London. <http://content.tfl.gov.uk/strategic-cycling-analysis.pdf>.

Transport for London. 2018. "Congestion Charge Factsheet." Transport for London, London.

Varian, Hal R. 2006. "Beyond Insurance: Weighing the Benefits of Driving vs. the Total Costs of Driving." *New York Times*, November 16. <https://www.nytimes.com/2006/11/16/business/16scene.html>.

Wikipedia. 2019a. "Bicycle-Sharing System." https://en.wikipedia.org/wiki/Bicycle-sharing_system.

Wikipedia. 2019b. "Cycling in Copenhagen." https://en.wikipedia.org/wiki/Cycling_in_Copenhagen.

Wilson, David Gordon. 1992. "Transportation Systems Based on HPVs." In *Proceedings of the Fourth IHPVA Scientific Symposium*, ed. Chester R. Kyle, Jean A. Seay, and Joyce S. Kyle. San Luis Obispo, CA: International Human Powered Vehicle Association.

Index

- Abbott, Alan, 33–34, 153, 497–498
Acceleration, 135–136, 148, 153, 179, 187, 443, 466
Actuator-disk theory, 504
Adenosine triphosphate, 53, 60–62
Aerobic metabolism, 69, 95
Aerobic power, 64, 71–73, 86, 150
Aerodynamic resistance, air drag, 171–175, 213–215, 229–232
Aerodynamic lift, 218, 250–254
Air density, 149, 216
Air pressure, atmospheric, 223–224
All-terrain bicycle, 26–27, 479
Altitude, 131–132, 134, 149–152, 223
Altitude training, 151, 165
Anaerobic metabolism, 72, 95
Anaerobic power, 53–56
Anaerobic threshold, 63
Anaerobic work capacity, 51, 74
Angle of internal friction, 287
Apparent wind, 45, 250
Arm-powered recumbent, 468–469
Aspect ratio, 252–253
ATP. *See* Adenosine triphosphate
- Backward pedaling, 97–98
Balancing, 349–350, 356–364
Ball bearing, 272–275
Basal metabolic rate (BMR), 81–84, 200–202, 503
Basal metabolism, 75–76, 81–82, 201
- Batteries, 444–445
Bicycle
 boom, 13, 26
 drivers, 531
 elevator, 133
 infrastructure, 528–534
 usage, 528–532
 riding skills, 360–362
Bicycles on public transport, 539–540
Bicycling myths. *See* Myths
Big circuits, 137
Bike-share systems, 540–542
Blasius (laminar) line, 219–220
Blood doping, 170
Blood levels, 63–65, 69–71
Body surface area, 82, 112
Boundary layer, 219–221, 224–226, 239. *See also* Blasius (laminar) line; Schoenherr (turbulent) line
Bowden cable, 339–340
Brachistochrone, 144–145
Braking
 and brakes, 322–347
 distance, 331–332
 power, 342–344
Breathing rate, 78–79, 87
Bump resistance, 182–187
Buoyant tracks, 500
- Camber thrust, of tires, 312
Capsizing, of vehicle, 377, 380

- Capstan, 4–5
- Carbohydrate, 61–71, 76–77
- Carbon dioxide, 76–78
- Cargo bike, 492–494, 537–539
- Cargo scooter, 463–465. *See also*
Chukudu
- Centrifugal force, centripetal
acceleration, 355
- Chain drive, 396–405, 429–434
- Chukudu, 458–459
- Climbing, 132–133, 177–178
- Coastdown test. *See* Rollout test
- Cocontraction, muscle, 81
- Coefficient
of drag, 173–174, 216–218, 225–227,
230–237, 241–243
of friction, 275, 289, 319–320, 430
of lift, 253
of rolling resistance, 263–268, 277,
280, 284, 289, 297–306
- Cohesion, soil, 287–290
- Commuter race, 134
- Commuting, 529
- Compact long wheelbase, 367, 480–
481
- Computer simulations, 90, 140, 191,
376, 506
- Conduction, heat, 111, 344–345
- Constant elevation, 138
- Constant (speed or torque) pedaling,
44–45
- Constrained motion, 92, 94, 108–109
- Contact patch, 265, 279–286, 294–296,
309–310
- Contraction, muscle, 57–59, 80
- Convective cooling, 112–114, 330, 344
- Cooling with heat pump, 120
- Cornering stiffness, 310
- Countersteering, 358–360
- Crank length, 100–102
- Creatine phosphate, 53, 60–61
- Critical power (CP), 51–52. *See also*
Functional threshold power (FTP)
- Crosswind, sidewind, 244–250
- Cup-and-cone bearing, 273–274
- Cycle paths, 529–534
- Daedalus 119 km flight, 511–512
- Dandy horse, 9. *See also* Draisine,
Draisienne
- Decavitator hydrofoil, 499
- Deceleration, 269, 321, 332–334
- Derailleur gearing, 25, 276, 401, 413,
431–434
- Differential gear, 19, 436, 440
- Direct drive, 415
- Disk brake, 324–326
- Doping, 159–165
- Downwind-faster-than-the-wind, 248
- Drafting, 152–153, 240–243
- Drag area, 173–174, 215, 229–233
- Drag race, 136
- Drag versus Reynolds number, 225
- Drais, Karl von, 6–10, 362, 395
- Draisine, Draisienne, 8–14, 395, 467
- Draisine, railway, 474–479
- Drum correction formula, 267–268
- Durometer, 293. *See also* Shore
(hardness) values
- E-(electric) bicycle, 31–37, 165–166,
435–447
- E-(micro)scooter, 466, 532, 542–544
- Eccentric contraction (negative work),
58, 81, 92, 207, 418
- Electrical series hybrid, 437–438
- Electrical transmission, 424–429
- Elliptical chainwheels, 103–105
- Energy cost, 80, 83–85, 204, 207–209
- Energy storage, 94, 130, 134, 144–145,
421, 510
- Ergometer, 42–47, 53–56, 94
- Erythropoietin (EPO), 79, 161, 164
- Exercise bicycle, 46, 517
- External costs and benefits, 524–526
- Extreme power levels, 46

- Fat (fuel), 60, 65–66, 75–77
- Fat tires, 157, 286, 291, 299, 470
- Fiber
- dietary, 75
 - muscle, 57, 67–75
 - in tires, 181, 278, 296, 308
- Flying boat (ground effect), 501
- Flying start, 135–136, 146–147, 508
- Flywheel, 42–46, 53–56, 158. *See also* Gyroscope
- Fork offset, 364–365, 367–368
- Freewheel, types of, 397
- Freight bicycle. *See* Cargo bike
- Frontal area, 173–174, 216–219, 229–235
- Functional electrical stimulation, 468
- Functional threshold power (FTP), 50–52. *See also* Critical power (CP)
- Gear ratio, 4, 17, 398, 412–414
- Geoid, 138
- Glucose, 61–65, 67–69, 512
- Glycogen, 61, 64–69, 72, 74
- Gossamer Albatros Channel flight, 509–510
- Gray rubber, 292
- Grease, 272, 274–275
- Ground (rolling) resistance, 181–182, 264, 285–291
- Gyroscope, 349–350, 356–357, 377, 384
- Handcar. *See* Draisine, railway
- Hand cranking, 95–96, 468–469
- Headwind, 175, 188
- Health benefits and costs, 447, 525–526
- Heart rate, 66, 79
- Heat engine, body is not, 85
- Heat index, humidex formulas, 117
- Helicopter, 513–514
- Hertzian contact, 281, 283, 292
- High-power aerobic metabolism, 69
- High-wheel (ordinary) bicycle, 2, 14–18, 20–21
- Hobby horse. *See* Draisine, Draisienne
- Horsepower, 203–205
- Hovercraft, 501
- Hub gear, 23, 400, 410–415, 431–432
- Hub motor, 36, 328, 438–444
- Hybrid power, 155. *See also* E-(electric) bicycle
- Hydraulic actuation, 325–326, 340–341, 420–421
- Hydrofoil, 496–500
- Hysteresis, viscoelastic, 181, 278, 296
- Ice skating, 8, 157, 209
- IHPVA, 130–131, 140, 498. *See also* WHPVA; WRRRA
- Inclinometer, 179–180
- Indirect calorimetry, 48, 76–77
- Induced drag, 252, 501
- Inertia, 42–45, 54–56, 135, 172, 191
- Kick scooter, 208–209, 457–468
- Kickbike, 458
- Kickboard, 208–209, 461–463
- Lactate, 61–65, 68–74, 79. *See also* OBLA (onset of blood-lactate accumulation)
- Laminar profile, 215, 220, 508
- Lessing, Hans-Erhard, 2, 10, 13
- Lever-tension wheel, 15–16
- Lift, 221, 250–253, 495
- Lift-to-drag ratio, 252–254, 499–506
- Locomotion, 202–204
- Long John, 493–494, 537–538. *See also* Cargo bike
- Long-wheelbase recumbent, 335–336, 366–367, 480–481
- Lubricant, 275, 422, 434. *See also* Grease
- Luggage scooter. *See* Cargo scooter
- Mechanical series hybrid, 35, 436
- Mechanical trail, 361, 365

- Metabolic efficiency, 61–62, 75–77, 83–85, 200–202, 394
- Metabolic power, 76–77, 88
- Metabolism, 69
- Michaux, Pierre, 13, 396
- Microscooter. *See* Kick scooter
- Minute volume (MV), 77–78
- Moon bicycle, 154
- Moped, 32, 35, 204, 426
- Motor doping, 158, 165–166
- Motor efficiency, 424–428
- Motor neuron, motor unit, 57, 59, 67
- Mountain bike. *See* All-terrain bicycle
- Muscles, overview, 57–59, 80–81. *See also* Fiber, muscle
- Musclair passenger flight, 510
- Myths, 1–2, 10, 362
- NACA profiles, 215, 220. *See also* Streamlined shape
- Negative work. *See* Eccentric contraction (negative work)
- OBLA (onset of blood-lactate accumulation), 63–64, 71, 79. *See also* Lactate
- On-bicycle power measuring, 47–49, 193–198
- Online tools, 66, 82, 90, 105, 116–117, 150, 176, 191
- Ordinary (bicycle). *See* High-wheel (ordinary) bicycle
- Oxygen, 62, 70, 72, 76, 79, 85–87, 150, 160
- Pacing, 152–153
- Paddle wheel, 504
- Papadopoulos, Jim, vii–ix, 363, 387
- Parallel hybrid e-bicycle, 435–436
- Partially faired HPV, 131, 238, 489
- PAS power assist system, 33
- Passing distance, minimum, 244
- Patents, 9, 24, 28–29, 33, 105, 267, 342, 360, 400, 405–407, 424, 429
- Pedal force, 89–91
- Pedal generator, 424, 428
- Pedal smoothness, 108
- Pedelec, 33–37, 436–440. *See also* E-(electric) bicycle
- Peloton, 242–243
- Pendulum test, 270–271
- Pennation, 57
- Penny-farthing. *See* High-wheel (ordinary) bicycle
- Perspiration, 111–113
- Phase-change materials, 119
- Phases of speed variation, 141, 144
- Phosphocreatine, 60–61
- Plain bearing, 275–276
- Pneumatic tire, 24, 294–313
- Pneumatic trail, 309–311
- Polygon effect, 404
- Polytetrafluoroethylene, 275, 340
- Polyurethane, 292–294
- Power-duration data, 48–53
- Pressure, 173, 222
- Pressure bulbs, 286
- Pressure drag, 173, 213–216
- Pressure recovery, 213–214, 236
- Propeller, 108–109, 248–249, 497–499, 504–506
- Protein, contractile, and food, 60–61, 67, 75, 77
- Public bicycle. *See* Bike-share systems
- Pyruvate, 62–64
- Quadracycle, 18, 352, 483, 487, 493
- Radial tire, 271, 307
- Radiation, thermal, 111–113, 330
- Rail HPV, 156–157, 473–479, 534–537
- Railway wheel, 264, 281–285
- Reaction wheel, 349
- Rear steering, 358, 363, 369, 382

- Recumbent HPV types, 480–483
Recumbent position, 27–31, 96–97, 232–233
Regenerative braking, 328–329
Respiratory quotient, 76–77
Resting metabolic rate (RMR), 81. *See also* Basal metabolic rate (BMR)
Reynolds number, 113, 219–229, 239–240
Riderless bicycle, 362–363, 375
Road train, 489–492
Roadster (utility) bicycle, 188
Road train, 489–492
Roller bearing, 272–275. *See also* Ball bearing
Roller-cam, 327
Roller chain, 399, 429
Roller skating, skate, 8, 11, 14, 461
Roller-cam, 327
Rolling resistance, 171, 180–181, 262–271, 276–308
Rollout (coastdown) test, 192, 198, 269–270, 299
Rowbike, 107
Rowing motion, 93–95, 419
Rumble strips, 185
Run-up, 135–137, 142–143, 147
Running, 204, 206–207
Running machine. *See* Draisine, Draisienne
Run-up, 135–137, 142–143, 147

Saddle height, 99–100
Safety
 bicycle, 10, 21, 23–24
 internal and external, 321, 487
 margin of, 301
 relative, in numbers, 532–533
Sailing, 247–250, 255–257
Schoenherr (turbulent) line, 220
Scooter, folding with saddle, 466–467
Scrub torque, 309, 313

Scything, 455–456
Semirecumbent. *See* Recumbent position
Sensitivity (relative rate of roll), 371
Separated flow, 214, 221–222
Shaft drive, 415, 417, 512
Shimmy, 383–388
Shore (hardness) values, 208, 293
Short-wheelbase recumbent, 235, 337, 367–368, 480–481
Skateboard. *See* Kickboard
Skating. *See* Ice skating; Roller skating, skate
Skiing, skis, 209–210, 289, 470
Skin or surface friction, 173, 213–215, 217–220, 239
Slip, lateral, 309–312
Slip, longitudinal, 108, 320–321, 504
Slope effects, 137–146, 176–179
Solar bicycle race, 155
Solid wheels and tires, 262, 264, 281–285, 291–294, 303
Standard acceleration of gravity, 176, 205
Standard US atmosphere, 216, 224
Standing start, 136, 148
Steam bicycle, 31
Streamlined shape, 213–215, 223, 225–229, 253
Submerged buoyancy, 501–502
Swinging-lever drive, 106–108
System boundary, 83–85

Tailwind, 175, 247, 498
Tandem, 240–241, 243–244, 489
Tension spoking, 15–16
Terminal velocity, 138, 344–345
Thermic effect of food, 75
Tidal volume (lung), 78
Tire construction, 307
Tire-on-tire test, 267–268
Traghetti, 502
Trail, mechanical trail, 364–365
Trailer, 383–385, 440, 495, 539

- Transmission efficiency, 172, 427–435
Treadwheel, treadmill, 5–7, 42–43
Tricycle, 18–20, 352–354, 381, 483
True wind, 175, 250
Tubeless tires, 308
Twisted chain, 403, 497
- Union Cycliste Internationale (UCI),
30, 130
Units, ix, 81, 216, 332
Upright cycling position, 231–232
- Velocar, 30
Velocipede. *See* Draisine, Draisienne
Velocipedio, software, 191
Velocity Dolphin, 34–36. *See also*
Mechanical series hybrid
Velogemel (bicycle sled), 470–471
Velomobile, 484–489
Vertical kilometer, 133
Virtual cycling, 179, 517
Viscosity, 222–224
VO₂max, 70, 79–80, 87, 150
- Walking, 206–208
Weir formula, 77, 82
Wetted area, 217
Wheel flop, 365, 367–368, 372
Wheels, optimal number, 304
WHPVA, 131, 140, 146, 233. *See also*
IHPVA; WRRRA
Wilsonomics, 526–527
Wind resistance. *See* Air resistance, air
drag
Windchill, 114, 116
Wing section. *See* Streamlined shape
Wingate test, 53–54, 56
Work metabolism, 83
Working efficiency and metabolism,
75, 83
WRRRA, 131. *See also* IHPVA; WHPVA
- Yuloh, 502